Anpassung des humanpathogenen Pilzes *Candida albicans* an wirtspezifische Umgebungsbedingungen durch den Transkriptionsfaktor Ace2

Inaugural-Dissertation

zur Erlangung des Doktorgrades
der Mathematisch-Naturwissenschaftlichen Fakultät
der Heinrich-Heine-Universität Düsseldorf

vorgelegt von

Lasse van Wijlick
aus Viersen

Düsseldorf, November 2016

aus dem Institut für Molekulare Mykologie

der Heinrich-Heine-Universität Düsseldorf

Gedruckt mit der Genehmigung der
Mathematisch-Naturwissenschaftlichen Fakultät
der Heinrich-Heine-Universität Düsseldorf

Referent: Prof. Dr. Joachim F. Ernst

Korreferent: Prof. Dr. Walter Däubener

Korreferent: Prof. Dr. Joachim Morschhäuser

Tag der mündlichen Prüfung: 25.01.2017

Inhaltsverzeichnis

1 Einleitung

1.1 *Candida albicans* – ein opportunistischer humanpathogener Pilz

Der Hefepilz *Candida albicans* gehört aus phylogenetischer Sicht zum Phylum der *Ascomycetes*, den Schlauchpilzen; er ist insbesondere nah mit der Klasse der *Saccharomycetes* verwandt (Petersen *et al.*, 2000) und besiedelt meist asymptomatisch den menschlichen Körper als Kommensale. Bei etwa 75 % der gesunden Bevölkerung ist *C. albicans* Bestandteil der Mikroflora des Darms, der Mundhöhle und des Urogenitaltraktes (Odds, 1988; Ghannoum *et al.*, 2010). Zu den humanmedizinisch relevanten Spezies der Gattung *Candida* gehören neben *C. albicans C. glabrata*, *C. tropicalis*, *C. krusei* und *C. parapsilosis*, die untereinander eine große Heterogenität aufweisen (Kullberg & Arendrup, 2015). Anders als bei primären humanpathogenen Pilzen, wie beispielsweise Vertretern der Gattungen *Histoplasma spp*. oder *Blastomyces spp*., sind Vertreter der Gattung *Candida* nicht in der Lage, Krankheitssymptome in gesunden Menschen zu verursachen, sie zählen zu den opportunistischen Krankheitserregern. Ändert sich der Immunstatus eines Menschen, z. B. infolge einer medikamentösen Behandlung, kann der Pilz zum Krankheitserreger werden und schwerwiegende Symptome auslösen. Paradoxerweise ist es derselbe, zuvor als Kommensale lebende *Candida*-Pilz, der nach der Schwächung des Immunsystems zum lebensbedrohlichen Pathogen wird (Eggimann & Pittet, 2006). Dem Wechsel von einer asymptomatischen Besiedlung zu einer krankhaften Infektion liegt häufig eine Störung des mikrobiellen Gleichgewichts zugrunde (Dysbiose), die zu einer Zunahme der Kolonisation durch *C. albicans* führen kann (Huffnagle & Noverr, 2013).

Durch *C. albicans* ausgelöste Infektionen lassen sich grundsätzlich in oberflächliche und systemische Infektionen unterteilen. Obwohl *C. albicans* Bestandteil der humanen Mikroflora ist, gehört der Pilz zu den häufigsten Verursachern von symptomatisch verlaufenden Pilzinfektionen (Gudlaugsson *et al.*, 2003). Oberflächliche Mykosen treten häufig bei immunsupprimierten Patienten auf, z. B. bei HIV-Patienten (Cassone & Cauda, 2012). Neben einem geschwächten Immunsystem tragen auch Stoffwechselerkrankungen, wie Diabetes mellitus oder Autoimmunkrankheiten, die wie bei der Psoriasis eine chronische Entzündung der Haut zur Folge haben, zu einem erhöhten Risiko bei (Waldman *et al.*, 2001; Darwazeh *et al.*, 1990). Zu den häufigsten oberflächlichen Mykosen zählen die vaginale Candidose und die oropharyngeale Candidose, die auch chronisch auftreten können (Sobel, 1988; Fischer, 2012). Bei Schädigung der schützenden Gewebe kann *Candida* durch Penetration des Epithels in den Blutstrom gelangen und in andere Organe disseminieren (Phan *et al.*, 2000; Wachtler *et al.*, 2011). Insbesondere bei immungeschwächten Patienten kann die Verbreitung zu einer

systemischen Candidose führen, die mit einer hohen Mortalitätsrate von 46-75 % assoziiert ist (Brown & Netea, 2012). Dabei kann *C. albicans* die Leber, Niere, Milz und die Augen infizieren. Jährlich werden weltweit über 400.000 systemisch verlaufende *C. albicans*-Infektionen registriert. Damit ist das Ausmaß systemischer Mykosen vergleichbar mit dem der durch *Plasmodium*-Parasiten verursachten Tropenkrankheit Malaria und der durch *Mycobacterium tuberculosis* verursachten Tuberkulose (Brown *et al.*, 2012).

Die Diagnostik von *C. albicans* gestaltet sich schwierig, denn es muss zwischen der normalen Besiedlung und einer akuten Infektion unterschieden werden. Neben der Kombination von histologischen Nachweismethoden und dem β-Glukan Nachweis, im Blut, einem Bestandteil der Zellwand des Pilzes, werden zunehmend kulturunabhängige Nachweismethoden entwickelt, die eine schnellere Identifikation des Pathogen erlauben (Perfect, 2013). Spezifische Nachweise einer invasiven Mykose liefert dabei z. B. die quantitative real-time PCR-basierte Diagnostik, die eine höhere Sensitivität als bisherige Diagnostik-Techniken aufweist und in der Lage ist, verschiedene *Candida spp*. zu unterscheiden (Nguyen *et al.*, 2012). Eine neuartige Entwicklung für den Nachweis von invasiven Mykosen basiert auf der Aktivierung von pilzspezifischen Immunzellen. Dabei wird die Frequenz, mit der diese Zellen den sogenannten CD154-Liganden exprimieren ($CD154^+$ T-Zellen), als Indikator verwendet (Bacher *et al.*, 2015). Die Behandlung von invasiven oder oberflächlichen *C. albicans*-Infektionen erfolgt in der Regel unmittelbar nach dem Nachweis der Infektion mit den Antimykotika aus den Klassen der Echinocandine (z. B. Micafungin, Caspofungin), der Polyene (z. B. liposomales Amphotericin B) oder alternativ der Azole (Fluconazol). Obwohl die Entwicklung von effizienten Antimykotika in den vergangen Jahren Fortschritte gemacht hat, ist die Anzahl resistenter *Candida*-Isolate in den Vereinigten Staaten und einigen europäischen Ländern angestiegen; insbesondere zeigt sich ein Anstieg in der Resistenz gegen Azole (Pappas *et al.*, 2009; Ruhnke *et al.*, 2011).

1.2 Pathogenitätsfaktoren von *C. albicans*

Faktoren, die auf Pilz- und Wirtseite den Übergang von *C. albicans* zum Pathogen ermöglichen, sind weitestgehend unbekannt. Aktuelle Studien weisen darauf hin, dass *C. albicans* seine Pathogenitätsfaktoren umgebungsabhängig reprimiert, um die Besiedlung im Gastrointestinaltrakt aufrechtzuerhalten (Doedt *et al.*, 2004; Pierce & Kumamoto, 2012). Neben einem intakten Immunsystem spielt auch die Besiedlung von probiotischen Bakterien im Darm eine wichtige Rolle für die Aufrechterhaltung der kommensalen Lebensweise von *C. albicans*. Es konnte gezeigt werden, dass *C. albicans* in Abwesenheit der schützenden

Bakteriengemeinschaft den Wechsel zum Pathogen vollzieht (Mendonca *et al.*, 2012; Koh, 2013). Zu den wichtigsten Pathogenitätsmechanismen von *C. albicans* zählen beispielsweise die Adhäsion an Wirtsepithele, der Wechsel von der Hefeform zur Hyphe- oder Opaque-Zellform (*White-Opaque-Switch*), die Biofilmbildung, die Sekretion von Proteasen, sowie die Maskierung von zelleigenen Oberflächenproteinen als Schutzmechanismus vor dem Immunsystem. Darüber hinaus verfügt *C. albicans* über eine ausgeprägte metabolische und Stress-induzierende Anpassungsfähigkeit.

1.2.1 Der Polymorphismus von *C. albicans*

Von besonderer Bedeutung für die Anpassung von *C. albicans* an sich ändernde Umweltbedingungen ist die Fähigkeit, seine Morphologie zu verändern. Diese Eigenschaft wird als Polymorphismus bezeichnet und erlaubt *C. albicans*, zusätzlich zu intrazellulären Anpassungsmechanismen, z. B. der Anreicherung von Sekundärmetaboliten wie Glycerol bei der Antwort auf osmotischen Stress, seine morphologische Form den Umwelteigenschaften anzupassen. Eine Vielzahl von Morphotypen von *C. albicans* konnte bereits identifiziert werden (Abb.1.1): Hefe, Hyphe, Pseudohyphe, Chlamydosporen, GUT und Opaque.

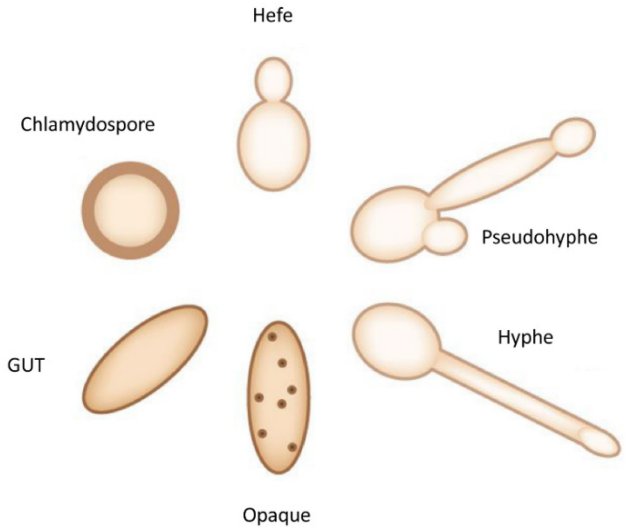

Abb.1.1 Morphologische Vielfalt von *C. albicans*. *C. albicans* weist eine Vielzahl von Morphotypen auf, die es dem Pilz erlauben sich an spezifische Umweltbedingung anzupassen. Die Hefe-Zellform begünstigt die Vermehrung und Verbreitung von *C. albicans*, während die Hyphe-Zellform die Penetration und Invasion von Gewebe und Organen ermöglicht. Die Opaque-Zellform stellt die paarungs-kompetente Zellform von *C. albicans* dar. Die GUT-Zellform zeichnet sich durch die besonders gute Anpassung an das Darmmilieu aus und begünstigt das kommensale Wachstum. Chlamydosporen stellen Überdauerungsformen dar und zeichnen sich durch eine besonders dicke Zellwand und die kugelige Zellform aus. Pseudohyphen entstehen infolge von unipolarem Wachstum, ohne die Abspaltung der Tochterzelle von der Mutterzelle. Die Grafik wurde Gow (2013) entnommen.

Ausgelöst wird der Wechsel in eine andere Zellform durch externe Reize, die durch Rezeptoren an Signaltransduktionswege vermittelt werden und zur Aktivierung von Transkriptionsfaktoren führen. Die kürzlich beschriebene GUT-Zellform (***G**astrointestinally-Ind**U**ced **T**ransition*) weist eine große Ähnlichkeit zu der Opaque-Zellform auf. Beide Zellformen unterscheiden sich jedoch grundlegend in ihrem transkriptionellen Profil, wie auch in ihrer Funktion. Während die Opaque-Zellform die paarungs-kompetente Zellform von *C. albicans* darstellt, zeichnet sich die GUT-Zellform durch eine besonders gute Anpassung an das Darmmilieu aus und unterstützt das kommensale Wachstum von *C. albicans* (Pande *et al.*, 2013; Miller & Johnson, 2002; Gow, 2013). Die Aufrechterhaltung des kommensalen Wachstums wird dabei durch die aktive Reprimierung von Pathogen-assoziierten Genen begünstigt. Interessanterweise wird das jeweilige transkriptionelle Programm beider Zellformen maßgeblich durch den Transkriptionsfaktor Wor1 reguliert (Pande *et al.*, 2013; Morschhauser, 2010). In der Hefeform vermehrt sich *C. albicans* durch Knospung und anschließende Abschnürung der neugebildeten Tochterzelle von der Mutterzelle. Echte Hyphen entstehen durch apikales Wachstum. Der dabei wachsende Keimschlauch ist septiert und weist parallel verlaufende Zellwände auf, während bei Pseudohyphen die elongierte Zellform Einschnürungen aufweist. Diese filamentöse Wachstumsform entsteht in Folge einer mehrfachen, unipolaren Knospung, ohne die folgende Abschnürung der Tochterzelle (Odds, 1988; Ernst, 2000). Chlamydosporen sind große, runde Zellen mit einer deutlich verstärkten Zellwand und werden nur unter bestimmten nährstofflimitierenden Bedingungen gebildet (Staib & Morschhauser, 2007). Die verschiedenen Zellformen erfüllen unterschiedliche Funktionen bei der Pathogenese des Pilzes. Die Hefeform begünstigt hauptsächlich die Vermehrung und Verbreitung über die Blutbahn, während die Hyphenform die Penetration von Epithelgewebe ermöglicht (Cutler, 1991; Hostetter, 1994). Darüber hinaus weist die Hyphenform eine erhöhte Adhärenz auf und ermöglicht es *C. albicans* aus Phagozyten zu entkommen (Vazquez-Torres & Balish, 1997). Die Funktion von Chlamydosporen ist ungeklärt, möglicherweise stellt diese Zellform eine Überdauerungsform dar.

1.2.2 Der Hefe-Hyphe-Wechsel

Der Wechsel zwischen der Hefe- und Hyphe-Zellform wird durch eine Vielzahl von Faktoren ausgelöst und spielt eine zentrale Rolle beim Übergang des kommensalen Wachstums zum invasiven Pathogen. Zu diesen Bedingungen gehören Serum, Stickstofflimitierung, eine erhöhte CO_2-Konzentration, ein neutraler bis basischer pH-Wert, die Exposition mit N-Acetyl-D-Glukosamin (GlcNAc) und eine Temperatur von 37 °C (Cottier & Muhlschlegel, 2009;

Huang, 2012). Gesteuert wird der morphologische Wechsel durch eine ebenso hohe Anzahl von Signaltransduktionswegen, die häufig miteinander vernetzt sind und teilweise überlappende Gen-Sets regulieren (Sudbery, 2011). Die wohl bedeutendsten Signaltransduktionswege sind der cAMP-Proteinkinase-A-Signalweg (cAMP-PKA) und der Cek1-Mitogen-Aktivierte-Proteinkinase-Signalweg (Cek1-MAPK).

Der cAMP-PKA-Signalweg wird durch erhöhte Temperaturen und CO_2-Konzentrationen aktiviert. Dabei wirken diese direkt auf die Adenylatzyclase Cyr1 und stimulieren die Bildung von cAMP aus ATP (Bockmuhl & Ernst, 2001). Weitere Signale, die den PKA-Signalweg aktivieren sind Serum und GlcNAc, die auf Ras1 wirken, eine GTPase, die der Adenylatzyclase vorgeschaltet ist (Feng *et al.*, 1999). Nährstoffmangel stimuliert den PKA-Signalweg über den G-Protein-gekoppelten, membranständigen Rezeptor Gpr1 (Maidan *et al.*, 2005). Durch die zunehmende Konzentration des Botenstoffs cAMP bindet dieser an die regulatorische Untereinheit der PKA Bcy1 und bewirkt dadurch die Dissoziation von den katalytischen Untereinheiten Tpk1 und Tpk2 (Abb.1.2). Ihrerseits phosphorylieren und aktivieren Tpk1 und Tpk2 u. a. den Transkriptionsfaktor Efg1 (Sonneborn *et al.*, 2000; Bockmuhl & Ernst, 2001). In Abhängigkeit des Signals wirkt Efg1 entweder stimulierend oder reprimierend auf die Hyphenbildung. Die Regulation der Efg1-Aktivität ist sehr komplex und wird durch verschiedene Umweltfaktoren beeinflusst. Efg1 gehört zu den APSES-Proteinen und weißt die für diese Proteingruppe typische basic-Helix-Loop-Helix (bHLH)-Domäne auf, die sowohl die Dimerisierung von Efg1 als auch die DNA-Bindung vermittelt (Stoldt *et al.*, 1997; Doedt *et al.*, 2004). In der Gegenwart von Sauerstoff wird Efg1 für die Initiierung der Hyphenbildung benötigt. Bei Sauerstoffausschluss (Hypoxie) hingegen, z. B. bei eingebettetem Wachstum in einer Agarmatrix, wirkt Efg1 als Repressor der Hyphenbildung. Diese Funktion ändert sich jedoch bei erhöhten Temperaturen. Oberhalb von 35 °C wird Efg1 auch für die hypoxische Filamentierung benötigt (Sonneborn *et al.*, 1999; Setiadi *et al.*, 2006; Giusani *et al.*, 2002). Hypoxische Bedingungen treten in fast allen Körpernischen auf und die Anpassungsfähigkeit von *C. albicans* an niedrige Sauerstoffkonzentrationen ist von großer Bedeutung für das Überleben im Wirt und die Pathogenese (Ernst & Tielker, 2009). Nach der Initiierung der Hyphenbildung konnte negative Autoregulation durch Efg1 an seinem eigenen Promotor nachgewiesen werden, die darauf hinweist, dass Efg1 grundsätzlich auch eine reprimierende Funktion in der späteren Phase der Hyphenbildung einnimmt (Tebarth *et al.*, 2003). Als Zielgene von Efg1 wurden u. a. die Hyphenregulatoren *TEC1*, *CZF1*, *EED1* und *NRG1* identifiziert (Lassak *et al.*, 2011).

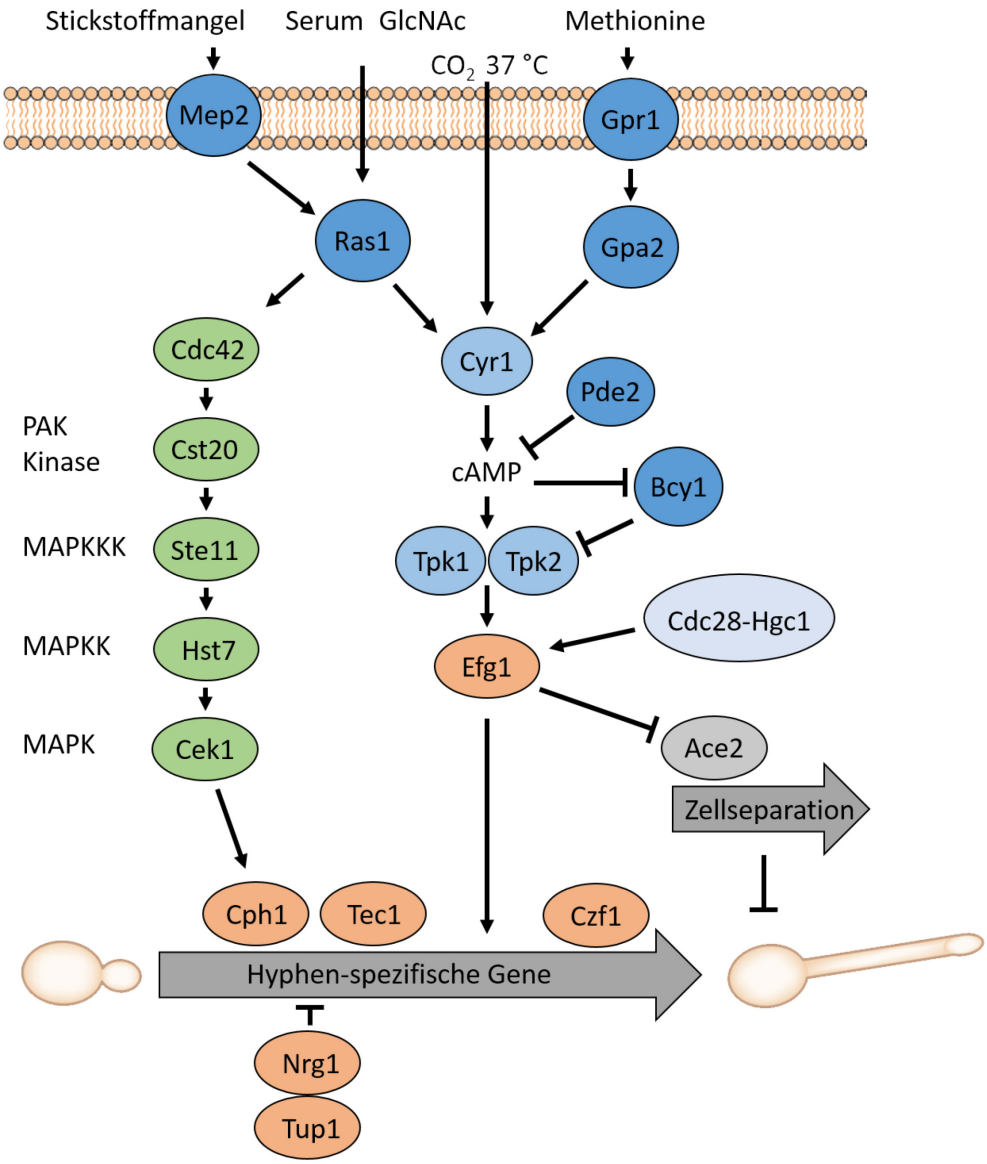

Abb.1.2 Regulation der Hyphenbildung in *C. albicans*. Übersicht über den cAMP-PKA (hell blau) und den Cek1 MAPK-Signalweg (grün), die parallel verlaufen und gemeinsam mit weiteren Transkriptionsaktivatoren und Repressoren (rot) die Hyphenbildung in *C. albicans* regulieren. Nähere Erläuterungen befinden sich im Text. Die Grafik wurde aus Sudbery (2011) entnommen und modifiziert.

Darüber hinaus konnte gezeigt werden, dass die Tpk-Untereinheiten unterschiedliche Funktionen ausüben, z. B. wird Tpk1 für die Hyphenbildung auf festen Nährmedien benötigt, während Tpk2 nur für die Hyphenbildung in flüssigen Nährmedien benötigt wird (Bockmuhl & Ernst, 2001). Außerdem konnte kürzlich gezeigt werden, dass die Tpk Untereinheiten selbst an regulatorische Promotorbereiche von morphogenesespezifischen Genen binden, die auch als Zielgene von Efg1 identifiziert wurden (Schaekel *et al.*, 2013). Auf diese Weise könnten die Proteinkinasen zur Rekrutierung und schließlich Aktivierung von Efg1 bereits an den Zielgenen beitragen und eine schnelle Anpassung von *C. albicans* begünstigen. Der genaue Mechanismus, über den die Proteinkinasen in den Zellkern gelangen ist unklar, diese Form der Regulation könnte auch für andere Signalwege von Bedeutung sein.

Der Cek1 MAPK-Signalweg wird vermutlich auch über die Ras1 GTPase aktiviert, die mit der GTPase Cdc42 interagiert (Abb.1.2), und besteht aus dem MAPK-Modul Cst20, Ste11, Hst7 und Cek1(Csank *et al.*, 1998; Leberer *et al.*, 2001). Bei der Aktivierung des Signalweges wird über eine Phosphorylierungskaskade die endständige Kinase Cek1 phosphoryliert, die ihrerseits den Transkriptionsfaktor Cph1 aktiviert (Csank *et al.*, 1998). Im Gegensatz zum PKA-Signalweg wird der Cek1 MAPK-Signalweg nur für die Hyphenbildung auf Oberflächen benötigt, z. B. auf festen Nährmedien, denen Mannitol als Kohlenstoffquelle zugesetzt wurde. In flüssigen Nährmedien, die mit Serum versetzt wurden, weist die *cph1* Mutante keinen Defekt in der Hyphenbildung auf (Liu *et al.*, 1994). Der Phosphorylierungsstatus der Cek1 Kinase wird durch die MAPK-Phosphatase Cpp1 negativ reguliert und reprimiert auf diese Weise die Aktivierung des Signalwegs (Csank *et al.*, 1997). Es wurde aber auch eine Cek1-unabhängige Funktion von Cpp1 für die Hyphenmorphogenese beschrieben, bei der Cpp1 an der Regulation von hyphenspezifischen Genen beteiligt ist, die interessanterweise Zielgene von Efg1 darstellen (Schroppel *et al.*, 2000).

Weitere Signalwege, die einen Einfluss auf die Hyphenmorphogenese haben, sind der Rim101-Signalweg, der Hog1 (*high osmolarity glycerol*) MAPK-Signalweg, der TOR (*target of rapamycin*)-Signalweg und der RAM (*regulation of Ace2 and morphogenesis*)-Signalweg. Zielgene des RAM-Signalwegs werden u. a. für die Zellseparation während des Hefe- und Pseudohyphenwachstums benötigt, dazu gehört insbesondere *CHT3*, das für eine Chitinase kodiert und *SCW11* (Kelly *et al.*, 2004). Reguliert werden diese Gene durch den Transkriptionsfaktor Ace2, der in der späten M- bzw. frühen G1-Phase des Zellzyklus in den Zellkernen von Tochterzellen lokalisiert und die Genexpression aktiviert (Sbia *et al.*, 2008). Damit das apikale Wachstum während der Hyphenbildung nicht unterbrochen wird, aktiviert der aus Cdc28 und der Cyklin-abhängigen Kinase Hgc1 bestehende Komplex den Transkriptionsfaktor Efg1 (Abb.1.2). Durch die Phosphorylierung von Efg1 an der Position T179, bindet Efg1 an regulatorische Sequenzen von Ace2-aktivierten Zielgenen und reprimiert deren Transkription, wodurch die Zellteilung verhindert wird (Wang *et al.*, 2009).

Auch post-transkriptionelle Mechanismen sind von Bedeutung für den Hefe-Hyphe-Wechsel, z. B. für die Stabilität von spezifischen mRNA Molekülen (Verma-Gaur & Traven, 2016). Für den hyphenregulierenden Transkriptionsfaktor Ume6 konnte kürzlich gezeigt werden, dass die Translation durch eine Sekundärstruktur innerhalb des 5‘-untranslatierten Bereichs (UTR) beeinflusst wird. Auf diese Weise wird das *UME6*-Transkript nur nach der Initiierung der Hyphenmorphogenese translatiert und bewirkt die Aufrechterhaltung des Hyphenwachstums durch Ume6 (Cleary *et al.*, 2012; Childers *et al.*, 2014).

Die besondere Bedeutung der beiden Transkriptionsfaktoren Efg1 und Cph1 bei der Hyphenbildung wird durch den Phänotyp der *cph1 efg1* Doppelmutante deutlich, die unter fast allen *in vitro*-Bedingungen nicht in der Lage ist Hyphen zu bilden (Lo *et al.*, 1997). Dieses Ergebnis deutet darauf hin, dass die beiden Signalwege parallel verlaufen und unabhängig voneinander zum Wechsel von der Hefe- und Hyphe-Zellform beitragen. Neben ihrer Funktion bei der Hyphenbildung weisen sowohl die *cph1* als auch die *efg1* Mutante erhöhte Sensitivitäten gegen die Zellwand-destabilisierende Substanzen auf (Eisman *et al.*, 2006). Der Cek1 MAPK-Signalweg wird darüber hinaus für die Anpassung von Zellwandschäden benötigt (Roman *et al.*, 2007). Für Efg1 konnte gezeigt werden, dass der Transkriptionsfaktor einen direkten Einfluss auf die Biosynthese der Zellwand ausübt (Sohn *et al.*, 2003). Die Zellwand von *C. albicans* ist von zentraler Bedeutung für die morphologische Vielfalt des Pilzes und zugleich Angriffspunkt des Immunsystems.

1.3 Zellwandeigenschaften von *C. albicans*

Die Zellwand von *C. albicans* kann in eine innere und äußere Schicht unterteilt werden. Die innere Schicht der Pilz-Zellwand setzt sich aus Chitin, β1,3-Glukan und β1,6-Glukan zusammen. Die äußere Schicht besteht hauptsächlich aus Mannosepolymeren, die kovalent mit Glykoproteinen verknüpft sind (Abb.1.3). Der Widerstand gegen den Zellturgor und die damit verbundene Aufrechterhaltung der Zellform wird durch die strukturellen Komponenten Chitin und β1,3-Glukan vermittelt (Shepherd, 1987; Chaffin *et al.*, 1998). Die Mannosepolymere der äußeren Schicht schützen durch ihre geringe Permeabilität die innere Zellwand vor Angriffen des Immunsystems und tragen zur Resistenz gegen Antimykotika bei, die sich gegen Bestandteile der Zellwand und Glykostrukturen richten. Die Zellwand von *C. albicans* ist jedoch kein starres Gebilde, sondern sie stellt vielmehr ein äußerst komplexes und dynamisches Organell dar. In Folge von Stress-induzierter Anpassung, aber auch bei der Zytokinese, der Sporulation und der Hyphenbildung, wird die Zellwand modelliert und synthetisiert (Smits *et al.*, 2001). Die Zellwandbestandteile bilden unterschiedliche Anteile am Zellwandtrockengewicht. Den größten Anteil mit etwa 40 % des Trockengewichts bildet das β1,3-Glukan, ein lineares Polymer aus Glukoseeinheiten. Mit bis zu 20 % des Trockengewichts stellt das β1,6-Glukan, das aus verzweigten Glukoseeinheiten besteht, einen kleineren Anteil dar. Chitin, ein unverzweigtes β1,4-verknüpftes *N*-Acetylglukosamin-Polymer verbindet das β1,3-Glukan und das β1,6-Glukan und trägt damit wesentlich zur Stabilität der Zellwand bei. Mit einem Anteil von etwa 2 % am Trockengewicht bildet Chitin den geringsten Anteil an der

Zellwand. Die Zellwandproteine der äußeren Zellwand sind vielfach *N*- und *O*-glykosyliert und stellen etwa 40 % des Zellwandtrockengewichts dar (Klis *et al.*, 2001; Klis *et al.*, 2002).

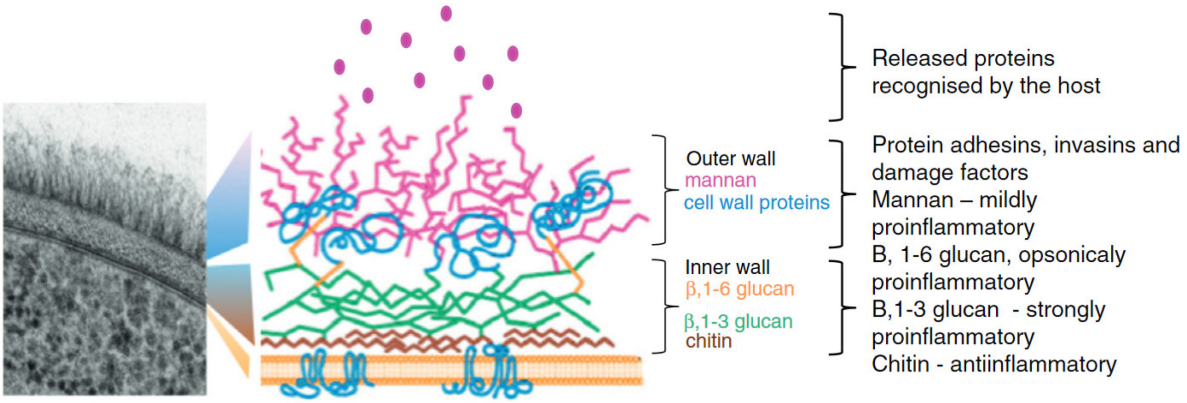

Abb.1.3 Zusammensetzung der Zellwand von *C. albicans*. Die elektronenmikroskopische Aufnahme zeigt einen Ausschnitt aus der *C. albicans*-Zellwand. Die innere Schicht der Zellwand besteht aus β1,3-Glukan, β1,6-Glukan und einem geringen Chitinanteil. Die äußere Schicht der Zellwand besteht aus Mannoproteinen, die kovalent entweder mit dem β1,3-Glukan (Pir-Proteine) oder dem β1,6-Glukan (GPI-Proteine) verknüpft sind und nicht kovalent gebundenen Scwp Proteinen. Die jeweiligen Zellwandbestandteile bewirken aktivierende oder supprimierende Immunreaktionen. Die Grafik wurde Gow & Hube (2012) entnommen.

Zellwandproteine können kovalent, entweder über den Rest eines GPI (*Glycosyl-phosphatidyl-inositol*) Ankers mit dem β1,6-Glukan der Zellwand verbunden sein, oder wie es bei den Pir- (*Protein with internal repeats*) Proteinen der Fall ist, über eine Transglutaminasereaktion kovalent mit dem β1,3-Glukan (Richard *et al.*, 2002; Ecker *et al.*, 2006). Im Gegensatz dazu sind die Scwp (*Soluble cell wall proteins*) Zellwandproteine nicht kovalent mit der Zellwand verknüpft, erfüllen aber wichtige Aufgaben bei der Modellierung der Zellwand, z. B. für die Synthese von Chitin durch Chitinsynthasen und die Degradation von Chitin durch Chitinasen (Munro & Gow, 2001; Chaffin, 2008). Einige Zellwandproteine tragen zur Struktur der Zellwand bei, während andere Zellwandproteine spezifischere Funktionen aufweisen, die essentiell für die Pathogenität von *C. albicans* sind. Die Zellwandproteine Hwp1 und Als3 vermitteln beispielsweise die Adhäsion an Wirtsgewebe (Staab & Sundstrom, 1998; Nobile *et al.*, 2006; Almeida *et al.*, 2008). Die Aspartat-Proteasen Sap1-8 werden sekretiert und bewirken die Degradation von Wirtsgewebe. Dadurch werden einerseits verwertbare Kohlenstoffquellen freigesetzt, andererseits wird dadurch auch die Gewebeinvasion erleichtert (Naglik *et al.*, 2003). Ein weiteres Beispiel ist das Zellwandprotein Sod5, eine Superoxid-Dismutase, die *C. albicans* vor oxidativem Stress schützt (Martchenko *et al.*, 2004).

Zudem wird die Zusammensetzung der Zellwandbestandteile durch die Morphologie beeinflusst, z. B. weisen Hyphenzellen einen Chitin Anteil von bis zu 10 % auf. Dieses verteilt sich jedoch gleichmäßiger als bei Hefezellen, deren Hauptanteil des Chitins in den Knospungsnarben lokalisiert ist (Munro *et al.*, 1998; Munro & Gow, 2001). Außerdem

unterscheidet sich das Mannan von Hefen und Hyphen, sowohl chemisch, als auch in seinen physikalischen Eigenschaften und trägt damit zu unterschiedlichen Immunreaktionen bei (Cheng *et al.*, 2011).

1.3.1 Interaktion mit dem Immunsystem

Die Zellwandbestandteile von *C. albicans* stellen Antigene dar, die von spezialisierten Zellen des Immunsystems erkannt werden können (Netea *et al.*, 2008). Das Immunsystem hat zur Erkennung dieser konservierten Strukturen, den PAMPs (*pathogen associated molecular patterns*), eine Reihe wirksamer Rezeptoren entwickelt, die im allgemeinen als *Pattern Recognition Receptors* (PRRs) bezeichnet werden und an der Oberfläche von Makrophagen und dendritischen Zellen lokalisiert sind. Die verschiedenen Zellwandbestandteile werden von unterschiedlichen PRRs erkannt. Dectin-1 und Dectin-2 gehören zu den C-Typ Lektin Rezeptoren und erkennen β-Glukan und α-Mannan (Saijo & Iwakura, 2011; Yoshikawa *et al.*, 2016). Der Toll-like Rezeptor 2 (TLR2) und TLR4 erkennen sowohl Phospholipomannan als auch *O*-glykosidisch verknüpftes Mannan (Netea *et al.*, 2006; Lionakis & Netea, 2013). Gemeinsam mit Dectin-1 ist auch TLR2 an der Erkennung von β1,3-Glukan beteiligt und führt zu einer verstärkten Aktivierung des Immunsystems (Dennehy *et al.*, 2008). Darüber hinaus spielt bei der Erkennung von Mannan das Lektin Galectin-3, das MRP (*Mannose Receptor Protein*), Mincle (*macrophage induced c-type lectin*) und DC-SIGN (*dendritic cell-specific ICAM-3-grabbing non-integrin-1*) eine wichtige Rolle (Miramon *et al.*, 2013). Die Immunerkennung von Chitin ist noch nicht vollständig geklärt, involviert aber die PRRs TLR2 und Dektin-1 (Lee *et al.*, 2008). In Abhängigkeit der erkannten Zellwandkomponente werden unterschiedlich starke Entzündungsreaktionen ausgelöst. Das β-Glukan, insbesondere β1,3-Glukan, löst eine starke Entzündungsreaktion aus (Abb.1.3), während Mannanpolymere und das β1,6-Glukan nur eine milde Aktivierung bewirken (Gow & Hube, 2012). Die Erkennung von Chitin durch das Immunsystem kann sowohl entzündungsfördernd, als auch -hemmend wirken. Dabei spielt die Länge der Chitin Moleküle eine Rolle (Lenardon *et al.*, 2010; Da Silva *et al.*, 2009). Auf diese Weise trägt die Gesamtheit der Zellwandbestandteile zu einer einzigartigen immunologischen Signatur von *C. albicans* bei, die auch durch die morphologische Form beeinflusst wird. Beispielsweise lösen Hefe- und Hyphezellen unterschiedlich starke Immunreaktionen aus und unterscheiden sich in den aktivierten Signalwegen (Gantner *et al.*, 2005; Gow & Hube, 2012). *C. albicans* Zellen in der Hyphe-Form führen zu einer besonders starken Induktion der IL-4 Produktion, während Hefezellen,

vermutlich durch die erhöhte β1,3-Glukan Exposition an den Knospungsnarben, zu einer verstärkten Dectin-1 Aktivierung führen (Gantner *et al.*, 2005; van der Graaf *et al.*, 2005).
Neben den strukturellen Komponenten der Zellwand spielen auch die Zellwandproteine eine wichtige Rolle bei der Erkennung durch das Immunsystem. Darüber hinaus weisen einige Zellwandproteine Funktionen bei der Immunkontrolle auf. Durch die Sekretion des löslichen Zellwandproteins Pra1 wird beispielsweise das Komplementsystem der Immunantwort inhibiert (Zipfel *et al.*, 2011). Ein weiteres Beispiel ist das Msb2-Mucin, das durch Abspaltung der extrazellulären-Domäne in die Umgebung sekretiert wird und u. a. mit den antimikrobiellen Peptiden LL-37 und Histatin-5, die von Effektorzellen des Immunsystems sezerniert werden, interagieren kann und in der Lage ist diese zu inaktivieren. Auf diese Weise wird *C. albicans*, wie auch andere sich in der näheren Umgebung befindliche Mikroorganismen, effektiv vor Angriffen des Immunsystems geschützt (Szafranski-Schneider *et al.*, 2012). Die protektive Wirkung des Msb2 Proteins wird dabei durch den Glykosylierungsstatus des Proteins wesentlich beeinflusst, so wies das Msb2 Protein eine verminderte protektive Wirkung in einem Stamm auf, der defekt für die Pmt1-vermittelte *O*-Mannosylierung ist (Swidergall *et al.*, 2013).

1.3.2 Glykosylierung

Die Glykosylierung stellt eine äußerst wichtige Form der Proteinmodifikation dar. Schätzungsweise wird die Hälfte aller Proteine durch Zuckerstrukturen modifiziert (Apweiler *et al.*, 1999). Diese Form der Proteinmodifikation ist in allen Bereichen des Lebens konserviert und die katalytischen Enzyme, die für die Glykosylierungsreaktionen benötigt werden, die Glykosyltransferasen und Glykosidasen, finden sich sowohl bei Archaeen, Prokaryoten, als auch in allen Eukaryoten (Spiro, 2002). Bei Menschen sind mindestens 30 Krankheiten bekannt, die im Zusammenhang mit fehlender oder fehlerhafter Glykosylierung stehen (Jaeken, 2010). Die häufigsten Glykosylierungstypen sind die *O*- und *N*-Glykosylierung (Abb.1.4). Auch die Modifikation mit dem Rest eines GPI-Ankers stellt eine Form der Glykosylierung dar. Dabei wird der GPI-Anker, der sich aus einem Saccharid-Rückgrat, dem Phosphoethanolamin-Linker und dem Phosphatidylinositol-„Tail“ zusammensetzt, über das Phosphoethanolamin an den Carboxy-Terminus des Glykoproteins geknüpft (Canivenc-Gansel *et al.*, 1998). Die Modifikation mit GPI-Ankern ermöglicht beispielsweise die Verankerung des modifizierten Proteins in der Plasmamembran und ist insbesondere bei Protozoen eine der häufigsten Modifikationen von Membranproteinen (Guha-Niyogi *et al.*, 2001).

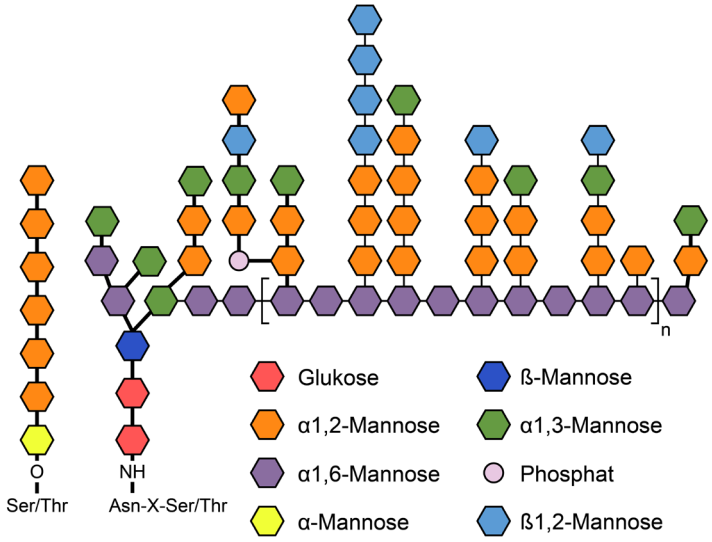

Abb.1.4 Struktur der *N*- und *O*-Glykane in *C. albicans*. Nach der initialen Verknüpfung der α-Mannose durch die Protein-*O*-Mannosyltransferasen kann die Saccharidkette bei der *O*-Glykosylierung um bis zu sechs weitere α1,2-Mannosen verlängert werden. Die Saccharidkette kann bei der *N*-Glykosylierung sehr komplexe Strukturen ausbilden. Die Grafik wurde Hall & Gow (2013) entnommen und modifiziert.

Die Funktionen von Glykosylierungen sind sehr vielfältig und stellen wichtige Modifikation für sowohl biologische, als auch physiologische Prozesse dar. Beispielsweise helfen Zuckermodifikationen bei der Qualitätskontrolle während der Proteinfaltung und tragen zur Stabilität von Proteinen bei. Zudem ist die Glykosylierung auch bei der Erkennung von biologisch wirksamen Molekülen, wie dem Insulin im Menschen von Bedeutung (Xu & Ng, 2015; Collier *et al.*, 1993; Maggi *et al.*, 1998). In *C. albicans* wird die *O*-Mannosylierung für das vollständige pathogene Potential benötigt (Rouabhia *et al.*, 2005). Die Glykosylierung betrifft hauptsächlich sekretorische Proteine, die entlang des Sekretionsweges im Endoplasmatischen Retikulum (ER) und Golgi-Apparat glykosyliert werden und üblicherweise in der Plasmamembran der Zellwand lokalisiert sind oder ins Medium freigesetzt werden. Auf diese Weise trägt die Glykosylierung auch zur Erkennung durch das Immunsystem bei (Hall & Gow, 2013).

1.3.3 *N*-Glykosylierung

Bei der *N*-Glykosylierung in *C. albicans* werden zunächst zwei GlcNAc-Reste, danach aber ausschließlich Mannosen auf die Zielproteine übertragen; der Ablauf ist prinzipiell sehr ähnlich zu dem in höheren Eukaryoten. Zunächst erfolgt die Synthese der linearen Saccharidkette auf der zytosolischen Seite des ER, die aus der Abfolge Man_5-$GlcNAc_2$ besteht. Als Trägermolekül fungiert Dolichol-Phosphat (Dol-P), das gemeinsam mit der Vorläufer-Saccharidkette auf die luminale Seite des ER translociert wird. Dort wird die Saccharidkette zu der Abfolge Glc_3-

Man_5-$GlcNAc_2$ vervollständigt. Die reife Saccharidkette wird vom Trägermolekül Dol-P durch den OST-Komplex über eine *N*-glykosidische Bindung auf einen Asparagin-Rest des Zielproteins übertragen. Dabei wird die Konsensus-Sequenz Asn-X-Thr/Ser erkannt. Es werden nur etwa 30-65 % der im Protein vorkommenden *N*-Glykosylierungsstellen modifiziert (Tanner & Lehle, 1987; Petrescu *et al.*, 2004). Im Golgi-Apparat findet anschließend die Verlängerung der Kern-Saccharidkette statt, die sehr komplexe Strukturen ausbilden kann (Abb.1.4). Es können bis zu 200 Mannosereste an die Kette gebunden werden (Lipke & Ovalle, 1998). Damit trägt die *N*-Glykosylierung zur Diversität des Proteoms bei. Dabei können die Längen der Zuckerketten, die Struktur und die Komposition unterschiedlich sein. Bei *C. albicans* wird die Kettenverlängerung im Golgi durch die Verknüpfung einer Mannose an die Saccharidkette durch die Mannosyltransferase Och1 initiiert. Entsprechend weisen *och1*-Mutanten keine äußeren Saccharidketten auf, sondern nur den Saccharidkern. Auf den Verlust der äußeren Saccharidkette reagiert *C. albicans* mit der Einlagerung von zusätzlichem Chitin und Glukan in der Zellwand (Netea *et al.*, 2006; Bates *et al.*, 2006). *C. albicans* Mutanten mit Defekten in Enzymen, die an der Kettenverlängerung beteiligt sind, weisen eine veränderte Virulenz auf und sind sensitiver gegen Zellwand-destabilisierenden Substanzen (Mora-Montes *et al.*, 2007; Mora-Montes *et al.*, 2010). Die äußeren Mannanketten schützen folglich *C. albicans* vor Angriffen des Immunsystems und tragen zu einer erfolgreichen Besiedlung des Wirtes bei. Interessanterweise werden *N*-Mannan-Strukturen im Gegensatz zu *O*-Mannan von dem C-Typ Lektin MRP, das von dendritischen Zellen exprimiert wird, erkannt und beeinflussen direkt die Produktion des entzündungsfördernden Zytokins IL-6. *O*-Mannan-Strukturen werden dagegen von TLR4 erkannt (Netea *et al.*, 2006; Netea *et al.*, 2008).

1.3.4 *O*-Mannosylierung

Wie bei der *N*-Glykosylierung werden bei der *O*-Glykosylierung bei *C. albicans* Mannosen auf das Zielprotein übertragen. Eine spezifische Konsensus-Sequenz ist nicht bekannt. Die Mannose-Moleküle werden jedoch ausschließlich *O*-glykosidisch mit der Hydoxylgruppe von Serin- und Threonin-Aminosäuren des Zielproteins verknüpft. *O*-glykosidische Proteinmodifikationen in höheren Eukaryoten weisen eine hohe Vielfalt der verknüpften Zuckermoleküle auf, z. B. werden neben Mannose auch Fucose, *N*-Acetylgalactosamin, Sialinsäure und GlcNAc auf das Zielprotein übertragen. Das Vorläufermolekül GDP-Mannose wird von Dpm1, der Dolicholphosphat-Mannose-Synthase auf das Trägermolekül Dol-P übertragen. Von der zytosolischen Seite des ER wird das Trägermolekül mit der verknüpften Mannose, Dol-P-Man, mit Hilfe der Flippase durch die Membran auf die luminale Seite des ER

transloziert. Die initiale Anknüpfung der ersten Mannose wird von den Protein-*O*-Mannosyltransferasen (Pmt) katalysiert und erfolgt bereits während der Translokation des Zielproteins in das ER-Lumen durch die Sekretionspore Sec61 (Tanner & Lehle, 1987). Die *O*-Mannosylierung bei *C. albicans* erfolgt demnach kotranslational. In höheren Eukaryoten erfolgt die *O*-Glykosylierung fast ausschließlich erst nach der vollständigen Faltung des Proteins, posttranslational im Golgi. In Pilzen wird die Verknüpfung der ersten- und zweiten-Mannose an die α-Mannosekette von den α1,2-Mannosyltransferasen Mnt1 und Mnt2, die teilweise redundante Funktionen aufweisen, im Golgi-Apparat katalysiert (Abb.1.4). Bei *C. albicans* kann die α-Mannosekette um bis zu sechs Mannosen verlängert werden (Buurman *et al.*, 1998; Munro *et al.*, 2005). Mutanten mit Defekten in der Biosynthese des *O*-Mannans oder des *N*-Mannans, weisen verminderte Virulenz auf. Zudem zeigen diese Mutanten Defekte in der Fähigkeit zu adhärieren und sind häufig sensitiver gegen Antimykotika und zellwandschädigende Substanzen (Timpel *et al.*, 1998; Timpel *et al.*, 2000; Prill *et al.*, 2005; Munro *et al.*, 2005).

1.3.5 Protein-*O*-Mannosyltransferasen in *C. albicans*

Protein-*O*-Mannosyltransferasen (Pmts) bilden eine konservierte Proteinfamilie innerhalb der Eukaryoten und wurden u. a. in *Drosophila melanogaster* und dem *Homo sapiens* nachgewiesen. Darüber hinaus wurden Pmt-Homologe auch in verschiedenen Prokaryoten identifiziert, z. B. in Mykobakterien und Corynebakterien (Lyalin *et al.*, 2006; Willer *et al.*, 2002; Mahne *et al.*, 2006; Espitia *et al.*, 2010). In *C. albicans* wurden fünf Isoformen identifiziert, die aufgrund ihrer Aminosäurebeschaffenheit in die drei Pmt-Unterfamilien Pmt1, Pmt2 und Pmt4 unterschieden werden können (Abb.1.5). Dabei sind die Isoformen Pmt1 und Pmt5 Mitglieder der Pmt1-Unterfamilie, Pmt2 und Pmt6 Mitglieder der Pmt2-Unterfamilie und Pmt4 ist das alleinige Mitglied der gleichnamigen Pmt4-Unterfamilie (Ernst & Prill, 2001). Dennoch weisen die Pmt-Isoformen nur teilweise redundante Funktionen auf. Dies äußerst sich in den Phänotypen der *pmt*-Mutanten, die sehr spezifisch sind, z. B. ist das *PMT2*-Gen essentiell für das Wachstum von *C. albicans*, während die anderen *PMT*-Gene keinen erkennbaren Einfluss auf das Wachstum ausüben. Erst der gleichzeitige Verlust von *pmt1* und *pmt4* zeigt einen synergistischen Effekt und führt zum Verlust der Lebensfähigkeit in *C. albicans* (Prill *et al.*, 2005). Auch die Fähigkeit, von der Hefe- in die Hyphe-Zellform zu wechseln, wird auf individuelle Weise durch die Pmt-Isoformen unterstützt. Mit Ausnahme der *pmt5*-Mutante weisen die übrigen *pmt*-Mutanten entweder einen teilweisen Verlust der Hyphenbildung auf festen Nährmedien auf oder haben die Fähigkeit der Hyphenbildung vollständig verloren

(Timpel *et al.*, 1998; Prill *et al.*, 2005). Damit einhergehend weisen *pmt*-Mutanten eine verminderte Virulenz auf, z. B. erwies sich die *pmt1*-Mutante als avirulent in einem systemischen Mausinfektionsmodell (Rouabhia *et al.*, 2005). Die Pmt-Proteine tragen auch zur Resistenz vor zellwandschädigenden Substanzen bei; so weisen die *pmt1*- und *pmt4*-Mutante, wie auch die heterozygote *pmt2*/*PMT2*-Mutante eine erhöhte Sensitivität gegen Antimykotika auf (Prill *et al.*, 2005).

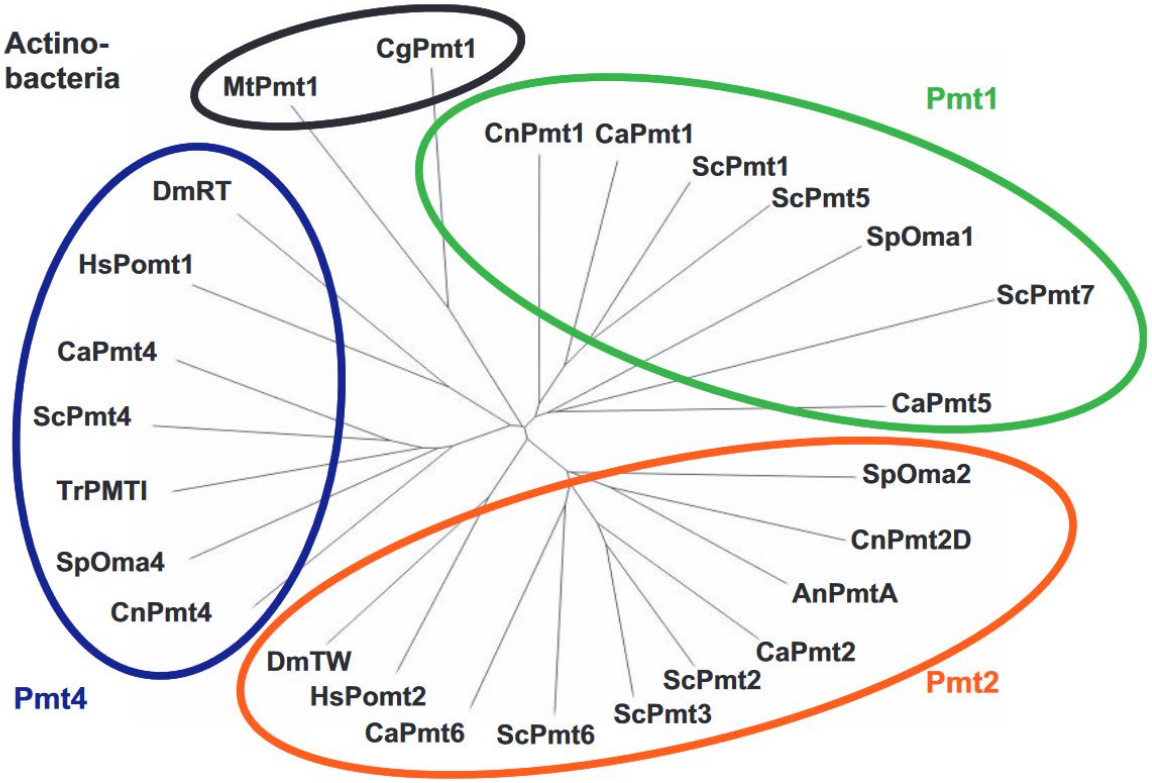

Abb.1.5 Phylogenetischer Stammbaum der Pmt-Proteine. Auf Grundlage der Aminosäurebeschaffenheit wurde die Verwandtschaft der Pmt-Proteine aus verschiedenen Organismen bestimmt und ergab die drei Unterfamilien der Pmt1-, Pmt2- und Pmt4-Proteine. An, *Aspergillus nidulans*; Ca, *Candida albicans*; Cg, *Corynebacterium glutamicum*; Cn, *Cryptococcus neoformans*; Dm, *Drosophila melanogaster*; Hs, *Homo sapiens*; Mt, *Mycobacterium tuberculosis*; Sc, *Saccharomyces cerevisiae*; Sp, *Schizosaccharomyces pombe*; Tr, *Trichoderma reesei*. Die Grafik wurde aus Lengeler *et al*. (2008) entnommen.

Die spezifischen Phänotypen sind vermutlich auf Pmt-Isoform-abhängige Zielproteine zurückzuführen, deren Unterglykosylierung in den jeweiligen *pmt*-Mutanten zu einem Funktionsverlust führt, z. B. könnte die fehlende Mannosylierung eines Sensors in der *pmt6*-Mutante für den Defekt der Hyphenbildung verantwortlich sein, der aufgrund der fehlenden Mannosylierung nicht länger in der Lage ist, einen Signalweg der Hyphenbildung zu aktivieren (Timpel *et al.*, 2000; Ernst, 2000).

Über die Zielproteine der *O*-Mannosylierung in *C. albicans* ist bisher wenig bekannt. Für das vSNARE Protein Sec20, das am retrograden Transport von Proteinen vom Golgi zum ER beteiligt ist, konnte nachgewiesen werden, dass *O*-Mannosylierung für die Stabilität des Proteins wichtig ist (Weber *et al.*, 2004). In der Hefe *S. cerevisiae* konnte bewiesen werden, dass die *O*-Mannosylierung der Zellwandproteine Utr2 und Gas1 eine protektive Wirkung vor der Wirkung der Aspartyl-Endopeptidase Yps1 (CaSap9) vermittelt. Die proteolytische Spaltung dieser Protease beruht auf der Erkennung von spezifischen Ser/Thr-reichen Domänen der Zielproteine. Die *O*-Mannosylierung der Ser/Thr-reichen Domäne vermindert die Erkennung durch die Protease und verhindert die Abspaltung der Zellwandproteine. Dabei wird die protektive Wirkung nur von den Pmt-Isoformen Pmt2 und Pmt4 vermittelt (Dube *et al.*, 2015). Das wohl bekannteste Zielprotein der *O*-Mannosylierung im Menschen stellt das Protein α-Dystroglykan dar, das im Zusammenhang mit dem Walker-Warburg-Syndrom steht, einer Krankheit, die zu Muskeldystrophie und einer Fehlbildung des Gehirns und der Augen führt (van Reeuwijk *et al.*, 2005; Barresi & Campbell, 2006). Das α-Dystroglykan ist ein membranständiges Protein, das an der Oberfläche von Skelettmuskelzellen oder Zellen im Gehirn den Kontakt zwischen der Zelle und der extrazellulären Matrix herstellt. Dabei wird die *O*-Mannosylierung des Proteins für die Interaktion mit den Matrixproteinen Neurexin und Laminin benötigt (Reed, 2009). Ausgelöst wird die Krankheit durch Mutationen in einem der beiden Gene *POMT1* oder *POMT2*, die für die Protein-*O*-Mannosyltransferasen des Menschen kodieren. Die Funktion der Mannosyltransferasen ist im Menschen, im Gegensatz zu *C. albicans*, nicht redundant. Es gibt Hinweise, dass beide Isoformen für die *O*-Mannosylierung benötigt werden (Hewitt, 2009).

Durch die Entwicklung von noch sensitiveren massenspektrometrischen Methoden ist es bei einer Proteom-Analyse in *S. cerevisiae* gelungen über 500 Proteine zu identifizieren, die eine Modifikation mit *O*-Mannan aufweisen (Neubert *et al.*, 2016). Die dabei identifizierten Proteine sind hauptsächlich Zellwand und Zellmembran assoziierte Proteine. Es konnten aber auch Proteine identifiziert werden, die komplexe molekulare Funktionen ausüben, die häufig mit dem ER assoziiert sind, z. B. wie dem Proteintransport (Sec12, Sec20), Mechanismen zur Überprüfung der Faltung von Proteinen (Kar2), der ER-Stressanpassung (Ire1), sowie der *O*- und *N*-Glykosylierung (Pmt1, Ost1, Mnn1 und Och1). Proteine, die an der Zellwand-Organisation und der Stressanpassung beteiligt sind, waren deutlich überrepräsentiert (Neubert *et al.*, 2016). Die Identifikation von Enzymen, die an der *N*-Glykosylierung beteiligt sind, als Zielproteine der *O*-Mannosylierung ist besonders interessant und könnte auf eine gegenseitige Regulation beider Formen der Glykosylierung hinweisen.

1.3.6 Signalwegaktivierung bei defekter Glykosylierung

Die Zellwand von *C. albicans* ist während der Kolonisation des menschlichen Körpers ständigen Angriffen durch das Immunsystem ausgesetzt. Der Erhalt und die Erneuerung der Zellwand, insbesondere der äußeren schützenden *O*- und *N*-Mannosepolymere, ist von entscheidender Bedeutung für das Überleben des Pilzes. Eine schnelle Anpassungsfähigkeit wird durch MAPK-Signalwege vermittelt, die in Folge von Änderungen in der Zellwand aktiviert werden und eine schnelle Regulation von kompensatorischen Mechanismen auslösen. In Folge von Glykosylierungsschäden werden der Cek1 MAPK-, der PKC (Protein Kinase C)- und der UPR (*unfolded-protein-response*)-Signalweg aktiviert (Travers *et al.*, 2000; Navarro-Garcia *et al.*, 1995; Cullen *et al.*, 2000). Der Cek1 MAPK-Signalweg ist der Hauptsignalweg, der sowohl bei defekter *O*-Mannosylierung als auch bei defekter *N*-Glykosylierung aktiviert wird. Der Verlust von *CEK1* führt zu einer Veränderung der Zellwandstruktur und damit einhergehend weist die *cek1*-Mutante eine hohe Sensitivität gegenüber *N*- und *O*-Glykosylierungsinhibitoren und Angriffen von Immunzellen auf (Roman *et al.*, 2009; Roman *et al.*, 2016). Glykosylierungsdefekte werden von dem Mucin Msb2 und dessen assoziierten Protein Sho1 detektiert und führen zur Aktivierung des MAP-Kinase-Moduls. In *S. cerevisiae* ist die Signalweg-Aktivierung von Cdc42 abhängig. Die Interaktion von Cdc42 mit Msb2 konnte in *C. albicans* bislang nicht nachgewiesen werden (Cullen *et al.*, 2004; Roman *et al.*, 2009). Das Msb2 Protein ist ein Typ I-Transmembranprotein, das durch eine Transmembranregion in eine zytosolische- und eine extrazelluläre-Domäne geteilt wird (Szafranski-Schneider, 2011). Die hochglykosylierte, extrazelluläre-Domäne, die typisch für Mucine ist, steht in engem Kontakt mit den Mannosepolymeren der Zellwandproteine und nimmt möglicherweise auf diese Weise Änderungen und Schäden in der Zellwand wahr. Das Signal wird von Msb2-Sho1 auf die Kinase Cst20 übertragen. Die Phosphorylierung der PAK (*p21-activated kinase*) Cst20 führt zur Aktivierung der Phosphorylierungskaskade und bewirkt die Aktivierung der MAPKKK Ste11, der MAPKK Hst7 und folglich der MAPK Cek1. Die Phosphorylierung von Cek1 wird in Folge von defekter *O*- und *N*-Glykosylierung stimuliert, z. B. nach der Behandlung mit dem Pmt1-Inhibitor oder Tunicamycin, einem Inhibitor der *N*-Glykosylierung. Außerdem konnte die Stimulation der Cek1 Phosphorylierung auch in der *pmt1*- und *pmt4*-Mutante nachgewiesen werden (Cantero *et al.*, 2007; Roman *et al.*, 2009). Dabei ist die Phosphorylierung von Cek1 in jedem Fall von Msb2 abhängig, denn in der *msb2*-Mutante konnte keine Phosphorylierung von Cek1 detektiert werden (Roman *et al.*, 2009). In *S. cerevisiae* wird in Folge von *O*-Glykosylierungsdefekten der PKC-Signalweg aktiviert. Die zur Cek1 MAPK homologe Kinase Kss1 in *S. cerevisiae* wird u. a. in Folge von

N-Glykosylierungsdefekten phosphoryliert und ist Teil des SVG (sterile vegetative growth)-Signalwegs (Arroyo *et al.*, 2011; Lee & Elion, 1999).

In der *pmt1*-Mutante und nach der Behandlung mit dem Pmt1-Inhibitor, konnte eine transkriptionelle Anpassung beobachtet werden, die zu einer gesteigerten Expression der Signalwegkomponenten *HAC1*, *KAR2* und *DDR48* des UPR-Signalwegs führte (Cantero *et al.*, 2007; Cantero & Ernst, 2011). Die Aktivierung des UPR-Signalwegs wurde auch nach der Behandlung mit Tunicamycin beobachtet und deutet darauf hin, dass Glykosylierung und die Faltung von Proteinen im ER miteinander verknüpfte Prozesse sind (Wimalasena *et al.*, 2008). Aktuelle Transkriptomanalysen bei der Anpassung an defekte Proteinglykosylierung in *S. cerevisiae* und *C. albicans* weisen darauf hin, dass es einen kompensatorischen Mechanismus zwischen der *O*-Mannosylierung und der *N*-Glykosylierung gibt (Cullen *et al.*, 2006; Arroyo *et al.*, 2011). Detaillierte Transkriptanalysen konnten zeigen, dass *C. albicans* zur Anpassung an defekte *N*-Glykosylierung die Expression des *PMT1*-Gens, das für die Protein-*O*-Mannosyltransferase1-Isoform kodiert, steigert (Cantero & Ernst, 2011). Auch innerhalb der *PMT*-Gene gibt es Anzeichen für kompensatorische transkriptionelle Anpassungen, z. B. wies die heterozygote *pmt2*/*PMT2*-Mutante eine erhöhte Expression des *PMT4*-Gens auf. Eine erhöhte Expression von *PMT2* konnte dagegen in der *pmt1*-Mutante nachgewiesen werden. In der *pmt4*-Mutante war die Expression von *PMT1* erhöht (Cantero *et al.*, 2007). Über die Transkriptionsfaktoren, die unterhalb der Signalwege agieren und eine solche Anpassung regulieren, ist bislang wenig bekannt. Die Funktion von Cph1, einem bekannten Substrat der Cek1-MAPK (1.2.2), bei der Anpassung an Glykosylierungsdefekte ist unklar. In *C. albicans* wurde der Transkriptionsfaktor Ace2 identifiziert, der ein wichtiges Element bei der Regulation von *PMT*-Genen darstellt (Cantero & Ernst, 2011).

1.3.7 Funktion des Transkriptionsfaktors Ace2 bei der Regulation von *PMT*-Genen

Aus einer Kollektion von mehr als 328 Stämmen, die Defekte in bekannten und potentiellen Transkriptionsfaktoren aufweisen, waren die *ace2*- und die *cna1*-Mutante als einzige Mutanten nicht in der Lage sich von der Behandlung des Pmt1-Inhibitors zu erholen. Die Funktion der Phosphatase Calcineurin (Cna1) bei der Anpassung und Erholung der Pmt1-Inhibition ist ungeklärt. Es konnte aber bewiesen werden, dass die bekannten Substrate Crz1 und Crz2 nicht an der Anpassung beteiligt sind. Die *ace2*-Mutante wies eine veränderte Expression der *PMT*-Gene auf (Karababa *et al.*, 2006; Cantero *et al.*, 2007; Cantero & Ernst, 2011). Der Transkriptionsfaktor-Ace2 ist Teil des RAM-Signalweges, der für das polarisierte Wachstum, bei der Zellwandbiosynthese und bei der Zytokinese von Bedeutung ist (Song *et al.*, 2008).

Sensitive Transkriptanalysen ergaben, dass sowohl Msb2, Cek1 als auch Ace2 für die basale Expression von *PMT2* und *PMT4* verantwortlich sind (Abb.1.6).

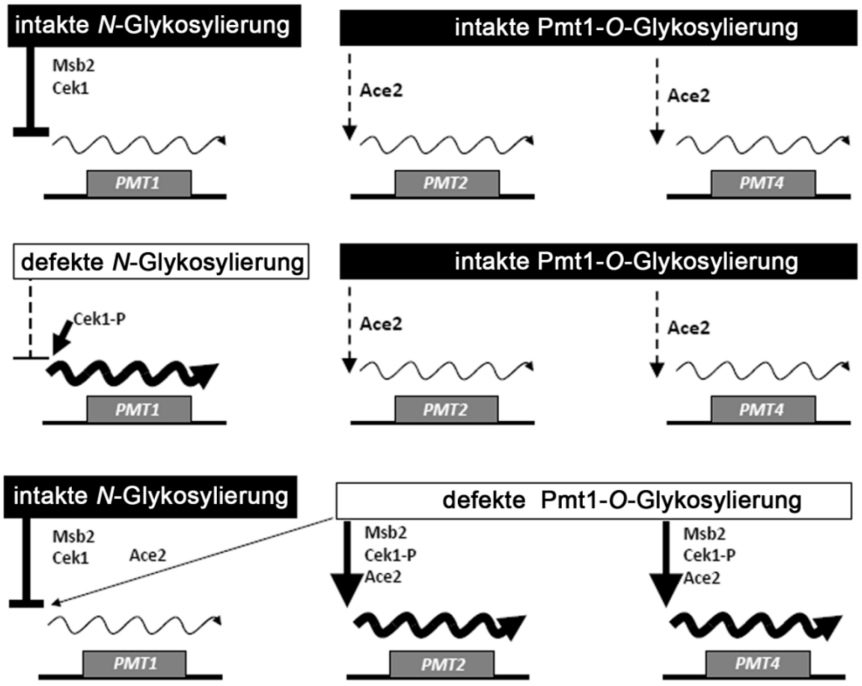

Abb.1.6 Modell für die Regulation der *PMT*-Gene durch den Msb2-Cek1-Ace2-Signalweg. Das Modell zeigt die transkriptionelle Regulation der *PMT*-Gene. Basierend auf ihren relativen Transkriptspiegeln sind Pmt1, Pmt2 und Pmt4 die Haupt-Isoformen in *C. albicans*. Die Transkription des *PMT1*-Gens wird durch den Signalweg bei intakter Zellwand reprimiert. Schäden in der Zellwand und den damit assoziierten Mannosepolymeren werden von dem Sensorprotein Msb2 wahrgenommen und an die Cek1-MAPK vermittelt. Die Phosphorylierung von Cek1 (Cek1-P) wird in Folge von defekter *N*- und *O*-Glykosylierung stimuliert. Die Regulation der *PMT*-Gene erfolgt hingegen spezifisch. Bei defekter *N*-Glykosylierung wird die Transkription von *PMT1* dereprimiert, während bei defekter Pmt1-*O*-Glykosylierung die Transkription von *PMT2* und *PMT4* induziert wird. Der Transkriptionsfaktor Ace2 reguliert dabei sowohl die basale Transkription von *PMT1*, *PMT2* und *PMT4* in intakten Zellen, als auch die Stressinduzierte Transkription. Die Grafik wurde Cantero & Ernst (2011) entnommen und modifiziert.

Des Weiteren werden die drei Proteine auch für die induzierte Expression von *PMT2* und *PMT4* bei defekter, durch die Pmt1-Isoform vermittelter, *O*-Mannosylierung benötigt. Die Expression von *PMT1* konnte, anders als in einem Kontrollstamm, in der *msb2*-, der *cek1*- und der *ace2*-Mutante nach der Behandlung mit Tunicamycin nicht weiter induziert werden. Demnach wirkt der Signalweg unter normalen Wachstumsbedingungen reprimierend auf die Expression von *PMT1*, wird aber gleichzeitig auch für die stimulierte, de-reprimierte Expression von *PMT1* bei defekter *N*-Glykosylierung benötigt (Cantero & Ernst, 2011).

In darauf aufbauenden Studien konnte gezeigt werden, dass Ace2 ein positiver Regulator der *PMT2*- und *PMT4*-Transkription ist (Van Wijlick, 2012). Die reprimierende Wirkung von Ace2 auf die Expression des *PMT1*-Gens konnte unter *ACE2*-Überexpressionsbedingungen nicht nachgewiesen werden. Die Fusion des *ACE2*-Promotors mit einem Reportergen wies eine Induktion des Ace2-Promotors in Abhängigkeit von defekter *N*- und *O*-Glykosylierung auf

(Van Wijlick, 2012). Der Ace2-Transkriptionsfaktor scheint demnach ein positiver Regulator der *PMT*-Genexpression zu sein, der bei Schädigung der *O*- und *N*-Mannosepolymere an der Zelloberfläche von *C. albicans* aktiviert wird. In einer Transkriptomanalyse der *ace2*-Mutante wurden zudem die *PMT*-Gene *PMT2*, *PMT4* und *PMT6* als unterexprimierte Gene identifiziert (Mulhern *et al.*, 2006).

1.3.8 Der Transkriptionsfaktor Ace2

Der Transkriptionsfaktor Ace2 weist nahe seines Carboxy-Terminus zwei C_2H_2-Zinkfinger-Domänen auf, die für die DNA-Bindung benötigt werden (Calderon-Norena *et al.*, 2015). Bislang wurde Ace2 nur als Ziel-Transkriptionsfaktor des RAM-Signalwegs identifiziert, der in Eukaryoten konserviert ist (Nelson *et al.*, 2003). Mutanten des RAM-Signalwegs, nicht aber die *ace2*-Mutante, weisen Defekte bei der Initiierung des polarisierten Wachstums auf (Kelly *et al.*, 2004; Song *et al.*, 2008). Zu Ace2 homologe Proteine wurden in den Modell-Hefen *S. cerevisiae* und *S. pombe*, aber auch in relevanten Pilzpathogenen, wie z. B. *C. glabrata*, *Aspergillus fumigatus* und *Cryptococcus neoformans*, nachgewiesen (Nelson *et al.*, 2003; Saputo *et al.*, 2012). Bei *C. albicans* wird die Aktivität von Ace2 u. a. von der Kinase Cbk1 reguliert, die der Familie der AGC-Kinasen angehört und als terminale Kinase des RAM-Signalwegs identifiziert wurde (Song *et al.*, 2008). Die Cbk1-Kinase liegt in einem Komplex mit der Kinase Mob2 vor und wird abhängig vom Zellzyklus durch Phosphorylierung von der GC (*germinal center*)-Kinase Kic1, aktiviert (Gutierrez-Escribano *et al.*, 2011). Eine direkte Interaktion von Ace2 und Cbk1 konnte bei *C. albicans* bislang nur aufgrund einer auf Haploinsuffizienz basierender genetischer Analyse nachgewiesen werden (Bharucha *et al.*, 2011; Saputo *et al.*, 2012). Die Aktivität von Ace2 wird zudem durch die Kinase Cdc28 und die Phosphatase Cdc14 bestimmt, den zentralen Regulatoren des *mitotic exit network* (MEN), welche die asymmetrische Verteilung von Ace2 regulieren (Brace *et al.*, 2011). Die Cyklin-abhängige Kinase Cdc28 phosphoryliert Ace2 und verhindert dadurch den vorzeitigen Zellkern-Import während der Synthese- und G2-Phase des Zellzyklus (Mazanka & Weiss, 2010). In der späten Metaphase vermittelt die Phosphatase Cdc14 die Dephosphorylierung dieser Phosphatgruppe und bewirkt den Import von Ace2 in die Zellkerne neugebildeter Tochterzellen (Clemente-Blanco *et al.*, 2006). Die Cbk1-Kinase phosphoryliert den Transkriptionsfaktor Ace2 an einer konservierten Stelle der NES (Nuclear Export Sequence) und verhindert den Export von Ace2 aus dem Zellkern (Bourens *et al.*, 2008; Sbia *et al.*, 2008). Mitglieder des RAM-Signalwegs weisen bei Defekten einen charakteristischen Phänotyp auf. Die Zellen trennen sich nach der Zytokinese nicht voneinander, sondern bilden lange Zellketten.

Dieser Phänotyp äußert sich durch pyramidenförmige Kolonien auf festen Nährmedien, welche durch die fehlende Expression von Chitinasen und Glukanasen, die während der Zellteilung durch Ace2 stimuliert werden, entstehen (Kelly *et al.*, 2004).

Darüber hinaus weist die *ace2*-Mutante eine Vielzahl von interessanten Phänotypen auf, die für die Pathogenität von *C. albicans* entscheidend sind. Bei *C. glabrata*, einem nahen Verwandten von *C. albicans*, wurde das zu Ace2 homologe Protein als Virulenzfaktor identifiziert. Die Deletion von *ACE2* bewirkte einen hypervirulenten Phänotyp in einem systemischen Mausinfektionsmodell. Auch im Schimmelpilz *A. fumigatus* löst die Deletion des zu *ACE2* homologen Gens eine erhöhte Virulenz aus (Ejzykowicz *et al.*, 2009). Bei *C. albicans* dagegen verursachte die Deletion von *ACE2* den gegenteiligen Effekt, die sich als avirulent erwies (Kamran *et al.*, 2004; Kelly *et al.*, 2004; MacCallum *et al.*, 2006). Der Transkriptionsfaktor Ace2 scheint neben der konservierten Funktion, wie z. B. der Zytokinese, die in allen Pilzen durch Ace2 reguliert wird, noch Spezies-spezifische Funktionen entwickelt zu haben. Interessanterweise konnten bei *C. albicans* zwei Ace2-Isoformen nachgewiesen werden (Calderon-Norena *et al.*, 2015). Durch eine alternative Translations-Initiation entsteht neben dem vollständigen Ace2-Protein auch eine um 54 Aminosäuren verkürzte-Isoform, welche durch die Initiation der Translation an der Methionin Position 55 entsteht; diese ist die transkriptionell aktive-Isoform. In einigen klinischen Isolaten konnte sogar eine konservierte Mutation nachgewiesen werden, die zu einem Stop-Codon an Position 9 der Aminosäurekette führt und zwangsläufig die Translation der kurzen Ace2-Isoform begünstigt (Calderon-Norena *et al.*, 2015). Für das vollständige Ace2-Protein wurde eine N-terminale potentielle Transmembrandomäne vorhergesagt, die sowohl die Lokalisation von Ace2, als auch die Funktion dieser Isoform beeinflusst. Im Gegensatz zu der kurzen Ace2-Isoform, die im Zellkern von Tochterzellen nachgewiesen werden konnte, lokalisiert die Volllängen Ace2-Isoform während der Bildung von Hyphen an den Septinringen und wird u. a. für die Eingliederung des Septins Sep7 in den Septinring benötigt (Calderon-Norena *et al.*, 2015). Bei anderen Hefepilzen konnte in den Aminosäuresequenzen der zu Ace2 homologen Proteine keine potentielle Transmembrandomäne identifiziert werden; die beiden unterschiedlichen Ace2-Isoformen könnten demnach zu Spezies-spezifischen Funktionen des Transkriptionsfaktors Ace2 in *C. albicans* beitragen.

Weitere Prozesse, an denen Ace2 beteiligt ist, sind die Bildung von Biofilmen und die Hyphenmorphogenese. Beide Prozesse stellen wichtige Virulenzeigenschaften von *C. albicans* dar. Die *ace2*-Mutante war nicht in der Lage, unter hypoxischen Bedingungen Hyphen zu bilden und wies Defekte in der Biofilmbildung auf (Kelly *et al.*, 2004; Stichternoth & Ernst,

2009). Möglicherweise besteht auch hier ein Zusammenhang zur Regulation der *PMT*-Gene, denn die *pmt*-Mutanten weisen vergleichbare Defekte auf. Beispielsweise ist die *pmt1*-Mutante nicht in der Lage, unter anaeroben Bedingungen Hyphen zu bilden und sie erwies sich, wie auch die *ace2*-Mutante, als avirulent in einem Mausinfektionsmodell (Prill *et al.*, 2005). Im Gegensatz zur *ace2*-Mutante zeigte die *cbk1*-Mutante keine ungewöhnliche Expression der *PMT*-Gene auf (Cantero, 2010). Kürzlich wurde eine Interaktion des RAM-Signalweges und Ace2 mit dem PKA-Signalweg beschrieben. Gemeinsam mit dem Transkriptionsfaktor Efg1 reguliert Ace2 die Expression von metabolischen Genen der Glykolyse und der Respiration, und von hyphenspezifischen Genen (Mulhern *et al.*, 2006; Saputo *et al.*, 2014; Wang *et al.*, 2009). Wie die Aktivität von Ace2 bei diesen vielseitigen biologischen Prozessen koordiniert wird, ist ungeklärt. Auch über die Zielgene von Ace2 ist wenig bekannt.

1.4 Zielsetzung

In Anbetracht der vielfältigen Funktionen von Ace2, die eng mit der Pathogenität von *C. albicans* assoziiert sind, sollten in dieser Arbeit die zugrundeliegenden molekularen Mechanismen untersucht werden, über die der Transkriptionsfaktor zur Virulenz des Pilzes beiträgt. Schwerpunkte waren dabei die Funktion von Ace2 bei der Regulation der *PMT*-Gene und der Beitrag von Ace2 zur Hyphenmorphogenese von *C. albicans* unter hypoxischen Wachstumsbedingungen.

Jede der fünf Protein-O-Mannosyltransferasen unterstützt auf individuelle Weise das Wachstum, den Schutz vor Antimykotika und die Virulenz von *C. albicans* (Lengeler *et al*., 2008). Die *PMT*-Gene sind wichtige Zielgene des Cek1-MAPK-Signalweges, der bei defekter Glykosylierung aktiviert wird und *PMT*-Gene zur Kompensation reguliert. Das Sensorprotein Msb2 und die MAP-Kinase Cek1 sind maßgeblich an der kompensatorischen Regulation der *PMT*-Gene beteiligt. Als weiterer Regulator konnte der Transkriptionsfaktor Ace2 identifiziert werden, der sowohl die basale als auch die kompensatorische Transkription von *PMT*-Genen vermittelt (Cantero & Ernst, 2011). Ein Ziel dieser Arbeit bestand darin die Funktion von Ace2 innerhalb des Msb2-Cek1 Signalweges zu untersuchen und zu ermitteln, ob Msb2, Cek1 und Ace2 einen linearen Signalweg bilden, der gemeinsam die Antwort auf Glykosylierungsdefekte reguliert.

Eine weitere wichtige Virulenzeigenschaft von *C. albicans* ist die Fähigkeit, zwischen der Hefe- und der Hyphe-Zellform zu wechseln. Die *ace2*-Mutante erwies sich in einem Mausinfektionsmodell als avirulent und war unter hypoxischen Wachstumsbedingungen nicht in der Lage, den Wechsel von der Hefe- in die Hyphe-Zellform zu vollziehen (Kelly *et al.*, 2004). Bislang wurde angenommen, dass die fehlende metabolische Anpassung in der *ace2*-Mutante dafür verantwortlich sei, denn Ace2 reguliert sowohl glykolytische als auch respiratorische Gene (Mulhern *et al.*, 2006). Neuere Studien weisen aber auf einen direkten regulatorischen Mechanismus hin, bei dem Ace2 gemeinsam mit dem Hyphenregulator Efg1 spezifische Morphogenesegene reguliert (Saputo *et al.*, 2014). Ein weiteres Ziel dieser Arbeit bestand darin, die Funktion von Ace2 bei der Hyphenmorphogenese unter hypoxischen Wachstumsbedingungen zu untersuchen.

2 Ergebnisse

Der humanpathogene Pilz *C. albicans* ist während der Kolonisierung des menschlichen Körpers ständigen Umgebungsschwankungen ausgesetzt. Die Anpassung an diese Umweltbedingungen, zu denen die Verfügbarkeit von Nährstoffen, erhöhte CO_2-Konzentrationen im Blut, die Verfügbarkeit von molekularem Sauerstoff in den unterschiedlichen Körpernischen, die Limitierung von Spurenelementen, aber auch Angriffe durch das Immunsystem zählen, ist von großer Bedeutung für das Überleben des Pilzes (Brock, 2009; Ernst & Tielker, 2009). Sensoren, die in der Zellwand von *C. albicans* lokalisiert sind, übermitteln äußere Einflüsse auf Signalwege, die eine Anpassung des Pilzes induzieren (Roman *et al.*, 2007; Roman *et al.*, 2009). Ein wichtiger Anpassungsmechanismus ist der Wechsel von der Hefe- zur Hyphe-Zellform, der es *C. albicans* ermöglicht, Angriffen des Immunsystems zu entgehen und in nährstoffreichere Gewebe vorzudringen (Phan *et al.*, 2000; Jimenez-Lopez & Lorenz, 2013). Die Erhaltung der Zellwandintegrität ist für die Wechselwirkung des Pilzes mit der Umwelt von besonderer Bedeutung. Die Zellwand ist von einem Zuckergerüst umgeben, das hauptsächlich aus Mannosepolymeren besteht, die glykosidisch mit Zellwandproteinen verknüpft sind. Die Anknüpfung des ersten Mannoserestes wird bei der *O*-Mannosylierung von Protein-*O*-Mannosyltransferasen (Pmt) katalysiert (Prill *et al.*, 2005; Lengeler *et al.*, 2008). Neben der *O*-Mannosylierung stellt die *N*-Glykosylierung die häufigste Form der Glykosylierung in Eukaryoten dar. Defekte in der *N*- und *O*-Glykosylierung werden in *C. albicans* von dem Sensorprotein Msb2 erkannt und aktivieren den Cek1 MAPK-Signalweg. Die *PMT*-Gene stellen wichtige Zielgene dar, die bei der Anpassung an defekte Glykosylierung reguliert werden (Cantero *et al.*, 2007). Neben dem Sensorprotein Msb2 und der MAP-Kinase Cek1 wurde der Transkriptionsfaktor Ace2 identifiziert, der auf noch unbekannte Weise wesentlich an der Regulation von *PMT*-Genen beteiligt ist (Cantero & Ernst, 2011). Neben dieser Funktion konnte für Ace2 auch eine Beteiligung an dem Wechsel von der Hefe- zur Hyphe-Zellform nachgewiesen werden, die im Zusammenhang mit dem zuvor identifizierten Hyphenregulator Efg1 steht und von der Verfügbarkeit von Sauerstoff abhängig ist (Stoldt *et al.*, 1997; Setiadi *et al.*, 2006; Kelly *et al.*, 2004; Saputo *et al.*, 2014).

Im Rahmen dieser Arbeit sollte die Funktion von Ace2 bei der Regulation der *PMT*-Gene und der Beitrag von Ace2 zur Hyphenmorphogenese von *C. albicans* unter hypoxischen Wachstumsbedingungen untersucht werden.

2.1 Manuskripte

2.1.1 Zusammenfassung Manuskript I

Candida albicans responds to glycostructure damage by Ace2-mediated feedback regulation of Cek1 signaling

In *C. albicans* werden Schäden an den Glykostrukturen der Zellwand durch den Cek1 MAPK-Signalweg an den Transkriptionsfaktor Ace2 vermittelt, der zur Kompensation die Transkription von Genen stimuliert, die u. a. für Protein-*O*-Mannosyltransferasen (Pmt) kodieren. In dieser Arbeit wurde die genomweite Bindung von Ace2 unter Glykostress-Bedingungen untersucht. Dabei war es möglich, Zielgene von Ace2 zu identifizieren, die unter der transkriptionellen Kontrolle von Ace2 zur Regulation der *PMT*-Gene beitragen. Unter den identifizierten Zielgenen befanden sich zudem Gene, die für Komponenten des Cek1 MAPK-Signalweges kodieren. Die Transkriptanalyse dieser Gene ergab, dass der Signalweg als Antwort auf defekte *N*-Glykosylierung transkriptionell, in Abhängigkeit von Ace2, hochgeregelt wird. Unter diesen Bedingungen konnte außerdem die physische Interaktion von Ace2 mit der PAK Cst20, die stromaufwärts der MAPK Cek1 liegt, festgestellt werden. Es konnte gezeigt werden, dass Cst20 die stimulierende Aktivität von Ace2 im Zellkern inhibiert und auf diese Weise zu einer negativen Rückkopplung des Cek1-Signalweges beiträgt.

2.1.2 Zusammenfassung Manuskript II

Hypoxia and temperature regulated morphogenesis in *Candida albicans*

Es ist bekannt, dass Hypoxie an Stellen von Infektionen auftritt und die Verfügbarkeit von Sauerstoff ein kritischer Faktor für die Pathogenese ist, sowohl für den Pilz als auch für den Wirt. Die vergleichende Analyse der genomischen Bindestellen von Ace2 und dem Hyphenregulator Efg1 unter hypoxischen Wachstumsbedingungen ergab, dass beide Transkriptionsfaktoren eine Vielzahl von gleichen Zielgenen in *C. albicans* teilen. Um den Einfluss von Hypoxie bei der Genregulation von Ace2-Efg1-Zielgenen zu untersuchen, wurde eine Transkriptanalyse durchgeführt. Die Ergebnisse weisen darauf hin, dass Efg1 als Repressor und Ace2 als Induktor der Genexpression wirkt. Darüber hinaus konnte gezeigt werden, dass die positive Wirkung von Ace2 maßgeblich von der Verfügbarkeit von CO_2 abhängig ist, während Efg1 unabhängig von CO_2 als Repressor wirkt. Zwei der identifizierten Zielgene von Ace2-Efg1, *BCR1* und *BRG1* wurden in vorherigen Studien als normoxische Regulatoren der

Morphogenese identifiziert. Darüber hinaus konnte gezeigt werden, dass beide Regulatoren an den Promotor von *EFG1* binden. Um zu klären, ob eine Rückkopplungsregulation zwischen *EFG1-ACE2* und *BCR1*/*BRG1* besteht, wurde die Transkription von *ACE2* und *EFG1* in der *bcr1* und *brg1* Mutante bestimmt. Zusammenfassend weisen die Ergebnisse darauf hin, dass die Genexpression von *EFG1*, *ACE2*, *BCR1* und *BRG1* untereinander gekoppelt ist und jeder Transkriptionsfaktor die Expression seiner Ko-Regulatoren beeinflusst. Um zu untersuchen, ob die Mitglieder des Efg1-Ace2 transkriptionellen Netzwerkes eine Funktion für die Hyphenmorphogenese haben, wurde der Kolonie-Phänotyp von entsprechenden Mutanten bestimmt. Die Ergebnisse zeigen, dass die Hyphenmorphogenese von *C. albicans* unter hypoxischen Bedingungen durch Efg1 und Bcr1 reprimiert wird und der stimulatorischen Wirkung von Ace2 und Brg1 entgegenwirkt. Die regulatorischen Mechanismen unter Hypoxie weisen darauf hin, dass *C. albicans* die Hyphenmorphogenese in sauerstoffarmen Körpernischen unterdrückt.

2.1.3 Zusammenfassung Manuskript III

Dom34 links translation to protein *O*-mannosylation

Die Translation und die Glykosylierung von Proteinen sind zwei essentielle biologische Prozesse in eukaryotischen Zellen. Für den humanpathogenen Pilz *C. albicans* konnte in dieser Arbeit erstmals eine direkte Verbindung zwischen diesen beiden Prozessen nachgewiesen werden, die durch das Protein Dom34 vermittelt wird. Das Dom34-Protein ist Mitglied der Dom34/Pelota-Proteinfamilie und ist am *No-Go decay* (NGD) Prozess beteiligt, der die Qualität von mRNA-Molekülen während der Translation kontrolliert. Durch die Freisetzung von blockierten Ribosomen von der mRNA und durch die Spaltung der mRNA beeinflusst Dom34 die generelle Translation. In dieser Arbeit wurde Dom34 als RNA-Bindeprotein identifiziert, das spezifisch mit der 5‘-UTR eines Transkriptes einer Protein-*O*-Mannosyltransferase interagiert und die Initiierung der Translation dieses Transkriptes verbessert. Demnach scheint Dom34 neben seiner generellen Funktion bei der Translation auch eine spezialisierte Funktion für die Translation zu erfüllen: der Verbesserung der Translation von spezifischen Transkripten, zu denen auch das *PMT1* Transkript zählt. Auf diese Weise unterstützt Dom34 die Anpassung von *C. albicans* bei Glykostress und trägt zu einer schnellen Erholung des Pilzes bei Schäden der Zellwand bei.

2.1.4 Zusammenfassung Manuskript IV

Signaling domains of mucin Msb2 in *Candida albicans*

Das Mucin Msb2 ist über eine Transmembrandomäne in der Zytoplasmamembran verankert, die das Protein in eine zytosolische- und eine extrazelluläre-Domäne teilt. Msb2 wurde als Sensor für Schäden von Glykostrukturen der Zellwand identifiziert und aktiviert in *C. albicans* den Cek1 MAPK-Signalweg. In dieser Arbeit wurden die Proteindomänen des Msb2 Sensorproteins systematisch deletiert. Dabei konnten zahlreiche Funktionen von Msb2 den Domänen zugeordnet werden und neue Funktionen identifiziert werden. Zelluläre Prozesse, an denen Msb2 beteiligt ist, umfassen neben der Aktivierung des Cek1 MAPK-Signalweges auch die Resistenz vor Antimykotika, die Regulation von stressinduzierten Genen, zu denen insbesondere das *PMT1*-Gen zählt, und die Hyphenmorphogenese.

2.1.5 Zusammenfassung Manuskript V

A surprising role for the Sch9 protein kinase in chromosome segregation in *Candida albicans*

Die Protein Kinase Sch9 gehört zu den AGC Kinasen und liegt stromabwärts des TORC1 (*target of rapamycin complex 1*)-Signalwegs, der in allen Eukaryoten das Zellwachstum in Abhängigkeit des Nährstoffangebotes reguliert. In *C. albicans*, einem humanpathogenen Hefepilz, ist die Kinase Sch9 zudem an der Regulation der hypoxischen Hyphenbildung beteiligt. Dabei ist die Funktion von Sch9 von einer erhöhten CO_2 Verfügbarkeit abhängig. Bei der Analyse der genomweiten Bindung von Sch9 wurde in *C. albicans* überraschenderweise die Assoziation von Sch9 mit den Zentromerregionen aller acht Chromosomen identifiziert. Die Bindung trat unabhängig von der O_2 und CO_2 Verfügbarkeit auf. In *S. cerevisiae*, einer nicht pathogenen Hefe, konnte die Bindung an die Zentromerregionen nicht nachgewiesen werden. Es stellte sich heraus, dass Sch9 an der Chromosomensegregation von *C. albicans* beteiligt ist.

2.2 Manuskript I: *Candida albicans* responds to glycostructure damage by Ace2-mediated feedback regulation of Cek1 signaling

Lasse van Wijlick, Marc Swidergall, Philipp Brandt, Joachim F. Ernst

Erstautor

Beitrag zum Manuskript: 85 %

Lasse van Wijlick hat den größten Teil der Experimente geplant, durchgeführt und ausgewertet. Er hat die Daten interpretiert und die Schlussfolgerungen formuliert. Des Weiteren hat er das Manuskript zum Großteil geschrieben und alle Abbildungen erstellt.

Veröffentlich in: Mol Microbiol, September 2016; DOI: 10.1111/MMI.13494.

Impact Factor: 3.761 (2015)

Molecular Microbiology (2016) 00(00), 00–00 ■

doi:10.1111/mmi.13494
First published online 2016

Candida albicans responds to glycostructure damage by Ace2-mediated feedback regulation of Cek1 signaling

Lasse van Wijlick,[1,2] Marc Swidergall,[1†] Philipp Brandt[1] and Joachim F. Ernst[1,2*]
[1]*Department Biologie, Molekulare Mykologie, and* [2]*Manchot Graduate School Molecules of Infection, Heinrich-Heine-Universität, 40225 Düsseldorf, Germany.*

Summary

Candida albicans **uses the Cek1 MAPK pathway to restore cells from damage of its cell wall glycostructures. Defective protein *N*- or *O*-glycosylation activates Cek1 and the transcription factor Ace2 as its downstream target, to upregulate genes encoding protein *O*-mannosyltransferases (Pmt proteins). In unstressed cells, Cek1-Ace2 activity blocks expression of *PMT1*, which is de-repressed by tunicamycin. Genomic binding targets of Ace2 included *ZCF21*, which was upregulated by Ace2 and found to repress *PMT1* transcription in unstressed cells. Surprisingly, genes encoding components of the Cek1 pathway including *MSB2*, *CST20*, *HST7*, *CEK1* and *ACE2* were also identified as Ace2 targets indicating Ace2-mediated transcriptional amplification of pathway genes under *N*-glycosylation stress. In this condition, physical interaction of the Ace2 protein with the upstream MAPKKK Cst20 was detected. Cst20-GFP showed stress-induced import from the cytoplasm into the nucleus and phosphorylation of Ace2. Interestingly, forced nuclear localization of Cst20 inhibited Cek1-Ace2 signaling, while forced cytoplasmic localization of Cst20 retained full signaling activity, suggesting that nuclear Cst20 downregulates the Cek1 pathway. Collectively, the results indicate that Ace2 is a versatile multifunctional transcriptional regulator, which activates glycostress responses of *C. albicans* by both positive forward and negative feedback regulation of Cek1 signaling.**

Accepted 30 August, 2016. *For Correspondence: E-mail joachim.ernst@uni-duesseldorf.de; Tel. +49(211)811-5176; Fax +49(211) 811-5176. †Present address: Division of Infectious Diseases, Los Angeles Biomedical Research Institute at Harbor-UCLA Medical Center, Torrance, CA 90502, USA.

Introduction

The cell wall of the pathogen *Candida albicans* is a complex and highly dynamic organelle that determines the outcome of the interaction of the fungus with the human host. It contains a network of carbohydrate-based polymers that acts as a scaffold, an armor and an environmental gate (Ernst and Pla, 2011). A network of chitin and β-glucans provides physical strength, while glycoproteins covalently attached to glucan sense and transmit environmental cues to the interior of cells. Cell wall proteins are extensively *O*- and *N*-glycosylated (Chaffin, 2008) and support a great variety of functions, such as adhesion and biofilm formation (Chandra *et al.*, 2001), immune recognition (Luo *et al.*, 2010; Sheth *et al.*, 2011), cell wall composition (de Groot *et al.*, 2004) and morphogenesis (Heilmann *et al.*, 2011). In order to survive in the complex host environment, *C. albicans* has evolved rescue pathways to overcome defects in its glycostructures that are caused by attacks of the immune system and by host hydrolases.

Cellular adaptation to glycostress is mediated by the cell integrity pathway (PKC), the unfolded-protein response pathway and the Cek1 MAP kinase pathway (Navarro-Garcia *et al.*, 1995; Cullen *et al.*, 2000; Travers *et al.*, 2000; Levin, 2011). Damage of glycostructures are sensed by the membrane protein Msb2 and its associated protein Sho1 and results in activation of the Cek1 MAP kinase module (Román *et al.*, 2009), which in turn activates compensatory transcriptional activities. Cek1 phosphorylation in *C. albicans* is stimulated in response to defective *O*- and *N*-linked glycosylation (Cantero *et al.*, 2007; Román *et al.*, 2009), while in *S. cerevisiae* blocked protein *O*-mannosylation activates the cell wall integrity pathway (Arroyo *et al.*, 2011). The cell wall structure is severely altered in *cek1* mutants, which becomes highly sensitive to the *N*-glycosylation inhibitor tunicamycin and to attack of immune cells and molecules (Román *et al.*, 2009, 2016) suggesting that

Cek1 mediated signaling is required to maintain glycosylation homeostatis of cell wall proteins and cell wall remodeling in *C. albicans*. Partial deletions of the Msb2 sensor protein revealed specific sequences required for induction or repression of Cek1 phosphorylation (Swidergall *et al.*, 2015) to maintain basal resistance to antifungals and regulation of the protective fungal glycoshield.

Genes encoding protein *O*-mannosyltransferases (Pmt proteins) were identified as downstream targets of Cek1 signaling, which compensate for glycostructure damages in the cell wall (Cantero and Ernst, 2011). Pmt proteins catalyze the first step in the process of protein-*O*-mannosylation, whereby mannose residues are linked to threonine or serine residues of secretory proteins (Lengeler *et al.*, 2008). The genome of *C. albicans* encodes 5 Pmt isoforms that by their homologies can be divided into 3 subfamilies, comprising the Pmt1- (Pmt1, Pmt5), Pmt2- (Pmt2, Pmt6) and Pmt4-subfamily (Pmt4) (Prill *et al.*, 2005). Defects in *O*-mannosylation were found to reduce the fitness and virulence of *C. albicans* (Timpel *et al.*, 1998; Prill *et al.*, 2005; Rouabhia *et al.*, 2005) and greatly contribute to host immune detection (Mora-Montes *et al.*, 2010; Sheth *et al.*, 2011). Recently, it was reported that expression of *PMT* genes is differentially regulated, because a Pmt1-inhibitor (Orchard *et al.*, 2004) enhanced expression of *PMT2* and *PMT4*, while treatment with the *N*-glycosylation inhibitor tunicamycin de-repressed *PMT1* expression (Cantero and Ernst, 2011). A compensatory function among different Pmt-isoforms had already reported by Cantero *et al.* (2007). The *PMT4* transcript was found to be upregulated in a *PMT2*/*pmt2* strain and expression of *PMT2* was upregulated in the *pmt1* mutant strain, suggesting mutual regulation among *C. albicans PMT* genes. However, Pmt isoforms mainly do not have redundant functions, as mutants lacking single Pmt isoforms exhibit specific *in vitro* and *in vivo* phenotypes (Rouabhia *et al.*, 2005; Prill *et al.*, 2005). For example, in the Pmt2-subfamily Pmt2 but not Pmt6 is essential for growth, although Pmt6 regulates morphogenesis (Timpel *et al.*, 2000; Prill *et al.*, 2005).

Besides Msb2 and Cek1 the transcription factor Ace2 was discovered as an additional element regulating *PMT* genes in *C. albicans*. Out of 328 mutants defective in known and putative transcription factors only the *ace2* mutant turned out to be unable to recover from Pmt1-inhibition and showed abnormal *PMT* transcription (Cantero and Ernst, 2011). The mechanism by which the transcription factor Ace2 orchestrates glycostress-dependent signaling of *C. albicans* remained unclear. Ace2 was first identified in *S. cerevisiae* as target of the regulation of Ace2 and morphogenesis (RAM) pathway, which is conserved in fungi and ensures cell separation (Kurischko *et al.*, 2005). Recently, cross-interaction of the RAM pathway with the PKA pathway was reported, in which Ace2 and the major hyphal regulator Efg1 determine morphogenesis of *C. albicans* in specific environments (Wang *et al.*, 2009; Bharucha *et al.*, 2011; Saputo *et al.*, 2014; Desai *et al.*, 2015). In this article we report that the transcription factor Ace2 functions downstream of the Cek1 MAP kinase pathway and is required to overcome impaired *N*- and *O*-glycosylation in *C. albicans*. This activity does not require the Cph1 transcription factor, which functions downstream of Cek1 to induce hyphal filamentation in some conditions (Liu *et al.*, 1994; Desai *et al.*, 2015). Importantly, Ace2 was found to regulate the Cek1 pathway by positive feedback and to trigger *PMT1* gene repression via the Zcf21 transcription factor. In addition, negative regulation of Ace2 by the upstream MAPKKK Cst20 suggests that Ace2 is involved in both positive- and negative-feedback mechanisms of the Cek1 pathway.

Results

ACE2 *overexpression rescues glycostructure signaling in Cek1 pathway mutants*

C. albicans mutants lacking the sensor Msb2, the MAP kinase Cek1, the transcription factor Ace2 or the *O*-mannosyltransferase Pmt1 are highly sensitive to cell wall-perturbing agents (Cantero *et al.*, 2007; Román *et al.*, 2009; Cantero and Ernst, 2011). To support the concept that these components form a linear MAPK signaling pathway responding to defects in glycostructures, the effects of *ACE2* overexpression on mutant sensitivities to tunicamycin, the Pmt1-inhibitor and caspofungin were examined. While the *ace2* mutant carrying an empty control vector (pBI-1) showed the expected inhibitor sensitivities, these defects were rescued by ectopic genomic integration of plasmid pPCK1p-ACE2-URA3 carrying *ACE2* under control of the *PCK1* promoter (Fig. 1A). Overexpression of *ACE2* in the genetic background of *msb2*, *hst7* and *pmt1* mutants alleviated their high sensitivities, at least partially (Fig. 1A and B). In contrast, overexpression of *ACE2* was not able to suppress sensitivities of the *cek1* mutant suggesting that basal activation/phosphorylation by Cek1 is required for suppression. These results are consistent with Ace2 being a downstream target of the Cek1 MAPK signaling pathway that acts to fortify glycostructures in *C. albicans*.

Genes encoding the major Pmt isoforms Pmt1, Pmt2 and Pmt4, catalyzing *O*-mannosylation of secretory proteins are known downstream target genes of Cek1 signaling in *C. albicans*; it has been reported that in the *ace2* mutant, *PMT2* and *PMT4* transcript levels are greatly reduced both in unstressed cells and in cells

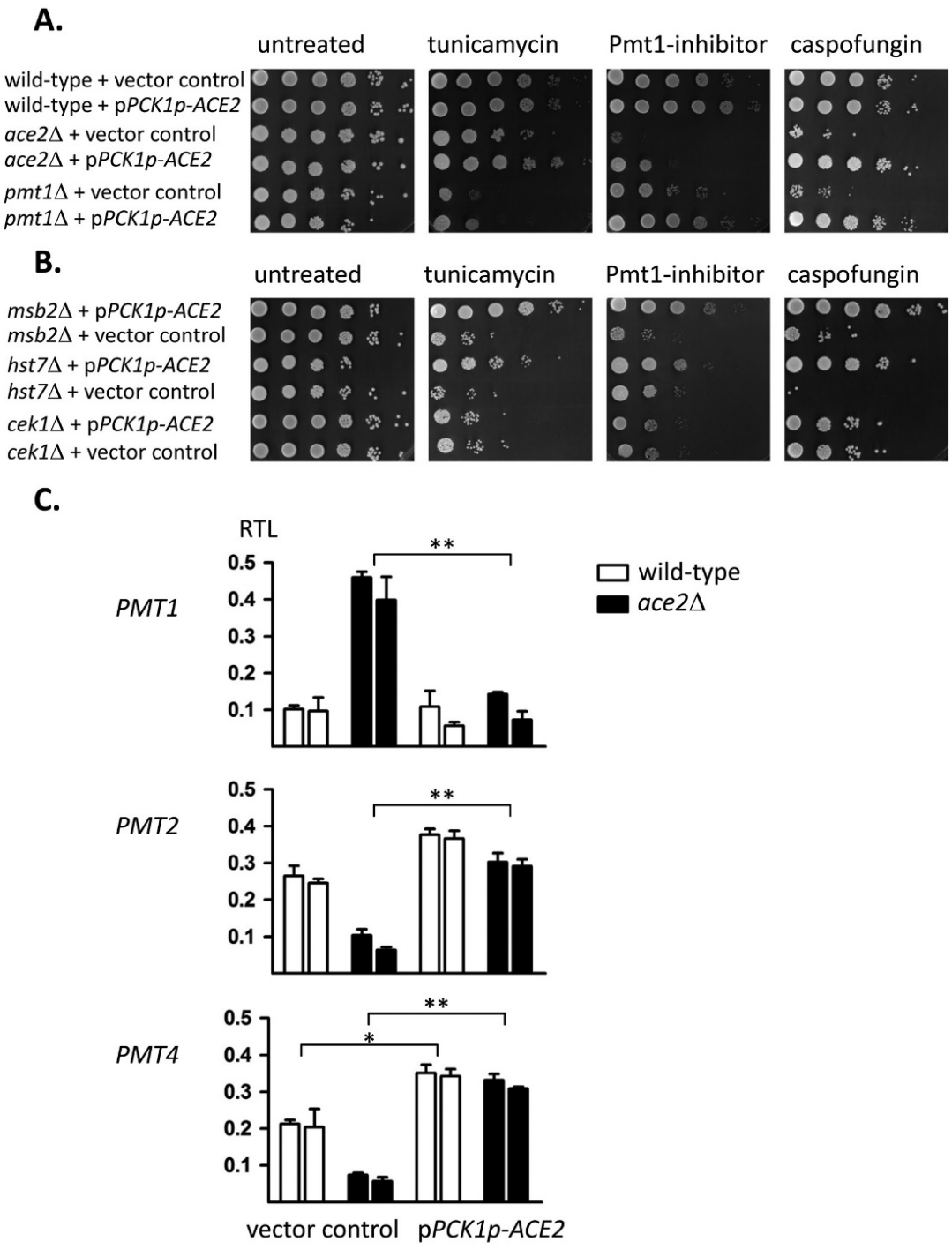

Fig. 1. *ACE2* Overexpression suppresses glycosylation defects. Strains CAI4 (wild-type), CLvW008 (*ace2*/*ace2*), CAP1-3121 (*pmt1*/*pmt1*), FCCa28 (*msb2*/*msb2*), hst7 (*hst7*/*hst7*) and CK43B-16L (*cek1*/*cek1*) were transformed with either plasmid pPCK1p-ACE2-URA3 or the empty vector pBI-1. Plasmids were linearized and integrated into the *LEU2* locus.
A. Sensitivity phenotypes of the *ace2* and *pmt1* mutant.
B. and of the *msb2*, *hst7* and *cek1* mutant were examined by serial spot dilutions of the strains. For activation (de-repression) of the *PCK1* promoter glucose-free SCAA (0.67% yeast nitrogen base, 2% casamino acids) medium was used and either supplemented with tunicamycin (2 μg/ml), caspofungin (50 ng/ml) or the Pmt1-inhibitor (4 μM).
C. Transcriptional regulation of *PMT* genes in strains overexpressing *ACE2*. Transformants of strains *ace2* or the reference strain CAI4 harbouring either the control plasmid pBI-1 or the *ACE2* overexpression plasmid were precultured in YPD medium and used for inoculation of 50 ml SCAA cultures. After 4 h incubation at 30°C cultures were harvested and used for preparation of total RNA. Two biological replicates and three technical replicates were assayed by qPCR using gene-specific oligonucleotides. Each bar represents the mRNA level of the indicated gene in an independent transformant expressed as means ± SEM relative to the *ACT1* transcript (relative transcript level, RTL). A *t*-test was used to calculate the statistical relevance: *, $p < 0.05$; **, $p < 0.01$; ***, $p < 0.001$.

lacking Pmt1-mediated *O*-mannosylation, as compared to a wild-type strain; in contrast, the *PMT1* transcript level was increased in unstressed *ace2* cells indicating that *PMT1* expression is normally repressed by Ace2, while de-repression occurs in case of defective *N*-glycosylation (Cantero *et al.*, 2007; Cantero and Ernst, 2011). Correspondingly, *ACE2* overexpression strongly induced expression levels of *PMT2* and *PMT4* in both wild-type and the *ace2* mutant strains, while the *PMT1* transcript was downregulated (Fig. 1C). It thus appears that the Cek1 MAP kinase pathway uses the transcription factor Ace2 to regulate *PMT* transcription, by inducing or by repressing *PMT* transcription in a Pmt isoform-specific manner.

Genomic Ace2 targets include genes encoding Cek1 signaling components

The genomic localization sites of Ace2 under normoxia and hypoxia have been determined previously (Desai *et al.*, 2015). Here, we explored genomic targets of Ace2 under glycostress conditions during growth in the presence of tunicamycin by *in vivo* genome-wide ChIP on chip analyses. For this purpose a strain producing HA-tagged Ace2 (CLvW004) from its native chromosomal locus was used in combination with a control strain producing untagged Ace2 (BWP17); tunicamycin did not affect growth rates of both strains at the employed concentration (0.5 μg/ml). In total, 264 significant binding regions of Ace2-HA had been identified previously in untreated yeast cells grown under normoxia, which were mostly located upstream of ORFs on all eight chromosomes (Desai *et al.*, 2015). Block of *N*-glycosylation by tunicamycin did not significantly change the genomic localization of Ace2-HA; 201 significant binding regions were detected with 269 corresponding ORFs on all eight chromosomes. While binding sites obtained under both conditions largely overlap (Fig. 2A), 58 sites were exclusively identified in cells grown in the presence of tunicamycin. Binding sites are specified in Supporting Information Table S1.

Gene ontology analysis of the deduced Ace2-target ORFs revealed enrichment of genes with function in DNA binding and in transferase activity, biofilm formation and stress response (Fig. 2B). Upstream regions of ORFs encoding DNA binding proteins were mostly bound by Ace2-HA not only under tunicamycin treatment but also under unstressed conditions, as described previously (Desai *et al.*, 2015). An exception is *ACE2* itself, which was found to bind the Ace2-HA protein in its promoter only under tunicamycin treatment suggesting autoregulation (see below). Five other genes involved in stress responses were identified as Ace2-HA targets including genes encoding components of the Cek1 MAP kinase cascade including the sensor protein Msb2, the Ste20 homolog Cst20 and the MAPKK Hst7 (underlined in Fig. 2B GO term, Process). Ace2-HA bound to the *HST7* promoter only under tunicamycin-stress at a single site, while interestingly, two binding sites were identified in the *MSB2* promoter occurring under tunicamycin stress (distal site) or during unstressed growth (proximal site) (Fig. 3A). ChIP-qPCR experiments using precipitated chromatin of the strain expressing HA-tagged Ace2 verified the presence of Ace2-HA at the indicated positions (Fig. 3B). Other genes identified among Ace2 targets encode proteins with signal transducer activity including Wsc2 and Ypd1, involved in cell wall integrity stress response (Verna *et al.*, 1997) and osmotic stress response (Calera *et al.*, 2000) respectively.

Within genes specifying transferase activity, a subset encoding glycosyltransferases including Pmt6, Alg2, Stt3 and the α1,3-mannosyltransferases Mnn1, Mnn11, Mnn22 and Mnn26 was identified (underlined in Fig. 2B GO term, Function); the Pmt6 isoform has a minor role for protection against glycostress (Cantero *et al.*, 2007; Cantero and Ernst, 2011) but contributes significantly to biofilm formation (Peltroche-Llacsahuanga *et al.*, 2006) and virulence of *C. albicans* (Timpel *et al.*, 2000; Rouabhia *et al.*, 2005). The Alg2 mannosyltransferase is essential for *N*-linked glycosylation (Huffaker and Robbins, 1983) and Stt3 is a structural component of the oligosaccharyltransferase complex (Zufferey *et al.*, 1995;

A.

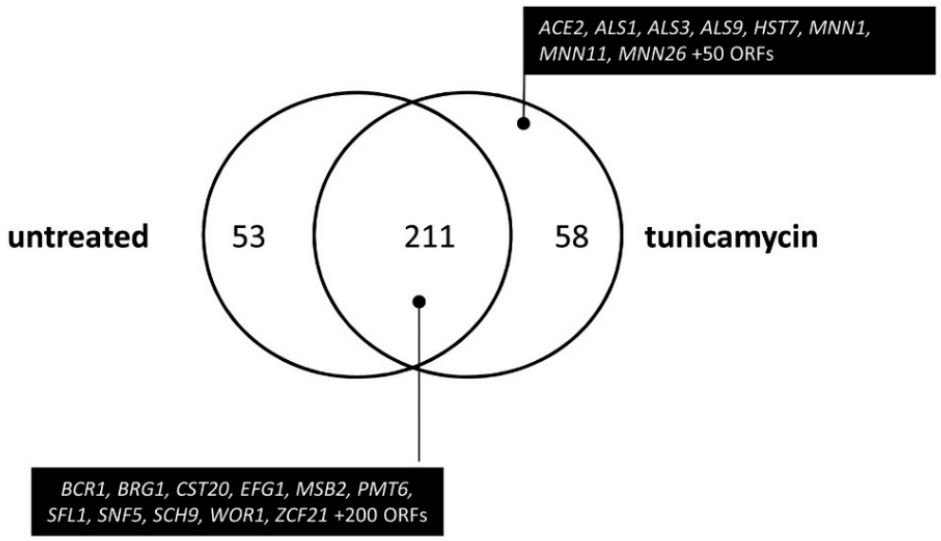

B.

GO term	Ace2-HA binding genes obtained under tunicamycin stress annotated to the term		
(genome frequency)	Name	Frequency	*P* value
A. Process			
Response to stress (7.3 %)	***ACE2***, ACT1, ***ALS9***, BCR1, ***BDF1***, BRG1, MMS2, ORF19.2673, ***CDC5***, MSH1, ***VAC14***, CSR1, CST20, EFG1, GLC7, ***HST7***, ***MDS3***, MPS1, ***MSB2***, NAM7, PMT6, RAD14, RNH35, RTA2, RTF1, ***RTT109***, SCH9, ***SHA3***, ***SNF5***, SNQ2, SOH1, ***SWC4***, SWI1, ***TSA1B***, VPS51, ***WAL1***, WSC2, YPD1, ***ZCF13***	19.3 %	0.05
Biofilm formation (1.1 %)	ADH1, ***ALS1***, ALS2, ***ALS3***, ***ALS9***, BCR1, BRG1, EED1, ORF19.2527, CSR1, ***EAP1***, EFG1, FCR3, ***MDS3***, PMT6, ***SNF5***, SOH1, TRY2, TRY3, TRY5, WOR1	10.9 %	0.01
B. Function			
Transferase activity (7.2 %)	***ABC1***, ACT1, ADH1, ALG2, MMS2, ORF19.5809, ORF19.4066, ORF19.2673, ORF19.3840, SET5, ORF19.223, MIP1, CDC34, ***CDC5***, CIS2, ***COQ3***, OAR1, CST20, ***FAS1***, FEN1, FUN31, ***HST7***, MET1, ***MNN1***, ***MNN11***, MNN22, ***MNN26***, MPS1, PKH3, PMT6, ***RTT109***, SCH9, ***SHA3***, SKY2, ***STT3***, ***SWC4***, TRM1, URK1, YPD1	19.7 %	0.05
DNA binding (7 %)	***ACE2***, AGE2, BCR1, ***BDF1***, BRG1, TRA98, SWI3, ***ORF19.1667***, MIP1, BDP1, ORF19.173, MSH1, CSR1, CUP9, EFG1, FCR3, FLO8, IFH1, ***ISW2***, NAM7, PUT3, RAD14, ***REP1***, RTF1, SFL1, STB3, ***SWC4***, SWI1, TRY5, WOR1, WOR3, ***ZCF13***, ZCF21	14.0 %	0.05

Fig. 2. Genomic binding sites for Ace2-HA.
A. Venn diagram showing the number of genes bound by Ace2-HA in presence of tunicamycin and untreated condition. Genomic binding regions of Ace2-HA were derived from ChIP chip experiments comparing strains CLvW004 (*ace2/ACE2*^{3HA}) and BWP17.
B. GO categories of identified Ace2-HA target genes under tunicamycin stress conditions. The CGD GO Term Finder (http://www.candidagenome.org/cgi-bin/GO/goTermFinder) was used to identify common functions and processes Ace2-HA target genes contribute to; the analysis was performed in May 2014. Genome frequencies of genes corresponding to GO terms are expressed as percentages, relative to 6,525 ORFs in the *C. albicans* genome; the frequency of genes corresponding to a specific GO category are expressed relative to the total number of 269 genes with an Ace2-HA binding region present in their upstream regions. *P* values for categories were calculated according to the GO Term Finder tool, which uses a hyper geometric distribution with multiple hypothesis correction. The *p* value cut-off used was 0.05. Underlined names indicate genes encoding proteins with glycosyltransferase activity or signal transducer activity. Genes obtained only under tunicamycin induced stress are highlighted in bold.

Chavan *et al.*, 2003). The four mannosyltransferases Mnn1, Mnn11, Mnn22 and Mnn26 are required for addition of mannose moieties of *N*- and *O*-linked oligosaccharides (Romero *et al.*, 1999); in *C. albicans* 12 members of the *MNN1* and *MNN2* family mostly share redundant functions (Bates *et al.*, 2013).

In conclusion, the identified set of Ace2 target genes is involved directly or indirectly in regulation of *O*- and *N*-linked glycosylation, thereby assuring cell wall maintenance and biofilm formation of *C. albicans*. Surprisingly, direct binding of Ace2-HA to promoter sequences of genes encoding the three major Pmt isoforms Pmt1, Pmt2 and Pmt4 was not detected under any growth condition.

Ace2 regulates Cek1 pathway genes under glycostress

To verify Ace2-dependent regulation of Cek1 pathway genes, their transcript levels were compared in the *ace2* mutant and wild-type cells, grown without and with glycostress by tunicamycin. The expression of *MSB2*, *CST20*, *HST7*, and *CEK1* genes were all affected by the presence of Ace2 under both conditions (Fig. 3C). Transcripts of the four genes were strongly upregulated by tunicamycin in the wild-type but not in the *ace2* mutant strain. Remarkably, the *CEK1* transcript was upregulated almost 12-fold by tunicamycin, which did not occur in the *ace2* mutant strain (Fig. 4A). Genes for the two upstream components Msb2 and Hst7 were already moderately de-repressed in the absence of Ace2 (indicating a repressor function of Ace2 in the absence of glycostress) but their transcript levels were not induced further in the mutant by tunicamycin indicating a second, inducer function of Ace2 under glycostress. In support of transcript analyses, the shed Msb2 protein exodomain (Szafranski-Schneider *et al.*, 2012) was increased in the medium of stressed wild-type and *ace2* mutant strains, although no further increase occurred in the *ace2* mutant, in the presence of tunicamycin (Supporting Information Fig. S1).

Similar to *ace2* mutants, mutants lacking the Msb2 upstream sensor of the Cek1 pathway did not upregulate *CST20*, *HST7* and *CEK1* transcripts in response to tunicamycin stress. This result suggested that information on defective *N*-glycosylation is transmitted through Msb2 to downstream elements of the Cek1 pathway. Remarkably, even upregulation of the *ACE2* transcript by tunicamycin was found to require Msb2, again placing Ace2 functions downstream of the Cek1 pathway. A reporter gene fusion of the *ACE2* promoter with the *lacZ* gene was stimulated during exposure with the *N*-glycosylation inhibitor tunicamycin and the Pmt1-inhibitor (Fig. 4B) indicating that *ACE2* transcript upregulation is due to enhanced *ACE2* promoter activity and not post-transcriptional regulation. In combination with Ace2 binding to its own promoter (Fig. 2A) the results suggest positive autoregulation of *ACE2* transcription via the Cek1 signaling pathway under glycostress. Increased phosphorylation and levels of Ace2 would consequently boost the overall output of the Cek1 pathway further, by increasing transcription of genes in the pathway. Thus, Ace2 provides positive feed-back on Cek1 signaling to rapidly respond to glycostress conditions.

Cph1 is a transcription factor acting downstream of Cek1 during hyphal morphogenesis under some conditions (Liu *et al.*, 1994; Desai *et al.*, 2015), which has been described to downregulate *CEK1*, *CST20*, *HST7* and *STE11* genes under oxidative stress (Maiti *et al.*, 2015). To explore the role of Cph1 in glycostress signaling, transcript levels of relevant genes were examined in a *cph1* mutant strain. Deletion of *CPH1* did not influence tunicamycin-induced upregulation of *PMT1*, *ACE2* and *CEK1* transcripts (Supporting Information Fig. S2) indicating that Cph1 is not involved in glycostress signaling; *PMT2* transcript levels were also not affected. The results indicate, however, that Cph1 mediates a moderate downregulation of the *CEK1* transcript under non-stressed conditions (Supporting Information Fig. S2).

Zcf21 functions downstream of Ace2 to repress PMT1

Although the Ace2-binding motif CAGCW (Desai *et al.*, 2015) is present in upstream regions of *PMT1*, *PMT2*

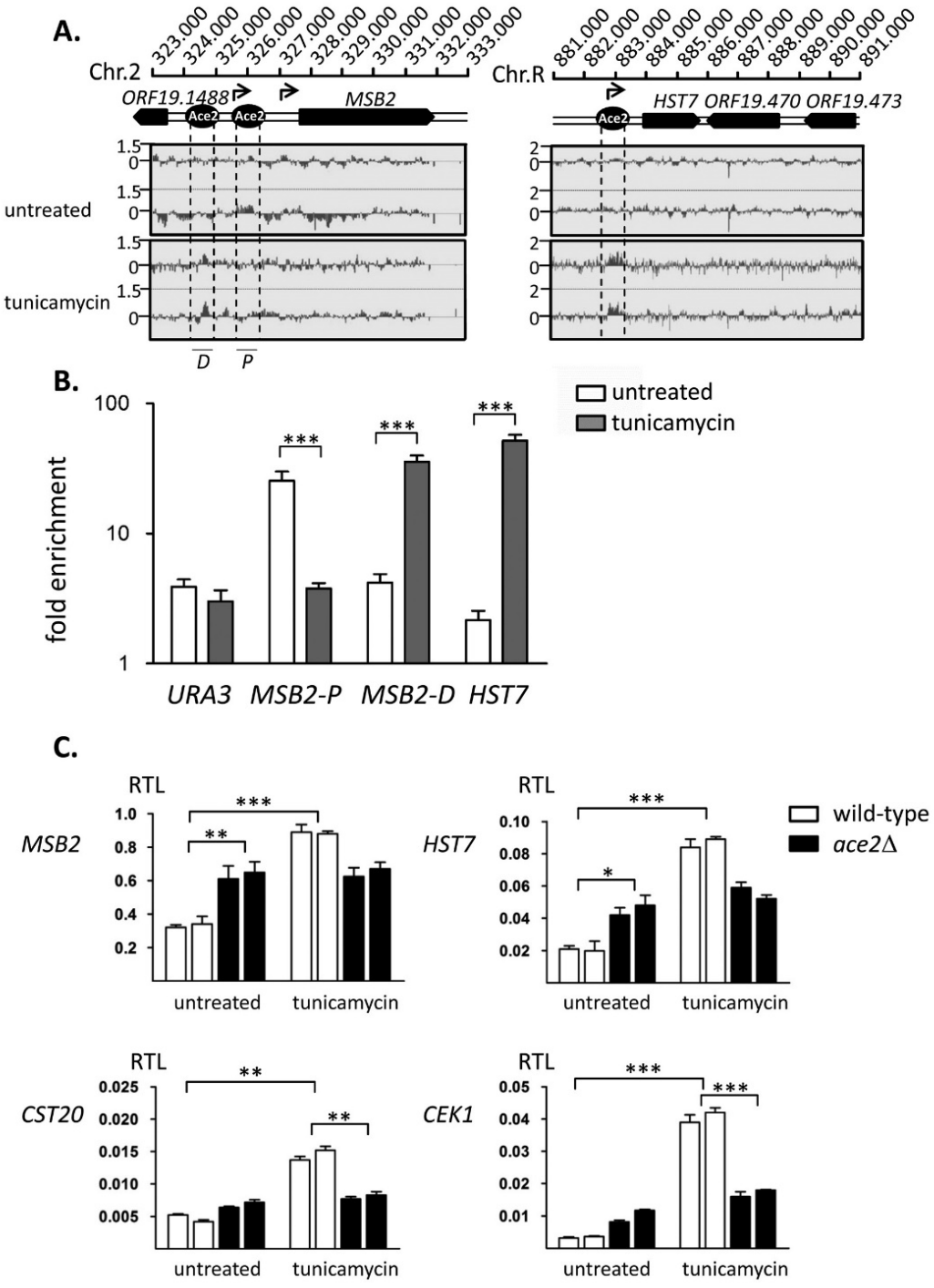

Fig. 3. Ace2 binds to regulatory sequences of genes encoding Cek1 MAP kinase members.
A. Ace2-HA binding to *MSB2* and *HST7* chromosomal loci. The genomic localization of Ace2-HA was determined by ChIP chip assays of strain CLvW004 in the presence and absence (untreated) of the *N*-glycosylation inhibitor tunicamycin, using strain BWP17 as the reference (no-tag control). Coordinates of *MSB2* and *HST7* with their respective neighbouring genes are shown on top. Round circles indicate the position of the obtained Ace2-HA binding site; distal (*D*) and proximal (*P*) binding sites in the *MSB2* upstream region are marked. Plots of scaled $\log_2$ ratios of Ace2-HA occupancy for two replicates are shown for each condition. Transcript start sites are indicated by kinked arrows.
B. Enrichment of Ace2-HA at *MSB2* and *HST7* chromosomal loci. qPCR was used to calculate the fold enrichment of Ace2-HA at the *MSB2* and *HST7* binding sites shown in (A). A sequence in the *URA3* upstream region was used as a background control.
C. Transcriptional regulation of *MSB2*, *HST7*, *CST20* and *CEK1*. Strains SC5314 (wild-type) and MK106 (*ace2*) were precultured in YPD medium and used for inoculation of 50 ml fresh YPD cultures, either supplemented with tunicamycin (1 μg/ml) or left untreated. Following 4 h incubation at 30°C, cells were harvested and total RNA was isolated. Relative transcript levels of *MSB2*, *HST7*, *CST20* and *CEK1* were determined by qPCR.

and *PMT4*, direct binding of Ace2-HA to promoters of *PMT* genes was not detected (see above). To exclude that nevertheless Ace2 operates via this motif to regulate *PMT1* expression, the *lacZ* reporter gene was placed downstream of a modified *PMT1* promoter lacking the Ace2 motif. However, transformants carrying this fusion still upregulated *lacZ* expression in the presence of tunicamycin (data not shown). It was concluded that Ace2 regulates *PMT1* transcription indirectly, through the activity of another, yet unknown transcription factor.

To identify the unknown transcription factor we focused on the genomic Ace2-HA target genes described above. Known phenotypes of respective mutants were used to reduce the size of the group (34 genes) to a set of 4 potential candidates, namely *BCR1*, *SNF5*, *ZCF14* and *ZCF21*. Among these genes, only *ZCF21* encoding a zinc finger domain-containing transcription factor showed a significant change in its transcript level in the presence of glycosylation inhibitors. In wild-type cells, tunicamycin led to lowered *ZCF21* transcript levels, while the Pmt1-inhibitor had no effect (Fig. 5A) indicating that *ZCF21* expression is repressed specifically by defective *N*-glycosylation. In an *ace2* mutant the *ZCF21* transcript only occurred at low repressed levels indicating that the positive function of Ace2 in upregulating *ZCF21* transcript levels during unstressed growth conditions and impaired *O*-glycosylation did not occur. In contrast, deletion of *zcf21* did not influence basal or stress-induced levels of the *ACE2* transcript. Thus, *ACE2* regulates *ZCF21* but not vice-versa.

To clarify how Zcf21 regulates transcripts of *PMT* genes, transcript levels of *PMT1* and *PMT4* genes were determined in the *zcf21* mutant strain grown in the presence and absence of glycosylation inhibitors. Consistent with earlier reports (Cantero and Ernst, 2011) the *PMT1* transcript was highly upregulated (de-repressed) in the presence of tunicamycin, but was not affected by the Pmt1-inhibitor (Fig. 5B). In the *zcf21* mutant, however, the *PMT1* transcript were drastically increased under all conditions and did not further change after treatment with the *N*-glycosylation inhibitor tunicamycin; a similar pattern was observed for the *ace2* mutant. The results suggest that both, Ace2 and Zcf21, function as repressors of *PMT1* gene under unstressed conditions, presumably because Ace2 increases levels of Zcf21, which directly binds to and represses *PMT1* transcription. This assumption is supported by the finding that an identical *PMT1* transcript pattern was detected in the *ace2 zcf21* double mutant as compared to the single mutants (Fig. 5B), which agrees with the function of both regulators function in one linear rather than in two parallel pathways. In addition, *PCK1*-promoter-driven overexpression of *ZCF21* in the double mutant repressed the *PMT1* transcript efficiently, while *ACE2* overexpression had no effect (Fig. 5C). Consistent with the finding that the *pmt4 pmt1* double mutant is not viable (Prill *et al.*, 2005), overexpression of *ZCF21*, but not of *ACE2* increased sensitivity to tunicamycin, the Pmt1-inhibitor and caspofungin in the *pmt4* mutant background, compared to the empty vector control (Fig. 5D).

In contrast to the effects on *PMT1* expression, *PMT4* transcript levels were only affected by the presence of Ace2, acting as an inducer, but not by Zcf21 (Fig. 5B). Taken together, the above described results suggest that in *C. albicans* the transcription factor Zcf21 functions as a downstream target of Ace2 to specifically repress expression of *PMT1*. Molecular mechanisms, by which Ace2 regulates *PMT2* and *PMT4* genes are yet unknown and need to be clarified.

Ace2 interactors include the MAPKKK Cst20

The search for functional interactors of Ace2 was continued by screening a random *C. albicans* genomic library fused to the Gal4 activation domain in a yeast two-hybrid approach (James *et al.*, 1996), using bait plasmid pBD-Ace2 that encodes a fusion of the Gal4 binding domain to Ace2. Library plasmids from 46 Ade^+ transformants were recovered and retransformed with empty plasmid pGBD-C1 (James *et al.*, 1996) to exclude auto-activation by the insert protein. The genomic insert in library plasmids carrying Ace2

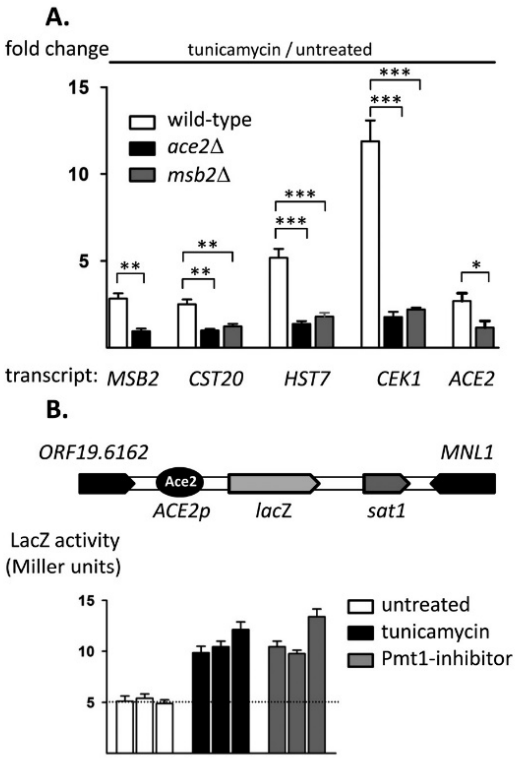

Fig. 4. Ace2 is a glycostress-dependent regulator of genes encoding Cek1 MAP kinase pathway members.
A. Transcriptional regulation of genes encoding Cek1 MAPK members. Strains SC5314, MK106 (*ace2*) and Fcc28 (*msb2*) were treated as described for (Fig. 3C), relative transcript levels (RTL) were determined by qPCR and used to calculate the $\log_2$ mean fold-change in expression under *N*-glycosylation block (tunicamycin) compared to untreated conditions. Each bar represents the mean of at least three independent biological replicates ± SEM.
B. *ACE2* promoter activity in response to glycostress. The reporter gene *lacZ* was used to replace one *ACE2* allel in strain CLvW001 to study activity of the native *ACE2*-promoter. The strain was grown in YPD medium containing tunicamycin (1 μg/ml), the Pmt1-inhibitor (4 μM) or was left untreated. For background correction strain BWP17 was used. After 4 h incubation the cells were collected and their β-galactosidase activity (Miller units) was determined. The assay was performed with three independent biological replicates, each representing one bar. The dotted line indicates basal *ACE2*-promoter activity in YPD medium without any inhibitor.

interactors were sequenced and revealed that they encoded sequences of 8 different proteins (Supporting Information Fig. S3A). Remarkably, one insert encoded 225 residues of the Cst20 protein kinase (Supporting Information Fig. S3B), which represents the MAPKKK of the MAPK Cek1, i. e. a protein functioning upstream of Ace2 in the glycostress signaling pathway. Co-immunoprecipitation of Ace2 and Cst20 using a strain producing chromosomal HA-tagged Ace2 and V5-tagged Cst20 (CLvW216) grown in the presence of tunicamycin confirmed the interaction of both proteins (Fig. 6A). Immunoblotting of cell extracts revealed Cst20-V5 and Ace2-HA in cell extracts with apparent masses of 135 kDa and 120 kDa, respectively, and immunoprecipitation of Ace2-HA detected Cst20-V5 in the precipitate (Fig. 6A).

The functional relevance of the Ace2-Cst20 interaction was examined by comparing the phosphorylation status of Ace2 in the *cst20* mutant and in the wild-type background (strain CLvW217). For this purpose, both chromosomal *CST20* copies were deleted in the *ace2*/*ACE2*^{3HA} genetic background generating strain CLvW215. Following immunoprecipitation of HA-tagged Ace2, protein extracts were divided, treated or not treated with lambda phosphatase and separated by SDS-PAGE. Coomassie blue-staining detected a mobility shift of Ace2-HA by the phosphatase treatment in the wild-type background, which became less distinctive in the *cst20* mutant background (Fig. 6B); this result is a first hint suggesting that Ace2 is a phosphorylation substrate of the Cst20 kinase, although further analyses are required to fortify this conclusion and to establish, if Cst20 acts directly or indirectly on Ace2. Previous phosphoproteomic analysis had identified at least 18 phosphorylated residues in the Ace2 protein (Willger *et al.*, 2015) suggesting that Ace2 is highly phosphorylated by multiple kinases including Cst20.

To obtain further evidence for the relevance of the Ace2-Cst20 interaction the intracellular localization of Cst20 was investigated. Strain CLvW219 producing GFP-tagged Cst20 was constructed and its biosynthesis was verified by immunoblotting using anti-GFP antibody (Supporting Information Fig. S4A); protein functionality was verified in the heterozygous mutant strain (*cst20*/*CST20*^{GFP}) by its inhibitor sensitivities (Fig. 7A and B). Fluorescence microscopy of unstressed cells revealed Cst20-GFP mainly at the tip of cells that did recently had undergone budding (Fig. 6C) in agreement with results obtained for the homologous protein Ste20 in *S. cerevisiae* (Peter *et al.*, 1996). In contrast, cells grown in the presence of tunicamycin showed co-localization of Cst20-GFP with the nucleus (Fig. 6C). Thus, re-localization of Cst20 from the cytoplasm to the nucleus under glycostress sets the stage for its potential interaction with the Ace2 transcription factor. Previously, an exclusive nuclear localization of Ace2 in yeast-daughter and filamentous cells of *C. albicans* had been reported (Kelly *et al.*, 2004; Sbia *et al.*, 2008; Saputo *et al.*, 2014). To investigate the subcellular localization of Ace2 during glycostress, strain CLvW228 producing GFP-tagged Ace2 was used. Fluoresence microscopy verified localization of Ace2-GFP in the

nucleus of daughter cells under untreated growth conditions, while cells exposed to tunicamycin showed nuclear localization of Ace2-GFP in both, yeast-daughter and mother cells (Fig. 6C). These results suggest that glycostress induces cell cycle independent accumulation of Ace2 in *C. albicans* mother cells, possibly reflecting enhanced *ACE2*-promoter activity and increased Ace2 biosynthesis.

Taken together, the results demonstrate that Ace2 and the MAPKKK Cst20 co-localize with the nucleus

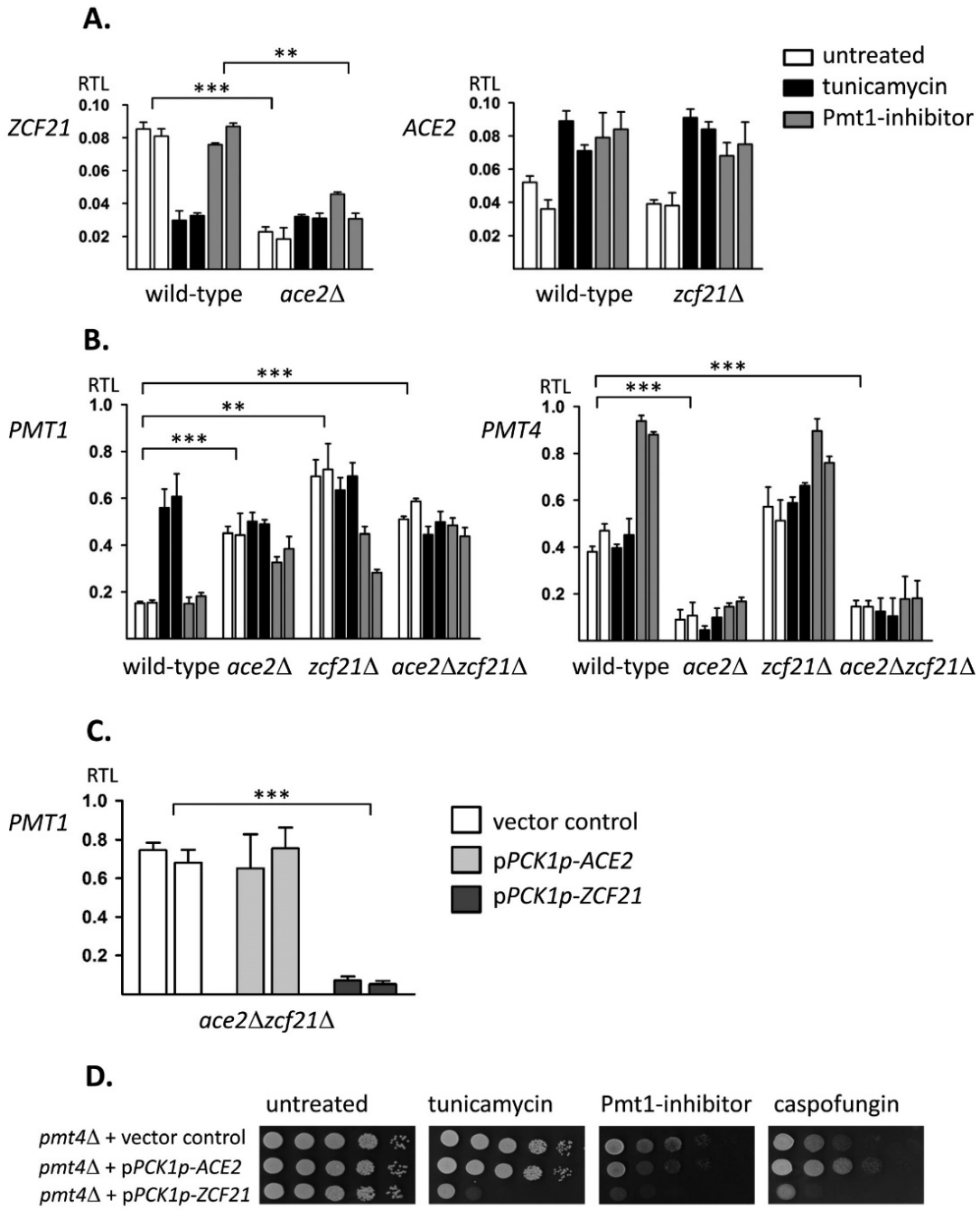

Fig. 5. Ace2 controls transcription of Zcf21 to mediate repression of *PMT1*.
A. Transcriptional regulation of *ZCF21*, *ACE2* and
B. *PMT* genes. Strains SC5314 (wild-type), MK106 (*ace2*), zcf21 (*zcf21*) and CLvW131 (*ace2 zcf21*) were precultured in YPD medium and used to inoculate 50 ml YPD cultures either containing tunicamycin (1 μg/ml), the Pmt1-inhibitor (4 μM) or left untreated. After 4 h incubation at 30°C cells were collected and used for preparation of total RNA. Relative transcript levels (RTL) of indicated genes in corresponding strains were assayed by qPCR, as described in Fig. 1.
C. Transcriptional regulation of *PMT1* in strains overexpressing *ACE2* or *ZCF21*. Strain CLvW131 (*ace2 zcf21*) was either transformed with plasmid pPCK1p-ACE2-SAT1, pPCK1p-ZCF21-SAT1 or pBI-SAT1 (empty vector). Plasmids were linearized and integrated into the *LEU2* locus. The corresponding transformants were precultured in YPD medium and used to inoculate 50 ml SCAA medium. Total RNA was isolated after 4 h incubation at 30°C and relative transcript levels of *PMT1* were determined.
D. Sensitivity phenotypes of the *pmt4* mutant harbouring *ACE2* or *ZCF21* overexpression plasmids. Plasmids pPCK1-ACE2-URA3, pPCK1-ZCF21-URA3 and the empty vector pBI-URA3 were linearized and transformed into strain PP46-4285 (*pmt4*). Phenotypes of the respective transformants were investigated in a serial spot dilution test on SCAA agar plates containing tunicamycin (2 μg/ml), the Pmt1-inhibitor (4 μM) or caspofungin (50 ng/ml).

under glycostress, allowing direct interaction of Ace2-Cst20 under these conditions.

Cst20-Ace2 interaction in the nucleus downregulates glycostress signaling

Molecular interactions of Ace2 and Cst20 proteins in the nucleus of tunicamycin-stressed cells raised the question on the biological importance of this interaction. A double mutant strain CLvW211 (*ace2 cst20*) was constructed and its sensitivity phenotypes were compared to the *ace2* and *cst20* single mutants CLvW209 and MK106 respectively. Both types of strains increased sensitivities similarly to inhibitors tunicamycin, the Pmt1-inhibitor and to caspofungin (Fig. 6D); thus, a synthetic defective phenotype was not found. Furthermore, overexpression of *ACE2* alone was able to suppress sensitivities of the double mutant. These results are consistent with the above conclusion (Fig. 1) that Ace2 functions downstream of Cst20 in the Cek1 pathway and suggest that at elevated Ace2 levels its interaction with Cst20 is not necessary for Ace2 to generate glycostress resistance.

In another approach to assess the relevance of Ace2-Cst20 interaction the influence of the cellular localization of Cst20 on glycostress phenotypes was studied. Cst20 does not contain a conventional NLS (nuclear localization signal) or NES (nuclear export sequence). To direct intracellular localization of Cst20, strains producing Cst20-GFP fusions with added heterologous NLS- (nuclear localization signal) or NES- (nuclear export sequence) sequences were constructed. We used the NLS of the simian virus 40 (SV40) large T-antigen (Kalderon *et al.*, 1984) or the NES of the protein kinase A inhibitor PKI (Wen *et al.*, 1995) fused C-terminally to Cst20-GFP for this purpose (Supporting Information Fig. S4B); both signal sequences have been widely used to analyze nuclear shuttling of proteins in *S. cerevisiae* (Miller and Cross, 2000; Hahn *et al.*, 2008; Sun *et al.*, 2011). The synthesis of the Cst20-GFP^{NES} and Cst20-GFP^{NLS} fusion proteins was confirmed by immunoblotting using anti-GFP antibody (Supporting Information Fig. S4C). Fluorescence microscopy revealed strong nuclear accumulation of Cst20-GFP^{NLS} in the nucleus of untreated cells, while Cst20-GFP^{NES} remained in the cytoplasm of cells treated with tunicamycin (Supporting Information Fig. S4D), thus reversing the regular localization of Cst20-GFP not carrying NLS/NES sequences (Fig. 6C).

The strain encoding the Cst20-GFP^{NLS} fusion protein was highly sensitive to the glycosylation inhibitors, similar to the *cst20* mutant (Fig. 7A). Surprisingly, this high sensitivity remained in a strain harboring an additional functional copy of *CST20* (*CST20/CST20-GFP-NLS*) suggesting that the NLS-fusion acts as a dominant repressor of the protein without the NLS. In contrast, the strain encoding the Cst20-GFP^{NES} fusion protein showed resistances comparable to the reference strain (Fig. 7A), suggesting that its cytoplasmic localization is required for Cek1 signaling in response to glycostress. The results confirm that indeed cytoplasmic localization is required for Cst20 function in response to glycostress, but indicate also that Cst20 has a second function within the nucleus to prevent glycostress signaling.

To further investigate the influence of cellular localization of Cst20, we determined tunicamycin-induced changes in the *CEK1* transcript level in cells producing Cst20-GFP without or with NLS- or NES-sequences. The heterozygous *cst20* mutant strain expressing unmodified Cst20-GFP showed wild-type *CEK1* ratios (Fig. 7B), whereas no up-regulation of *CEK1* was detected in the homozygous *cst20* mutant suggesting that Cst20, like Msb2 and Ace2 (Fig. 5A), is required for upregulation of the signaling pathway. Strains producing Cst20-GFP^{NES} variants showed even higher *CEK1* transcript ratios as compared to the wild-type, suggesting that cytoplasmic localization of Cst20 advantages positive regulation or prevents negative regulation. Consistent with this phenotype, strains expressing Cst20-GFP^{NLS} variants showed significantly lower *CEK1* trancript ratios, comparable to the *cst20* mutant, irrespective of the presence of unmodified Cst20 (*CST20/CST20-GFP-NLS*) in these cells.

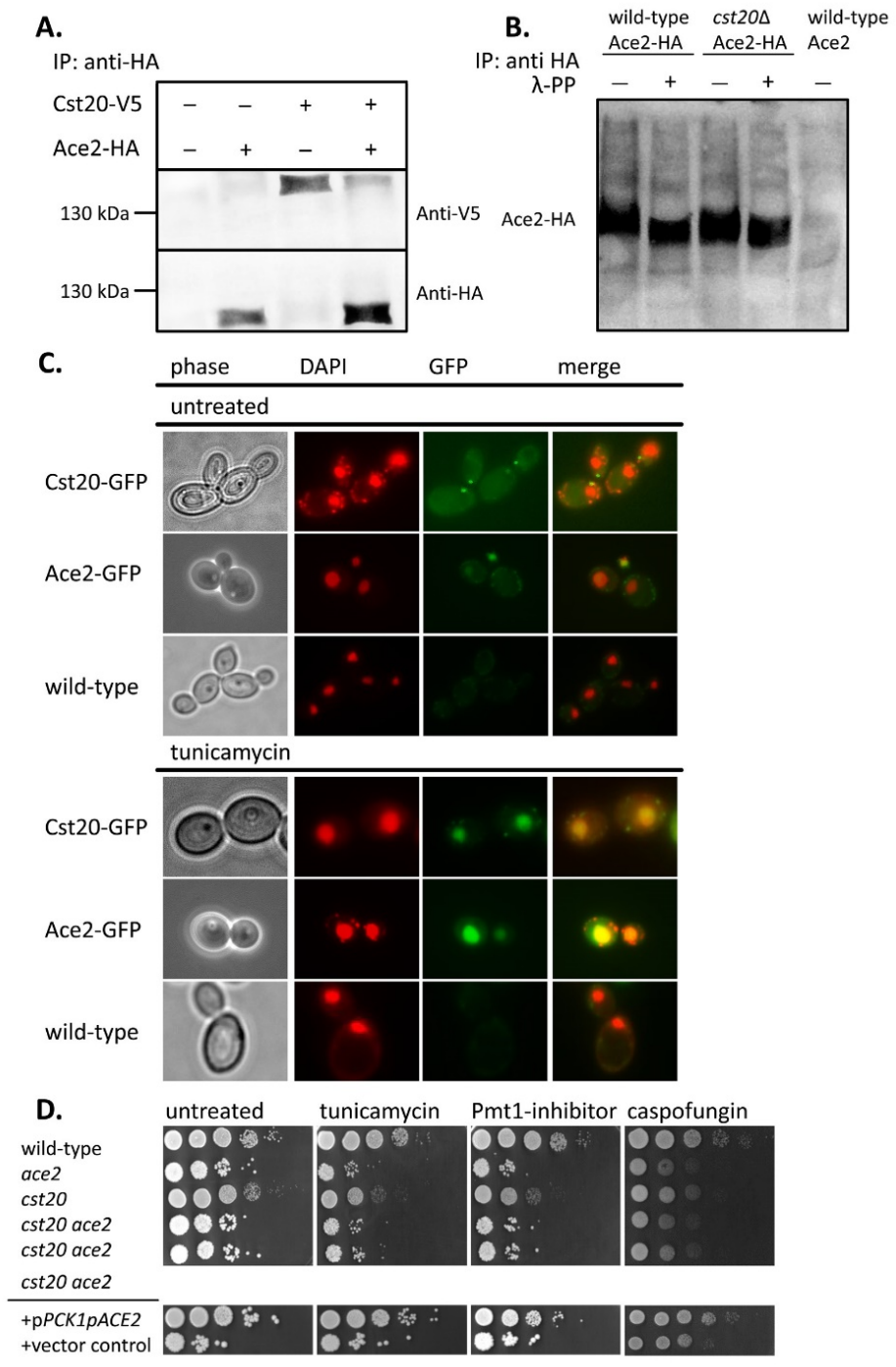

Fig. 6. Ace2 interacts with the upstream MAPKKK Cst20.
A. Co-immunoprecipitation. Whole cell extracts of strain CLvW216 producing Ace2-HA and Cst20-V5 from their chromosomal locus were used for immunoprecipitation using anti-HA affinity gel (IP: anti-HA). The strains were grown in YPD medium supplemented with tunicamycin (1 μg/ml). Immunoprecipitated samples were immunoblotted and developed using anti-HA or anti-V5 antibodies (±).
B. Phosphorylation of Ace2-HA. Both chromosomal copies of *CST20* were deleted to generate strain CLvW215 (*cst20/cst20*; *ace2/ACE2*^{3HA}). Strain CLvW217 producing wild-type Ace2-HA and strain CLvW215 producing Ace2-HA in absence of Cst20 were grown in YPD medium supplemented with tunicamycin (1 μg/ml). Cell extracts were used for immunoprecipitation with anti-HA affinity gel (IP: anti-HA). Lambda protein phosphatase (λ-PP) was used to release phosphate groups from residues in the immunoprecipitated Ace2-HA protein. Phosphatase treated and untreated (±) Ace2-HA samples were resolved by gradient SDS-PAGE and visualized by Coomassie blue staining. Protein extracts of strain CLvW006 were used to detect background bands.
C. Localization of Cst20-GFP and Ace2-GFP. Fluorescence microscopy of strains producing GFP modified Cst20 or Ace2 was used to investigate the subcellular localization of Cst20-GFP and Ace2-GFP. Strains CLvW219 (*cst20/CST20*^{GFP}), CLvW228 (*ace2/ACE2*^{GFP}) and CLvW208 (control strain) were incubated in SCAA medium for 4 h, supplemented with tunicamycin (1 μg/ml) or left untreated. Representative images of cells producing either Ace2-GFP or Cst20-GFP (green) are shown for both conditions. DAPI was used for nuclear staining (red) and images were merged to visualize co-localization of both signals.
D. Sensitivity phenotypes of *cst20* mutant strains. Strain SC5314 (wild-type), MK106 (*ace2*), CLvW209 (*cst20*), CLvW211 (*cst20 ace2*) and strains CLvW224 and CLvW225, harbouring either plasmid pPCK1-ACE2-SAT1 or pBI-SAT1, were precultured in YPD medium and corresponding phenotypes were investigated in a serial spot dilution test on SCAA agar plates containing either caspofungin (50 ng/ml), tunicamycin (2 μg/ml) or the Pmt1-inhibitor (4 μM).

In non-stressed cells, basal Cek1 signaling pathway serves to downregulate *PMT1* expression and to upregulate *PMT2/4* expression (Cantero and Ernst, 2011). Cst20 contributes to these activities since the *PMT1* and *PMT4* transcript levels were increased or lowered, respectively, in the *cst20* mutant. Similar to the *CEK1* transcript, the *PMT4* transcript was lowered in strains producing the Cst20-GFP-NLS but not the -NES variant (Fig. 7C) indicating that Cst20 is required for basal *PMT4* expression in the cytoplasm, but that it represses basal transcription of *PMT4* once it enters the nucleus. Ace2 was also found to be required for basal expression of *PMT2* and *PMT4* (Fig. 1C; Cantero and Ernst, 2011), indicating that interaction of Cst20 with Ace2 might cause the repression. In contrast to regulation of *PMT2* and *PMT4*, Ace2 was found to mediate repression of *PMT1* (Fig. 1C). To test if nuclear tanslocation of Cst20 prevents Ace2 mediated repression of *PMT1*, we examined the relative expression level of *PMT1* in strains expressing different *CST20-GFP* variants. As expected, variants expressing NLS modified Cst20-GFP showed significantly increased transcript levels of *PMT1* (Fig. 7C).

Above results had revealed that Ace2, as a deduced downstream target of Cek1, represses *PMT1* expression (Fig. 5A) and upregulates *PMT2/4* expression in unstressed cells (Fig. 1C; Cantero and Ernst, 2011). Furthermore, Ace2 was found to interact physically with Cst20 in the nucleus of stressed cells. Collectively, the results indicate that cytoplasmic Cst20 in unstressed cells allows Cek1-Ace2 signaling, while nuclear translocation of Cst20 under tunicamycin-stress inactivates Ace2 activity.

Discussion

In the human host, *C. albicans* cells are attacked by hydrolytic enzymes and antimicrobial peptides that damage its glycostructures (Gow and Hube, 2012; Swidergall and Ernst, 2014), e. g. glycoproteins or glucan in the fungal cell wall. The Cek1 signaling pathway serves to restore or compensate for such damages by upregulating fortifying enzymes by two different mechanisms: *C. albicans* either represses gene expression in unstressed cells (as for *PMT1*) or induces expression under glycostress (as for *PMT2/PMT4*) (Cantero *et al.*, 2007; Cantero and Ernst, 2011). By de-repression and/or induction of *PMT* genes, protein-*O*-mannosylation is increased and cells can survive. The exodomain of the sensor Msb2, in contact with the cell wall, senses defects in glycostructures and initiates a phosphorylation cascade consisting of MAPKKK Cst20, MAPKK Hst7 and the MAPK Cek1 (Román *et al.*, 2009; Cantero and Ernst, 2011); in addition, nuclear targeting of the cytoplasmic tail of Msb2 (Swidergall *et al.*, 2015) may contribute to the rescue. The importance of Cek1 signaling is supported by the supersensitive phenotypes to glycosylation and cell wall inhibitors of all mentioned pathway components. Here, we describe events downstream of Cek1 activity that help to upregulate and eventually downregulate the transcriptional output of rescue signaling.

The transcription factor Ace2 has multiple functions in cell separation (Wang *et al.*, 2009), biofilm formation (Stichternoth and Ernst, 2009; Nobile *et al.*, 2012) and hyphal morphogenesis (Kelly *et al.*, 2004; Mulhern *et al.*, 2006; Saputo *et al.*, 2014; Desai *et al.*, 2015) and is known to function in a co-regulated transcriptional hub with the Efg1, Brg1 and Bcr1 transcription factors (Wang *et al.*, 2009; Saputo *et al.*, 2014; Desai *et al.*, 2015). Ace2 also has an important role in glycostructure signaling, since *ace2* mutants show the same inhibitor sensitivities as mutants lacking any of the above-mentioned components of the Cek1 pathway (Cantero and Ernst, 2011). Here we have shown that *ace2 cst20* double mutants show no synthetic defective phenotype compared to single mutants and that *ACE2* induction by

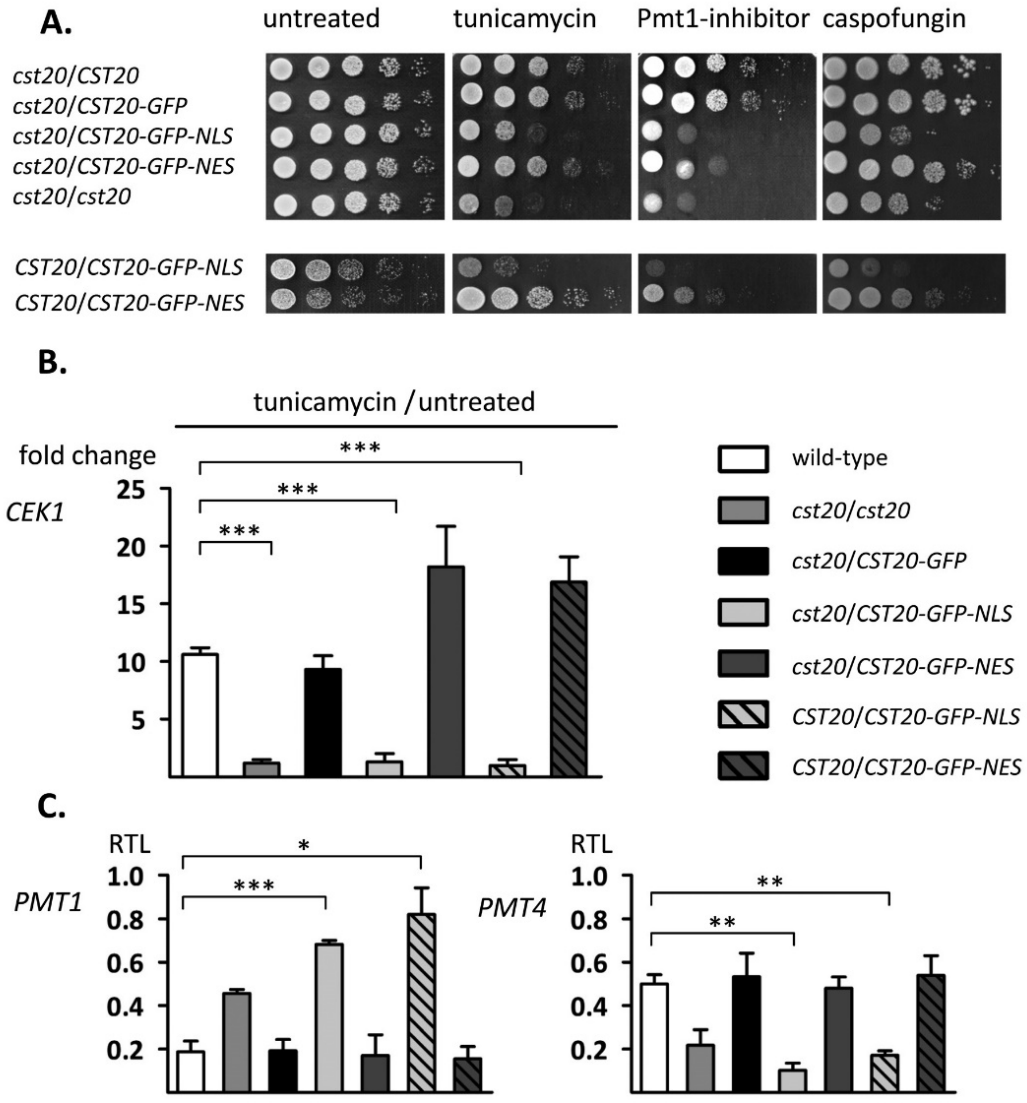

Fig. 7. Dual function of Cst20 for glycostress signaling.
A. Sensitivity phenotypes of strains expressing Cst20-GFP variants containing NES and NLS sequences under glycostress conditions. Chromosomal *CST20* in strains CLvW208 (*cst20/CST20*) and SC5314 (wild-type) was modified with GFP, GFP^{NLS} and GFP^{NES}. The strains were precultured in YPD medium and respective phenotypes were examined by spot dilution test on SCAA agar plates supplemented with either caspofungin (50 ng/ml), tunicamycin (2 μg/ml) or the Pmt1-inhibitor (4 μM).
B. Transcriptional regulation of *CEK1*.
C. *PMT* genes in strains expressing Cst20-GFP variants containing NES and NLS sequences. The indicated strains were grown in YPD medium and used to inoculate 50 ml SCAA medium, either supplemented with (B) tunicamycin (1 μg/ml) or (C) left untreated. After 4 h incubation at 30°C cells were collected and total RNA was isolated. Relative transcript levels of *CEK1*, *PMT1* and *PMT4* were determined as described for Fig. 4. The relative transcript levels (RTL) of *CEK1* was used to calculate the $\log_2$ fold-change (tunicamycin/untreated). Each bar represents the mean of at least three independent biological replicates ± SEM.

tunicamycin requires Msb2, suggesting that Ace2 functions as a downstream component in a linear pathway of Cek1 signaling comprising Msb2, Cst20, Hst7 and Cek1 proteins. Corresponding to this notion, *ACE2* overexpression restored the sensitivity phenotypes of all mutants in the Cek1 pathway except in the *cek1* mutant, indicating that Ace2 activation requires phosphorylation by Cek1 and that an increase in Ace2 levels obviates the necessity for Ace2 activation by upstream components. Ace2 was found to contain 18 phosphorylated

residues (Willger *et al.*, 2015), which may be due to the action of Cek1 and other kinases, including Cst20 (discussed below). Previously, it was shown that *ACE2* overexpression is able to suppress the sensitivity phenotypes of the *pmt1* mutant (Cantero and Ernst, 2011), which probably is mediated by induced expression of *PMT2/PMT4* genes. In contrast, *ACE2* overexpression had no effect on *PMT1* expression, which instead was strongly increased by deletion of *ACE2* (Cantero and Ernst, 2011). The transcription factor Cph1 is a known downstream element of Cek1 signaling, which is required for hyphal morphogenesis under normoxic and hypoxic conditions (Liu *et al.*, 1994; Desai *et al.*, 2015). In contrast, we have shown here that Cph1 is not required for glycostress signaling leading to *PMT1* upregulation but merely functions to downregulate *CEK1* transcript level under non-stressed conditions. On the other hand, the activity of the Cek1 pathway is likely to get adjusted by other signaling pathways, as in the case of the homologous filamentous growth pathway in *S. cerevisiae* (Borneman *et al.*, 2006; Chavel *et al.*, 2010; Chavel *et al.*, 2014).

Putative Ace2 target genes have previously been identified in unstressed cells by determination of genomic Ace2 binding sites (Desai *et al.*, 2015). Most target genes were identical under non-stressed and tunicamycin stress, as described here, although for some genes (e.g. *MSB2*), different promoter binding sites suggesting different transcription initiation sites were found in both conditions. Surprisingly, genes encoding proteins of the Cek1 pathway including *MSB2*, *CST20*, *HST7* and *ACE2* were identified among Ace2 targets suggesting feedback regulation by Ace2 on transcription of these genes. This concept was verified by showing for each pathway gene a strongly increased transcript level upon tunicamycin treatment, which did not occur in the absence of Ace2. Likewise, an *ACE2* promoter fusion to a reporter gene was upregulated by tunicamycin indicating enhanced transcriptional initiation as the underlying mechanism. These results are indicative of positive transcriptional feedback loops of Ace2 on most upstream components of the Cek1 pathway. In a similar manner, the cell wall integrity pathway of the apathogenic yeast *S. cerevisiae* appears regulated, since a positive feedback by the Rlm1 transcription factor on its encoding gene and on that for the upstream Slt2 MAPK was reported recently (García *et al.*, 2016). Positive feedback regulation is expected to strongly boost the activity of MAPK pathways by increasing levels of the respective pathway components.

Genomic targets of Ace2 included genes encoding various components involved in stress responses and glycosylation, but surprisingly not the genes encoding the major Pmt isoforms Pmt1, Pmt2 or Pmt4. Only the promoter of *PMT6* encoding a minor but relevant Pmt isoform (Timpel *et al.*, 2000; Rouabhia *et al.*, 2005) was bound by Ace2. This result suggested that the major *PMT* genes are not regulated directly by Ace2, but by one or more yet unknown transcription factors. Among Ace2 genomic targets, *ZCF21* encoding a transcription factor relevant for mouse kidney colonization and commensalism (Pérez and Johnson, 2013) was identified as a likely downstream target of Ace2. In the absence of inhibitors, Ace2 upregulates *ZCF21* expression, which in turn downregulates *PMT1* expression (but not *PMT4* expression). This regulatory pattern explains, why cells lacking Ace2, Zcf21 or both proteins strongly upregulate *PMT1*, while overexpression of *ZCF21*, but not overexpression of *ACE2*, downregulates this gene. It has been reported previously that a *pmt1 pmt4* double mutant is not viable (Prill *et al.*, 2005); the supersensitive phenotype of a *pmt4* mutant overexpressing *ZCF21* described here fully agrees with the specific repressive action of Zcf21 on *PMT1* expression. In agreement, the Zcf21 transcription factor was found to primarily function as a repressor of its target genes (Böhm *et al.*, 2016).

The activity of signaling pathways is typically transient, partly because its output activities abolish the need for continued signaling; in other cases, downregulation of signaling is initiated by activity of the signaling pathway itself (Molina *et al.*, 2010). The *C. albicans* Cek1 pathway realizes the latter pattern in a unique mechanism: during pathway activation and its Ace2-mediated amplification, the upstream Cst20 MAPKKK is increasingly imported into the nucleus, where it interacts with Ace2 and blocks its functions. Hereby, feedback upregulation of *CEK1* and probably other pathway genes is removed and the activity of the pathway decreases. During this pathway downregulation, *PMT1* expression is upheld at high levels, since Ace2 no longer induces production of the Zcf21 repressor; thus, compensating activities to tunicamycin stress are maintained. Strong supportive evidence for these events was obtained by directing Cst20 to either cytoplasm or nucleus by added NES or NLS sequences respectively. While NES fusions did not influence *PMT* expression and basal resistance to glycostress consistent with pathway activation, the NLS fusion turned out to strongly inhibit signaling and lead to supersensitive cells. Remarkably, Cst20-NLS even generated a dominant-negative phenotype in the presence of native Cst20 suggesting an effective block of Ace2 function and thereby, downregulation of Cek1 signaling. Consistent with these findings, an added nuclear function of Cst20 homologs has been reported for Ste20 in *S. cerevisiae* (Ahn *et al.*, 2005) and MST in mammalian cells (Lee and Yonehara, 2002). Furthermore, a fraction of kinases normally

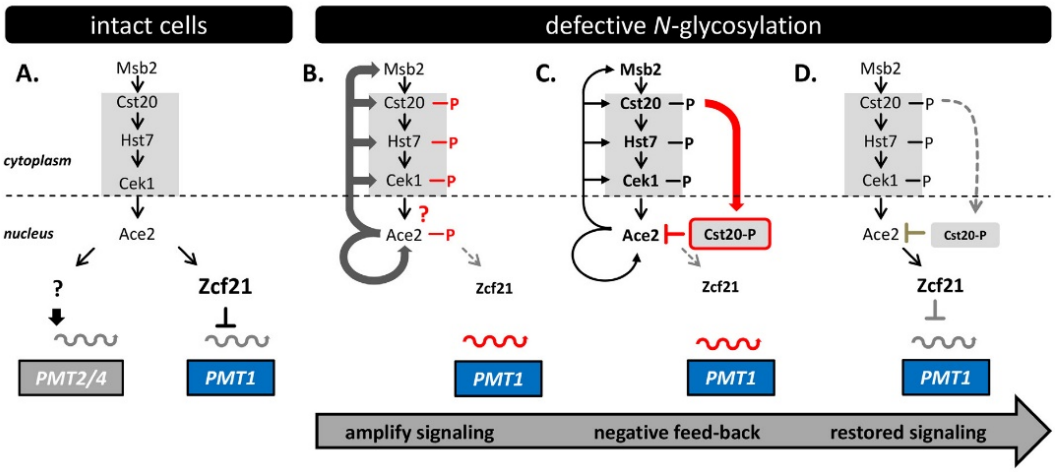

Fig. 8. Model for regulation of the Cek1 MAP kinase pathway under glycostress.
A. In intact cells, the Cek1 MAP kinase pathway and the transcription factor Ace2 ensure basal expression of genes encoding Pmt-isoforms Pmt1, Pmt2 and Pmt4. The Cek1-Ace2 pathway represses *PMT1* indirectly via the transcription factor Zcf21.
B. If damage of *N*-linked glycostructures occurs, e.g., in the presence of tunicamycin, the phosphorylation cascade is activated and stimulates phosphorylation of the Cek1 MAP kinase resulting in Ace2-Zcf21-mediated relief of *PMT1* repression. In a positive feed-back loop, Ace2 stimulates expression of genes encoding Cek1 pathway components and its own expression, enabling *C. albicans* to amplify Cek1-mediated signaling. Activation of Ace2 by Cek1 has not been proven experimentally and might involve other kinases.
C. During constant glycostress, components of the Cek1 pathway amass (bold characters) and the upstream MAPKKK Cst20 accumulates in the nucleus and inhibits the positive action of Ace2, thereby promoting downregulation of the Cek1 pathway; de-repressed *PMT1* expression is not affected and continues until glycostructures at the cell surface are completely restored.
D. Negative feed-back regulation limits the extent and duration of the signaling event and restores homeostasis, which is required to maintain sensitivity of the pathway, allowing *C. albicans* to quickly respond to new environmental cues. Expression of *PMT2* and *PMT4* is not regulated by defects in *N*-linked glycosylation but by defective Pmt1-*O*-mannosylation and involves an unknown downstream factor. Note that Ace2 also regulates metabolism and filamentous growth of *C. albicans* by alternative pathways in other environments (not shown in the figure).

acting in the cytoplasm also is present in the nucleus of *S. cerevisiae* and *C. albicans* cells, often in association with dedicated transcription factors, directly at their target genes (Pokholok *et al.*, 2006; Bharucha *et al.*, 2008; Schaekel *et al.*, 2013). Cst20 might mediate inhibition of Ace2 by phosphorylation or by physically blocking Ace2 from binding to its target genes. However, directing Cst20 to the nucleus did not completely inhibit Ace2 functions since cell division occurred normally in these cells, thus indicating target specificity for this inhibitory function. Moreover, it is not clear if Cst20 directly or indirectly phosphorylates Ace2 and if other kinases might also be involved in this complex process and contribute to Ace2 activity under glycostress. The discovery of numerous phosphorylated residues in Ace2 (Willger *et al.*, 2015) suggests that Ace2 phosphorylation reflects multiple environmental cues. Interestingly, alternative translational initiation has been shown recently to generate two Ace2 isoforms with different functions (Calderón-Noreña *et al.*, 2015). Our preliminary results suggest that the full length protein, encompassing a potential N-terminal transmembrane domain is required for glycostress signaling (L. v. Wijlick and J. F. Ernst, unpublished results).

The current working model describes activities of the Cek1 pathway, both in unstressed and glycostructure-stressed *C. albicans* cells (Fig. 8). In unstressed cells, all components of the Cek1 pathway including Ace2 are needed to repress expression of certain genes, as exemplified by *PMT1*. During unstressed growth, Cek1 levels and its degree of phosphorylation are low. In this situation, Ace2 phosphorylated at low basal levels induces *ZCF21* expression that encodes the most downstream identified component that is responsible for *PMT1* repression and upregulates *PMT2/PMT4* genes to basal expression levels. If glycostress occurs by damage of *N*- or *O*-glycosylation or glucan structures, the phosphorylation status of pathway components increases (Román *et al.*, 2009). In the subsequent wave of activation, highly activated/phosphorylated Ace2 triggers transcriptional upregulation of all genes for upstream components to further boost the activity of the pathway. In the case of defective *N*-glycosylation in the presence of tunicamycin, the highly phosphorylated form of Ace2 no longer promotes *ZCF21* expression; therefore, *PMT1* transcription is de-repressed. One possible de-repression mechanism may be 'squelching' of the Zcf21 repressor by surplus levels of Ace2 under glycostress (Cahill *et al.*, 1994).

Redirection of the transcriptional program under glycostress may also be mediated in parts by the cytoplasmic tail of the Msb2 sensor protein, which is directed to the nucleus in this condition (Swidergall *et al.*, 2015). In the case of defective *O*-glycosylation in the presence of the Pmt1-inhibitor, activated Ace2 boosts expression of *PMT2/PMT4* levels beyond basal levels. It thus appears that the type of glycostructure damage decides on the outcome of Ace2-mediated signaling by activating either *PMT1* or *PMT2/PMT4* expression. While Zcf21 appears to render Ace2-specificity for defective *N*-glycosylation, a corresponding specificity factor for defective *O*-glycosylation remains to become identified. Finally, downregulation of the Cek1 pathway activities can occur on the one hand, when its output processes have restored glycostructure defects, e.g. by fortifying the cell wall. In addition, an active downregulation mechanism can occur, characterized by nuclear accumulation of Cst20, which may occur especially following transcriptional amplification of the pathway. Nuclear Cst20 phosphorylates and inhibits Ace2, which prevents upregulation of pathway genes. However, it is yet unclear if this mechanism is specific for defective *N*-glycosylation and if it reflects a graded response to glycostructure damage or if it only occurs beyond a threshold of damage/pathway activation. Clearly, other regulatory inputs including the Efg1/Bcr1/Brg1 regulatory hub (Saputo *et al.*, 2014; Desai *et al.*, 2015) and its co-regulators, e.g. in the RAM and PKA pathways (Bharucha *et al.*, 2011; Saputo *et al.*, 2014; Desai *et al.*, 2015), may also contribute to Ace2 activity and glycostress responses.

Experimental procedures

Strains and media

C. albicans strains used are listed in Table 1. Strains were grown in liquid YPD (1% yeast extract, 2% peptone, 2% glucose) or SCAA (0.67% yeast nitrogen base, 2% casamino acids) medium. Semisolid media contained 2% agar. Medium used for spot dilution growth tests was supplemented with the indicated amounts of inhibitors.

Construction of cst20 mutant strains

To generate *cst20* mutant strains plasmid pSFS5 containing a modified *sat1* flipper cassette was used (Sasse *et al.*, 2011). Oligonucleotides used are listed in Supporting Information Table S2 and plasmids are listed in Supporting Information Table S3. The upstream and downstream region of the *CST20* ORF was amplified with oligonucleotide pairs F1/F2 and F3/F4 by PCR, using genomic DNA of strain SC5314 and cloned into the *Sac*I/*Sac*II and *Apa*I/*Xho*I sites of plasmid pSFS5, generating the outer-deletion cassette containing plasmid pCLvW100. Similarly, oligo pairs F5/F6 and F7/F8 were used to generate plasmid pCLvW101, containing the inner-deletion cassette. Enzymes *Apa*I and *Sac*I were used to release the respective cassette; the first *CST20* allel was deleted by subsequent transformation of the outer deletion cassette. Integration of the cassette was confirmed by colony PCR using oligonucleotides FLP1, binding within the FLP1 gene on the cassette and CST20-UTR5, binding upstream of the CST20 ORF. Transformants were grown in YCB-BSA medium (20 g yeast carbon base, 4 g bovine serum albumin, 2 g yeast extract per liter) to induce excision of the cassette by FLP-mediated recombination. 100 µl of the cells were spotted on YPD plates containing 25 µg/ml nourseothricin to identify strains that lost the resistance, by their small colony size. Following transformation with the inner deletion cassette, the second *CST20* allel was deleted. Deletion of *CST20* was confirmed by Southern blot analysis. This approach was used to construct heterozygous and homozygous *cst20* mutant strains in background strains SC5314, CAI4, the homozygous *ace2* mutant MK106 and in the heterozygous *ace2* mutant CLvW006.

Construction of ace2 mutant strains

For deletion of *ACE2*, plasmids pCLvW90 and pCLvW91 were used, described by Desai *et al.* (2015). Briefly, both plasmids contain deletion cassettes based on a modified *sat1* flipper cassette (Sasse *et al.*, 2011) flanked with *ACE2* upstream and downstream sequences, resulting in an inner- and outer-deletion cassette. Digestion with *Sac*I and *Apa*I releases the cassettes, respectively; sequential transformation of the outer cassette, eviction of the cassette by activation of the *FLP1* gene, followed by transformation of the inner cassette was used to delete both copies of *ACE2* in strains zcf21 (*zcf21/zcf21*), resulting in strain CLvW131. For epitope-tagging of Ace2 one *ACE2* allele was disrupted in strains CAI4 resulting in the heterozygous *ace2* mutant strains CLvW006 (*ace2/ACE2*). Integration and excision of the cassette was confirmed by colony PCR and Southern blot analysis.

C. albicans *strains overproducing* ACE2 *and* ZCF21

To generate vectors allowing overexpression of *ACE2* or *ZCF21*, the coding region of both genes was amplified by genomic PCR using oligonucleotide pair ACE2-BglII rev/for, adding *Bgl*II sites to the end of the *ACE2* encoding sequence and oligonucleotide pair ZCF21-BglII rev/for, adding *Bgl*II sites to the terminal end of the *ZCF21* encoding sequence. Respectively, both fragments were cut with *Bgl*II and ligated downstream of the *PCK1* promoter in plasmid pBI-1 (Stoldt *et al.*, 1997), referred as pBI-URA3. Resulting plasmids were named pPCK1p-ACE2-URA3 and pPCK1p-ZCF21-URA3. In addition, plasmid pBI-1 was modified to allow selection in prototrophic strains. Therefore the *sat1* encoding gene, flanked with *ACT1* promoter and *ACT1* terminator sequences was PCR amplified (*ACT1p-sat1-ACT1t*) with oligonucleotides SAT1-PstI-rev/for and ligated into the *Pst*I linearized vector pBI-1 to generate plasmid pBI-SAT1. *Bgl*II fragments containing sequences of *ACE2* and *ZCF21* were ligated into plasmid pBI-SAT1 generating

Table 1. *C. albicans* strains.

Strain	Genotype or description	Source
SC5314	wild-type	Fonzi and Irwin, 1993
CAI4	as SC5314, but *ura3Δ::imm434/ura3Δ::imm434*	Fonzi and Irwin, 1993
CAF2-1	as SC5314, but *ura3Δ::imm434/URA3*	Fonzi and Irwin, 1993
BWP17	*ura3Δ::imm434/ura3Δ::imm434, his1Δ::hisG/his1Δ::hisG arg4Δ::hisG/arg4Δ::hisG*	Wilson *et al.*, 1999
MK106	as SC5314, but *ace2Δ::FRT/ace2Δ::FRT*	Kelly *et al.*, 2004
CLvW001	as BWP17, but *ace2Δ::lacZ-SAT1/ACE2*	Desai *et al.*, 2015
CLvW004	as CLvW001, but *ace2Δ::SAT1/ACE2^{HA}::URA3*	Desai *et al.*, 2015
CLvW006	as CAI4, but *ace2Δ::FRT/ACE2*	Desai *et al.*, 2015
CLvW008	as CLvW006, but *ace2Δ::FRT/ace2Δ::FRT*	Desai *et al.*, 2015
CLvW188	as CLvW008, but *LEU2/LEU2*::pPCKp-ACE2-URA3(*PCK1p-ACE2*)	this work
CLvW189	as CLvW008, but *LEU2/LEU2*::pBI-1 (empty vector)	this work
CLvW190	as CAI4, but *LEU2/LEU2*::pPCKp-ACE2-URA3(*PCK1p-ACE2*)	this work
CLvW191	as CAI4, but *LEU2/LEU2*::pBI-1 (empty vector)	this work
CAP1-3121	as CAI4, but *pmt1Δ::hisG/pmt1Δ::hisG*	Timpel *et al.*, 1998
CLvW192	as CAP1-3121, but *LEU2/LEU2*::pPCKp-ACE2-URA3(*PCK1p-ACE2*)	this work
CLvW193	as CAP1-3121, but *LEU2/LEU2*::pBI-1 (empty vector)	this work
FCCa28	as CAI4, but *msb2Δ::hisG/msb2Δ::hisG*	Szafranski *et al.*, 2012
CLvW194	as FCCa28, but *LEU2/LEU2*::pPCKp-ACE2-URA3(*PCK1p-ACE2*)	this work
CLvW195	as FCCa28, but *LEU2/LEU2*::pBI-1 (empty vector)	this work
CK43B-16L	as CAI4, but *cek1Δ::hisG/cek1Δ::hisG*	Csank *et al.*, 1998
CLvW196	as CK43B-16L, but *LEU2/LEU2*::pPCKp-ACE2-URA3(*PCK1p-ACE2*)	this work
CLvW197	as CK43B-16L, but *LEU2/LEU2*::pBI-1 (empty vector)	this work
hst7	as BWP17, but *hst7Δ::UAU1/hst7Δ::URA3*	Blankenship *et al.*, 2010
CLvW198	as hst7, but *LEU2/LEU2*::pPCKp-ACE2-SAT1(*PCK1p-ACE2-SAT1*)	this work
CLvW199	as hst7, but *LEU2/LEU2*::pBI-SAT1 (empty vector)	this work
zcf21	*arg4Δ/arg4Δ leu2Δ/leu2Δ his1Δ/his1Δ zcf21Δ::HIS1/zcf21Δ::LEU2*	Homann *et al.*, 2009
CLvW131	as zcf21, but *ace2Δ::FRT/ace2Δ::FRT*	this work
CLvW200	as CLvW131, but *LEU2/LEU2*::pPCKp-ACE2-SAT1(*PCK1p-ACE2-SAT1*)	this work
CLvW201	as CLvW131, but *LEU2/LEU2*::pPCKp-ZCF21-SAT1(*PCK1p-ZCF21-SAT1*)	this work
CLvW202	as CLvW131, but *LEU2/LEU2*::pBI-SAT1 (empty vector)	this work
PP46-4285	as CAI4, but *pmt4Δ::hisG/pmt4Δ::hisG*	this work
CLvW203	as PP46-4285, but *LEU2/LEU2*::pPCKp-ACE2-URA3(*PCK1p-ACE2-URA3*)	this work
CLvW204	as PP46-4285, but *LEU2/LEU2*::pPCKp-ZCF21-URA3(*PCK1p-ZCF21-URA3*)	this work
CLvW205	as PP46-4285, but *LEU2/LEU2*::pBI-1(empty vector)	this work
CLvW206	as CAI4, but *cst20Δ::FRT/CST20*	this work
CLvW207	as CLvW206, but *cst20Δ::FRT/cst20Δ::FRT*	this work
CLvW208	as SC5314, but *cst20Δ::FRT/CST20*	this work
CLvW209	as CLvW208, but *cst20Δ::FRT/cst20Δ::FRT*	this work
CLvW210	as MK106, but *cst20Δ::FRT/CST20*	this work
CLvW211	as CLvW210, but *cst20Δ::FRT/cst20Δ::FRT*	this work
CLvW213	as CLvW006, but *cst20Δ::FRT/CST20*	this work
CLvW214	as CLvW213, but *cst20Δ::FRT/cst20Δ::FRT*	this work
CLvW215	as CLvW214, but *ace2Δ::FRT/ACE2^{HA}::URA3*	this work
CLvW216	as CLvW213, but *ace2Δ::FRT/ACE2^{HA}::URA3; cst20Δ::FRT/CST20^{V5}::SAT1*	this work
CLvW217	as CLvW006, but *ace2Δ::FRT/ACE2^{HA}::URA3*	this work
CLvW218	as CLvW208, but *cst20Δ::FRT/CST20^{GFP}::SAT1*	this work
CLvW219	as SC5314, but *CST20/CST20^{GFP}::SAT1*	this work
CLvW220	as CLvW208, but *cst20Δ::FRT/CST20$^{GFP-NLS}$::SAT1*	this work
CLvW221	as SC5314, but *CST20/CST20$^{GFP-NLS}$::SAT1*	this work
CLvW222	as CLvW208, but *cst20Δ::FRT/CST20$^{GFP-NES}$::SAT1*	this work
CLvW223	as SC5314, but *CST20/CST20$^{GFP-NES}$::SAT1*	this work
CLvW224	as CLvW209, but *LEU2/LEU2*::pPCKp-ACE2-SAT1(*PCK1p-ACE2-SAT1*)	this work
CLvW225	as CLvW209, but *LEU2/LEU2*::pBI-SAT1(empty vector)	this work
CLvW226	as CAI4, but *MSB2/MSB2*::pES11a (*HpaI-MSB2^{HA}-URA3-HpaI*)	this work
CLvW227	as CLvW008, but *MSB2/MSB2*::pES11a (*HpaI-MSB2^{HA}-URA3-HpaI*)	this work
CLvW228	as CLvW006, but *ace2Δ::FRT/ACE2^{GFP}::URA3*	this work
JKC19	as CAI4, but *cph1Δ::/cph1Δ::URA3*	Liu *et al.*, 1994

plasmids pPCK1p-ACE2-SAT1 and pPCK1p-ZCF21-SAT1. Enzymes *Bst*EII or *Eco*RV were used for linearization of the plasmids to allow integration into the *LEU2* locus of the respective transformed strains (Table 1). Integration was verified by colony PCR using oligonucleotides Colo-LEU2-rev and Colo-AMP-for.

C. albicans *strains producing HA-tagged Ace2 and V5-tagged Cst20*

For co-immunoprecipitation a strain expressing hemagglutinin-epitope (HA) modified Ace2 and V5-epitope modified Cst20 was constructed. For c-terminal tagging of Cst20, plasmid

pFC-V5 (Ullmann *et al.*, unpublished) was used as template for PCR amplification of *V5-sat1* sequences using oligonucleotide pair CST20 V5 for/rev. The oligonucleotides added homologous sequences of the 3'-end and sequences of the 3'-UTR of the *CST20* allele to the amplified sequence, allowing recombination mediated chromosomal integration. Similarly, for c-terminal modification of Ace2, oligonucleotide pair ACE2HAFor and ACE2HARev was used to amplify the triple HA-encoding sequence from plasmid p3HA-URA3 (Prill *et al.*, 2005). The fragments were transformed into the heterozygous *ace2 cst20* mutant strain CLvW213 to generate strain CLvW216, producing HA-tagged Ace2 and V5-tagged Cst20. Chromosomal integration of both fragments was confirmed by Southern blot analysis.

C. albicans *strains producing Cst20- and Ace2-GFP fusions*

For localization studies of the Cst20 protein, strains expressing the Cst20-GFP fusion protein were constructed. The plasmid pNIM1R-GFP (Prieto *et al.*, 2014) was used as template to PCR amplify the *GFP* and *sat1* encoding region. The oligonucleotide pair CST20 GFP rev/for added homologous sequences of the 3'-end and sequences of the 3'-UTR of the *CST20* allele to the amplified sequence, allowing c-terminal tagging of Cst20. In order to modify GFP with either a NLS or NES sequence, oligonucleotide GFP NotIXhoI rev was combined with oligo GFP NLS BglII for or GFP NES BglII for, respectively and used to amplify the GFP encoding sequence from plasmid pNIM1R-GFP. The oligo GFP NLS BglII for contains the sequence of the SV40 large T-antigen NLS sequence and the oligo GFP NES BglII for contains the sequence of the PKI NES sequence, thereby adding the sequence to the 3'-end of the amplicon. The fragments were cut with enzymes *Bgl*II and *Xho*I and ligated into the *Bgl*II and *Sal*I cut plasmid pNIM1R-GFP, replacing the unmodified *GFP* sequence. In addition, the *Sal*I site was exchanged for a *Not*I site, resulting in plasmids pGFP-NLS-SAT1 and pGFP-NES-SAT1. The plasmids were used as template with oligonucleotide pair CST20 GFP rev/for to PCR amplify the respective *GFP* modified sequence and *sat1* encoding region. The fragments were transformed into strains SC5314, generating strains CLvW219, CLvW221 and CLvW223 and in the heterozygous *cst20* mutant strain CLvW208, generating strains CLvW218, CLvW220 and CLvW222.

For localization of the Ace2 protein during glycostress conditions, strains producing Ace2-GFP were constructed. The oligonucleotide pair ACE2 GFP rev/for was used to amplify the GFP encoding sequence from plasmid pGFP-URA3 (Gerami-Nejad *et al.*, 2001) and for addition of homologous *ACE2* sequences of the 3'-end of the *ACE2* allele to allow c-terminal tagging of Ace2. The fragment was transformed into the heterozygous *ace2* mutant strain CLvW006, generating strain CLvW228. Colony-PCR was used to verify correct integration.

Yeast two hybrid

To identify potential interaction partners of Ace2, the classical yeast two-hybrid system was used (James *et al.*, 1996). The genomic sequence encoding *ACE2* was amplified by PCR with oligos ACE2-BglI for/rev, adding *Bgl*II restriction sites to the terminal end of the fragment. The *Bgl*II fragment was ligated into the bait vector pGBD, generating plasmid pBD-ACE2 and into the Gal4 activating domain containing vector pGAD, generating plasmid pAD-ACE2. Both plasmids were transformed into *S. cerevisiae* strain PJ69-4A (James *et al.*, 1996) to test dimerisation of Ace2. To exclude auto-activation, plasmids pBD-ACE2 and the empty vector pGAD were transformed. Both plasmid combinations did not result in any positive transformants, indicating that Ace2 is not forming dimers and the binding domain-Ace2 fusion protein is not self-activating expression of reporter genes tested. To screen for potential interaction partners a plasmid encoded random genomic library fused to the Gal4 activation domain was used. Genomic DNA fragments of *C. albicans* strain CAI4 were generated by digestion of genomic DNA with enzymes *Taq*I, *Mae*II, *Hin*1I, *Aci*I and *Msp*I and ligated into plasmids pGAD-C1, -C2 and -C3 generating three genomic library plasmid pools, pDYC-C1, -C2 and -C3 (Timpel C., Weber I. and Ernst JF., unpublished). Each plasmid pool, pDYC-C1 to C3 was transformed into *S. cerevisiae* strain PJ69-4A, in combination with plasmid pBD-ACE2. Positive transformants were selected by adenine prototrophic growth and ß-galactosidase (LacZ) activity (James *et al.*, 1996). Plasmid inserts encoding potential interactors of Ace2 were sequenced and identified by BLAST analyses in the Candida Genome Database (http://www.candidagenome.org).

Immunoprecipitation

For detection of Ace2-HA exponential cultures were grown for 4h in 50 ml YPD containing tunicamycin (1 µl/ml) or left untreated. Cells were harvested and washed with ice cold TBS. For co-immunoprecipitation cells were fixed with formaldehyde (1%) for 60 min at 30°C; cells were quenched with glycine (125 mM) for 10 min and washed with ice cold TBS. Lysis buffer (50 mM HEPES-KOH pH 7.5, 140 mM NaCl, 1 mM EDTA, 1% Triton-X-100, 0.1% Na-deoxycholate; Complete protease inhibitor EDTA-free, Roche) and glass beads were added and cells were disrupted using 5 runs at 6.5 m/s for 1 min in a Fastprep 24 (MP Biomedicals) with 5 min incubation on ice between. Lysates were centrifuged for 1 min at 13,000 rpm at 4°C to remove cell debris and glass beads. 300 µl of the crude cell extract were incubated over night with 30 µl of EZview™ Red Anti-HA Affinity Gel (Sigma Aldrich) at 4°C on a rotator. Samples were collected by centrifugation and washed three times with lysis buffer. After addition of 6x SDS sample buffer and heating at 95°C for 10 min, eluted proteins were separated by SDS-PAGE using 12% or 4-20% acrlyamide gels (Pierce) and transferred to a PVDF membrane or stained with Coomassie-Blue (Bio-Rad). Transferred proteins were analyzed with the following antibodies: Anti-HA High Affinity (rat monoclonal, 1:5000, Roche), followed by treatment with horseradish peroxidise-labelled secondary antibody Goat Anti rat (1:10,000, Thermo Scientific); Anti-V5 (mouse monoclonal, 1:2500, AbD Serotec), followed by Goat Anti mouse Poly-HRP

(1:10,000, Pierce) antibodies. Signals were detected with an ImageQuant LAS 400 mini imager (GE Healthcare).

Chromatin immunoprecipitation on microarray (ChIP on chip)

To detect chromosomal binding regions of Ace2-HA the ChIP chip procedure was performed as described previously by Lassak *et al.* (2011). Strain CLvW004, producing HA-tagged Ace2 and strain BWP17, producing unmodified Ace2 were precultured in YPD medium and used to inoculate 100 ml YPD medium. To block *N*-glycosylation the medium was supplemented with tunicamycin (0.5 μg/ml). Three independent cultures of each strain were allowed to grow for 4 h at 30°C. Genomic localization of Ace2-HA was determined using anti-HA antibody for immunoprecipitation. Significant genomic binding sites of Ace2-HA were defined as probes containing four or more signals above the background in a 500 bp sliding window. The degree of significance was thereby dependent on the false discovery rate. For evaluation and visualization of the micro-array reads, the program SignalMap (1.9) was used. Only the most significant peaks (FDR $\leq$ 0.05) overlapping in at least two replicates were defined as Ace2-HA binding region. In an identical approach we determined genomic localization of Ace2-HA without block of N-glycosylation, referred as untreated, published in Desai *et al.* (2015).

ChIP-qPCR

To verify binding regions of Ace2-HA obtained by ChIP chip experiments chromatin immunoprecipitation followed by quantitave PCR (qPCR) was performed with site specific oligonucleotides specified in Supporting Information Table S2. Chromatin of strains was immunoprecipited as described above (ChIP on chip). The qPCR was performed in a Mx3000P instrument (Stratagene) using EvaGreen QPCR-MIX II (Bio-Budget) and 400 pmol/μl forward and reverse oligonucleotide primer each. The Taq-Polymerase was activated for 10 min at 95°C. Following denaturation, steps were repeated at 95°C for 30 s, annealing was performed at 60°C for 20 s and elongation at 72°C for 30 s. After 40 cycles a dissociation curve was performed to detect product specificity. A standard curve was used to determine the oligonucleotide primer efficiency. The qPCR experiments were done using two or three biological replicates, which were assayed in triplicate. The mean fold enrichment for Ace2-HA was calculated relative to the respective no-tag control (chromatin precipitated of strain BWP17) and normalized to the input sample, taking the oligonucleotide efficiency into consideration.

Fluorescence microscopy

Strains producing Ace2-GFP, Cst20-GFP or GFP containing NES and NLS modifications were precultured in SCAA medium and used to inoculate fresh SCAA medium and allowed to grow in darkness for 4 h (OD_{600} = 0.4-0.5). Cells were washed twice with PBS and DAPI (diamidino-2-phenylindole; 1 μg/ml) was added for nuclear staining. Following 20 min incubation at room temperature, cell samples were again washed twice with PBS and 20 μl were fixed to polylysine-coated glass slides. For inspection of GFP and DAPI fluorescence the Axioskop 40 (Zeiss) microscope was used. ImageJ software (http://imagej.nih.gov/ij/) was used for evaluation of images.

Acknowledgements

We thank A. D. Johnson for sending the *zcf21* mutant strain and J. Pla and E. Roman for sharing vectors pNIM1R-GFP. This project was supported by the Jürgen Manchot Stiftung Düsseldorf and the Deutsche Forschungsgemeinschaft (ER47/13-1).

Author contributions

LvW and JFE designed the study; LvW, MS and PB acquired the data; LvW and JFE analysed and interpreted the data; LvW and JFE wrote the manuscript.

References

Ahn, S.H., Cheung, W.L., Hsu, J.Y., Diaz, R.L., Smith, M.M., and Allis, C.D. (2005) Sterile 20 kinase phosphorylates histone H2B at serine 10 during hydrogen peroxide-induced apoptosis in *S. cerevisiae*. *Cell* **120**: 25–36.

Arroyo, J., Hutzler, J., Bermejo, C., Ragni, E., García-Cantalejo, J., Botías, P., *et al.* (2011) Functional and genomic analyses of blocked protein *O*-mannosylation in baker's yeast. *Mol Microbiol* **79**: 1529–1546.

Bates, S., Hall, R.A., Cheetham, J., Netea, M.G., MacCallum, D.M., Brown, A.J., *et al.* (2013) Role of the *Candida albicans MNN1* gene family in cell wall structure and virulence. *BMC Res Notes* **6**: 294.

Bharucha, N., Chabrier-Rosello, Y., Xu, T., Johnson, C., Sobczynski, S., Song, Q., *et al.* (2008) Analysis of the yeast kinome reveals a network of regulated protein localization during filamentous growth. *Mol Biol Cell* **19**: 2708–2717.

Bharucha, N., Chabrier-Rosello, Y., Johnson, C., Sobczynski, S., Song, Q., *et al.* (2011) A large-scale complex haploinsufficiency-based genetic interaction screen in *Candida albicans*: analysis of the RAM network during morphogenesis. *PLoS Genet* **7**: e1002058.

Blankenship, J.R., Fanning, S., Hamaker, J.J., and Mitchell, A.P. (2010) An extensive circuitry for cell wall regulation in *Candida albicans*. *PLoS Pathog* **6**: e1000752.

Böhm, L., Muralidhara, P., and Pérez, J.C. (2016) A *Candida albicans* regulator of disseminated infection operates primarily as a repressor and governs cell surface remodeling. *Mol Micrbiol* **100**: 328–344.

Borneman, A.R., Leigh-Bell, J.A., Yu, H., Bertone, P., Gerstein, M., and Snyder, M. (2006) Target hub proteins serve as master regulators of development in yeast. *Genes Dev* **20**: 435–448.

Cahill, M.A., Ernst, W.H., Janknecht, R., and Nordheim, A. (1994) Regulatory squelching. *FEBS Lett* **344**: 105–108.

Calderón-Noreña, D.M., González-Novo, A., Orellana-Muñoz, S., Gutiérrez-Escribano, P., Arnáiz-Pita, Y., Dueñas-Santero, E., *et al.* (2015) A single nucleotide polymorphism uncovers a novel function for the transcription factor Ace2 during *Candida albicans* hyphal development. *PLoS Genet* **11**: e1005152.

Calera, J.A., Herman, D., and Calderone, R. (2000) Identification of YPD1, a gene of *Candida albicans* which encodes a two-component phosphohistidine intermediate protein. *Yeast* **16**: 1053–1059.

Cantero, P.D., and Ernst, J.F. (2011) Damage to the glycoshield activates PMT-directed O-mannosylation via the Msb2-Cek1 pathway in *Candida albicans*. *Mol Microbiol* **80**: 715–725.

Cantero, P.D., Lengsfeld, C., Prill, S.K.H., Subanović, M., Román, E., and Ernst, J.F. (2007) Transcriptional and physiological adaptation to defective protein-*O*-mannosylation in *Candida albicans*. *Mol Microbiol* **64**: 1115–1128.

Chaffin, W.L. (2008) *Candida albicans* cell wall proteins. *Microbiol Mol Biol Rev* **72**: 495–544.

Chandra, J., Kuhn, D.M., Mukherjee, P.K., Hoyer, L.L., McCormick, T., and Ghannoum, M.A. (2001) Biofilm formation by the fungal pathogen *Candida albicans*: development, architecture, and drug resistance. *J Bacteriol* **183**: 5385–5394.

Chavan, M., Rekowicz, M., and Lennarz, W. (2003) Insight into functional aspects of Stt3p, a subunit of the oligosaccharyl transferase. Evidence for interaction of the N-terminal domain of Stt3p with the protein kinase C cascade. *J Biol Chem* **278**: 51441–51447.

Chavel, C.A., Caccamise, L.M., Li, B., and Cullen, P.J. (2014) Global regulation of a differentiation MAPK pathway in yeast. *Genetics* **198**: 1309–1328.

Chavel, C.A., Dionne, H.M., Birkaya, B., Joshi, J., and Cullen, P.J. (2010) Multiple signals converge on a differentiation MAPK pathway. *PLoS Genet* **6**: e1000883.

Csank, C., Schröppel, K., Leberer, E., Harcus, D., Mohamed, O., Meloche, S., *et al.* (1998) Roles of the Candida albicans mitogen-activated protein kinase homolog, Cek1p, in hyphal development and systemic candidiasis. *Infect Immun* **66**: 2713–2721.

Cullen, P.J., Schultz, J., Horecka, J., Stevenson, B.J., Jigami, Y., and Sprague, G.F. Jr. (2000) Defects in protein glycosylation cause SHO1-dependent activation of a STE12 signaling pathway in yeast. *Genetics* **155**: 1005–1018.

de Groot, P.W., de Boer, A.D., Cunningham, J., Dekker, H.L., de Jong, L., Hellingwerf, K.J., *et al.* (2004) Proteomic analysis of *Candida albicans* cell walls reveals covalently bound carbohydrate-active enzymes and adhesins. *Eukaryot Cell* **3**: 955–965.

Desai, P.R., van Wijlick, L., Kurtz, D., Juchimiuk, M., and Ernst, J.F. (2015) Hypoxia and Temperature Regulated Morphogenesis in *Candida albicans*. *PLoS Genet* **11**: e1005447.

Ernst, J.F., and Pla, J. (2011) Signaling the glycoshield: Maintenance of the *Candida albicans* cell wall. *Int J Med Microbiol* **301**: 378–383.

Fonzi, W.A., and Irwin, M.Y. (1993) Isogenic strain construction and gene mapping in *Candida albicans*. *Genetics* **134**: 717–728.

García, R., Sanz, A.B., Rodríguez-Peña, J.M., Nombela, C., and Arroyo, J. (2016) Rlm1 mediates positive autoregulatory transcriptional feedback that is essential for Slt2-dependent gene expression. *J Cell Sci* **129**: 1649–1660.

Gerami-Nejad, M., Berman, J., and Gale, C.A. (2001) Cassettes for PCR-mediated construction of green, yellow, and cyan fluorescent protein fusions in *Candida albicans*. *Yeast* **9**: 859–864.

Gow, N.A., and Hube, B. (2012) Importance of the *Candida albicans* cell wall during commensalism and infection. *Curr Opin Microbiol* **15**: 406–412.

Hahn, S., Maurer, P., Caesar, S., and Schlenstedt, G. (2008) Classical NLS Proteins from *Saccharomyces cerevisiae*. *J Mol Biol* **379**: 678–694.

Heilmann, C.J., Sorgo, A.G., Siliakus, A.R., Dekker, H.L., Brul, S., de Koster, C.G., *et al.* (2011) Hyphal induction in the human fungal pathogen *Candida albicans* reveals a characteristic wall protein profile. *Microbiology* **157**: 2297–2307.

Homann, O.R., Dea, J., Noble, S.M., and Johnson, A.D. (2009) A phenotypic profile of the *Candida albicans* regulatory network. *PLoS Genet* **12**: e1000783.

Huffaker, T.C., and Robbins, P.W. (1983) Yeast mutants deficient in protein glycosylation. *Proc Natl Acad Sci* **80**: 7466–7470.

James, P., Halladay, J., and Craig, E.A. (1996) Genomic libraries and a host strain designed for highly efficient two-hybrid selection in yeast. *Genetics* **144**: 1425–1436.

Kalderon, D., Roberts, B.L., Richardson, W.D., and Smith, A.E. (1984) A short amino acid sequence able to specify nuclear location. *Cell* **39**: 499–509.

Kelly, M., MacCallum, D.M., Clancy, S.D., Odds, F.C., Brown, A.J., and Butler, G. (2004) The *Candida albicans CaACE2* gene affects morphogenesis adherence and virulence. *Mol Microbiol* **53**: 969–983.

Kurischko, C., Weiss, G., Ottey, M., and Luca, F.C. (2005) A role for the *Saccharomyces cerevisiae* regulation of Ace2 and polarized morphogenesis signaling network in cell integrity. *Genetics* **171**: 443–455.

Lassak, T., Schneider, E., Bussmann, M., Kurtz, D., Manak, J.R., Srikantha, T., *et al.* (2011) Target specificity of the *Candida albicans* Efg1 regulator. *Mol Microbiol* **82**: 602–618.

Lee, K.K., and Yonehara, S. (2002) Phosphorylation and dimerization regulate nucleocytoplasmic shuttling of mammalian STE20-like kinase (MST). *J Biol Chem* **277**: 12351–12358.

Lengeler, K., Tielker, D., and Ernst, J.F. (2008) Protein-*O*-mannosyltransferases in virulence and development. *Cell Mol Life Sci* **65**: 528–544.

Levin, D.E. (2011) Regulation of cell wall biogenesis in *Saccharomyces cerevisiae*: the cell wall integrity signaling pathway. *Genetics* **189**: 1145–1175.

Liu, H., Köhler, J., and Fink, G.R. (1994) Suppression of hyphal formation in *Candida albicans* by mutation of a *STE12* homolog. *Science* **266**: 1723–1726.

Luo, G., Ibrahim, A.S., Spellberg, B., Nobile, C.J., Mitchell, A.P., and Fu, Y. (2010) *Candida albicans* Hyr1p confers resistance to neutrophil killing and is a potential vaccine target. *J Infect Dis* **201**: 1718–1728.

Maiti, P., Ghorai, P., Ghosh, S., Kamthan, M., Tyagi, R.K., and Datta, A. (2015) Mapping of functional domains and characterization of the transcription factor Cph1 that mediate morphogenesis in *Candida albicans*. *Fungal Genet Biol* **83**: 45–57.

Miller, M.E., and Cross, R. (2000) Distinct Subcellular Localization Patterns Contribute to Functional Specificity of the Cln2 and Cln3 Cyclins of *Saccharomyces cerevisiae*. *Mol Cell Biol* **20**: 542–555.

Molina, M., Cid, V.J., and Martín, H. (2010) Fine regulation of *Saccharomyces cerevisiae* MAPK pathways by post-translational modifications. *Yeast* **27**: 503–511.

Mora-Montes, H.M., Bates, S., Netea, M.G., Castillo, L., Brand, A., Buurman, E.T., *et al.* (2010) A multifunctional mannosyltransferase family in *Candida albicans* determines cell wall mannan structure and host-fungus interactions. *J Biol Chem* **285**: 12087–12095.

Mulhern, S.M., Logue, M.E., and Butler, G. (2006) *Candida albicans* transcription factor Ace2 regulates metabolism and is regulated for filamentation in hypoxic conditions. *Eukaryot Cell* **5**: 2001–2013.

Navarro-Garcia, F., Sanchez, M., Pla, J., and Nombela, C. (1995) Functional characterization of the *MKC1* gene of *Candida albicans*, which encodes a mitogen-activated protein kinase homolog related to cell integrity. *Mol Cell Biol* **15**: 2197–2206.

Nobile, C.J., Fox, E.P., Sorrells, T.R., Mitrovich, Q.M., Hernday, A.D., Andes, D.R., *et al.* (2012) A recently evolved transcriptional network controls biofilm development in *Candida albicans*. *Cell* **148**: 126–138.

Orchard, M.G., Neuss, J.C., Galley, C.M., Carr, A., Porter, D.W., Smith, P., *et al.* (2004) Rhodanine-3-acetic acid derivatives as inhibitors of fungal protein mannosyl transferase 1 (PMT1). *Bioorg Med Chem Lett* **14**: 3975–3978.

Peltroche-Llacsahuanga, H., Goyard, S., D'entfert, C., Prill, S.K., and Ernst, J.F. (2006) Protein *O*-mannosyltransferase isoforms regulate biofilm formation in *Candida albicans*. *Antimicrob Agents Chemother* **50**: 3488–3491.

Pérez, J.C., and Johnson, A.D. (2013) Regulatory circuits that enable proliferation of the fungus *Candida albicans* in a mammalian host. *PLoS Pathog* **9**: e1003780.

Peter, M., Neiman, A.M., Park, H.O., van Lohuizen, M., and Herskowitz, I. (1996) Functional analysis of the interaction between the small GTP binding protein Cdc42 and the Ste20 protein kinase in yeast. *Embo J* **15**: 7046–7059.

Pokholok, D.K., Zeitlinger, J., Hannett, N.M., Reynolds, D.B., and Young, R.A. (2006) Activated signal transduction kinases frequently occupy target genes. *Science* **313**: 533–536.

Prieto, D., Román, E., Correia, I., and Pla, J. (2014) The HOG pathway is critical for the colonization of the mouse gastrointestinal tract by *Candida albicans*. *PLoS One* **9**: e87128.

Prill, S.K., Klinkert, B., Timpel, C., Gale, C.A., Schröppel, K., and Ernst, J.F. (2005) *PMT* family of *Candida albicans*: five protein mannosyltransferase isoforms affect growth, morphogenesis and antifungal resistance. *Mol Microbiol* **55**: 546–560.

Román, E., Cottier, F., Ernst, J.F., and Pla, J. (2009) Msb2 signaling mucin controls activation of Cek1 mitogen-activated protein kinase in *Candida albicans*. *Eukaryot Cell* **8**: 1235–1249.

Román, E., Correia, I., Salazin, A., Fradin, C., Jouault, T., Poulain, D., *et al.* (2016) The Cek1-mediated MAP kinase pathway regulates exposure of α–1,2 and β–1,2–mannosides in the cell wall *of Candida albicans* modulating immune recognition. *Virulence* **18**: 1–20.

Romero, P.A., Lussier, M., Véronneau, S., Sdicu, A.M., Herscovics, A., and Bussey, H. (1999) Mnt2p and Mnt3p of *Saccharomyces cerevisiae* are members of the Mnn1p family of alpha-1,3-mannosyltransferases responsible for adding the terminal mannose residues of *O*-linked oligosaccharides. *Glycobiology* **9**: 1045–1051.

Rouabhia, M., Schaller, M., Corbucci, C., Vecchiarelli, A., Prill, S.K.H., Giasson, L., *et al.* (2005) Virulence of the fungal pathogen *Candida albicans* requires the five isoforms of protein mannosyltransferases. *Infect Immun* **73**: 4571–4580.

Saputo, S., Kumar, A., and Krysan, D.J. (2014) Efg1 directly regulates *ACE2* expression to mediate cross talk between the cAMP/PKA and RAM patwhways during *Candida albicans* morphogenesis. *Eukaryot Cell* **13**: 1169–1180.

Sasse, C., Schillig, R., Dierolf, F., Weyler, M., Schneider, S., Mogavero, S., *et al.* (2011) The transcription factor Ndt80 does not contribute to Mrr1-, Tac1-, and Upc2-mediated fluconazole resistance in *Candida albicans*. *PLoS One* **6**: e25623.

Sbia, M., Parnell, E.J., Yu, Y., Olsen, A.E., Kretschmann, K.L., Voth, W.P., *et al.* (2008) Regulation of the yeast Ace2 transcription factor during the cell cycle. *J Biol Chem* **283**: 11135–11145.

Schaekel, A., Desai, P.R., and Ernst, J.F. (2013) Morphogenesis-regulated localization of protein kinase A to genomic sites in *Candida albicans*. *BMC Genomics* **14**: 842.

Sheth, C.C., Hall, R., Lewis, L., Brown, A.J., Odds, F.C., Erwig, L.P., and Gow, N.A. (2011) Glycosylation status of the *C. albicans* cell wall affects the efficiency of neutrophil phagocytosis and killing but not cytokine signaling. *Med Mycol* **49**: 513–524.

Stichternoth, C., and Ernst, J.F. (2009) Hypoxic adaptation by Efg1 regulates biofilm formation by *Candida albicans*. *Appl Environ Microbiol* **75**: 3663–3672.

Stoldt, V.R., Sonneborn, A., Leuker, C.E., and Ernst, J.F. (1997) Efg1p, an essential regulator of morphogenesis of the human pathogen *Candida albicans*, is a member of a conserved class of bHLH proteins regulating morphogenetic processes in fungi. *Embo J* **16**: 1982–1991.

Sun, Z., Diaz, Z., Fang, X., Hart, M.P., Chesi, A., Shorter, J., *et al.* (2011) Molecular Determinants and Genetic Modifiers of Aggregation and Toxicity for the ALS Disease Protein FUS/TLS. *PLoS Biol* **9**: e1000614.

Swidergall, M., and Ernst, J.F. (2014) Interplay between *Candida albicans* and the Antimicrobial Peptide Armory. *Eukaryot Cell* **13**: 950–957.

Swidergall, M., van Wijlick, L., and Ernst, J.F. (2015) Signaling domains of mucin Msb2 in *Candida albicans*. *Eukaryot Cell* **14**: 359–370.

Szafranski-Schneider, E., Swidergall, M., Cottier, F., Tielker, D., Román, E., Pla, J., *et al.* (2012) Msb2 shedding protects *Candida albicans* against antimicrobial peptides. *PLoS Pathog* **8**: e1002501.

Timpel, C., Strahl-Bolsinger, S., Ziegelbauer, K., and Ernst, J.F. (1998) Multiple functions of Pmt1p-mediated protein *O*-mannosylation in the fungal pathogen *Candida albicans*. *J Biol Chem* **273**: 20837–20846.

Timpel, C., Zink, S., Strahl-Bolsinger, S., Schröppel, K., and Ernst, J.F. (2000) Morphogenesis, adhesive properties, and antifungal resistance depend on the Pmt6

protein mannosyltransferase in the fungal pathogen *Candida albicans*. *J Bacteriol* **182**: 3063–3071.
Travers, K.J., Patil, C.K., Wodicka, L., Lockhart, D.J., Weissman, J.S., and Walter, P. (2000) Functional and genomic analyses reveal an essential coordination between the unfolded protein response and ER-associated degradation. *Cell* **101**: 249–258.
Verna, J., Lodder, A., Lee, K., Vagts, A., and Ballester, R. (1997) A family of genes required for maintenance of cell wall integrity and for the stress response in *Saccharomyces cerevisiae*. *Proc Natl Acad Sci USA* **94**: 13804–13809.
Wang, A., Raniga, P.P., Lane, S., Lu, Y., and Liu, H. (2009) Hyphal chain formation in *Candida albicans*: Cdc28-Hgc1 phosphorylation of Efg1 represses cell separation genes. *Mol Cell Biol* **29**: 4406–4416.
Wen, W., Meinkoth, J.L., Tsien, R.Y., and Taylor, S.S. (1995) Identification of a signal for rapid export of proteins from the nucleus. *Cell* **82**: 463–473.
Willger, S.D., Liu, Z., Olarte, R.A., Adamo, M.E., Stajich, J.E., Myers, L.C., *et al.* (2015) Analysis of the *Candida albicans* Phosphoproteome. *Eukaryot Cell* **14**: 474–485.
Wilson, R.B., Davis, D., and Mitchell, A.P. (1999) Rapid hypothesis testing with *Candida albicans* through gene disruption with short homology regions. *J Bacteriol* **181**: 1868–1874.
Zufferey, R., Knauer, R., Burda, P., Stagljar, I., Te Heesen, S., Lehle, L., *et al.* (1995) STT3, a highly conserved protein required for yeast oligosaccharyl transferase activity in vivo. *EMBO J* **14**: 4949–4960.

Supporting information

Additional supporting information can be found in the online version of this article at the publisher's website.

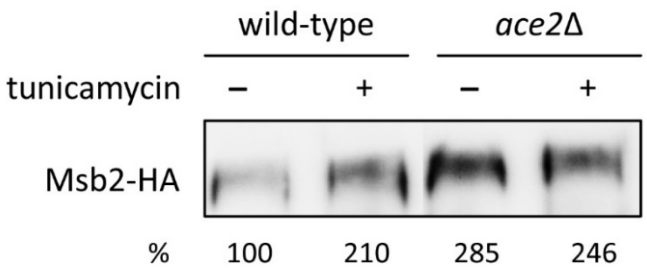

Fig.S1. Shedding of Msb2. Deletion of *ACE2* effects biosynthesis of Msb2. The MSB2-HA expression vector pES11a was digested with *Hpa*I and integrated into the *MSB2* locus, allowing transcriptional control of the native *MSB2* promoter in strain CAI4 (wild-type) and CLvW008 *(ace2*). The strains were grown in YPD-medium supplemented with tunicamycin (1 µg/ml) to enhance shedding of Msb2-HA. After 4 h growth, 20 µl spent medium of each culture was supplemented with 6x SDS sample buffer, heated at 80 °C for 5 min and loaded on a 12 % acrylamide gel (Pierce). After separation the proteins were transferred to a PVDF membrane. Transferred proteins were analyzed with the following antibodies: Anti-HA High Affinity (rat monoclonal, 1:5000, Roche), followed by treatment with HRP-conjugated secondary antibody Goat Anti rat (1:10000, Thermo Scientific). Intensities of the bands were used to determine the shedded Msb2-HA protein amount (%) using ImageJ software (http://imagej.nih.gov/ij/).

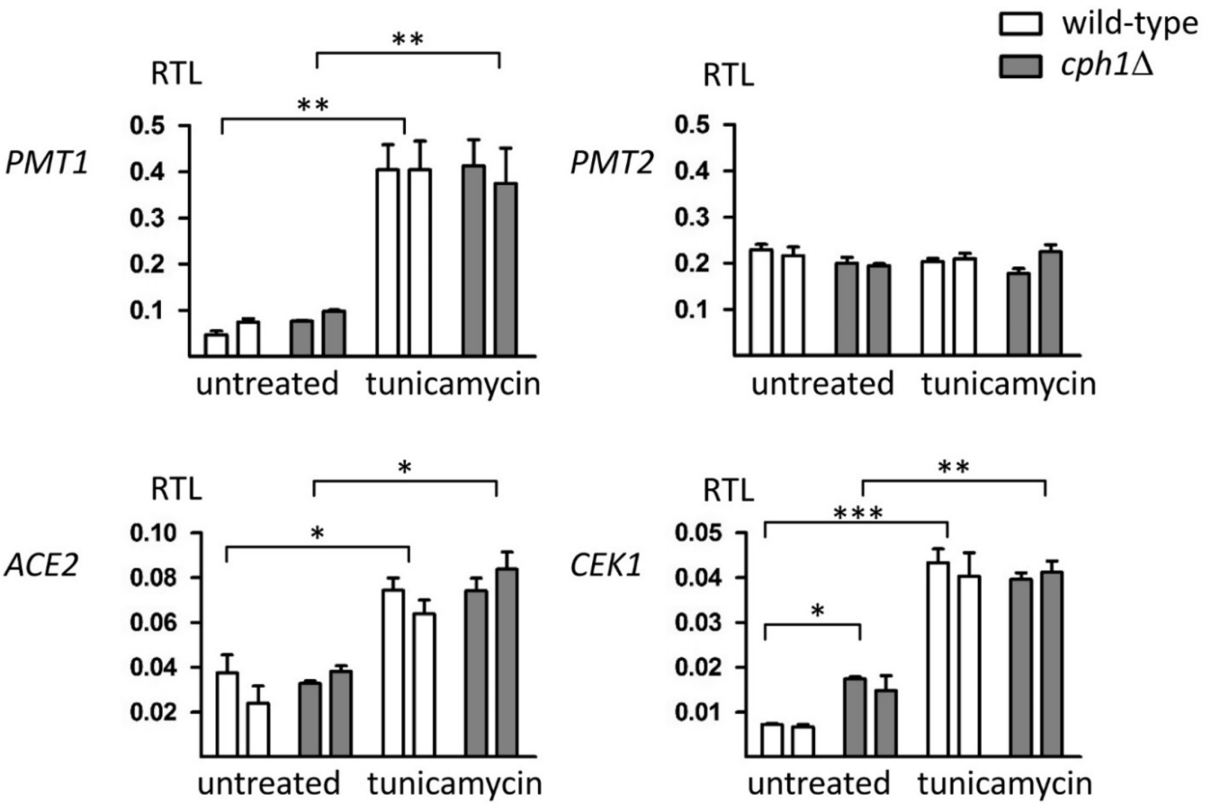

Fig.S2. The Cph1 transcription factor is not required for transcriptional regulation of Cek1 signaling target genes under glycostress. To investigate if the transcription factor Cph1, a known Cek1 MAPK substrate is involved in regulation of glycostress response genes, relative transcript levels (RTL) of *PMT1*, *PMT2*, *ACE2* and *CEK1* were determined by qPCR in the *cph1* mutant (JKC19) and the wild-type strain (CAF2-1). The cultures were precultured in YPD medium and used for inoculation of 50 ml fresh YPD cultures. The medium was either supplemented with tunicamycin (1 µg/ml) or left untreated and cultures were allowed to grow for 4 h at 30 °C. The cells were collected and total RNA was isolated, transcribed into cDNA and used for subsequent qPCR. The *ACT1* transcript was used to normalize the indicated transcripts. The experiment was performed with two replicates, represented as individual bars as means ± SEM of three technical replicates. Statistical relevance was calculated using a t-test: *, $P < 0.05$; **, $P < 0.01$; ***, $P < 0.001$.

A.

Identified AD fusion proteins interacting with Ace2 BD fusion protein in Y2H

Homology	Assignment	Gene	Sequence length (bp)	Function
390/410 (95 %)	*ORF19.5595*	*SHE3*	1560	mRNA-binding protein localizing specific mRNAs to daughter yeast cells and hyphal tips
236/244 (97 %)	*ORF19.3626*		2115	Uncharacterized
995/999 (99 %)	*ORF19.7391*	*OCH1*	1158	Alpha-1,6-mannosyltransferase
673/684 (98 %)	*ORF19.931*		2085	Uncharacterized
1039/1073 (97 %)	*ORF19.5557*	*MNN4*	2619	Mannosyltransferase
711/711 (100 %)	*ORF19.7631*	*SLD5*	711	GINS-complex subunit
598/601 (99 %)	*ORF19.3656*	*COX15*	1440	Cytochrome oxidase assembly protein
674/675 (99 %)	*ORF19.4242*	*CST20*	3687	Ste20 homolog; Cdc42p-acivated signal transducing kinase; involved in Cst20-Hst7-Cek1 MAPK pathway

B.

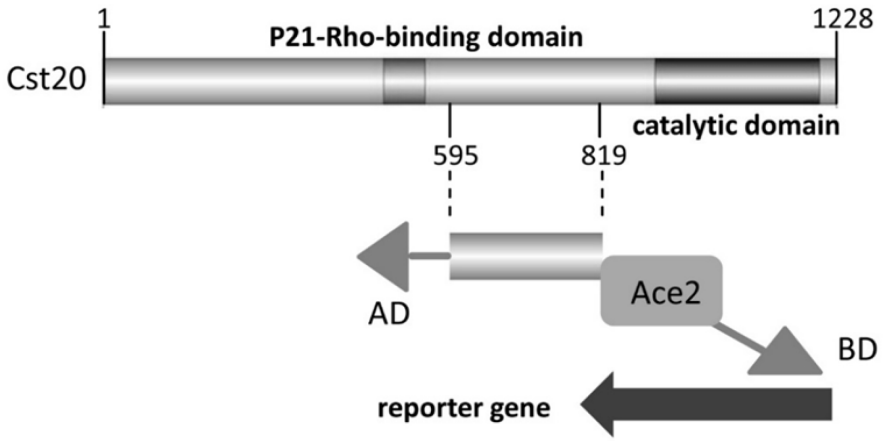

Fig.S3. Ace2 interaction partners identified by yeast-two-hybrid (Y2H) screening. (**A**) Table with potential interaction partners of Ace2. The yeast two-hybrid system was used to identify potential interaction partners of Ace2. Plasmid pBD-ACE2 encoding the Gal4 binding-domain (BD) fused to Ace2 was co-transformed into *S. cerevisiae* strain PJ69-4A with a plasmid encoded random *C. albicans* genomic library fused to the Gal4 activation domain (AD). Positive transformants were selected by adenine prototrophy and ß-galactosidase activity. Inserts of plasmids encoding potential interaction partners of Ace2 were sequenced and identified by BLAST analyses in the Candida Genome Database. The table lists the 8 identified potential interaction partners of Ace2; the respective gene annotation, length of the ORF, length of the insert with the corresponding homology to the identified *C. albicans* gene and the hypothetical function of the encoded protein is indicated. (**B**) Cst20 fragment interacting with Ace2. Among the identified interaction partners a 675 bp-long fragment shared 99% homology with a partial sequence of *ORF19.4242* encoding Cst20. The identified fragment encodes amino acids 595 – 819 and is situated between the P21-Rho-binding domain and the catalytic domain of Cst20 (http://www.candidagenome.org).

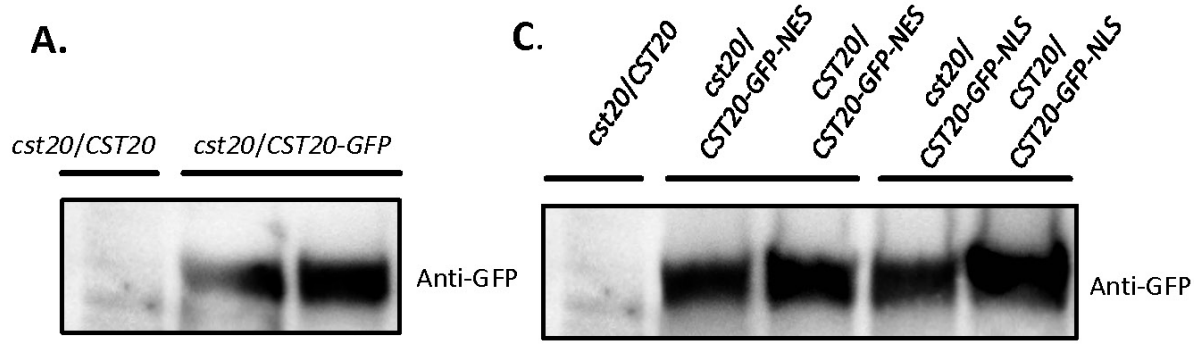
A.
cst20/CST20
cst20/CST20-GFP
Anti-GFP
C.
cst20/CST20
cst20/ CST20-GFP-NES
CST20/ CST20-GFP-NES
cst20/ CST20-GFP-NLS
CST20/ CST20-GFP-NLS
Anti-GFP

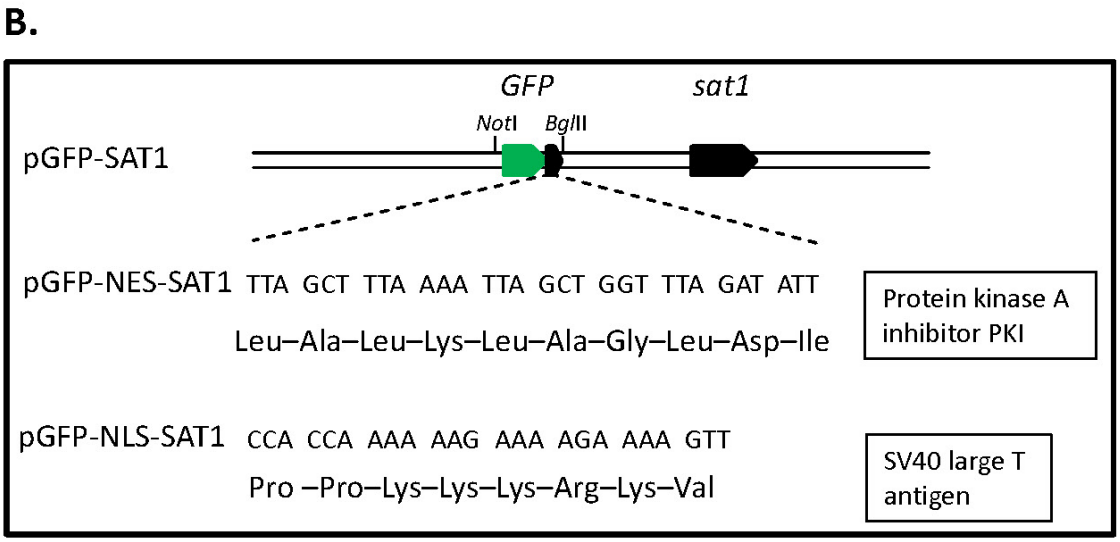
B.
GFP
sat1
NotI
BglII
pGFP-SAT1
pGFP-NES-SAT1 TTA GCT TTA AAA TTA GCT GGT TTA GAT ATT
Leu–Ala–Leu–Lys–Leu–Ala–Gly–Leu–Asp–Ile
Protein kinase A inhibitor PKI
pGFP-NLS-SAT1 CCA CCA AAA AAG AAA AGA AAA GTT
Pro –Pro–Lys–Lys–Lys–Arg–Lys–Val
SV40 large T antigen

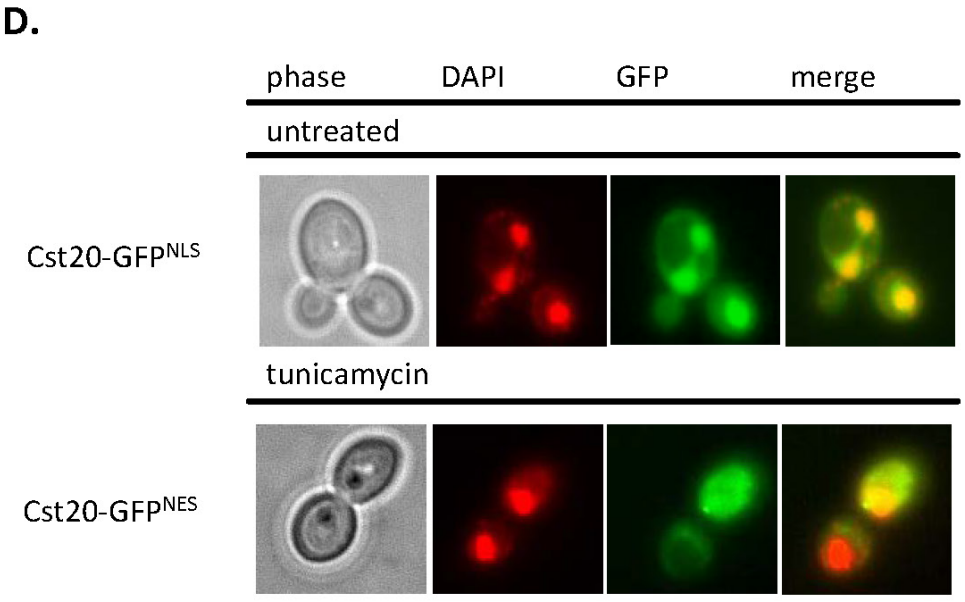
D.
phase
DAPI
GFP
merge
untreated
Cst20-GFPNLS
tunicamycin
Cst20-GFPNES

Fig.S4. Expression of Cst20-GFP variants containing NES and NLS sequences. Chromosomal *CST20* in the wild-type strains SC5314 and the heterozygous *cst20* mutant strain CLvW208 (*cst20/CST20*) was modified with *GFP, GFP-NLS* and *GFP-NES* containing sequences. (**A**) Synthesis of Cst20-GFP or (**C**) Cst20-GFP^{NLS} and -GFP^{NES} was examined by immunoblotting. Strains were grown in SCAA medium containing tunicamycin (1 µg/ml) until OD_{600} = 0.4-0.6 was reached. Protein extracts were isolated and used for subsequent immunoprecipitation using anti-rabbit Dynabeads (Thermo Scientific) coupled with anti-GFP antibody (derived from rabbit, monoclonal). Precipitated proteins were separated by SDS-PAGE on 12% acrylamide gels (Pierce) and transferred to a PVDF membrane following immunodetection with anti-GFP antibody (1:1000) and treatment with HRP-conjugated secondary goat anti-rabbit antibody (1:10000, Thermo Scientific). Signals were detected with an ImageQuant LAS 400 mini imager. (**B**) Modification of GFP with NLS and NES encoding sequences. The NLS-encoding sequence of the Simian virus 40 (SV40) large T-antigen and the NES-encoding sequence of the protein kinase A inhibitor PKI was optimized for translation in *C. albicans* and fused to the C-terminal region of GFP, resulting in plasmids pGFP-NLS-SAT1 and pGFP-NES-SAT1. *Not*I and *Bgl*II restriction sites were used for in-frame cloning of insert DNA, allowing *tet* promoter-driven overexpression (Tet-OFF). (**D**) Localization of Cst20GFP containing NLS and NES modifications. Fluorescence microscopy was used to monitor subcellular localization of Cst20-GFP variants modified with either NLS or NES sequences. Strains CLvW221 (*cst20/CST20*$^{GFP\text{-}NLS}$) and CLvW222 (*cst20/CST20*$^{GFP\text{-}NES}$) were incubated in SCAA medium for 4 h, supplemented with tunicamycin (1 µg/ml) or left untreated. Representative images of cells producing Cst20$^{GFP\text{-}NLS}$ or Cst20$^{GFP\text{-}NES}$ (green) are shown for both conditions. DAPI was used for nuclear staining (red) and images were merged to visualize co-localization of both signals.

Table S1. Binding of Ace2-HA to chromosomal sequences of *C. albicans* under tunicamycin stress conditions. Strain CLvW004 producing Ace2-HA from its chromosomal ORF and reference strain BWP17 were grown in YPD medium supplemented with 0.5 µg/ml tunicamycin at 30 °C. Chromosomal cross-linking of proteins was done and chromatin was fragmented before immunoprecipitation. For immunoprecipitation anti-HA antibody was used and the precipitated chromatin was spotted on a *C. albicans* whole-genome tiling microarray. Regions showing significant enrichment of Ace2-HA binding compared to control strain BWP17 are listet along with their nearest neighbouring ORFs. Other proteins binding to the same chromosomal region are indicated and are taken from Desai *et al*., 2015. Binding targets of Ace2-HA obtained uniquely under tunicamycin stress conditions are indicated with green background color. Accordingly to transcriptomal data obtained by Mulhern *et al*., 2006 and Roman *et al*., 2016, up- and down-regulation of genes is indicated of identified Ace2-HA target genes.

Chr	binding region	size (bp)	left ORF	gene name	left ORF position	additional binding proteins	transcriptom	right ORF	gene name	right ORF Position	additional binding proteins	transcriptom
1	7841..8275	434	*ORF19.13531*	*CTA2*		Ace2-HA untreated						
1	87268..87643	375	*ORF19.6054*	*BUL2*	87249<--85081	Ace2-HA untreated		*ORF19.6053*	*CIS2*	87901-->89811	Ace2-HA untreated	
1	91736..93009	1273	*ORF19.6049*					*ORF19.6048*		93971-->94900	Ace2-HA untreated	
1	195160..197323	2136	*ORF19.6010*	*CDC5*	193405<--191444							
1	281746..283031	1285						*ORF19.3331*	*ABC1*	282447-->284147		
1	386515..386762	247	*ORF19.4536*		386295<--384805	Ace2-HA untreated						
1	443876..445132	1256	*ORF19.3669*	*SHA3*								
1	504408..504615	207	*ORF19.2927*	*MNN11*	503456<--502635		yeast (up)					
1	771329..772704	1375	*ORF19.1133*		771008<--767144	Ace2-HA untreated						
1	1065969..1066247	278	*ORF19.4062*	*TRY2*	1066194<--1067309	Ace2-HA untreated						
1	1081669..1082323	654						*ORF19.4056*	*BRG1*	1082699-->1083970	Ace2-HA untreated	*cek1* (down)
1	1121797..1122154	357	*ORF19.432*		1119669..1118293			*ORF19.430*		1123222-->1123881		
1	1174050..1174323	273	*ORF19.2494*		1174293<--1175759	Ace2-HA untreated						
1	1291466..1293116	1650						*ORF19.2662*	*ATC218*	1293702-->1293097	Ace2-HA untreated	
1	1390429..1390775	346	*ORF19.6261*		1389741<--1382920	Ace2-HA untreated						
1	1410577..1410731	154						*ORF19.6250*	*SCD6*	1411731-->1412744		
1	1497356..1497593	237	*ORF19.6203*	*PUT3*	1497166<--1494230	Ace2-HA untreated						
1	1552870..1554106	1236						*ORF19.4443*	*YPD1*	1553615-->1554169	Ace2-HA untreated	
1	1867832..1868037	205	*ORF19.397*		1867699<--1867256	Ace2-HA untreated		*ORF19.398*		1867970-->1868443	Ace2-HA untreated	
1	2229588..2229837	249						*ORF19.4884*	*WOR1*	2230568-->2232925	Ace2-HA untreated	
1	2282001..2282196	195						*ORF19.4903*	*GPI12*	2282393-->2283454	Ace2-HA untreated	
1	2553541..2553862	321	*ORF19.1155*	*DPP1*	2553615<--2552761	Ace2-HA untreated	*cek1* (up)	*ORF19.1154*		2554349-->2554822	Ace2-HA untreated	
1	2577684..2577955	271	*ORF19.1140*		2577623<--2576997	Ace2-HA untreated	yeast (up)					
1	2749592..2749753	161	*ORF19.3756*	*CHR1*	2749710<--2747789	Ace2-HA untreated	yeast (up)	*ORF19.3755*		2749829-->2750491	Ace2-HA untreated	
1	2752108..2752359	251						*ORF19.6362*		2752616-->2757016	Ace2-HA untreated	
1	2759309..2759592	283	*ORF19.6358*	*MMS2*	2759325<--2758829	Ace2-HA untreated		*ORF19.6357*	*MAD1*	2759790-->2761880	Ace2-HA untreated	
1	2764327..2764726	399	*ORF19.6356*	*PRP6*	2764649<--2761914	Ace2-HA untreated		*ORF19.6355*	*RRB1*	2764846-->2766399	Ace2-HA untreated	
1	2774136..2774509	373	*ORF19.6350*		2773130<--2772588	Ace2-HA untreated		*ORF19.6349*	*RVS99*	2774849-->2775856	Ace2-HA untreated	
1	2788755..2788926	171	*ORF19.6343*	*FEN1*	2788244<--2787231	Ace2-HA untreated		*ORF19.6342*		2789607-->2790092	Ace2-HA untreated	
1	2803025..2803506	481	*ORF19.4917*		2803179<--2802532	Ace2-HA untreated						
1	2805639..2805969	330	*ORF19.4918*	*TRA98*	2805372<--2803813	Ace2-HA untreated		*ORF19.4919*	*CTN4*	2805700-->2807010	Ace2-HA untreated	
1	2807712..2808181	469						*ORF19.4921*	*YFW1*	2808006-->2810177	Ace2-HA untreated	
1	2854713..2854982	269						*ORF19.4936.1*			Ace2-HA untreated	
1	2934342..2934758	416	*ORF19.4970*		2933952<--2932225	Ace2-HA untreated						
1	3011053..3011437	384	*ORF19.5006.1*	*SNC2*	3010047<--3009640	Ace2-HA untreated		*ORF19.5007*	*ACT1*	3011501-->3013289	Ace2-HA untreated	
1	3163835..3164032	197	*ORF19.7521*	*REP1*	469116<--471743							
2	32744..32988	244	*ORF19.2107.1*	*WSC4*	33351<--33620	Ace2-HA untreated		*ORF19.2108*	*PGA9*	32587-->31637	Ace2-HA untreated	
2	62620..62860	240	*ORF19.2090*	*ECM16*	62936<--59145	Ace2-HA untreated		*ORF19.2089*	*NYV1*	63257-->64177	Ace2-HA untreated	

2	234732..234914	182	*ORF19.1990*		234444<--232552	Ace2-HA untreated							
2	302891..303122	231	*ORF19.1478*	*STT3*	301509<--299254			*ORF19.1480*		305495-->306025	Ace2-HA untreated		
2	305109..305421	312	*ORF19.1479*		304225<--301883	Ace2-HA untreated		*ORF19.1490*	*MSB2*	327702-->331931		*cek1* (down)	
2	325097..325750	653						*ORF19.1490*	*MSB2*	327702-->331931	Ace2-HA untreated		
2	327015..327177	162						*ORF19.5841*		536330-->537088	Ace2-HA untreated	hyphae (down)	
2	535888..536244	356	*ORF19.5842*		535695<--534910	Ace2-HA untreated		*ORF19.5811*	*MET1*	586286-->587971	Ace2-HA untreated		
2	585599..586161	562	*ORF19.5812*		585586<--584321	Ace2-HA untreated		*ORF19.5809*		588296-->589657	Ace2-HA untreated		
2	587969..588273	304						*ORF19.4488*	*SWI3*	965485-->968400	Ace2-HA untreated		
2	828388..828888	500	*ORF19.829*	*SCH9*	827878<--825515	Ace2-HA untreated		*ORF19.24*	*RTA2*	1317217-->1318578	Ace2-HA untreated	CAF2-1(up), *cek1* (up)	
2	963789..963998	209	*ORF19.4490*	*RPL17*	961980<--961423	Ace2-HA untreated	CAF2-1 (down),	*ORF19.35*	*SKY2*	1341138-->1344068	Ace2-HA untreated		
2	1316490..1317142	652						*ORF19.1863*		1554724-->1556511	Ace2-HA untreated		
2	1340887..1341353	466						*ORF19.2214*	*MRPL7*	1568309-->1569172		yeast (up)	
2	1554104..1554409	305	*ORF19.1864*		1551800<--1549956	Ace2-HA untreated		*ORF19.3605*		1771101-->1771826	Ace2-HA untreated		
2	1567094..1567257	163						*ORF19.223*		1797689-->1800073	Ace2-HA untreated		
2	1770659..1770967	308	*ORF19.3606*		1770360<--1769839	Ace2-HA untreated		*ORF19.203*	*STB3*	1842959-->1844470	Ace2-HA untreated		
2	1797354..1797663	309	*ORF19.225*		1796447<--1795362	Ace2-HA untreated							
2	1842607..1842881	274	*ORF19.204*		1840229<--1839615	Ace2-HA untreated		*ORF19.4079*		1883767-->1884558	Ace2-HA untreated		
2	1857917..1858111	194	*ORF19.4066*		1856790<--1854379	Ace2-HA untreated		*ORF19.4090*		1898301-->1896796	Ace2-HA untreated		
2	1869326..1869531	205	*ORF19.4072*	*IFF6*	1869204<--1865944			*ORF19.1401*	*EAP1*	1951311-->1953272			
2	1883592..1883939	347						*ORF19.1396*	*AGE2*	1960782-->1961945	Ace2-HA untreated		
2	1896579..1897081	502						*ORF19.5467*		13756-->14265	Ace2-HA untreated		
2	1952336..1952793	457											
2	1959173..1959431	258	*ORF19.1397*		1958642<--1957932	Ace2-HA untreated							
3	13097..13527	430	*ORF19.5468*			Ace2-HA untreated							
3	32454..32637	193	*ORF19.5445*	*GLO3*	31575<--30220								
3	396501..396690	189	*ORF19.1667*		394543<--390791								
3	719128..719320	192	*ORF19.337*	*VTI1*	719561<--717785								
3	759789..759949	160	*ORF19.355*	*TCD4*	758825<--757554								
3	877355..877585	230	*ORF19.5864*	*URK1*	877338<--875701	Ace2-HA untreated		*ORF19.5865*		877626-->880223	Ace2-HA untreated		
3	892929..893238	309	*ORF19.5871*	*SNF5*	893071<--890979	Ace2-HA untreated	hyphae (down)						
3	896473..897684	1211	*ORF19.5871*	*SNF5*	893060<--890970		hyphae (down)	*ORF19.5875*	*VAM3*	899620-->900480			
3	1118625..1118860	235						*ORF19.5992*	*WOR2*	1118847-->1120187	Ace2-HA untreated		
3	1233227..1233512	285						*ORF19.6986*		1234039-->1236246	Ace2-HA untreated		
3	1448683..1448835	152	*ORF19.7401*	*ISW2*	1441679<--1438509			*ORF19.7398*	*TSA1B*	1452471-->1453061		*cek1* (up)	
3	1456021..1456182	161	*ORF19.7421*	*CYP5*	1455477<--1454866								
3	1475513..1475883	370						*ORF19.7436*	*AAF1*	1477326-->1479164	Ace2-HA untreated		
3	1491955..1492166	211	*ORF19.7441*		1491938<--1491012	Ace2-HA untreated		*ORF19.7442*		1492186-->1493082	Ace2-HA untreated		
3	1510669..1511153	484						*ORF19.7451*	*FUN31*	1511052-->1515023	Ace2-HA untreated		
3	1680349..1680567	218						*ORF19.6760*	*MDS3*	1683073-->1687224			
3	1731713..1731910	197						*ORF19.6734*	*TCC1*	1730057-->1732303	Ace2-HA untreated		
4	48034..48219	185	*ORF19.5657*	*SWI1*	48100<--45137	Ace2-HA untreated							
4	131436..131638	202	*ORF19.4167*		127111<--126572	Ace2-HA untreated		*ORF19.4166*	*ZCF21*	131941-->133830	Ace2-HA untreated		
4	248259..248536	277	*ORF19.4668*		248276<--246123	Ace2-HA untreated							
4	282782..283309	527						*ORF19.4649*		283241-->286831	Ace2-HA untreated		
4	420730..420888	158						*ORF19.4579*		421115-->422041	Ace2-HA untreated		
4	480605..481016	411						*ORF19.2765*		480632-->481273	Ace2-HA untreated	yeast (down)	
4	538595..538903	308	*ORF19.2739*		538696<--536978	Ace2-HA untreated							
4	555823..556043	220	*ORF19.2731*		553564<--553226	Ace2-HA untreated	yeast (down)	*ORF19.2730*		553936-->555756	Ace2-HA untreated		
4	569822..570064	242	*ORF19.2725*		567226<--566924	Ace2-HA untreated		*ORF19.2724*		571920-->573416	Ace2-HA untreated		
4	591730..592160	430	*ORF19.2712*	*HCA4*	591191<--588894								

4	665440..665998	558	*ORF19.2674*		665137<--664109	Ace2-HA untreated		*ORF19.2673*		665706-->666725	Ace2-HA untreated			
4	901830..902078	248	*ORF19.1429*	*SOH1*	901816<--901376	Ace2-HA untreated		*ORF19.1428*		902225-->902740	Ace2-HA untreated			
4	958836..959072	236	*ORF19.3840*		959031<--954805	Ace2-HA untreated		*ORF19.3839*		961031-->962392	Ace2-HA untreated			
4	982132..982341	209						*ORF19.3823*		982321-->987258				
4	990641..990855	214	*ORF19.3821*		990526<--989339	Ace2-HA untreated								
4	1020888..1021863	975	*ORF19.3803*	*MNN22*	1020679<--1018910	Ace2-HA untreated	yeast (down)	*ORF19.3802*	*PMT6*	1022709-->1025207	Ace2-HA untreated	yeast (d), cek1 (d)		
4	1048206..1048473	267	*ORF19.3794*	*CSR1*	1044143<--1042287	Ace2-HA untreated		*ORF19.3793*		1048418-->1049593	Ace2-HA untreated			
4	1335245..1335458	213	*ORF19.4411*	*HOS1*	1334577<--133267			*ORF19.4413*	*CMD1*	1338201-->1338872				
5	17762..17961	199	*ORF19.5683*		15979<--15636			*ORF19.5681*		18148-->18882				
5	30117..30380	263	*ORF19.979*	*FAS1*	29661<--23548		yeast (up)							
5	32454..32632	178	*ORF19.979*	*FAS1*	29661<--23548	Ace2-HA untreated	yeast (up)							
5	34138..35335	1197	*ORF19.978*	*BDF1*	32849<--30720			*ORF19.974*	*ROT2*	36656-->39271				
5	53308..53791	483	*ORF19.964*	*SMC4*	53010<--48904									
5	94280..94512	232	*ORF19.940*		93594<--89881	Ace2-HA untreated		*ORF19.939*	*NAM7*	95043-->98102	Ace2-HA untreated			
5	217717..218023	306	*ORF19.1972*	*SET5*	217288<--215867	Ace2-HA untreated		*ORF19.1971*	*TRY3*	218221-->219705	Ace2-HA untreated			
5	364803..365136	333	*ORF19.6294*	*MYO1*	368537<--362691									
5	380339..380796	457	*ORF19.3207*	*CCN1*	379761<--377680	Ace2-HA untreated								
5	406103..406467	364	*ORF19.3195*	*HIP1*	404636<--402837	Ace2-HA untreated		*ORF19.3193*	*FCR3*	407979-->409178	Ace2-HA untreated			
5	443455..443624	169	*ORF19.3174*		443369<--440835	Ace2-HA untreated								
5	453619..453945	326	*ORF19.3170*		453571<--451385	Ace2-HA untreated								
5	513893..514105	212	*ORF19.4239*		513647<--511632	Ace2-HA untreated								
5	522151..522532	381	*ORF19.4242*	*CST20*	521590<--517904	Ace2-HA untreated								
5	596483..596710	227	*ORF19.4279*	*MNN1*	591842<--589440									
5	599825..600166	341	*ORF19.4282*	*IFH1*	598167<--597259	Ace2-HA untreated								
5	676680..677025	345	*ORF19.4334*	*PGA58*	677230<--676508									
5	760111..760266	155	*ORF19.2646*	*ZCF13*	759778<--756050			*ORF19.2645*		760524-->760844				
5	1107056..1107300	244						*ORF19.3997*	*ADH1*		Ace2-HA untreated	yeast (down)		
6	4563..5065	502						*ORF19.6337*		5545-->6489	Ace2-HA untreated			
6	60497..60663	166	*ORF19.1195*	*MIP1*	60013<--57662	Ace2-HA untreated	yeast (up)	*ORF19.1196*	*PKH3*	60921-->63506	Ace2-HA untreated	yeast (down)		
6	107748..107995	247						*ORF19.4199*		107932-->109503	Ace2-HA untreated			
6	173917..174207	290						*ORF19.90*		174680-->176944	Ace2-HA untreated			
6	304142..304599	457	*ORF19.3434*	*TRY5*	301246<--298277	Ace2-HA untreated		*ORF19.3433*	*OYE23*	304843-->306063	Ace2-HA untreated	yeast (down)		
6	319400..319632	232	*ORF19.3431*		317782<--314096	Ace2-HA untreated		*ORF19.3430*	*BUD21*	319776-->320810	Ace2-HA untreated			
6	339382..339625	243						*ORF19.3421.1*		339664-->340248	Ace2-HA untreated			
6	349369..349608	239	*ORF19.3420*		348886<--348503	Ace2-HA untreated		*ORF19.3419*	*MAE1*	350713-->352605	Ace2-HA untreated	yeast (down)		
6	384287..384762	475	*ORF19.3400*	*COQ3*	383593<--382610									
6	421895..422171	276						*ORF19.3505*		422337-->424733	Ace2-HA untreated	hyphae (up)		
6	430038..430268	230	*ORF19.3501*		429691<--426551	Ace2-HA untreated		*ORF19.3499*		434464-->434967	Ace2-HA untreated			
6	444405..444602	197	*ORF19.3494*		444313<--443213	Ace2-HA untreated		*ORF19.3453*		444683-->447643	Ace2-HA untreated			
6	549988..550214	226	*ORF19.5537*	*WSC2*	548965<--547667	Ace2-HA untreated		*ORF19.5539*		552727-->553569	Ace2-HA untreated			
6	603094..603382	288	*ORF19.5568*	*VPS51*	603308<--602358	Ace2-HA untreated		*ORF19.5569*		603848-->606529	Ace2-HA untreated			
6	630120..630398	278						*ORF19.5584*		630618-->633050	Ace2-HA untreated			
6	640292..640524	232	*ORF19.5586*		640372<--637424	Ace2-HA untreated								
6	730739..730929	190	*ORF19.5705*	*NAM2*	730549<--727964	Ace2-HA untreated	yeast (up)	*ORF19.5710*		731035-->734520	Ace2-HA untreated			
6	754997..755190	193						*ORF19.5723*	*POX1*	756971-->758962				
6	793026..793519	493						*ORF19.5741*	*ALS1*	791472-->795254				
6	799768..800467	699						*ORF19.5742*	*ALS9*	798023-->803695				
6	821237..821408	171	*ORF19.5753*	*HGT10*	819180<--817540	Ace2-HA untreated	yeast (up)							
6	837437..837820	383	*ORF19.5759*		836974<--832487	Ace2-HA untreated	yeast (up)							
6	867771..868136	365	*ORF19.5775*		864791<--863253	Ace2-HA untreated		*ORF19.1221*	*ALG2*	876496-->877833	Ace2-HA untreated			

6	875889..876332	443			897780<--894497	Ace2-HA untreated		*ORF19.1221*		876496-->877833	Ace2-HA untreated		
6	898101..898410	309	*ORF19.4557*										
6	962825..962993	168	*ORF19.1093*	*FLO8*	962206<--959828	Ace2-HA untreated							
6	969214..969419	205						*ORF19.1097*	*ALS2*	971475-->976745	Ace2-HA untreated	CAF2-1(d), *cek1* (d)	
6	1028365..1028747	382	*ORF19.2160*		1027136<--1025391	Ace2-HA untreated		*ORF19.2163*		1028841-->1031354	Ace2-HA untreated		
7	51967..52153	196	*ORF19.7089*	*PMR1*	51214<--48461								
7	132431..132677	246						*ORF19.7047*	*RTF1*	132567-->134273	Ace2-HA untreated		
7	147491..147734	243						*ORF19.7041*		148191-->150485	Ace2-HA untreated		
7	197995..198262	267						*ORF19.7020*	*KEX1*	198461-->200569	Ace2-HA untreated		
7	226954..227152	198	*ORF19.7006*		226654<--223297	Ace2-HA untreated	yeast (down)						
7	235013..235204	191	*ORF19.6896*		232413<--230875	Ace2-HA untreated							
7	312089..312282	193						*ORF19.6580*		312573-->313265	Ace2-HA untreated		
7	329445..329682	237						*ORF19.6573*		329718-->336476	Ace2-HA untreated		
7	350127..350842	715	*ORF19.6563*		349795<--347816	Ace2-HA untreated		*ORF19.6562*	*RNH35*	350992-->352287	Ace2-HA untreated		
7	375318..375638	320	*ORF19.6551*		375267<--374593	Ace2-HA untreated		*ORF19.6550*		375747-->376631	Ace2-HA untreated		
7	410407..410669	262	*ORF19.6530*		409253<--408390	Ace2-HA untreated		*ORF19.6529*	*CDC34*	411057-->411791	Ace2-HA untreated		
7	413027..413320	293	*ORF19.6528*		412926<--412315	Ace2-HA untreated							
7	437730..438044	314	*ORF19.6518*		437290<--435305	Ace2-HA untreated		*ORF19.6517*	*RAD14*	438040-->439230	Ace2-HA untreated		
7	451625..451894	269	*ORF19.6514*	*CUP9*	450912<--449878	Ace2-HA untreated							
7	465046..465507	461						*ORF19.6506*		465072-->467138	Ace2-HA untreated		
7	476843..477195	352	*ORF19.6498*		476933<--475905	Ace2-HA untreated							
7	493528..493763	235						*ORF19.6486*		493963-->494421	Ace2-HA untreated		
7	519989..520286	297	*ORF19.6472*		519627<--519139	Ace2-HA untreated		*ORF19.6470*		520558-->521115	Ace2-HA untreated		
7	632455..633164	709						*ORF19.5169*		633454-->635175	Ace2-HA untreated		
7	720181..720422	241	*ORF19.5124*	*RBR3*	721424<--716736		hyphae (down)						
7	800343..800508	165						*ORF19.6692*	*MNN26*	800431-->802701			
7	857431..857623	192	*ORF19.7194*		856999<--856073								
7	864303..864578	275	*ORF19.7187*	*MAM33*	862917<--862123		yeast (up)						
R	8643..8842	199	*ORF19.7545*		7566<--4884	Ace2-HA untreated		*ORF19.7544*		9111-->9863	Ace2-HA untreated		
R	103208..103399	191	*ORF19.7492*	*SWC4*	104010<--102103			*ORF19.7491*	*RTT109*	104234-->105313			
R	172196..172884	688	*ORF19.3283*	*OAR1*	172342<--171653	Ace2-HA untreated							
R	201809..202075	266	*ORF19.3265.1*			Ace2-HA untreated		*ORF19.3265*	*TRM1*	202225-->203895	Ace2-HA untreated		
R	324799..325013	214						*ORF19.2519*	*NNF1*	325676-->326266			
R	334667..334909	242	*ORF19.2527*		334491<--333205	Ace2-HA untreated		*ORF19.2528*	*BDP1*	334922-->336910	Ace2-HA untreated		
R	509931..510278	347	*ORF19.3742*		509369<--508644	Ace2-HA untreated		*ORF19.3740*		510511-->511359	Ace2-HA untreated		
R	556779..557328	549						*ORF19.173*		556964-->560266	Ace2-HA untreated		
R	757854..758091	237						*ORF19.2378*	*PKR1*	759807-->760160			
R	874612..874814	202						*ORF19.467*	*WOR3*	878593-->880521	Ace2-HA untreated		
R	883948..884149	201						*ORF19.469*	*HST7*	884043-->885812			
R	926791..927553	762	*ORF19.496*	*MSH1*	926380<--923609	Ace2-HA untreated		*ORF19.498*	*EAF7*	928331-->929716	Ace2-HA untreated	yeast (up)	
R	963503..963739	236						*ORF19.522*	*PIM1*	963564-->966800	Ace2-HA untreated	yeast (up)	
R	1024221..1024515	294						*ORF19.6318*		1026963-->1027295			
R	1125308..1125600	292	*ORF19.556*		1124656<--1124237	Ace2-HA untreated		*ORF19.557*		1125739-->1126764	Ace2-HA untreated		
R	1157158..1157584	426	*ORF19.5286*		1156504<--1155638	Ace2-HA untreated		*ORF19.5285*		1158030-->1158629	Ace2-HA untreated		
R	1259394..1260341	947	*ORF19.454*	*SFL1*	1258170<--1255753	Ace2-HA untreated							
R	1271946..1272327	381						*ORF19.451*		1274207-->1276684	Ace2-HA untreated		
R	1372318..1372553	235	*ORF19.723*	*BCR1*	1370542<--1368320	Ace2-HA untreated							
R	1469903..1470143	240	*ORF19.1847*		1469576<--1467687	Ace2-HA untreated							
R	1536906..1536504	599	*ORF19.1816*	*ALS3*	1535813<--1532346		*cek1* (down)	*ORF19.1815*		1538777-->1539514		hyphae (up)	
R	1612428..1613147	719						*ORF19.6124*	*ACE2*	1611767-->1614118			

R	1659779..1660018	239	*ORF19.6286*		1659219<--1658623	Ace2-HA untreated		*ORF19.6285*	*GLC7*	1660942-->1661934	Ace2-HA untreated		
R	1718524..1718725	201						*ORF19.610*	*EFG1*	1723620-->1725197	Ace2-HA untreated		
R	1723278..1723663	385						*ORF19.610*	*EFG1*	1723620-->1725197	Ace2-HA untreated	*cek1* (down)	
R	1759755..1759942	187	*ORF19.589*		1759114<--1758464	Ace2-HA untreated		*ORF19.6365*	*PTP1*	1760210-->1761328	Ace2-HA untreated		
R	1768496..1768880	384						*ORF19.6374*	*ATP10*	1770183-->1771313			
R	1817697..1817862	165						*ORF19.6411*	*VAC14*	1818771-->1821443			
R	1885618..1886042	424						*RDN18*			Ace2-HA untreated		
R	1888916..1889176	260	*RDN5*			Ace2-HA untreated		*RDN18*			Ace2-HA untreated		
R	1892603..1893207	604	*RDN5*			Ace2-HA untreated		*RDN58*			Ace2-HA untreated		
R	1919596..1919753	157	*ORF19.7293*	*MPS1*	1919006<--1916934	Ace2-HA untreated							
R	2034320..2034587	267	*ORF19.6608*		2034660<--2032492	Ace2-HA untreated	yeast (down)						
R	2051577..2052070	493	*ORF19.6599.1*		2049950<--2049756			*ORF19.6598*	*WAL1*	2050368-->2052509		*cek1* (down)	
R	2106048..2106312	264						*ORF19.7561*	*EED1*	2106249-->2108912	Ace2-HA untreated	yeast (d), *cek1* (d)	

Table S2. Oligonucleotides

name	**sequence** (5'-3')
ZCF21-rev	AGATCTTCAAGTGATCAATTTGGAAAT
ZCF21-for	AGATCTATGATGGATATTTATCAGAAGG
ACE2-BglI rev	GGAAGATCTCTATTGCAACATTAAAAACTC
ACE2-BglI for	GGAAGATCTATGCATTGGAAATTTCTGAAC
Colo-LEU2 -rev	CACACTGATGCTGCTCAGG
Colo-Amp -for	GTTGGCCGCAGTGTTATC
SAT1-PstI-rev	AATACTGCAGCTATAGGGCGAATTGGAG
SAT1-PstI-for	AATACTGCAGCAGCTATGACCATGATTAC
FLP1	CCCAAGCTTGACCAAGGCTTTGAACTATC
CST20-UTR5	GGTGATTTCTATTGTTTC
F1 CST20 rev XhoI	AAACTCGAGAAGTATGCTCATGATAGGC
F2 CST20 for ApaI	ATAGGGCCCCACACATACACACTTATTAAC
F3 CST20 for SacII	ATACCGCGGGAGTGAATCTGATTAATG
F4 CST20 rev SacI	AAAGAGCTCCATACGCCCATATCGTCTC
F5 CST20 rev XhoI	AAACTCGAGCGTTTTTTTGGTTTCTTTGG
F6 CST20 for ApaI	ATAGGGCCCAGCACCACCACCACCAATAC
F7 CST20 rev SacII	ATACCGCGGTCAACCACCATGATGTTGAG
F8 CST20 for SacI	AAAGAGCTCTTACACCAAGAGGTCCAAAG
CST20 V5 rev	CCAATATATTGACAGCAGTAGAATTTAGGGTTCTTGTTGTTCTTCTTTTTT TAAATGTTTTTATTTCTAGGATAACTCCACCCTCGACATTTTATGATGGA
CST20 V5 for	TTACTGAATGTGATGATGTATCGTCGTTAAGTCCATTAGTGAAAATTGCT CGATTGAAAAAAATGAGTGAATCTGATGGTGGAGGTAAGCCTATC
ACE2HArev	GCAATCTCTAACAGAAGTGAACATAGAATTAATAAACTGGCAGTAAATC AAACGATATAAAATAAAAAAGAATAATAGCTAGAAGGACCACCTTTGAT TG
ACE2HAfor	CAGTGGTTGAGAGGATAGAAAAACAGTTGCTACAGGAAGATAAGAGTG TTACTGAGGAGTTTTTAATGTTGCAATCGGGTGGTGGTCGGATCCCCGG GTTAATTAAC
GFP NotIXhoI rev	CTACTCGAGCTAGCGGCCGCGATGAGTAAGGGAGAAGAAC
GFP NLS BglII for	TCCAGATCTTTAAACTTTTCTTTTCTTTTTTGGTGGTTTGTATAGTTCATCC ATGCC
GFP NES BglII for	TCCAGATCTTTAAATATCTAAACCAGCTAATTTTAAAGCTAATTTGTATAG TTCATCCATGCC
CST20 GFP rev	CCAATATATTGACAGCAGTAGAATTTAGGGTTCTTGTTGTTCTTCTTTTTT TAAATGTTTTTATTTCTAGGATAACTCCACCCCACCAAACCCAAAAAAAG AG
CST20 GFP for	TTACTGAATGTGATGATGTATCGTCGTTAAGTCCATTAGTGAAAATTGCT CGATTGAAAAAAATGAGTGAATCTGATATGAGTAAGGGAGAAGAAC
CST20-URT3 rev	ACATAGGTGGTAGAATATGG
SAT1 for	AGCGATGTACTGGTACTG
ACE2 GFP rev	GCAATCTCTAACAGAAGTGAACATAGAATTAATAAACTGGCAGTAAATC AAACGATATAAAATAAAAAAGAATAATAGCTAGAAGGACCACCTTTGAT TGTAAATAGTAATAATTACCAC

ACE2 GFP for	CAGTGGTTGAGAGGATAGAAAAACAGTTGCTACAGGAAGATAAGAGTG TTACTGAGGAGTTTTTAATGTTGCAATCGGGTGGTGGTATGTCTAAAGGT GAAGAATTATT
qPCR oligonucleotides	
ACT1-RT-rev	TGGACAAATGGTTGGTCAAG
ACT1-RT-for	TTGGATTCTGGTGATGGTGT
PMT1-RT-for	GCTGCTGAACCTGTTGAAGA
PMT1-RT-rev	CATCAGCAACTTGTGGGTCT
PMT2-RT -for	CCATGATGGCTACTAACAATG
PMT2-RT -rev	CCCATCCACACATTCTAATACC
PMT4-RT-for	TTGGAAACATCATTGGGTTC
PMT4-RT-rev	TTGATCTTGCTCTGTCGCTT
PMT5-RT-for	CCCTTATGCATCTCCTCCAT
PMT5-RT-rev	CACCAAATATGGCCAGGAAT
PMT6-RT-for	ATTTGTTGGTTGTTGGCATC
PMT6-RT-rev	TGATTGACTGTTTGCTGGGT
ZCF21-RT-for	GCACAGCCATCACAACTACC
ZCF21-RT-rev	ACCGAAGGTTGACTCATTGG
CEK1-RT-for	TTAGAAATTGTTGGAGAAGGAGCAT
CEK1-RT-rev	GCAACTTTTTGTTGTGATGGTTTATG
HST7-RT-for	CAGCTTCATCGCAGTCTCC
HST7-RT-rev	GGAAACTCAGGATCGGTGC
CST20-RT-for	TCATATTGCACCTGCTCCTC
CST20-RT-rev	CATTATTCTCACCGCCAAAC
MSB2-RT-for	AGTTACCGCAGTTGCTCCTT
MSB2-RT-rev	CTCGATGGTGTCTCAGCAAT
ACE2-RT-for	CGCCGAATCAAAAAGACTTC
ACE2-RT-rev	CGCACATTGTATCGACGAGT
MSB2 P ChIP-for	ATACAAGGCCGAATACCGAG
MSB2 P ChIP-rev	GATTGCTTGCCGGAACTATC
MSB2 D ChIP-for	TTTGATACCCACCCCTTC
MSB2 D ChIP-rev	TTTCTCTGTATGTGTTTGATTC
HST7 ChIP-for	CTCCACCTCAACAATGAC
HST7 ChIP-rev	AGGCACTGGTGGTAAATC
URA3-5'-ChIP-for	AGAAGTTGAAAATGCCGTTGAC
URA3-5'-ChIP-rev	CGTCAACACTGTTAAACTTATC

Table S3. Plasmids

Plasmid	Description	Source
***C. albicans* plasmids**		
pBI-1	*PCK1p* for overexpression, *URA3*, Amp^R, *LEU2*	Stoldt *et al.*, 1997
pPCKp-ACE2-URA3	as pBI, but *PCK1p-ACE2-ACT1t*	this work
pPCKp-ZCF21-URA3	as pBI, but *PCK1p-ZCF21-ACT1t*	this work
pBI-SAT1	as pBI, but *ACT1p-sat1-ACT1t*	this work
pPCKp-ACE2-URA3	as pBI-SAT1, but *PCK1p-ACE2-ACT1t*	this work
pPCKp-ZCF21-URA3	as pBI-SAT1, but *PCK1p-ZCF21-ACT1t*	this work
pSFS5	*sat1*, Amp^R, *SAP2p-FLP1*, *sat1* based flipper cassette	Sasse *et al.*, 2010
pCLvW90	as pSFS5, but containing the outer *ACE2* deletion cassette (*Sac*I/*Apa*I)	Desai *et al.*, 2015
pCLvW91	as pSFS5, but containing the inner *ACE2* deletion cassette (*Sac*I/*Apa*I)	Desai *et al.*, 2015
pCLvW100	as pSFS5, but containing the outer *CST20* deletion cassette (*Sac*I/*Apa*I)	this work
pCLvW101	as pSFS5, but containing the inner *CST20* deletion cassette (*Sac*I/*Apa*I)	this work
pFC-V5	*V5*, *ACT1p-sat1-ACT1t*, Amp^R	Ullman *et al.*, unpublished
p3HA-URA3	*3HA*, *URA3*, Amp^R	Prill *et al.*, 2005
pNIM1R-GFP	*TETp-GFP*, ACT1p-sat1 *ACT1t*, Amp^R, *ADH1*, TET-OFF plasmid containing GFP	Prieto *et al.*, 2014
pGFP-NLS-SAT1	as pNIM1R-GFP, but *TETp-GFP-NLS*	this work
pGFP-NES-SAT1	as pNIM1R-GFP, but *TETp-GFP-NLS*	this work
pDS1044-1	*ACT1p* for overexpression, *URA3*, Amp^R, *LEU2*	D. Sanglard
pES11a	as pDS1044-1, but *ACT1p-MSB2-HA-ACT1t*, *URA3*, *LEU2*	Szafranski-Schneider *et al.*, 2012
pGFP-URA3	*GFP*, *URA3*, Amp^R	Gerami-Nejad *et al.*, 2001
***S. cerevisiae* plasmids**		
pGBD-C1	Amp^R, *TRP1*, yeast two hybrid plasmid containing *ADH1p-GAL4-BD-ADH1t*	James *et al.*, 1996
pGAD-C1	Amp^R, *LEU2*, yeast two hybrid plasmid containing *ADH1p-GAL4-AD-ADH1t*	James *et al.*, 1996
pBD-ACE2	as pGBD-C1, but *ADH1p-GAL4-BD-ACE2-ADH1t*	this work
pAD-ACE2	as pGBD-C1, but *ADH1p-GAL4-AD-ACE2-ADH1t*	this work
pGAD-C2	as pGAD-C1, but reading frame shift (1 bp)	James *et al.*, 1996
pGAD-C3	as pGAD-C1, but reading frame shift (2 bp)	James *et al.*, 1996
pDYC-C1	as pGAD-C1, but genomic DNA fragments (0.5 – 3.0 kb) from *C. albicans* strain CAI4 after treatment with enzymes *Taq*I, *Mae*II, *Hinf*I, *Aci*I and *Msp*I and cloned to the *GAL4-AD*	Timpel C., Weber Y. and Ernst J. F., unpublished
pDYC-C2	as pDYC-C1, but reading frame shift (1 bp)	Timpel C., Weber Y. and Ernst J. F., unpublished
pDYC-C3	as pDYC-C1, but reading frame shift (2 bp)	Timpel C., Weber Y. and Ernst J. F., unpublished

2.3 Manuskript II: Hypoxia and temperature regulated morphogenesis in *Candida albicans*

Prashant R. Desai, **Lasse van Wijlick**, Dagmar Kurtz, Mateusz Juchimiuk, Joachim F. Ernst

Geteilter Erstautor

Beitrag zum Manuskript: 40 %

Lasse van Wijlick hat einen Großteil der Experimente geplant, durchgeführt und ausgewertet. Des Weiteren hat er die entsprechenden Abbildungen (Fig.6.A-C, Fig.7.A-B, Fig.8.A-E, Fig.9.A-B, Fig.10.A, Fig.S4.A-B, Fig.S5, Fig.S6.A-B, Fig.S7 und Fig.S8) erstellt, die Ergebnisse interpretiert und Schlussfolgerungen für das Manuskript formuliert. Darüber hinaus hat er Teile des Manuskripts geschrieben.

Veröffentlicht in: PLoS Genetics, August 2015; 11(8): e1005447.

Impact Factor: 7.528 (2014)

PLOS | GENETICS

RESEARCH ARTICLE

Hypoxia and Temperature Regulated Morphogenesis in *Candida albicans*

Prashant R. Desai[1☯], Lasse van Wijlick[1,2☯], Dagmar Kurtz[1], Mateusz Juchimiuk[1], Joachim F. Ernst[1,2*]

1 Department Biologie, Molekulare Mykologie, Heinrich-Heine-Universität, Düsseldorf, Germany, **2** Manchot Graduate School Molecules of Infection, Heinrich-Heine-Universität, Düsseldorf, Germany

☯ These authors contributed equally to this work.
* Joachim.ernst@uni-duesseldorf.de

OPEN ACCESS

Citation: Desai PR, van Wijlick L, Kurtz D, Juchimiuk M, Ernst JF (2015) Hypoxia and Temperature Regulated Morphogenesis in *Candida albicans*. PLoS Genet 11(8): e1005447. doi:10.1371/journal.pgen.1005447

Editor: Geraldine Butler, University College Dublin, IRELAND

Received: February 21, 2015

Accepted: July 15, 2015

Published: August 14, 2015

Data Availability Statement: All 16 files are available at the Candida Genome Database (http://www.candidagenome.org/download/systematic_results/Desai_2014/).

Funding: This work was supported by the Deutsche Forschungsgemeinschaft (Er47/11-1) to JFE, the Jürgen Manchot Stiftung Düsseldorf (http://www.moi.hhu.de/) to JFE and the ERA-NET PathoGenoMics project OXYstress (www.pathogenomics-era.net/FundedProjects3rdJoint) to JFE. The funders had no role in study design, data collection and analysis, decision to publish, or preparation of the manuscript.

Abstract

Candida albicans is a common commensal in the human gut but in predisposed patients it can become an important human fungal pathogen. As a commensal, *C. albicans* adapts to low-oxygen conditions and represses its hyphal development by the transcription factor Efg1, which under normoxia activates filamentation. The repressive hypoxic but not the normoxic function of Efg1 required its unmodified N-terminus, was prevented by phosphomimetic residues at normoxic phosphorylation sites T179 and T206 and occurred only at temperatures ≤35°C. Genome-wide binding sites for native Efg1 identified 300 hypoxia-specific target genes, which overlapped partially with hypoxic binding sites for Ace2, a known positive regulator of hypoxic filamentation. Transcriptional analyses revealed that *EFG1*, *ACE2* and their identified targets *BCR1* and *BRG1* encode an interconnected regulatory hub, in which Efg1/Bcr1 act as negative and Ace2/Brg1 act as positive regulators of gene expression under hypoxia. In this circuit, the hypoxic function of Ace2 was stimulated by elevated CO_2 levels. The hyperfilamentous phenotype of *efg1* and *bcr1* mutants depended on Ace2/Brg1 regulators and required increased expression of genes encoding Cek1 MAP kinase and its downstream target Cph1. The intricate temperature-dependent regulatory mechanisms under hypoxia suggest that *C. albicans* restricts hyphal morphogenesis in oxygen-poor body niches, possibly to persist as a commensal in the human host.

Author Summary

Candida albicans is an important cause of human disease that occurs if the fungus proliferates strongly on skin surfaces or in several internal organs causing superficial and systemic mycosis. Remarkably, at low cell numbers, *C. albicans* is also a normal inhabitant of mucosal surfaces and the gut and it is believed that its transition from the commensal to the virulent, highly proliferative state is a key event that initiates fungal disease. In the gut and other body niches, *C. albicans* adapts to an oxygen-poor environment, which downregulates its virulence traits including the ability to form hyphae. We report on a set of four transcription factors in *C. albicans* that form an interdependent regulatory circuit, which

Competing Interests: The authors have declared that no competing interests exist.

downregulates filamentation specifically under hypoxia at slightly lowered body temperatures (≤ 35°C). Disturbance of this circuit is expected to initiate the fungal virulence and proliferation in predisposed patients.

Introduction

Candida albicans is a regular fungal inhabitant of the human gastrointestinal tract and the skin [1–3] but in predisposed patients it can also cause life-threatening systemic disease [4]. Systemic candidiasis occurs if resident fungi translocate to the blood and proliferate massively in extraintestinal organs [5,6]. Currently, the requirements for *C. albicans* commensalism are being investigated using murine models of colonization, in which fungi are fed orally and monitored during transit and following exit of the gut [7–11]. In all studies, *C. albicans* cells growing in the gut lumen were found to propogate in the yeast form and not in the alternative hyphal form. Transciptomal analyses revealed that *C. albicans* adapts to conditions in the mouse gut or in internal organs by upregulation of genes related to growth, stress-resistance and cell surface components [12]. Several proteins required for gut colonization were identified by their defective mutant phenotypes [9,10,12]. In contrast, mutants lacking the transcription factor Efg1 or its homologue Efh1 were found to hyperproliferate in the murine gut [7–9], while overproduction of the Efg1-antagonist Wor1 stimulated excessive proliferation [9]. These results suggested that *C. albicans* limits its gastrointestinal growth by the repressive transcriptional activity of the Efg1 protein [8]. Gut mucosal damage, deficiencies in immune defenses and defects of the gut probiotic microbiome have been described as essential preconditions to allow translocation and systemic dissemination of *C. albicans* originating from the gut [11,13]. Despite this knowledge, the environmental cues and signaling pathways favouring commensal growth of *C. albicans* and its transition to the invasion and dissimination states are largely unclear.

Oxygen-poor locations are frequent in the human host and some niches including the gut may be anoxic [14,15], while other tissues including tissue of exposed skin are hypoxic [16,17]. Hypoxia has also been verified in the mouse gastrointestinal tract [18]. *C. albicans* adapts to hypoxia by increasing glycolytic and decreasing respiratory metabolism; furthermore, increased expression of genes required for the oxygen-dependent biosynthesis of compounds including ergosterol and unsaturated fatty acids procures maximal use of residual oxygen [19–21]. Under hypoxia, genes required for ergosterol biosynthesis are induced by the transcription factor Upc2 [20,22], while the transcription factors Efg1 and Ace2 both upregulate glycolysis and downregulate oxidative activities [19,23,24]. Efg1 is required for rapid transcriptomal adaptation to hypoxia [25], it controls the regulation of many hypoxic genes and prevents inappropriate hypoxic regulation of normoxic genes [14,19]. Besides their hypoxic metabolic functions, Efg1 and Ace2 also regulate the yeast-to-hypha transition, an important virulence trait of *C. albicans*, in an oxygen-dependent manner. Under normoxia, *efg1* mutants are unable to form hyphae indicating that Efg1 acts as an inducer of morphogenesis [26,27]. In contrast, Efg1 represses hyphal growth under hypoxia, which is apparent by hyperfilamentous growth of *efg1* mutants during hypoxic growth on an agar surface [19,23,28] or during embedment in agar [4,29] but not during growth in liquid media. The increased hyperfilamentous phenotype of an *efg1 efh1* double mutant demonstrated further that the Efg1 homolog Efh1 acts synergistically with Efg1 [23]. The function of Efg1 as a hypoxic repressor was strikingly temperature-dependent since *efg1* mutants were hyperfilamentous at temperatures ≤ 35°C, while at 37°C they were unable to form hyphae under both hypoxia and normoxia [19]. In contrast to Efg1,

the Ace2 protein was found to be largely dispensable for hyphal morphogenesis under normoxia [30–32] but it was required for filamentation under hypoxia [30,32]. Thus, Efg1 and Ace2 have opposing functions under hypoxia and recent results suggested that Efg1 represses *ACE2* expression [32], as well as expression of Ace2 target genes [32,33] under normoxia.

Both described hypoxic functions of Efg1, i. e. to regulate yeast proliferation of *C. albicans in vitro* and in the mouse gut *in vivo*, may be directed by similar if not identical regulatory circuits. In support of this notion, as compared to the wild-type strain, an *efg1* mutant not only was hyperproliferative in the mouse gut [7–9] but it also showed increased extraintestinal dissemination in animals exposed to hypoxia [34] and increased virulence in orally-inoculated mice [35]; in contrast, the virulence of the *efg1* mutant was strongly reduced in the systemic model of bloodstream-infection, i. e. under increased oxygen levels [27,35]. Hypoxia by decreased blood flow in individual gut villi had previously been shown to favor invasion and translocation of *C. albicans* across enterocytes [36]. Conceivably, the hypoxic repressor functions of Efg1 are relevant not only at temperatures <37°C, i.e. for fungal colonization of exposed skin tissue but also for translocation across gut epithelia. Here we identify a transcriptional regulatory hub describing the functions of Efg1 under hypoxia that controls the proliferation and morphogenesis of *C. albicans* in oxygen-limiting environments.

Results

Efg1 hypoxic function requires its unmodified N-terminus

Under hypoxia, Efg1 has been described as a temperature-dependent regulator of morphogenesis because it suppresses filamentation during surface growth at temperatures ≤35°C [19], while at 37°C it is required for hyphal growth [19] as under normoxia [26,27]. Properties of the *efg1* mutant were re-confirmed by growth on the surface of YPS agar, which under normoxia does not induce hypha formation in *C. albicans* [37]. Under hypoxia (0.2% O_2), the *efg1* mutant was unable to filament at 37°C, while it showed vigorous hyphal outgrowth at 34, 30 and 25°C; in contrast, under normoxia no filamentation was observed at 25°C (Fig 1A). At 37°C under hypoxia, the defective filamentation of an *efg1* homozygous mutant on YPS agar was fully restored not only by native Efg1 but also by an N-terminally HA-tagged Efg1 variant (Fig 1A) or by an Efg1 variant carrying a N-terminal deletion (Fig 1B), as under normoxia [38]. In contrast, at 25, 30 or 34°C the synthesis of HA-Efg1 did not prevent hyperfilamentation in an *efg1* genetic background, while native unmodified Efg1 had this activity (Fig 1A). The repressing function of authetic Efg1 was slightly reduced by deleting residues 9 to 74 (ΔN-Efg1) since colonies grown at 25°C (but not at 30 or 34°C) showed residual filamentation (Fig 1B). Thus, the morphogenetic repressor function of Efg1 requires its native N-terminus.

The structural requirements for hypoxic Efg1 functions were explored further by single-site mutated variants mutated for residues T206 and T179. T206 fits the consensus sequence for phosphorylation by PKA [39] and T179 is considered as the phosphorylation site of the Cdc28-Hgc1 kinase complex [33]; phosphorylation of both residues is needed for efficient hypha formation under normoxia [33,39]. *EFG1* versions encoding T206A, T206E, T179A and T179E variants were integrated into the genome of an *efg1* mutant and filamentation phenotypes of transformants were examined. All Efg1 variants were produced at similar levels during hypoxic growth (Fig 1C) as under normoxia [38], which was assayed by immunoblotting of cell extracts using a newly generated anti-Efg1 antiserum (S1 Fig). Interestingly, at 25, 30 and 34°C, both non-phosphorylatable variants T206A and T179A effectively repressed filamentation, while Efg1 variants mimicking phosphorylation (T206E and T179E) were unable to act as repressors (Fig 1B). This result suggests that opposite to its normoxic functions, the

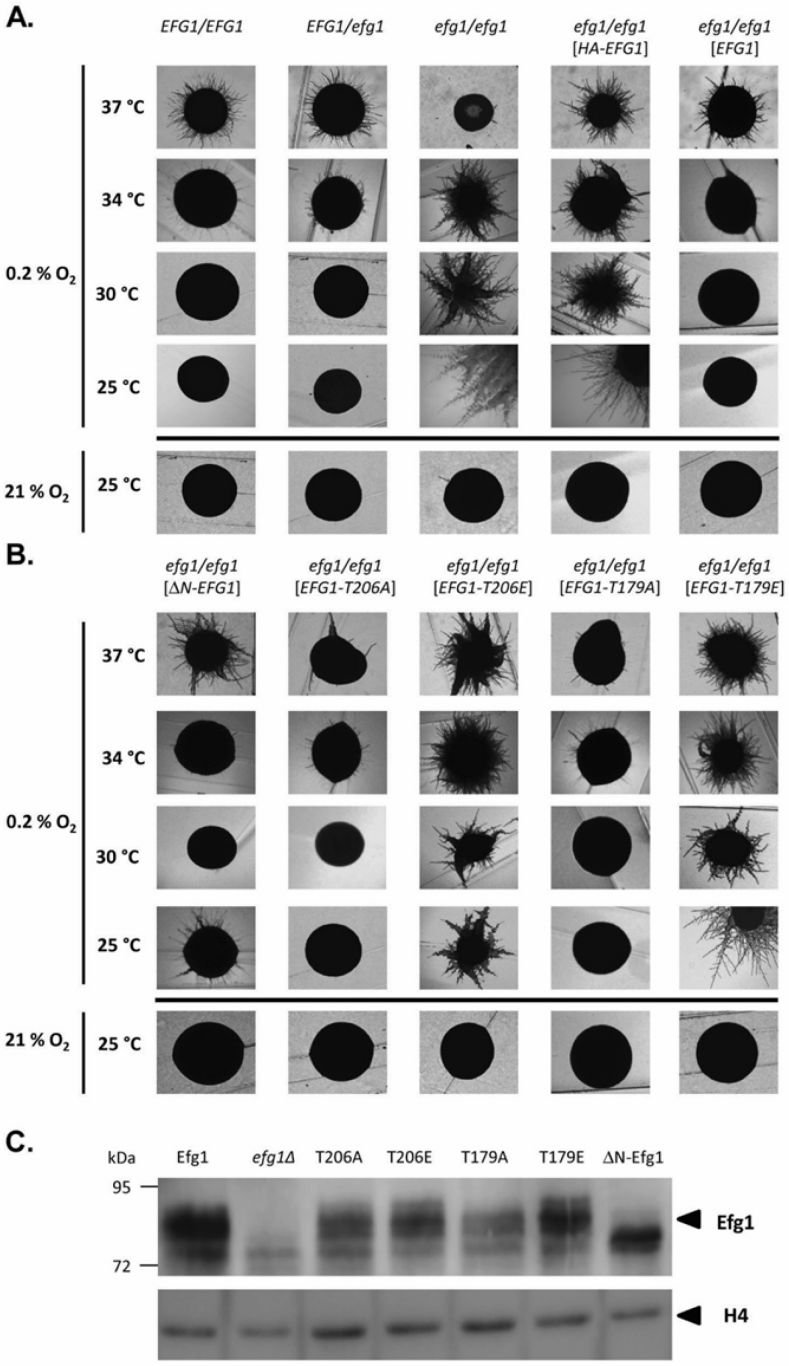

Fig 1. Hypoxia and temperature dependent filamentation regulated by Efg1 variants. (A, B) Colony phenotypes. Strains were grown under hypoxia (0.2% O_2) on the surface of YPS agar at 37°C (3 d), 34°C (3 d), 30°C (3 d) or 25°C (4 d) and under normoxia (21% O_2) at 25°C (4 d). (C) Efg1 immunoblot. Strains were

grown on YPS agar for 60 h at 25°C before cell harvesting by scraping off the colonies. 75 μg of protein in cell extracts were separated by SDS-PAGE (8% acrylamide) and immunoblots were developed using anti-Efg1 antiserum. Levels of histone H4 (loading control) were detected by anti-histone H4 antibodies. Strains tested were CAF2-1 (*EFG1/EFG1*), BCA0901 (*EFG1/efg1*), HLC52 (*efg1/efg1*), HLCEEFG1 (*efg1/efg1* [*HA-EFG1*]), HLCPEFG1 (*efg1/efg1* [*EFG1*]), HLCNEFG1 (*efg1/efg1* [*ΔN-EFG1*]), HLCEEFG1T206A (*efg1/efg1* [*EFG1-T206A*]), HLCEEFG1T206E (*efg1/efg1* [*EFG1-T206E*]), HLCEEFG1T179A (*efg1/efg1* [*EFG1-T179A*]) and HLCEEFG1T179E (*efg1/efg1* [*EFG1-T79E*]).

doi:10.1371/journal.pgen.1005447.g001

phosphorylated forms of Efg1 are inactive in hypoxic repression, while the non-phosphorylated forms are active.

Collectively, the results suggest that normoxic and hypoxic functions of Efg1 have different structural requirements. An unmodified native N-terminus of Efg1 and the lack of T206/T179 phosphorylation appear essential for its repressive functions under hypoxia at temperatures slightly below 37°C.

Genomic binding of native and HA-tagged Efg1 under hypoxia

The above experiments had shown that native but not HA-tagged Efg1 is active for morphogenetic repression under hypoxia at 25°C and 30°C. Next, we sought to identify genes that are hypoxically repressed by Efg1 but not HA-Efg1 under hypoxia. For this purpose genomic binding sites for both Efg1 versions were determined by ChIP chip analyses and compared. Binding of native Efg1 was determined in the Efg1$^+$ strain CAF2-1 using anti-Efg1 antibody for immunoprecipitation and the *efg1* mutant HLC52 [27] as the background control strain; binding of HA-Efg1 was established using anti-HA antibody and strain CAF2-1 as the reference control [40]. Cells were grown at 30°C (i. e. a temperature compatible with the hypoxic repressor function of Efg1) in liquid glucose-containing YPD medium. This experimental setup was chosen to focus on hypoxia-regulated targets under clearly defined conditions using uniformly exponentially-growing yeast cells and to exclude other targets, e. g. related to differential filamentation. Furthermore, normoxic targets for HA-Efg1 had been previously determined in identical conditions [40] and provided a useful dataset for comparisons.

Genomic binding sites for native Efg1 (221 sites corresponding to 300 ORFs) greatly outnumbered those for HA-tagged Efg1 (100 sites corresponding to 118 ORFs) and surprisingly little overlap was found for sites binding both proteins (23 sites); 198 sequences were exclusively bound by native Efg1 under hypoxia (Fig 2A). Little overlap was also detected between targets of HA-Efg1 under hypoxia and normoxia [40] (S2 Fig). Binding sites for both proteins are specified in S1 Table and are available at (http://www.candidagenome.org/download/systematic_results/Desai_2014/). Hypoxic binding occurred exclusively in promoter regions upstream of ORFs, marking these genes as potential regulatory targets (in case of divergently transcribed genes both ORFs were considered as regulatory targets). A significant subset of identified genes has a known or suspected role in hyphal growth of *C. albicans* (shaded area in Fig 2A). Genes binding both Efg1 and HA-Efg1 included *EFG1* itself [40], as well as seven genes encoding general morphogenetic regulators comprising *NRG1*, *TCC1* and *TYE7*. Forty-one genes were only bound by native Efg1 but not by HA-Efg1 under hypoxia including *BCR1*, *CEK1*, *CPH2*, *CYR1*, *STE11* and *TPK1*. Consensus sequences in promoters binding Efg1 proteins were calculated using the program RSAT dyad analysis [41] and revealed an enrichment for CA-containing motifs for both Efg1 and HA-Efg1 (Fig 2B) that may represent binding sites. This result suggests that although target promoters differ, untagged and tagged Efg1 proteins bind to identical sequences under hypoxia. Interestingly, the binding sequences resemble CA-containing sequences bound by HA-Efg1 during hyphal induction under normoxia but

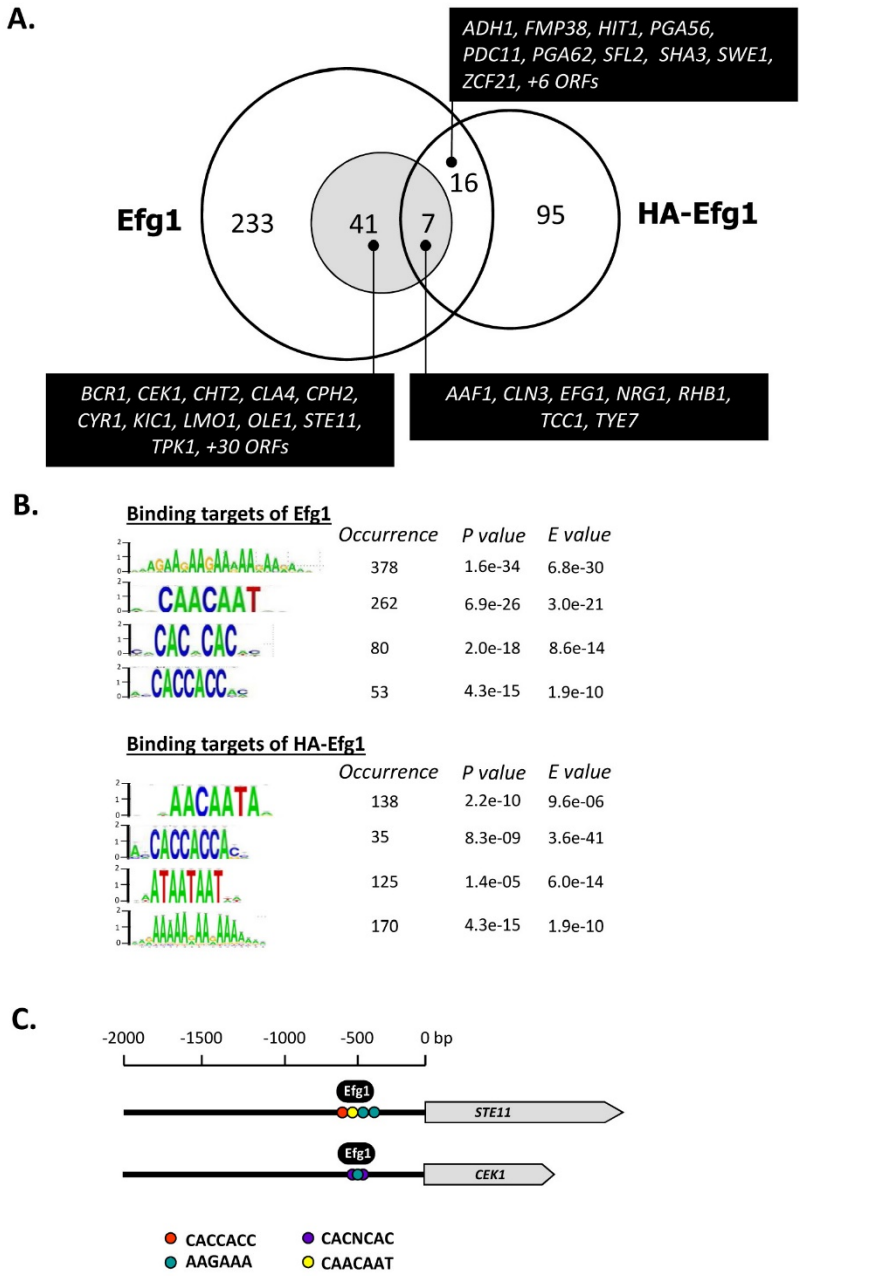

Fig 2. Genomic binding sites for Efg1. (A) Venn diagram listing numbers of genes bound by untagged Efg1 (Efg1) and HA-Efg1 under hypoxia. For Efg1, genomic binding sites were derived from ChIP chip experiments comparing strains CAF2-1 (*EFG1/EFG1*) and HLC52 (*efg1/efg1*); for HA-Efg1, strains HLCEEFG1 (*efg1/efg1* [*HA-EFG1*]) and DSC11 (*efg1/efg1* [*EFG1*]) were compared. The shaded circle encompasses genes in filamentous growth. (B) The program RSAT dyad analysis [43] was used to predict the DNA binding motif of Efg1 and HA-Efg1 from genomic binding regions. Predicted dyads for Efg1 and HA-Efg1 binding sites under hypoxic growth were ranked and the top-ranked sequences are shown with their P-/E-values. (C) Position of Efg1 binding sites in promoter regions. Arrows indicate ORFs of genes *STE11*,

CEK1 and *CPH1* and consensus sequences representing potential Efg1 binding sites in promoter regions are indicated by colored circles. The position of identified Efg1 binding (black oval) in *STE11* and *CEK1* promoters is indicated.

doi:10.1371/journal.pgen.1005447.g002

differ from the major binding site (EGR-box TATGCATA) in normoxically grown, yeast-form cells [40].

Gene ontology (GO) analysis of genes binding native Efg1 under hypoxia revealed an enrichment for genes involved in filamentation and transcription factor activity (Fig 3), as expected from the Venn diagram (Fig 2A). Several of these genes had previously been identified as targets of HA-tagged Efg1 grown under normoxia in liquid [40] or during biofilm formation [42]. Gene ontology assignments for HA-Efg1 are shown in S3 Fig.

Transcriptional regulation under hypoxia

The above results had indicated a subset of genes bound by native but not HA-tagged Efg1, which are known to be involved in the yeast-to-hypha transition. Efg1 binding in promoter regions of these genes suggested that they are transcriptionally regulated by Efg1, explaining the hypoxic repressor function of Efg1 on hyphal morphogenesis. To verify this notion, transcript levels of selected genes were monitored during the shift from normoxia to hypoxia in Efg1$^+$ cells (CAF2-1) and *efg1* mutant cells (HLC52). Genes *STE11*, *CEK1* and *CPH1* encode members of the Cek1 MAP kinase cascade, which is needed for hypha formation of *C. albicans* mainly during surface growth [43–45]; Efg1 binding occurs in the promoter region of *STE11* and *CEK1* genes at the CA-type consensus binding sequences (Fig 2C). Transcripts of genes *CYR1* and *TPK1* were also analyzed that encode adenylate cyclase and PKA isoform 1, respectively, which are members of the cAMP-dependent pathway of filamentation [46,47]. In addition, the *KIC1* transcript encoding a presumed regulator of the Ace2 transcription factor [48] was assayed since Ace2 stimulates hypoxic filamentation [30] (see below).

In the control strain, transcripts for the Cek1 MAP kinase, its downstream transcription factor Cph1 and for the Kic1 protein were present at low levels but increased temporarily at 10–20 min following the hypoxic shift (Fig 4). Remarkably, in *efg1* mutant cells, these transcripts were strongly upregulated suggesting hypoxic repression by Efg1. A completely different pattern of regulation was detected for the *STE11* gene encoding a kinase upstream of Cek1, as well as for the *CYR1* adenylate cyclase gene. Transcript levels for both of these genes decreased strongly during the hypoxic shift in the Efg1$^+$ strain and were significantly downregulated in the *efg1* mutant. Thus, the regulation of both *STE11* and *CYR1* did not fit the pattern of an Efg1-repressed but rather of an Efg1-induced gene; in addition, expression of both genes was down- and not upregulated during the course of hypoxic exposure. The *TPK1* transcript also was downregulated under hypoxia but the absence of Efg1 did not affect its levels. Collectively, these results suggest that under hypoxia Efg1 downregulates *CEK1*, *CPH1* and *KIC1* transcript levels to suppress filamentation, which becomes evident by the *efg1* mutant phenotype (Fig 1). Efg1 binding to *STE11*, *CYR1* and *TPK1* promoters may have other functions that are not directly related to repression of hypoxic filamentation.

Efg1 represses Cek1-dependent filamentation under hypoxia

To verify the transcriptional data we analyzed levels of the Cek1 MAPK protein and of its phosphorylated form by immunoblotting in wild-type and mutant strains grown under hypoxia and normoxia. Under hypoxia, the total amount of Cek1 and of its phosphorylated form (Cek1-P) was strongly increased in the *efg1* mutant as compared to the wild-type strain, while under normoxia Cek1 levels were unaltered in the mutant and Cek1-P was not detected

GO term (genome frequency)	Efg1 binding genes annotated to the term Name	Frequency	*P* value
A. Process			
Growth (8.8 %)	*AAF1*[ac] *ADA2* BCR1*[bc] *BMH1 BNI4 CAS4 CCN1*[c] *CEK1 CHT2 CLA4*[c] *CLN3*[ac] *CPH2 CYR1 DBF2* EFG1*[ac] *ENO1 ERG13 ERG3 FTR1 GLN3 GZF3 HGT1*[c] *IRO1 KIC1 LMO1 MP65 MSS4 MYO2 NDH51 NRG1*[ac] *OLE1*[c] *PCL5 PDX1*[c] *RAP1 RBD1 RFG1*[ac] *RHB1*[a] *RHO1 ROB1 STE11 STE4 STP2*[c] *TCC1*[ac] *TOP1 TPK1*[c]* *TYE7*[c] *ZCF17 ORF19.2397.3 ORF19.4459*[ac] *ORF19.6705*	17.4 %	0.001
Filamentous growth (8.5 %)	*AAF1*[ac] *ADA2* BCR1*[bc] *BMH1 BNI4 CAS4 CCN1*[c] *CEK1 CHT2 CLA4*[c] *CLN3*[ac] *CPH2 CYR1 DBF2* EFG1*[ac] *ENO1 ERG13 ERG3 GLN3 GZF3 HGT1*[c] *IRO1 KIC1 LMO1 MP65 MSS4 MYO2 NDH51 NRG1*[ac] *OLE1*[c] *PCL5 PDX1*[c] *RAP1 RBD1 RFG1*[ac] *RHB1*[a] *ROB1 STE11 STE4 STP2*[c] *TCC1*[ac] *TOP1 TPK1*[c]* *TYE7*[c] *ZCF17 ORF19.2397.3 ORF19.4459*[a] *ORF19.6705*	16.7 %	0.037
Symbiosis, encompassing mutualism through parasitism (2 %)	*AAF1*[ac] *ADA2* ADH1 BCR1*[bc] *CAP1* CLA4 CPH2 CYR1 EFG1*[ac] *ENO1 FBA1 FTR1 HYR1 MET6 MP65 NRG1*[ac] *PGK1 SSA2 TDH3 XOG1*	7 %	0.001
B. Function			
Nucleic acid binding transcription factor activity (2.6 %)	*ADA2* BCR1*[bc] *CAP1* CAS4 CBF1*[a] *CPH2 EFG1*[ac] *GLN3 GZF3 NRG1*[ac] *RAP1 RFG1*[ac] *ROB1 RPN4 SFU1 STP2 TYE7*[c] *ZCF17 ZCF21 ORF19.173 ORF19.1757 ORF19.4972*	7.3 %	0.012
Sequence-specific DNA binding (6.5 %)	*ADA2* BCR1*[bc] *BMH1 CAP1* CBF1*[a] *EFG1*[ac] *GLN3 GZF3 NRG1*[ac] *RAP1 RFG1*[ac] *ROB1 RPN4 SFU1 STP2 TYE7*[c] *WOR3 ORF19.173 ORF19.1757*	13.8 %	0.028

Fig 3. GO categories of genes binding Efg1 under hypoxia. GO terms for Efg1 binding targets were identified in ChIP chip data using the CGD GO Term Finder tool (http://www.candidagenome.org/cgi-bin/GO/goTermFinder); the analysis was conducted in June 2013. Genome frequencies of genes corresponding to GO terms are expressed as percentages (gene number relative to 6,525 genes in the *C. albicans* genome; the frequency of genes binding Efg1 that correspond to a specific GO term are expressed relative to the total number of 287 genes binding Efg1). Superscripts of genes indicate known gene functions: a, Efg1 binding under yeast normoxia [40]; b, Efg1 binding in hypha-inducing conditions [40]; c, Efg1 binding in biofilm-inducing conditions [42]; *genes regulated by Efg1 during GI tract colonisation [8]. Blue Lettering indicates common target genes bound by Efg1 and HA-Efg1 under hypoxia. *P* values for overrepresented categories were calculated using a hyper geometric distribution with multiple hypothesis correction according to the GO Term Finder tool. The *P* value cutoff used was 0.05.

doi:10.1371/journal.pgen.1005447.g003

(Fig 5A). This result matches the observed increase in the *CEK1* transcript level in the *efg1* mutant (Fig 4B). Activation of MAP kinase activity was specific for Cek1 since the Mkc1 phosphorylation status was unaffected by the presence of Efg1 (Fig 5A).

To test if during hypoxic surface growth, excessive filamentation by the Cek1-Cph1 pathway is suppressed by the Efg1 protein we examined filamentation phenotypes under hypoxia in strains lacking or overproducing potential regulator proteins. We observed that a *cph1* mutant and colonies of an *efg1 cph1* double mutant did not form hyphae, unlike the hyperfilamentous *efg1* mutant (Fig 5B). In addition, overexpression of *STE11* and *CPH1* genes encoding members of the Cek1 signaling pathway by an anhydrotetracyclin-inducible promoter stimulated filamentation in the wild-type genetic background (Fig 5C). In this experiment, the failure of overexpressed *CEK1* to induce filamentation may reflect low activity of non-phosphorylated Cek1 in the absence of activation by an upstream kinase. Collectively, the results provide strong evidence that Efg1 represses hypha formation of *C. albicans* under hypoxia by repressing the biosynthesis and activity of the Cek1 MAP kinase pathway.

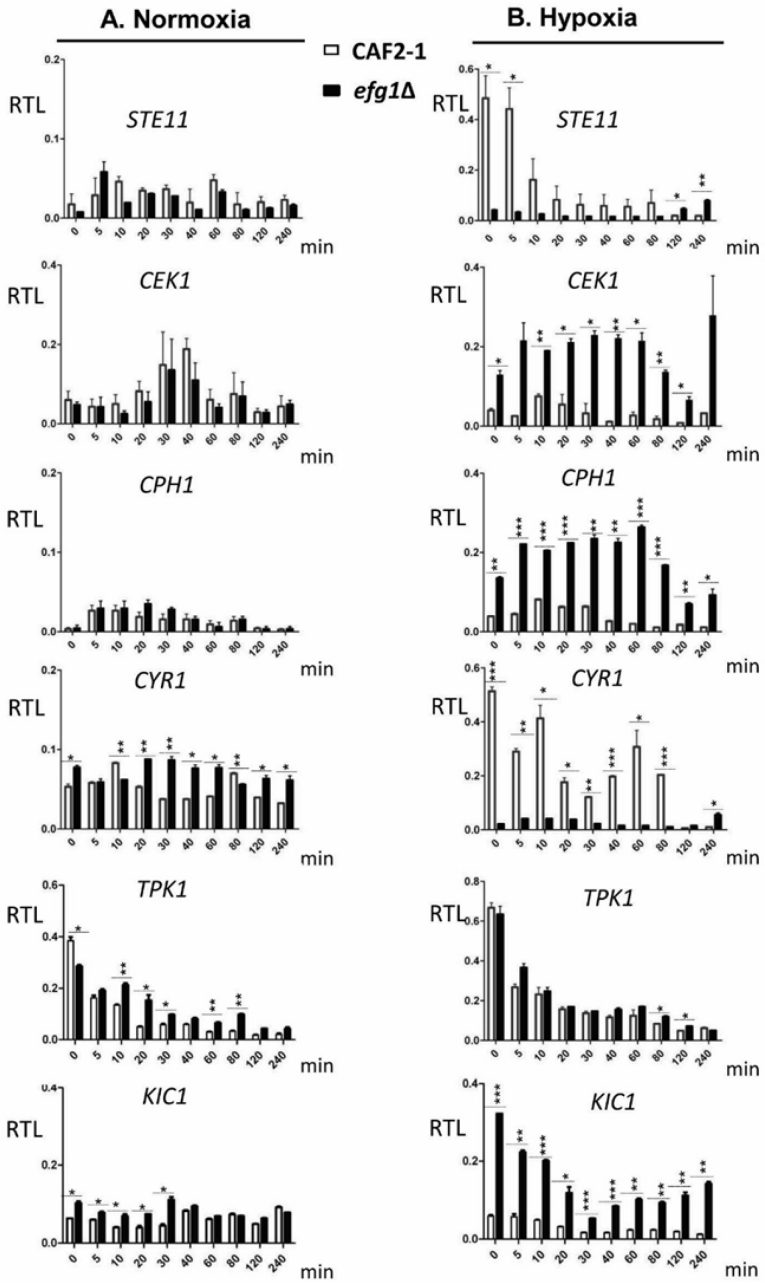

Fig 4. Transcriptional regulation of Efg1 target genes under normoxia and hypoxia. Strains were precultured under normoxia at 30°C in YPD medium and used for inoculation of 200 ml YPD cultures for normoxia, or under 0.2% O_2 for hypoxia. Cultures were incubated at 30°C under normoxia or hypoxia, and at the indicated times 20 ml of culture was withdrawn and used for preparation of total RNA. At each time point, two biological replicates and three technical replicates were assayed by qPCR using gene-specific primers. mRNA levels are expressed as means ± SEM of transcript levels relative to the *ACT1* transcript (RTL), for normoxia (A) and hypoxia (B) grown cultures. A two-tailed, unpaired *t* test comparing the RTL values of

control strain CAF2-1 and *efg1* mutant HLC52 was used to determine the statistical relevance. *, $P < 0.05$; **, $P < 0.01$; ***, $P < 0.001$.

doi:10.1371/journal.pgen.1005447.g004

Intersection of Ace2 and Efg1 regulatory circuits

Ace2 is a transcription factor that under hypoxia, unlike Efg1 at lower temperatures, is required for filamentation [30]. Efg1 represses the transcription of *ACE2* and of Ace2-dependent genes and binds to the *ACE2* promoter under normoxia [31, 32]. On the other hand, Ace2 and Efg1 have similar functions to stimulate glycolysis and to repress oxidative metabolism [23, 30]. These results suggested that Ace2 and Efg1 regulatory circuits overlap to jointly control filamentation of *C. albicans* under hypoxia. To verify this notion we compared genomic binding sites of Ace2 and Efg1 in cells grown under hypoxia. Strain CLvW004 (*ACE2-HA/ace2*) was constructed, which synthesizes the Ace2 protein with an added C-terminal triple HA-tag. This strain did not show any of the known *ace2* mutant phenotypes for antimycin A resistance, wrinkled colony growth [24,30] and sensitivity to the Pmt1 *O*-mannosylation inhibitor [49] indicating that the Ace2-HA fusion protein is functional (S4 Fig). For the identification of hypoxic Ace2 genomic binding sites, based on preliminary results, a broad ChIP chip screening strategy was chosen to identify all hypoxic targets including those targets requiring the presence of CO_2. For this purpose genomic binding sites for Ace2-HA in strain CLvW004 were determined following growth in 0.2% O_2/ 6% CO_2 and related to results of strain BWP17 synthesizing unmodified Ace2 for background correction; in parallel, normoxic binding sites were determined. Binding sites for Ace2 are listed in S2 and S3 Tables and deposited at http://www.candidagenome.org/download/systematic_results/Desai_2014/.

296 significant genomic Ace2 binding sites were identified in *C. albicans* promoter regions, while no binding occurred within ORFs (Fig 6A). The majority of binding sites (>80%) was identical in cells grown under hypoxia or normoxia (S5 Fig). Analysis with the RSAT program dyad analysis [41] revealed potential consensus binding sequences CAACAA, CACCAC, CAGCW and ATCAT for Ace2 (Fig 6B). The sequence CAGCW is similar to the CCAGC motif deduced from transcriptomal analyses of Ace2 [30] and matches the binding sequence of *S. cerevisiae* Ace2 [50]. Interestingly, the CAACAA and CACCAC motifs had also been observed as potential binding sites for native and tagged Efg1 (Fig 2B) suggesting that these sequences are targeted by both Ace2 and Efg1. Genomic positions for both proteins correspond to binding motifs, mostly to the CACCAC sequence, in a selected group of promoters (Fig 6C).

53 promoters bound both Ace2-HA and Efg1 and/or HA-Efg1 under hypoxia (Fig 7A). Gene ontology analysis of the corresponding genes revealed their preferential function as transcription factors to regulate processes of cell adhesion, biofilm formation and morphogenesis (Fig 7B). The transcription factors Brg1 [51] and Bcr1 [52] are known to regulate morphogenesis under normoxia but they also appear to function under hypoxia because they are under joint control of both Ace2 and (HA-) Efg1 in this environment (Fig 7B). Other common hypoxic Ace2/Efg1 target genes encode regulators with more specific functions including Aaf1 [53], Adh1 [54], Eed1 [55], Tye7 [56], Rfg1 [57], Wor2 [58], Wor3 [59] and Zcf21 [60]. In control experiments, binding targets were verified by qPCR following ChIP demonstrating strong enrichment of binding sites for Efg1, HA-Efg1 or Ace2-HA in a selected group of target promoters (S6 Fig). By this sensitive method, binding of HA-Efg1 (in addition to Efg1) was also detected at the *BCR1* promoter; furthermore, these data demonstrated the specificity of antibodies used for immunoprecipitation since anti-Efg1 antibody precipitated both Efg1 and HA-Efg1, while anti-HA antibody was specific for HA-Efg1 and Ace2-HA (S6 Fig).

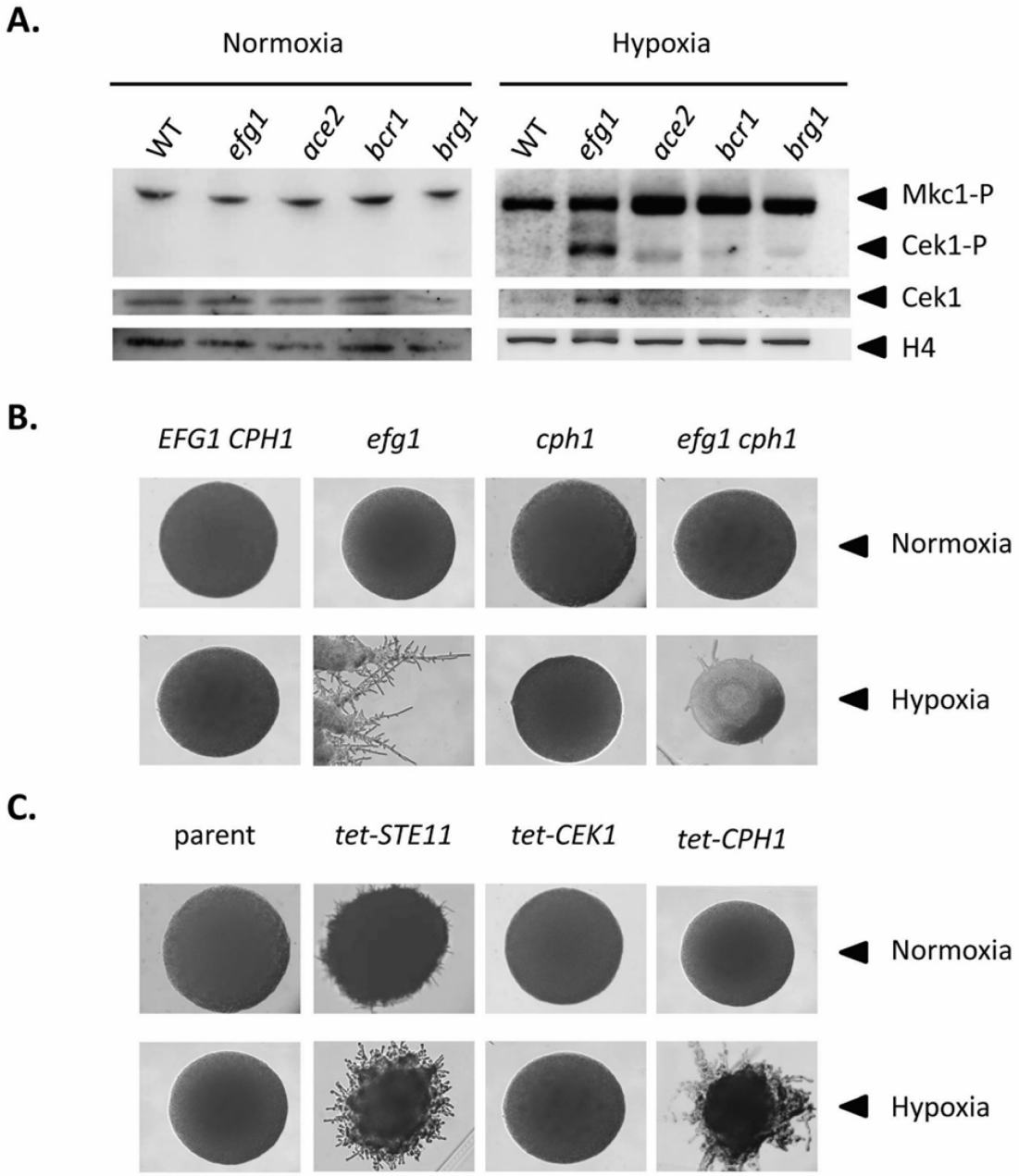

Fig 5. Hypoxic filamentation is activated by the Cek1 pathway. (A) Levels of MAP kinases in *C. albicans* mutants. *C. albicans* strains CAF2-1 (WT), HLC52 (*efg1*), MK106 (*ace2*), CJN702 (*bcr1*) and TF022 (*brg1*) were plated on YPS agar plates and incubated for 60 h at 25°C under normoxia or hypoxia (0.2% O_2). Colonies were scraped off the agar and cell extracts were used for immunoblotting. Anti-phospho-p44/42 antibody was used to detect the phosphorylated forms of MAP kinases Mkc1p and Cek1p. Total Cek1 (Cek1) and histone H4 levels (loading control) were detected by anti-Cek1 and anti histone H4 antibodies, respectively. (B, C) Phenotypes of *C. albicans* strains with altered expression of Efg1 target genes. Filamentation phenotypes were monitored following growth on YPS agar at 25°C under normoxia or hypoxia (0.2% O_2) for 3 d. (B) Mutant phenoypes. Comparisons of control strain CAF2-1 (*EFG1 CPH1*) and homozygous mutants HLC52 (*efg1*), JKC19 (*cph1*), HLC54 (*efg1 cph1*). (C) Overexpression phenotypes. Transformants expressing genes *STE11*, *CEK1* and *CPH1* under control of a tetracycline inducible promoter were grown on YPS medium containing 3 μg/ml anhydrotetracycline. Strains included CDC2907 (parent control), CECSTE11 (*tet-STE11*), CECCEK1 (*tet-CEK1*) and CDCCPH1 (*tet-CPH1*).

doi:10.1371/journal.pgen.1005447.g005

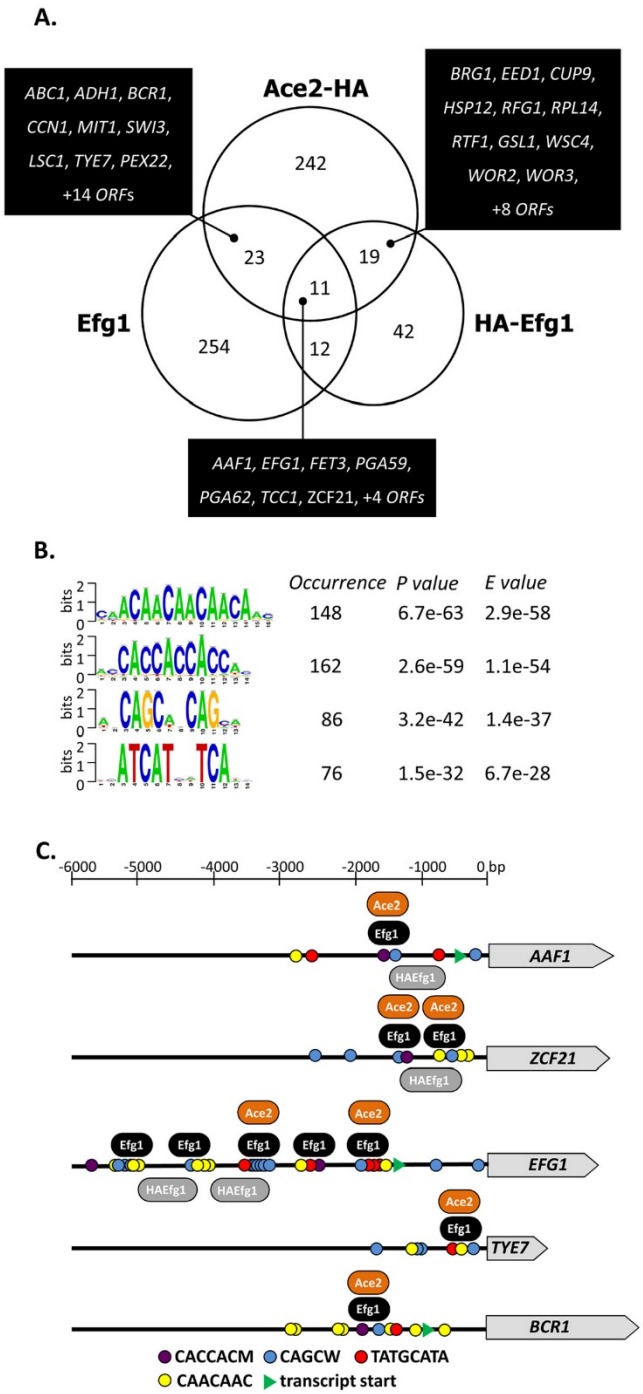

Fig 6. Genomic binding sites for Ace2. (A) Venn diagram showing numbers of genes bound by untagged Efg1 (Efg1), HA-Efg1 and Ace2-HA under hypoxia. For Efg1, genomic binding sites were derived from ChIP

chip experiments comparing strains CAF2-1 (*EFG1/EFG1*) and HLC52 (*efg1/efg1*), for Ace2-HA, strains CLvW004 (*ACE2-HA/ace2*) and BWP17 were compared. A set of 34 genes is common for Efg1 and Ace2-HA. (B) The program RSAT dyad-analysis [41] was used to predict the DNA binding motif of Ace2-HA from genomic binding regions. Predicted dyads for Ace2-HA binding sites under hypoxic growth were ranked and the top-ranked sequences are shown with their respective *P*- and *E*-values. (C) Position of Efg1 and Ace2-HA binding sites in promoter regions of target genes. Arrows indicate ORFs of genes *AAF1*, *TYE7*, *ZCF21*, *EFG1* and *BCR1*. Consensus sequences representing potential Efg1 and Ace2-HA binding sites in promoter regions are indicated by colored circles. The position of common identified sequences for Efg1 (black oval) and Ace2-HA (orange oval) binding in *AAF1*, *TYE7*, *ZCF21*, *EFG1* and *BCR1* promoters is indicated.

doi:10.1371/journal.pgen.1005447.g006

In addition, 242 genes were identified that only bound Ace2-HA but not (HA-)Efg1. This group was enriched for genes involved in glycolysis and oxidative metabolism (e. g. *PFK2*, *ACO1*, *LSC1*) confirming previous transcriptomal analyses [30]. Interestingly, genes involved in mitochondrial translation (*NAM2*, *ORF19.4929*, *ORF19.4705*, *EAF7*, *PIM1*) were also identified among Ace2 targets. The promoter of the *SCH9* gene encoding a kinase repressing hypha formation under hypoxia if CO_2 is present [37], was also identified as a hypoxic binding target of Ace2. Collectively, the group of "Ace2-only" genes appears to regulate metabolism and growth but also contains some genes for some relevant morphogenetic regulators including *FLO8* [61,62], *CAS5* [63], *SFL1* [64,65] and *WOR1* [58]. Conceivably, under hypoxia activation of *FLO8*, which is known to be required for CO_2 sensing [62], may be mediated by Ace2 (see below).

Efg1-Ace2 and its targets form an interdependent regulatory hub under hypoxia

Joint binding of Efg1 and Ace2 to target promoters under hypoxia suggested that both proteins regulate the respective genes on the transcriptional level. To clarify a specific role of hypoxia on gene regulation the transcript levels of selected Ace2-Efg1 target genes were determined under hypoxia and normoxia. Wild-type cells, as well as *ace2* and *efg1* mutant cells, were grown under normoxia and hypoxia (0.2% O_2) both in the absence or presence of CO_2 (6% CO_2); hypoxia in combination with elevated CO_2 levels was tested because previous results had suggested that this environment triggers specific patterns of gene expression [37]. Transcript levels were determined for Ace2-Efg1 target genes under hypoxia and normoxia (Fig 8).

First, mutual regulation of *EFG1* and *ACE2* was examined. In the wild-type strain, the *ACE2* transcript was strongly upregulated under hypoxia but only in the presence of CO_2; upregulation did not require CO_2 in the *efg1* mutant (Fig 8A) suggesting that Efg1 strongly represses *ACE2* under hypoxia also in the absence of CO_2. The *EFG1* transcript level was upregulated about twofold under hypoxia in the wild-type strain; this occurred even in the *ace2* mutant in the absence but not in the presence of CO_2. This mutual regulatory pattern of both genes indicated that under hypoxia, Efg1 acts as a transcriptional repressor independently of CO_2, while Ace2 requires CO_2 for its induction activity.

In a similar manner we analysed the hypoxic expression of two Ace2-Efg1 target genes encoding key morphogenetic regulators during biofilm formation under normoxia (*BCR1*, *BRG1*) (Fig 8B). Bcr1 is a positive regulator of biofilm formation, cell surface composition and filamentation [52,66,67], while Brg1 (Gat2) promotes hypha-specific gene expression during hyphal elongation [51,68,69] and promotes *ACE2* expression under normoxia [32]. The *BCR1* transcript was downregulated in the wild-type strain but upregulated in the *efg1* mutant under normoxia but more strongly under hypoxia revealing Efg1 as a strong hypoxic repressor of *BCR1*. In the *ace2* mutant the *BCR1* transcript was downregulated more strongly in the presence than in the absence of CO_2 suggesting that Ace2 upregulates *BCR1* in this environment,

A.

GO term (genome frequency)	Common Efg1, HA-Efg1 and Ace2-HA binding genes annotated to the term: Name	Frequency	*P* value
A. Process			
Cell adhesion (0.9 %)	*AAF1*, *BCR1*, *EED1*, *EFG1*, *orf19.4216*	9.4 %	0.036
Biofilm formation (2.2 %)	*ADH1*, *BCR1*, *BRG1*, *CSR1*, *EED1*, *EFG1*, *TYE7*	13.2 %	0.044
B. Function			
Nucleic acid binding transcription factor activity (3.4 %)	*BCR1*, *BRG1*, *CSR1*, *CUP9*, *EFG1*, *RFG1*, *TYE7*, *WOR2*, *ZCF21*, *orf19.173*	18.9 %	0.001
DNA binding (7 %)	*BCR1*, *BRG1*, *CSR1*, *CUP9*, *EFG1*, *RFG1*, *RTF1*, *TYE7*, *WOR3*, *ZCF21*, *orf19.173*, *orf19.4488*	22.6 %	0.014

B.

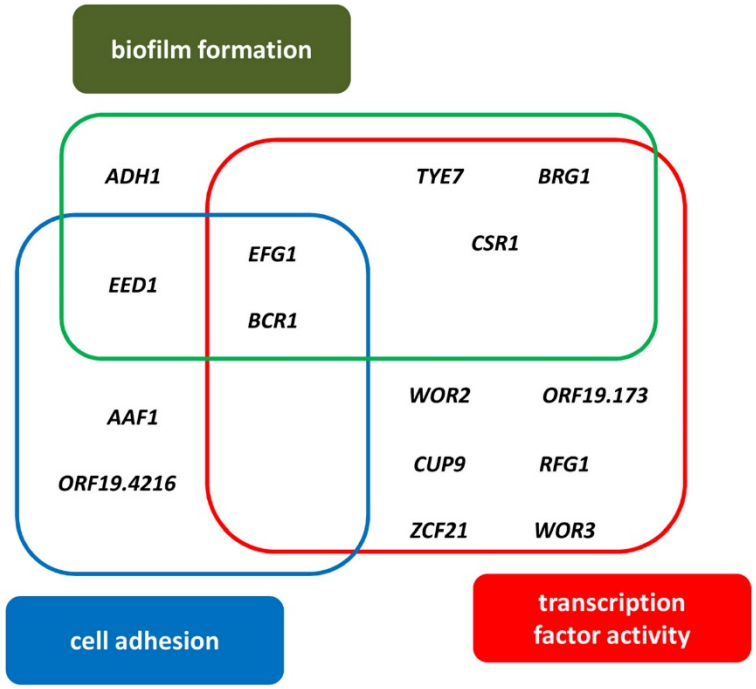

Fig 7. GO categories of common untagged Efg1 (Efg1), HA-Efg1 and Ace2-HA target genes under hypoxia. (A) GO terms for target genes identified by ChIP-chip analysis that are common for untagged Efg1, HA-Efg1 and Ace2-HA under hypoxia using the CGD GO Term Finder tool (http://www.candidagenome.org/cgi-bin/GO/goTermFinder); the analysis was conducted in May 2014. Genome frequencies of genes corresponding to GO terms are expressed as

percentages (gene number relative to 6,525 genes in the *C. albicans* genome; the frequency of genes that correspond to a specific GO term are expressed relative to the total number of 53 genes with either a binding region of untagged Efg1 or HA-Efg1 and Ace2-HA present in their 5'-UTR). *P* values for overrepresented categories were calculated using a hyper geometric distribution with multiple hypothesis correction according to the GO Term Finder tool. The *P* value cutoff used was 0.05. Colors indicate genes binding only untagged Efg1 (red), only HA-tagged Efg1 (blue) or both Efg1 versions (black). (B) Scheme depicting overlap between GO categories for common Efg1 and Ace2 target genes.

doi:10.1371/journal.pgen.1005447.g007

counteracting Efg1-mediated repression. In contrast to *BCR1* regulation, *BRG1* expression was upregulated in the wild-type strain under hypoxia and this upregulation was even enhanced in an *efg1* mutant but reduced in the *ace2* mutant. Thus, although *BCR1* and *BRG1* genes are regulated differently under hypoxia, Efg1 and Ace2 regulate these genes similarly, with Efg1 acting as repressor and Ace2 as an inducer of gene expression. Other genes encoding relevant transcription factors, including Tye7 [56], Aaf1 [53] and Zcf21 [60,70], were also controlled by Efg1/Ace2 (S7 Fig); these proteins regulate glycolysis, biofilm formation and/or commensalism of *C. albicans*.

In a previous report Bcr1 and Brg1 had been shown to bind to the *EFG1* promoter [42] suggesting feedback regulation between *EFG1-ACE2* and *BCR1/BRG1* genes under normoxia. To clarify the regulation under hypoxia *ACE2* and *EFG1* transcript levels were determined in *bcr1* or *brg1* mutants. The *ACE2* transcript was strongly downregulated in the *brg1* mutant in all conditions and largely increased in the *bcr1* mutant (not further increasing the already elevated level under hypoxia/CO_2) (Fig 8C). Thus, Brg1 activates and Bcr1 represses *ACE2* transcript levels. Brg1 also functions as an activator of the *EFG1* transcript under hypoxia, which did not increase in the *brg1* mutant in this condition.

On the other hand, gene products of *BCR1* and *BRG1* also mutually acted as negative regulators since the hypoxic downregulation of the *BCR1* transcript did not occur in a *brg1* mutant (showing even transcript upregulation) and the *BRG1* transcript was upregulated in the *bcr1* mutant under hypoxia (Fig 8D). Under normoxia, however, the *BRG1* transcript was strongly reduced in the *bcr1* mutant indicating that Bcr1 is a normoxic inducer but a hypoxic repressor for *BRG1*. Collectively, the results indicate that *EFG1*, *ACE2*, *BCR1* and *EFG1* genes form an interconnected regulatory hub, in which each participant regulates expression of the co-regulators. The transcriptional output of this unit is specific for hypoxia and is influenced significantly by CO_2 levels.

The Efg1-Ace2 regulatory hub regulates hyphal morphogenesis via the Cek1 pathway under hypoxia

The above transcript analyses had revealed that both *CEK1* and *CPH1* genes are repressed by Efg1 under hypoxia (Fig 4). Because Efg1 is part of an interconnected regulatory hub we re-examined the hypoxic/normoxic ratios of both transcripts in the respective mutant backgrounds (Fig 8E). In the wild-type strain, *CEK1* and *CPH1* transcripts were lowered in a hypoxic atmosphere without CO_2 but reached normoxic levels in the presence of CO_2 (Fig 8E). The repressive effect of Efg1 on both genes in this environment was clearly evident by strongly increased transcript levels in the *efg1* mutant. Under normoxia the Efg1 co-regulators Ace2, Bcr1 and Brg1 did not greatly influence *CEK1* or *CPH1* transcript levels. However, under hypoxia these regulators all repressed the *CEK1* transcript, while the *CPH1* transcript was downregulated only by Bcr1 (and Efg1). Consistently, protein levels of Cek1 and its phosphorylated form Cek1-P was upregulated under hypoxia (Fig 5A). Collectively, these results confirm the conclusion that Efg1 and its co-regulators control the Cek1 MAP kinase pathway.

To examine if and how members of the Efg1-Ace2 regulatory hub influence hyphal morphogenesis the colony phenotypes of control and mutant strains were recorded. Cells were

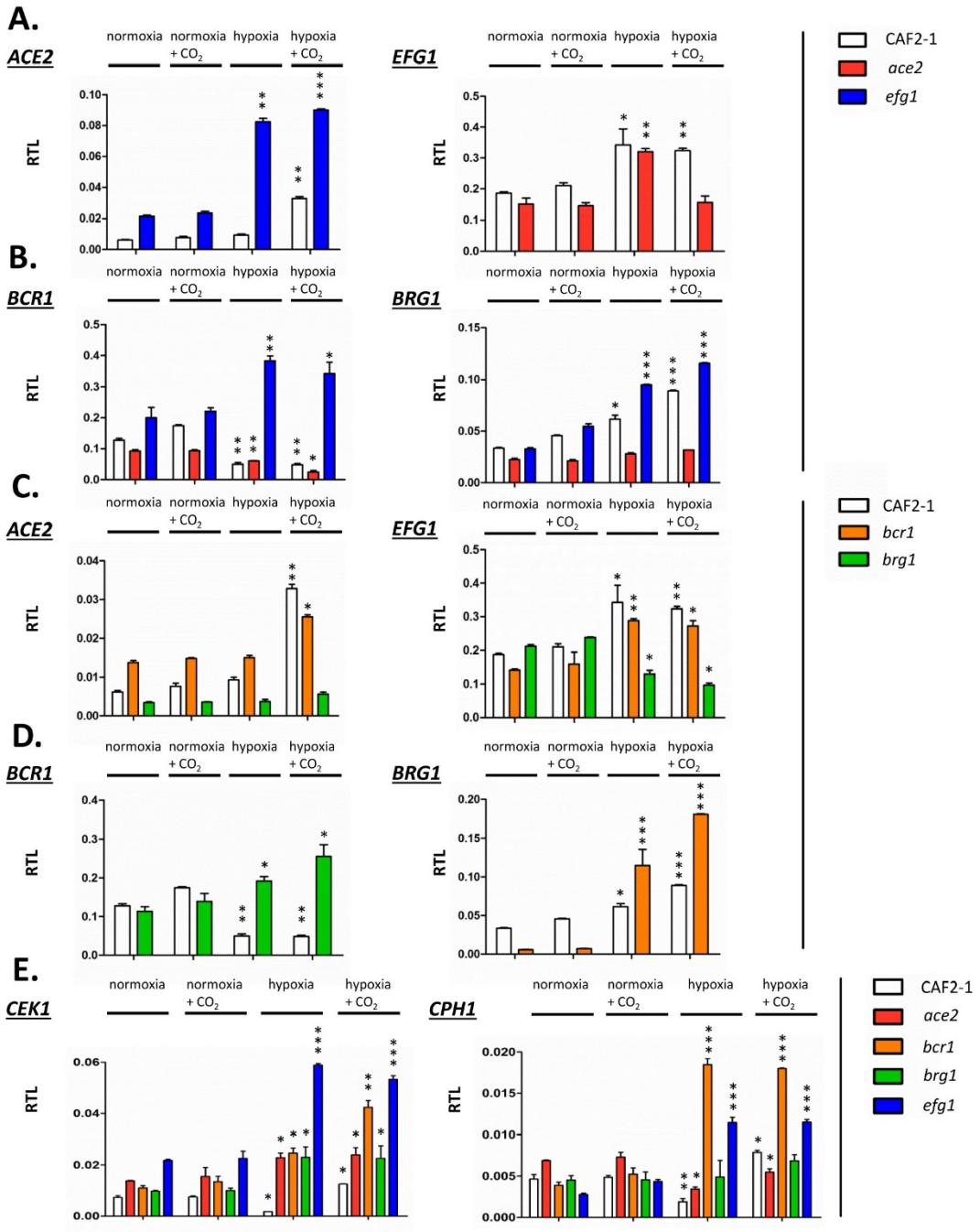

Fig 8. Transcriptional regulation of Efg1 and Ace2 target genes under hypoxia. Strains CAF2-1 (control), the *ace2* mutant MK106 and the *efg1* mutant HLC52 were precultured under normoxia at 30°C in YPD medium and used for inoculation of 100 ml YPD cultures. Cultures were incubated at 30°C under normoxia, under normoxia with addition of CO_2 (6%), under hypoxia (0.2% O_2) or under hypoxia with addition of CO_2 (0.2% O_2, 6% CO_2) until OD_{600} = 0.5 and total RNA was then isolated. Relative transcript levels were determined using *ACT1* transcript as the reference, as described in Fig 4. (A) Relative

transcript levels (RTL) for the *ACE2* transcript in strains CAF2-1 and HLC52 (*efg1*) and for the *EFG1* transcript in strains CAF2-1 and MK106 (*ace2*). (B to D) Relative transcript levels for the indicated transcripts in strains CAF2-1 (control), HLC52 (*efg1*), MK106 (*ace2*), CJN702 (*bcr1*) and strain TF022 (*brg1*). (E) Relative levels of *CEK1* and *CPH1* transcripts. Error bars represent standard deviation of the means. A two-tailed, unpaired t test comparing the cycle threshold values of samples grown in hypoxic and normoxic conditions for each mutant was used to determine the statistical relevance: *, $P < 0.05$; **, $P < 0.01$; ***, $P < 0.001$.

doi:10.1371/journal.pgen.1005447.g008

grown on YPS agar under hypoxia or normoxia, in the absence or presence of 6% CO_2 and at 25°C or 37°C. Under hypoxia, the control strain CAF2-1 showed no or sparse filamentation at 25°C but strong hypha formation at 37°C (Fig 9A). The *efg1* mutant was hyperfilamentous at 25°C but non-filamentous at 37°C verifying the previously reported dual repressor/activator role of Efg1 [19,23,29]. Strong hypha formation was also observed for the *bcr1* mutant at 25°C but unlike the *efg1* mutant, this mutant had a hyperfilamentous phenotype at 37°C. Both *ace2* and *brg1* mutant were defective in filamentation; this defect occurred for the *ace2* mutant in all conditions, whereas the *brg1* mutant was able to filament at 37°C in the presence of CO_2. Interestingly, under normoxia the wild-type strain presented vigorous filamentation at 37°C, while all single mutants showed complete or partial (*ace2* mutant) filamentation defects (S8 Fig). Thus, the Efg1, Ace2, Bcr1 and Brg1 regulators determine morphogenesis under both hypoxia and normoxia.

To establish if the hyperfilamentous phenotype of the *efg1* and *bcr1* mutants at 25°C requires Ace2 and/or Brg1 proteins double mutants were constructed and tested (Fig 9B). The construction of a homozygous *efg1 ace2* double mutant failed repeatedly suggesting that a *C. albicans* strain lacking both Efg1 and Ace2 is not viable; therefore, an *ace2/ace2 efg1/EFG1* heterozygous mutant (CLvW047) was constructed. Filamentation of the *efg1/EFG1* heterozygote was slightly but reproducibly increased at 25°C as compared to the control strain, while filamentation was reduced in strain CLvW047. The hyperfilamentous phenotype of the *bcr1* mutant (especially in the presence of CO_2) was also reduced in the *bcr1 ace2* double mutant. These results suggest that the increased hypha formation of *efg1* and *bcr1* mutants requires Ace2. The Brg1 protein is also needed for this phenotype because *efg1 brg1* and *bcr1 brg1* double mutants were completely defective for filamentation at 25°C; at 37°C, Brg1 was also needed for the *bcr1* phenotype in the absence of CO_2. In summary, the results indicate that hyphal morphogenesis of *C. albicans* under hypoxia is effectively repressed by Efg1 and Bcr1, counteracting the stimulatory effects of the Ace2 and Brg1 proteins.

Discussion

C. albicans is an opportunistic pathogen that inhabits the human host as a harmless commensal but that also can turn into a serious pathogen, which causes tenacious superficial and deadly systemic fungal disease. Candidiasis is typically caused by the strong proliferation of the same *C. albicans* strain that had inhabited the patient as a commensal before [6] raising questions about the molecular events that occur in the pathogen during the commensal-to-pathogen transition. As a commensal, *C. albicans* colonizes the gut and partly also mucosal surfaces [2,71–73]. Recent results have suggested that the fungus actively restrains its proliferation in the gut by transcriptional regulators Efg1 and Efh1 [7,8,74], while the Wor1 protein enhances gut colonization [9]. Events in the gut occur in oxygen-poor conditions (partly under anoxia) and mostly at elevated carbon dioxide concentrations [14,15]. Here we describe a transcriptional hub that downregulates filamentous growth of *C. albicans* and favors proliferation of its yeast form under hypoxic conditions. Surprisingly, this repressive activity involves regulators including Efg1, which positively regulate filamentation under normoxia.

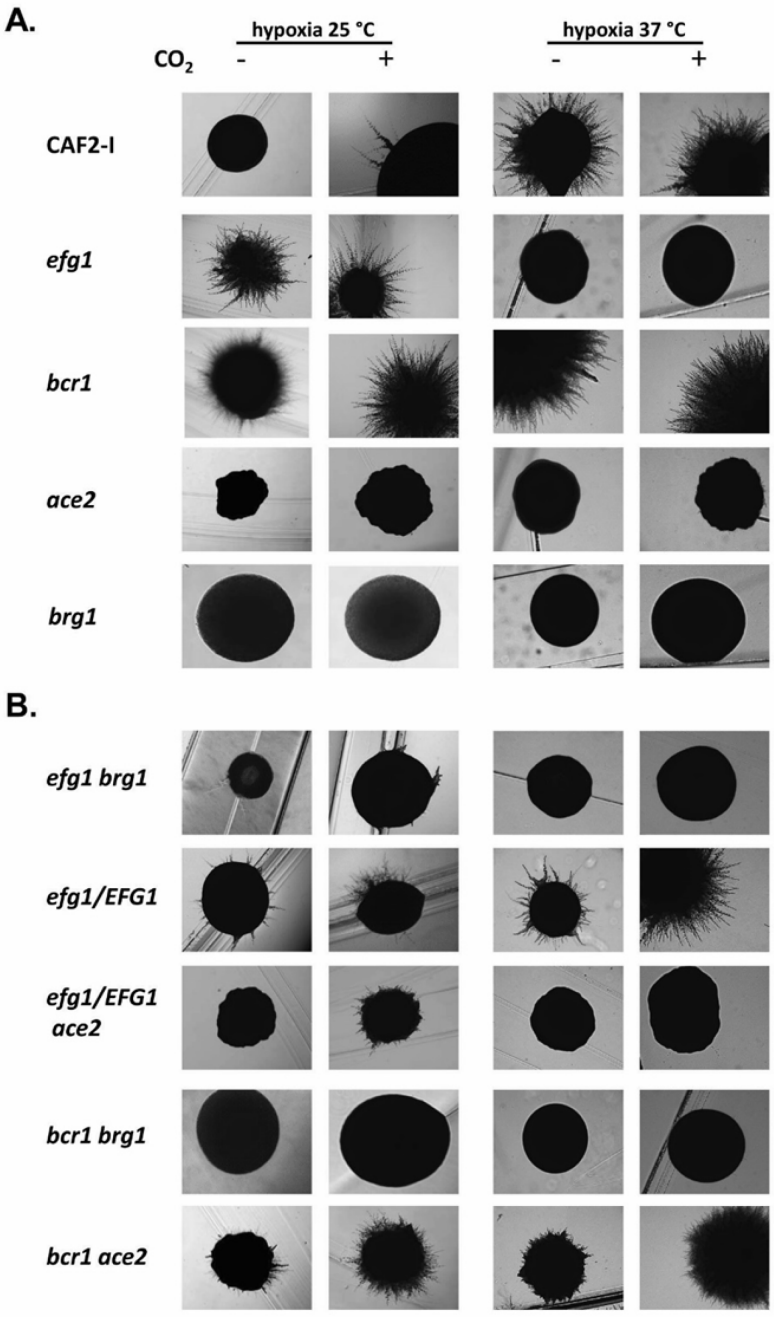

Fig 9. Hypoxic phenotypes of mutants lacking hypoxic regulators. The strains were grown under hypoxia (0.2% O_2) or hypoxia with 6% CO_2 on YPS agar for 4 d at 25°C or at 37°C for 3 d. (A) Strains included CAF2-1 (control), homozygous single mutants HLC52 (*efg1*), CJN702 (*bcr1*), MK106 (*ace2*) and TF022 (*brg1*). (B) Double knockout strains PDEB4 (*efg1 brg1*), PDBB4 (*bcr1 brg1*) and CLvW024 (*bcr1 ace2*) were tested. *ACE2* could not be disrupted in an *efg1* mutant background; therefore, the heterozygous mutant strain CLvW047 (*efg1/EFG1*, *ace2/ace2*) was constructed and its phenotype was compared to the *efg1/EFG1* strain DSC11.

doi:10.1371/journal.pgen.1005447.g009

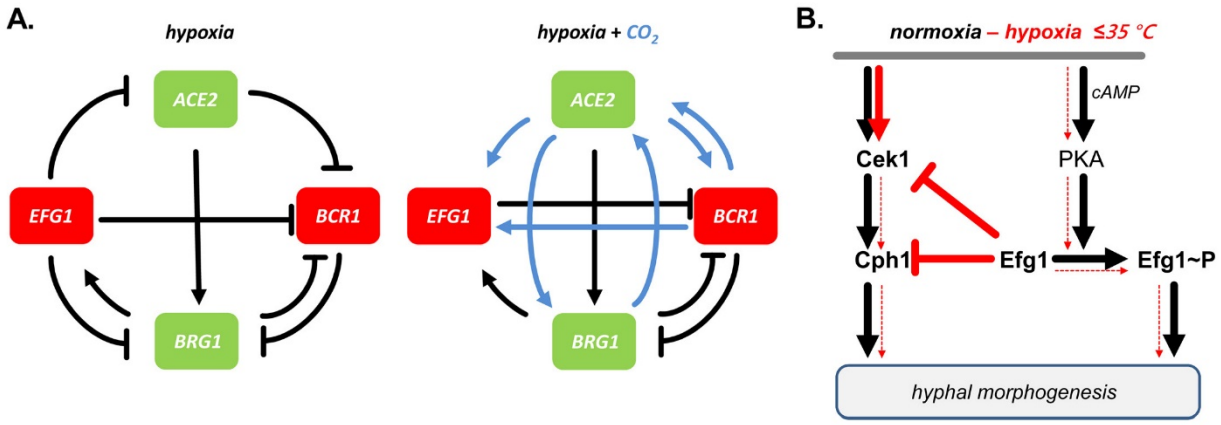

Fig 10. Models for transcriptional regulation and morphogenesis under hypoxia. (A) Transcriptional circuits. Hypoxic repressors Efg1 and Bcr1 (red) and hypoxic activators Ace2 and Brg1 (green) are mutually connected in regulatory circuits to regulate hypha formation of *C. albicans*. Note that regulatory circuits differ depending on the availability of CO_2 (blue arrows). (B) Morphogenetic signaling pathways. Under normoxia both Cek1 and PKA kinase pathways trigger hypha formation; Efg1 phosphorylation provides a major signalling input. Under hypoxia, at temperatures ≤ 35°C, low levels of Efg1 phosphorylation block the Cek1 pathway, thereby preventing hyphal induction by both pathways.

doi:10.1371/journal.pgen.1005447.g010

Efg1 directs several aspects of morphogenesis and metabolism in *C. albicans*. It has an important transcriptional role under hypoxia since it contributes to but also prevents hypoxic regulation of many genes [14,19]. The change to a hypoxia-specific pattern of gene expression requires Efg1 at an early time-point following a shift to hypoxia [25]. It is known that Efg1 has a dual role on hyphal morphogenesis: under hypoxia it acts as a hyphal repressor during growth on agar at temperatures ≤ 35°C [19,23,28], while under normoxia, Efg1 is a strong inducer of hypha formation [26,27]. The Efg1 signaling pathway under normoxia comprises adenylate cyclase Cyr1 activity that increases cAMP levels [46,47], which activates PKA isoforms Tpk1/Tpk2 and in turn Efg1 by phosphorylation of residue T206 [39]; an additional phosphorylation of T179 by the Cdc28-Hgc1 complex was also described to occur during hyphal morphogenesis [33]. Here we report that the hypoxic repressor function of Efg1 has specific structural requirements. Efg1 lost its repressor activity, when its N-terminal end was modified by extension and partially by deletion, while under normoxia such variants were active in hyphal induction [38]. Interestingly, chlamydospore formation, which is induced by oxygen limitation, also was found to require an undeleted N-terminus of Efg1 [28]. In addition, phosphomimetic residues at Efg1 phosphorylation sites (T179E, T206E) blocked the hypoxic repressor activity, while the corresponding alanine replacement variants were fully active in repression but inactive for the normoxic induction of hyphae [33,39]. This result corresponds to the lowered *CYR1* and *TPK1* transcript levels under hypoxia, which predicts lowered PKA activity and reduced T206 phosphorylation, thus resulting in enhanced hypoxic repressor activity of Efg1. With regard to Efg1 target sequences, the deduced CA-rich hypoxic binding sites did not match the major normoxic binding site TATGCATA for the yeast growth form, although Efg1 binds to CA- sequences shortly after hyphal induction [40]. Thus, the different functions of Efg1 as a hypoxic repressor involve different recognition and target sequences, as compared to normoxia.

Previously, synergistic and antagonistic functions of Efg1 and Ace2 transcription factors have been described. Both proteins enhance glycolytic and oxidative patterns of gene expression [23,30] and positively influence filamentation under normoxia [26,27,30–32]. In contrast,

under hypoxia Efg1 represses hypha formation [19,23,28], while Ace2 acts as an inducer [30,32]. Efg1 represses *ACE2* transcript levels, possibly by direct binding of Efg1 to the *ACE2* promoter [32]. To further characterize the functional intersection of both regulators we used ChIP chip analyses to compare their genomic binding patterns under hypoxia. A significant overlap of target genes was identified and the deduced Ace2 binding sequences in promoters included sequences resembling the ACCAGC motif for *S. cerevisiae* Ace2 [50] but also the above discussed CA-sequences representing hypoxic binding sites for Efg1. Interestingly, the group of genes targeted by both (HA-)Efg1 and Ace2 included important regulators of hyphal growth, biofilm formation and cell adhesion. Targets included the *EFG1* promoter, which thereby was confirmed not only as an autoregulatory target for Efg1 [40] but also identified as an Ace2 target. Confirming this result, Ace2 was required for upregulation of the *EFG1* transcript in a hypoxic CO_2-containing atmosphere, while Efg1 repressed the *ACE2* transcript as under normoxia [32]. We analyzed the mode of joint target gene regulation by the Efg1/Ace2 proteins by focusing on *BCR1* [52,66,67] and *BRG1 (GAT2)* [51,68,69], which regulate filamentation and were found to get hypoxically down- and, respectively, upregulated. Surprisingly, these genes were not only targets but also regulators of Efg1/Ace2 and they negatively regulated each other, thereby generating an interconnected regulatory loop (Fig 10A). Efg1 acted as hypoxic repressor of *BCR1/BRG1* and also of two other target genes (*TYE7*, *ZCF21*), while it was an inducer of *AAF1* expression (S3 Fig). In general, Ace2 activated hypoxic expression of all of these genes, especially in the presence of CO_2. Transcripts of hypoxia-upregulated genes including *EFG1*, *BRG1* and *TYE7* and of hypoxia-downregulated genes including *BCR1*, *AAF1* and *ZCF21* were all reduced if *ace2* mutant cells were grown hypoxically in the presence of CO_2. Interestingly, Ace2 bound strongly to the promoter of the *FLO8* gene, which encodes a CO_2 sensor interacting with Efg1 [38,62] that is required for white-to-opaque switching and for filamentous growth [61]. Thus, the lack of oxygen combined with an increased level of CO_2 generates an environment that elicits a specific regulatory response in *C. albicans*. These results are reminiscent of and confirm previous results for the hypoxia-specific, CO_2-dependent functions of Sch9 kinase [37] and the Ume6 regulator [75].

The morphogenetic output of the described hypoxic regulatory hub was tested by examining hypha formation on agar. The results confirmed that Ace2 is a positive factor for filamentation under hypoxia and partly also under normoxia [30,32], while Efg1 has a dual repressor/activator function under hypoxia/normoxia. Similar to Efg1, Bcr1 acted as a repressor of hypha formation at 25°C, especially in the presence of CO_2. Transcript data suggested that in this environment, Ace2 stimulates *BCR1* expression to ensure efficient blockage of hypha formation. Brg1 was needed for hypha formation at 37°C under hypoxia, but only in the absence of CO_2; in its presence, Brg1 was dispensable for filamentation. The *BRG1* transcript was repressed by Efg1 and activated by Ace2, largely independent of CO_2. As shown by the phenotypes of double mutants the increased filamentation of *efg1* and *bcr1* mutants depended on the activity of both Brg1 and Ace2. Thus, under hypoxia *C. albicans* restrains the stimulatory actions of both Brg1 and Ace2 on hyphal morphogenesis, using Efg1 and Bcr1 as repressors. While this study puts its focus on hypha formation, it is likely that other adaptation processes occurring under hypoxia, especially re-direction of metabolism to a fermentative mode, are regulated by transcription factors that link to the Efg1-Ace2 regulatory hub. Relevant transcription factors for this function could include Tye7 [56], Aaf1 [53] and Zcf21 [60], proteins that regulate glyolysis, biofilm formation and/or commensalism.

Which signaling pathway of morphogenesis is downregulated by Efg1 or Bcr1 proteins? Transcript analyses revealed that the genes encoding MAP kinase Cek1, its downstream target Cph1 and the kinase Kic1 are downregulated specifically under hypoxia by Efg1. The Cek1/Cph1 pathway is known to permit filamentation under normoxia during surface growth of

C. albicans [43–45], while in *S. cerevisiae*, Kic1 is part of the RAM pathway that activates Ace2 activity [48]. The repressive action of Efg1 and its co-regulators on the Cek1 pathway was verified by demonstrating that Efg1, Ace2, Bcr1 and Brg1 all act as repressors of *CEK1* transcript levels, while the *CPH1* transcript was especially repressed by Bcr1 and Efg1. Furthermore, Efg1- and Ace2-mediated repression of the Cek1 protein in its non-phosphorylated and phosphorylated form was also demonstrated. Confirming these results, an *efg1 cph1* double mutant was unable to filament, while overexpression of *CPH1* in a wild-type genetic background triggered hypha formation under hypoxia. These results clearly indicate that *C. albicans* actively suppresses filamentation mediated by the Cek1 pathway in certain oxygen-poor conditions to promote proliferation of the yeast form (Fig 10B). We have discovered this suppression *in vitro* slightly below the core body temperature (i. e. $< 37°C$) but this activity may also occur in the special molecular environment of the gastrointestinal tract or in hypoxic skin tissue [16,17]. Nevertheless, this scenario does not exclude that upregulation of hypoxic filamentation may occur under hypoxia, e. g. if the repressive action of Efg1 is blocked by the Czf1 protein [4]. In this situation, other regulators including Mss11 and Rac1, which were identified by their embedded growth phenotypes [76,77], may also promote hypoxic filamentation. A similar hyperfilamentous phenotype was also reported for mutants lacking the kinase Sch9, although elevated CO_2-levels were required in this case [37]. In the human gut, locally increased filamentation could favor anchoring of *C. albicans* to the epithelium and trigger strong fungal proliferation and systemic invasion mediated by invasion-specific regulators including Eed1 [8,55]. These events may initiate the pathogenic stage of fungal colonization, which will ultimately become apparent by the symptoms of disease. It appears that as a commensal *C. albicans* attempts to avoid immune responses and to maintain its residency by downregulation of filamentation and possibly other virulence traits. Strengthening of fungal commensalism, e. g. by novel therapeutic molecules or by probiotic microbes could become a promising strategy to combat serious fungal disease.

Materials and Methods

Strains and media

C. albicans strains are listed in S4 Table. Strains were grown in liquid YP medium (1% yeast extract, 2% peptone) containing 2% glucose (YPD) or 2% sucrose (YPS); solid media contained 2% agar. An Invivo200 hypoxia chamber (Ruskinn) was used for hypoxic growth under 0.2% O_2 [37]; liquid media were pre-equilibrated overnight under hypoxia before inoculation. Strains overexpressing genes using tetracyclin-inducible promoters were grown in/on YPS medium containing 3 μg/ml anhydrotetracycline.

C. albicans strains expressing *EFG1* variants

Oligonucleotides are listed in S5 Table. Plasmid pTD38-HA contains promoter and coding region for an N-terminally hemagglutinin (HA)-tagged Efg1 [38]. In this plasmid, HA-encoding sequences reside on a *Bgl*II and *Bam*HI fragment, which were removed in plasmid pPRDEFG1, in which the native *EFG1* ORF is preceded by a *Bam*HI site. Other plasmids carrying *EFG1* genes encoding Efg1 variants without HA tag were constructed in two steps, as in the case of pPRDNEFG1, in which nucleotides 25 and 222 of the *EFG1* ORF are deleted encoding a variant lacking residues Y9 to G74 of Efg1. Primers EFG1BamHIFor and EFG1BamHIRev were used for PCR amplification of the ORF of this variant, using plasmid pBI-HAHYD-D1 [38] as the template. The *Bam*HI-digested PCR fragment was inserted downstream of the *EFG1* promoter by ligation with the large *Bgl*II fragment of pTD38-HA to generate plasmid p2621NΔEFG1. The *Pac*I-*Spe*I fragment of this plasmid carrying the junction of the *EFG1*

promoter and its ORF was then used to replace the corresponding fragment in pTD38-HA. By this procedure, the mutated *EFG1* ORF was joined to its 3´-UTR. Similarly, the mutated *EFG1* alleles encoding the T206A and T206E mutations were transferred from plasmids pDB1 and pDB2 [39] into pTD38-HA to generate plasmids pPDEFG1T206A and pPDEFG1T206E. Analogous plasmids encoding T179A and T179E Efg1 variants were constructed by mutating the *EFG1* ORF by primer pairs EFG1179AFor/Rev and T179Efor/rev, respectively, using site-directed mutagenesis (QuikChange kit, Stratagene). The resultant plasmids pPDEFG1T179E and pPDEFG1T179A encode T179A and T79E variants of Efg1, respectively. All constructs were sequenced using primers EFG1seqFor, EFG1seqRev and Efg1SeqM to confirm the presence of the mutations within *EFG1*.

Plasmids were integrated into the chromosomal *EFG1* locus of *efg1* mutant HLC67 by transformation following digestion with *Pac*I in the *EFG1* promoter [38]. Their correct chromosomal integration was verified by PCR of gDNA using primers UTREfg1For and Efg1seqM.

C. albicans strains expressing HA-tagged Ace2

For localization studies of Ace2 a heterozygous mutant strain was constructed first. One *ACE2* ORF was replaced with a *lacZ-ACT1p-SAT1* cassette. The cassette was amplified from plasmid pStLacZ-SAT. All PCR products were separated on an agarose gel and purified using the QIAquick Gel Extraction Kit (Qiagen) before transformation. The oligonucleotides (lacZACE2for/lacZACE2rev) used for amplification, tagged the cassette with 90 bp of flanking sequence complementary to the *ACE2* ORF. The strain BWP17 was transformed and transformants were screened for nourseothricin resistance. Integration of the *lacZ-ACT1p-SAT1* cassette and replacement of the *ACE2* ORF was verified by Southern blot analysis using a probe for *SAT1*. The resulting heterozygous strain CLvW001 (*ace2-lacZ-ACT1p-SAT1/ACE2*) was used for C terminal tagging of Ace2. Oligonucleotides ACE2HAFor and ACE2HARev were used to amplify the triple HA-encoding sequence from plasmid p3HA-URA3 thereby adding homologous sequences of the 3‘- end of the *ACE2* ORF and 5‘-UTR of the *ACE2* allele to the amplicon. Strain CLvW001 was transformed for C terminal tagging of the remaining *ACE2* allele. Correct chromosomal integration at the *ACE2* locus was confirmed by colony-PCR using oligonucleotides ACE2For and HARev and by Southern blot analysis. The resulting strain CLvW004, expressing C-terminal HA-tagged Ace2 at the native locus was used to study chromosomal localization of Ace2-HA.

Construction of *ACE2* deletion strains

For the deletion of *ACE2* in the *bcr1* and *efg1* mutant background and in strain CAI4, plasmid pSFS5 was used, containing a modified *SAT1* flipper cassette [78]. The *ACE2* upstream and downstream regions were amplified with the oligonucleotide pairs CAF1ApaI/CAF2XhoI and CAR1SacII/CAR2SacI, for construction of the inner deletion cassette, and oligonucleotide pairs CAF3ApaI/CAF4XhoI and CAR3SacII/CAR4SacI for construction of the outer deletion cassette; the *ace2* mutant strain MK106 described by Kelly *et al.* [24] was used as the reference strain. gDNA of strain SC5314 was used to generate PCR products, which were digested with the indicated restriction enzymes and cloned on both sites of the *SAT1* flipper cassette in pSFS5 [78] resulting in plasmids pCLvW90 (inner cassette) and pCLvW91 (outer cassette). The deletion cassettes in plasmids pCLvW90 and pCLvW91 were released by digestion with *Sac*I and *Apa*I and used for transformation of strains using first the fragment containing the outer cassette and, after excision of the *SAT1* flipper cassette, with the second fragment containing the inner cassette. Integration of the deletion cassette was confirmed by colony PCR using oligonucleotides FLP1, which binds within the *FLP1* gene, and ACE2UTR5, which binds

upstream of the *ACE2* ORF. Transformants containing the *ACE2* deletion cassette were grown overnight in liquid YCB-BSA medium (20 g yeast carbon base, 4 g bovine serum albumin and 2 g yeast extract per liter) to induce excision of the cassette by FLP-mediated recombination; corresponding strains were identified by their small colony size on YPD plates containing 25 μg/ml nourseothricin. After excision of the second *SAT1* flipper cassette, deletion of both *ACE2* alleles was confirmed by Southern blot analysis. With this approach both *ACE2* alleles were deleted in the *bcr1* mutant strain CJN702 [52] resulting in strain CLvW024 and in CAI4 resulting in strain CLvW008. However, deletion of the second *ACE2* allele in the *efg1* mutant HLC52 [27] was not successful.

In an additional approach we tried to generate the *ace2 efg1* double knockout strain by deleting *EFG1* in the *ace2* mutant strain CLvW008 with the Ura-blaster disruption technique [79] but again we were not able to obtain a homozygous mutant strain suggesting that the double knockout is lethal. The *URA3* deletion cassette used for this approach was released from plasmid pBB503 [80] by digestion with *Hin*dIII and *Kpn*I. The fragment was purified and transformed into strain CLvW008 and transformants were selected for uridine prototrophy on SD agar. Integration of the cassette was confirmed by colony-PCR. In the resulting strain CLvW041 one chromosomal copy of *EFG1* was replaced by the sequence of *URA3* flanked by *hisG* sequences (*efg1*::*hisG-URA3-hisG*/*EFG; ace2*::*FRT*/*ace2*::*FRT*). Attempts to delete the second *EFG1* allele after removal of *URA3* [79] were not successful.

Construction of *BRG1* deletion strains

For deletion of *BRG1* gene in *efg1* (HLC52) and *bcr1* (CJN702) mutants the upstream region of the *BRG1* ORF was amplified by genomic PCR using primers BRG1 5UTRKpnIFor/KpnIRev and cloned into the *Kpn*I site of plasmid pSFS5 to generate pSFS5-B5. The *BRG1* downstream region was amplified using primers BRG13UTRNot1For/SacIRev and cloned into *Not*I and *Sac*I sites of pSFS5-B5 to generate pSFS5-B5B3. The *Kpn*I-*Sac*I fragment of this plasmid was used to transform *efg1* and *bcr1* mutant strains, selecting transformants on YPD agar containing nourseothricin (200 μg/ml). Correct genomic integration was confirmed by colony PCR using oligonucleotides FLP1, which binds within the *FLP1* gene, and BRG1UpFor, which binds upstream of the *BRG1* promoter region. Verified heterozygous transformants were grown in YCB-BSA medium to evict the disruption cassette and retransformed with the disruption fragment, as described [78]. Deletion of both *BRG1* alleles was confirmed by negative colony PCR using primer BRG1UpFor, which binds upstream to the *BRG1* ORF and BRG1midrev that is specific for the *BRG1* ORF. *BRG1* alleles were deleted in *efg1* (HLC52) and *bcr1* (CJN702) mutant strains resulting in strains PDEB4 (*efg1 brg1*) and PDBB4 (*bcr1 brg1*) respectively.

C. albicans strains overproducing signalling components

The plasmids pClp10TETSTE11, pClp10TETCEK1 and pClpTETCPH1 [81] encoding Ste11, Cek1 and Cph1 proteins were linearized with *Stu*I within the *RPS1* sequence and transformed into *C. albicans* CEC2907 [81] selecting for uridine prototrophy; the resultant strains were named CECSTE11, CECCEK1 and CECCPH1. Correct plasmid integration at the *RPS1* locus was confirmed by colony PCR using primers ClpUL and ClpUR.

Generation of an anti-Efg1 antiserum

A rabbit polyclonal anti-Efg1 antiserum was generated using His_{10}-tagged Efg1 produced in *E. coli*. The *EFG1* ORF (allele *ORF19.8243*) residing on a *Xho*I-*Bam*HI fragment was subcloned into pET19b (Novagen), downstream of the T7 RNA polymerase promoter. The resulting plasmid encoded a His_{10}-Efg1 fusion but contained a single CUG codon (residue 449) that encodes

serine in *C. albicans* but leucine in *E. coli*. This codon was changed to a UCG serine codon by site-directed mutagenesis using oligonucleotides pET19Serinhin/her, resulting in plasmid pET19-His-Efg1Kodon, which was transformed into *E. coli* Rosetta 2 (DE3)pLysS (Merck). Transformants were grown and the T7 promoter was induced according to instructions of the manufacturer. Cells were resuspended in buffer (20 mM CAPSO pH 9.5, 1 M NaCl, 1 mM EDTA, 20 mM imidazol, 0.1% Triton X100) and broken using 3 passages through a French press cell (Slaminco Spectronic Instruments). Crude extracts were cleared by centrifugation and applied to HisTrap columns connected to an ÄKTA prime plus fraction collector (GE Healthcare). The His_{10}-Efg1 fusion protein was eluted using CAPSO buffer containing 250 mM imidazol. Purified protein (100 µg) was injected on days 1, 14, 28 and 56 in 2 New Zealand White rabbits (performed by Eurogentec, Belgium). One rabbit generated high anti-Efg1 titers in ELISA tests and in immunoblottings (dilution 1:5000).

Immunodetection

YPD precultures were grown under normoxia overnight at 30°C in YPD medium and were used to inoculate 40 ml of YPD medium, which had been preincubated overnight under hypoxia (0.2% O_2). Starting with an initial density of OD_{600} = 0.1 cells were grown at 30°C under hypoxia to an OD_{600} = 1. Cells were harvested, frozen at -70°C for 1 h and then thawed by addition of 500 ml of CAPSO buffer (20 mM CAPSO pH 9,5, 1 M NaCl, 1 mM EDTA, 20 mM imidazole, 0,1% Triton X-100) containing protease inhibitor (Cocktail Complete, Mini, EDTA-free/Roche). Cells were broken at 4°C by shaking with one volume of glass beads (0.45 mm) in a FastPrep-24 shaker (MP Biomedicals) using 4–6 cycles for 40 s at 6.5 ms^{-1}; between cycles cells were placed on ice for 5 min. Debris was removed by centrifugation at 13,000 rpm for 5 min and protein in the supernatant was determined using the Bradford assay. 45 µg of the crude cell extract was separated by SDS-PAGE (8% polyacrylamide) and analysed by immunoblotting using anti-Efg1 antiserum (1:5,000) or anti-histone H4 (Abcam; 1:5,000) to detect histone H4 as loading control. Total Cek1 levels were detected by immunoblotting using anti-Cek1 antiserum [10], while phosphorylated Cek1 was detected using monoclonal rabbit anti-phospho-p44/42 antibody (Cell Signaling Technology). Anti-rabbit-IgG-HRP conjugate (1:10,000) was used as secondary antibody in all blottings. Signals generated by the chemiluminescent substrate (SuperSignal West Dura; Pierce) were detected by a LAS-4000 mini imager (Fujifilm) and evaluated by the Multi Gauge Software (Fujifilm).

Chromatin immunoprecipitation on microchips (ChIP chip)

The ChIP chip procedure was performed as described by Lassak *et al.* [40], except that the strains and antibodies used for immunoprecipitation were different. Two independent cultures were assayed for each combination of strains. Precultures were grown overnight under normoxia at 30°C in YPD medium and were shifted to YPD medium precalibrated under hypoxia (0.2% O_2, 30°C). The cells were allowed to grow from OD_{600} = 0.1 to 1. Two sets of strains were analysed: (1) wild-type strain CAF2-1 as test strain and *efg1* mutant HLC52 as control strain were compared to determine the genomic localization of untagged Efg1, using anti-Efg1 antibody for chromatin immunoprecipitation; (2) Strain HLCEEFG1 producing HA-tagged Efg1 as test strain and DSC11 (Efg1 producing) as control strain were compared to determine the genomic localization of HA-Efg1 using anti-HA antibody for chromatin immunoprecipitation. *C. albicans* genomic tiling microarrays were probed pairwise by immunoprecipitated chromatin as described previously [40]. For localization studies of Ace2, precultures were grown overnight under normoxia at 30°C in YPD medium and were used to inoculate medium preincubated under normoxia or hypoxia (0.2% O_2) with addition of 6% CO_2. Strain

CLvW004, producing HA-tagged Ace2 from its native locus and control strain BWP17 were used to determine the genomic localization of Ace2-HA using anti-HA antibody for immunoprecipitation. Significant binding peaks were defined as probes containing four or more signals above background in a 500 bp sliding window; the degree of significance depended on the FDR value. Results were visualized using the program SignalMap (version 1.9). The most significant binding peaks (FDR $\leq$ 0.05) for Efg1 (202 peak genomic binding sites), HA-Efg1 (106 peak genomic binding sites) and Ace2-HA (272 peak genomic binding sites), which coincided in both replicates, were analysed by the program RSAT dyad-analysis to predict DNA binding sequence [40].

Supporting Information

S1 Fig. Activity of rabbit anti-Efg1 antiserum. (A) Immunoblotting. Extracts of *efg1* mutant HLC67 (lane 2) and control strain CAF2-1 (lane 3) were separated by SDS-PAGE and blots were probed with anti-Efg1 antiserum (1: 5000). For comparison, 250 ng of *E. coli*-produced His_{10}-Efg1 protein was used (lane 1). (B) Immunoprecipitation. Efg1 was immunoprecipitated using anti-Efg1 antiserum and protein G-coated agarose beads. Immunoprecipitates from the control strain CAF2-1 (lane 1) and the *efg1* mutant HLC67 (lane 2) were analysed by immunoblotting using anti-Efg1 antiserum. The arrow indicates the migration of Efg1.
(PDF)

S2 Fig. Intersection of genomic binding sites for Efg1 and HA-Efg1 under hypoxia and normoxia. For Efg1, genomic binding sites were derived from ChIP chip experiments comparing strains CAF2-1 (*EFG1/EFG1*) and HLC52 (*efg1/efg1*); for HA-Efg1, strains HLCEEFG1 (*efg1/efg1* [*HA-EFG1*]) and CAF2-1 were compared. Normoxic binding sites for HA-Efg1 were obtained from Lassak *et al.* [40]. The shaded circle encompasses genes in filamentous growth.
(PDF)

S3 Fig. GO categories of genes binding HA-Efg1 under hypoxia. GO terms for Efg1 binding targets were identified in ChIP chip data using the CGD GO Term Finder tool (http://www.candidagenome.org/cgi-bin/GO/goTermFinder); the analysis was conducted in June 2013. Genome frequencies of genes corresponding to GO terms are expressed as percentages (gene number relative to 6,525 genes in the *C. albicans* genome; the frequency of genes binding Efg1 that correspond to a specific GO term are expressed relative to the total number of 106 genes binding HA-Efg1). Superscripts: a, Efg1 binding in yeast normoxia [40]; b, Efg1 binding in hyphae inducing conditions [40]; c, Efg1 binding in biofilm inducing conditions [42]. *P* values for overrepresented categories were calculated using a hyper geometric distribution with multiple hypothesis correction according to the GO Term Finder tool website (http://www.candidagenome.org/help/goTermFinder.shtml). The *P* value cutoff used was 0.05.
(PDF)

S4 Fig. Functionality of the HA tagged Ace2 protein. To verify the functionality of C-terminal HA-tagged Ace2 the phenotypes of three isolates of strain CLvW004 (*ACE2-HA/ace2*) was compared to mutant strain MK106 (*ace2/ace2*), wild-type strain BWP17 (*ACE2/ACE2*) and the heterozygous strain CLvW001 (*ACE2/ace2*). (A) Drop dilution assay for sensitivity to 4 μM Pmt1-inhibitor [49] and resistance to antimycin A (20 μg/ml). The agar plates were photographed after 2 d incubation at 30°C. The *ace2* mutant strain Mk106 shows enhanced sensitivity to the Pmt1-inhibitor and is less susceptible to the respiratory inhibitor antimycin A [30]. (B) Colonies of the indicated strains were photographed following growth for 2 d at 30°C on YPD agar. The *ace2* mutant strain Mk106 shows the wrinkled colony phenotype described previously [24]. Phenotypes of strains CLvW004.1–3 correspond to the heterozygous strain

CLvW001 indicating that the Ace2-HA protein in these strains is functional.
(PDF)

S5 Fig. Genomic binding sites for Ace2 under hypoxia and normoxia. Venn diagram showing numbers of genes bound by HA-tagged Ace2 under normoxic conditions (30°C, YPD) and hypoxic conditions (30°C, YPD 0.2% O_2 and 6% CO_2). Binding regions with the corresponding ORFs are listed in S2 and S3 Table. Genomic binding sites were derived from ChIP chip experiments comparing strains ClvW004 (*ACE2-HA/ace2*) and BWP17 (non tag control).
(PDF)

S6 Fig. Genomic localization of Ace2 and Efg1 on target promoters. (A) Binding positions identified by ChIP chip experiments. Binding positions of Efg1 (black ovals), Ace2-HA (orange ovals) and HA-Efg1 positions (grey ovals) identified by ChIP chip experiments are shown schematically. (B) Quantitation of Ace2, HA-Efg1 and Efg1 enrichment by ChIP on target promoters. Following ChIP the respective fold enrichment was determined by qPCR using oligonucleotide pairs shown by red arrows in A. Chromatin of strains CAF2–1 (Efg1) and HLCEEFG1 (HA-Efg1) was immunoprecipitated using anti-Efg1 and anti-HA antibody, respectively, as described in S1 Table. For Ace2 enrichment anti-HA antibody was used for immunoprecipitation of strain CLvW004 (Ace2-HA), as described in S2 Table. In a control experiment, ChIP followed by qPCR was also done using anti-Efg1 antibody on extracts of strain HLCEEFG1 (HA-Efg1). qPCR experiments were done using two biological replicates, which were assayed in triplicate. The mean fold enrichment (± standard deviation) for each protein was calculated relative to the respective no tag or mutant strain and normalized to the input sample. Statistical relevance is indicated by asterisks: *, $P < 0.05$; **, $P < 0.01$; ***, $P < 0.001$. The results verify the presence of proteins on target promoters; in addition, the presence of HA-Efg1 on the *BCR1* promoter, which was not found in the ChIP chip experiment, was revealed by the ChIP-qPCR experiment.
(PDF)

S7 Fig. Transcriptional regulation of selected Efg1 and Ace2 target genes under hypoxia. Strains CAF2-1 (control), the *ace2* mutant MK106 and the *efg1* mutant HLC52 were precultured under normoxia at 30°C in YPD medium and used for inoculation of 100 ml YPD cultures. Cultures were incubated at 30°C under normoxia, or normoxia with addition of CO_2 (6% CO_2), or under hypoxia (0.2% O_2), or under hypoxia with addition of CO_2 (0.2% O_2, 6% CO_2) until $OD_{600} = 0.5$ and total RNA was then isolated. Relative transcript levels were determined using *ACT1* transcript as the reference as described in Fig 4. Relative transcript levels (RTL) for the *AAF1*, *TYE7* and *ZCF21* transcripts in strains CAF2-1 (control), HLC52 (*efg1*) and MK106 (*ace2*). Error bars represent standard deviation of the means. A two-tailed, unpaired *t* test comparing the cycle threshold values of samples grown in hypoxic and normoxic conditions for each mutant respectively was used to determine the statistical relevance: *, $P < 0.05$; **, $P < 0.01$; ***, $P < 0.001$.
(PDF)

S8 Fig. Normoxic phenotypes of mutants lacking hypoxic regulators under hypoxia. The strains were grown under normoxia without or with 6% CO_2 on YPS agar for 4 d at 25°C or at 37°C for 3 d. Strains included CAF2-1 (control), homozygous single mutants HLC52 (*efg1*), CJN702 (*bcr1*), MK106 (*ace2*), TF022 (*brg1*) and double knockout strains PDEB4 (*efg1 brg1*), PDBB4 (*bcr1 brg1*) and CLvW024 (*bcr1 ace2*). *ACE2* could not be disrupted in an *efg1* mutant background; therefore, the heterozygous mutant strain CLvW047 (*efg1/EFG1*, *ace2/ace2*) was constructed and its phenotype was compared to the *efg1/EFG1* strain DSC11.
(PDF)

S1 Table. Binding of Efg1 to chromosomal sequences of *C. albicans* under hypoxia. Strain CAF2-1 producing wild-type Efg1 was grown in YPD medium at 30°C under hypoxic conditions (0.2% O_2), chromosomal cross-linking of proteins was done. Fragmented chromatin was immunoprecipitated using anti-Efg1 antibody and used as probe for tiling microarrays covering the *C. albicans* genome. Regions showing significantly increased binding of Efg1 compared to control strain HLC52 (*efg1/efg1*) are listed along with their nearest neigbouring ORFs designated left or right ORF if situated at descending and, respectively, ascending chromosomal coordinates. ORF orientations are indicated by the arrows. Other proteins binding to the same chromosomal region are also indicated. Binding regions within coding regions are marked in purple lettering and green shading indicates multiple binding regions. *, significant binding regions that do not overlap in both replicates.
(XLSX)

S2 Table. Binding of Ace2-HA to chromosomal sequences of *C. albicans* under hypoxia and CO_2. Strain CLvW004 producing Ace2-HA from its chromosomal ORF and reference strain BWP17 were grown in YPD medium at 30°C under hypoxic conditions and in presence of elevated CO_2 levels (0.2% O_2 and 6% CO_2). Chromosomal cross-linking of proteins was done and chromatin was fragmented before immunoprecipitation. For immunoprecipitation anti-HA antibody was used and the precipitated chromatin was spotted on a *C. albicans* whole-genome tiling microarray. Regions showing significant enrichment of Ace2-HA binding compared to control strain BWP17 are listet along with their nearest neighbouring ORFs. Other proteins binding to the same chromosomal region are indicated and are taken from Lassak *et al.* [40]. Binding targets of wild-type Efg1 or HA-Efg1 shared with Ace2-HA are indicated with red background color. Accordingly to transcriptomal data obtained by Mulhern *et al.* [30], up- and down-regulation of genes is indicated of identified Ace2-HA target genes.
(XLSX)

S3 Table. Binding of Ace2-HA to chromosomal sequences of *C. albicans* under normoxia. Strain CLvW004 producing Ace2-HA from its chromosomal ORF and reference strain BWP17 were grown in YPD medium at 30°C under normoxic conditions. Chromosomal cross-linking of proteins was done and chromatin was fragmented before immunoprecipitation. For immunoprecipitation anti-HA antibody was used and the precipitated chromatin was spotted on a *C. albicans* whole-genome tiling microarray. Regions showing significant enrichment of Ace2-HA binding compared to control strain BWP17 are listet along with their nearest neighbouring ORFs. Other proteins binding to the same chromosomal region are indicated and are taken from Lassak *et al.* [40]. Binding targets of wild-type Efg1 or HA-Efg1 shared with Ace2-HA are indicated with red background color, binding targets of Ace2-HA obtained uniquely under normoxic conditions are indicated with green background color. Accordingly to transcriptomal data obtained by Mulhern *et al.* [30], up- and down-regulation of genes is indicated of identified Ace2-HA target genes.
(XLSX)

S4 Table. *C. albicans* strains.
(PDF)

S5 Table. Oligonucleotides.
(PDF)

Acknowledgments

We thank C. D´Enfert, S. Noble and A. Mitchell for providing strains and/or plasmids. We are grateful to E. Román and J. Pla for supplying the anti-Cek1 antibody.

Author Contributions

Conceived and designed the experiments: JFE. Performed the experiments: PRD LvW DK MJ. Analyzed the data: PRD LvW JFE. Wrote the paper: PRD LvW JFE.

References

1. Scanlan PD, Marchesi JR. Micro-eukaryotic diversity of the human distal gut microbiota: qualitative assessment using culture-dependent and-independent analysis of faeces. ISME J. 2008; 2: 1183–1193. doi: 10.1038/ismej.2008.76 PMID: 18670396
2. Ghannoum MA, Jurevic RJ, Mukherjee PK, Cui F, Sikaroodi M, Naqvi A, et al. Characterization of the oral fungal microbiome (mycobiome) in healthy individuals. PLoS Pathog. 2010; 6: e1000713. doi: 10.1371/journal.ppat.1000713 PMID: 20072605
3. Iliev ID, Funari VA, Taylor KD, Nguyen Q, Reyes CN, Strom SP et al. Interactions between commensal fungi and the C-type lectin receptor Dectin-1 influence colitis. Science. 2012; 336: 1314–1317. doi: 10.1126/science.1221789 PMID: 22674328
4. Brown DH Jr, Giusani AD, Chen X, Kumamoto CAFilamentous growth of *Candida albicans* in response to physical environmental cues and its regulation by the unique *CZF1* gene. Mol Microbiol. 1999; 34: 651–662. PMID: 10564506
5. Odds FC, Davidson AD, Jacobsen MD, Tavanti A, Whyte JA, Kibbler CC, et al. *Candida albicans* strain maintenance, replacement, and microvariation demonstrated by multilocus sequence typing. J Clin Microbiol. 2006; 44: 3647–3658. PMID: 17021093
6. Miranda LN, van der Heijden IM, Costa SF, Sousa AP, Sienra RA, Gobara S, Santos CR, Lobo RD, Pessoa VP Jr, Levin AS. *Candida* colonisation as a source for candidaemia. J Hosp Infect. 2009; 72: 9–16. doi: 10.1016/j.jhin.2009.02.009 PMID: 19303662
7. White SJ, Rosenbach A, Lephart P, Nguyen D, Benjamin A, Tzipori S, et al. Self-regulation of *Candida albicans* population size during GI colonization. PLoS Pathog. 2007; 3: e184. PMID: 18069889
8. Pierce JV, Dignard D, Whiteway M, Kumamoto CA. Normal adaptation of *Candida albicans* to the murine gastrointestinal tract requires Efg1p-dependent regulation of metabolic and host defense genes. Eukaryot Cell. 2013; 12: 37–49. doi: 10.1128/EC.00236-12 PMID: 23125349
9. Pande K, Chen C, Noble SM. Passage through the mammalian gut triggers a phenotypic switch that promotes *Candida albicans* commensalism. Nat Genet. 2013; 45: 1088–1091. doi: 10.1038/ng.2710 PMID: 23892606
10. Prieto D, Román E, Correia I, Pla J. The HOG pathway is critical for the colonization of the mouse gastrointestinal tract by *Candida albicans*. PLoS One. 2014; 9: e87128. doi: 10.1371/journal.pone.0087128 PMID: 24475243
11. Koh AY. Murine models of *Candida* gastrointestinal colonization and dissemination. Eukaryot Cell. 2013; 12: 1416–1422. doi: 10.1128/EC.00196-13 PMID: 24036344
12. Rosenbach A, Dignard D, Pierce JV, Whiteway M, Kumamoto CA. Adaptations of Candida albicans for growth in the mammalian intestinal tract. Eukaryot Cell. 2010; 9: 1075–1086. doi: 10.1128/EC.00034-10 PMID: 20435697
13. Jawhara S, Thuru X, Standaert-Vitse A, Jouault T, Mordon S, Sendid B, Desreumaux P, Poulain D. Colonization of mice by *Candida albicans* is promoted by chemically induced colitis and augments inflammatory responses through galectin-3. J Infect Dis. 2008; 197: 972–980. doi: 10.1086/528990 PMID: 18419533
14. Ernst JF, Tielker D. Responses to hypoxia in fungal pathogens. Cell Microbiol. 2008; 11: 183–190. doi: 10.1111/j.1462-5822.2008.01259.x PMID: 19016786
15. Grahl N, Cramer RA Jr. Regulation of hypoxia adaptation: an overlooked virulence attribute of pathogenic fungi? Med Mycol. 2010; 48: 1–15. doi: 10.3109/13693780902947342 PMID: 19462332
16. Peyssonnaux C, Boutin AT, Zinkernagel AS, Datta V, Nizet V, Johnson RS. Critical role of HIF-1alpha in keratinocyte defense against bacterial infection. J Invest Dermatol. 2008; 128: 1964–1968. doi: 10.1038/jid.2008.27 PMID: 18323789
17. Evans SM, Schrlau AE, Chalian AA, Zhang P, Koch CJ. Oxygen levels in normal and previously irradiated human skin as assessed by EF5 binding. J Invest Dermatol. 2006; 126: 2596–2606. PMID: 16810299
18. He G, Shankar RA, Chzhan M, Samouilov A, Kuppusamy P, Zweier JL. Noninvasive measurement of anatomic structure and intraluminal oxygenation in the gastrointestinal tract of living mice with spatial and spectral EPR imaging. Proc Natl Acad Sci U S A. 1999; 96: 4586–45891. PMID: 10200306

19. Setiadi ER, Doedt T, Cottier F, Noffz C, Ernst JF. Transcriptional response of *Candida albicans* to hypoxia: linkage of oxygen sensing and Efg1p-regulatory networks. J Mol Biol. 2006; 361: 399–411. PMID: 16854431

20. Synnott JM, Guida A, Mulhern-Haughey S, Higgins DG, Butler G. Regulation of the hypoxic response in *Candida albicans*. Eukaryot Cell. 2010; 9: 1734–1746. doi: 10.1128/EC.00159-10 PMID: 20870877

21. Sellam A, van het Hoog M, Tebbji F, Beaurepaire C, Whiteway M, Nantel A. Modeling the transcriptional regulatory network that controls the early hypoxic response in *Candida albicans*. Eukaryot Cell. 2014; 13: 675–690. doi: 10.1128/EC.00292-13 PMID: 24681685

22. Silver PM, Oliver BG, White TC. Role of *Candida albicans* transcription factor Upc2p in drug resistance and sterol metabolism. Eukaryot Cell. 2004; 3: 1391–1397. PMID: 15590814

23. Doedt T, Krishnamurthy S, Bockmühl DP, Tebarth B, Stempel C, Russell CL, et al. APSES proteins regulate morphogenesis and metabolism in *Candida albicans*. Mol Biol Cell. 2004; 15: 3167–3180. PMID: 15218092

24. Kelly MT, MacCallum DM, Clancy SD, Odds FC, Brown AJ, Butler G. The *Candida albicans CaACE2* gene affects morphogenesis, adherence and virulence. Mol Microbiol. 2004; 53: 969–983. PMID: 15255906

25. Stichternoth C, Ernst JF. Hypoxic adaptation by Efg1 regulates biofilm formation by *Candida albicans*. Appl. Environ. Microbiol. 2009; 75: 3663–3672. doi: 10.1128/AEM.00098-09 PMID: 19346360

26. Stoldt VR, Sonneborn A, Leuker C, Ernst JF. Efg1, an essential regulator of morphogenesis of the human pathogen *Candida albicans*, is a member of a conserved class of bHLH proteins regulating morphogenetic processes in fungi. EMBO J. 1997; 16: 1982–1991. PMID: 9155024

27. Lo HJ, Köhler JR, DiDomenico B, Loebenberg D, Cacciapuoti A, Fink GR. Nonfilamentous *C. albicans* mutants are avirulent. Cell. 1997; 90: 939–949. PMID: 9298905

28. Sonneborn A, Bockmühl DP, Ernst JF. Chlamydospore formation in *Candida albicans* requires the Efg1p morphogenetic regulator. Infect Immun. 1999; 67: 5514–5517. PMID: 10496941

29. Giusani AD, Vinces M, Kumamoto CA. Invasive filamentous growth of *Candida albicans* is promoted by Czf1p-dependent relief of Efg1p-mediated repression. Genetics. 2002; 160: 1749–1753. PMID: 11973327

30. Mulhern SM, Logue ME, Butler G. *Candida albicans* transcription factor Ace2 regulates metabolism and is required for filamentation in hypoxic conditions. Eukaryot Cell. 2006; 5: 2001–2013. PMID: 16998073

31. Bharucha N, Chabrier-Rosello Y, Xu T, Johnson C, Sobczynski S, Song Q et al. A large-scale complex haploinsufficiency-based genetic interaction screen in *Candida albicans*: analysis of the RAM network during morphogenesis. PLoS Genet. 2011; 7: e1002058. doi: 10.1371/journal.pgen.1002058 PMID: 22103005

32. Saputo S, Kumar A, Krysan DJ. Efg1 directly regulates *ACE2* expression to mediate cross-talk between the cAMP/PKA and RAM pathways during *Candida albicans* morphogenesis. Eukaryot Cell. 2014; 13: 1169–1180. doi: 10.1128/EC.00148-14 PMID: 25001410

33. Wang A, Raniga PP, Lane S, Lu Y, Liu H. Hyphal chain formation in *Candida albicans*: Cdc28-Hgc1 phosphorylation of Efg1 represses cell separation genes. Mol Cell Biol. 2009; 29: 4406–4416. doi: 10.1128/MCB.01502-08 PMID: 19528234

34. Kim AS, Garni RM, Henry-Stanley MJ, Bendel CM, Erlandsen SL, Wells CL. Hypoxia and extraintestinal dissemination of *Candida albicans* yeast forms. Shock. 2003; 19: 257–262. PMID: 12630526

35. Bendel CM, Hess DJ, Garni RM, Henry-Stanley M, Wells CL. Comparative virulence of *Candida albicans* yeast and filamentous forms in orally and intravenously inoculated mice. Crit Care Med. 2003; 31: 501–507. PMID: 12576958

36. Gianotti L, Alexander JW, Fukushima R, Childress CP. Translocation of *Candida albicans* is related to the blood flow of individual intestinal villi. Circ Shock. 1993; 40: 250–257. PMID: 8375026

37. Stichternoth C, Fraund A, Setiadi E, Giasson L, Vecchiarelli A, Ernst JF. Sch9 kinase integrates hypoxia and CO_2 sensing to suppress hyphal morphogenesis in *Candida albicans*. Eukaryot Cell. 2011; 10: 502–511. doi: 10.1128/EC.00289-10 PMID: 21335533

38. Noffz CS, Liedschulte V, Lengeler K, Ernst JF. Functional mapping of the *Candida albicans* Efg1 regulator. Eukaryot Cell. 2008; 7: 881–893. doi: 10.1128/EC.00033-08 PMID: 18375615

39. Bockmühl DP, Ernst JF. A potential phosphorylation site for an A-type kinase in the Efg1 regulator protein contributes to hyphal morphogenesis of *Candida albicans*. Genetics. 2001; 157: 1523–30. PMID: 11290709

40. Lassak T, Schneider E, Bussmann M, Kurtz D, Manak JR, Srikantha T, et al. Target specificity of the *Candida albicans* Efg1 regulator. Mol Microbiol. 2011; 82: 602–618. doi: 10.1111/j.1365-2958.2011.07837.x PMID: 21923768

41. Van Helden J, Rios AF, Collado-Vides J. Discovering regulatory elements in non-coding sequences by analysis of spaced dyads. Nucleic Acids Res. 2000; 28: 1808–1818. PMID: 10734201

42. Nobile CJ, Fox EP, Nett JE, Sorrells TR, Mitrovich QM, Hernday AD, et al. A recently evolved transcriptional network controls biofilm development in *Candida albicans*. Cell.2012; 148: 126–138. doi: 10.1016/j.cell.2011.10.048 PMID: 22265407

43. Liu H, Köhler J, Fink GR. Suppression of hyphal formation *in Candida albicans* by mutation of a STE12 homolog. Science. 1994; 266: 1723–1726. Erratum in Science. 1995;267:217. PMID: 7992058

44. Csank C, Schröppel K, Leberer E, Harcus D, Mohamed O, Meloche S, et al. Roles of the *Candida albicans* mitogen-activated protein kinase homolog, Cek1p, in hyphal development and systemic candidiasis. Infect Immun. 1998; 66: 2713–2721. PMID: 9596738

45. Ernst JF. Transcription factors in *Candida albicans*—environmental control of morphogenesis. Microbiology. 2000; 146: 1763–1774. PMID: 10931884

46. Rocha CR, Schröppel K, Harcus D, Marcil A, Dignard D, Taylor BN, et al. Signaling through adenylyl cyclase is essential for hyphal growth and virulence in the pathogenic fungus *Candida albicans*. Mol Biol Cell. 2001; 12: 3631–3643. PMID: 11694594

47. Bockmühl DP, Krishnamurthy S, Gerads M, Sonneborn A, Ernst JF. Distinct and redundant roles of the two protein kinase A isoforms Tpk1p and Tpk2p in morphogenesis and growth of *Candida albicans*. Mol Microbiol. 2001; 42: 1243–1257. PMID: 11886556

48. Saputo S, Chabrier-Rosello Y, Luca FC, Kumar A, Krysan DJ. The RAM network in pathogenic fungi. Eukaryot Cell. 2012; 11: 708–717. doi: 10.1128/EC.00044-12 PMID: 22544903

49. Cantero PD, Ernst JF. Damage to the glycoshield activates *PMT*-directed *O*-mannosylation via the Msb2-Cek1 pathway in *Candida albicans*. Mol Microbiol. 2011; 80: 715–725. doi: 10.1111/j.1365-2958.2011.07604.x PMID: 21375589

50. Badis G, Chan ET, van Bakel H, Pena-Castillo L, Tillo D, Tsui K et al. A library of yeast transcription factor motifs reveals a widespread function for Rsc3 in targeting nucleosome exclusion at promoters. Mol Cell. 2008; 32: 878–887. doi: 10.1016/j.molcel.2008.11.020 PMID: 19111667

51. Du H, Guan G, Xie J, Sun Y, Tong Y, Zhang L, et al. Roles of *Candida albicans* Gat2, a GATA-type zinc finger transcription factor, in biofilm formation, filamentous growth and virulence. PLoS One. 2012; 7: e29707. doi: 10.1371/journal.pone.0029707 PMID: 22276126

52. Nobile CJ, Mitchell AP. Regulation of cell-surface genes and biofilm formation by the *C. albicans* transcription factor Bcr1p. Curr Biol. 2005; 15: 1150–1155. PMID: 15964282

53. Fu Y, Filler SG, Spellberg BJ, Fonzi W, Ibrahim AS, Kanbe T, et al. Cloning and characterization of CAD1/AAF1, a gene from *Candida albicans* that induces adherence to endothelial cells after expression in *Saccharomyces cerevisiae*. Infect Immun. 1998; 66: 2078–2084. PMID: 9573092

54. Bertram G, Swoboda RK, Gooday GW, Gow NA, Brown AJ. Structure and regulation of the *Candida albicans ADH1* gene encoding an immunogenic alcohol dehydrogenase. Yeast. 1996; 12: 115–127. PMID: 8686375

55. Martin R, Moran GP, Jacobsen ID, Heyken A, Domey J, Sullivan DJ, et al. The *Candida albicans*-specific gene *EED1* encodes a key regulator of hyphal extension. PLoS One. 6:e18394. Mol Microbiol. 2011;53: 969–983. doi: 10.1371/journal.pone.0018394 PMID: 21512583

56. Bonhomme J, Chauvel M, Goyard S, Roux P, Rossignol T, d'Enfert C. Contribution of the glycolytic flux and hypoxia adaptation to efficient biofilm formation by *Candida albicans*. Mol Microbiol. 2011; 80: 995–1013. doi: 10.1111/j.1365-2958.2011.07626.x PMID: 21414038

57. Kadosh D, Johnson AD. Rfg1, a protein related to the *Saccharomyces cerevisiae* hypoxic regulator Rox1, controls filamentous growth and virulence in *Candida albicans*. Mol Cell Biol. 2001; 21: 2496–2505. PMID: 11259598

58. Zordan RE, Miller MG, Galgoczy DJ, Tuch BB, Johnson AD. Interlocking transcriptional feedback loops control white-opaque switching in *Candida albicans*. PLoS Biol. 2007; 5: e256 PMID: 17880264

59. Lohse MB, Hernday AD, Fordyce PM, Noiman L, Sorrells TR, Hanson-Smith V, et al. Identification and characterization of a previously undescribed family of sequence-specific DNA-binding domains. Proc Natl Acad Sci U S A. 2013; 110: 7660–7665. doi: 10.1073/pnas.1221734110 PMID: 23610392

60. Pérez JC, Kumamoto CA, Johnson AD. *Candida albicans* commensalism and pathogenicity are intertwined traits directed by a tightly knit transcriptional regulatory circuit. PLoS Biol. 2013; 11: e1001510. doi: 10.1371/journal.pbio.1001510 PMID: 23526879

61. Cao F, Lane S, Raniga PP, Lu Y, Zhou Z, Ramon K, et al. The Flo8 transcription factor is essential for hyphal development and virulence in *Candida albicans*. Mol Biol Cell. 2006; 17:295–307. PMID: 16267276

62. Du H, Guan G, Xie J, Cottier F, Sun Y, Jia W, et al. The transcription factor Flo8 mediates CO_2 sensing in the human fungal pathogen *Candida albicans*. Mol Biol Cell. 2012; 23: 2692–2701. doi: 10.1091/mbc.E12-02-0094 PMID: 22621896

63. Bruno VM, Kalachikov S, Subaran R, Nobile CJ, Kyratsous C, Mitchell AP. Control of the *C. albicans* cell wall damage response by transcriptional regulator Cas5. PLoS Pathog. 2006; 2: e21. PMID: 16552442

64. Bauer J, Wendland J. *Candida albicans* Sfl1 suppresses flocculation and filamentation. Eukaryot Cell. 2007; 6:1736–1744. PMID: 17766464

65. Li Y, Su C, Mao X, Cao F, Chen J. Roles of *Candida albicans* Sfl1 in hyphal development. Eukaryot Cell. 2007; 6: 1736–1744.

66. Gutiérrez-Escribano P, Zeidler U, Suárez MB, Bachellier-Bassi S, Clemente-Blanco A, Bonhomme J, et al. The NDR/LATS kinase Cbk1 controls the activity of the transcriptional regulator Bcr1 during biofilm formation in *Candida albicans*. PLoS Pathog. 2012; 8: e1002683. doi: 10.1371/journal.ppat.1002683 PMID: 22589718

67. Guan G, Xie J, Tao L, Nobile CJ, Sun Y, Cao C, et al. Bcr1 plays a central role in the regulation of opaque cell filamentation in *Candida albicans*. Mol Microbiol. 2013; 89: 732–750. doi: 10.1111/mmi.12310 PMID: 23808664

68. Lu Y, Su C, Liu H. A GATA transcription factor recruits Hda1 in response to reduced Tor1 signaling to establish a hyphal chromatin state in *Candida albicans*. PLoS Pathog. 2012; 8: e1002663. doi: 10.1371/journal.ppat.1002663 PMID: 22536157

69. Su C, Lu Y, Liu H. Reduced TOR signaling sustains hyphal development in *Candida albicans* by lowering Hog1 basal activity. Mol Biol Cell. 2013; 24: 385–397. doi: 10.1091/mbc.E12-06-0477 PMID: 23171549

70. Vandeputte P, Ischer F, Sanglard D, Coste AT. In vivo systematic analysis of *Candida albicans* Zn2-Cys6 transcription factors mutants for mice organ colonization. PLoS ONE. 2011; 6: e26962. doi: 10.1371/journal.pone.0026962 PMID: 22073120

71. Mukherjee PK, Sendid B, Hoarau G2, Colombel JF, Poulain D, Ghannoum MA. Mycobiota in gastrointestinal diseases. Nat Rev Gastroenterol Hepatol. 2015; 12: 77–87. doi: 10.1038/nrgastro.2014.188 PMID: 25385227

72. Seed PC. The Human Mycobiome. Cold Spring Harb Perspect Med. 2014; 5(5).

73. Brown GD, Denning DW, Gow NA, Levitz SM, Netea MG, White TC. Hidden killers: human fungal infections. Sci Transl Med. 2012; 4: 165rv13.

74. Pierce JV, Kumamoto CA. Variation in *Candida albicans EFG1* expression enables host-dependent changes in colonizing fungal populations. MBio. 2012; 3: e00117–12. doi: 10.1128/mBio.00117-12 PMID: 22829676

75. Lu Y, Su C, Solis NV, Filler SG, Liu H. Synergistic regulation of hyphal elongation by hypoxia, CO(2), and nutrient conditions controls the virulence of *Candida albicans*. Cell Host Microbe. 2013; 14: 499–509 doi: 10.1016/j.chom.2013.10.008 PMID: 24237696

76. Su C, Li Y, Lu Y, Chen J. Mss11, a transcriptional activator, is required for hyphal development in *Candida albicans*. Eukaryot Cell. 2009; 8: 1780–1791. doi: 10.1128/EC.00190-09 PMID: 19734367

77. Hope H, Bogliolo S, Arkowitz RA, Bassilana M. Activation of Rac1 by the guanine nucleotide exchange factor Dck1 is required for invasive filamentous growth in the pathogen *Candida albicans*. Mol Biol Cell. 2008; 19: 3638–3651. doi: 10.1091/mbc.E07-12-1272 PMID: 18579689

78. Sasse C, Schillig R, Dierolf F, Weyler M, Schneider S, Mogavero S, et al. The transcription factor Ndt80 does not contribute to Mrr1-, Tac1-, and Upc2-mediated fluconazole resistance in *Candida albicans*. PLoS One. 2011; 6: e25623. doi: 10.1371/journal.pone.0025623 PMID: 21980509

79. Fonzi WA, Irwin MY. Isogenic strain construction and gene mapping in *Candida albicans*. Genetics. 1993; 134: 717–728. PMID: 8349105

80. Braun BR, Johnson AD. *TUP1*, *CPH1* and *EFG1* make independent contributions to filamentation in *Candida albicans*. Genetics. 2000; 155: 57–67. PMID: 10790384

81. Chauvel M, Nesseir A, Cabral V, Znaidi S, Goyard S, Bachellier-Bassi S, et al. A versatile overexpression strategy in the pathogenic yeast *Candida albicans*: identification of regulators of morphogenesis and fitness. PLoS One. 2012; 7: e45912. doi: 10.1371/journal.pone.0045912 PMID: 23049891

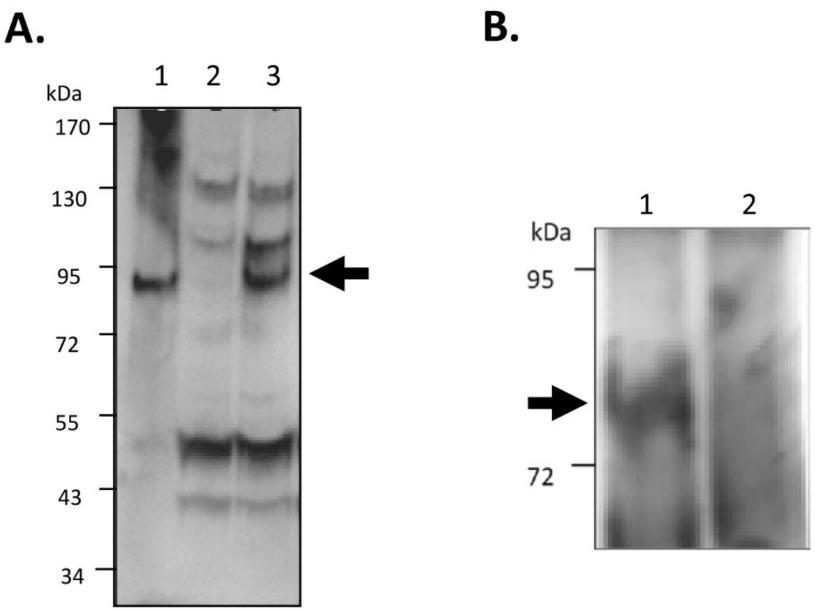

S1 Fig. Activity of rabbit anti-Efg1 antiserum. A. Immunoblotting. Extracts of *efg1* mutant HLC67 (lane 2) and control strain CAF2-1 (lane 3) were separated by SDS-PAGE and blots were probed with anti-Efg1 antiserum (1 : 5000). For comparison, 250 ng of *E. coli*-produced His_{10}-Efg1 protein was used (lane 1). **B.** Immunoprecipitation. Efg1 was immunoprecipitated using anti-Efg1 antiserum and protein G-coated agarose beads. Immunoprecipitates from the control strain CAF2-1 (lane 1) and the *efg1* mutant HLC67 (lane 2) were analysed by immunoblotting using anti-Efg1 antiserum. The arrow indicates the migration of Efg1.

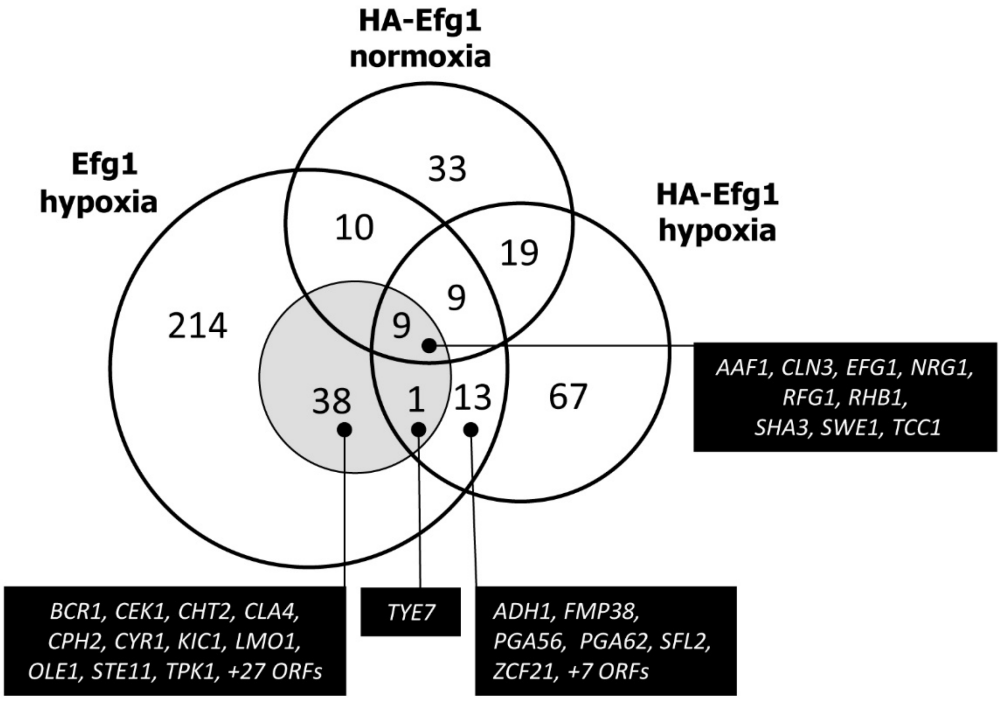

S2 Fig. Intersection of genomic binding sites for Efg1 and HA-Efg1 under hypoxia and normoxia. For Efg1, genomic binding sites were derived from ChIP chip experiments comparing strains CAF2-1 (*EFG1/EFG1*) and HLC52 (*efg1/efg1*); for HA-Efg1, strains HLCEEFG1 (*efg1/efg1* [*HA-EFG1*]) and CAF2-1 were compared. Normoxic binding sites for HA-Efg1 were obtained from Lassak *et al.* [40]. The shaded circle encompasses genes in filamentous growth.

GO term[1] (genome frequency)	HA-Efg1 binding genes annotated to the term[2] Name	Frequency[3]	*P* value[4]
A. Process			
Regulation of multi-organism process (1.6 %)	*AHR1 ALS1 BMH1 BRG1 CBK1 CRZ2[a] CSR1 CZF1[a] DEF1[a] EFG1[ac] SHA3[a] TEC1[a] TYE7*	11.4 %	1.39e-05
Regulation of filamentous growth (2.6 %)	*AHR1 BMH1 BRG1 CBK1 CLN3 CZF1 DEF1 EFG1[ac] NRG1[ac] RFG1[ac] RME1 TEC1[a] TYE7 WOR2[a]*	12.3 %	0.00066
Regulation of biosynthetic process (10.9 %)	*AAF1[ac] ADAEC AHR1 BMH1 BRG1 CBF1[a] CBK1 CLN3 CRZ2[a] CSR1 CUP9 CZF1 EFG1[ac] GZF3 HTB1 NRG1[ac] RFG1[ac] RME1 RPS23A RTF1 SBP1 SFU1 SHA3[a] TCC1[ac] TEC1[a] TYE7, WOR2[a] ZCF21 ORF19.4375*	25.4 %	0.00532
***B*. Function**			
Nucleic acid binding transcription factor activity (3.4 %)	*AHR1 BRG1 CBF1[a] CRZ2[a] CSR1 CUP9 CZF1 EFG1[ac] GZF3 NRG1[ac] RFG1[ac] RME1 SFU1 TEC1[a] TYE7 WOR2 ZCF21*	14 %	3.25e-05
Sequence-specific DNA binding (2.9 %)	*AHR1 BMH1 BRG1 CBF1[a] CSR1 CUP9 EFG1[ac] GZF3 NRG1[ac] RFG1[ac] RME1 SBP1 SFU1 TEC1[a] TYE7 WOR3*	14.9 %	1.83e-05

S3 Fig. GO categories of genes binding HA-Efg1 under hypoxia. GO terms for Efg1 binding targets were identified in ChIP chip data using the CGD GO Term Finder tool (http://www.candidagenome.org/cgi-bin/GO/goTermFinder); the analysis was conducted in June 2013. Genome frequencies of genes corresponding to GO terms are expressed as percentages (gene number relative to 6,525 genes in the *C. albicans* genome; the frequency of genes binding Efg1 that correspond to a specific GO term are expressed relative to the total number of 106 genes binding HA-Efg1). Superscripts: a, Efg1 binding in yeast normoxia [40]; b, Efg1 binding in hyphae inducing conditions [40]; c, Efg1 binding in biofilm inducing conditions [42]. *P* values for overrepresented categories were calculated using a hyper geometric distribution with multiple hypothesis correction according to the GO Term Finder tool website (http://www.candidagenome.org/help/goTermFinder.shtml). The *P* value cutoff used was 0.05.

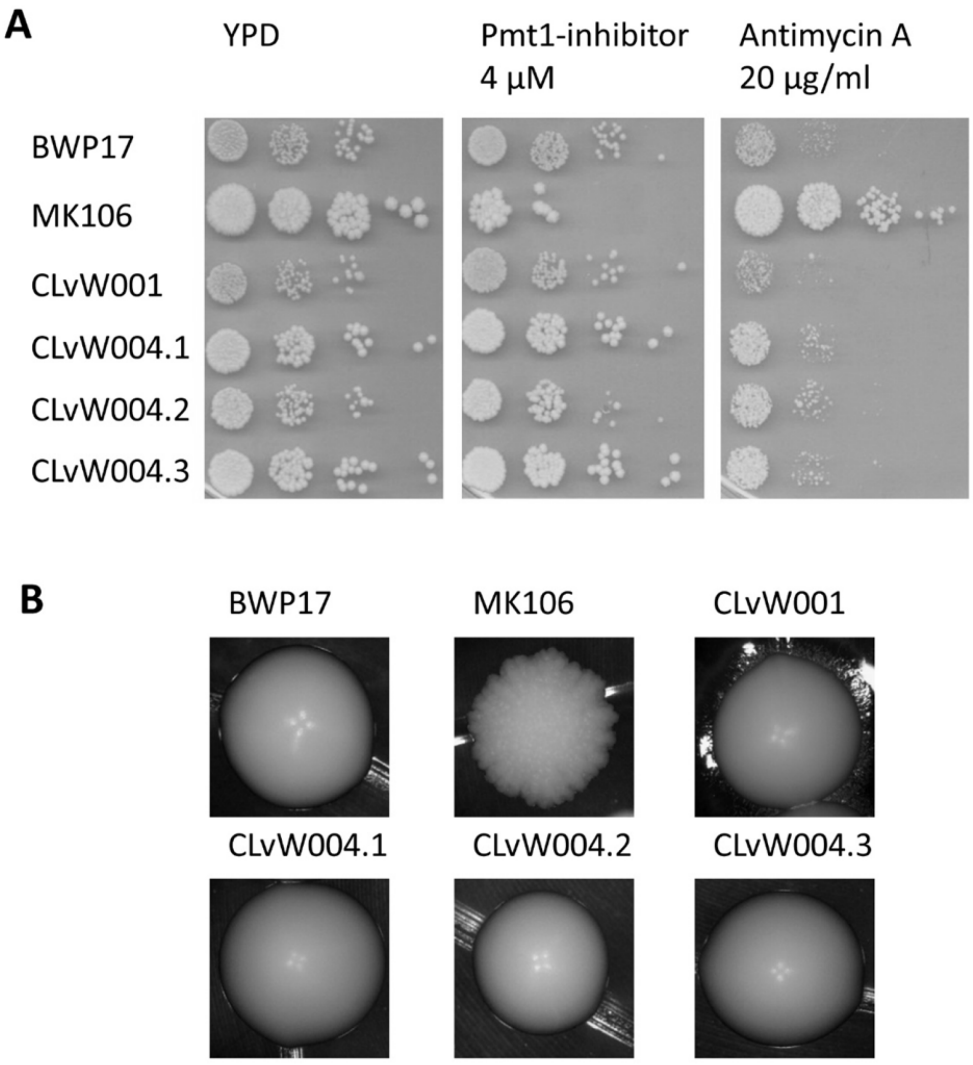

S4 Fig. Functionality of the HA tagged Ace2 protein. To verify the functionality of C-terminal HA-tagged Ace2 the phenotypes of three isolates of strain CLvW004 (*ACE2-HA/ace2*) was compared to mutant strain MK106 (*ace2/ace2*), wild-type strain BWP17 (*ACE2/ACE2*) and the heterozygous strain CLvW001 (*ACE2/ace2*). (A) Drop dilution assay for sensitivity to 4 µM Pmt1-inhibitor and resistance to antimycin A (20 µg/ml). The agar plates were photographed after 2 d incubation at 30 °C. The *ace2* mutant strain Mk106 shows enhanced sensitivity to the Pmt1-inhibitor [49] and is less susceptible to the respiratory inhibitor antimycin A [30]. (B) Colonies of the indicated strains were photographed following growth for 2 d at 30 °C on YPD agar. The *ace2* mutant strain Mk106 shows the wrinkled colony phenotype described previously [27]. Phenotypes of strains CLvW004.1-3 correspond to the heterozygous strain CLvW001 indicating that the Ace2-HA protein is functional.

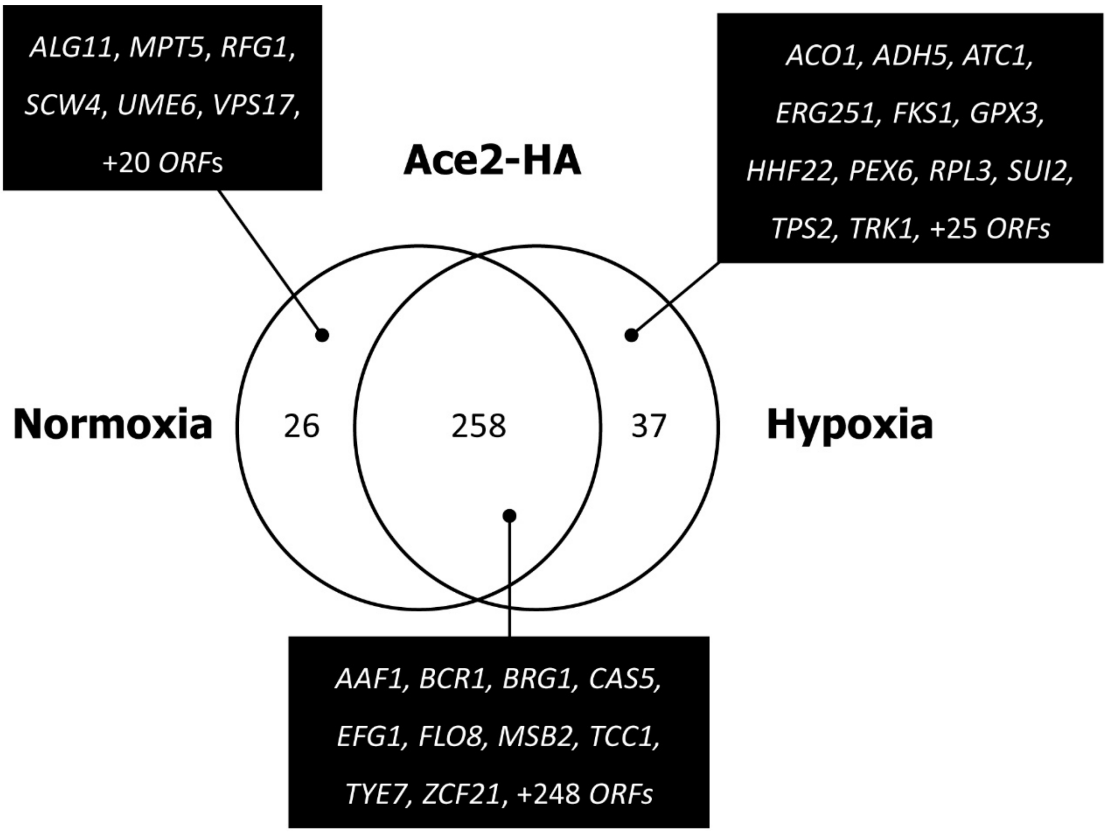

S5 Fig. **Genomic binding sites for Ace2**. Venn diagram showing numbers of genes bound by HA-tagged Ace2 under normoxic conditions (30 °C, YPD) and hypoxic conditions (30 °C, YPD 0.2 % O_2 and 6 % CO_2). Binding regions with the corresponding ORFs are listed in supplementary table S2 and S3. Genomic binding sites were derived from ChIP chip experiments comparing strains CLvW004 (*ACE2-HA/ace2*) and BWP17 (non tag control). For both conditions, 258 genes are common.

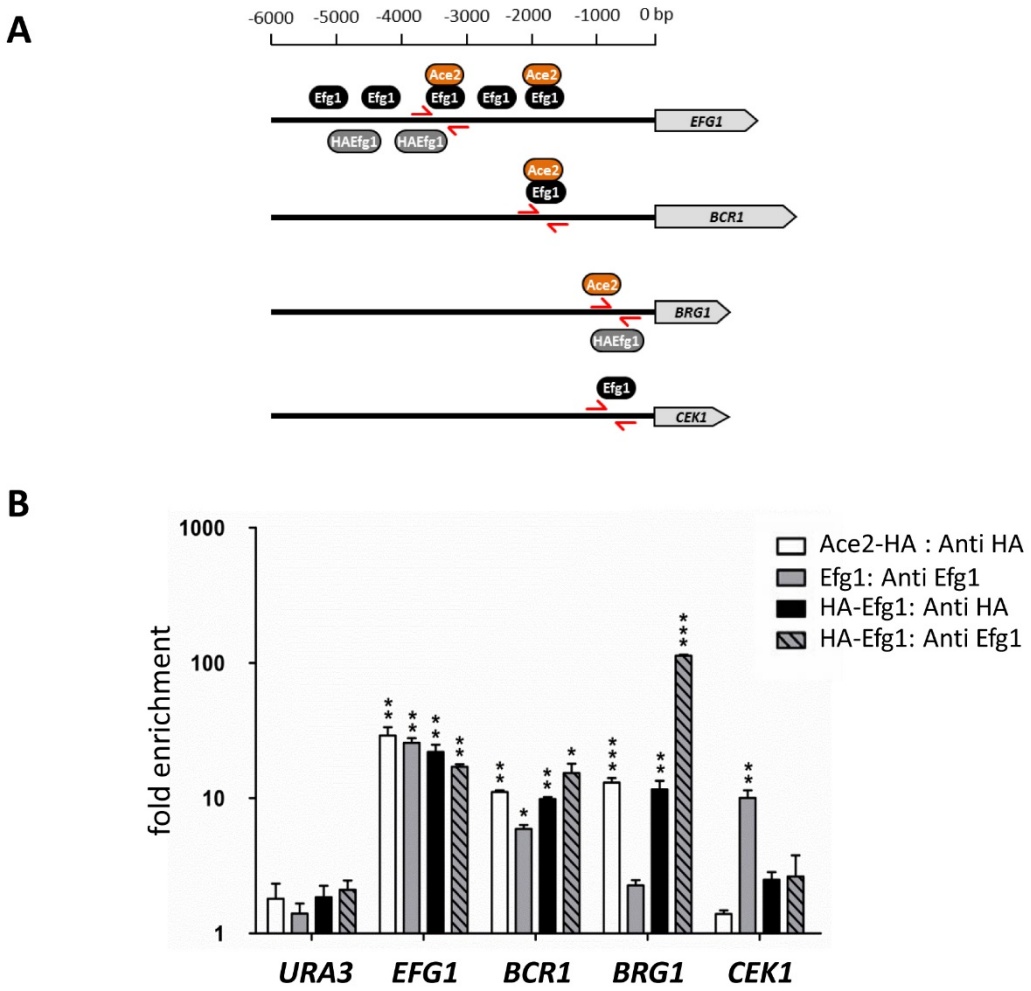

S6 Fig. Genomic localization of Ace2 and Efg1 on target promoters. (A) Binding positions identified by ChIP chip experiments. Binding positions of Efg1 (black ovals), Ace2-HA (orange ovals) and HA-Efg1 positions (grey ovals) identified by ChIP chip experiments are shown schematically. (B) Quantitation of Ace2, HA-Efg1 and Efg1 enrichment by ChIP on target promoters. Following ChIP the respective fold enrichment was determined by qPCR using oligonucleotide pairs shown by red arrows in A. Chromatin of strains CAF2 -1 (Efg1) and HLCEEFG1 (HA-Efg1) was immunoprecipitated using anti-Efg1 and anti-HA antibody, respectively, as described in S1 Table. For Ace2 enrichment anti-HA antibody was used for immunoprecipitation of strain CLvW004 (Ace2-HA), as described in S2 Table. In a control experiment, ChIP followed by qPCR was also done using anti-Efg1 antibody on extracts of strain HLCEEFG1 (HA-Efg1). qPCR experiments were done using two biological replicates, which were assayed in triplicate. The mean fold enrichment (± standard deviation) for each protein was calculated relative to the respective no tag or mutant strain and normalized to the input sample. Statistical relevance is indicated by asterisks: *, $P < 0.05$; **, $P < 0.01$; ***, $P < 0.001$. The results verify the presence of proteins on target promoters; in addition, the presence of HA-Efg1 on the *BCR1* promoter, which was not found in the ChIP chip experiment, was revealed by the ChIP-qPCR experiment.

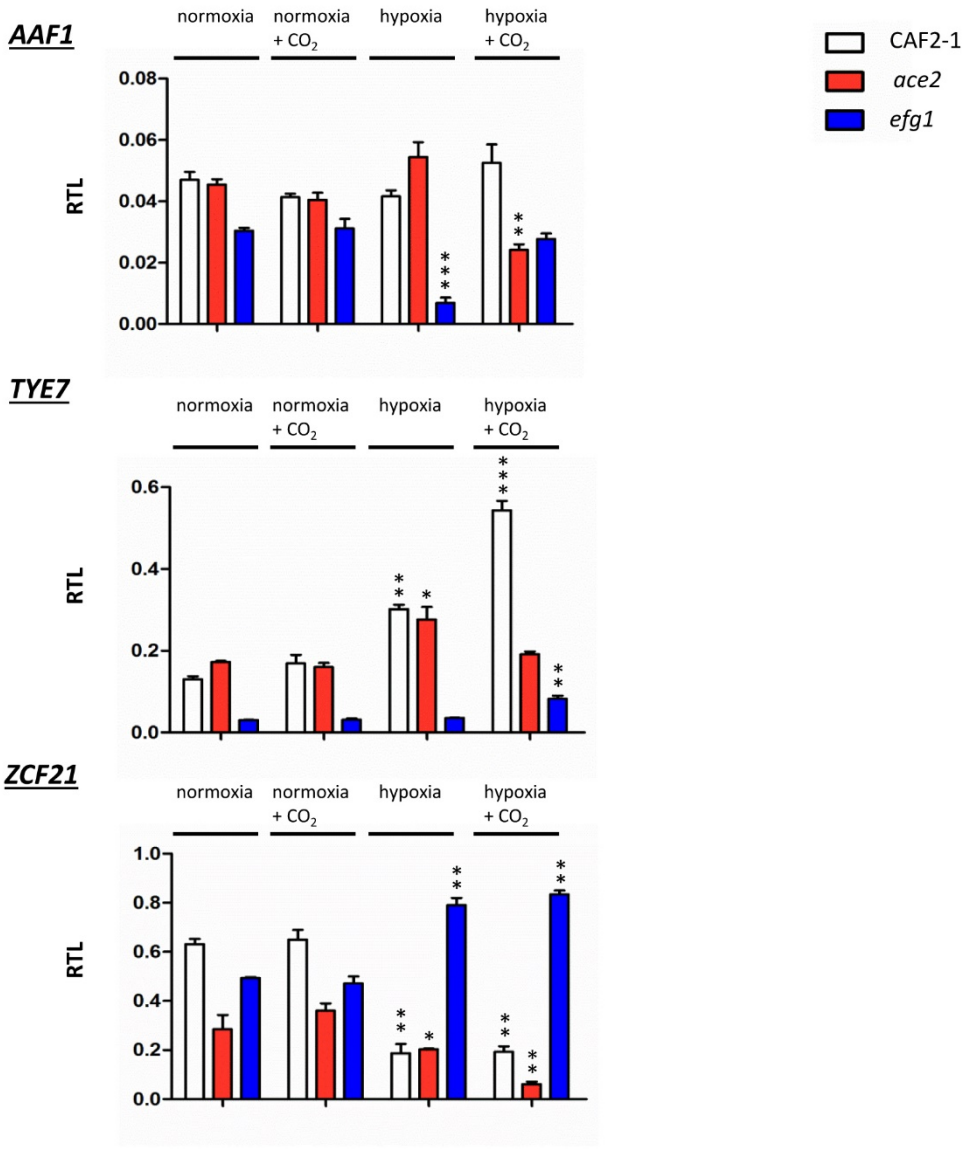

S7 Fig. Transcriptional regulation of selected Efg1 and Ace2 target genes under hypoxia. Strains CAF2-1 (control), the *ace2* mutant MK106 and the *efg1* mutant HLC52 were precultured under normoxia at 30 °C in YPD medium and used for inoculation of 100 ml YPD cultures under normoxia, or normoxia with addition of CO_2 (6 % CO_2), or under hypoxia (0.2 % O_2), or under hypoxia with addition of CO_2 (0.2 % O_2, 6 % CO_2). Cultures were incubated at 30 °C in the respective condition until OD_{600}= 0.5 and total RNA was then isolated. Relative transcript levels were determined using *ACT1* transcript as the reference as described in Fig. 4. Relative transcript levels (RTL) for the *AAF1*, *TYE7* and *ZCF21* transcripts in strains CAF2-1 (control), HLC52 (*efg1*) and MK106 (*ace2*). Error bars represent standard deviation of the means. A two-tailed, unpaired *t* test comparing the cycle threshold values of samples grown in hypoxic and normoxic conditions for each mutant respectively was used to determine the statistical relevance: *, $P < 0.05$; **, $P < 0.01$; ***, $P < 0.001$.

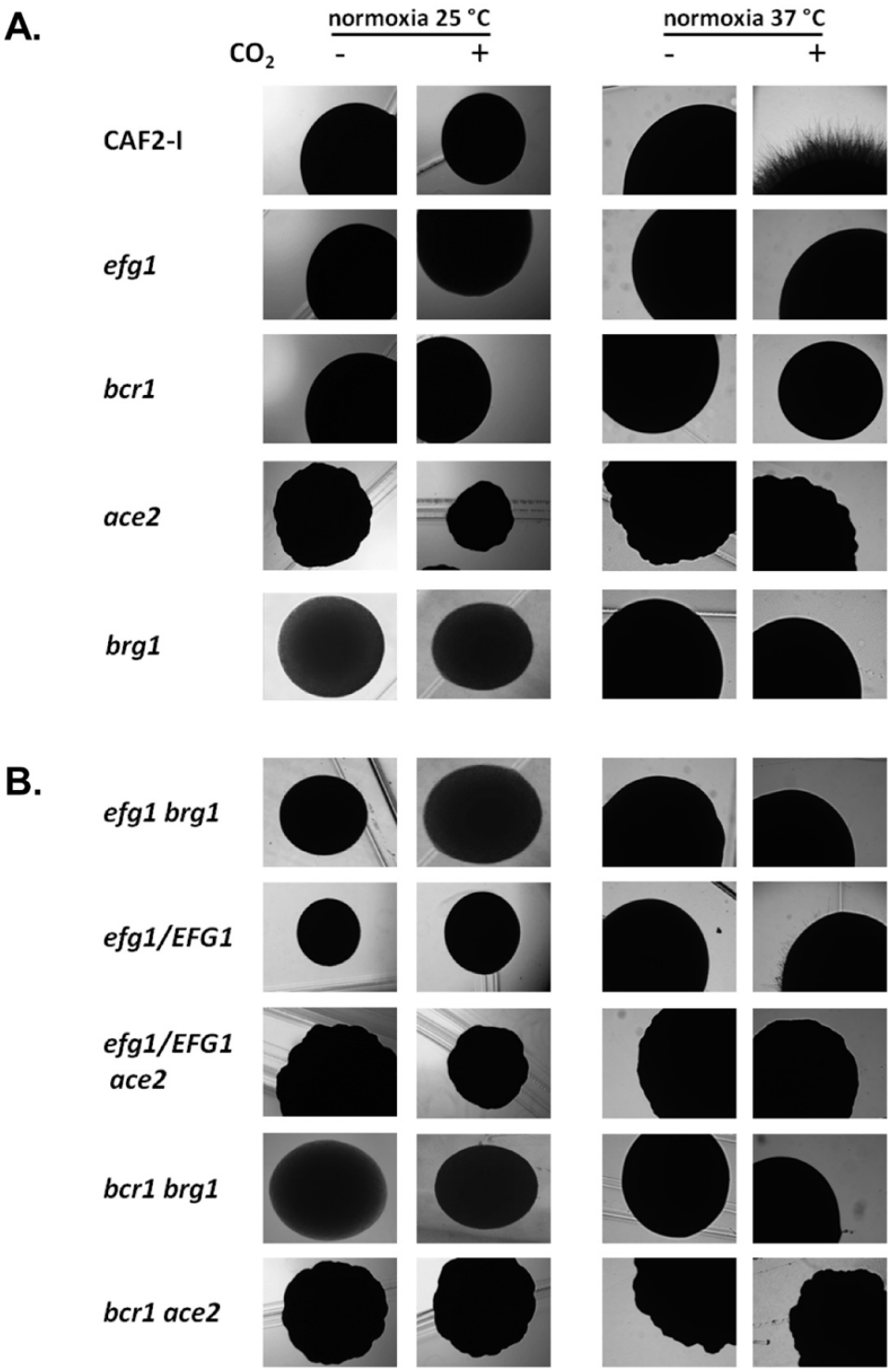

S8 Fig. Normoxic phenotypes of mutants lacking hypoxic regulators under hypoxia. The strains were grown under normoxia without or with 6 % CO_2 on YPS agar for 4 d at 25 °C or for 3d at 37 °C. Strains included CAF2-1 (control), homozygous single mutants HLC52 (*efg1*), CJN702 (*bcr1*), MK106 (*ace2*), TF022 (*brg1*) and double knockout strains PDEB4 (*efg1 brg1*), PDBB4 (*bcr1 brg1*) and CLvW024 (*bcr1 ace2).* *ACE2* could not be disrupted in an *efg1* mutant background; therefore, the heterozygous mutant strain CLvW047 (*efg1/EFG1, ace2/ace2*) was constructed and its phenotype was compared to the *efg1/EFG1* strain DSC11.

S1 Table. Binding of HA-Efg1 to chromosomal sequences of *C. albicans* under hypoxia. Strain HLCEEFG1 producing HA-Efg1 was grown in YPD medium at 30 °C under Hypoxic conditions (0.2% O_2), chromosomal cross-linking of proteins was done. Fragmented chromatin was immunoprecipitated using anti-Efg1 antibody and used as probe for tiling microarrays covering the *C. albicans* genome. Regions showing significantly increased binding of Efg1 compared to control strain CAF2-1 (WT) are listed along with their nearest neigbouring ORFs designated left or right ORF if situated at descending and, respectively, ascending chromosomal coordinates. ORF orientations are indicated by the arrows. Other proteins binding to the same chromosomal region are also indicated. Binding regions within coding regions are marked in purple lettering and green shading indicates multiple binding regions. *, significant binding regions did not overlap in both replicates.

Chr	binding region	size (bp)	left ORF	gene name	left ORF position	additional binding proteins	right ORF	gene name	right ORF Position	additional binding proteins
1	267520..269120	1600	*ORF19.3325*		265492<--267474					
1	447360..447760	2480	*ORF19.3669*	*SHA3*	442472<--444259	Efg1 (Normoxia)				
1	534560..537040	2480	*ORF19.2942*	*DIP5*	532457<--534217					
1	536080..536960	1040					*ORF19.2943.5*		536985-->537284	
1	674080..675120	1040	*ORF19.3013*	*CDC12*	672554<--673909					
1	675200..676640	1440	*ORF19.3014*	*BMH1*	675145<--675939					
1	719080..719640	560					*ORF19.3043*		719686-->720741	
1	817680..818320	640	*ORF19.4459*		813949<--815640	Efg1 (Normoxia)				
1	1081920..1082320	400					*ORF19.4056*	*BRG1*	1082678-->1083949	
1	1088040..1088920	880	*ORF19.450*		1085006<--1085239	Efg1 (Normoxia)				
1	1165207..1165400	193	*ORF19.411*		1163651<--1164670		*ORF19.410.3*		1166924-->1167627	
1	1167680..1169040	1360	*ORF19.2495*	*GSL1*	1169252<--1173967					
1	1195340..1195660	320	*ORF19.2478.1*		1195221<--1196758					
1	1409085..1409335	250	*ORF19.6253*	*RPS23A*	1409046<--1409483					
1	1565580..1566240	660	*ORF19.4438*	*RME1*	1578967<--1580490			*CEN1*	1563083-->1565967	
1	2106070..2106540	470	*ORF19.4820*		2107090<--2108712					
1	2193920..2194750	830	*ORF19.4867*	*SWE1*	2189160<--2192696	Efg1 (Normoxia)	*ORF19.4869*	*SFU1*	2195405-->2196958	
1	2299520..2300000	480	*ORF19.4909*	*CBK1*						
1	2401600..2403400	1800	*ORF19.2333*		2399724<--2401214		*ORF19.2332*		2403598-->2404392	
1	2300000..2300720	720	*ORF19.4909.1*	*RPL42*	2300032<--2300710					
1	2433560..2433750	190					*ORF19.2310.1*	*RPL29*	2434130-->2434321	
1	2434320..2434560	240					*ORF19.2310*		2434657-->2435635	
1	2588300..2590400	2100					*ORF19.5282*		2593345-->2594787	
1	2698160..2698360	200	*ORF19.5226*	*WRS1*	2696598<--2697872					
1	2698360..2698720	360	*ORF19.5225.2*		2698355<--2699181					
1	2839320..2839860	540	*ORF19.4931*		2836544<--2838889		*ORF19.4931.1*	*RPL14*	2839943-->2840692	
1	2869020..2869180	160	*ORF19.4941*	*TYE7*	2869020<--2869829					
1	2870360..2871320	960	*ORF19.4942*							
1	3164200..3164360	160	*ORF19.7251*	*WSC4*						
2	28680..28770	90	*ORF19.2111.2*	*RPL38*	28566<--28802					
2	28920..29170	250	*ORF19.2111*		28906<--28802					
2	162460..162850	390	*ORF19.2024*		163117<--163476	Efg1 (Normoxia)				
2	164030..164235	205	*ORF19.2023*	*HGT7*	164467<--166107	Efg1 (Normoxia)				
2	744840..745940	1100	*ORF19.868*	*ADAEC*	740829<--742466	Efg1 (Normoxia)	*ORF19.867*		747283-->748896	

2	1333020..1333500	480	*ORF19.33*		1332647<--1332957							
2	1394900..1395150	250	*ORF19.2231*		1392837<--1393616							
2	1887340..1887550	210						*ORF19.4081*		1889255-->1889755		
2	1927620..1929200	1580							*CEN2*	1927255-->1930214		
2	2190200..2190430	230	*ORF19.5341*		2189961<--2190749							
3	127980..128450	470	*ORF19.5383*	*PMA1*	133120<--135807							
3	153360..153680	320	*ORF19.3071*	*MIH1*	155056<--157740							
3	538240..538600	610	*ORF19.234*	*PHA2*	537221<--538228							
3	539100..539380	360	*ORF19.236*	*RPL9B*	538929<--539504							
3	818360..818680	280	*ORF19.6925*	*HTB1*	817960<--818352			*ORF19.6924*	*HTA1*	818897-->819295		
3	826740..827380	320	*ORF19.2812*		826589<--828100							
3	855640..856520	800						*ORF19.5854*	*SBP1*	856949-->857797	Efg1 (Normoxia)	
3	941400..941960	880	*ORF19.5904*	*RPL19A*	941386<--942394							
3	955800..956340	540	*ORF19.5908*	*TEC1*	949870<--952101	Efg1 (Normoxia)						
3	1117920..1118050	130	*orf19.5991*			Efg1 (Normoxia)		*ORF19.5992*	*WOR2*	1118833-->1120173	Efg1 (Normoxia)	
3	1125110..1125270	160	*ORF19.5994*	*RHB1*	1126576<--1127130	Efg1 (Normoxia)						
3	1356690..1357440	750	*ORF19.7380*			Efg1 (Normoxia)		*ORF19.7381*	*AHR1*	1362620-->1364494	Efg1 (Normoxia)	
3	1475390..1475880	490	*ORF19.7436*	*AAF1*	1477306<--1479144	Efg1 (Normoxia)						
3	1721900..1723700	1800	*ORF19.6736*			Efg1 (Normoxia)						
3	1727110..1728860	1750	*ORF19.6734*	*TCC1*	1730057<--1732303	Efg1 (Normoxia)						
3	1759380..1759730	350	*ORF19.6715*		1757968<--1758276	Efg1 (Normoxia)		*ORF19.6713*		1761919-->1763124	Efg1 (Normoxia)	
4	128200..131300	3100	*ORF19.4166*	*ZCF21*	131943<--133832							
4	479920..480720	800	*ORF19.2765*	*PGA62*	480635<--481276							
4	569300..571200	1900	*ORF19.2725*		566926<--567228			*ORF19.2724*		571922-->573418	Efg1 (Normoxia)	
4	574900..577300	2400	*Orf19.2723*	*HIT1*	577406<--577852	Efg1 (Normoxia)						
4	780000..780850	850	*ORF19.1313*		773035<--774255			*ORF19.1311*	*SPO75*	782925-->785510		
4	992100..992900	800						*ORF19.3821*		992579-->996216		
4	1048400..1048520	120	*ORF19.3794*	*CSR1*	1042268<--1044124							
4	1099800..1100460	660	*ORF19.740*	*HAP41*	1097336<--1099281	Efg1 (Normoxia)						
4	1425000..1425960	960						*ORF19.2842*		1426618-->1429254		
4	1470300..1471000	700	*ORF19.2877*	*PDC11*	1468241<--1469944	Efg1 (Normoxia)						
4	1504610..1504748	138	*ORF19.3134*		100282<--100722			*ORF19.3133*	*GUT2*	1507275-->1509227		
4	1522500..1523000	500	*ORF19.2876*	*CZF1*	1471203<--1472237	Efg1 (Normoxia)						
5	250650..251292	642	*ORF19.1960*	*CLN3*	244214<--245611			ORF19.1959		253350-->254321		
5	469320..469800	480						ORF19.4216		473411-->473917		
5	855300..855950	650	*ORF19.1105.3*		855473<--855730							
5	896460..896700	240	*ORF19.1286*		896484<--896840							
5	997800..998460	660	*ORF19.3942.1*	*RPL43A*	997147<--997746							
5	998280..998460	180	*ORF19.3944*	*GRR1*	998281<--1000623							
5	1046310..1046610	300	*ORF19.3968*		1051721<--1052032				*CEN5*	468716-->471745		
6	90040..91350	1310	*ORF19.4211*	*FET3*	87506<--89365	Efg1 (Normoxia)		*ORF19.4210*		92713-->94104	Efg1 (Normoxia)	
6	173880..174244	364		*orf19.20*								
6	217480..217640	160							*FAD2*	218253-->219563		

6	403520..403660	140	*ORF19.687.1*	*RPL25*	402823<--403696		*ORF19.5741*	*ALS1*	791472-->795254		
6	788340..788835	495									
6	980890..982000	1110		*CEN6*	980040<--983792						
7	109660..110040	380	*ORF19.7055*		106320<--106646	Efg1 (Normoxia)	*ORF19.7054*		114110-->114475	Efg1 (Normoxia)	
7	132100..132560	460					*ORF19.7047*	*RTF1*	132567-->134273		
7	426420..427230	810		*CEN7*	425812<--428712						
7	451320..451680	360	*ORF19.6514*	*CUP9*	449876<--450910	Efg1 (Normoxia)					
7	917000..917900	900					*ORF19.7150*	*NRG1*	918848-->919780	Efg1 (Normoxia)	
R	338600..339100	500	*ORF19.2529.1*		338130<--338318	Efg1 (Normoxia)					
R	515580..516720	1140	*ORF19.3737*		512535<--514916						
R	589800..590000	200	*ORF19.2822*		585256<--586101	Efg1 (Normoxia)	*ORF19.2823*	*RFG1*	600293-->602095	Efg1 (Normoxia)	
R	839300..839900	600	*ORF19.4375*		839137<--839925						
R	840300..840650	300	*ORF19.4375.1*	*RPS30*	840283<--840810						
R	874600..876000	1400	*ORF19.467*		878587<--880515						
R	1315980..1316160	180	*ORF19.3868*		1315882<--1316235	Efg1 (Normoxia)					
R	1529050..1529250	200	*ORF19.2360*	*CRZ2*	1514505<--1521155						
R	1607700..1609200	1500	*ORF19.6127*	*LPD1*	1606104<--1607579		*ORF19.6126*	*KGD2*	1609238-->1610563		
R	1714600..1717600	3000	*ORF19.610*	*EFG1*	1723589<--1725166	Efg1 (Normoxia)					
R	1772000..1772650	650	*ORF19.6375*	*RPS20*	1772309<--1772668						
R	2103400..2106000	2600	*ORF19.7561*	*DEF1*	2106215<--2108878	Efg1 (Normoxia)					
R	2168900..2169600	700	*ORF19.7592*	*FAA4*	2172618<--2174708	Efg1 (Normoxia)					

S1 Table. Binding of Efg1 to chromosomal sequences of *C. albicans* under hypoxia. Strain CAF2-1 producing wild-type Efg1 was grown in YPD medium at 30 °C under hypoxic conditions (0.2% O_2), followed by chromosomal cross-linking of proteins. Fragmented chromatin was immunoprecipitated using anti-Efg1 antibody and used as probe for tiling microarrays covering the *C. albicans* genome. Regions showing significantly increased binding of Efg1 compared to control strain Hlc52 (*efg1/efg1*) are listed along with their nearest neigbouring ORFs designated left or right ORF if situated at descending and, respectively, ascending chromosomal coordinates. ORF orientations are indicated by the arrows. Other proteins binding to the same chromosomal region are also indicated. Binding regions within coding regions are marked in purple lettering and green shading indicates multiple binding regions. *, significant binding regions did not overlap in both replicates.

Chr	binding region	size (bp)	left ORF	gene name	left ORF position	additional binding proteins	right ORF	gene name	right ORF Position	additional binding proteins
1	41740..42160	420	*ORF19.6080*	*BFA1*	40485<--41771		*ORF19.6079*		42606-->43505	
1	161400..164000	2600	*ORF19.6022*		160946<--162676		*ORF19.6021*	*IHD2*	167084-->167830	
1	238530..238840	310	*ORF19.3305*	*ZCF17*	236100<--238300					
1	281757..282429	672	*ORF19.3330.3*	*POX18*	280432<--280830		*ORF19.3331*	*ABC1*	282488-->284148	
1	293789..295440	1641	*ORF19.3336*		296059<--296517	Efg1 (Normoxia)				
1	343880..345560	1680	*ORF19.3358*	*LSC1*	342949<--343920		*ORF19.3359*	*ARP8*		
1	405320..406158	838	*ORF19.4528*		403100<--403700		*ORF19.4527*	*HGT1*	406700-->408300	
1	438840..442620	3780	*ORF19.3668*	*HGT2*	434400<--436100					
1	468060..469140	1080					*ORF19.3681*		469200-->471700	
1	496987..497743	756	*ORF19.3694*		496220<--496250					
1	513480..514940	1460	*ORF19.2929*	*GSC1*	506000<--511600					
1	624356..625250	894	*ORF19.2990*	*XOG1*	622280<--623598		*ORF19.2991*	*HOL1*	628104-->629850	
1	642960..643280	320	*ORF19.3001*	*TEM1*	642020<--642720		*ORF19.3002*	*RPS1*		
1	676300..677320	1020	*ORF19.3014*	*BMH1*	675150<--675950					
1	801402..801789	387	*ORF19.1028*	*ELA1*	798250<--799400		*ORF19.1027*	*PDR16*	801800-->802900	
1	811500..813800	2300	*ORF19.4457*	*BNI4*	806500<--811500					
1	817700..818450	750	*ORF19.4459*		813950<--815600	Efg1 (Normoxia)				
1	831858..832160	302					*ORF19.4468*		832180-->832700	
1	871387..871611	224	*ORF19.1051*	*HTA2*	870750<--871150		*ORF19.1052*		872000-->872400	
1	879390..879720	330	*ORF19.1057*		879400<--878800		*ORF19.1058*			
1	881900..882250	350	*ORF19.1060*		881450<--881950			*HHT21*	882240-->882660	
1	889200..892950	3750	*ORF19.1064*	*ASC2*	886000<--889200					
1	892300..892950	650	*ORF19.1065*	*SSA2*	890400<--892400					
1	896950..898000	1050					*ORF19.1069*	*RPN4*	898000-->899500	
1	913960..914230	270	*ORF19.5197*	*APE2*	911200<--914300					
1	945500..946100	600	*ORF19.6852*		943720<--944530		*ORF19.6852.1*		946320-->946508	
1	993420..993780	360	*ORF19.767*	*ERG3*	991690<--992840					
1	1032864..1033900	1036	*ORF19.48*		1028320<--1032500					
1	1035900..1036850	950	*ORF19.50*		1033920<--1035920		*ORF19.51*		1036980-->1040960	
1	1376850..1377800	950	*ORF19.6265.1*	*RPS14B*	1375920<--1376750		*ORF19.6265*	*RPS22A*	1377105-->1377500	
1	1833360..1833780	420	*ORF19.5114.1*		1832950<--1833140					
1	1835820..1836540	720	*ORF19.5117*	*OLE1*	1834360<--1835812					
1	1865684..1866220	536	*ORF19.395*	*ENO1*	1864240<--1865570		*ORF19.396*	*EAF6*	1866510-->1867150	
1	1913970..1914750	780	*ORF19.4737*	*TPO3*	1914900<--1916600					

1	1933440..1933890	450	*ORF19.4748*	*MSL1*	1933050<--1933450		*ORF19.4749*		1933890-->1935570			
1	2052390..2053200	810	*ORF19.4792*		2050140<--2051810		*ORF19.4793*		2050000-->2051800			
1	2098500..2099800	1300	*ORF19.4818*		2102700<--2104290							
1	2193660..2193990	330	*ORF19.4867*	*SWE1*	2189160<--2192700	Efg1 (Normoxia)	*ORF19.4869*	*SFU1*	2195410-->2196960			
1	2252800..2254800	2000	*ORF19.4890*	*CLA4*	2249520<--2252470							
1	2256940..2257500	560	*ORF19.4892*	*TPK1*	2255640<--2256855							
1	2300880..2301120	240	*ORF19.4909.1*	*RPL42*	2300031<--2300730							
1	2307550..2307860	310	*ORF19.4912*		2305310<--2307240		*ORF19.984*	*PHO8*	2309140-->2310647			
1	2401200..2402900	1700	*ORF19.2333*		2399740<--2401214		*ORF19.2332*		2403600-->2404380			
1	2406060..2406510	450		*ADA2*	2404450<--2405790			*RPS17B*	2406591-->2407383			
1	2437190..2437750	560					*ORF19.2309*	*RPL2*	2438200-->2440300			
1	2441250..2441950	700	*ORF19.2308*		2442020<--2443140							
1	2491650..2492070	420	*ORF19.667.1*		2492140<--2492760							
1	2514000..2514450	450	*ORF19.657*	*SAM2*	2513620<--2514780							
1	2682800..2683800	1000	*ORF19.5234*	*RBD1*	2680634<--2682643		*ORF19.5233*		2683788-->2684135			
1	2694600..2695800	1200	*ORF19.5228*	*RIB3*	2694013<--2694636		*ORF19.5227*		2695968-->2696465			
1	2776700..2776800	100					*ORF19.6348*		2776744-->2779569			
1	2852850..2853620	770	*ORF19.4936*		2853604<--2853999							
1	2869900..2871300	1400	*ORF19.4941*	*TYE7*	2869020<--2869829		*ORF19.4942*		2871337-->2871705			
1	2890500..2891200	700	*ORF19.4952*		2891695<--2892633							
1	2910180..2910390	210	*ORF19.4960*		2907412<--2908446		*ORF19.4961*	*STP2*	2911732-->2913486			
1	2943300..2943800	500	*ORF19.4972*		2935625<--2937571		*ORF19.4975*	*HYR1*	2944794-->2947553			
1	2992290..2993110	820	*ORF19.4997*	*KIS2*	2987895<--2990032		*ORF19.4998*	*ROB1*	2993348-->2996389			
1	3023800..3026000	2200	*ORF19.5014*		3022829<--3023536		*ORF19.5015*	*MYO2*	3026140-->3030825			
1	3034100..3035260	1160	*ORF19.5017*	*DUR32*	3031584<--3033599		*ORF19.5019*		3035261-->3037345			
1	3040660..3041150	490	*ORF19.5021*	*PDX1*	3039105<--3040358		*ORF19.5022*		3041593-->3043548			
1	3051300..3051700	400	*ORF19.5024*	*GND1*	3045995<--3048182		*ORF19.5025*	*MET3*	3051624-->3053207			
1	3071600..3072800	1200					*ORF19.5032*	*SIM1*	3074225-->3075343			
1	3080420..3081050	630					*ORF19.5035*		3078708-->3080366			
1	3112130..3112640	510	*ORF19.7218*	*RBE1*	3108246<--3109061		*ORF19.7219*	*FTR1*	3113806-->3114951			
2	163500..164100	600										
2	465977..466288	311	*ORF19.1555*	*SAC3*	464538<--468209							
2	557960..558130	170	*ORF19.5826*		557079<--558713							
2	593190..594270	1080	*ORF19.5806*	*ALD5*	591488<--592987							
2	626356..626850	494	*ORF19.5785*		628280<--629158							
2	671450..671950	500	*ORF19.906*	*ROM2*	665520<--669665							
2	672552..672732	180					*ORF19.905*	*AVT7*	672821-->674143			
2	774413..775099	686					*ORF19.852*	*SAP98*	775519-->776613			
2	783780..784740	960					*ORF19.849*		785985-->788531			
2	798300..798510	210	*ORF19.8464*	*STE11*	795730<--798201							
2	803500..803730	230	*ORF19.841*		802020<--804110							
2	815640..816150	510	*ORF19.835*		813549<--815909							
2	878200..878680	480	*ORF19.804*		877222<--878202							

2	883790..884532	742					ORF19.799	STE4	884534->885907	
2	901800..902400	600	ORF19.1592		901037<-901795		ORF19.1591	ERG10	902615->903823	
2	954210..955076	866	ORF19.4495	NDH51	952547<-954019		ORF19.4494	KTR2	955166->956605	
2	962090..962430	340	ORF19.4490	RPL17B	961440<-961997		ORF19.4488		965502->968417	
2	974900..975120	220	ORF19.144	SNU114	971804<-974872					
2	997380..997680	300					ORF19.191	KIC1	997849->1000524	
2	1024676..1024873	197	ORF19.3521	ARH2	1023164<-1023958		ORF19.3522		1026295->1026600	
2	1105360..1106040	680	ORF19.3568	RXT3	1102641<-1104197		ORF19.3569		1106693->1107811	
2	1301983..1302022	39	ORF19.17	SCP1	1301325<-1301909					
2	1345393..1345665	272	ORF19.35.1		1345203<-1345445					
2	1362880..1363240	360	ORF19.1223	DBF2	1357902<-1360034		ORF19.1224	FRP3	1365218->1366075	
2	1367600..1368080		ORF19.225	PEX22	1367053<-1367676		ORF19.3152	AMO2	1317756->1373771	
2	1377930..1379250	1320		LSP1	1379510<-1380463					
2	1482160..1482580	420	ORF19.2284		1481535<-1482554					
2	1661980..1662640	660					ORF19.2165		1662652->1663488	
2	1723000..1723500	500					ORF19.3627		1722702->1723421	
2	1825800..1827300	1500	ORF19.207	PGA55	1823947<-1828161					
2	1879160..1880200	1040		MET10	1872707<-1875991		ORF19.4077	MIT1	1880524->1882158	
2	1991080..1991630	550	ORF19.1375	LEU42	1992242<-1993957					
2	2055040..2055440	400	ORF19.1779	MP65	2053567<-2054703		ORF19.1778		2056276->2056590	
2	2066600..2066980	380					ORF19.1773	RAP1	2066997->2068286	
2	2075585..2075817	232					ORF19.1769	PLP2	2075839->2076636	
2	2088225..2088375	150					ORF19.1765		2088810->2090066	
2	2100600..2101320	720	ORF19.1759	PHO23	2099138<-2100586		ORF19.1757		2102914->2104665	
3	152960..153300	340					ORF19.3071	MIH1	155056->157740	
3	162240..162640	400	ORF19.1288	FOX2	157976<-160696		ORF19.1289	SCT1	162857->165169	
3	174030..174380	350					ORF19.6164		174381->174707	
3	208320..208440	120					ORF19.2506		209733->211526	
3	216009..216160	151					ORF19.2509.1		216500->216709	
3	235900..236060	160	ORF19.158		232341<-233667		ORF19.3153	MSS4	236576->238752	
3	245700..247800	2100	ORF19.3156		240982<-244245					
3	291720..292320	600	ORF19.1715	IRO1						
3	295400..296000	600	ORF19.1714	PGA44						
3	305450..305620	170	ORF19.1709		304792<-305175		ORF19.1708		306821-> 307480	
3	333720..335600	1880	ORF19.1693		324275<-332767		ORF19.1691		335872-> 336459	
3	338760..339040	280	ORF19.1690	TOS1	336918<- 338324		ORF19.1687		342684-> 344987	
3	364700..364850	150	ORF19.1676		362744<-363830		ORF19.1675		365359-> 366561	
3	417640..418000	360	ORF19.1658		414753<-416640					
3	478200..478480	280	ORF19.1624		474903<- 477388		ORF19.1623	CAP1	479014-> 480513	
3	500340..501430	1090	ORF19.1616	FGR23	499572<-502916					
3	510700..511380	680	ORF19.1611		509772<-510704		ORF19.1610		511399 ->512532	
3	517080..517280	200	ORF19.1608	AYS1	514997<-516763					
3	528720..528980	260	ORF19.229		527185<-528719					

3	550800..551065	265	ORF19.242.2	SAP8	548234<--549451		ORF19.242.1		551642--> 551830			
3	888466..888730	264	ORF19.5870	CTP1	887091<--888046							
3	1125000..1125400	400	ORF19.5994	RHB1	1126576<--1127130	Efg1 (Normoxia)						
3	1475328..1475640	312	ORF19.7436	AAF1	1477306<--1479144	Efg1 (Normoxia)						
3	1573640..1574000	360	ORF19.6816		1572570<--1573418		ORF19.6814	TDH3	1574973--> 1573418			
3	1721700..1722200	500	ORF19.6736		1719447<--1721336	Efg1 (Normoxia)						
3	1728270..1728540	270	ORF19.6734	TCC1	1730057<--1732303	Efg1 (Normoxia)						
4	39220..39840	620	ORF19.5653	ATP2	39465<--41389							
4	51040..51360	320	ORF19.5660.1		50930<--51211		ORF19.5661	PTC1	51522--> 52574			
4	128500..131800	3300	ORF19.4167		126574<--127113		ORF19.4166	ZCF21				
4	238480..240240	1760	ORF19.4673	BMT9	234413<--236764		ORF19.4672		240313--> 240615			
4	245400..246120	720	ORF19.4669	AAT22	244153<--245382							
4	255300..255540	240	ORF19. 4660	RPS6A	255674<--256809							
4	261750..262900	1150	ORF19.4657		263911<--265413							
4	316700..317200	500	ORF19.4632	RPL20B	315765<--316283							
4	347120..347520	400	ORF19.4618	FBA1	346020<--347099		ORF19.4617		348197--> 348733			
4	479840..480120	280	ORF19.2765	PGA62	480635<--481276		ORF19.2767	PGA59	471123--> 471464			
4	563934..569250	316	ORF19.2726		558959<--559897							
4	570720..570920	200	ORF19.2725		566926<--567228		ORF19.2724		571922--> 573418	Efg1 (Normoxia)		
4	575480..575680	200	ORF19.2723	HIT1	577406<--577852	Efg1 (Normoxia)						
4	638800..639360	560	ORF19.2686		633978<--635720		ORF19.2685	PGA54	639770--> 640798			
4	1436070..1436220	150	ORF19.2888		1434188<--1434862		ORF19.2887		1436372--> 1436986			
4	1439500..1440400	900	ORF19.2886	CEK1	1437788<-- 1439056							
4	1470230..1470720	490	ORF19.2877	PDC11	1468241<--1469944	Efg1 (Normoxia)	ORF19.2876	CBF1	1471203--> 1472237	Efg1 (Normoxia)		
5	33240..33780	540					ORF19.978	BDF1	30720--> 32849			
5	100700..101900	1200	ORF19.938		103156<--104601							
5	149940..151960	2020	ORF19.922	ERG11	148120<--149706							
5	161820..162000	180	ORF19.568	SPE2	159627<--160775		ORF19.570	IFF8	164521--> 16665			
5	208830..209040	210	ORF19.1978	GIT2	206349<--207953							
5	246700..247400	700	ORF19.1960	CLN3	244214<--245611							
5	254580..254730	150	ORF19.1958		253350<--255256							
5	342270..342900	630	ORF19.4148		340785<--342233		ORF19.4149.1		342916--> 351076			
5	351360..351720	360	ORF19.4152	CEF3	347719<--351076		ORF19.4153		353433--> 355034			
5	380340..380820	480	ORF19.3207	CCN1	377678<--379759							
5	854600..855500	900	ORF19.1106		848594<--850948							
5	871800..872160	360	ORF19.3215		872183<--872572							
5	921800..923800	2000	ORF19.3895	CHT2	919805<--921556		ORF19.3897					
5	947340..947820	480	ORF19.3911	SAH1	946010<--947362							
5	950100..952000	1900	ORF19.3912	GLN3	947849<--949897							
5	953460..954180	720	ORF19.3914		952095<--953387							
5	955800..956340	540	ORF19.3915		954174<--955478		ORF19.3916		956373--> 957956			
5	997800..998250	450	ORF19.3942.1	RPL43A.3	997147<--997796							
5	1040800..1041030	230	ORF19.3967	PFK1	1041235<--1044198							

S	1046000..1046320	320	*ORF19.11451*									
S	1047900..1050900	3000	*ORF19.11451*									
S	1085800..1087100	1300	*ORF19.3983*		1080849<--1083059			*ORF19.11467*				
S	1106700..1107550	850	*ORF19.3997*	*ADH1*	1107937<--1108986							
S	1138640..1139360	720	*ORF19.4012*	*PCL5*	1139318<--1140232							
6	31740..32580	840	*ORF19.1187*	*CPH2*	32572<--35133							
6	60500..60650	150	*ORF19.1195*		57658<--60009		*ORF19.1196*			60917-->63502		
6	90200..90850	650	*ORF19.4211*	*FET3*	87506<--89365	Efg1 (Normoxia)	*ORF19.4210*			92713-->94104	Efg1 (Normoxia)	
6	128632..129240	608	*ORF19.3653*	*FAT1*	129850<--131802							
6	133550..134300	750	*ORF19.3651*	*PGK1*	132037<--133290							
6	164070..165060	990	*ORF19.3649*	*CAN3*			*ORF19.85*	*GPX2*	165076-->165567			
6	173880..174320	440	*ORF19.90*			Efg1 (Normoxia)						
6	189000..191070	2070	*ORF19.96*	*TOP1*	186586<--188928		*ORF19.97*	*CAN1*	191821-->192821			
6	208530..209160	630	*ORF19.111*	*CAN2*	206049<--207755							
6	412860..413550	690	*ORF19.691*	*GPD2*	411560<--412675							
6	417460..417900	440	*ORF19.3508*		416316<--417449		*ORF19.3507*	*MCR1*	418020-->418925			
6	693120..693800	680	*ORF19.5618*		691040<--692998		*ORF19.5619*		693815--> 695932			
7	109500..109850	350	*ORF19.7055*		16320<--106646	Efg1 (Normoxia)	*ORF19.7054*		114110-->114475		Efg1 (Normoxia)	
7	128350..129050	700	*ORF19.7049*	*CYB5*	129228<--129608							
7	201940..202140	200	*ORF19.7018*	*RPS18*	202217<--203082							
7	378060..378480	420	*ORF19.6548*	*ISU1*	377224<--377787		*ORF19.6547*		379041-->379388			
7	669290..669420	130	*ORF19.5148*	*CDC35*	662738<--667810		*ORF19.5147*	*LMO1*	669600-->671519			
7	701550..702300	750	*ORF19.5132*		700597<--700977		*ORF19.5131*		703314-->705476			
7	730600..730800	200	*ORF19.1345*	*LIP8*	727502<--728884		*ORF19.1344*		731818-->732482			
7	768300..740500	2200	*ORF19.6705*		771047<--774184							
7	852520..852860	340	*ORF19.7196*		853153<--854634							
7	912200..913300	1100	*ORF19.7152*		907588<--908685	Efg1 (Normoxia)	*ORF19.7151*		915533-->915967		Efg1 (Normoxia)	
7	916400..917200	800	*ORF19.7150*	*NRG1*	918848<-- 919780	Efg1 (Normoxia)						
7	917800..918200	400	*ORF19.7150*	*NRG1*	918848<--919780	Efg1 (Normoxia)						
R	69500..70900	1400	*ORF19.7506*		67793<--76707		*ORF19.7504*		72120-->73049			
R	79260..79620	360	*ORF19.7502*		75931<--76707	Efg1 (Normoxia)						
R	114000..115000	1000	*ORF19.7489*		108226<--112632							
R	204530..204760	230	*ORF19.3264.1*		206338<--206502							
R	371460..371670	210	*ORF19.2551*	*MET6*	368753<--371056							
R	547770..548220	450	*ORF19.3719*		548260<--548730							
R	555500..556600	1100	*ORF19.173*		556961<--560263							
R	596200..596538	338	*ORF19.2823*	*RFG1*	600293<--602095	Efg1 (Normoxia)	*ORF19.2822*		585256-->586101		Efg1 (Normoxia)	
R	631700..631980	280	*ORF19.2833*	*PGA34*	630066<--630659							
R	649980..651120	1140	*ORF19.2842*	*GZF3*	647412<--649544		*ORF19.2843*	*RHO1*	653856-->654452			
R	688500..689300	800	*ORF19.2862*	*RIB1*	687001<--688029							
R	729900..730140	240	*ORF19.9934*									
R	730500..731060	560	*ORF19.2397.3*		731817<--732989							
R	777360..777610	250	*ORF19.4393*	*CIT1*	777837<--779333							

R	842820..843420	600	*ORF19.4376*		841223<--841970							
R	877050..877620	570	*ORF19.467*		878587<--880515							
R	894570..894760	190	*ORF19.475*		894751<--895851	Efg1 (Normoxia)	*ORF19.474*		892936-->894237	Efg1 (Normoxia)		
R	1047130..1047310	180	*ORF19.13687*		1044415<--1046835							
R	1146180..1146580	400	*ORF19.5289*		1146111<--1146425							
R	1372080..1372560	480	*ORF19.723*	*BCR1*	1368310<--1370352		*ORF19.721*		1378138-->1380198			
R	1660050..1660380	330	*ORF19.3665*		1658591<--1659187		*ORF19.6285*	*GLC7*	1660910-->1661902			
R	1716800..1717600	800	*ORF19.610*	*EFG1*	1723589<--1725166	Efg1 (Normoxia)						
R	1718130..1718940	810	*ORF19.610*	*EFG1*	1723589<--1725166	Efg1 (Normoxia)						
R	1719360..1719780	420	*ORF19.610*	*EFG1*	1723589<-- 1725166	Efg1 (Normoxia)						
R	1721760..1721940	180	*ORF19.610*	*EFG1*	1723589<--1725166	Efg1 (Normoxia)						
R	1953120..1953680	560	*ORF19.7312*	*ERG13*	19514430<--1952785							
R	2157930..2158620	690	*ORF19.7585*	*INO1*	2155634<--2157196		*ORF19.7586*	*CHT3*	2161835-->2163538			
R	2168900..2169400	500	*ORF19.7592*	*FAA4*	2172618<--2174708	Efg1 (Normoxia)						
R	2204300..2204700	400	*ORF19.7610*	*PTP3*	2206947<--2209715							

S2 Table. Binding of Ace2-HA to chromosomal sequences of *C. albicans* under hypoxia and addition of CO_2. Strain CLvW004 producing Ace2-HA from its chromosomal ORF and reference strain BWP17 were grown in YPD medium at 30 °C under hypoxic conditions and in presence of elevated CO_2 levels (0.2 % O_2 and 6 % CO_2). Chromosomal cross-linking of proteins was done and chromatin was fragmented before immunoprecipitation. For immunoprecipitation anti-HA antibody was used and the precipitated chromatin was spotted on a *C. albicans* whole-genome tiling microarray. Regions showing significant enrichment of Ace2-HA binding compared to control strain BWP17 are listet along with their nearest neighbouring ORFs. Other proteins binding to the same chromosomal region are indicated and are taken from Lassak *et al*. [40]. Binding targets of wild-type Efg1 or HA-Efg1 shared with Ace2-HA are indicated with red background color. Accordingly to transcriptomal data obtained by Mulhern *et al*. [30], up- and down-regulation of genes is indicated of identified Ace2-HA target genes.

Chr	binding region	size (bp)	left ORF	gene name	left ORF position	additional binding proteins	transcriptom	right ORF	gene name	right ORF Position	additional binding proteins	transcriptom
1	7841..8275	434	*ORF19.13531*	*CTA2*	10718<--11485							
1	87268..87643	375	*ORF19.6054*	*BUL2*	87249<--85081			*ORF19.6053*	*ECM38*	87901-->89811		
1	91736..93009	1273						*ORF19.6048*		93971-->94900		
1	386515..386762	247	*ORF19.4536*		386295<--384805							
1	443876..445132	1256	*ORF19.3669*	*SHA3*	444229<--442442							
1	771329..772704	1375	*ORF19.1133*		771008<--767144							
1	1065969..1066247	278	*ORF19.4062*	*TRY2*	1066194<--1067309							
1	1081669..1082323	654						*ORF19.4056*	*BRG1*	1082699-->1083970	HA-Efg1 (hypoxia)	
1	1174050..1174323	273	*ORF19.2494*		1174293<--1175759							
1	1291466..1293116	1650						*ORF19.2662*	*ATC218*	1293702-->1293097		
1	1390429..1390775	346	*ORF19.6261*		1389741<--1382920							
1	1497356..1497593	237	*ORF19.6203*		1497166<--1494230							
1	1552870..1554106	1236						*ORF19.4443*		1553615-->1554169		
1	1867832..1868037	205	*ORF19.397*		1867699<--1867256			*ORF19.398*		1867970-->1868443		
1	2229588..2229837	249						*ORF19.4884*	*WOR1*	2230568-->2232925	HA-Efg1 (normoxia)	
1	2282001..2282196	195						*ORF19.4903*	*GPI12*	2282393-->2283454		
1	2553541..2553862	321	*ORF19.1155*	*DPP1*	2553615<--2552761			*ORF19.1154*		2554349-->2554822		
1	2577684..2577955	271	*ORF19.1140*		2577623<--2576997		yeast (up)					
1	2749592..2749753	161	*ORF19.3756*	*CHR1*	2749710<--2747789		yeast (up)	*ORF19.3755*		2749829-->2750491		
1	2752108..2752359	251						*ORF19.6362*		2752616-->2757016		
1	2759309..2759592	283	*ORF19.6358*	*MMS2*	2759325<--2758829			*ORF19.6357*	*MAD1*	2759790-->2761880		
1	2764327..2764726	399	*ORF19.6356*	*PRP6*	2764649<--2761914			*ORF19.6355*	*RRB1*	2764846-->2766399		
1	2774136..2774509	373	*ORF19.6350*		2773130<--2772588			*ORF19.6349*	*RVS99*	2774849-->2775856		
1	2788755..2788926	171	*ORF19.6343*	*FEN1*	2788244<--2787231			*ORF19.6342*		2789607-->2790092		
1	2803025..2803506	481	*ORF19.4917*		2803179<--2802532							
1	2805639..2805969	330	*ORF19.4918*	*TRA98*	2805372<--2803813			*ORF19.4919*	*CTN4*	2805700-->2807010		
1	2807712..2808181	469						*ORF19.4921*	*YFW1*	2808006-->2810177		
1	2854713..2854982	269						*ORF19.4936.1*		2854984-->2855199		
1	2871462..2871716	809	*ORF19.4941*	*TYE7*	2869648<--2868839	Efg1 (hypoxia)						
1	2934342..2934758	416	*ORF19.4970*		2933952<--2932225							
1	3011053..3011437	384	*ORF19.5006.1*	*SNC2*	3010047<--3009640			*ORF19.5007*	*ACT1*	3011501-->3013289		
1	231980..232506	526	*ORF19.3302*		229786<--227684	HA-Efg1 (normoxia)						
1	267962..269100	1138	*ORF19.3325*	*GLG21*	267472<--265490	HA-Efg1 (hypoxia)	yeast (down)					
1	534538..537448	2910	*ORF19.2942*	*DIP52*	534219<--532460							
1	709163..709459	296						*ORF19.3038*	*TPS2*	709534-->712200		yeast (down)
1	944334..947063	2729	*ORF19.6852*		944553<--943726	Efg1 (hypoxia)						
1	1168052..1169064	1012						*ORF19.2495*	*GSL1*	1169273-->1173989	HA-Efg1 (hypoxia)	
1	1483827..1484221	394	*ORF19.6214*	*ATH1*	1483075<--1479839			*ORF19.6213*		1484856-->1485758		
1	1539849..1540065	216	*ORF19.4450*	*ZCF23*	1538490<--1536790			*ORF19.4449*	*LYS7*	1540781-->1541527		

1	1557823..1558176	353	*ORF19.4441*	*DNA43*	1557992<--1556196			*ORF19.4440*		1558228-->1560747			
1	1585052..1585329	277	*ORF19.4436*	*GPX2*	1584961<--1584446		yeast (down)						
1	2474390..2475561	1171	*ORF19.675.1*		2473989<--2473852			*ORF19.675*		2475630-->2476268			haphae (down)
1	163192..163956	764	*ORF19.6022*		162676<--160946								
1	290470..291182	712	*ORF19.3334*	*RPS2*	290460<--289711		hyphae (up)	*ORF19.3335*		291859-->292461			
1	308710..309143	433	*ORF19.3341*		308500<--306632			*ORF19.3342*		309136-->310986			
1	344379..344729	350	*ORF19.3358*	*LSC1*	343919<--342948	Efg1 (hypoxia)	hyphae (up)	*ORF19.3359*		345578-->348778			yeast (up)
1	473351..475375	2024						*ORF19.3682*	*CAX4*	474953-->475678			yeast (down)
1	619987..620177	190						*ORF19.2989*		620167-->621195		Efg1 (hypoxia)	
1	281746..283031	1285						*ORF19.3331*	*ABC1*	282447-->284147	Efg1 (hypoxia)	HA-Efg1 (hypoxia)	
1	718672..719605	933						*ORF19.3043*	*TGL2*	719688-->720743	HA-Efg1 (hypoxia)		
1	893816..894200	384	*ORF19.1066*		893769<--893005			*ORF19.1067*		895187-->895972			
1	1122505..1122672	167	*ORF19.431*		1122320<--1119993								
1	1250416..1250835	419	*ORF19.2452*		1249532<--1248285		yeast (up)	*ORF19.2451*	*PGA45*	1251622-->1253010			yeast (up)
1	1512469..1513395	926						*ORF19.6196*		1513369-->1513935			
1	1610668..1610890	222						*ORF19.4423*		1611113-->1614334			
1	2595231..2595559	328						*ORF19.5281*		2595412-->2599074			
1	2620707..2620948	241	*ORF19.5269*		2620599<--2619208			*ORF19.5268*	*NUT2*	2621047-->2621559			
1	2767288..2767489	201	*ORF19.6354*		2767135<--2766485			*ORF19.6353*	*LPF40*	2767870-->2769948			
1	2790207..2790434	227						*ORF19.6341*	*RIB7*	2790384-->2791298			
1	2831400..2831561	161	*ORF19.4928*		2829632<--2827377			*ORF19.4929*		2832124-->2835648			yeast (up)
1	2839170..2839331	161	*ORF19.4931*		2838924<--2836579	HA-Efg1 (hypoxia)		*ORF19.4931.1*		2839978-->2840727	HA-Efg1 (hypoxia)		
1	2890707..2891612	905						*ORF19.4952*		2891732-->2892670	Efg1 (hypoxia)		
1	2896486..2896938	452	*ORF19.4954*	*PPA1*	2896192<--2895602			*ORF19.4955*	*SPS2*	2896843-->2898429			
1	2931444..2931724	280	*ORF19.4969*	*XRN1*	2930822<--2926240								
1	3017160..3017444	284	*ORF19.5010*	*DIM1*	3017120<--3016140		yeast (up)	*ORF19.5011*		3017953-->3020229			
1	3076372..3076521	149	*ORF19.5033*	*ATG12*	3076363<--3075869			*ORF19.5034*	*YBP1*	3076776-->3078707			
1	3163635..3164032	197	*ORF19.7251*	*WSC4*	3164394<--3162919	HA-Efg1 (hypoxia)							
2	32744..32988	244	*ORF19.2107.1*	*STF2*	33351<--33620		hyphae (down	*ORF19.2108*	*PGA9*	32587-->31637			
2	62620..62860	240	*ORF19.2090*	*ECM16*	62936<--59145			*ORF19.2089*	*NYV1*	63257-->64177			
2	234732..234914	182	*ORF19.1990*		234444<--232552								
2	305109..305421	312	*ORF19.1479*		304225<--301883			*ORF19.1480*		305495-->306025			
2	535888..536244	356	*ORF19.5842*		535695<--534910			*ORF19.5841*		536330-->537088		hyphae (down)	
2	585599..586161	562	*ORF19.5812*		585586<--584321			*ORF19.5811*	*MET1*	586286-->587971			
2	587969..588273	304						*ORF19.5809*		588296-->589657			
2	828388..828888	500	*ORF19.829*	*SCH9*	827878<--825515								
2	963789..963998	209	*ORF19.4490*	*RPL17*	961980<--961423	Efg1 (hypoxia)		*ORF19.4488*	*SWI3*	965485-->968400	Efg1 (hypoxia)		
2	1316490..1317142	652						*ORF19.24*	*RSB11*	1317217-->1318578			
2	1340887..1341353	466						*ORF19.35*	*SKY2*	1341138-->1344068	Tpk2-HA (hyphae)		
2	1770659..1770967	308	*ORF19.3606*		1770360<--1769839			*ORF19.3605*		1771101-->1771826			
2	1797354..1797663	309	*ORF19.225*		1796447<--1795362	Efg1 (hypoxia)		*ORF19.223*		1797689-->1800073			
2	1842607..1842881	274	*ORF19.204*		1840229<--1839615			*ORF19.203*		1842959-->1844470			
2	1857917..1858111	194	*ORF19.4066*		1856790<--1854379								
2	1883592..1883939	347						*ORF19.4079*		1883767-->1884558			
2	1896579..1897081	502						*ORF19.4090*		1898301-->1896796			
2	1959173..1959431	258	*ORF19.1397*		1958642<--1957932			*ORF19.1396*	*AGE2*	1960782-->1961945			
2	116183..116795	612						*ORF19.2057*	*YTA12*	117048-->119588		yeast (up)	
2	155250..155786	536	*ORF19.2031*		155268<--154526			*ORF19.2030*		155823-->156296			
2	327015..327177	162						*ORF19.1490*	*MSB2*	327702-->331931			
2	572071..572863	792						*ORF19.5818*	*SUR2*	573066-->574094		hyphae (down)	

2	660174..660417	243	*ORF19.909*	*STP4*	660179<--659049		hyphae (down)			791066-->792154			
2	789975..790975	1000						*ORF19.847*					
2	822632..823052	420	*ORF19.832*		822404<--819356								
2	919877..920124	247						*ORF19.4513*		920879-->922069			
2	956685..956995	310						*ORF19.4492*	*EBP2*	956922-->958202			
2	1104636..1105023	387	*ORF19.3568*	*RXT3*	1104183<--1102627								
2	1164935..1165312	377	*ORF19.6881*		1164794<--1164147			*ORF19.6882*	*OSM1*	1165487-->1166998		hyphae (down)	
2	1187147..1187465	318	*ORF19.6893*		1187201<--1185839								
2	1554538..1554886	348	*ORF19.1864*		1554405<--1552246			*ORF19.1863*		1554715-->1556503			
2	1680188..1680349	161	*ORF19.1351*		1679933<--1679193								
2	1685026..1685304	278	*ORF19.1348*		1685131<--1684568								
2	1802346..1802508	162	*ORF19.220*	*PIR1*	1801740<--1800700		hyphae (down)						
2	1876679..1876854	175	*ORF19.4076*	*MET10*	1875988<--1872704		hyphae (down)						
2	1879647..1879982	335						*ORF19.4077*	*MIT1*	1880521-->1882155	Efg1 (hypoxia)		
2	1893206..1893376	170	*ORF19.4085*		1893261<--1892620			*ORF19.4086*		1893505-->1894155			
2	2139486..2139660	174	*ORF19.1742*		2138454<--2137432								
2	623114..623431	317	*ORF19.5789*		622945<--622277			*ORF19.5788*		623651-->626379			
2	749035..749443	408						*ORF19.866*	*RAD30*	749865-->751787			
2	1077383..1077657	274	*ORF19.3553*		1077153<--1076170								
2	1111969..1113009	1040						*ORF19.3573*		1112912-->1116385			
2	1888295..1888470	175						*ORF19.4081*		1889252-->1889752	HA-Efg1 (hypoxia)		
2	1921625..1921782	157						*ORF19.1601*		1921931-->1923100			
3	13097..13527	430	*ORF19.5468*		12501<--12190			*ORF19.5467*		13756-->14265			
3	877355..877585	230	*ORF19.5864*		877338<--875701			*ORF19.5865*		877626-->880223			
3	776603..777066	463						*ORF19.6951*	*DPL1*	777441-->779210			yeast (down)
3	807277..807523	246	*ORF19.6930*	*SIC1*	807031<--806315			*ORF19.6929*		807898-->808425			
3	1038620..1039215	595	*ORF19.5952*		1038697<--1037381			*ORF19.5953*	*SFP1*	1041453-->1042790			
3	1072160..1072466	306	*ORF19.5965*		1072248<--1069021			*ORF19.5966*		1072444-->1072785			
3	1093084..1093262	178						*ORF19.5978*		1093310-->1094524			
3	1305553..1305863	310	*ORF19.7362*		1302603<--1300389			*ORF19.7363*		1306218-->1308440			
3	1445006..1445426	420						*ORF19.7400*		1446629-->1451336			
3	1496185..1496554	369	*ORF19.7444*		1494922<--1493897			*ORF19.7445*		1496429-->1497916			
3	1727020..1727262	242						*ORF19.6734*	*TCC1*	1730074-->1732320	HA-Efg1(n and h), Efg1(hypoxia)		
3	892929..893238	309	*ORF19.5871*		893071<--890979		hyphae (down)						
3	1118625..1118860	235						*ORF19.5992*	*WOR2*	1118847-->1120187	HA-Efg1 (normoxia and hypoxia)		
3	1233227..1233512	285						*ORF19.6986*		1234039-->1236246			
3	1475513..1476883	370						*ORF19.7436*	*AAF1*	1477326-->1479164	HA-Efg1(n and h), Efg1(hypoxia)		
3	1491955..1492166	211	*ORF19.7441*		1491938<--1491012			*ORF19.7442*		1492186-->1493082			
3	1510669..1511153	484						*ORF19.7451*		1511052-->1515023			
4	48034..48219	185	*ORF19.5657*	*SWC1*	48100<--45137								
4	131436..131638	202	*ORF19.4167*		127111<--126572			*ORF19.4166*	*ZCF21*	131941-->133830	HA-Efg1 (hypoxia), Efg1 (hypoxia)		
4	248259..248536	277	*ORF19.4668*		248276<--246123								
4	282782..283309	527						*ORF19.4649*		283241-->286831			
4	420730..420888	158						*ORF19.4579*		421115-->422041			
4	480605..481016	411						*ORF19.2765*	*PGA62*	480632-->481273	HA-Efg1 (hypoxia),	yeast (down)	
4	538595..538903	308	*ORF19.2739*		538696<--536978								
4	555823..556043	220	*ORF19.2731*		553564<--553226			*ORF19.2730*		553936-->555756			
4	569822..570064	242	*ORF19.2725*		567226<--566924	HA-Efg1 (normoxia and hypoxia)		*ORF19.2724*		571920-->573416	HA-Efg1(n and h), Efg1(hypoxia)		
4	665440..665998	558	*ORF19.2674*		665137<--664109			*ORF19.2673*		665706-->666725			
4	901830..902078	248	*ORF19.1429*		901816<--901376			*ORF19.1428*		902225-->902740			

4	958836..959072	236	*ORF19.3840*		959031<-954805			*ORF19.3839*		961031->962392			
4	982132..982341	209						*ORF19.3823*		982321->987258			
4	990641..990855	214	*ORF19.3821*		990526<-989339	HA-Efg1 (hypoxia)							
4	1020888..1021863	975	*ORF19.3803*	*MNN24*	1020679<-1018910		yeast (down)	*ORF19.3802*	*PMT6*	1022709->1025207		yeast (down)	
4	1048206..1048473	267	*ORF19.3794*	*CSR1*	1044143<-1042287	HA-Efg1 (hypoxia)		*ORF19.3793*		1048418->1049593			
4	156748..157165	417	*ORF19.4706*		156361<-155864			*ORF19.4705*		157320->158915		yeast (up)	
4	318539..318875	336	*ORF19.4631*	*ERG251*	318193<-317228		hyphae (down)						
4	673775..674045	270	*ORF19.2670*		673767<-672892		yeast (down)						
4	772472..772673	201	*ORF19.1314*		772094<-770685		yeast (down)						
4	119205..119456	251	*ORF19.4173*		119171<-117582								
4	125737..125901	164	*ORF19.4169*		125651<-125256			*ORF19.4168*		126013->126516			
4	149067..149317	250						*ORF19.4711*		150355->152169			
4	167790..168189	399	*ORF19.4702*		167605<-166703			*ORF19.4701*		168466->169392			
4	241195..241666	471						*ORF19.4670*	*CAS5*	241403->243868			
4	263241..263484	243						*ORF19.4657*		263907->265409	Efg1 (hypoxia)		
4	277969..278128	159						*ORF19.4651*		278269->278688			
4	294547..294757	210						*ORF19.4643*		294803->301954			
4	336726..336904	178	*ORF19.4624*		336394<-335036								
4	342226..342418	192	*ORF19.4622*		342120<-340963								
4	449574..449864	290	*ORF19.4560*	*BFR1*	449237<-447849			*ORF19.2775*	*IDI1*	450181->451035			
4	681943..682094	151						*ORF19.2665*		682598->686252			
4	806517..806676	159	*ORF19.1298*		806323<-803789			*ORF19.1297*		807459->809654			
4	972793..973252	459	*ORF19.3829*		972279<-970633								
4	1263263..1263475	212						*ORF19.1258*		1264022->1264735			
4	1269196..1269522	326	*ORF19.1259*		1269246<-1264915								
4	1301093..1301343	250	*ORF19.1274*		1298570<-1296879			*ORF19.1275*		1302092->1304095			
5	30117..30380	263	*ORF19.979*	*FAS1*	29661<-23548		yeast (up)						
5	94280..94512	232	*ORF19.940*		93594<-89881			*ORF19.939*		95043->98102			
5	217717..218023	306	*ORF19.1972*		217288<-215867	Efg1 (hypoxia)		*ORF19.1971*		218221->219705			
5	380339..380796	457	*ORF19.3207*	*CCN1*	379761<-377680	Efg1 (hypoxia)							
5	406103..406467	364	*ORF19.3195*	*HIP1*	404636<-402837		hyphae (down	*ORF19.3193*	*FCR3*	407979->409178	Tpk2-HA (hyphae)		
5	443455..443624	169	*ORF19.3174*		443369<-440835								
5	453619..453945	326	*ORF19.3170*		453571<-451385								
5	465380..466233	853	*ORF19.3161*		465405<-464443								
5	472765..473253	488						*ORF19.4216*	*HSP12*	473414->473920	HA-Efg1 (hypoxia)		
5	155228..155460	232	*ORF19.921*		153233<-151176			*ORF19.920*		156807->158162		yeast (up)	
5	175021..175219	198						*ORF19.576*		175559->176047			
5	347903..348110	207	*ORF19.4151*		347572<-345242								
5	529019..529265	246	*ORF19.4245*		527060<-525714			*ORF19.4246*		529711->531504			
5	568004..568222	218	*ORF19.4266*		568051<-566677								
5	851168..851516	348	*ORF19.1106*		850957<-848603	Efg1 (hypoxia)							
5	513893..514105	212	*ORF19.4239*		513647<-511632								
5	522151..522532	381	*ORF19.4242*	*CST20*	521590<-517904								
5	599825..600166	341	*ORF19.4282*		598167<-597259								
5	1107056..1107300	244						*ORF19.3997*	*ADH1*	1107881->1108930	Efg1 (hypoxia)	yeast (down)	
6	4563..5065	502						*ORF19.6337*		5545->6489			
6	60497..60663	166	*ORF19.1195*		60013<-57662	Efg1 (hypoxia)	yeast (up)	*ORF19.1196*		60921->63506	Efg1 (hypoxia)	yeast (down)	
6	107748..107995	247						*ORF19.4199*		107932->109503			
6	173917..174207	290						*ORF19.90*		174680->176944	Efg1 (hypoxia), HA-Efg1 (normoxia)		
6	304142..304599	457	*ORF19.3434*		301246<-298277			*ORF19.3433*	*OYE23*	304843->306063		yeast (down)	

6	319400..319632	232	*ORF19.3431*		317782<-314096				*ORF19.3430*	*BUD21*	319776->320810			
6	339382..339625	243							*ORF19.3421.1*		339664->340248			
6	349369..349608	239	*ORF19.3420*		348886<-348503				*ORF19.3419*	*MAE1*	350713->352605		yeast (down)	
6	378815..379061	246	*ORF19.3405*		378232<-376640				*ORF19.3404*		379021->380502			
6	421895..422171	276							*ORF19.3505*		422337->424733			
6	430038..430268	230	*ORF19.3501*		429691<-426551				*ORF19.3499*		434464->434967		hyphae (up)	
6	444405..444602	197	*ORF19.3494*		444313<-443213				*ORF19.3453*		444683->447643			
6	549988..550214	226	*ORF19.5537*		548965<-547667				*ORF19.5539*		552727->553569			
6	603094..603382	288	*ORF19.5568*		603308<-602358				*ORF19.5569*		603848->606529			
6	630120..630398	278							*ORF19.5584*		630618->633050			
6	640292..640524	232	*ORF19.5586*		640372<-637424									
6	730739..730929	190	*ORF19.5705*	*NAM2*	730549<-727964		yeast (up)	*ORF19.5710*			731035->734520			
6	821237..821408	171	*ORF19.5753*	*HGT10*	819180<-817540		yeast (up)							
6	837437..837820	383	*ORF19.5759*		836974<-832487		yeast (up)							
6	867771..868136	365	*ORF19.5775*		864791<-863253				*ORF19.1221*		876496->877833			
6	875889..876332	443							*ORF19.1221*		876496->877833			
6	898101..898410	309	*ORF19.4557*		897780<-894497									
6	90037..90595	558	*ORF19.4211*	*FET3*	89370<-87511	HA-Efg1 (normoxia and hypoxia)			*ORF19.4210*		92718->94109	HA-Efg1(n and h), Efg1(hypoxia)		
6	711941..712284	343							*ORF19.5627*		712343->713449			
6	954958..955148	190	*ORF19.1090*		954989<-954642				*ORF19.1091*		955216->957288			
6	962825..962993	168	*ORF19.1093*	*FLO8*	962206<-959828									
6	969214..969419	205							*ORF19.1097*	*ALS2*	971475->976745			
6	1028365..1028747	382	*ORF19.2160*		1027136<-1025391				*ORF19.2163*		1028841->1031354			
7	132431..132677	246							*ORF19.7047*	*RTF1*	132567->134273	HA-Efg1 (hypoxia)		
7	147491..147734	243							*ORF19.7041*		148191->150485			
7	197995..198262	267							*ORF19.7020*	*KEX1*	198461->200569			
7	226954..227152	198	*ORF19.7006*		226654<-223297		yeast (down)							
7	235013..235204	191	*ORF19.6896*		232413<-230875									
7	312089..312282	193							*ORF19.6580*		312573->313265			
7	329445..329682	237							*ORF19.6573*		329718->330476			
7	350127..350842	715	*ORF19.6563*		349795<-347816				*ORF19.6562*		350992->352287			
7	375318..375638	320	*ORF19.6551*		375267<-374593				*ORF19.6550*		375747->376631			
7	389345..389658	313	*ORF19.6540*	*PFK2*	388801<-385961		yeast (down)		*ORF19.6539*		390350->391846			
7	392764..392967	203	*ORF19.6538*		392514<-392023				*ORF19.6537*		393006->393698			
7	419339..419895	556							*ORF19.6525*		419663->421988			
7	410407..410669	262	*ORF19.6530*		409253<-408390				*ORF19.6529*	*CDC34*	411057->411791			
7	413027..413320	293	*ORF19.6528*		412926<-412315									
7	437730..438044	314	*ORF19.6518*		437290<-435305				*ORF19.6517*		438040->439230			
7	451625..451894	269	*ORF19.6514*	*CUP9*	450912<-449878	HA-Efg1 (normoxia and hypoxia)								
7	465046..465507	461							*ORF19.6506*		465072->467138			
7	476843..477195	352	*ORF19.6498*		476933<-475905									
7	493528..493763	235							*ORF19.6486*		493963->494421			
7	519989..520286	297	*ORF19.6472*		519627<-519139				*ORF19.6470*		520558->521115			
7	632455..633164	709							*ORF19.5169*		633454->635175			
R	8643..8842	199	*ORF19.7545*		7566<-4884				*ORF19.7544*		9111->9863			
R	172196..172884	688	*ORF19.3283*		172342<-171653									
R	201809..202075	266	*ORF19.3265.1*		201735<-201475				*ORF19.3265*		202225->203895			
R	334667..334909	242	*ORF19.2527*		334491<-333205				*ORF19.2528*		334922->336910			
R	509931..510278	347	*ORF19.3742*		509369<-508644				*ORF19.3740*	*PGA23*	510511->511359			
R	556779..557328	549							*ORF19.173*		556964->560266	Efg1 (hypoxia)		

R	874612..874814	202						ORF19.467	WOR3	878593-->880521	HA-Efg1 (hypoxia)		
R	926791..927553	762	ORF19.496		926380<--923609			ORF19.498	EAF7	928331-->929716		yeast (up)	
R	963503..963739	236						ORF19.522	PIM1	963564-->966800		yeast (up)	
R	1125308..1125600	292	ORF19.556		1124656<--1124237			ORF19.557		1125739-->1126764			
R	1157158..1157584	426	ORF19.5286		1156504<--1155638			ORF19.5285		1158030-->1158629			
R	1259394..1260341	947	ORF19.454	SFL1	1258170<--1255753								
R	1271946..1272327	381						ORF19.451		1274207-->1276684			
R	1372318..1372553	235	ORF19.723	BCR1	1370542<--1368320	Efg1 (hypoxia)							
R	1469903..1470143	240	ORF19.1847		1469576<--1467687								
R	1659779..1660018	239	ORF19.6286		1659219<--1658623			ORF19.6285	GLC7	1660942-->1661934			
R	1718524..1718725	201						ORF19.610	EFG1	1723620-->1725197	HA-Efg1(n and h), Efg1(hypoxia)		
R	1723278..1723663	385						ORF19.610	EFG1	1723620-->1725197	HA-Efg1(n and h), Efg1(hypoxia)		
R	1759755..1759942	187	ORF19.589	VPS21	1759114<--1758464			ORF19.6365	PTP1	1760210-->1761328			
R	1885618..1886042	424						RDN18					
R	1888916..1889176	260	RDN5					RDN18					
R	1892603..1893207	604	RDN5					RDN58					
R	1919596..1919753	157	ORF19.7293		1919006<--1916934								
R	2106048..2106312	264						ORF19.7561	EED1	2106249-->2108912	HA-Efg1 (normoxia	yeast (down)	
R	456371..456650	279	ORF19.2608		455035<--454025								
R	1229936..1230397	461	ORF19.6630		1229108<--1228704								
R	1234621..1234953	332						ORF19.6626		1235075-->1235701			
R	1461771..1461933	162	ORF19.1854	HHF22	1461360<--1461043			ORF19.1853	HHT2	1462318-->1462728			
R	1741688..1741957	269	ORF19.600		1741164<--1737995								
R	1787351..1787780	429	ORF19.6385	ACO1	1785923<--1783590		yeast (up)						
R	1832192..1832373	181	ORF19.6415.1		1831395<--1831225			ORF19.6417		1832500-->1835028			
R	78276..78466	190	ORF19.7502		76707<--75931	Efg1 (hypoxia), HA-Efg1 (normoxia)							
R	580631..580875	244	ORF19.2822		586104<--585259	HA-Efg1 (normoxia and hypoxia)		ORF19.2823	RFG1	600296-->602099	HA-Efg1 (normoxia and hypoxia)		
R	1093988..1094309	321						ORF19.646	GLN1	1095535-->1096656		yeast (down)	
R	1196472..1196912	440	ORF19.5843		1194914<--1194066	hyphae (down)							
R	1200478..1200718	240	ORF19.6653		1200545<--1198899			ORF19.6652		1201138-->1202460			
R	1445167..1445556	389						ORF19.707		1445481-->1447400			
R	1477563..1477801	238	ORF19.1843		1477285<--1475594			ORF19.1842		1479665-->1484341			
R	1955700..1956129	429	ORF19.7313		1955547<--1954102			ORF19.7314		1957926-->1958723			

S3 Table. Binding of Ace2-HA to chromosomal sequences of *C. albicans* under normoxia. Strain CLvW004 producing Ace2-HA from its chromosomal ORF and reference strain BWP17 were grown in YPD medium at 30 °C under normoxic conditions. Chromosomal cross-linking of proteins was done and chromatin was fragmented before immunoprecipitation. For immunoprecipitation anti-HA antibody was used and the precipitated chromatin was spotted on a *C. albicans* whole-genome tiling microarray. Regions showing significant enrichment of Ace2-HA binding compared to control strain BWP17 are listet along with their nearest neighbouring ORFs. Other proteins binding to the same chromosomal region are indicated and are taken from Lassak *et al*. [40]. Binding targets of wild-type Efg1 or HA-Efg1 shared with Ace2-HA are indicated with red background color, binding targets of Ace2-HA obtained uniquely under normoxic conditions are indicated with green background color. Accordingly to transcriptomal data obtained by Mulhern *et al*. [30], up- and down-regulation of genes is indicated of identified Ace2-HA target genes.

Chr	binding region	size (bp)	left ORF	gene name	left ORF position	additional binding proteins	transcriptom	right ORF	gene name	right ORF Position	additional binding proteins	transcriptom
1	7841..8275	434	*ORF19.13531*	*CTA2*	10718<--11485							
1	87268..87643	375	*ORF19.6054*	*BUL2*	87249<--85081			*ORF19.6053*	*ECM38*	87901-->89811		
1	91736..93009	1273						*ORF19.6048*		93971-->94900		
1	310988..311305	317						*ORF19.3344*	*VPS17*	311194-->312753		
1	386515..386762	247	*ORF19.4536*		386295<--384805							
1	443876..445132	1256	*ORF19.3669*	*SHA3*	444229<--442442							
1	481694..482321	627	*ORF19.3689*		486470<--484839							
1	529487..531017	1530						*ORF19.2941*	*SCW4*	530180-->531916		
1	771329..772704	1375	*ORF19.1133*		771008<--767144							
1	859362..860358	996	*ORF19.1041*		859401<--857914							
1	1065969..1066247	278	*ORF19.4062*	*TRY2*	1066194<--1067309							
1	1081669..1082323	654						*ORF19.4056*	*BRG1*	1082699-->1083970	HA-Efg1 (hypoxia)	
1	111654..111936	282	*ORF19.6041*	*RPO41*	111026<--107124		yeast and hyphae (up)					
1	1174050..1174323	273	*ORF19.2494*		1174293<--1175759							
1	1291466..1293116	1650						*ORF19.2662*	*ATC218*	1293702-->1293097		
1	1317798..1320016	2218	*ORF19.1822*	*UME6*	1316979<--1314448	HA-Efg1 (normoxia)						
1	1390429..1390775	346	*ORF19.6261*		1389741<--1382920							
1	1497356..1497593	237	*ORF19.6203*		1497166<--1494230							
1	1552870..1554106	1236						*ORF19.4443*		1553615-->1554169		
1	1867832..1868037	205	*ORF19.397*		1867699<--1867256			*ORF19.398*		1867970-->1868443		
1	2229588..2229837	249						*ORF19.4884*	*WOR1*	2230568-->2232925	HA-Efg1 (normoxia)	
1	2282001..2282196	195						*ORF19.4903*	*GPI12*	2282393-->2283454		
1	2553541..2553862	321	*ORF19.1155*	*DPP1*	2553615<--2552761			*ORF19.1154*		2554349-->2554822		
1	2577684..2577955	271	*ORF19.1140*		2577623<--2576997		yeast (up)					
1	2749592..2749753	161	*ORF19.3756*	*CHR1*	2749710<--2747789		yeast (up)	*ORF19.3755*		2749829-->2750491		
1	2752108..2752359	251						*ORF19.6362*		2752616-->2757016		
1	2759309..2759592	283	*ORF19.6358*	*MMS2*	2759325<--2758829			*ORF19.6357*	*MAD1*	2759790-->2761880		
1	2764327..2764726	399	*ORF19.6356*	*PRP6*	2764649<--2761914			*ORF19.6355*	*RRB1*	2764846-->2766399		
1	2774136..2774509	373	*ORF19.6350*		2773130<--2772588			*ORF19.6349*	*RVS99*	2774849-->2775856		
1	2788755..2788926	171	*ORF19.6343*	*FEN1*	2788244<--2787231			*ORF19.6342*		2789607-->2790092		
1	2803025..2803506	481	*ORF19.4917*		2803179<--2802532							
1	2805639..2805969	330	*ORF19.4918*	*TRA98*	2805372<--2803813			*ORF19.4919*	*CTN4*	2805700-->2807010		
1	2807712..2808181	469						*ORF19.4921*	*YFW1*	2808006-->2810177		
1	2854713..2854982	269						*ORF19.4936.1*		2854984-->2855199		
1	2871462..2871716	809	*ORF19.4941*	*TYE7*	2869648<--2868839	Efg1 (hypoxia)						
1	2934342..2934758	416	*ORF19.4970*		2933952<--2932225							
1	2971929..2972206	277						*ORF19.4991*	*MPT5*	2976172-->2978988		
1	3011053..3011437	384	*ORF19.5006.1*	*SNC2*	3010047<--3009640			*ORF19.5007*	*ACT1*	3011501-->3013289		
1	163192..163956	764	*ORF19.6022*		162676<--160946							
1	290470..291182	712	*ORF19.3334*	*RPS2*	290460<--289711		hyphae (up)	*ORF19.3335*		291859-->292461		
1	308710..309143	433	*ORF19.3341*		308500<--306632			*ORF19.3342*		309136-->310986		

1	344379..344729	350	*ORF19.9368*	*LSC1*	343919<-342948	Efg1 (hypoxia)	hyphae (up)	*ORF19.3359*		345578->348778				
1	473351..475375	2024						*ORF19.3682*	*CAX4*	474953->475678		yeast (up)		
1	619987..620177	190						*ORF19.2989*		620167->621195		yeast (down)		
1	718672..719605	933						*ORF19.3043*	*TGL2*	719688->720743	HA-Efg1 (hypoxia)			
1	893816..894200	384	*ORF19.1066*		893769<-893005			*ORF19.1067*		895187->895972				
1	1122505..1122672	167	*ORF19.431*		1122320<-1119993									
1	1250416..1250835	419	*ORF19.2452*		1249532<-1248285		yeast (up)	*ORF19.2451*	*PGA45*	1251622->1253010		yeast (up)		
1	1512469..1513395	926						*ORF19.6196*		1513369->1513935				
1	1610668..1610890	222						*ORF19.4423*		1611113->1614334				
1	2595231..2595559	328						*ORF19.5281*		2595412->2599074				
1	2620707..2620948	241	*ORF19.5269*		2620599<-2619208			*ORF19.5268*	*NUT2*	2621047->2621559				
1	2767288..2767489	201	*ORF19.6354*		2767135<-2766485			*ORF19.6353*	*LPF40*	2767870->2769948				
1	2790207..2790434	227						*ORF19.6341*	*RIB7*	2790384->2791298				
1	2831400..2831561	161	*ORF19.4928*		2829632<-2827377			*ORF19.4929*		2832124->2835648		yeast (up)		
1	2839170..2839331	161	*ORF19.4931*		2838924<-2836579	HA-**Efg1 (hypoxia)**		*ORF19.4931.1*		2839978->2840727	HA-Efg1 (hypoxia)			
1	2890707..2891612	905						*ORF19.4952*		2891732->2892670	Efg1 (hypoxia)			
1	2896486..2896938	452	*ORF19.4954*	*PPA1*	2896192<-2895602			*ORF19.4955*	*SPS2*	2896843->2898429				
1	2931444..2931724	280	*ORF19.4969*	*XRN1*	2930822<-2926240									
1	3017160..3017444	284	*ORF19.5010*	*DIM1*	3017120<-3016140		yeast (up)	*ORF19.5011*		3017953->3020229				
1	3076372..3076521	149	*ORF19.5033*	*ATG12*	3076363<-3075869			*ORF19.5034*	*YBP1*	3076776->3078707				
1	3163835..3164032	197	*ORF19.7261*	*WSC4*	3164394<-3162919	HA-Efg1 (hypoxia)								
1	32744..32988	244	*ORF19.2107.1*	*STF2*	33351<-33620		hyphae (down)	*ORF19.2108*	*PGA9*	32587->31637				
2	62620..62860	240	*ORF19.2090*	*ECM16*	62936<-63145			*ORF19.2089*	*WY1*	63257->64177				
2	234732..234914	182	*ORF19.1990*		234444<-232552									
2	305109..305421	312	*ORF19.1479*		304225<-301883			*ORF19.1480*		305495->306025				
2	535888..536244	356	*ORF19.5842*		535695<-534910			*ORF19.5841*		536330->537088		hyphae (down)		
2	585599..586161	562	*ORF19.5812*		585586<-584321			*ORF19.5811*	*MET1*	586286->587971				
2	587969..588273	304						*ORF19.5809*		588296->589657				
2	828388..828888	500	*ORF19.829*	*SCH9*	827878<-825515									
2	963789..963998	209	*ORF19.4490*	*RPL17*	961980<-961423	Efg1 (hypoxia)		*ORF19.4488*	*SWI3*	965485->968400	Efg1 (hypoxia)			
2	1316490..1317142	652						*ORF19.24*	*RSB11*	1317217->1318578				
2	1340887..1341353	466						*ORF19.35*	*SKY2*	1341138->1344068				
2	1770659..1770967	308	*ORF19.3606*		1770360<-1769839			*ORF19.3605*		1771101->1771826				
2	1797354..1797663	309	*ORF19.226*		1796447<-1795362	Efg1 (hypoxia)		*ORF19.223*		1797689->1800073				
2	1842607..1842881	274	*ORF19.204*		1840229<-1839615			*ORF19.203*		1842959->1844470				
2	1857917..1858111	194	*ORF19.4066*		1856790<-1854379									
2	1883592..1883939	347						*ORF19.4079*		1883767->1884558				
2	1896579..1897081	502						*ORF19.4090*		1898301->1896796				
2	1959173..1959431	258	*ORF19.1397*		1958642<-1957932			*ORF19.1396*	*AGE2*	1960782->1961945				
2	116183..116795	612						*ORF19.2057*	*YTA12*	117048->115588		yeast (up)		
2	155250..155786	536	*ORF19.2031*		155268<-154526			*ORF19.2030*		155823->156296				
2	327015..327177	162						*ORF19.1490*	*MSB2*	327702->331931				
2	336007..336287	280	*ORF19.1491*	*SNU71*	335997<-334153			*ORF19.1492*	*PRP39*	336552->338519				
2	429195..429403	208	*ORF19.1634*	*ZRT3*	427370<-429145									
2	549769..550317	548	*ORF19.6831*		549458<-548142			*ORF19.6830*	*LHS1*	550341->553139				
2	572071..572863	792						*ORF19.6818*	*SUR2*	573066->574094		hyphae (down)		
2	660174..660417	243	*ORF19.909*	*STP4*	660179<-659049		hyphae (down)							
2	789975..790975	1000						*ORF19.847*		791066->792154				
2	822632..823052	420	*ORF19.832*		822404<-819356									
2	919877..920124	247						*ORF19.4513*		920879->922069				
2	956685..956995	310						*ORF19.4492*	*EBP2*	956922->958202				
2	1009610..1009989	379						*ORF19.4128*		1010681->1011985				

2	1104636..1105023	387	*ORF19.3568*	*RXT3*	1104183<..1102627								
2	1164935..1165312	377	*ORF19.6881*		1164794<..1164147			*ORF19.6882*	*OSM1*	1165487->1166998		hyphae (down)
2	1187147..1187465	318	*ORF19.6893*		1187201<..1185839								
2	1403997..1404286	289						*ORF19.2237*		1404254->1404933			
2	1554538..1554886	348	*ORF19.1864*		1554405<..1552246			*ORF19.1863*		1554715->1556503			
2	1632520..1632667	147						*ORF19.2181*		1632178->1632708			
2	1680188..1680349	161	*ORF19.1351*		1679933<..1679193								
2	1685026..1685304	278	*ORF19.1348*		1685131<..1684568								
2	1802346..1802508	162	*ORF19.220*	*PIR1*	1801740<..1800700	hyphae (down)							
2	1876679..1876854	175	*ORF19.4076*	*MET10*	1875988<..1872704	hyphae (down)							
2	1879647..1879982	335					*ORF19.4077*	*MIT1*		1880521->1882155	Efg1 (hypoxia)		
2	1893206..1893376	170	*ORF19.4085*		1893261<..1892620		*ORF19.4086*			1893505->1894155			
2	2139486..2139660	174	*ORF19.1742*		2138454<..2137432								
2	13097..13527	430	*ORF19.5468*		12501<..12190		*ORF19.5467*			13756->14265			
2	877355..877585	230	*ORF19.5864*		877338<..875701		*ORF19.5865*			877626->880223			
3	776603..777066	463					*ORF19.6951*	*DPL1*		777441->779210		yeast (down)	
3	807277..807523	246	*ORF19.6930*	*SIC1*	807031<..806315		*ORF19.6929*			807898->808425			
3	1038620..1039215	595	*ORF19.5952*		1038697<..1037381		*ORF19.5953*	*SFP1*		1041453->1042790			
3	1072160..1072466	306	*ORF19.5965*		1072248<..1069021		*ORF19.5966*			1072444->1072785			
3	1093084..1093262	178					*ORF19.5978*			1093310->1094524			
3	1305553..1305863	310	*ORF19.7362*		1302603<..1300389		*ORF19.7363*			1306218->1308440			
3	1445006..1445426	420					*ORF19.7400*			1446629->1451336			
3	1496185..1496554	369	*ORF19.7444*		1494922<..1493897		*ORF19.7445*			1496429->1497916			
3	1727020..1727262	242					*ORF19.6734*	*TCC1*		1730074->1732320	HA-Efg1 (n and h), Efg1 (hypoxia)		
3	892929..893238	309	*ORF19.5871*		893071<..890979	hyphae (down)							
3	1118625..1118860	235					*ORF19.6992*	*WOR2*		1118847->1120187	HA-Efg1 (normoxia and hypoxia)		
3	1233227..1233512	285					*ORF19.6996*			1234039->1236246			
3	1475513..1475883	370					*ORF19.7436*	*AAF1*		1477326->1479164	HA-Efg1 (n and h), Efg1 (hypoxia)		
3	1491955..1492166	211	*ORF19.7441*		1491938<..1491012		*ORF19.7442*			1492186->1493082			
3	1510669..1511153	484					*ORF19.7451*			1511052->1515023			
3	48034..48219	185	*ORF19.5657*	*SWC1*	48100<..45137								
3	131436..131638	202	*ORF19.4167*		127111<..126572		*ORF19.4166*	*ZCF21*		131941->133830	HA-Efg1 (hypoxia), Efg1 (hypoxia)		
4	248259..248536	277	*ORF19.4668*		248276<..246123								
4	282782..283309	527					*ORF19.4649*			283241->286831			
4	420730..420888	158					*ORF19.4579*			421115->422041			
4	480605..481016	411					*ORF19.2765*	*PGA62*		480632->481273	HA-Efg1 (hypoxia), yeast (down)		
4	538595..538903	308	*ORF19.2739*		538696<..536978								
4	543774..546002	2228	*ORF19.2737*		545945<..543717	yeast (down)							
4	551457..551678	221					*ORF19.2733*			551575->553128			
4	555823..556043	220	*ORF19.2731*		553564<..553226		*ORF19.2730*			553936->555756			
4	569822..570064	242	*ORF19.2725*		567226<..566924	HA-Efg1 (n and h), Efg1 (hypoxia)	*ORF19.2724*			571920->573416	HA-Efg1 (n and h), Efg1 (hypoxia)		
4	665440..665998	558	*ORF19.2674*		665137<..664109		*ORF19.2673*			665706->666725			
4	901830..902078	248	*ORF19.1429*		901816<..901376		*ORF19.1428*			902225->902740			
4	958836..959072	236	*ORF19.3840*		959031<..954805		*ORF19.3839*			961031->962392			
4	982132..982341	209					*ORF19.3823*			982321->987258			
4	990641..990855	214	*ORF19.3821*		990526<..989339	HA-Efg1 (hypoxia)							
4	1020888..1021863	975	*ORF19.3803*	*MNN24*	1020679<..1018910		yeast (down)	*ORF19.3802*	*PMT6*	1022709->1025207		yeast (down)	
4	1048206..1048473	267	*ORF19.3794*	*CSR1*	1044143<..1042287	HA-Efg1 (hypoxia)		*ORF19.3793*		1048418->1049593			
4	119205..119456	251	*ORF19.4173*		119171<..117582								
4	125737..125901	164	*ORF19.4169*		125651<..125256			*ORF19.4168*		126013->126516			
4	149067..149317	250						*ORF19.4711*		150355->152169			
4	167790..168189	399	*ORF19.4702*		167605<..166703			*ORF19.4701*		168466->169392			

4	241195..241666	471							ORF19.4670	CAS5	241403->243868			
4	263241..263484	243							ORF19.4657		263907->265409	Efg1 (hypoxia)		
4	277969..278128	159							ORF19.4651		278269->278688			
4	294547..294757	210							ORF19.4643		294803->301954			
4	336726..336904	178	ORF19.4624		336394<-335036									
4	342226..342418	192	ORF19.4622		342120<-340963									
4	449574..449864	290	ORF19.4560	BFR1	449237<-447849				ORF19.2775	IDI1	450181->451035			
4	681943..682094	151							ORF19.2665		682598->686252			
4	806517..806676	159	ORF19.1298		806323<-803789				ORF19.1297		807459->809654			
4	972793..973252	459	ORF19.3829		972279<-970633									
4	1263263..1263475	212							ORF19.1258		1264022->1264735			
4	1269196..1269522	326	ORF19.1269		1269246<-1264915									
4	1301093..1301343	250	ORF19.1274		1298570<-1296879				ORF19.1275		1302092->1304095			
4	30117..30380	263	ORF19.979	FAS1	29661<-23548		yeast (up)							
4	94280..94512	232	ORF19.940		93594<-89881				ORF19.939		95043->98102			
5	102915..103182	267							ORF19.938		103156->104601	Efg1 (hypoxia)		
5	217717..218023	306	ORF19.1972		217288<-215867				ORF19.1971		218221->219705			
5	380339..380796	457	ORF19.3207	CCN1	379761<-377680	Efg1 (hypoxia)								
5	406103..406467	364	ORF19.3195	HIP1	404636<-402837		hyphae (down)		ORF19.3193	FCR3	407979->409178			
5	443455..443624	169	ORF19.3174		443369<-440835									
5	453619..453945	326	ORF19.3170		453571<-451385									
5	155228..155460	232	ORF19.921		153233<-151176				ORF19.920		156807->158162			yeast (up)
5	175021..175219	198							ORF19.576		175559->176047			
5	347903..348110	207	ORF19.4151		347572<-345242									
5	529019..529265	246	ORF19.4245		527060<-525714				ORF19.4246		529711->531504			
5	568004..568222	218	ORF19.4266		568051<-566677									
5	851168..851516	348	ORF19.1106		850957<-848603	Efg1 (hypoxia)								
5	861451..861765	314	ORF19.3219		861340<-859535									
5	513893..514105	212	ORF19.4239		513647<-511632									
5	522151..522532	381	ORF19.4242	CST20	521590<-517904									
5	599825..600166	341	ORF19.4282		598167<-597259									
5	1107056..1107300	244							ORF19.3997	ADH1	1107881->1108930	Efg1 (hypoxia)	yeast (down)	
5	4563..5065	502							ORF19.6337		5545->6489			
5	60497..60663	166	ORF19.1105		60013<-57662	Efg1 (hypoxia)	yeast (up)		ORF19.1196		60921->63506	Efg1 (hypoxia)	yeast (down)	
6	97579..97753	174	ORF19.4208	RAD52	97417<-95723									
6	107748..107995	247							ORF19.4199		107932->109503			
6	173917..174207	290							ORF19.90		174680->176944	Efg1 (hypoxia), HA-Efg1 (normoxia)		
6	304142..304599	457	ORF19.3434		301246<-298277				ORF19.3433	OYE23	304843->306063		yeast (down)	
6	319400..319632	232	ORF19.3431		317782<-314096				ORF19.3430	BUD21	319776->320810			
6	339382..339625	243							ORF19.3421.1		339664->340248			
6	349369..349608	239	ORF19.3420		348886<-348503				ORF19.3419	MAE1	350713->352605		yeast (down)	
6	421895..422171	276							ORF19.3505		422337->424733			
6	430038..430268	230	ORF19.3501		429691<-426551				ORF19.3499		434464->434967		hyphae (up)	
6	444405..444602	197	ORF19.3494		444313<-443213				ORF19.3453		444683->447643			
6	474206..474375	169	ORF19.3468	ALG11	472898<-471069				ORF19.3469		474238<-475425			
6	549988..550214	226	ORF19.5537		548965<-547667				ORF19.5539		552727->553569			
6	603094..603382	288	ORF19.5568		603308<-602358				ORF19.5569		603848->606529			
6	630120..630398	278							ORF19.5584		630618->633050			
6	640292..640524	232	ORF19.5596		640372<-637424									
6	730739..730929	190	ORF19.5705	NAM2	730549<-727964		yeast (up)		ORF19.5710		731035->734520			
6	821237..821408	171	ORF19.5753	HGT10	819180<-817540		yeast (up)							
6	837437..837820	383	ORF19.5769		836974<-832487		yeast (up)							

6	867771..868136	365	*ORF19.5775*		864791<-863253			*ORF19.1221*		876496->877833		
6	875889..876332	443						*ORF19.1221*		876496->877833		
6	898101..898410	309	*ORF19.4557*		897780<-894497							
6	90037..90595	558	*ORF19.4211*	*FET3*	89370<-87511	HA-Efg1 (n and h), Efg1 (hypoxia)		*ORF19.4210*		92718->94109	HA-Efg1 (n and h), Efg1 (hypoxia)	
6	711941..712284	343						*ORF19.5627*		712343->713449		
6	954958..955148	190	*ORF19.7090*		954989<-954642			*ORF19.7091*		955216->957288		
6	962825..962993	168	*ORF19.7093*	*FLO8*	962206<-959828							
6	969214..969419	205						*ORF19.7097*	*ALS2*	971475->976745		
6	1028365..1028747	382	*ORF19.2160*		1027136<-1025391			*ORF19.2163*		1028841->1031354		
6	132431..132677	246						*ORF19.7047*	*RTF1*	132567->134273	HA-Efg1 (hypoxia)	
6	147491..147734	243						*ORF19.7041*		148191->150485		
7	179372..179581	209	*ORF19.7027*		179318<-176562	yeast (down)						
7	197995..198262	267						*ORF19.7020*	*KEX1*	198461->200569		
7	226954..227152	198	*ORF19.7006*		226654<-223297	yeast (down)						
7	235013..235204	191	*ORF19.6896*		232413<-230875							
7	312089..312282	193						*ORF19.6580*		312573->313265		
7	329445..329682	237						*ORF19.6573*		329718->336476		
7	350127..350842	715	*ORF19.6563*		349795<-347816			*ORF19.6562*		350992->352287		
7	375318..375638	320	*ORF19.6551*		375267<-374593			*ORF19.6550*		375747->376631		
7	389345..389658	313	*ORF19.6540*	*PFK2*	388801<-385961	yeast (down)		*ORF19.6539*		390350->391846		
7	392764..392967	203	*ORF19.6538*		392514<-392023			*ORF19.6537*		393006->393698		
7	419339..419895	556						*ORF19.6525*		419663->421988		
7	410407..410669	262	*ORF19.6530*		409253<-408390			*ORF19.6529*	*CDC34*	411057->411791		
7	413027..413320	293	*ORF19.6528*		412926<-412315							
7	437730..438044	314	*ORF19.6518*		437290<-435305			*ORF19.6517*		438040->439230		
7	451625..451894	269	*ORF19.6514*	*CUP9*	450912<-449878	HA-Efg1 (normoxia and hypoxia)						
7	465046..465507	461						*ORF19.6506*		465072->467138		
7	476843..477195	352	*ORF19.6498*		476933<-475905							
7	493528..493763	235						*ORF19.6486*		493963->494421		
7	519989..520286	297	*ORF19.6472*		519627<-519139			*ORF19.6470*		520558->521115		
7	632455..633164	709						*ORF19.5169*		633454->635175		
7	8643..8842	199	*ORF19.7545*		7566<-4884			*ORF19.7544*		9111->9863		
7	864303..864578	275						*ORF19.7186*	*CLB4*	864775<-863315		
7	172196..172884	688	*ORF19.3283*		172342<-171653							
R	201809..202075	266	*ORF19.3265.1*		201735<-201475			*ORF19.3265*		202225->203895		
R	334667..334909	242	*ORF19.2527*		334491<-333205			*ORF19.2528*		334922->336910		
R	509931..510278	347	*ORF19.3742*		509369<-508644			*ORF19.3740*	*PGA23*	510511->511359		
R	556779..557328	549						*ORF19.173*		556964->560266	Efg1 (hypoxia)	
R	598390..599287	897						*ORF19.2823*	*AFG1*	600293<-602095	HA-Efg1 (n and h), Efg1 (hypoxia)	
R	874612..874814	202						*ORF19.467*	*WOR3*	878593->880521	HA-Efg1 (hypoxia)	
R	926791..927553	762	*ORF19.496*		926380<-923609			*ORF19.498*	*EAF7*	928331->929716		yeast (up)
R	963503..963739	236						*ORF19.522*	*PIM1*	963564->966800		yeast (up)
R	1125308..1125600	292	*ORF19.556*		1124656<-1124237			*ORF19.557*		1125739->1126764		
R	1157158..1157584	426	*ORF19.5286*		1156504<-1155638			*ORF19.5285*		1158030->1158629		
R	1259394..1260341	947	*ORF19.454*	*SFL1*	1258170<-1255753							
R	1271946..1272327	381						*ORF19.451*		1274207->1276684		
R	1285179..1285413	234	*ORF19.3852*		1285014<-1282627							
R	1372318..1372553	235	*ORF19.723*	*BCR1*	1370542<-1368320	Efg1 (hypoxia)						
R	1469903..1470143	240	*ORF19.1847*		1469576<-1467687							
R	1659779..1660018	239	*ORF19.6286*		1659219<-1658623			*ORF19.6285*	*GLC7*	1660942->1661934		
R	1718524..1718725	201						*ORF19.610*	*EFG1*	1723620->1725197	HA-Efg1 (n and h), Efg1 (hypoxia)	
R	1723278..1723663	385						*ORF19.610*	*EFG1*	1723620->1725197	HA-Efg1 (n and h), Efg1 (hypoxia)	

R	1759755..1759942	187	*ORF19.589*	*VPS21*	1759114<-1758464			*ORF19.6365*	*PTP1*	1760210->1761328			
R	1885618..1886042	424						*RDN18*					
R	1888916..1889176	260	*RDN5*					*RDN18*					
R	1892603..1893207	604	*RDN5*					*RDN58*					
R	1919596..1919753	157	*ORF19.7293*		1919006<-1916934								
R	2034320..2034587	267						*ORF19.6608*		2034582<--2032414	HA-Efg1 (hyphae)	yeast (down)	
R	2106048..2106312	264						*ORF19.7661*	*EED1*	2106249->2108912	HA-Efg1 (normoxia	yeast (down)	
R	78276..78466	190	*ORF19.7502*		76707<-75931	Efg1 (hypoxia), HA-Efg1 (normoxia)		*ORF19.2823*	*RFG1*	600296-->602099	HA-Efg1 (normoxia and hypoxia)		
R	590631..590875	244	*ORF19.2822*		586104<-585259	HA-Efg1 (normoxia and hypoxia)		*ORF19.646*	*GLN1*	1095535->1096656		yeast (down)	
R	1093988..1094309	321					hyphae (down)						
R	1196472..1196912	440	*ORF19.5843*		1194914<-1194066			*ORF19.6652*		1201138->1202460			
R	1200478..1200718	240	*ORF19.6663*		1200545<-1198899			*ORF19.707*		1445481->1447400			
R	1445167..1445556	389						*ORF19.1842*		1479665->1484341			
R	1477563..1477801	238	*ORF19.1843*		1477285<-1475594			*ORF19.7314*		1957926->1958723			
R	1955700..1956129	429	*ORF19.7313*		1955547<-1954102								

S4 Table. *C. albicans* strains

Strain	Genotype	reference/source
SC5314	wild-type	[1]
CAF2-1	*URA3/ura3::imm434*	[1]
CAI4	*ura3::imm434/ura3::imm434*	[1]
HLC52	Like CAI4 but *efg1::hisG/efg1::hisG-URA3-hisG*	[2]
HLC67	Like CAI4 but *efg1::hisG/efg1::hisG*	[2]
HLC46	Like CAI4 but *EFG1/efg1::hisG-URA3-hisG*	[2]
BCA0901	Like CAI4, but *EFG1/efg1::hisG-URA3-hisG*	[3]
JKC19	Like CAI4, but *cph1::hisG/cph1::hisG-URA3-hisG*	[4]
HLC54	Like CAI4 but *cph1::hisG/cph1::hisG efg1/efg1::hisG-URA3-hisG*	[2]
HLCE	Like HLC67 but *efg1::hisG/efg1::* [*EFG1p-URA3*]	[5]
HLCEEFG1	Like HLC67, but *efg1::hisG/efg1::*[*EFG1p-HA-EFG1-URA3*] (pTD38 HA/Pac1 integrated in *EFG1p*)	[5]
HLCPEFG1	Like HLC67, but *efg1::hisG/efg1::*[*EFG1p-EFG1-URA3*] (pPRDA208C/Pac1 integrated in *EFG1p*)	this study
HLCNEFG1	Like HLC67, but *efg1::hisG/efg1::*[*EFG1p-ΔN-EFG1-URA3*] (pPDNEFG1/Pac1 integrated in *EFG1p*)	this study
HLC67[pDB1]	Like HLC67, but *LEU2/leu2::PCK1p-EFG1*^{T206A}*-URA3*	[6]
HLC67[pDB2]	Like HLC67, but *LEU2/leu2::PCK1p-EFG1*^{T206E}*-URA3*	[6]
HLCEEFG1T206A	Like HLC67, but *efg1::hisG/efg1::*[*EFG1p-EFG1*^{T206A}*-URA3*] (pPDEFG1T206A/Pac1 integrated in *EFG1p*)	this study
HLCEEFG1T206E	Like HLC67, but *efg1::hisG/efg1::*[*EFG1p-EFG1*^{T206E}*-URA3*] (pPDEFG1T206E/Pac1 integrated in *EFG1p*)	this study
HLCEEFG1T179A	Like HLC67, but *efg1::hisG/efg1::*[*EFG1p-EFG1*^{T179A}*-URA3*] (pPDEFG1T179A/Pac1 integrated in *EFG1p*)	this study
HLCEEFG1T179E	Like HLC67, but *efg1::hisG/efg1::*[*EFG1p-EFG1*^{T179E}*-URA3*] (pPDEFG1T179E/Pac1 integrated in *EFG1p*)	this study

CEC2907	Like CAI4, but *his1::hisG/HIS1 arg4::hisG/ARG4 ADH1/adh1::TDH3p-carTA::SAT1*	[7]
CECSTE11	Like CEC2907, but *RPS1/RPS1::TETp-STE11-URA3* (pClp10TETSTE11/StuI integrated in *RPS1* locus)	this study
CECCEK1	Like CEC2907, but *RPS1/RPS1::TETp-CEK1-URA3* (pClp10TETCEK1/StuI integrated in *RPS1* locus)	this study
CECCPH1	Like CEC2907, but *RPS1/RPS1::TETp-CPH1-URA3* (pClp10TETCPH1/StuI integrated in *RPS1* locus)	this study
DSC11	*efg1::hisG/efg1::hisG::EFG1-dpl200 ura3::imm434/ura3::imm434::URA3*	[8]
BWP17	*ura3::imm434/ura3::imm434, his1::hisG/his1::hisG arg4::hisG/arg4::hisG*	[9]
MK106	Like SC5314, but *ace2::FRT/ace2::FRT*	[10]
CLvW001	Like BWP17, but *ace2::lacZ-SAT1/ACE2*	this study
CLvW004	Like CLvW001, but *ace2::SAT1/ACE2*^{HA}*::URA3*	this study
CLvW008	Like CAI4, but *ace2::FRT/ace2::FRT*	this study
SN250	*ura3Δ::imm434::URA3-IRO1/ura3Δ::imm434 arg4::hisG/arg4::hisG his1::hisG/his1::hisG leu2::hisG::CdHIS1/leu2::hisG::CmLEU2*	[11]
CLvW047	Like CLvW008, but *efg1::hisG-URA3-hisG/EFG1*	this study
CJN702	Like Bwp17, but *his1::hisG/his1::hisG::pHIS1 bcr1::URA3/bcr1::ARG4*	[12]
CLvW024	Like CJN702, but *ace2::FRT/ace2::FRT*	this study
TF022	*ura3Δ::imm434::URA3-IRO1/ura3Δ::imm434 arg4::hisG/arg4::hisG his1::hisG/his1::hisG leu2::hisG/leu2::hisG brg1Δ::CmLEU2/brg1Δ::CdHIS1*	[13]
PDEB4	Like HLC52, but *brg1::FRT/brg1::FRT*	this study
PDBB4	Like CJN702, but *brg1::FRT/brg1::FRT*	this study

References

1. Fonzi WA, Irwin MY. Isogenic strain construction and gene mapping in *Candida albicans*. Genetics. 1993;134: 717-728.

2. Lo HJ, Köhler JR, DiDomenico B, Loebenberg D, Cacciapuoti A, Fink GR. Nonfilamentous *C. albicans* mutants are avirulent. Cell. 1997;90: 939-949.
3. Braun BR, Johnson AD. *TUP1, CPH1* and *EFG1* make independent contributions to filamentation in *Candida albicans*. Genetics. 2000;155: 57-67.
4. Liu H, Köhler J, Fink GR. Suppression of hyphal formation *in Candida albicans* by mutation of a STE12 homolog. Science. 1994;266: 1723-1726. Erratum in Science. 1995;267:217.
5. Noffz CS, Liedschulte V, Lengeler K, Ernst JF. Functional mapping of the *Candida albicans* Efg1 regulator. Eukaryot Cell. 2008;7: 881-893.
6. Bockmühl DP, Ernst JF. A potential phosphorylation site for an A-type kinase in the Efg1 regulator protein contributes to hyphal morphogenesis of *Candida albicans*. Genetics. 2001;157: 1523-30.
7. Chauvel M, Nesseir A, Cabral V, Znaidi S, Goyard S, Bachellier-Bassi S, et al. A versatile overexpression strategy in the pathogenic yeast *Candida albicans*: identification of regulators of morphogenesis and fitness. PLoS One. 2012;7: e45912.
8. Park H, Myers CL, Sheppard DC, Phan QT, Sanchez AA, Edwards JE, Filler SG. Role of the fungal Ras-protein kinase A pathway in governing epithelial cell interactions during oropharyngeal candidiasis. Cell Microbiol 2005;7: 499–510.
9. Wilson RB, Davis D, Mitchell AP. Rapid hypothesis testing with *Candida albicans* through gene disruption with short homology regions. J Bacteriol. 1999;181: 1868-1874.

10. Kelly MT, MacCallum DM, Clancy SD, Odds FC, Brown AJ, Butler G. The *Candida albicans CaACE2* gene affects morphogenesis, adherence and virulence. Mol Microbiol. 2004;53: 969-983.
11. Noble SM, French S, Kohn LA, Chen V, Johnson AD. Systematic screens of a *Candida albicans* homozygous deletion library decouple morphogenetic switching and pathogenicity. Nat Genet. 2010;42: 590-598.
12. Nobile CJ, Mitchell AP. Regulation of cell-surface genes and biofilm formation by the *C. albicans* transcription factor Bcr1p. Curr Biol. 2005;15: 1150-1155.
13. Homann OR, Dea J, Noble SM, Johnson AD. A phenotypic profile of the *Candida albicans* regulatory network. PLoS Genet. 2009;5: e1000783.

S5 Table. List of oligonucleotides

name	sequence
pET19Serinhin	5′-GTATGGGTATCAATCGAATTATTACCAGGG-3′
pET19Serinher	5′-CCCTGGTAATAATTCGATTGATACCCATAC-3′
EFG1BamHIFor	5′-ACTACGCGGATCCATGTCAACGTATTCTATACCC -3′
EFG1BamHIRev	5′-GGTATGCGGATCCCTTTTCTTCTTTGGCAACAG-3′
Efg1179AFor	5′GTATCGACAATGCAACAACCAGCTCCTGTTCAGGATACGTTGAAC-3′
Efg1179ARev	5′ GTTCAACGTATCCTGAACAGGAGCTGGTTGTTGCATTGTCGATAC-3′
UTREFG1For	5′-GCGTTAGTCTCAATTGAACAGATAG-3′
EFG1seqFor	5′-GACAACCAGGTCAACAGACTG-3′
EFG1seqRev	5′-CAGTGGCAGCCTTGGTATTTAC-3′
EFG1seqM	5′-CAATTCTACCAGTGGACCTTC-3′
Clp UL	5′ -ATACTACTGAAATTTCCTGACTTTC-3′
ClpUR	5′ –ATTACTATTTACAATCAAAGGTGGTC-3′
lacZACE2For	5′-ACTGAAATGCAATCTTCTCTCCCACTCGAGCAAACACTCTCTCCATG AAAAACCAACTTGTGGCAGAAGTCTCGACATTTTATGATGGAATG-3′
lacZACE2Rev	5′-ATTTAGTGAAGGAGGTGCAAAAGTTGGGAAAGTAAATGA GAAAAAGAAAAAATGGTAAATAAAATACTTGAAAGGTATTTCATGAAC ATGACTGAAAAAATTC-3′
ACE2HAFor	5′-CAGTGGTTGAGAGGATAGAAAAACAGTTGCTACAGGAAG ATAAGAGTGTTACTGAGGAGTTTTTAATGTTGCAATCGGGTGGTGGTC GGATCCCCGGGTTAATTAAC-3′
ACE2HARev	5′-GCAATCTCTAACAGAAGTGAACATAGAATTAATAAACTG GCAGTAAATCAAACGATATAAAATAAAAAAGAATAATAGCTAGAAGG ACCACCTTTGATTG-3′
ACE2For	5′-GATTAATGGATCTCCCGATTGG-3′
HARev	5′-CTAGAAGGACCACCTTTGATTG 3′
CAF1ApaI	5′-TATATGGTGTAAATCTCACTG-3′
CAF2XhoI	5′-TTTCCAATGCATCTCGAGTGAAGG-3′
CAR1SacII	5′-AGACTTCTGCCGCGGGTTGGTTTT-3′
CAR2SacI	5′-ATTTGTTGGGAGCTCCACAACACT-3′
CAF3ApaI	5′-TTTCGAAAGGGCCCTCTTTCTTT-3′
CAF4XhoI	5′-ATCATTGGCCTCGAGACTTAAAAA-3′
CAR3SacII	5′-GCAAATGTCCGCGGGGTAAAGA-3′
CAR4SacI	5′-CAACATTAAGAGCTCCTCAGTAAC-3′
FLP1	5′-TTCCGTTATGTGTAATCATCC-3′
ACE2UTR5	5′-ATATGGTAAGCTTCAGTTCG-3′
ACE2RTFor	5′-CGCCGAATCAAAAAGACTTC-3′
ACE2RTRev	5′-CGCACATTGTATCGACGAGT-3′
EFG1RTFor	5′-TAACGGAACCAAATTGCTCA-3′
EFG1RTRev	5′-CACCTCGAGGATTGACAGAA-3′
AAF1RTFor	5′-GCCCTTGGTGGTACATCTTT-3′
AAF1RTRev	5′-GATGGATGAGTGGATGTTGC-3′
TYE7RTFor	5′-GATTGCAAATTCTGTTCCGA-3′
TYE7RTRev	5′-AATAGGATTTGGTGGTTGGC-3′
BCR1RTFor	5′-AATGCCTGCAGGTTATTTGG-3′
BCR1RTRev	5′-GTTCTTGACCACCACCCATT-3′
ZCF21RTFor	5′-AGATCTATGATGGATATTTATCAGAAGG- 3′
ZCF21RTRev	5′-AGATCTTCAAGTGATCAATTTGGAAAT- 3′
ACT1RTFor	5′-TTGGATTCTGGTGATGGTGT-3′

ACT1RTRev	5′-TGGACAAATGGTTGGTCAAG-3′
STE11 RTFor	5′-GCTCATGATCGCCATTCTAC-3′
STE11 RTRev	5′-CTCAATCCGGCATAGTCAGA-3′
CPH1 RTFor	5′-AGATGCCTTGGAACGAGATT-3′
CPH1RTRev	5′-TGGAAGACTCGTCGTAATGG-3′
CEK1RTFor	5′-ACAACAACAACAGGCAGCAG-3′
CEK1RTRev	5′-TCCATATGCTCCTTCTCCAA-3′
CYR1 RTFor	5′-AAGAATCCCGAAACAGGAGA-3′
CYR1 RTRev	5′-CTTGTTCTGGCACGTTTGTT-3′
TPK1 RTFor	5′-TTGGATTTGCTAAAGAAGTTCAA-3′
TPK1 RTRev	5′-ACCAAATGACCACCAATCAA-3′
KIC1 RTFor	5′-CAACCAACCACCCACAATTA-3′
KIC1 RTRev	5′-GGTGACGTATTCAACGAGGA-3′
BRG1 RTFor	5′-AGAGGTCCAAAGGGTGTGAG-3′
BRG1 RTRev	5′-TACCTCTTCTGCTGCCAATG-3′
BRG15 UTR KpnI For	5′-CATGCGAGGTACCGCCGGAGATTCAGAGCTCTTAC-3′
BRG15UTR KpnI Rev	5′-CATTCGGGTACCAATTTGAATTTCTGGAATAGTAG-3′
BRG13UTR Not1 For	5′-CATGCTGCGGCCGCGTATTCCTGTTGCTTACCC-3′
BRG13UTR SacI Rev	5′-CATCGACGAGCTCGTCGTCTGGACGATCTGATTTGCTCTC-3′
BRG1UpFor	5′-GTAATGTGTGCACTACACAATAACC-3′
BRG1MidRev	5′-GTGTAACCCACATTAGGTGGCATACC-3′
URA3 CHIP For	5′-GGAGTTGGATTAGATGATAAAGGTGATGG-3′
URA3 CHIP Rev	5′-GGACCACCTTTGATTGTAAATAGTAATA-3′
EFG1 CHIP For	5′-CAACTTGGTCCAAGAATTC-3′
EFG1 CHIP Rev	5′-TATGGGTTATATTCTTGGTAGTC-3′
BCR1 CHIP For	5′-GTCCTCCCCATCCAACTA-3′
BCR1 CHIP Rev	5′-CAAAAATAGGGTAGGCAATAGA-3′
BRG1 CHIP For	5′-GCCGGAGATTCAGAGCTC-3′
BRG1 CHIP Rev	5′-ACTGAGAACAGGCAATCTCC-3′
CEK1 CHIP For	5′-GCATCGTCGAATATGTACAACC-3′
CEK1 CHIP Rev	5′-GGCGGGTTAGATGATGAAAT-3′

2.4 Manuskript III: Dom34 links translation to protein *O*-mannosylation

Lasse van Wijlick, Rene Geissen, Jessica Hilbig, Quentin Lagadec, Pilar D. Cantero, Eugen Pfeifer, Mateusz Juchimiuk, Sven Kluge, Stephan Wickert, Paula Alepuz, Joachim F. Ernst

Erstautor

Beitrag zum Manuskript: 40 %

Lasse van Wijlick hat einen Teil der Experimente durchgeführt und ausgewertet. Darüber hinaus hat er die Daten interpretiert, Hypothesen für das Manuskript formuliert und Abbildungen (Fig.3.B, Fig.4.A-C, Fig.5.B und Fig.S6.A-B) erstellt. Außerdem hat er Teile des Manuskripts geschrieben.

Veröffentlicht in: PLoS Genetics, October 2016; 12(10): e1006395.

Impact Factor: 7.528 (2014)

PLOS | GENETICS

RESEARCH ARTICLE

Dom34 Links Translation to Protein *O*-mannosylation

Lasse van Wijlick[1,2], René Geissen[1], Jessica S. Hilbig[1], Quentin Lagadec[1], Pilar D. Cantero[1], Eugen Pfeifer[1], Mateusz Juchimiuk[1], Sven Kluge[1], Stephan Wickert[1], Paula Alepuz[3,4], Joachim F. Ernst[1,2]*

1 Department Biologie, Molekulare Mykologie, Heinrich-Heine-Universität, Düsseldorf, Germany, **2** Manchot Graduate School Molecules of Infection, Heinrich-Heine-Universität, Düsseldorf, Germany, **3** Departamento de Bioquímica y Biología Molecular, Universitat de València, Burjassot Spain, **4** ERI Biotecmed. Universitat de València, Burjassot Spain

* joachim.ernst@uni-duesseldorf.de

OPEN ACCESS

Citation: van Wijlick L, Geissen R, Hilbig JS, Lagadec Q, Cantero PD, Pfeifer E, et al. (2016) Dom34 Links Translation to Protein *O*-mannosylation. PLoS Genet 12(10): e1006395. doi:10.1371/journal.pgen.1006395

Editor: David Kadosh, University of Texas Health Science Center at San Antonio, UNITED STATES

Received: June 28, 2016

Accepted: September 29, 2016

Published: October 21, 2016

Data Availability Statement: All relevant data are within the paper and its Supporting Information files.

Funding: Funded by the Deutsche Forschungsgemeinschaft (SPP1160), the Manchot Graduate School Molecules of Infection (MOI II) and ERA-NET Pathogenomics project "Glycoshield" to JFE and by the Spanish Ministerio de Ciencia e Innovación (BFU2013-48643-C3-3-P) to PA. The funders had no role in study design, data collection and analysis, decision to publish, or preparation of the manuscript.

Abstract

In eukaryotes, Dom34 upregulates translation by securing levels of activatable ribosomal sub-units. We found that in the yeast *Saccharomyces cerevisiae* and the human fungal patho-gen *Candida albicans*, Dom34 interacts genetically with Pmt1, a major isoform of protein *O*-mannosyltransferase. In *C. albicans*, lack of Dom34 exacerbated defective phenotypes of *pmt1* mutants, while they were ameliorated by Dom34 overproduction that enhanced Pmt1 protein but not *PMT1* transcript levels. Translational effects of Dom34 required the 5′-UTR of the *PMT1* transcript, which bound recombinant Dom34 directly at a CA/AC-rich sequence and regulated *in vitro* translation. Polysomal profiling revealed that Dom34 stimu-lates general translation moderately, but that it is especially required for translation of tran-scripts encoding Pmt isoforms 1, 4 and 6. Because defective protein *N*- or *O*-glycosylation upregulates transcription of *PMT* genes, it appears that Dom34-mediated specific transla-tional upregulation of the *PMT* transcripts optimizes cellular responses to glycostress. Its translational function as an RNA binding protein acting at the 5′-UTR of specific transcripts adds another facet to the known ribosome-releasing functions of Dom34 at the 3′-UTR of transcripts.

Author Summary

Fungi respond to damages of their glycostructures in their cell wall by transcriptional upregulation of genes that specify compensatory activities. Upon block of protein *N*-glycosylation, the human fungal pathogen *Candida albicans* increases transcription of *PMT1* encoding a major isoform of protein *O*-mannosyltransferase. Here we demonstrate that the Dom34 protein aids in glycostress responses by upregulating the translation of several *PMT* isoform transcripts. Dom34 has previously been implicated in mechanisms to secure high levels of ribosomal subunits that promote translation in general, e. g. by no-go decay at the 3′-UTR of transcripts. By binding to the 5′-UTR and activating translational initiation of *PMT* transcripts we add a novel mode of action and suggest a preferred class of

Competing Interests: The authors have declared that no competing interests exist.

targets for the translational activities of the Dom34 protein. The combination of transcriptional and Dom34-mediated translational upregulation of *PMT* genes optimizes effective recovery and survival of fungal cells upon glycostress.

Introduction

In eukaryotes, secretory proteins can get *O*-mannosylated at serine or threonine residues by protein mannosyltransferases (Pmt proteins). This modification occurs during or shortly after translation, during transit across the secretory pore complex into the ER lumen. *O*-mannosylation initiates the typical type of fungal *O*-chains, which mature in the Golgi. In mammalian cells *O*-mannosylation is a rare but important process, while the bulk of *O*-chains is formed post-translationally in the Golgi [1,2]. Seven and five Pmt isoforms forming Pmt1, 2 and 4 subfamilies have been described in the yeast *Saccharomyces cerevisiae* and the human fungal pathogen *Candida albicans*, respectively [1–3]. Pmt isoforms are largely specific for their protein substrates and the lack of the Pmt2 isoform in *C. albicans* or at least two isoforms in *S. cerevisiae* prevents growth [3,4]. In *C. albicans*, each Pmt isoform affects one or another aspect of fungal growth, morphogenesis and virulence [3,5]. Impaired *O*-mannosylation in *pmt1* mutants or upon Pmt1 inhibition of a wild-type strain leads to transcriptional upregulation of *PMT2* and *PMT4* genes, while inhibition of *N*-glycosylation by tunicamycin upregulates *PMT1* expression [6–8]. In both glycostress conditions, the increased levels of underglycosylated proteins also trigger the unfolded protein response (UPR), e. g. by increasing levels of the Kar2 chaperon and matured *HAC1* transcript [6,7]. UPR induction is known to lower overall translation in yeast cells, although translation of some transcripts is increased [9].

In *S. cerevisiae*, the Dom34 protein is involved in the "no-go decay" (NGD) process, which is one of at least three mechanisms responding to the quality of translated mRNA. NGD relieves stalled translational complexes arising e. g. by secondary structures or rare codons through dissociation of ribosomal subunits and cleavage of mRNA [10,11]. Dom34 also rescues ribosomes that accumulate at the 3′-UTR of transcripts [12,13]. To promote subunit dissociation and peptidyl-tRNA drop-off from stalled ribosomes, Dom34 co-operates with its associated GTPase Hbs1 [10,11]. Very likely, this function of Dom34 is possible because of its high homology to the translational termination factor eRF1, as well as the structural similarities of the Dom34-Hbs1 and eRF1:eRF3 complexes that can occupy the ribosomal A-site. *S. cerevisiae* strains carrying single mutations for Dom34 or Hbs1 grow normally, while their combination with mutations impairing components of 40S (but not 60S) ribosomal subunits [14], mutations delaying translation by phosphorylation of eIF2 [15] and yet undefined mutations [16], leads to severe impairment of growth. The scarcity of 40S subunits due to "stuck" 80S ribosomes and the resultant impaired translational initiation has been suggested as the mechanism causing slow growth of *dom34 hbs1* double mutants [14]. The homology of Dom34 to eRF1 only regards its central and C-terminal domains, while its N-terminal domain adopts a Sm-fold that is characteristic of RNA degradation or recognition domains [17,18]. However, recent results indicated that Dom34 is not the endonuclease that degrades mRNA in stalled ribosomes [19]. Besides NGD, other mechanisms including separation of free 80S ribosomes [14,20] and non-functional rRNA decay (NRD) [21,22] depend on Dom34 to maintain a sufficient supply of ribosomes for translation.

Based on the previous discovery of a *S. cerevisiae* mutant with defective protein *O*-mannosylation [23] we report here a novel function of Dom34 in translational upregulation of the *PMT1* transcript in *C. albicans*. By promoting the translational initiation of the *PMT1*

transcript, which under glycostress is strongly increased [6–8], Dom34 contributes to optimize the overall output of Pmt1 activity that helps to recover from damage to its glycostructures. Its mode of action as an RNA binding protein for specific transcripts differs from the previously described general roles and mechanisms of Dom34 in promoting translation in eukaryotes. By this action, Dom34 functionally links two essential processes in eukaryotic cells, translation and *O*-mannosylation.

Results

Identification of Dom34 as contributor of Pmt1 function in *S. cerevisiae*

Previously, a *S. cerevisiae* mutant (M577) defective in *O*-mannosylation of a heterologous protein (hIGF-1) and some homologous secretory proteins had been identified [23]. The mannosylation defect was recessive and segregated 2:2 in crosses to a wild-type strain suggesting that it was caused by mutation of a single gene. Because M577 did not show easily scorable phenotypes, *pmt1* or *pmt2* mutations were introduced to explore synthetic phenotypes with mutations affecting *O*-mannosylation. This approach was led by the finding that *pmt1 pmt2* double mutants, but not the single mutants, are resistant to the K1 killer toxin [24]. In agreement, we found that Pmt$^+$- strains YE449 and mutant M577, as well as the *pmt1* and *pmt2* single mutants were toxin-sensitive (blue/dark appearance of colonies on indicator plates), while the *pmt1 pmt2* double mutant was completely resistant to the toxin (white appearance of colonies on indicator plates) (Fig 1Aa). Importantly, similar to the *pmt1 pmt2* double mutant, the *pmt1* derivative of mutant M577 but not of the parental strain YE449 was completely toxin-resistant. Because the *pmt2* derivative of M577 retained sensitivity, the results indicated that the unknown mutation in M577 generates a synthetic protein-*O*-mannosylation phenotype in combination with a *pmt1* but not a *pmt2* mutation.

To identify the mutation in M577, its *pmt1* derivative was transformed with a genomic bank in vector YEp13 and 80,000 transformants were screened for re-appearance of sensitivity to K1 killer toxin. Among 78 initial transformant isolates, 17 carried the complementing activity on a genomic insertion within the bank plasmid. Two genomic loci occurred repeatedly in overlapping inserts (Fig 1B): 5 plasmids contained a region close to the centromere of chromosome XIV and 4 plasmids contained a region close to the centromere of chromosome IX. In both cases, the overlapping clones had a single gene in common: the chromosome XIV clones contained *DOM34*, while the chromosome IX-clones contained *YIL001w*.

To clarify if the K1 killer-resistance phenotype in strain M577 *pmt1* was caused by mutation of *DOM34*, we introduced *pmt1*, *dom34* and *yil001w* mutations singly or in combination into the genetic background of the parental strain YE449. At variance with an initial report [16] but in agreement with a subsequent report [15] we found that *dom34* single mutants did not show significant growth defects. Importantly, we detected that the *pmt1 dom34* mutant but not the *pmt1 yil001w* mutant was killer-resistant, resembling the M577 *pmt1* strain (Fig 1Ab). Transformation with either *PMT1*-, *DOM34*- or *YIL001w*-overexpressing vectors restored killer-sensitivity of the *pmt1 dom34* mutant (Fig 1Ac). These results suggested that in the parental strain M577, the *DOM34* gene is mutated, while *YIL001w* may represent an extragenic suppressor of the *pmt1* and *dom34* mutations. In support of this conclusion we found that a diploid constructed from haploids M577 *pmt1* and W21 (YE449 *pmt1 dom34*) was unable to sporulate, as expected for a homozygous *dom34* diploid [15]. Furthermore, sequencing of the *DOM34* ORF in mutant M577 revealed that it is mutated by insertion of a single T residue following position 366 generating a UAA stop codon leading to a truncated protein of 122 residues.

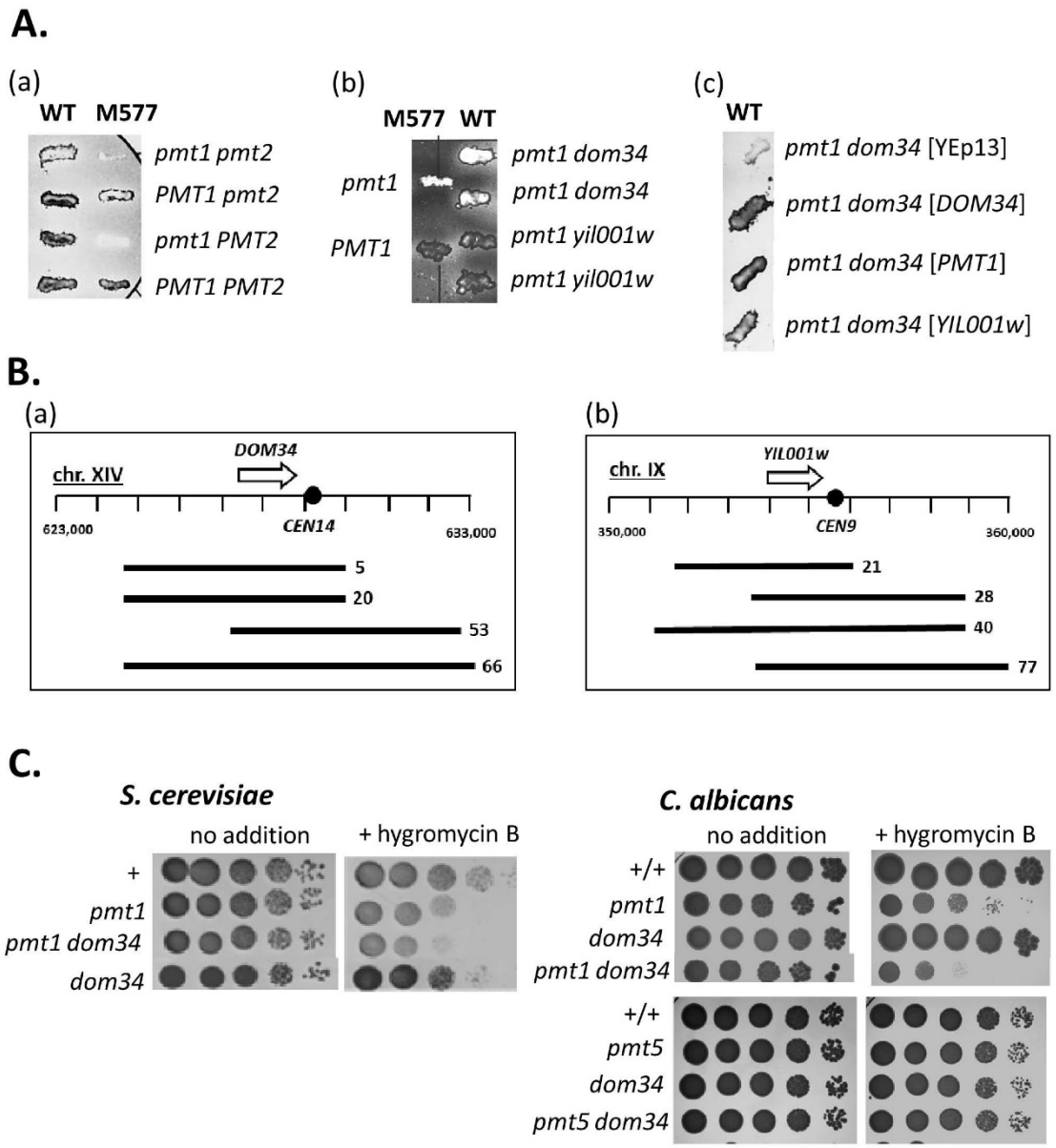

Fig 1. Genetic interactions of *dom34* and *pmt1* mutations. (A) Killer phenotypes of *S. cerevisiae* mutants. Strains were grown as streaks and replica-printed onto plates containing the killer K1-secreting strain RC130. Following incubation at 18˚C for 4–7 d, the appearance of streaks was blue (dead cells stained by methylene blue appear dark on figure), or white (live cells). Strains tested were the parental strain YE449 (WT) and its mutant M577 and *pmt1* and/or *pmt2* derivatives; in addition, mutant strains W21 (*pmt1 dom34*), W12 (*pmt1 yil001w*) and transformants of strain W21 carrying pSW20 (*PMT1*), p577/20 (*DOM34*) and pSW577/2 (*YIL001w*) were tested. **(B)** Inserts in genomic clones complementing the killer K1-resistance of strain M577 *pmt1*. Regions of chromosomes XIV and IX are shown, along with genomic inserts in YEp13 (numbered bars). **(C)** Hygromycin B sensitivity. Strains were serially diluted and spotted on YPD plates without or with hygromycin B (50 μg/ml). Growth was for 2 d at 30˚C. *S. cerevisiae* strains tested were YE449 (WT), YE449 *pmt1*, YE449 *dom34* and W21 (*pmt1 dom34*). *C. albicans* strains tested were CAF2-1 (WT), SPCa2 (*pmt1*/*pmt1*), JH47-1 (*dom34*/*dom34*), JH24-4 (*pmt1*/*pmt1 dom34*/*dom34*), SPCa10 (*pmt5*/*pmt5*) and JH5-3-1 (*dom34*/*dom34 pmt5*/*pmt5*).

doi:10.1371/journal.pgen.1006395.g001

Dom34 and Pmt1 cooperate to increase hygromycin B resistance

The above results had suggested that in *S. cerevisiae*, the activities of specific elements involved in translation (Dom34) and protein-*O*-mannosylation (Pmt1) are functionally linked. We subsequently found that this cooperation not only prevents resistance (to killer toxin K1) but also enhances resistance to hygromycin B (HygB). HygB is an aminoglycoside antibiotic known to block translation [25], which is particularly active to block growth of glycosylation mutants [26]. *dom34 pmt1* double mutants were significantly more sensitive than the *pmt1* single mutant, although the *dom34* single mutant did not show any sensitivity phenotype (Fig 1C).

To generalize Dom34-Pmt1 functional interactions and because *S. cerevisiae* contains a *DOM34* homolog (YCL001W-B) with unknown activity, we also studied the single *DOM34* gene in the human fungal pathogen *C. albicans* that contains a family of well-studied Pmt proteins [3]. A homologue of *S. cerevisiae DOM34, ORF19.2419* in the *C. albicans* genome encodes a protein with 36%, 39% and 40% sequence identity to Dom34 proteins of *S. cerevisiae*, *S. pombe* and human, respectively. Sequence similarities are observed in the 3 domains of these proteins including a Sm-fold in domain 1 and a sequence in domain 3, which were both suggested to bind RNA (S1 Fig [13,15]). Compared to its homologues, the CaDom34 protein lacks a potential NLS sequence (position 173–177 in ScDom34p). Strains were constructed that lack both alleles of *CaDOM34* in the wild-type background (SK47), in the *pmt1* background (SK24) and in the *pmt5* background (JH8-5-11) (disruption scheme in S2 Fig). Phenotypes were determined using mutant strains, in which *URA3* was reconstituted at its authentic locus [27].

Similar to *S. cerevisiae*, a homozygous *dom34* single mutation did not generate significant growth or morphogenetic defects in *C. albicans*; furthermore, this mutant was found not to be supersensitive to numerous tested antibiotics or inhibitors including HygB. On the other hand, the HygB-supersensitive phenotype of the *pmt1* mutant was significantly increased by an additional *dom34* mutation (Fig 1C). Thus, evidence in both yeast species supported a functional link between Dom34 and Pmt1 proteins to generate HygB resistance. However, for *S. cerevisiae* it cannot be excluded that the *DOM34* paralog *YCL001W-B* contributes to this phenotype. Therefore, and because of its importance as a human pathogen, we focused subsequent analyses on the *C. albicans DOM34* gene.

Overexpression of *DOM34* suppresses *pmt1* mutant phenotypes

The genetic interaction of *dom34* and *pmt1* mutations in *C. albicans* prompted experiments to study effects of *DOM34* overexpression in this fungus. The *DOM34* transcript level was determined by qPCR and showed an equal amount in homozygous *pmt4*, *pmt5*, *pmt6* and heterozygous *pmt2/PMT2* mutants as in the wild-type strain CAF2-1 but surprisingly, a 2–3 fold lower level in the *pmt1* mutant (Fig 2A; S3 Fig). A transformant of the *pmt1* mutant carrying plasmid pSK2 (*MET3p-DOM34*^{FLAG}) that was grown in SD medium contained about sixfold higher *DOM34* transcript levels than the untransformed strain and about threefold higher levels than the wild-type strain. Thus, using pSK2, a moderate overexpression of *DOM34* was achieved in *C. albicans*.

Overexpression of *DOM34*^{FLAG} was able to rescue several known *pmt1* mutant phenotypes [3]. The inability of *pmt1* mutant colonies to form hyphae was partially suppressed by *DOM34* overexpression, which was observed in > 80% of the colonies (Fig 2B). Furthermore, the sensitivity of *pmt1* mutants to HygB and to high temperature (42°C) was also partially suppressed (Fig 2Ca). Interestingly, however, suppression was not achieved using a derivative of pSK2 carrying a point mutation in the *DOM34* ORF that encodes the E21A variant Dom34 protein (Fig 2Cb). It has been suggested that this residue is important for RNase activity of Dom34 proteins [18].

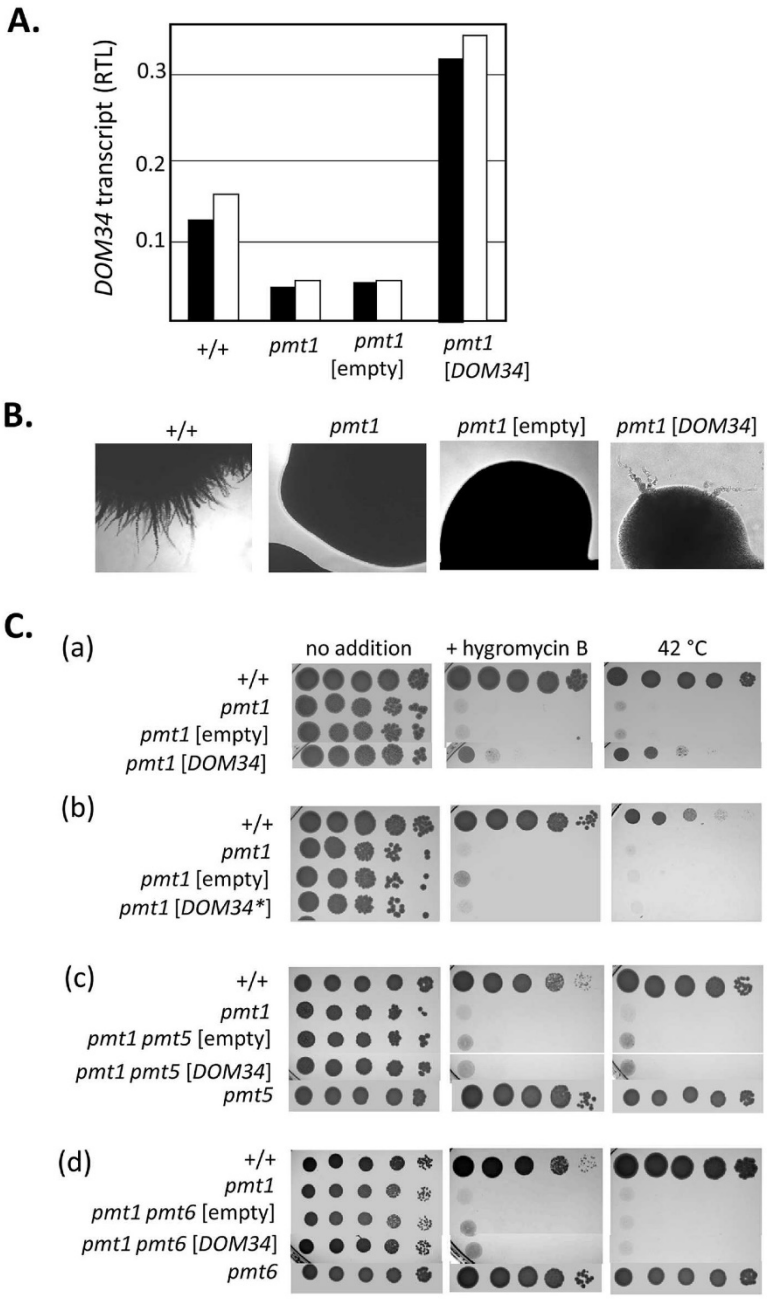

Fig 2. *DOM34* overexpression suppresses *pmt1* phenotypes. (A) Relative *DOM34* transcript level (RTL). Total RNA of strains CAF2-1 (+/+), SPCa2 (*pmt1*/*pmt1*), CAP1-3121[pSP38] (*pmt1*/*pmt1*[empty vector] and CAP1-3121[pSK2] (*pmt1*/*pmt1*[*DOM34*]) was isolated and amounts of the *DOM34* transcript were determined by qPCR using *ACT1* as the reference transcript. Two independent biological replicates of each strain were assayed. **(B)** Hypha formation of representative colonies grown on Spider medium for 2–5 d at 37˚C. Strain designations as in (A) **(C)** Effects of *DOM34* overexpression on *pmt* mutant phenotypes. Serially diluted cultures of strains were spotted and grown on YPD agar at 30˚C without or with 200 μg

hygromycin B,or at 42˚C without additions. *pmt1* single mutant host strains were transformed with expression vector pSK2 encoding wild-type Dom34 protein (a) or with pSK2mut encoding a E21A variant of Dom34 (Dom34*) (d). In addition, transformants of double mutant strains *pmt1 pmt5* (b) and *pmt1 pmt6* (c) were tested. Strains P15-274 (*pmt1*/*pmt1 pmt5*/*pmt5*), P15-274-1[pSP38] (*pmt1*/*pmt1 pmt5*/*pmt5*[empty vector], P15-274-1[pSK2] (*pmt1*/*pmt1 pmt5*/*pmt5*[*DOM34*]) were compared (b); in addition, strains CPP1121[pSP38] (*pmt1*/*pmt1 pmt6*/*pmt6*[empty vector]) and CPP1121[pSK2] (*pmt1*/*pmt1 pmt6*/*pmt6*[*DOM34*] were compared (c). Single mutant strains SPCa2 (*pmt1*/*pmt1*), SPCa10 (*pmt5*/*pmt5*), SPCa8 (*pmtD6*/*pmt6*) and the wild-type strain CAF2-1 (+/+) were used as reference strains.

doi:10.1371/journal.pgen.1006395.g002

We asked next if the suppression of *pmt1* mutant phenotypes by *DOM34* overexpression depended on the Pmt isoforms remaining in this strain. For this purpose, we constructed *pmt1 pmt5* and *pmt1 pmt6* double mutants, which both showed the supersensitive *pmt1* mutant phenotype (Fig 2Cc and 2Cd), while single *pmt5* or *pmt6* mutants are not supersensitive to HygB [3]. Interestingly, double mutant transformants carrying the *DOM34* overexpression plasmid pSK2 did not show any recovery of *pmt* mutant phenotypes (Fig 2Cc and 2Cd). This result indicates that Pmt5 or Pmt6 isoforms are required for the observed rescue by Dom34 overproduction. The relevance of the Pmt2 and Pmt4 isoforms could not be tested in this manner, because *PMT2* is an essential gene and *pmt1 pmt4* double mutants are not viable [3]. These experiments also revealed that unexpectedly, a *C. albicans* strain lacking all members of the Pmt1 subfamily (Pmt1 and Pmt5) is fully viable, although in *S. cerevisiae* heteromeric Pmt1-Pmt2 or Pmt1-Pmt5 complexes have been described to be essential for growth [28].

Dom34 stimulates Pmt protein but not transcript levels

Conceivably, Dom34 could have suppressed Pmt1 deficiencies by several mechanisms, especially by increasing transcription/transcript levels of several *PMT* genes including *PMT5* and/or *PMT6*, as suggested by the above experiments (Fig 2C). To explore this notion, we determined transcript levels in the *DOM34* overexpression strain and found that none of the *PMT* transcript levels was increased (S4A Fig). In addition, the absence of Dom34 did not decrease *PMT* transcript levels, while *PMT2/PMT4* transcript levels were increased in the *pmt1 dom34* double mutant, as described for the *pmt1* single mutant [6] (S4B Fig). Thus, increases and decreases of Dom34 levels were not related to *PMT* transcript levels. To explore effects on Pmt protein levels a *C. albicans* strain was constructed, in which one *PMT1* allele was fused to sequences encoding the hemagglutinin (HA)-epitope (Fig 3), which was subsequently transformed with the *DOM34* overexpression vector pSK2 or the corresponding empty vector. This strain produced considerably higher $Pmt1^{HA}$ protein levels as compared to a transformant carrying an "empty" control vector (Fig 3A). Scanning of band intensities revealed that *DOM34* overexpression increased the mean Pmt1-HA/actin ratio 1.78 fold ($p = 0.025$).

The 5′-UTR of the *PMT1* transcript encompasses 190 or 218 nt [29,30] and contains an intriguing CA/AC-rich sequence, which is ordered into three overlapping 11-mer ACAACCA CAAC repeats between nt -157 to -179 (Fig 3B, top). To examine if this sequence is involved in overproduction of the Pmt1 protein by *DOM34* overexpression we generated genomic fusions containing two different lengths of the *PMT1* upstream region joined to the *RLUC* reporter gene. One fusion did not contain most 5′-UTR sequences (pPdC3-HIS), while the second contained one full and one half of the 11-mer repeat (pPdC2-HIS) (Fig 3B top). These strains were transformed with the *DOM34* overexpression plasmid pSK2 or a control plasmid and luciferase activity of the double transformants was determined. The results revealed that the construct containing 5′-UTR sequences including the 11-mer repeat was stimulated significantly by

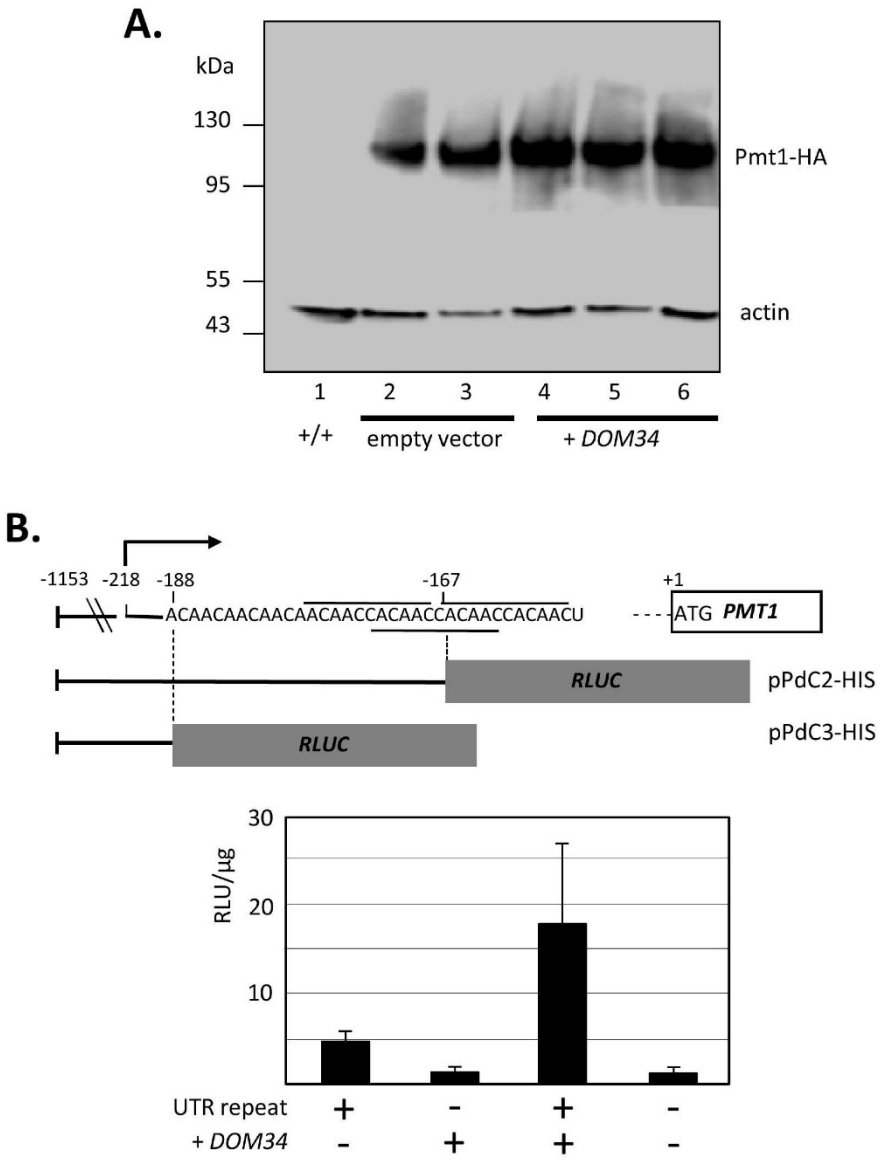

Fig 3. *Dom34* overexpression upregulates Pmt1 amounts and depends on 5′-UTR of *PMT1*. (A) Pmt1 amounts. Two independent strains of CIS23[pSP38] (*PMT1*/*PMT1*^{HA} [empty vector]) were compared with three independent strains of CIS23[pSK2] (*PMT1*/*PMT1*^{HA} [*DOM34*]); strain CAF2-1 (+/+) was used as negative reference strain. 5 µg of crude extract protein were separated by SDS-PAGE (10% acrylamide) and immunoblots were probed by rat anti-HA antibody (1:1000) and mouse anti-actin antibody (1:1000) followed by reaction with POD-coupled anti-rat and anti-mouse antibodies (1:20000). The signals of tagged Pmt1^{HA} and actin are indicated. **(B)** Importance of 5′-UTR on *PMT1* regulation. The 5′-start of the *PMT1* transcript at position -218 is indicated by the kinked arrow. Plasmids containing the *PMT1* promoter either including the 5′-end of the UTR from position -218 to -167 containing one of three 11-mer repeats (pPdC2-HIS) (under-/overlined sequences) or lacking this 5′-UTR sequence (pPdC3-HIS) in fusion to the *RLUC* reporter gene were integrated into the *PMT1* promoter of *C. albicans* strain RM1000 by transformation. These strains were additionally transformed with vectors pSK2 for *DOM34* overexpression or with the pSP38 empty control vector. Protein extracts of three independent double transformants were tested for luciferase activity, which was calculated as relative light units (RLU) per µg of protein.

doi:10.1371/journal.pgen.1006395.g003

DOM34 overexpression, while no activation occurred for the construct lacking UTR sequences (Fig 3B bottom).

As stated above, the *C. albicans* Dom34 protein lacks a consensus NLS sequence, suggesting that its primary action takes place outside of the nucleus. Furthermore, differential centrifugation of cell extracts identified HA-tagged Dom34^{11A} to a large extent in the soluble fraction (cytoplasm) (S5 Fig). Collectively, the results suggest that Dom34 overproduction stimulates translation of Pmt proteins. The site of the Dom34 stimulatory activity appears to lie in a specific sequence within the 5′-UTR of target transcripts, as exemplified by the Dom34-mediated regulation of the *PMT1-RLUC* fusion.

Dom34 is required for efficient translation of the *PMT1* transcript

We next carried out polysome analyses to establish the role of Dom34 in translation of *PMT1* and the *ACT1* housekeeping transcripts. For this purpose, cellular lysates of the control strain CAF2-1 and the *dom34* mutant JH47-2 were separated by sucrose gradient centrifugation to establish polysomal profiles (Fig 4A). Profile comparisons of both strains revealed that pre-polysomal fractions containing 40S, 60S and 80S rRNA were more pronounced in the *dom34* mutant than in the control strain; furthermore, polysomal peaks were lower in the mutant and decreased at >2n polysomes, whereas in the control strain, the 3n peak was even greater than the 2n peak. These results indicate that in the *dom34* mutant, translational efficiency is generally but moderately reduced.

To examine the efficiency of *PMT1* translation in control and *dom34* mutant cells, the fractions of the polysomal gradient were examined for the presence of the *PMT1* transcript by RT-qPCR, using a spiked-in control RNA as a reference. The result indicates clearly that the *PMT1* transcript in the *dom34* mutant is found predominantly in the pre-polysomal fraction, while in the control strain, significantly higher amounts reside in the polysomal fractions (Fig 4B). To establish if lower translational efficiency in the mutant concerns only the *PMT1* transcript, we also examined the transcript profile for the *PMT4* and *PMT6* transcripts, which also were enriched in the polysomal fraction in the presence of Dom34 (S6A Fig) indicating that Dom34 positively regulates the translation of several *PMT* transcripts. In comparison, translation of the transcript for the housekeeping gene *ACT1* appeared less affected by Dom34. These effects were quantitated the Kolmogorov-Smirnov test [31 (Fig 4C). By this algorithm, the calculated Dom34-dependent enrichment of transcripts in the polysomal fraction showed a statistically significant increase for the *PMT1* transcript ($D = 0.6$, p-value = 0.031), the *PMT4* transcript ($D = 0.5$, $p = 0.042$) and for the *PMT6* transcript ($D = 0.5$, $p = 0.066$); in contrast, a lower and insignificant enrichment was calculated for the *ACT1* transcript (D = 0.3, $p = 0.675$) (Fig 4C).

Collectively, the results suggest that Dom34 generally enhances but is not absolutely required for translation in *C. albicans*. The degree of Dom34-mediated translational enhancement differs between transcripts and may particularly affect specific groups of transcripts including transcripts for different Pmt isoforms. Interestingly, the 5′-UTR of all *PMT* transcripts (but not the 5′-UTR of the *ACT1* transcript) contains at least one CAAC motif, which in the above-described ACAACCACAAC repeat region of the *PMT1* 5′-UTR occurs eight times (S6B Fig). Conceivably, the positive action of Dom34 on translation of *PMT* transcripts is mediated by this sequence.

Dom34 regulates *in vitro* translation via the *PMT1* 5′-UTR

Recombinant Dom34 (S7 Fig) was added to a rabbit reticulocyte *in vitro* translation system, using RNA carrying the coding region for click beetle green luciferase (CBGluc), either containing or not containing the *PMT1* 5′-UTR (Fig 5Aa). As expected, protein products of

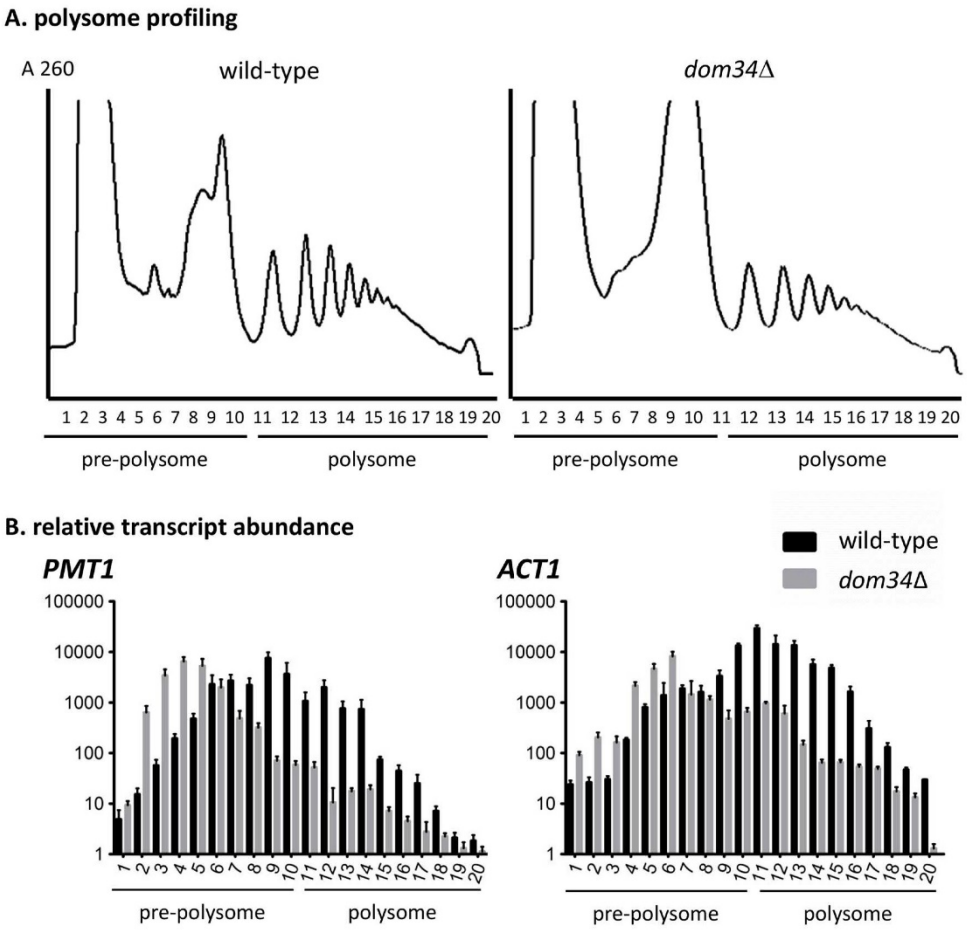

C. KS-test statistics

fraction / transcript	pre-polysome		polysome	
	D-value	*p*-value	*D*-value	*p*-value
ACT1	0.2	0.975	0.3	0.675
PMT1	0.4	0.135	0.6	0.031
PMT4	0.4	0.171	0.5	0.042
PMT6	0.5	0.022	0.5	0.066

Fig 4. Transcript fractionation on polysome gradients. (A) Cellular extracts of strain CAF2-1 (wild-type) and *dom34* mutant JH47-2 were centrifuged in a 10–50% sucrose gradient, which was subsequently fractionated. Nucleic acids in gradient fractions were detected by absorbance (A_{260}). Note that pre-polysome fractions contain 40S, 60S and 80S ribosomal RNA. **(B)** Occurrence of *ACT1* and *PMT1* transcripts in gradient fractions. Transcripts were detected by qPCR after adding a known amount of an *in vitro* generated transcript of CaCBGluc as calibrator. Each bar represents the normalized mean *ACT1* or *PMT1* transcript level of two independent experiments including the standard error of the

mean. **(C)** The Kolmogorov-Smirnov test was used to determine the distance "D-value" between the two distribution functions of the wild-type strain CAF2-1 and *dom34* mutant for polysomal and pre-polysomal fractions of *PMT1*, *PMT4*, *PMT6* and *ACT1*, respectively. Statistical relevance is indicated by the calculated *p*-value.

doi:10.1371/journal.pgen.1006395.g004

identical molecular masses of 60 kDa were obtained for both proteins (Fig 5Ab). Additional experiments indicated that the presence of the 5′-UTR augmented CBGluc biosynthesis, while added Dom34 reduced production, if the 5′-UTR was present, but not in its absence (Fig 5Ba). These effects were quantitated by measuring CBGluc luminescence of the samples, which demonstrated that in the presence of Dom34, for RNA containing the 5′-UTR, enzyme activity was decreased by about 40% in three independent measurements (Fig 5Bb and 5Bc). Next, using translational assays containing varying amounts of Dom34 protein, it was shown that already at 0.1 μM, Dom34 reduces translation efficiency significantly, while it fully inhibits translation at 0.25 μM. At higher concentrations of Dom34, CBGluc production increases and again to diminishes at 2.5 μM. These results demonstrate clearly that Dom34 is able to strongly influence translational activity via the *PMT1* 5′-UTR sequence. Use of a heterologous *in vitro* system may explain the concentration-dependent, negative rather than the expected positive action of Dom34 on translation.

Dom34 is able to bind and cleave endonucleolytically the *PMT1* 5'-UTR at distinct sites

To clarify the mechanisms how Dom34 influences translation we carried out electrophoretic mobility shift assays (EMSA) with recombinant Dom34 of the complete *PMT1* 5'-UTR sequence. The 5′-UTR was obtained by run off *in vitro* transcription using T7 polymerase using pRG01 as the template, which was cut by *Bgl*II at the 3′-end of the UTR. The 3′-[^{32}PpCp] end-labelled RNA was incubated with increasing amounts of Dom34, separated by native PAGE (5% acrylamide) and examined by autoradiography. The 5′-UTR RNA migrated very slowly compared to the control 6S RNA from *E. coli* which is not much shorter and has a well-known compact secondary structure [32] (Fig 6A). This suggests a more bulky secondary structure for the *PMT1* 5'-UTR. At concentrations above 0.3 μM, the binding of Dom34 to the UTR became visible resulting in two retarded complexes (I and II). The second complex appeared at high Dom34 concentrations suggesting that multiple proteins are bound to one RNA molecule. At 2.5 μM of Dom34, no free RNA remained suggesting that all of the UTR was bound or degraded; in contrast, little binding of Dom34 (or Dom34^{E21A}) to the 6S control RNA was observed (S8A and S8B Fig). Interestingly, starting already at very low concentrations of Dom34 (150 nM) some smaller-size degradation fragments of the UTR were observed (asterisks). Because the degradation products did not appear as sharp bands during native gel electrophoresis, we analyzed the same samples by denaturing gel electrophoresis (Fig 6B, right panel). Autoradiography clearly showed that already at 0.1 μM Dom34 the 5′-UTR is partially degraded and that the degradation products have distinct lengths of 1 to 40 nt and around 100 to 120 nt suggesting endonucleolytic cleavage rather than 3' or 5' exonucleolytic degradation. Exonuclease-mediated degradation from the 3′- end would have removed the 3′-labeling, which would have decreased amounts of full-length UTR RNA, while degradation from its 5′-end would have generated a smear of cleavage products. However, the results of denaturing gel electrophoresis indicate that the slight decrease of full-length UTR occurring at Dom34 concentrations > 0.6 μM is solely due to endonucleolytic fragmentation at specific sites. Under denaturing separation conditions protein-UTR interactions are disturbed, revealing the presence of full-length UTR that is not seen under native conditions. This result also provides an indirect proof for UTR binding by Dom34 at higher concentrations.

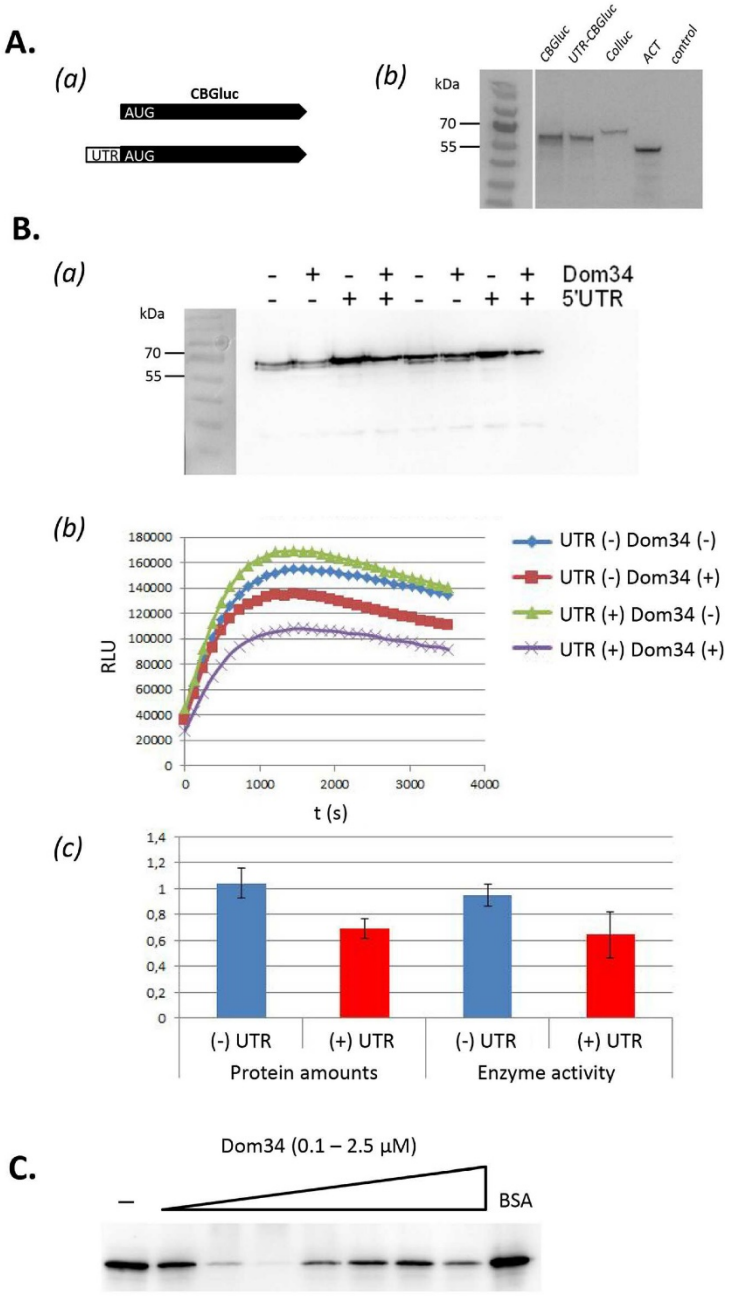

Fig 5. Dom34 inhibits translation when *PMT1* 5'-UTR is present. (A) Identical sizes of CBGluc proteins produced in an *in vitro* rabbit reticulocyte translational system using RNA templates containing or not containing the 5'-UTR of *PMT1*. *(a)* Scheme of RNA templates, *(b)* Protein products derived from *CBGluc* RNA without (*CBGluc*) or with (*UTR-CBGluc*) the 5'-UTR. Equal amounts of *in vitro* transcribed RNA were translated and labeled by incorporation of biotinylated lysine in the rabbit reticulocyte lysate; proteins were separated by SDS-PAGE and detected by using HRP-conjugated streptavidin. Further lanes contain protein

products of control RNAs (Promega) showing 61 kDa *Coleoptera* luciferase (*Colluc*) and 42 kDa mouse ß-actin (Ambion) (*ACT*) and a control without RNA template (*control*). **(B)** Dom34 regulates *in vitro* translation. *(a)* CBGluc production as in (A) using no or 2.5 μM final concentration of Dom34, in the presence or absence of the 5′-UTR, as indicated. *(b)* Time course of luminescence emitted by the *in vitro* translated CBGluc, *(c)* comparisons of CBGluc protein amounts and CBGluc enzyme activities (luminescence peaks at 1332 sec) in the presence of Dom34. Three independent experiments were analyzed; the activity of samples without added Dom34 was set to 1. **(C)** Concentration dependence of *in vitro* translation of *CBGluc* transcript containing the 5′-UTR by increasing amounts of Dom34 protein.

doi:10.1371/journal.pgen.1006395.g005

The 5′-UTR structure predicted by the RNAfold program (http://rna.tbi.univie.ac.at/cgi-bin/RNAfold.cgi) indicated that it contains several single-stranded regions including the presumed Dom34-binding CA/AC-rich sequence, as well as two double-stranded regions that compact the structure (S9A and S9B Fig). In the absence of Dom34, cleavage with single strand-specific RNase U2 confirmed that the CA/AC-region is unpaired, while in the presence of Dom34, this region was protected from RNase digestion, consistent with Dom34 binding in this region (S9C Fig).

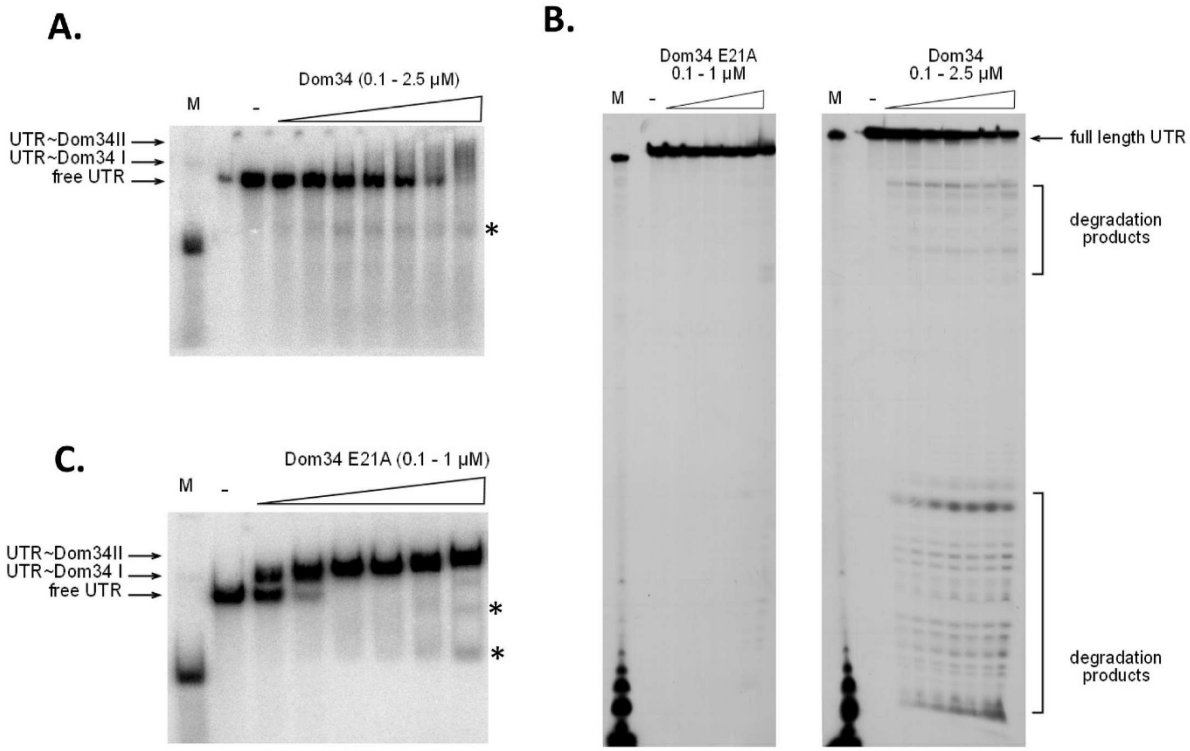

Fig 6. Dom34 is able to bind the *PMT1* 5′-UTR and cleave at distinct sites. Radioactive 3′ end-labeled RNA was incubated with increasing amounts of recombinantly produced Dom34 or Dom34^{E21A} proteins and after complex formation samples were split and analysed either by 6% native PAGE **(A, C)** or by 10% denaturing PAGE **(B)**. Dom34 or Dom34 E21A were present in final concentrations of 0.1/0.15/0.25/0.3/0.6/1/2.5 μM, while BSA as a specificity control was added also at 2.5 μM final concentration. For comparison of running behaviour under native and denaturing conditions 6S RNA from *E. coli* was loaded on the gel (M). Two UTR-Dom34 complexes (I, II) were observed under native separation conditions **(A, C)**, which also revealed potential RNA degradation fragments (unbound or bound to Dom34) (asterisks). Under denaturing conditions Dom34 but not the Dom34 E21A variant generated specific UTR degradation fragments **(B)**.

doi:10.1371/journal.pgen.1006395.g006

Furthermore, besides cutting the 50-UTR at position 80–100 from the 50-end, binding of Dom34 made paired regions more accessible to RNase attack, thus indicating that significant rearrangement of the 5′-UTR had occurred during Dom34 binding.

Specific sequences in Dom34 homologs have been suggested to be important for the transla-tional functions of Dom34 [17–20, 33]. A conserved glutamic acid residue in domain 1 (E21 in CaDom34) has been suggested to be important for RNase activity [18] and the importance of E21 for CaDom34 function was already shown above by the demonstration that the E21A vari-ant is unable to suppress *pmt1* phenotypes (Fig 2C). To test effects of the E21A mutation on binding or cleavage of the *PMT1* UTR the Dom34-E21A variant was recombinantly produced in *E. coli*. Binding of Dom34-E21A to purified 5'-UTR was observed at very low protein con-centrations (> 0.1 μM Dom34); estimation of an apparent K_D of about 100 nM deduced from these results demonstrates the very high affinity of Dom34-E21A to the UTR RNA, which is greater than the affinity observed for the wild-type Dom34 protein (Fig 6C). Importantly, mini-mal UTR cleavage is seen at concentrations > 0.6 μM of Dom34-E21A. The denaturing gel confirms this result, because only at 1 μM Dom34-E21A minimal degradation products become visible, while the amount of full-length RNA is not changed significantly (Fig 6B, left panel).

We conclude that Dom34 is an RNA binding protein, which favours certain RNA targets including the *PMT1* 5′-UTR. Furthermore, Dom34 has the capacity to endonucleolytically cleave bound target RNA and requires its E21 residue for this function.

Dom34 binds to a 5′-UTR oligonucleotide

The above experiments had indicated that Dom34 stimulates translation (Fig 4) and that a specific sequence containing three overlapping 11-mer repeats within the 5′-UTR of the *PMT1* is involved in this function (Fig 3). To explore if Dom34 directly interacts with this sequence we tested interaction of a corresponding RNA oligomer containing the repeat sequence with Dom34 protein in EMSA. These experiments showed a single retarded complex (complex I) with wild-type Dom34, which in the presence of lauryl sarcosinate (asterisks) split into two retarded complexes (I, II) (Fig 7). In contrast, BSA as a control protein did not bind the RNA oligonucleotide and the labelled RNA oligomer could be competed out using a 100-fold excess of unlabeled oligomer. The E21A Dom34 variant showed even enhanced binding compared to native Dom34, supporting its binding behavior to the full-length 5′-UTR (Fig 6). Furthermore, the $Dom34^{N317A}$ variant containing a mutation of a key residue in a sequence with high homology to RNA binding proteins [15] also bound to the 5′-UTR RNA oligomer as native Dom34. All Dom34 versions also led to a slight partial degradation of the labelled RNA oligonucleotide (smear emanating from free oligonucleotide); however, because a similar pattern was observed using the BSA control protein, it appears that no additional RNase activity is associated with Dom34.

Discussion

By NGD, NRD and 80S release mechanisms, Dom34 and co-regulatory molecules including Hbs1 maintain sufficient numbers of ribosomes and thereby assure efficient translation in eukaryotes [10,14]. However, recent *in vivo* results have indicated that Dom34 affects ribosome occupancy at only 11% of all genes and it is yet unknown, why stalled ribosomes on some tran-scripts are resolved by Dom34, while other transcripts with similar structural impediments are not affected [13]. A restricted rather than a general function of Dom34 in translation was also suggested by the finding that *S. cerevisiae dom34* mutants do not show a general growth pheno-type in all genetic backgrounds [15,16]. Thus, the target specificity of Dom34 for specific tran-scripts remains to be clarified. Results presented here indicate for the first time that Dom34

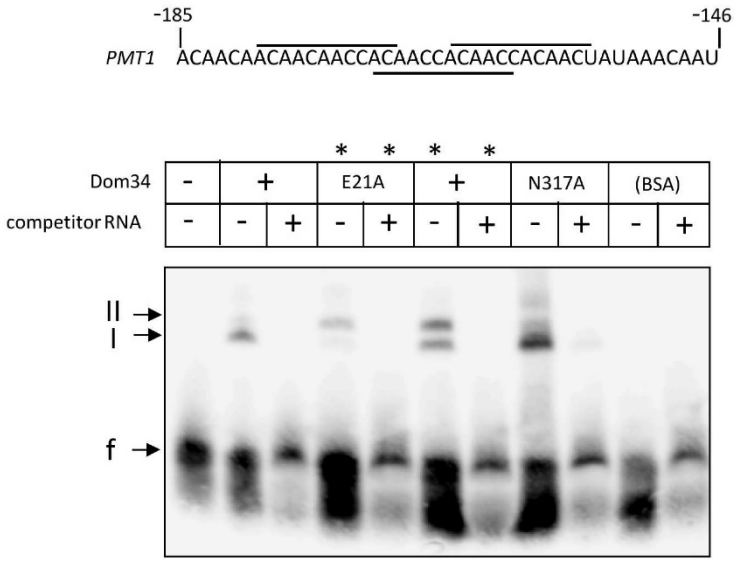

Fig 7. Dom34 binding to the 5′-UTR of the *PMT1* transcript. (Top) Sequence of oligonucleotide representing the 5′-end of the 5′-UTR of the *PMT1* transcript. (Bottom) EMSA of biotinylated 5′-UTR oligonucleotide in the absence or presence of *E. coli*-produced Dom34, its E21A variant and its N317A variant (protein/oligonucleotide molar ratio = 20). A specificity control reaction contains 2.5 μM BSA instead of Dom34. Unlabeled oligonucleotide in 100-fold excess was added as competitor in the indicated samples. The migration of unbound oligonucleotide (f) and two retarded complexes (I, II) was assayed by blotting of RNA separated by agarose gel electrophoresis onto a nylon membrane, which was developed by a chemiluminescent substrate to detected biotin. Binding reactions marked by an asterisk (*) were performed in the presence of 0.05% lauryl sarcosinate.

doi:10.1371/journal.pgen.1006395.g007

can serve as an RNA binding protein that could enhance translation of specific transcripts. These conclusions were obtained using the yeast *C. albicans* as experimental organism, which contains a single allele for a Dom34 protein with high similarity to orthologs in other organisms, while *S. cerevisiae*, because of its ancient genome duplication [34], contains in addition to *DOM34* a paralog (*YCL001W-B*) of unknown function.

Our results indicate on the one hand a general function of Dom34 on translation, since polysome gradients in the *dom34* mutant showed an increase of monosomes and decrease of polysomes, as compared to a wild-type strain. Furthermore, the abundance of the housekeeping *ACT1* transcript encoding actin was shifted slightly to the monosomal fraction in the *dom34* mutant suggesting reduced translation. However, the general translational effects of Dom34 appear to be moderate, since growth or morphogenesis of *C. albicans* was not affected in unstressed conditions. In contrast, in *pmt1* mutants with defective *O*-mannosylation that lack a major isoform of Pmt proteins [3], the contribution of Dom34 to growth phenotypes was clearly apparent. Protein-*O*-mannosylation is essential for fungal growth and its absence triggers the UPR response, because of the accumulation of underglycosylated, wrongly folded proteins in the ER lumen [6,7]. The *HAC1* transcript has recently been identified as a specific target of Dom34, which releases ribosomes stuck at the 3′-UTR [13]. One possible scenario explaining the genetic interaction of mutations in *DOM34* and *PMT1* is that Dom34, by its ribosome releasing function, assures efficient translation of the mature *HAC1* transcript. By this action, UPR responses could stimulate growth of *pmt1* mutant cells.

Aside from this general activity for maintenance of ribosome levels, our results suggest a specific stimulatory function of Dom34 on the translation of certain transcripts. As shown by the polysome profiling experiments, the translation of the *PMT1*, *PMT4* and *PMT6* transcripts were more strongly affected by the presence of Dom34 than that of the *ACT1* transcript. Furthermore, Dom34 binding to the 5′-UTR of the *PMT1* transcript and activation of a reporter gene by this sequence supported a direct positive role of Dom34 on the translational initiation of the *PMT1* transcript. This action is consistent with lowered Pmt1-mediated *O*-mannosylation of a heterologous protein (hIGF-1) during its massive overproduction in a *dom34* single mutant of *S. cerevisiae* [23]. In this overproduction condition, Dom34-mediated improvement of Pmt1 activity appears to be needed to obtain full *O*-mannosylation of target proteins. On the other hand, *DOM34* overexpression only rescued *pmt1* mutant phenotypes, if *PMT5* or *PMT6* genes were present, suggesting that the post-transcriptional stimulatory action of Dom34 is not exclusive for the *PMT1* transcript but applies to transcripts of several *PMT* genes, which was indeed confirmed for the *PMT4* and *PMT6* transcripts. Dom34 activity may be especially needed for translation of *PMT2* and *PMT4* transcripts, which in a compensatory response are upregulated in *pmt1* mutants [7]. On the other hand, stalled ribosomes were not found previously in a *dom34* mutant at any of the seven *S. cerevisiae PMT* transcripts [13], indicating that ribosome release by Dom34 is not a specific translational activation mechanism for *PMT* transcripts. The function of Dom34 as a relatively specific translational enhancer complements other posttranscriptional mechanisms in *C. albicans* that recently have been discovered to be essential for the biology and virulence of this fungus [35,36].

The ability of Dom34 to act as a RNA binding protein adds a new facet to the mode of action of Dom34 in eukaryotes. RNA binding was specific, because it did not occur with a control RNA, it was outcompeted efficiently and it occurred at low Dom34 concentrations. A stretch of residues in domain 3 of Dom34 had previously been shown to share high homology to RNA binding proteins [15,33]. However, mutation of a central residue in this sequence, N317 to N317A, did not affect binding of $Dom34^{N317A}$ to the 5′-UTR oligonucleotide suggesting that this Dom34 sequence may be important for binding to the 3′-UTR but not to the 5′-UTR of transcripts. The predicted structure of the 5′-UTR, which was supported by limited RNase digestion, was found to contain several single-stranded regions, one of which comprised a CA/AC-rich region with three ACAACCACAAC repeats. Binding of Dom34 protected the 5′-UTR at this region from RNase digestion and Dom34 bound to a corresponding oligonucleotide, thus identifying the CA/AC-rich region as the Dom34 binding site. Interestingly, 5′-UTR regions of all five transcripts for *C. albicans* Pmt isoform (but not the 5′-UTR of the *ACT1* control transcript) contained at least one CAAC repeat (eight in the *PMT1* 5′-UTR), which may constitute the minimum requirement for Dom34 binding.

Dom34 did not show a major general RNase activity in our experiments, in agreement with Passos *et al.* [19], although distinct levels of specific degradation products of the bound 5′-UTR were detected. A Dom34 mutant, in which the conserved glutamic acid residue (E21 in CaDom34) important for *in vitro* RNase activity [18] was altered (E21A), strongly bound to the 5′-UTR but did not cause its endonucleolytic degradation, suggesting that E21 is relevant for its RNase activity. In agreement, rescue of *pmt1* phenotypes did not occur with overexpression of the $DOM34^{E21A}$ allele, thus confirming the importance of the E21 residue for the function of Dom34. Dom34 binding to the CA/AC-rich sequence caused cleavage of the 5′-UTR by its RNase activity at a distant site, within predicted double-stranded regions causing a major structural alteration of the 5′-UTR. The mechanism, by which Dom34-mediated binding and cleavage of 5′-UTR sequences is able to stimulate translation of specific transcripts remains to

be established. Possibly, the actions of Dom34 on the 5′-UTR structure could improve the accessibility of the AUG codon to ribosomal factors and subunits. Whatever the mechanism may be, the results suggest that in addition to its general action at the 3′-UTR to release stalled ribosomes, Dom34 may act at the 5′-UTR of specific transcripts including *PMT* transcripts to stimulate translational initiation in glycostress conditions.

Methods and Materials

S. cerevisiae strains

S. cerevisiae strains are listed in S1 Table. To disrupt *PMT* genes in strain YE449, a 3.3 kb *Xba*I-*Sac*I fragment of pDIS2, carrying *pmt1*Δ::*URA3*, or/and a 2.4 kb *Hin*dIII-*Bam*HI fragment of pBDis [24], carrying *pmt2*Δ::*LEU2*, were used for transformation, selecting prototrophs [37]. To disrupt *DOM34* in strain YE449, a fragment generated by PCR on plasmid pUG6 [38] was used for transformation, selecting G418-resistance (PCR primers ScDOM34 disrupt for /rev). Oligonucleotides are listed in S2 Table. Likewise, to disrupt *YIL001w*, a PCR fragment generated by primers ScYIL001w disrupt for/rev was used. Correct integration of the disruption cassettes was verified by Southern blottings.

C. albicans strains

C. albicans strains are listed in S1 Table. For disruption of Ca*DOM34* its 5′- and 3′-regions flanking the ORF were inserted into pSFU1 to frame the *SAP2p-FLP* and *URA3* markers [39]. The *DOM34* 5′-region was amplified by genomic PCR on DNA of strain SC5314 using primers FPD34/RPD34 and the 3′-region was amplified using primers FDD34/RDD34. The resulting *DOM34* 5′-flanking region, as a *Sac*II-*Not*I fragment, and the 3′-flanking region, as a *Xho*I-*Apa*I fragment, were inserted into the respective sites of pSFU1 to generate pJB28. JB28 was cut with *Apa*I and *Sac*II and the large fragment was used for transformation of strain CAI4 or of *pmt1* mutant CAP1-3121 [40]. Correct integration in the resulting strains SK47 and SK24, respectively, was verified by diagnostic colony PCR and confirmed by Southern blottings, using the 5′-region flanking the *DOM34* ORF as the probe (S2 Fig). Removal of the *URA3* cassette and disruption of the second allele was carried out as described [41]. Following disruption of both *CaDOM34* alleles and eviction of the disruption cassette, *URA3* was reconstituted at its authentic locus by transformation with a genomic fragment [3] to generate strains JH47-1/2 and JH24-4/5. The *PMT5* gene was disrupted in the *dom34* background (strain SK47) or in the *pmt1* background (strain CAP1-3121) as previously described [3] to generate strains JH5-3-1 and P15-274, respectively.

To generate a *PMT1* gene encoding a C-terminally hemagglutinin (HA) epitope-marked Pmt1 protein PCR fragments were used containing the *sat1* selectable marker and flanked by regions of homology to *PMT1*. For tagging pSAT1-3HA was used as template, which was constructed by replacing the *URA3* gene in p3HA-URA [3] situated between *Pst*I and *Bgl*II sites with the *ACT1p-sat1-ACT1t*-cassette of pFC1 [42] on a *Pst*I to *Bam*HI fragment. PCR was done using primers CaPMT1del-for/-rev to generate a tagging fragment for Pmt1, which was chromosomally integrated by transformation of strain CAI4 selecting for nourseothricin resistance (*sat1*); resulting strain CIS23. For C-terminal HA-tagging of Dom34, an insertion fragment was generated by PCR using p3HA-URA as template and primers Dom34-HA-for/rev. The insertion fragment was transformed in strain CAI4 selecting for uridine prototrophy; resulting strains JHCa1-1 (-2). Correct integration of tagging cassettes was verified by diagnostic PCR of transformants.

Growth conditions and screening method

S. cerevisiae and *C. albicans* strains were grown in complex YPD and synthetic SD media [37]. For hyphal induction of *C. albicans* the strains were grown for 3–4 days at 37°C on Spider-medium [43] or on 2% agar containing 5% horse serum.

To compare killer sensitivities of several *S. cerevisiae* strains, YPD agar containing methylene blue and buffered to pH 4.5 was autoclaved, cooled to 50°C and 17 μl of a saturated culture of the killer K1- secreting strain RC130 was added before pouring plates [44]. Strains to be tested were pre-grown on YPD medium and replica printed onto these plates and grown at 18°C for 4–7 days. Sensitive strains appeared blue at this time, while resistant strains remained white. To complement killer K1-resistance of strain M577 *pmt1* by genomic clones, we transformed it with a genomic *S. cerevisiae* bank in YEp13 [45] and obtained 80 000 transformants on SD minimal medium. Colonies of transformants were replica-printed onto SD/methylene blue/pH 4.5-medium containing killer K1 strain RC180. Blue colonies were picked, their plasmid was isolated and retransformed into M577 *pmt1*. Among 78 initial transformants, 17 transformants were identified, whose plasmids restored Killer-sensitivity upon retransformation. Insert ends in these plasmids were sequenced using primers YEp13-Bamflank-A/-B, flanking the *Bam*HI insertion site of YEp13.

Yeast expression plasmids

The 7 kb *Bam*HI-*Xho*I fragment of pDM3 carrying a genomic *ScPMT1* fragment [46] was subcloned into YCplac111, to generate pSW20. Derivatives of YEp13 containing a 5.59 kb genomic insert carrying *ScDOM34* (pSW577/20) or containing a 4.55 kb genomic insert carrying *YIL001w* were used in some complementation experiments. Expression vectors encoding HA-tagged proteins were constructed by PCR amplification of ORFs and introducing them into YCpIF17 [47]. *DOM34* was amplified using primers ScDom34N/C, the 1.2 kb product was digested with *Eco*RI and *Pst*I and introduced into YCpIF17, resulting in plasmid pSW22. The *GAL1p-HA-DOM34* fragment of pSW22 was excised with *Xho*I and *Xba*I and inserted into YCplac111 (*Sal*I, *Xba*I) to generate pSW25. Likewise, *YIL001w* was amplified using primers YIL001wN/C, inserted into YCpIF17 to generate pSW21 and transferred into YCplac111 to generate pSW24.

To construct a *CaDOM34* expression vector its coding region was PCR amplified on gDNA using primers p1-DOM-FLAG and p2-DOM-FLAG. We then inserted the resulting *Pst*I-*Sph*I fragment downstream of the *MET3* promoter into a derivative of pFLAG-Met3 [48], which had been modified by adding the *CaARS2* replicator on an *Aat*II fragment [49]. The resulting plasmid pSK2 was modified further by oligonucleotide-directed mutagenesis to encode the Dom34-E21A variant; for this purpose, pSK2 was used as template with primers Dom34-Mut21for/rev in the QuikChange protocol (Stratagene) to generate pSK2mut. Using anti-FLAG antibody the FLAG-tagged Dom34 protein could be identified as a 45 kDa protein in immunoblottings of cellular extracts, although several cross-reacting proteins prevented immunocytological analyses.

Production of Dom34 in *E. coli*

The *C. albicans DOM34* ORF was inserted downstream of the T7 promoter, between the *Nde*I and *Xho*I restriction sites of expression vector pET22b (Invitrogen). The resulting vector pET22b-Dom34 encoded a Dom34 protein containing six histidine residues at its C-terminal end. The single CTG sequence encoding non-standard S288 in *C. albicans* was then altered to standard serine-encoding TCG by oligonucleotide-directed mutagenesis, using primers Dom34-Leu(mut)for/rev according to the QuikChange protocol (Agilent). The resulting vector

pET22b-Dom34+ was modified further similarly to encode variants potentially important for the function of Dom34. For the E21A variant and the N317A variant, oligonucleotides Dom34-Mut21fw/rev and Dom34Mut317fw/rev were used for mutagenesis. All expression vectors were verified by sequencing and transformed in *E. coli* strain Rosetta (Novagen).

Transformant cultures were grown to OD_{600} = 0.6 in LB medium containing 100 μg/ml ampicillin and 50 μg/ml chloramphenicol, 100 mM IPTG was added to induce the T7 promoter and cultures were incubated further at room temperature. Cell pellets were resuspended in buffer (50 mM TrisHCl/pH 7.9; 500 mM NaCl; 10% glycerol) containing protease inhibitors and disrupted by ultrasonication, followed by centrifugation (10,000 *x g* for 20 min). To assure the solubility of recombinant proteins, 0.5% lauryl sarcosinate was added to the buffer in some experiments. Soluble Dom34-His_6 proteins in the supernatant were purified by affinity chromatography using Histrap Crude-Agarose columns (GE) using 5 mM, 50 mM and 250 mM imidazole for elution. Elution fractions were collected using a ÄKTAprime collector (GE Healthcare) and analyzed by SDS-PAGE (4–20% acrylamide) followed by Coomassie Blue staining or by immunoblotting using an HRP-coupled anti-His tag antibody (Qiagen) (S7 Fig). About 2 mg of Dom34 variants with at least 95% purity were obtained.

qPCR

Relative transcript levels (RTL) of specific *C. albicans* genes were determined by quantitative reverse transcription PCR (qPCR) using the *ACT1* transcript as reference, as described [7,8]. Oligonucleotides designated RT (S2 Table) were used for this purpose.

In vitro translation

For the *in vitro* generation of transcripts, plasmid pUC18-T7CBG was constructed, which contains the promoter of bacteriophage T7 upstream of the coding region for click beetle green luciferase (CBGluc). For this purpose, primers CBG-Stu/Bam for/rev were used to amplify the coding region for CBGluc from plasmid CBGluc-pMK-RQ [50], which was inserted into pUC18T7 [51]. The resulting plasmid was modified further by insertion of the *PMT1* 5′-UTR sequence (-218 to -1 [29]) that was amplified using primers PMT1_5′UTR/-rev BglII_long from gDNA (strain CAF2-1); the resulting plasmid was named pRG01. Plasmids were linearized by *Bam*HI (pUC18-T7-CBG) or *Bgl*II (pRG01) downstream of the CBGluc coding region and were used as template for *in vitro* run-off transcription using T7 RNA polymerase (Ambion SP6 *in vitro* transcription kit) according to Gildehaus *et al.* [51]). The resulting transcripts were used for *in vitro* translation in a rabbit reticulocyte lysate kit (Promega L4960) that incorporates biotinylated lysine in the protein products (Promega Transcend Detection System). Divergent from the manufacturer's protocol the reaction was reduced to a total volume of 20 μl with 0.75 μl Transcend™ Biotin-Lysyl-tRNA. For each reaction 4.9 fmol RNA (244 nM) and variable amounts of Dom34 were preincubated for 10 min at RT and the reaction was started by adding a premix of reticulocyte-lysate, amino acids and RNasin. After 100 min at 30°C, 1 μl was separated by SDS-PAGE (10% acrylamide), followed by reaction with horseradish peroxidase-coupled streptavidin, as described by the manufacturer. Furthermore, CBGluc luminescence was measured by adding 45 μl of water to 5 μl of the translation mix, followed by addition of 50 μl Chroma-Glo substrate (Promega). Measurements were done in wells of 96-microtiter plates using TriStar LB 941 luminometer (Berthold Technologies) for 1 sec, as described [50].

Electrophoretic Mobility Shift Assay (EMSA)

Labelled RNA encompassing the 5′-UTR was obtained by multiple rounds of run-off transcription of pRG01 linearized by *Bgl*II and T7 RNA polymerase [48]. pUC18-T7-6S linearized by

*Stu*I served to generate 6S control RNA [51]. After purification on agarose-gels followed by glass wool-elution, the radioactive labeling at the 3′-end was performed by T4-RNA ligase-catalyzed addition of ^{32}P-pCp, as described [52]. If necessary, the labeled RNA was purified in a second step by electrophoresis on a 5% denaturing polyacrylamide gel. RNA-Dom34 complex formation was assayed by incubating 50–100 cps ^{32}P-labeled RNA together with variable amounts of Dom34 for 10 min at 30 °C, in 10 mM Tris-HCl/pH 8.0, 100 mM NaCl. Complexes were then challenged by adding of heparin (final concentration 50 ng/μl) for 10 min and sepa-rated on native 5% polyacrylamide gels or denaturing 10% polyacrylamide gels.

For EMSA of the *PMT1*-5′UTR RNA oligonucleotide, it was biotinylated using the Pierce RNA 3′ End Biotinylation Kit (Thermo Scientific) according to the instructions of the manufacturer. Protein-RNA binding assays were done using the LightShift Chemoluminescent RNA EMSA Optimization and Control Kit (Thermo Scientific). In a total volume of 20 μl, binding assays contained 20 nM biotinylated RNA oligonucleotide and 400 nM purified Dom34-His$_6$ (or its E21A or N317A variants), which were supplemented in part by 2 μM unlabelled oligonucleotide. Following incubation at room temperature for 20 min, 5 μl of 5x REMSA loading buffer was added and the assay components were separated by native PAGE (6% acrylamide) and electroblotted onto a nylon membrane; the biotinylated RNA was fixed on the membrane by a short UV treatment and was detected using the Chemiluminescent Nucleic Acid Detection Module Kit (Thermo Scientific).

Polysomal profiling

Cells of wild-type strain CAF2-1 and of *dom34*Δ mutant JH47-2 cells were grown exponentially in YPD media to OD_{600} 0.4–0.6. Preparation of cells and polysome gradients were performed as described by Garre *et al.* [53] with some modifications. A portion of the culture (80 ml) was recovered and chilled for 5 min on ice in the presence of 0.1 mg/ml cycloheximide (CHX). Cells were harvested by centrifugation at 6000 *x g* for 4 min at 4°C and resuspended in lysis buffer (20 mM Tris-HCl, pH 8, 140 mM KCl, 5 mM $MgCl_2$, 0.5 mM dithiothreitol, 1% Triton X-100, 0.1 mg/ml CHX, and 0.5 mg/ml heparin). After washing, cells were resuspended in 700 μl of lysis buffer, a 0.3 ml volume of glass beads was added, and cells were disrupted by shaking on a Vortex Genie 2 (setting 8) using 6 cycles for 40 s at 6.5 ms^{-1}. Between cycles cells were placed on ice for 5 min. Lysates were cleared by centrifuging twice for 5 min, first at 5,000 rpm, and then the supernatant was recovered and was centrifuged at 8,000 rpm. Finally, glycerol was added to the supernatant at a final concentration of 5%, before storing extracts at -70°C. Samples of 10–20 A_{260} units were loaded onto 10–50% sucrose gradients and were separated by ultracentrifugation for 2 h and 40 min at 35,000 rpm in a Beckman SW41 rotor at 4°C. Then, gradients were fractionated using isotonic pumping of 60% sucrose from the bottom, followed by a recording of the polysomal profiles by online UV detection at 260 nm (Density Gradient Fractionation System, Teledyne Isco, Lincoln, NE).

To analyze the RNA of the polysomal fractions, RNA from 200 μl of each fraction was extracted using GeneJet RNA extraction kit (STREK, Biotools). To each sample 1 μg of *in vitro* transcribed RNA (HiScribe™ T7 High Yield RNA Synthesis Kit, NEB) was added and used as spiked-in mRNA for normalization of the transcripts. After reverse transcription of the purified RNA (Maxima First Strand cDNA synthesis kit, Thermo Scientific) quantitative PCR (RT-qPCR) was performed using gene specific primer pairs to quantify mRNAs of *PMT1*, *PMT4*, *PMT6* and *ACT1*. For each fraction three technical replicates were assayed on a Mx3000P LightCycler (Stratagene), with 10 μl of cDNA, 4 μl EvaGreen QPCR-mix II (Bio-Budget) and 3 μl each of forward and reverse oligonucleotide primers (400 pmol/μl) in each reaction. The polymerase was activated at 95°C for 10 min, annealing was performed at 60°C for 15 s,

extension at 72°C for 30 s and the denaturation step was performed at 95°C for 30 s in a total of 50 cycles.

For the statistical assessment of the difference between the transcript distributions in the reference strain CAF2-1 and the *dom34* mutant strain, the Kolmogorov-Smirnov test (KS-test) was performed [31]. The KS-test was computed using the *ks.test* CRAN package in the *R* statistical software environment.

Supporting Information

S1 Fig. Structure of Dom34 proteins. Dom34/Pelota sequences of *S. cerevisiae* (ScDom34), *C. albicans* (CaDom34), *D. melanogaster* (DmPelota) and *S. pombe* (SpDom34) are aligned. The positions of domains 1–3 is indicated by the arrows and the circled numbers. The region suggested as a RNA binding sequence in domain 3 is underlined. The conserved glutamate in domain 1, presumed to act in RNase activity, is indicated by the thick arrow.
(PDF)

S2 Fig. Disruption of *DOM34* locus. (A) Scheme of wild-type *DOM34* locus, after disruption by the *FRT-URA3—FLP-FRT* cassette and after removal of the *URA3-FLP* sequences (top-to-bottom). **(B)** Southern blotting of genomic DNA in transformants. Total DNA was digested with *Cla*I and *Sal*I and blots were probed using a *DOM34* segment indicated by asterisks in (A). The fragment for the wild-type alleles is visible in lane 1, while the subsequent lanes demonstrate the course of disruption in derivative strains and the complete disruption of the two *DOM34* alleles in strain SK47 (lane 5).
(PDF)

S3 Fig. *DOM34* transcript levels in *pmt* mutant strains. Total RNA of strains CAF2-1 (+/+), SPCa2 (*pmt1*/*pmt1*), SPCa4 (*pmt2*/*PMT2*), SPCa6 (*pmt4*/*pmt4*), SPCa10 (*pmt5*/*pmt5*) and SPCa8 (*pmt6*/*pmt6*) was isolated and the relative *DOM34* transcript level (RTL) was determined by qPCR using the *ACT1* transcript as the reference. Values obtained for two biological replicates are shown as black and white bars.
(PDF)

S4 Fig. Influence of *DOM34* expression on *PMT* transcript levels. (A) Influence of *DOM34* overexpression was tested using strains CAF2-1 (+/+), SPCa2 (*pmt1*/*pmt1*), CAP1-3121 [pSP38] (*pmt1*/*pmt1*[empty vector]) and strain CAP1-3121[pSK2] (*pmt1*/*pmt1*[*DOM34*]). **(B)** Influence of *dom34* mutation was tested using strains CAF2-1 (+/+), SPCa2 (*pmt1*/*pmt1*), JH24-4 (*pmt1*/*pmt1 dom34*/*dom34*) and JH47-1 (*dom34*/*dom34*). Total RNA of all strains was isolated and relative transcript levels of the indicated *PMT* genes were determined by qPCR using the *ACT1* transcript as the reference. Values obtained for two independent biological replicates are shown as black and white bars.
(PDF)

S5 Fig. Immunoblot of HA-tagged Dom34. Cells of strains JHCa1-1 (*DOM34/DOM34*^{HA}) were fractionated by differential centrifugation. The periplasmic space (PE), crude extract (CE), pellet after centrifugation at 10,000 *x g* (P10; ER fraction), pellet after centrifugation of P10 supernatant at 100,000 *x g* (P100; Golgi fraction) and the corresponding supernatant (S100; cytoplasmic fraction) were obtained. Aliquots of each fraction were examined by SDS-PAGE (10% acrylamide) followed by immunoblotting using rat anti-HA antibody. The arrow indicates the migration of HA-tagged Dom34. As a control, an immunoblot of a crude extract of strain CIS23 (*PMT1/PMT1*^{HA}), producing HA-tagged Pmt1, is shown.
(PDF)

S6 Fig. Occurrence of *PMT4* and *PMT6* transcripts in polysome-gradient fractions. (A) The indicated transcripts were detected by qPCR after adding a known amount of an *in vitro* generated transcript of CaCBGluc as calibrator. Each bar represents the normalized mean *PMT4* or *PMT6* transcript level of two independent experiments including the standard error of the mean. **(B)** Incidence of "CAAC" and "ACCA" motifs in 5'-UTRs of *ACT1* and *PMT*-genes. The 5'-UTR sequences of *ACT1* (reference gene) and all *C. albicans PMT*-genes were analyzed for occurrence of the identified "CAAC" and "ACCA" motif (Fig 3B). Information about transcript start sites were taken from Tuch *et al.* (2010) and Bruno *et al.* (2010) [29,30]; the transcript with the longer 5'-UTR was chosen and respective sequences were obtained from CGD (http://www.candidagenome.org) assembly 21. Occurrence of the "CAAC" (underlined) and "ACCA" (line on top) motifs are highlighted in red at the indicated positions. The "CAAC" motif was identified in 5'-UTRs of all *PMT*-genes, but not in the 5'-UTR sequence of the reference gene *ACT1*.
(PDF)

S7 Fig. Purification of Dom34-His$_6$. *E. coli* Rosetta transformants carrying pET22b-Dom34+ were induced by IPTG and cell pellets were disrupted by ultrasonication. Soluble proteins in the cell extract were separated by affinity chromatography on Ni-NTA agarose, which was washed in buffer using 5 mM imidazole and eluted using 50 and 250 mM imidazole. Aliquots of fractions were separated by SDS-PAGE (4–20% acrylamide) and gels were stained using Coomassie Brilliant Blue R-250. Lanes show protein standards (S), cell pellet (Pe), flow-through (F), wash fractions (W1,2) and elution fractions (E1-5). The arrow marks the position of Dom34-His$_6$.
(PDF)

S8 Fig. Weak binding of native Dom34 (A) or the Dom34 E21A variant (B) to 6S RNA from *E. coli*. Radioactive 3' end-labeled 6S RNA was incubated with increasing amounts of Dom34; after complex formation samples were analysed by 6% native PAGE. As indicated Dom34 was present in final concentrations of 0.1/0.15/0.25/0.3/0.6/1 and 2.5 μM.
(PDF)

S9 Fig. Sequence and structure of the *PMT1* 5′-UTR. (A) UTR RNA sequence generated by *in vitro* transcription of plasmid pRG01 (linearized by *Bgl*II) using T7 RNA polymerase. Two G residues are added to 218 nt UTR sequence at its 5′-end by T7 RNA polymerase, while AGATC at the 3′-end reflects the *Bgl*II sequence. The transcript start site at -218 was determined by Tuch *et al.* [29], while an additional start site at -190 was reported by Bruno *et al.* [30] (underlined U in sequence). The CA/AC-rich region (Dom34 binding site) is marked in red font. **(B)** Predicted folding structure of *PMT1* UTR. The RNAfold program (http://rna.tbi.univie.ac.at/cgi-bin/RNAfold.cgi) was used for prediction and results were depicted as a centroid structure drawing encoding base-pair probabilities (colour code showing probabilities of base-pairing or single strandedness in predicted paired and unpaired regions, respectively). Numbered black arrows indicated predicted events upon Dom34 binding: (1) Binding of Dom34 to single-stranded region containing CA/AC-repeats, (2) opening of paired region by binding of Dom34, (3) opening of paired region and cleavage by Dom34, (4) cleavage by Dom34. **(C)** RNAse cleavage experiments supporting the predicted actions of Dom34. 3′-[^{32}P] end-labelled UTR RNA (50 cps) was incubated with RNases in the absence or presence of Dom34 for 1 min at 37°C; Dom34 was preincubated 10 min with the UTR before RNAse addition. Products were separated by 12% denaturing PAGE. Nucleotide positions are numbered from the UTR 5′-end as in (B). UTR, no RNAse (lane 1); UTR with 1 U RNAse T1 cleaving at G residues indicated in the left margin (lane 2); UTR with 0.5 U RNAse U2 specific for RNA

single strands (lane 3); UTR with 1 μM Dom34 (lane 4); UTR sequence ladder generated by partial hydrolysis with NaOH (lane 5); UTR with 0.25/0.5/1 U RNAse U2 (lanes 6–8); UTR incubated with 0.5 U RNAse U2 and 0.5/1/2.5 μM Dom34 (lanes 9–11). Note a prominent Dom34-mediated cleavage of the UTR around position 100. RNase U2 cleavage in position 30–60 (CA/AC-repeat region) confirms the predicted single-strandedness of the UTR in this position (lanes 7–9); Dom34 protects this region (lanes 10, 11), confirming its predicted binding at this site. Region 180–190 appears permanently single-stranded, while the predicted double-stranded regions 65–77 and around 170 become single-stranded upon Dom34 binding (lanes 9–11).
(PDF)

S1 Table. Strains.
(PDF)

S2 Table. Oligonucleotides.
(PDF)

Acknowledgments

We thank M. Gerads for excellent technical assistance and we acknowledge preparatory work on the project, which was carried out by J. van den Boom, J. Koopmeiners and I. Schmidt.

Author Contributions

Conceptualization: JFE LvW.

Funding acquisition: JFE PA.

Investigation: LvW RG JSH MJ PDC SW PA EP SK.

Methodology: LvW RG QL PA.

Supervision: JFE PA.

Writing – original draft: LvW JFE.

References

1. Lengeler KB, Tielker D, Ernst JF. Protein-*O*-mannosyltransferases in virulence and development. Cell Mol Life Sci. 2008; 65: 528–544. doi: 10.1007/s00018-007-7409-z PMID: 17975704
2. Willer T, Valero MC, Tanner W, Cruces J, Strahl S. *O*-mannosyl glycans: from yeast to novel associations with human disease. Curr Opin Struct Biol. 2003; 13: 621–630. doi: 10.1016/j.sbi.2003.09.003 PMID: 14568618
3. Prill SK-H, Klinkert B, Timpel C, Gale CA, Schröppel K, Ernst JF. *PMT* family of *Candida albicans*: five protein mannosyltransferase isoforms affect growth, morphogenesis and antifungal resistance. Mol Microbiol. 2005; 55: 546–560. doi: 10.1111/j.1365-2958.2004.04401.x PMID: 15659169
4. Gentzsch M, Tanner W. Protein-*O*-glycosylation in yeast: protein-specific mannosyltransferases. EMBO J. 1996; 15: 5752–5759.
5. Rouabhia M, Schaller M, Corbucci C, Vecchiarelli A, Prill SK-H, Giasson L, et al. Virulence of the fungal pathogen *Candida albicans* requires the five isoforms of protein mannosyltransferases. Infect Immun. 2005; 73: 4571–4580. doi: 10.1128/IAI.73.8.4571-4580.2005 PMID: 16040968
6. Cantero PD, Lengsfeld C, Prill SK-H, Subanovíc M, Román E, Pla J, et al. Transcriptional and physiological adaptation to defective protein-O-mannosylation in *Candida albicans*. Mol Microbiol. 2007: 64: 1115–1128. doi: 10.1111/j.1365-2958.2007.05723.x PMID: 17501932
7. Cantero PD, Ernst JF. Damage to the glycoshield activates *PMT*-directed *O*-mannosylation via the Msb2-Cek1 pathway in *Candida albicans*. Mol Microbiol. 2011; 80: 715–725. doi: 10.1111/j.1365-2958.2011.07604.x PMID: 21375589

8. van Wijlick L, Swidergall M, Brandt P, Ernst JF. *Candida albicans* responds to glycostructure damage by Ace2-mediated feedback regulation of Cek1 signaling. Mol Microbiol., in press. doi: 10.1111/mmi.13494 PMID: 27589033
9. Payne T, Hanfrey C, Bishop AL, Michael AJ, Avery SV, Archer DB. Transcript-specific translational regulation in the unfolded protein response of *Saccharomyces cerevisiae*. FEBS lett. 2008; 582: 503–509. doi: 10.1016/j.febslet.2008.01.009 PMID: 18206654
10. Doma MK, Parker R. Endonucleolytic cleavage of eukaryotic mRNAs with stalls in translation elongation. Nature. 2006; 440: 561–564. doi: 10.1038/nature04530 PMID: 16554824
11. Shoemaker CJ, Eyler DE, Green R. Dom34:Hbs1 promotes subunit dissociation and peptidyl-tRNA drop-off to initiate no-go decay. Science. 2010; 330: 369–372. doi: 10.1126/science.1192430 PMID: 20947765
12. Tsuboi T, Kuroha K, Kudo K, Makino S, Inoue E, Kashima I, et al. Dom34:hbs1 plays a general role in quality-control systems by dissociation of a stalled ribosome at the 3' end of aberrant mRNA. Mol Cell. 2012; 46: 518–259. doi: 10.1016/j.molcel.2012.03.013 PMID: 22503425
13. Guydosh NR, Green R. Dom34 rescues ribosomes in 3' untranslated regions. Cell. 2014; 156: 950–962. doi: 10.1016/j.cell.2014.02.006 PMID: 24581494
14. Bhattacharya A, McIntosh KB, Willis IM, Warner JR. Why Dom34 stimulates growth of cells with defects of 40S ribosomal subunit biosynthesis. Mol Cell Biol. 2010; 30: 5562–5571. doi: 10.1128/MCB.00618-10 PMID: 20876302
15. Carr-Schmid A, Pfund C, Craig EA, Goss Kinzy T. Novel G-protein complex whose requirement is linked to the translational status of the cell. Mol Cell Biol. 2002; 22: 2564–2574. doi: 10.1128/MCB.22.8.2564-2574.2002 PMID: 11909951
16. Davis L, Engebrecht J. Yeast *dom34* mutants are defective in multiple developmental pathways and exhibit decreased levels of polyribosomes. Genetics. 1998; 149: 45–56. PMID: 9584085
17. Graille M, Chaillet M, van Tilbeurgh H. Structure of yeast Dom34. A protein related to translation termination factor Erf1 and involved in no-decay. J Biol Chem. 2008; 283: 7145–7154. doi: 10.1074/jbc.M708224200 PMID: 18180287
18. Lee HH, Kim YS, Kim KH, Heo I, Kim SK, Kim O, et al. Structural and functional insights into Dom34, a key component of no-go mRNA decay. Mol Cell. 2007; 27: 938–950. doi: 10.1016/j.molcel.2007.07.019 PMID: 17889667
19. Passos DO, Doma MK, Shoemaker CJ, Muhlrad D, Green R, Weissman J, et al. Analysis of Dom34 and its function in no-go decay. Mol Cell. 2009; 20: 3025–3032. doi: 10.1091/mbc.E09-01-0028 PMID: 19420139
20. van den Elzen A.M., Schuller A., Green R., Séraphin B. Dom34-Hbs1 mediated dissociation of inactive 80S ribosomes promotes restart of translation after stress. EMBO J. 2014; 33, 265–276. doi: 10.1002/embj.201386123 PMID: 24424461
21. Cole SE, LaRiviere FJ, Merrikh CN, Moore MJ. A convergence of rRNA and mRNA quality control pathways revealed by mechanistic analysis of nonfunctional rRNA decay. Mol Cell. 2009; 34: 440–540. doi: 10.1016/j.molcel.2009.04.017 PMID: 19481524
22. van den Elzen AM, Henri J, Lazar N, Gas ME, Durand D, Lacroute F, et al. Dissection of Dom34-Hbs1 reveals independent functions in two RNA quality control pathways. Nat Struct Mol Biol. 2010; 17: 1446–1452. doi: 10.1038/nsmb.1963 PMID: 21102444
23. Finck M, Bergmann N, Jansson B, Ernst JF. Defective threonine-linked glycosylation of human insulin-like growth factor in mutants of the yeast *Saccharomyces cerevisiae*. Glycobiology. 1996; 6: 313–320. doi: 10.1093/glycob/6.3.313 PMID: 8724139
24. Lussier M, Gentzsch M, Sdicu AM, Bussey H, Tanner W. Protein *O*-glycosylation in yeast. The *PMT2* gene specifies a second protein *O*-mannosyltransferase that functions in addition to the *PMT1*-encoded activity. J Biol Chem. 1995; 270: 2770–2775. doi: 10.1074/jbc.270.6.2770 PMID: 7852348
25. González A, Jiménez A, Vázquez D, Davies JE, Schindler D. Studies on the mode of action of hygromycin B, an inhibitor of translocation in eukaryotes. Biochim Biophys Acta. 1978; 521: 459–469. PMID: 367435
26. Dean N. Yeast glycosylation mutants are sensitive to aminoglycosides. Proc Natl Acad Sci USA. 1995; 92: 1287–1291. doi: 10.1073/pnas.92.5.1287 PMID: 7877969
27. Lay J, Henry LK, Clifford J, Koltin Y, Bulawa CE, Becker JM. Altered expression of selectable marker *URA3* in gene-disrupted *Candida albicans* strains complicates interpretation of virulence studies. Infect Immun. 1998; 66: 5301–5306. PMID: 9784536
28. Girrbach V, Strahl S. Members of the evolutionary conserved *PMT* family of protein *O*-mannosyltransferases form distinct protein complexes among themselves. J Biol Chem. 2003; 278: 12554–12562. doi: 10.1074/jbc.M212582200 PMID: 12551906

29. Tuch BB, Mitrovich QM, Homann OR, Hernday AD, Monighetti CK, De La Vega FM, et al. The transcriptomes of two heritable cell types illuminate the circuit governing their differentiation. PLoS Genet. 2010; 6: e1001070. doi: 10.1371/journal.pgen.1001070 PMID: 20808890

30. Bruno VM, Wang Z, Marjani SL, Euskirchen GM, Martin J, Sherlock G, Snyder M. Comprehensive annotation of the transcriptome of the human fungal pathogen *Candida albicans* using RNA-seq. Genome Res. 2010; 20: 1451–1458. doi: 10.1101/gr.109553.110 PMID: 20810668

31. Lilliesfors HW. On the Kolmogorov-Smirnov test for normality with mean and variance unknown. J Am Stat Assoc. 1967; 62: 399–402.

32. Steuten B, Wagner R. A conformational switch is responsible for the reversal of the 6S RNA-dependent RNA polymerase inhibition in *Escherichia coli*. Biol Chem. 2012; 393: 1513–1522. doi: 10.1515/hsz-2012-0237 PMID: 23667906

33. Koonin EV, Bork P, Sander C. A novel RNA-binding motif in omnipotent suppressors of translation termination, ribosomal proteins and a ribosome modification enzyme? Nucleic Acids Res. 1994; 22: 2166–2167. doi: 10.1093/nar/22.11.2166 PMID: 7518079

34. Wolfe KH, Shields DC. Molecular evidence for an ancient duplication of the entire yeast genome. Nature. 1997; 387: 708–713. doi: 10.1038/42711 PMID: 9192896

35. Verma-Gaur J, Traven A. Post-transcriptional gene regulation in the biology and virulence of *Candida albicans*. Cell Microbiol. 2016; 18: 800–806. doi: 10.1111/cmi.12593 PMID: 26999710

36. Kadosh D. Control of *Candida albicans* morphology and pathogenicity by post-transcriptional mechanisms. Cell Mol Life Sci., in press. doi: 10.1007/s00018-016-2294-y PMID: 27312239

37. Sherman F, Fink G, Hicks J. Methods in Yeast Genetics. 1986. Cold Spring Harbor, NY; Cold Spring Harbor Laboratory Press.

38. Wach A, Brachat A, Pöhlmann R, Philippsen P. New heterologous modules for classical or PCR-based gene disruptions in *Saccharomyces cerevisiae*. Yeast. 1994; 10: 1793–1808. PMID: 7747518

39. Morschhäuser J, Michel S, Staib P. Sequential gene disruption in *Candida albicans* by FLP-mediated site-specific recombination. Mol Microbiol. 1999; 32: 547–556. PMID: 10320577

40. Timpel C., Strahl-Bolsinger S, Ziegelbauer K, Ernst JF. Multiple functions of Pmt1p-mediated protein *O*-mannosylation in the fungal pathogen *Candida albicans*. J Biol Chem. 1998; 273: 20837–20846. PMID: 9694829

41. Fonzi W, Irwin Y. Isogenic strain construction and gene mapping in *Candida albicans*. Genetics. 1993; 134: 717–728. PMID: 8349105

42. Setiadi ER, Doedt T, Cottier F, Noffz C, Ernst JF. Transcriptional response of *Candida albicans* to hypoxia: linkage of oxygen sensing and Efg1p-regulatory networks. J Mol Biol. 2006; 361: 399–411. doi: 10.1016/j.jmb.2006.06.040 PMID: 16854431

43. Köhler JR, Fink GR. *Candida albicans* strains heterozygous and homozygous for mutations in mitogen-activated protein kinase signaling components have defects in hyphal development. Proc Natl Acad Sci USA. 1996; 93: 13223–13228. PMID: 8917572

44. Brown JL, Kossaczka Z, Jiang B, Bussey H. A mutational analysis of killer toxin resistance in *Saccharomyces cerevisiae* identifies new genes involved in cell wall (1—>6)-beta-glucan synthesis. Genetics. 1993; 133: 837–849. PMID: 8462845

45. Nasmyth KA, Tatchell K. The structure of transposable yeast mating type loci. Cell. 1980; 19: 753–764. doi: 10.1016/S0092-8674(80)80051-1 PMID: 6244896

46. Strahl-Bolsinger S, Immervoll T, Deutzmann R, Tanner W. *PMT1*, the gene for a key enzyme of protein *O*-glycosylation in *Saccharomyces cerevisiae*. Proc Natl Acad Sci USA. 1993; 90: 8164–8168. doi: 10.1073/pnas.90.17.8164 PMID: 8367478

47. Foreman PK, Davis RW. Cloning vectors for the synthesis of epitope-tagged, truncated and chimeric proteins in *Saccharomyces cerevisiae*. Gene. 1994; 144: 63–68. doi: 10.1016/0378-1119(94)90204-6 PMID: 7517907

48. Umeyama T, Nagai Y, Niimi M, Uehara Y. Construction of FLAG tagging vectors for *Candida albicans*. Yeast. 2002; 19: 611–618. doi: 10.1002/yea.863 PMID: 11967831

49. Sonneborn A, Tebarth B, Ernst JF. Control of white-opaque phenotypic switching in *Candida albicans* by the Efg1p morphogenetic regulator. Infect Immun. 1999; 67: 4655–4660. PMID: 10456912

50. Kapitan M, Eichhof I, Lagadec Q, Ernst JF. Click beetle luciferases as dual reporters of gene expression in *Candida albicans*. Microbiology. 2016; 162: 1310–1320. doi: 10.1099/mic.0.000329 PMID: 27339610

51. Gildehaus N, Neusser T, Wurm R, Wagner R. Studies on the function of the riboregulator 6S RNA from *E. coli*: RNA polymerase binding, inhibition of *in vitro* transcription and synthesis of RNA-directed de novo transcripts. Nucleic Acids Res. 2007; 35: 1885–1896. doi: 10.1093/nar/gkm085 PMID: 17332013

52. Göringer HU, Bertram S, Wagner R. The effect of tRNA binding on the structure of 5 S RNA in *Escherichia coli*. A chemical modification study. J Biol Chem. 1984; 259: 491–496. PMID: 6200475

53. Garre E, Romero-Santacreu L, De Clercq N, Blasco-Angulo N, Sunnerhagen P, Alepuz P. Yeast mRNA cap-binding protein Cbc1/Sto1 is necessary for the rapid reprogramming of translation after hyperosmotic shock. Mol Biol Cell. 2012; 23: 137–150. doi: 10.1091/mbc.E11-05-0419 PMID: 22072789

S1 Table. Strains.

	Genotype or description	Source
C. albicans strains		
CAI4	*ura3Δ::imm434/ura3Δ::imm434*	[41]
CAF2-1	*ura3Δ::imm434/URA3*	[41]
RM1000	*ura3::imm434/ura3::imm434 iro1/iro1::imm434 his1::hisG/his1::hisG*	[54]
SK47	as CAI4 but *dom34Δ::FRT/dom34Δ::FRT*	this work
JH47-1 /-2	as CAI4 but *dom34Δ ::FRT/dom34Δ ::FRT ura3Δ ::imm434/URA3*	this work
SK24	as CAI4 but *pmt1Δ::hisG/pmt1Δ::hisG dom34Δ::FRT/dom34Δ::FRT*	this work
JH24-4	*pmt1Δ::hisG/pmt1Δ::hisG dom34Δ::FRT/ dom34Δ::FRT ura3Δ ::imm434/URA3*	this work
JH5-3-1	as SK47 but *pmt5Δ-hisG-URA3-hisG/pmt5Δ-hisG*	this work
P15-274	as SK47 but *pmt1Δ::hisG/pmt1Δ::hisG pmt5Δ-URA3/pmt5Δ-hisG*	this work
P15-274-1	as SK47 but *pmt1Δ::hisG/pmt1Δ::hisG pmt5Δ-hisG/pmt5Δ-hisG*	this work
CIS23	as CAI4 but *PMT1/PMT1^{HA}-SAT1*	this work
CAP1-3121	as CAI4, but *pmt1Δ::hisG /pmt1Δ::hisG*	[40]
SPCa2	as CAI4, but *pmt1Δ::hisG /pmt1Δ::hisG ura3Δ::imm434/URA3*	[3]
SPCa10	as CAI4, but *pmt5Δ::hisG/pmt5Δ::hisG ura3Δ::imm434/URA3*	[3]
CPP1121	as CAI4, but *pmt1Δ::hisG/pmt1Δ::hisG pmt6Δ-hisG/pmt6Δ-hisG*	[3]
SPCa8	as CAI4, but *pmt6Δ::hisG/pmt6Δ::hisG ura3Δ::imm434/URA3*	[3]
SPCa4	as CAI4, but *PMT2/pmt2Δ::hisG ura3Δ::imm434/URA3*	[3]
SPCa6	as CAI4, but *pmt4Δ::hisG/pmt4Δ::hisG ura3Δ::imm434/URA3*	[3]
JH-Ca1-1 /-2	as CAI4, but *DOM34/DOM34^{fIA}-URA3*	this work
S. cerevisiae strains		
YE449	*MATα leu2 ura3-52 prb1-112 pep4-3 cir^{0}*	[23]
YE449 *pmt1*	as YE449, but *pmt1::URA3*	this work
YE449 *pmt2*	as YE449, but *pmt2::LEU2*	this work
YE449 *pmt1 pmt2*	as YE449, but *pmt1::URA3 pmt2::LEU2*	this work

YE449 *dom34*	as YE449, but *dom34Δ::kanMX4*	this work
W21, W32	as YE449, but *pmt1Δ::URA3 dom34Δ::kanMX4*	this work
W12, W14	as YE449, but *pmt1Δ::URA3 yil001wΔ::kanMX4*	this work
M577	as YE449, but mutant isolate after EMS mutagenesis	[23]
M577 *pmt1*	as M577, but *pmt1::URA3*	this work
M577 *pmt2*	as M577, but *pmt2::LEU2*	this work
M577 *pmt1 pmt2*	as M577, but *pmt1::URA3 pmt2::LEU2*	this work
RC130	*MATa/MATα his1/his1* [*KIL-K1*] (K^+ R^+)	R. Chan, unpublished

S2 Table. Oligonucleotides.

name	sequence (5′-3′)
***S. cerevisiae* genes**	
ScDOM34 disrupt for	ATGAAGGTTATTAGTCTGAAAAAGGATTCTTTTAACAAAGCAGCT GAAGCTTCGTACGC
ScDOM34 disrupt rev	CTACTCCTCACCATCGTCTTCATCAAGATCGGGGAGCGGGGCATA GGCCACTAGTGGATCTG
ScYIL001w disrupt for	ATGGCAGATAAATTAATGGACAAAAATTTTGAAGAACTGTCAGCT GAAGCTTCGTACGC
ScYIL001w disrupt rev	TTATACATCAAGTTCCAGATCAGCTAGGATATTATCTAACGCATAG GCCACTAGTGGATCTG
ScDOM34N	TTTGAATTCTTATGAAGGTTATTAGTCTG
ScDOM34C	TTTCTGCAGGCTACTCCTCACCATCGTC
ScYIL001wN	TTTGAATTCTTATGGCAGATAAATTAATGG
ScYIL001wC	TTTCTGCAGGTTATACATCAAGTTCCAG
YEp13-Bamflank-A	ACTATCGACTACGCG
YEp13-Bamflank-B	CCGGATCCAGCAACCGCACCTGTG
***C. albicans* genes**	
FDP34	ATTCCGCGGTCCCAGAACCAATCAAGATTAATTACG
RPD34	ATTGCGGCCGCGTGGTGATGCTATAAGAATCTTTTCTG
FDD34	ATTCTCGAGGGAACTACATTATTTTTTATACGAGTT
RDD34	ATTGGGCCCTTCATTATGTTTTGCAGCAATTATGAT
Dom34-NdeI-FW	GGAATTCCATATGGCTGGCACAGTTCCTGGCCA
Dom34-XhoI-RV-Stopp	CGCTGAGGTCTTCTTCATCACTGTC
Dom34-Leu(mut)for	CTAAATTTTTGGAGGAGTCGGAGGCATTACAGCGC
Dom34-Leu(mut)rev	GCGCTGTAATGCCTCCGACTCCTCCAAAAATTTAG
Dom34Mut21fw	GCAATAACCTTGGTACCCGCTGATTCCGAGGATTTATGG
Dom34Mut21rev	CCATAAATCCTCGGAATCAGCGGGTACCAAGGTTATTGC
Dom34Mut317fw	AAAGGCATTAGCTATGGATGCAG
Dom34Mut317rev	CTGCATCCATAGCTAATGCCTTT
p1-DOM-FLAG	TTACTGCAGATGCAAGTTAAAAACAAAGC
p2-DOM-FLAG	TTAGCATGCCAAGTCTTCTTCATCACTG
Dom34-HA-for	GAATCTGGTGAACAATTGAATCAGTTGACGGGTATTGC TGCTTTATTGAAATATCCGATACCAGATCTTGATGACAGTGATGAA GAAGACGGTGGTGGTCGGATCCCCGGGTTAATT AA
Dom34-HA-rev	GGTTTAATACAGGACTATTTAATTCACGCCAGAAAGGG TAGAGTCTGGTATTTAGATAGGTATACACAACAAAAAC TCGTATAAAAAATAATACTCTAGAAGGACCACCTTTGA TTG
CaPmt1del-for	GAAAAGCAACAACAAGAACAACAACAAGAACAAGAACAGGTTGA AGATGAATCAGTGCATCAAGTTCAACAAGGTGGTGGTCGGATCCC CGGGTTAATTAA

CaPmt1del-rev	CAAATATGTAAAATGTGATGTGTAATATATGTTCATATTTCTCTTTC TGCAAAAGATAATTTCTTCTACTAAGTCTAGAAGGACCACCTTTGA TTG
Pmt1 5´UTR for	CAAGATTCTTTTTCAAGATTTTTC
Pmt1 5´UTR rev BglII long	AAAAAGATCTATTGAATGGGAAACTAAAATAAAAATAA
CBG-Stu for	CCTACAAGATCTATGGTTAAGAGAGAAAAAAACG
CBG-Bam rev	GGATCCTTAACCACCAGCTTTTTC
ACT1(RT)-rev	TGGACAAATGGTTGGTCAAG
ACT1(RT)-for	TTGGATTCTGGTGATGGTGT
PMT1-RT-for	GCTGCTGAACCTGTTGAAGA
PMT1-RT-rev	CATCAGCAACTTGTGGGTCT
PMT2-for-RTa	CCATGATGGCTACTAACAATG
PMT2-rev-RTa	CCCATCCACACATTCTAATACC
PMT4-RT-for	TTGGAAACATCATTGGGTTC
PMT4-RT-rev	TTGATCTTGCTCTGTCGCTT
PMT5-RT-for	CCCTTATGCATCTCCTCCAT
PMT5-RT-rev	CACCAAATATGGCCAGGAAT
PMT6-RT-for	ATTTGTTGGTTGTTGGCATC
PMT6-RT-rev	TGATTGACTGTTTGCTGGGT
DOM34-RT-for	GTTGAATGATGACGACGGAA
DOM34-RT-rev	CGTCGCTTCTAAACAAAGCA
PMT1 5'-UTR RNA	ACAACAACAACAACAACCACCACAACCACAACUAUAAACAAU

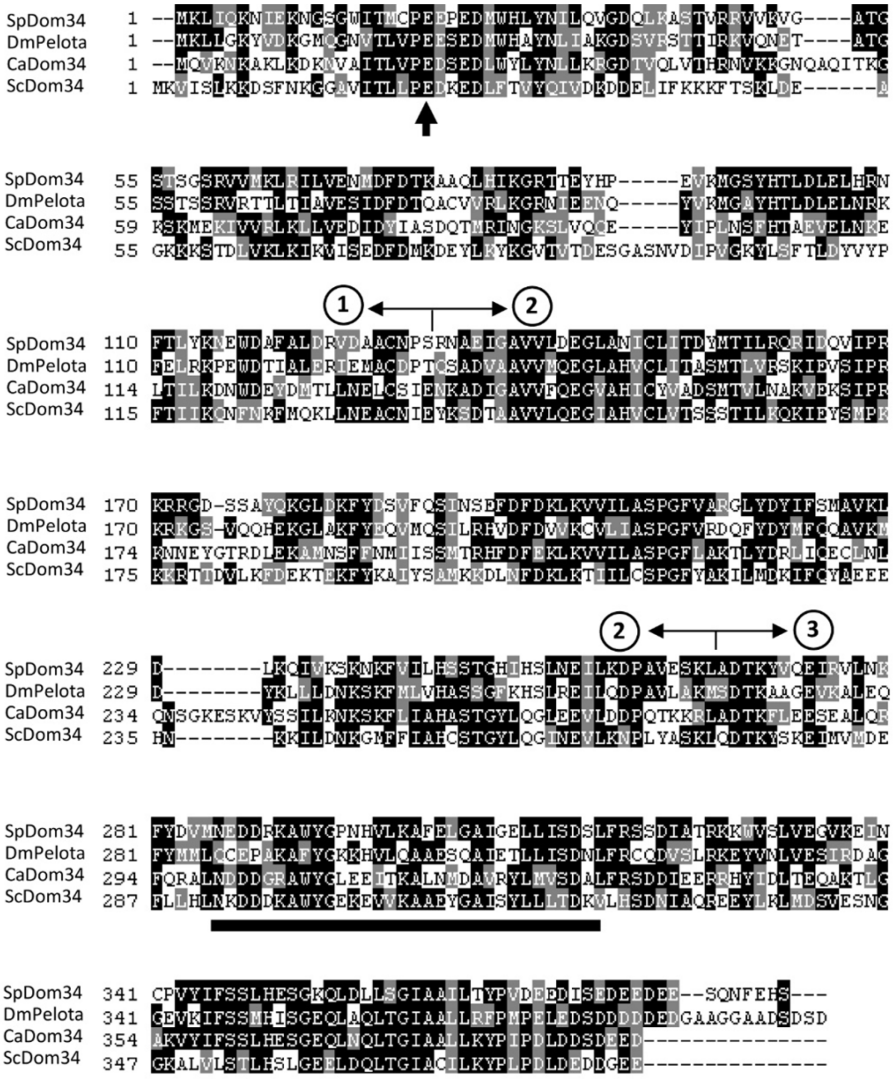

S1 Fig. Structure of Dom34 proteins. Dom34/Pelota sequences of *S. cerevisiae* (ScDom34), *C. albicans* (CaDom34), *D. melanogaster* (DmPelota) and *S. pombe* (SpDom34) are aligned. The positions of domains 1-3 is indicated by the arrows and the circled numbers. The region suggested as a RNA binding sequence in domain 3 isunderlined. The conserved glutamate in domain 1, presumed to act in RNase activity is indicated by the thick arrow.

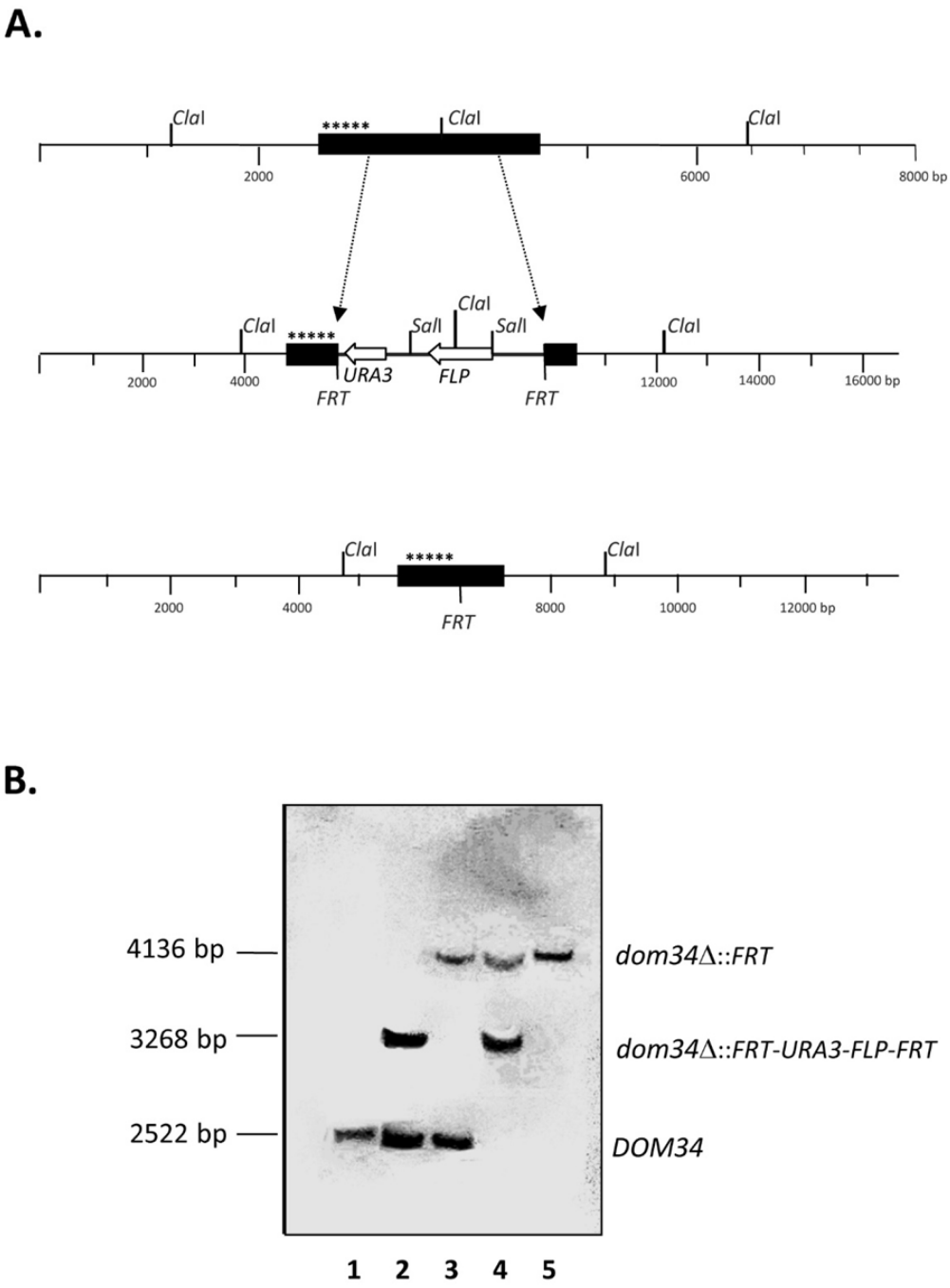

S2 Fig. Disruption of *DOM34* locus. (A) Scheme of wild-type *DOM34* locus, after disruption by the *FRT-URA3—FLP-FRT* cassette and after removal of the *URA3-FLP* sequences (top-to-bottom). **(B)** Southern blotting of genomic DNA in transformants. Total DNA was digested with *Cla*I and *Sal*I and blots were probed using a *DOM34* segment indicated by asterisks in (A). The fragment for the wild-type alleles is visible in lane 1, while the subsequent lanes demonstrate the course of disruption in derivative strains and the complete disruption of the two *DOM34* alleles in strain SK47 (lane 5).

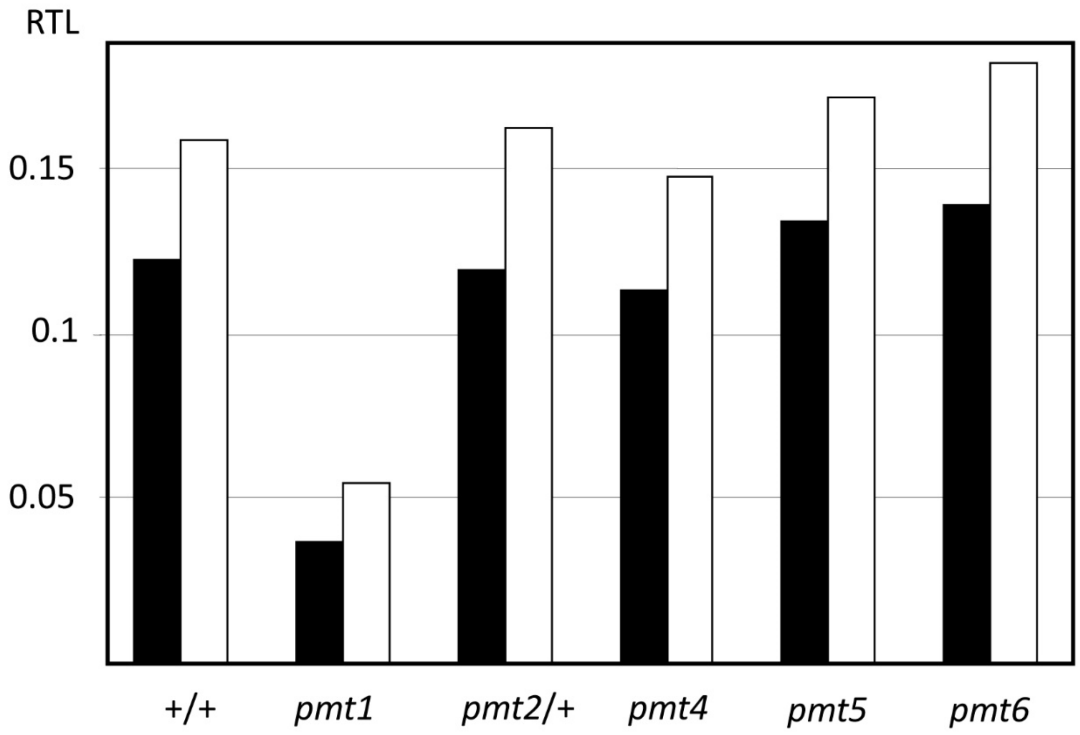

S3 Fig. *DOM34* transcript levels in *pmt* strains. Total RNA of strains CAF2-1 (+/+), SPCa2 (*pmt1*/*pmt1*), SPCa4 (*pmt2*/*PMT2*), SPCa6 (*pmt4*/*pmt4*), SPCa10 (*pmt5*/*pmt5*) and SPCa8 (*pmt6*/*pmt6*) was isolated and the relative *DOM34* transcript level (RTL) was determined by qPCR using the *ACT1* transcript as the reference. Values obtained for two biological replicates are shown as black and white bars.

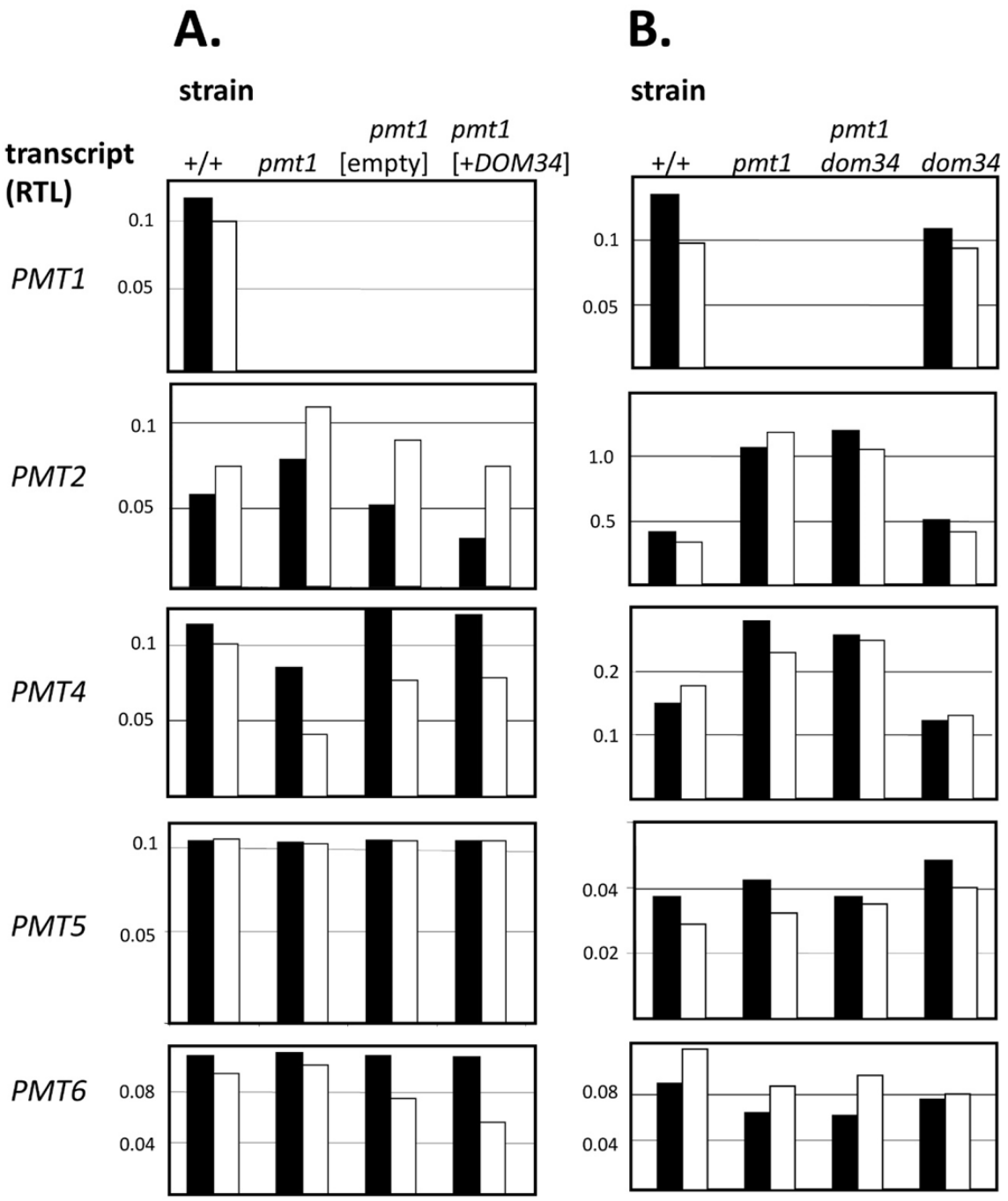

S4 Fig. Influence of *DOM34* expression on *PMT* transcript levels. (A) Influence of *DOM34* overexpression was tested using strains CAF2-1 (+/+), SPCa2 (*pmt1*/*pmt1*), CAP1-3121[pSP38] (*pmt1*/*pmt1*[empty vector] and strain CAP1-3121[pSK2] (*pmt1*/*pmt1*[*DOM34*]). **(B)** Influence of *dom34* mutation was tested using strains CAF2-1 (+/+), SPCa2 (*pmt1*/*pmt1*), JH24-4 (*pmt1*/*pmt1 dom34*/*dom34*) and JH47-1 (*dom34*/*dom34*). Total RNA of all strains was isolated and relative transcript levels of the indicated *PMT* genes were determined by qPCR using the *ACT1* transcript as the reference. Values obtained for two independent biological replicates are shown as black and white bars.

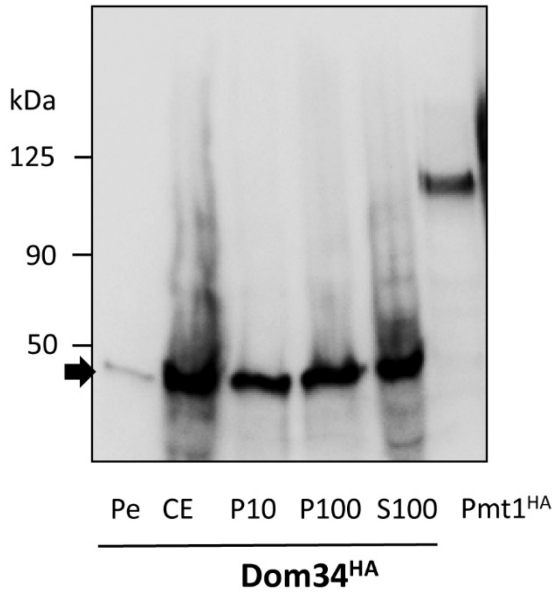

S5 Fig. Immunoblot of HA-tagged Dom34. Cells of strains JHCa1-1 (*Dom34/DOM34*^{HA}) were fractionated by differential centrifugation. The periplasmic space (PE), crude extract (CE), pellet after centrifugation at 10,000 *x g* (P10; ER fraction), pellet after centrifugation of P10 supernatant at 100,000 *x g* (P100; Golgi fraction) and the corresponding supernatant (S100; cytoplasmic fraction) were obtained. Aliquots of each fraction were examined by SDS-PAGE (10 % acrylamide) followed by immunoblotting using rat anti-HA antibody. The arrow indicates the migration of HA-tagged Dom34. As a control, an immunoblot of a crude extract of strain CIS23 (*PMT1/PMT1*^{HA}), producing HA-tagged Pmt1, is shown.

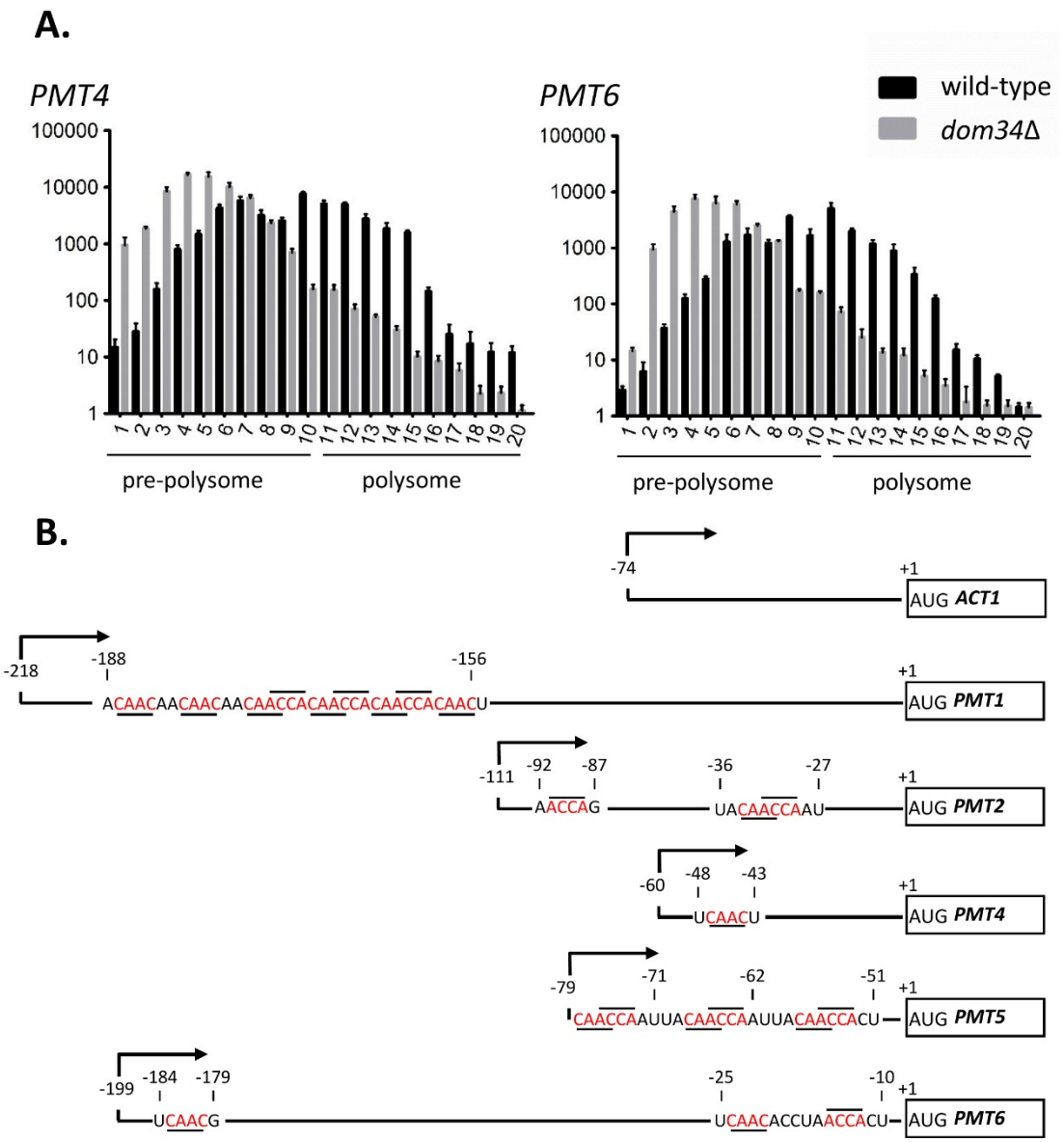

S6 Fig. Occurrence of *PMT4* and *PMT6* transcripts in polysome-gradient fractions. (A) The indicated transcripts were detected by qPCR after adding a known amount of an *in vitro* generated transcript of CaCBGluc as calibrator. Each bar represents the normalized mean *PMT4* or *PMT6* transcript level of two independent experiments including the standard error of the mean. **(B)** Incidence of "CAAC" and "ACCA" motifs in 5'-UTRs of *ACT1* and *PMT*-genes. The 5'-UTR sequences of *ACT1* (reference gene) and all *C. albicans PMT*-genes were analyzed for occurrence of the identified "CAAC" and "ACCA" motif (Fig. 3B). Information about transcript start sites were taken from Tuch *et al*. [29] and Bruno *et al*. [30]; the transcript with the longer 5'-UTR was chosen and respective sequences were obtained from CGD (http://www.candidagenome.org) assembly 21. Occurrence of the "CAAC" (underlined) and "ACCA" (line on top) motifs are highlighted in red at the indicated positions. The "CAAC" motif was identified in 5'-UTRs of all *PMT*-genes, but not in the 5'-UTR sequence of the reference gene *ACT1*.

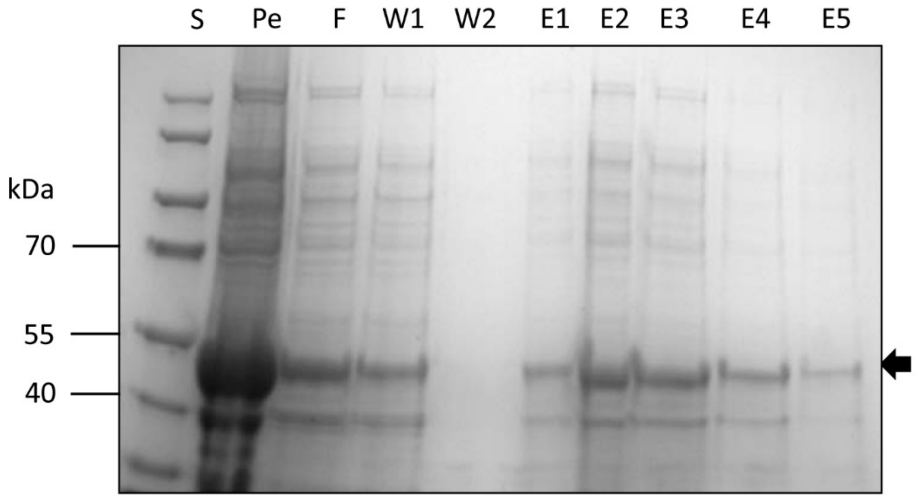

S7 Fig. Purification of Dom34-His$_6$. *E. coli* Rosetta transformants carrying pET22b-Dom34+ were induced by IPTG and cell pellets were disrupted by ultrasonication. Soluble proteins in the cell extract were separated by affinity chromatography on Ni-NTA agarose, which was washed in buffer using 5 mM imidazole and eluted using 50 and 250 mM imidazole. Aliquots of fractions were separated by SDS-PAGE (4-20 % acrylamide) and gels were stained using Coomassie Brilliant Blue R-250. Lanes show protein standards (S), cell pellet (Pe), flow-through (F), wash fractions (W1,2) and elution fractions (E1-5). The arrow marks the position of Dom34-His$_6$.

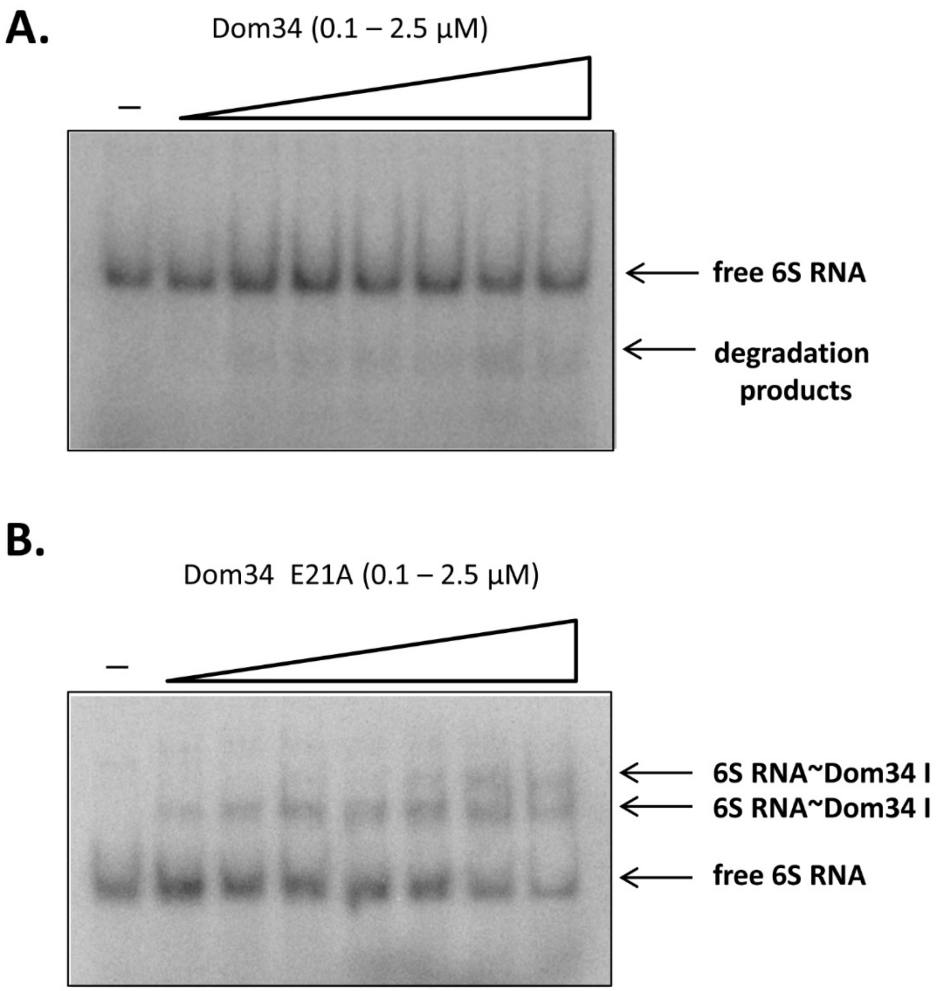

S8 Fig. Weak binding of native Dom34 (A) or the Dom34 E21A variant (B) to 6S RNA from *E. coli*. Radioactive 3‘ end-labeled 6S RNA was incubated with increasing amounts of Dom34; after complex formation samples were analysed by 6% native PAGE. As indicated Dom34 was present in final concentrations of 0.1/0.15/0.25/0.3/0.6/1 and 2.5 µM.

A.

1 20 40 60

*GG*CAAGAUUCUUUUUCAAGAUUUUUCAUUUUUACAACAACAACAACAACCACCACAACCACA

80 100 120

ACUAUAAACAAUUGAUAUAGCAUUAUCUUUUAAGAUUAUUGAAUAAAGGUCAAUUUAUAGCG

140 160 180

CCCCCCCUCACUCCACCUCCUACCGUCUUUCUUUCACGCAACUAAAACAAAUUUUUAUAUUU

200 218

UUAUUUUUAUUUUUAUUUUAGUUUCCCAUUCAAU*AGAUC*–3´

B.

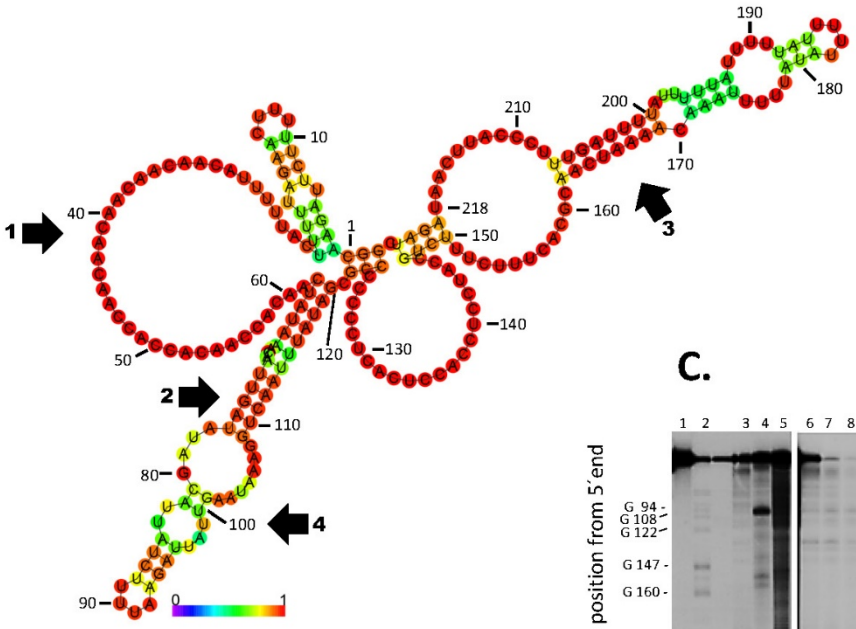

C.

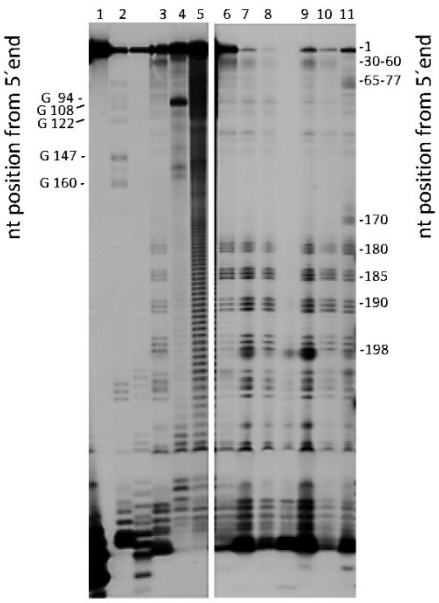

S9 Fig. Sequence and structure of the *PMT1* 5´-UTR. (A) UTR RNA sequence generated by *in vitro* transcription of plasmid pRG01 (linearized by *Bgl*II) using T7 RNA polymerase. Two G residues are added to 218 nt UTR sequence at its 5´-end by T7 RNA polymerase, while AGATC at the 3´-end reflects the *Bgl*II sequence. The transcript start site at -218 was determined by Tuch *et al.* [29], while an additional start site at -190 was reported by Bruno *et al.* [30] (underlined U insequence). The CA-enriched region (Dom34 binding site) is marked in red font. **(B)** Predicted folding structure of *PMT1* UTR. The RNAfold program (http://rna.tbi.univie.ac.at/cgi-bin/RNAfold.cgi) was used for prediction and results were depicted as a centroid structure drawing encoding base-pair probabilities (colour code showing probabilities of base-pairing or single strandedness in predicted paired and unpaired regions, respectively). Numbered black arrows indicated predicted events upon Dom34 binding: (1) Binding of Dom34 to single-stranded region containing CA-repeats, (2) opening of paired region by binding of Dom34, (3) opening of paired region and cleavage by Dom34 , (4) cleavage by Dom34. **(C)** RNase cleavage experiments supporting the predicted actions of Dom34. 3´-[^{32}P] end-labelled UTR RNA (50 cps) was incubated with RNases in the absence or presence of Dom34 for 1 min at 37 °C; Dom34 was preincubated 10 min with the UTR before RNase addition. Products were separated by 12 % denaturing PAGE. Nucleotide positions are numbered from the UTR 5´-end as in B. UTR, no RNase (lane 1); UTR with 1 U RNase T1 cleaving at G residues indicated in the left margin (lane 2); UTR with 0.5 U RNase U2 specific for RNA single strands (lane 3); UTR with 1 µM Dom34 (lane 4); UTR sequence ladder generated by partial hydrolysis with NaOH (lane 5); UTR with 0.25/0.5/1 U RNase U2 (lanes 6-8); UTR incubated with 0.5 U RNase U2 and 0.5/1/2.5 µM Dom34 (lanes 9-11). Note a prominent Dom34-mediated cleavage of the UTR around position 100. RNase U2 cleavage in position 30-60 (CA-repeat region) confirms the predicted single-strandedness of the UTR in this position (lanes 7-9); Dom34 protects this region (lanes 10, 11), confirming its predicted binding at this site. Region 180-190 appears permanently single-stranded, while the predicted double-stranded regions 65-77 and around 170 become single-stranded upon Dom34 binding (lanes 9-11).

2.5 Manuskript IV: Signaling domains of mucin Msb2 in *Candida albicans*

Marc Swidergall, **Lasse van Wijlick**, Joachim F. Ernst

Zweitautor

Beitrag zum Manuskript: 15 %

Lasse van Wijlick hat einen Teil der Experimente durchgeführt und interpretiert. Er hat die entsprechenden Hypothesen für das Manuskript formuliert und die entsprechenden Abbildungen (Fig.5 und Fig.9) erstellt.

Veröffentlicht in: Eukaryotic Cell, January 2015; EC.00264-14.

Impact Factor: 3.179 (2013)

EC Journals.ASM.org

Signaling Domains of Mucin Msb2 in *Candida albicans*

Marc Swidergall,[a] Lasse van Wijlick,[a,b] Joachim F. Ernst[a,b]

Department Biologie, Molekulare Mykologie, Heinrich-Heine-Universität Düsseldorf, Düsseldorf, Germany[a]; Manchot Graduate School, Molecules of Infection II, Heinrich-Heine-Universität Düsseldorf, Düsseldorf, Germany[b]

Candida albicans **adapts to the human host by environmental sensing using the Msb2 signal mucin, which regulates fungal morphogenesis and resistance characteristics. Msb2 is anchored within the cytoplasmic membrane by a single transmembrane (TM) region dividing it into a large N-terminal exodomain, which is shed, and a small cytoplasmic domain. Analyses of strains carrying deleted Msb2 variants revealed an exodomain segment required for cleavage, shedding, and all functions of Msb2. Phosphorylation of the mitogen-activated protein kinase (MAP kinase) Cek1 was regulated by three distinct regions in Msb2: in unstressed cells, N-terminal sequences repressed phosphorylation, while its induction under cell wall stress required the cytoplasmic tail (C-tail) and sequences N-terminally flanking the TM region, downstream of the proposed cleavage site. Within the latter Msb2 region, overlapping but not identical sequences were also required for hyphal morphogenesis, basal resistance to antifungals, and, in unstressed cells, downregulation of the *PMT1* transcript, encoding protein *O*-mannosyltransferase-1. Deletion of two-thirds of the exodomain generated a truncated Msb2 variant with a striking ability to induce hyperfilamentous growth, which depended on the presence of the Msb2-interacting protein Sho1, the MAP kinase Cek1, and the Efg1 transcription factor. Under cell wall stress, the cytoplasmic tail relocalized partially to the nucleus and contributed to regulation of 117 genes, as revealed by transcriptomic analyses. Genes regulated by the C-tail contained binding sites for the Ace2 and Azf1 transcription factors and included the *ALS* cell wall genes. We concluded that Msb2 fulfills its numerous functions by employing functional domains that are distributed over its entire length.**

Upon proliferation and dissemination in a host tissue or target cell, pathogens encounter different types of host cells, extracellular matrices, and molecules that participate in pathogen defense. Upon contact with fungal pathogens, the human host utilizes an efficient and complex immune response that acts in multiple layers, including pathogen recognition and production of soluble innate effectors (1). To survive and overcome host immunity, pathogenic fungi have evolved sophisticated strategies which include two major steps: immune evasion and tissue invasion (2). Polysaccharides and glycoproteins in the fungal cell wall are the first contact points between the fungus and human immune cells, representing pathogen-associated molecular patterns (PAMPs). PAMPs are detected by human pattern recognition receptors (PRRs) and respond to a variety of innate immune components (3), including antimicrobial peptides (AMPs), which constitute major weapons of innate immunity that can directly kill fungal pathogens (4, 5). In response to the host, modification of PAMPs by cell wall remodeling or by hypha formation alters their availability for PRRs in many fungal species (6). The cellular morphology of the important human fungal pathogen *Candida albicans* is determined by host contact, which regulates morphogenetic signaling pathways depending on the type and intensity of environmental cues in body niches (7).

Fungal signaling mucins are large, transmembrane glycoproteins that undergo posttranslational modifications, such as glycosylation and proteolytic processing, which are crucial for their cellular functions (8–13). The *C. albicans* mucin Msb2 triggers responses and rescue pathways required for hyphal morphogenesis and growth in the presence of antifungal compounds (8, 14). Msb2 is cleaved to release and shed its large glycosylated exodomain, which is able to bind AMPs with a high affinity and thereby to protect fungal cells (15). The yeast-to-hypha transition is regulated by several signal transduction cascades containing protein kinase A (PKA), mitogen-activated protein kinases (MAP kinases), and pH-responsive modules (16). Msb2 triggers hyphal morphogenesis via the Cek1 MAP kinase module. Defects in cell wall glycostructures affecting protein glycosylation and β1,3-glucan levels are sensed by Msb2 and transmitted to the Cek1 MAP kinase cascade regulating target genes, e.g., *PMT* genes, encoding protein-*O*-mannosyltransferases (14, 17). Intact *N*-glycosylation is detected by Msb2 and represses *PMT1* transcription, while defective *N*-glycosylation induces Cek1 phosphorylation and derepresses *PMT1* transcription. The responses to defective *O*-glycosylation also require Msb2 to upregulate *PMT2* and *PMT4* expression (17). Recently, the transcription factor Ace2 was implicated in the regulation of *PMT* genes (17).

The structure of signaling mucins consists of a large, highly glycosylated, rod-shaped extracellular domain that is connected to a small, cytosolic carboxy-terminal domain via a transmembrane (TM) region (9). Previous results indicated that the cytoplasmic tail (C-tail) of Msb2 in *C. albicans* is needed to activate Cek1 in response to cell wall defects (8). In the present work, a systematic deletion analysis of Msb2 identified a mosaic of functional regions in the Msb2 structure, which contribute to various

Received 27 November 2014 **Accepted** 23 January 2015

Accepted manuscript posted online 30 January 2015

Citation Swidergall M, van Wijlick L, Ernst JF. 2015. Signaling domains of mucin Msb2 in *Candida albicans*. Eukaryot Cell 14:359–370. doi:10.1128/EC.00264-14.

Address correspondence to Joachim F. Ernst, Joachim.ernst@uni-duesseldorf.de.

Supplemental material for this article may be found at http://dx.doi.org/10.1128/EC.00264-14.

doi:10.1128/EC.00264-14

TABLE 1 *C. albicans* strains used for this study

Strain	Genotype	Reference
AS1	CAI4, but *tpk2*Δ::*hisG*/*tpk2*Δ::*hisG*	41
CAF2-1	*ura3*Δ::*imm434*/*URA3*	42
CAI4	*ura3*::*imm434*/*ura3*::*imm434*	43
CK43B-16L	*ura3*/*ura3 cek1*Δ::*hisG*/*cek1*Δ::*hisG*	44
CKY157	*ura3*/*ura3 czf1*::*hisG*/*czf1*::*hisG*	45
HLC67	CAI4, but *efg1*::*hisG*/*efg1*::*hisG*	46
JKC18	CAI4, but *cph1*::*hisG*/*cph1*::*hisG*	47
IIHH6-4a	CAI4, but *tpk1*Δ::*hisG*/*tpk1*Δ::*hisG*	48
FCCa27	CAI4, but *msb2*Δ*1*::*hisG*/*msb2*Δ*1*::*hisG-URA3-hisG*	8
FCCa28	CAI4, but *msb2*Δ::*hisG*/*msb2*Δ::*hisG*	8
ESCa3	CAI4, but *msb2*Δ*1*::*hisG*/*msb2*Δ*1*::*hisG LEU2*/*LEU2*::pES11a(*ACT1p-MSB2*$^{HA\text{-}V5}$)	8
ESCa25	CAI4, but *msb2*Δ*1*::*hisG*/*msb2*Δ*1*::*hisG LEU2*/*LEU2*::pES14(*ACT1p-MSB2-*Δ*N*$^{HA\text{-}V5}$)	8
ESCa38	FCCa28, but *LEU2*/*LEU2*::pES16(*ACT1p-MSB2-*Δ*C*^{HA})	8
ESCa39	FCCa28, but *LEU2*/*LEU2*::pES17(*ACT1p-MSB2-*Δ*TM-C*^{HA})	8
REP22	*ura3*Δ::*imm434*/*ura3*Δ::*imm434 his1*Δ::*hisG*/*his1*Δ::*hisG-msb2*Δ::*FRT*/*msb2*Δ::*FRT sho1*::*hisG*/*sho1*::*hisG*	14
LvW1000	CAI4, but *LEU2*/*LEU2*::pDS1044-1 (empty vector)	This study
MSCa1	FCCa28, but *LEU2*/*LEU2*::pSM4(*ACT1p-MSB2*$^{\Delta 1293\text{–}1307}$)	This study
MSCa3	FCCa28, but *LEU2*/*LEU2*::pSM4(*ACT1p-MSB2*$^{\Delta 1278\text{–}1292}$)	This study
MSCa8	FCCa28, but *LEU2*/*LEU2*::pSM6(*ACT1p-MSB2*ΔN$^{514\text{–}680}$)	This study
MSCa29	FCCa28, but *LEU2*/*LEU2*::pSM7(*ACT1p-MSB2*ΔN$^{582\text{–}780}$)	This study
MSCa30	FCCa28, but *LEU2*/*LEU2*::pSM9(*ACT1p-MSB2*$^{\Delta 788\text{–}853}$)	This study
MSCa31	FCCa28, but *LEU2*/*LEU2*::pSM10(*ACT1p-MSB2*$^{\Delta 855\text{–}939}$)	This study
MSCa34	FCCa28, but *LEU2*/*LEU2*::pSM11(*ACT1p-MSB2*$^{\Delta 920\text{–}1087}$)	This study
MSCa35	FCCa28, but *LEU2*/*LEU2*::pSM12(*ACT1p-MSB2*$^{\Delta 1085\text{–}1282}$)	This study
MSCa37	FCCa28, but *LEU2*/*LEU2*::pSM14(*ACT1p-MSB2*ΔN$^{514\text{–}1087}$)	This study
MSCa38	CAI4, but *LEU2*/*LEU2*::pSM14(*ACT1p-MSB2 MSB2*ΔN$^{514\text{–}1087}$)	This study
MSCa39	CK43B-16L, but *LEU2*/*LEU2*::pSM14(*ACT1p-MSB2*ΔN$^{514\text{–}1087}$)	This study
MSCa40	CKY157, but *LEU2*/*LEU2*::pSM14(*ACT1p-MSB2*ΔN$^{514\text{–}1087}$)	This study
MSCa41	HLC67, but *LEU2*/*LEU2*::pSM14(*ACT1p-MSB2*ΔN$^{514\text{–}1087}$)	This study
MSCa42	JKC18, but *LEU2*/*LEU2*::pSM14(*ACT1p-MSB2*ΔN$^{514\text{–}1087}$)	This study
MSCa43	IIHH6-4a, but *LEU2*/*LEU2*::pSM14(*ACT1p-MSB2*ΔN$^{514\text{–}1087}$)	This study
MSCa44	AS1, but *LEU2*/*LEU2*::pSM14(*ACT1p-MSB2*ΔN$^{514\text{–}1087}$)	This study
MSCa45	FCCa28, but *LEU2*/*LEU2*::pSM15(*ACT1p-MSB2*ΔN-C$^{514\text{–}1087}$)	This study
MSCa46	FCCa28, but *LEU2*/*LEU2*::pSM16(*ACT1p-MSB2*ΔN-TMC$^{514\text{–}1087}$)	This study
MSCa47	REP22, but *LEU2*/*LEU2*::pSM14(*ACT1p- MSB2*ΔN$^{514\text{–}1087}$)	This study
MSCa48	FCCa28, but *LEU2*/*LEU2*::pSM17(*ACT1p-MSB2 MSB2*Δ$^{514\text{–}1087}$)	This study

cellular processes, including hypha formation, activation of the MAP kinase Cek1, basal antifungal resistance, and regulation of the transcriptome, including regulation of *PMT1*. Thus, the combined Msb2 activities help to protect *C. albicans* from immune reactions and treatment with antifungal compounds.

MATERIALS AND METHODS

Strains and media. *C. albicans* strains used for this study are listed in Table 1. *MSB2* expression vectors digested with EcoRV were integrated ectopically into the *LEU2* locus of strain FCCa28, which places *MSB2* alleles under transcriptional control of the *ACT1* promoter (8). Strains were grown on/in complex yeast extract-peptone-dextrose (YPD) or minimal supplemented SD medium (8). Standard drop dilution tests (10-fold dilutions to 10^{-5}) were used to determine sensitivity to inhibitors on YPD agar. Hypha formation was induced by growth at 37°C on YPM medium (1% yeast extract, 2% peptone, 2% mannitol).

***MSB2* expression vectors.** Expression vectors encoding Msb2 variants were constructed by primer-directed mutagenesis of plasmid pES11a (8), using a QuikChange kit (Stratagene). Sequences of oligonucleotide primers are listed in Table S1 in the supplemental material. Designations of deletion variants (with the encoding plasmids and mutagenic primers) were as follows: ΔD3 (plasmid pSM3; primer pair Msb2-15ASDel1 Fwd/Rev), ΔD4 (pSM4; Msb2-15ASDel2 Fwd/Rev), ΔD5 (pSM12; Msb2-Del12 Fwd/Rev), ΔD6 (pSM11; Msb2-Del11 Fwd/Rev), ΔD7 (pSM10; Msb2-Del10 Fwd/Rev), ΔD8 (pSM9; Msb2-Del9 Fwd/Rev), ΔD9 (pSM17; Msb2-Del6 Rev/Msb2-Del11 Fwd), ΔD11 (pSM14; Msb2-Del6 Rev/Msb2-Del11), ΔD14 (pSM7; Msb2-Del7 Fwd/Rev), and ΔD15 (pSM6; Msb2-Del6 Fwd/Rev). pSM15/16 was based on construct pSM14. pES16/17 (8) and pSM14 were cut with ApaI and Bsu36I. Fragments including stop codons upstream or downstream of the TM domain were ligated into pSM14, encoding the ΔD12 and ΔD13 variants. Plasmids were integrated into the *LEU2* locus of strain FCCa28. Integration into the *LEU2* locus was verified by colony PCR with primers Kolo AMP Fwd and Kolo LEU2 Rev.

RNA methods. RNAs were isolated from all cultures, and transcriptomic analyses were performed essentially as described previously (18). Cy3- and Cy5-labeled cDNAs generated from RNAs of strains ESCa3 and ESCa38 were cohybridized to *C. albicans* genomic arrays (Eurogentec, Belgium). The arrays were read and evaluated using GeneSpring software as described previously. Genes were considered to be significantly regulated ($P < 0.05$) if the expression ratios for strains ESCa3 and ESCa38 were ≥1.5 during caspofungin treatment (50 ng/ml; 30 min).

For quantitative PCR (qPCR) analyses, total RNA was isolated, treated with DNase I (Turbo DNase kit; Ambion), and purified using an RNA cleanup kit (Zymo Research). One to 2 μg of purified RNA was reverse transcribed into cDNA (Maxima First Strand cDNA synthesis kit; Thermo Scientific), using nuclease-free water (protocols of the suppliers were used for all steps). A parallel sample was not reverse transcribed as a control for

contaminated DNA. The qPCR assay was done using a model Mx3000P (Stratagene) machine, with 10 μl of cDNA sample (1:10), 4 μl EvaGreen QPCR-mix II (Bio-Budget), and 3 μl each of forward and reverse oligonucleotide primers (400 pmol/μl) in each reaction mixture. AmpliTaq polymerase was activated at 95°C for 10 min, and annealing was performed at 60°C for 20 s. The extension step was performed at 72°C for 30 s, and the denaturation step was performed at 95°C for 30 s; a total of 40 cycles were completed.

Protein methods. Strains were grown in 50 ml YPD or SD medium at 30°C to an optical density at 600 nm (OD_{600}) of 0.8 or 6 to 10, respectively, and cells were harvested by centrifugation. Cells were washed with water and resuspended in lysis buffer (50 mM HEPES, pH 7.5; 150 mM NaCl; 5 mM EDTA; 1% Triton X-100) containing protease inhibitors (Complete Mini; Roche). Cells were broken by shaking with glass beads at 4°C with a FastPrep homogenizer (MP Biochemicals). Cell debris and glass beads were separated from the crude cell extract by centrifugation. For immunoblotting, proteins were separated by SDS-PAGE (12% SDS, 4 to 20% acrylamide) and blotted to polyvinylidene difluoride (PVDF) membranes. Protein standards used were the PageRuler set (11 to 170 kDa; Fermentas) and the HiMark set (31 to 460 kDa; Invitrogen) of proteins. Membranes were probed using a rat anti-hemagglutinin (anti-HA) monoclonal antibody (1:2,000; Roche) and visualized using peroxidase-coupled goat anti-rat or anti-mouse antibody (1:10,000; Thermo Scientific) and the SuperSignal West Dura chemiluminescent substrate (Pierce). The membrane was processed as for immunoblotting, and the resulting signals were recorded using a Fujifilm LAS400 mini-image analyzer and evaluated with the Fujifilm Multi Gauge program. Signals were quantitated using ImageJ software (http://imagej.nih.gov/ij/).

MAP kinase activation assay. Strains were grown overnight to stationary phase in YPD medium and diluted in YPD medium to an OD_{600} of 0.1. Cells were grown to an OD_{600} of 0.8 at 37°C and incubated further for 1 h in the presence (+) or absence (−) of tunicamycin (2 μg/ml). Immunoblots were prepared as described previously, with verification of equal loading by Ponceau red staining of the membranes. Blots were probed with anti-phospho-p44/42 MAP kinase (Cell Signaling Technology) to detect phosphorylated Cek1 protein (8) or with a polyclonal Cek1 antibody to detect total Cek1 (14).

Fluorescence microscopy. Strains were grown in YPD at 30°C to an OD_{600} of 1 and were stained with calcofluor white (0.1% calcofluor white solution; Sigma) to visualize chitin. Cells (OD_{600} = 0.8) used for immunofluorescence microscopy were fixed with 4% formaldehyde, and 1 ml of cell suspension was treated with Zymolyase T100 (100 μg; 50 μl), glucuronidase (30 μl), and 10 mM dithiothreitol (DTT) for 30 min at 30°C. Cells were pelleted and treated with 0.1% Triton X-100 for 5 min at room temperature. Cells (20 μl) were fixed to polylysine-coated glass slides and washed with phosphate-buffered saline (PBS), followed by blocking of unspecific binding sites by use of 2% milk powder in PBS. The blocking solution was removed, and 40 μl of rat anti-V5 antibody (1:100; AbD Serotec) was allowed to react for 90 min at room temperature or overnight at 4°C in a wet chamber. Cells were washed, and fluorescein isothiocyanate (FITC)-coupled anti-mouse antibody (1:100; Sigma-Aldrich) in 0.2% milk powder was added and allowed to react for 90 min at room temperature. For nuclear staining, 20 μl 4′,6-diamidino-2-phenylindole (DAPI; 1 μg/ml) was added for 15 min at room temperature. Slides were washed with PBS, and a drop of antifade reagent (Pro-Long; Sigma) was added before covering the specimen with a coverslip, which was sealed with nail polish. Microscopic inspection of FITC and DAPI fluorescence was done using an Axioskop 40 microscope (Carl Zeiss, Goettingen, Germany), and the ImageJ program (http://imagej.nih.gov/ij/) was used for evaluation of fluorescence signals.

Antimicrobial peptide assays. Overnight cultures of *C. albicans* were diluted and grown in YPD at 30°C to an OD_{600} of 0.3. Cells were harvested by centrifugation and washed with and resuspended in PBS. Triplicate assay mixtures containing 5 μl cell suspension and 2 μg LL-37 (Sigma) in a total volume of 25 μl were incubated for 1.5 h at 37°C, diluted 500-fold, and plated on YPD. Numbers of CFU were determined after 2 days of growth at 30°C. Sensitivity to long-term exposure to LL-37 was determined by growing strains in the presence or absence of LL-37 (1 μg/200 μl; final concentration, 5 μg/ml). Triplicate assay mixtures were inoculated to an OD_{600} of 0.1 and were incubated for 7 h at 37°C on a rotary shaker at 115 rpm. To assess killing, the OD_{600} was measured and compared to that of untreated cells.

Statistical analysis. Statistical significance was determined using the unpaired *t* test (*, $P < 0.05$; **, $P < 0.01$; and ***, $P < 0.001$).

RESULTS

***C. albicans* strains producing Msb2 deletion variants.** The precursor of the membrane sensor protein Msb2 in *C. albicans* contains a single transmembrane (TM) region that separates a large, N-terminal glycosylated exodomain from a short, C-terminal cytoplasmic tail. The precursor is cleaved and the exodomain released in substantial amounts into the environment during planktonic and surface growth (8, 15, 19). Previous studies suggested that the N-terminal, TM, and cytoplasmic domains of Msb2 convey different cellular functions (8). To further define Msb2 functional domains, strains were constructed to produce additional Msb2 deletions; variants were designated ΔD1 to ΔD15 and included the previously described variants ΔN (ΔD10), ΔC (ΔD1), and ΔTM-C (ΔD2) (8) (Fig. 1). The respective *MSB2* alleles were chromosomally integrated into an *msb2* mutant strain and expressed under the control of the constitutive *ACT1* promoter (8), because preliminary results revealed that *MSB2* transcription is autoregulated via the Msb2-Cek1 pathway (L. van Wijlick and J. F. Ernst, unpublished results). Transformants produced all Msb2 variants at similar levels, although amounts of cell-associated/secreted proteins were different for certain variants (see below).

Hyphal morphogenesis and basal resistance to glycostress require specific Msb2 domains. As previously described, the *msb2* mutant and a strain producing an Msb2 variant lacking both the TM region and the cytoplasmic tail (ΔD2 variant) were not able to form hyphae on YPM agar, while removal solely of the cytoplasmic tail (ΔD1 variant) had no effect (8). Interestingly, a series of small deletions directly upstream of the TM region (ΔD3, ΔD4, and ΔD5 variants) led to defective hypha formation, indicating that the respective sequences (residues 1084 to 1308) collectively contribute to hyphal development (Fig. 2A). Defective hypha formation was not observed for any of the deletions further upstream, assigning Msb2 requirements for hyphal morphogenesis to a specific internal Msb2 segment.

Previous work indicated that *msb2* mutants are supersensitive to caspofungin and to other agents generating glycostress, including Congo red and Zymolyase (14). To define functional domains of Msb2 required for basal resistance, we tested the sensitivity of strains producing Msb2 variants to caspofungin and to low concentrations of tunicamycin, which blocks *N*-glycosylation. As expected, the *msb2* mutant was more sensitive than the wild-type strain to tunicamycin. Similarly, the Msb2 deletion series encompassing sequences immediately N-terminal to the TM region (ΔD3, ΔD4, and ΔD5 variants) was also more sensitive, while further upstream deletions (ΔD6 to ΔD10 variants) restored basal resistance (Fig. 1 and 2B). Collectively, the results indicate that basal resistance to glycostress requires specific internal Msb2 sequences, which coincide essentially with sequences required for hypha formation.

Shedding of the exodomain requires a specific Msb2 segment. To establish if specific sequences of Msb2 are needed for its

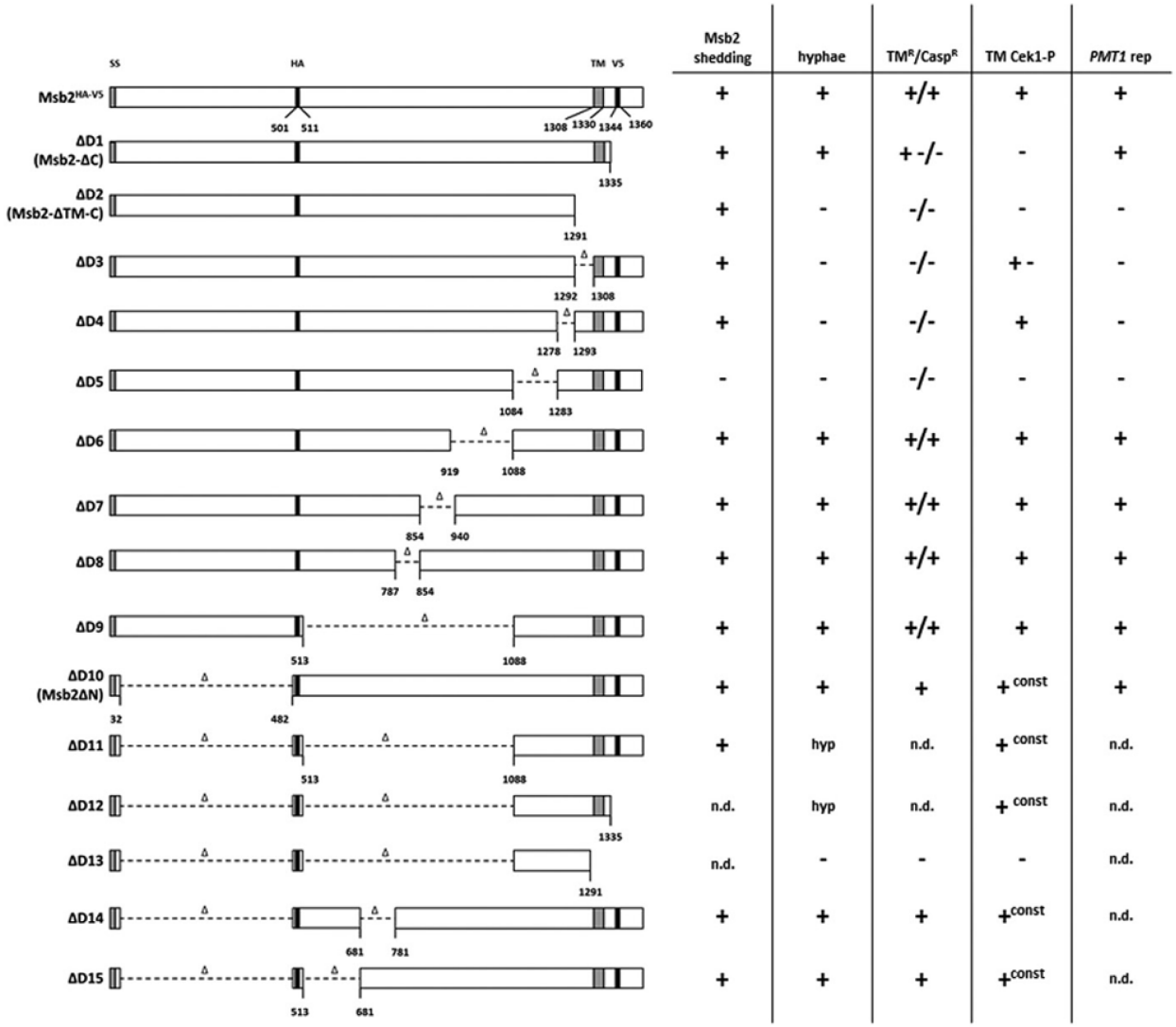

FIG 1 Structures and functions of Msb2 protein variants. Plasmids encoding Msb2 variants were chromosomally integrated into strain FCCa28, which produces the inactive Msb2-Δ1 variant via the *msb2Δ1* allele (8). The positions of the signal sequence (SS), the transmembrane region (TM), and HA and V5 epitope tags in Msb2 are indicated. The transformants (encoded variants) were strains ESCa3 ($Msb2^{HA-V5}$), ESCa38 (ΔD1), ESCa39 (ΔD2), MSCa1 (ΔD3), MSCa3 (ΔD4), MSCa34 (ΔD6), MSCa35 (ΔD5), MSCa30 (ΔD8), MSCa31 (ΔD7), MSCa48 (ΔD9), ESCa25 (ΔD10), MSCa37 (D11), MSCa45 (ΔD12), MSCa46 (ΔD13), MSCa29 (ΔD14), and MSCa8 (ΔD15). Data for strains ESCa25 (ΔD10; Msb2ΔN), ESCa38 (ΔD1; Msb2-ΔC), and ESCa39 (ΔD2; Msb2-ΔTM-C) have been reported previously (8). Listed Msb2 phenotypes include Msb2 shedding, hypha formation on YPM agar at 37°C, tunicamycin (TM^R) and caspofungin ($Casp^R$) resistances, phosphorylation of Cek1 induced by tunicamycin treatment (TM Cek1-P), and repression of *PMT1* expression (*PMT1* rep) under normal growth conditions. Hyperfilamentous growth (hyp) and constitutive phosphorylation of Cek1 during growth in YPD at 37°C (const) are listed. n.d., not determined.

shedding from *C. albicans* cells, we examined the presence of Msb2 in strains producing variants both in the growth medium and in association with cells. Because all Msb2 variants retained the HA epitope (Fig. 1), immunoblotting using an anti-HA antibody was performed. We discovered that only a single deletion variant (ΔD5), lacking 199 residues (residues 1085 to 1282), was not shed by such *C. albicans* cells, since the Msb2 signal was detected only in association with cells, not in the medium (Fig. 3). For all other Msb2 variants, evidence of shedding was observed by detecting both cell-associated Msb2 and Msb2 in the medium. These results suggest that proteolytic cleavage of Msb2 occurs between residues 1085 and 1282 as a precondition to allow shedding of the exodomain. This sequence is also required for all other Msb2-related phenotypes, suggesting that Msb2 shedding is essential for its functions.

Separate Msb2 sequences activate or suppress phosphorylated Cek1 levels. Msb2 has been described as an upstream element of a signaling pathway regulating levels of the phosphorylated form of the MAP kinase Cek1 (14). *msb2* mutants are unable to respond to glycostress provoked by defects in *N*- and *O*-protein glycosylation by increasing phosphorylated Cek1 (17). To identify the functional domains of Msb2 that mediate Cek1 regulation, we

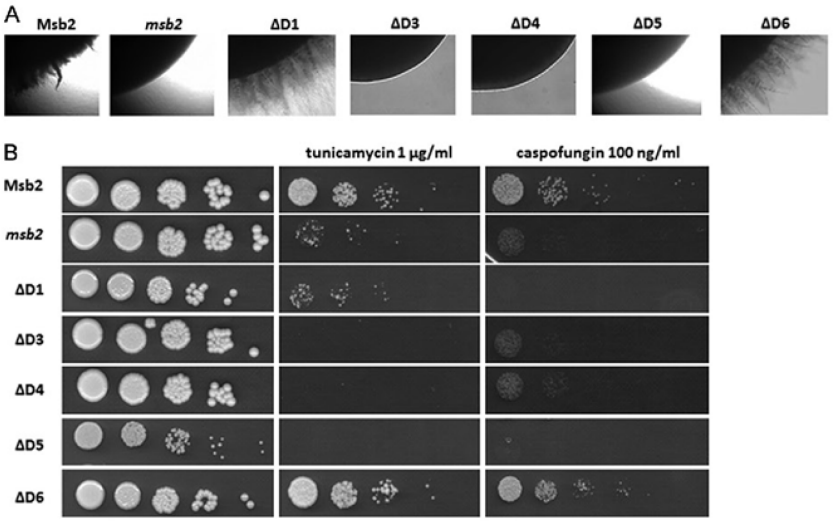

FIG 2 Msb2 variants affect morphogenesis and glycostress resistance. (A) Msb2 variants are defective in formation of hyphae on YPM agar. Colonies of strains were photographed following growth for 2 days at 37°C. Strains FCCa27 (*msb2*), ESCa38 (ΔD1), MSCa1 (ΔD3), MSCa3 (ΔD4), MSCa34 (ΔD6), and MSCa35 (ΔD5) were compared to ESCa3 ($Msb2^{HA\text{-}V5}$). (B) Sensitivities of strains to tunicamycin (1 μg/ml) and caspofungin (100 ng/ml) were tested by a drop dilution test.

examined the phosphorylation status of Cek1 by immunoblotting crude extracts of cells grown either without stress or in the presence of tunicamycin. Interestingly, under both conditions, separate Msb2 domains were found to be responsible for Cek1 regulation. First, under tunicamycin stress, the control strain (Msb2) revealed a strong upregulation of phosphorylated Cek1 and total Cek1, which did not occur in the *msb2* mutant and occurred at reduced levels in strains producing the ΔD3, ΔD4, and ΔD5 variants (defective in Msb2 shedding) or the ΔD13 variant (Fig. 4). In addition, the C-terminal deletion variants ΔD1 and ΔD2 were reported to be defective for upregulation of phosphorylated Cek1 with tunicamycin treatment (8). All other Msb2 variants were able to produce phosphorylated Cek1 as in control cells (Fig. 4; see Fig. S1 in the supplemental material). We concluded that the C-terminal region surrounding the transmembrane region of Msb2 is required to increase levels of phosphorylated Cek1 in response to glycostress by tunicamycin and also by caspofungin (see below).

The second, repressive function of the functional domains in Msb2 was detected by analyzing Cek1 in unstressed cells. Under these conditions, Cek1 and Cek1-P levels were low in both the control strain (Msb2) and the *msb2* mutant but were as high as those with tunicamycin induction in cells with the ΔD11, ΔD12, ΔD14, and ΔD15 Msb2 variants; no other deleted Msb2 variant showed this characteristic (Fig. 4). Collectively, the results indicate that N-terminal sequences of Msb2 prevent upregulation of Cek1 levels in unstressed cells, while its C-terminal sequences are crucial for increasing the levels of Cek1 and its phosphorylated form under glycostress conditions.

Msb2 domains repress transcription of *PMT1* in unstressed cells. Previous results indicated that the Msb2-Cek1 pathway regulates transcription of *PMT* genes, encoding protein *O*-mannosyltransferases (17). Specifically, the presence of Msb2 and Cek1 proteins was found to downregulate transcript levels of *PMT1*, encoding Pmt isoform 1. When *PMT1* transcript levels were ana-

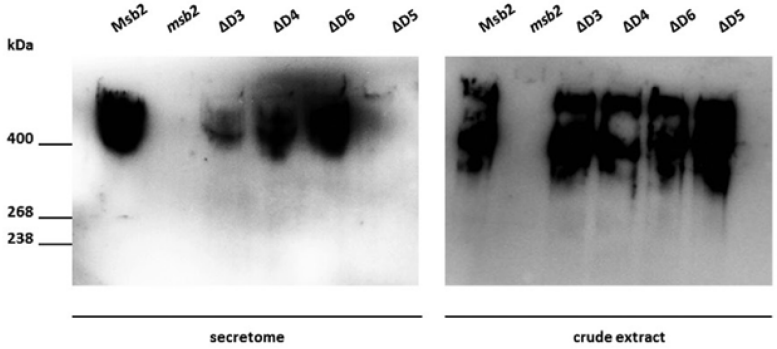

FIG 3 Msb2 shedding. Immunoblotting was performed to detect HA-tagged Msb2. Fifty-microgram samples of proteins in cell extracts and 15-μl aliquots of the secretome were separated in 4 to 20% SDS-PAGE gels, and immunoblots were incubated with rat anti-HA antibody. Strains tested included ESCa3 (Msb2; $MSB2^{HA\text{-}V5}$), FCCa27 (*msb2*), MSCa1 (ΔD3), MSCa3 (ΔD4), MSCa34 (ΔD6), and MSCa35 (ΔD5).

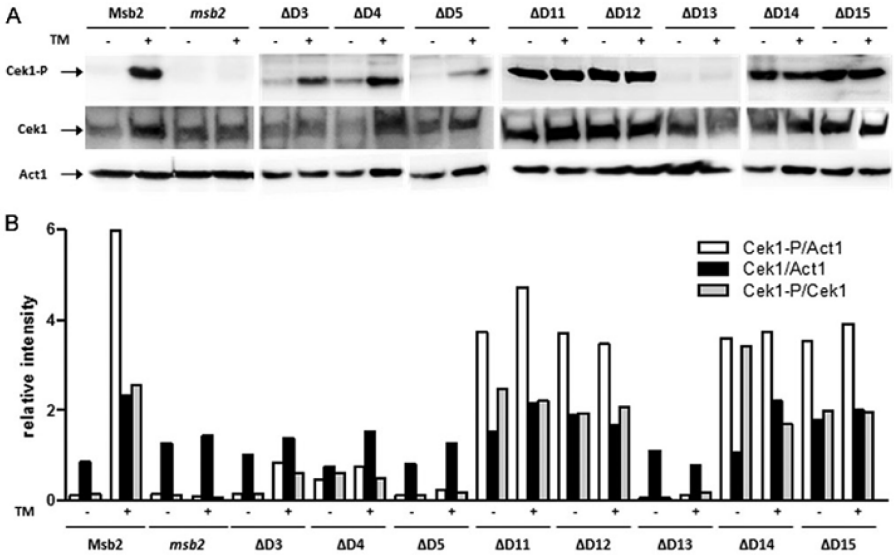

FIG 4 Levels of MAP kinase Cek1 in strains producing Msb2 variants. (A) Cells were grown to stationary phase, diluted in YPD medium, grown to an OD_{600} of 0.8 at 37°C, and incubated further for 1 h in the presence (+) or absence (−) of tunicamycin (2 μg/ml). Cell extracts (50 μg) were separated by SDS-PAGE, and immunoblots were incubated with anti-phospho-p44/42 MAP kinase antibody, which detects phosphorylated Cek1 (Cek1-P), or with a polyclonal antibody to detect total Cek1 (Cek1). The actin protein (Act1), detected by anti-Act1 antibody, was used as the loading control. Strains tested included ESCa3 (Msb2; *MSB2*$^{HA\text{-}V5}$), FCCa27 (*msb2*), MSCa1 (ΔD3), MSCa3 (ΔD4), MSCa35 (ΔD5), MSCa37 (D11), MSCa45 (ΔD12), MSCa46 (ΔD13), MSCa29 (ΔD14), and MSCa8 (ΔD15). (B) Relative intensities of Cek1-P and total Cek1 compared to Act1 and of Cek1-P compared to total Cek1. Band intensities were quantified using ImageJ software (http://imagej.nih.gov/ij/).

lyzed in tunicamycin-stressed cells, high levels were detected in the control strain, in the *msb2* mutant, and in all strains producing Msb2 variants (Fig. 5), suggesting that Msb2 is dispensable for upregulating *PMT1* transcripts under tunicamycin stress conditions. In unstressed cells, however, Msb2 appeared to have a repressive function, since the *PMT1* transcript level was low in the control strain but was upregulated in the *msb2* mutant strain. Furthermore, the ΔD2 to ΔD5 variants upregulated the *PMT1* transcript in unstressed cells, suggesting that the encompassed sequences (residues 1084 to 1308) mediate repression of *PMT1*. Low levels of phosphorylated Cek1 (Fig. 4) but derepressed high transcript levels of its downstream element *PMT1* in the *msb2* mutant and the *cek1* mutant (17) suggest that transcriptional repression of *PMT1* depends on Cek1 in its unphosphorylated form. The identified Msb2 sequences may transmit information on the intactness of glycostructures to Cek1 to permit downregulation of *PMT1* transcription.

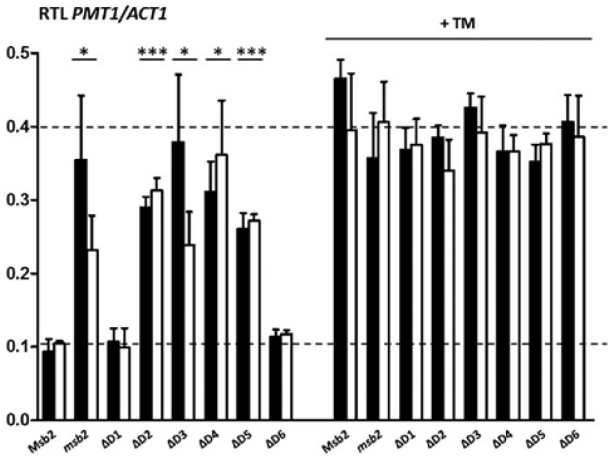

FIG 5 Regulation of *PMT1* transcripts in strains producing Msb2 variants. The level of the *PMT1* transcript relative to the *ACT1* transcript (RTL) was determined by qPCR for cells grown to an OD_{600} of 0.8 in the presence or absence of tunicamycin (0.5 μg/ml). Strains tested included ESCa3 (Msb2; *MSB2*$^{HA\text{-}V5}$), FCCa27 (*msb2*), ESCa38 (ΔD1), ESCa39 (ΔD2), MSCa1 (ΔD3), MSCa3 (ΔD4), MSCa34 (ΔD6), and MSCa35 (ΔD5). Means and standard deviations of results for two biological replicates (black and white bars) in triplicate assays are shown. Statistical significance was determined using the *t* test. *, $P < 0.05$; **, $P < 0.01$; ***, $P < 0.001$.

Msb2 sequences involved in basal resistance to LL-37. In previous studies, it was shown that the basal resistance of *C. albicans* to the AMP LL-37 depends on the shed Msb2 glycofragment (8, 15). In this study, we tested the ability of Msb2 variants to mediate resistance during short- and long-term exposures to LL-37. In experiments employing high LL-37 concentrations for short exposure times, we found that only the *msb2* mutant, not the strains producing Msb2 deletion variants, was supersensitive to LL-37 (Fig. 6A). Physiological concentrations of LL-37 are low but persist at sites of infection and inflammation (20). Therefore, we also incubated strains for 7 h in the presence or absence of low levels of LL-37 (5 μg/ml). In this experimental setting, the elevated sensitivity of the *msb2* mutant was confirmed (Fig. 6B). Remarkably, Msb2 variants lacking C-terminal sequences (ΔD1 to ΔD5 variants) were also more sensitive to LL-37. Thus, it appears that Msb2 sequences involved in basal glycostress resistance (Fig. 2B) also contribute to basal LL-37 resistance. In these experiments, we also examined the involvement of Cek1 in LL-37 resistance by including a *cek1* mutant. This mutant was supersensitive to LL-37

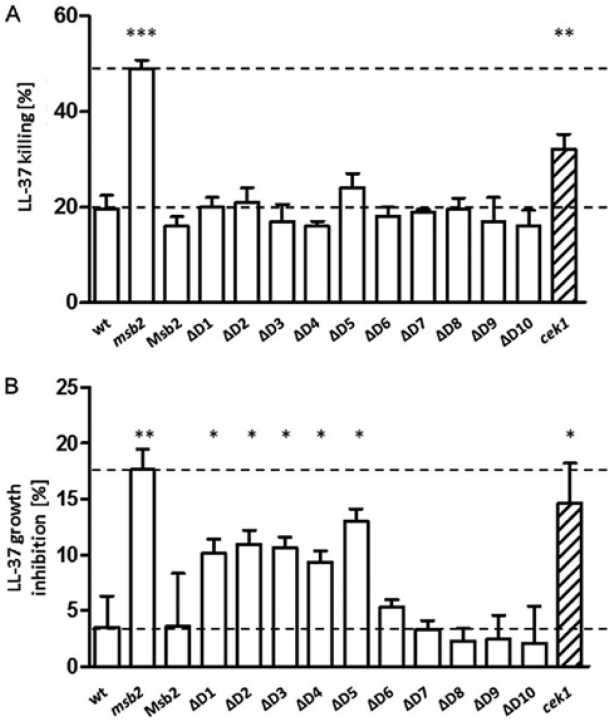

FIG 6 Shed Msb2 and Cek1 regulate basal LL-37 resistance. (A) Killing by short-term exposure to LL-37. Cells (OD_{600} = 0.3) were incubated with 2 μg LL-37 in a total volume of 25 μl for 1.5 h, followed by CFU determination. Killing by LL-37 is indicated as a percentage relative to the killing of untreated cultures. (B) Growth inhibition by long-term exposure to LL-37. Cells (OD_{600} of 0.1) were incubated with 1 μg LL-37 (5 μg/ml) in wells of a microtiter plate (total volume, 200 μl) for 7 h at 37°C before measurement of the OD_{600} by use of a microplate reader. The ratios of OD_{600} values for untreated and treated cultures are given as percentages. Strains tested included CAF2-1 (wt), FCCa27 (*msb2*), ESCa3 ($Msb2^{HA\text{-}V5}$), ESCa38 (ΔD1), ESCa39 (ΔD2), MSCa1 (ΔD3), MSCa3 (ΔD4), MSCa34 (ΔD6), MSCa35 (ΔD5), MSCa30 (ΔD8), MSCa31 (ΔD7), MSCa48 (ΔD9), ESCa25 (ΔD10), and CK43B-16 (*cek1*) (hatched bar). Dotted lines indicate values for the wild-type and *msb2* mutant strains. Means and standard deviations of results for triplicate assays are shown. Statistical significance was determined using the *t* test. *, $P < 0.05$; **, $P < 0.01$; ***, $P < 0.001$.

(Fig. 6) and did not prevent Msb2 shedding (data not shown), indicating that basal resistance to LL-37 is mediated not only by binding of LL-37 to the shed Msb2 exodomain (15) but also by other cell-associated Msb2 sequences that are required for Cek1 signaling.

Hyperfilamentous phenotype generated by Msb2 variants. Transformants producing the ΔD11 variant, in which most N-terminal sequences of the Msb2 exodomain are deleted (Fig. 1), were remarkably hyperfilamentous under all growth conditions, including those environments that normally do not induce hyphal morphogenesis (YPD and 30°C) (Fig. 7A). This phenotype was not observed with the ΔD9 and ΔD10 variants, in which only one of the two deleted segments of the ΔD11 variant is missing. Two partial deletions of the segment missing in the ΔD9 variant (ΔD14 and ΔD15 variants) did not reproduce the ΔD11 phenotype, indicating that other sequences in this region are involved in generating hyperfilamentation. To investigate if the cytoplasmic tail is required for hypha formation, we constructed the ΔD12 variant, lacking 103 C-terminal residues, and the ΔD13 variant, which also lacks the TM region. Because the ΔD12 variant but not the ΔD13 variant allowed hypha formation, it appears that the TM region but not the cytoplasmic tail of Msb2 is involved in triggering exaggerated hyphal induction.

Next, we investigated the activity of the ΔD11 variant in an $Msb2^{+}$ wild-type strain and in several mutant strains carrying known defects in hypha formation. The hyperfilamentation phenotype of the ΔD11 variant was dominant, since transformants of the wild-type strain showed extensive filamentation (Fig. 7B) and were able to shed Msb2 (see Fig. S1 in the supplemental material). Among mutants hosting the ΔD11 variant, only the *cek1* and *efg1* mutants were defective in hypha formation, while mutants lacking either PKA isoform (*tpk1* and *tpk2* mutants) or the transcription factor Czf1 or Cph1 showed strong filamentation. Thus, hyperfilamentation induced by the ΔD11 variant requires some elements that normally are required for hyphal morphogenesis. The Sho1 membrane protein, which controls the activity of Cek1 in cooperation with Msb2 (14), also appears to be required for ΔD11 hyperfilamentation, because in the *msb2 sho1* double mutant genetic background, only yeast growth was observed (Fig. 7B).

Cleavage and nuclear localization of the cytoplasmic tail of Msb2. The above-described experiments indicated that the cytoplasmic tail of Msb2 is needed for basal resistance against caspofungin (Fig. 2B) and to stimulate phosphorylation of Cek1 in response to stress (Fig. 4) (8). To explore the intracellular fate of the cytoplasmic tail of Msb2, we performed immunofluorescence microscopy of cells producing doubly tagged $Msb2^{HA\text{-}V5}$ (the V5 epitope is located within the middle of the cytoplasmic domain of Msb2) (Fig. 1). In unstressed cells, the cytoplasmic domain was detected on the cellular surface, most likely reflecting the localization in the plasma membrane of cells (Fig. 8A). Short-term exposure to caspofungin (50 ng/ml for 30 min) led to the appearance of the V5 epitope in the cytoplasm and in the nucleus (Fig. 8A, merged signals). Quantification revealed that about 70% of the Msb2 C-terminal domain localized to intracellular locations upon caspofungin treatment (Fig. 8B). These results suggested that under glycostress by caspofungin, the cytoplasmic tail of Msb2 is partially cleaved and enters the nucleus.

The cytoplasmic tail of Msb2 regulates transcriptional responses to glycostress. To further investigate the role of the Msb2 cytoplasmic tail, we first analyzed the activation of Cek1 under caspofungin stress conditions (Fig. 9A). We first tested different caspofungin concentrations, ranging from 10 to 100 ng/ml, during short-term exposure to determine conditions under which <10% of *C. albicans* cells were killed for both strains (data not shown). As in the case of glycostress by tunicamycin (Fig. 4), a strain producing the ΔD1 variant showed strongly reduced levels of phosphorylated Cek1 with treatment by caspofungin (50 ng/ml for 30 min) compared to those of the control strain. Genome-wide transcript profiling was then carried out on strain ESCa38, producing the ΔD1 variant, compared to the Msb2 wild-type strain ESCa3 grown under identical conditions in the presence of caspofungin. Genes for transcripts regulated differently in ESCa38 cells producing deleted Msb2 compared to ESCa3 cells producing full-length Msb2 are listed in Table S2 in the supplemental material. The deletion of the cytoplasmic tail of Msb2 altered the expression of 117 genes >1.5-fold, with 80 genes being upregulated and 37 being downregulated. Categorization of the regulated

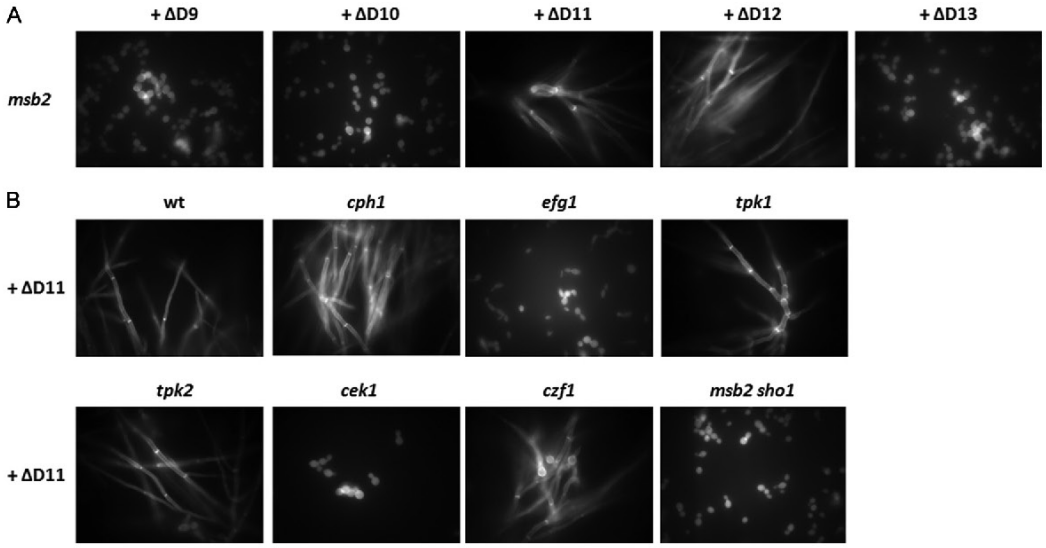

FIG 7 Msb2-Sho1 interactions induce hypha formation via Cek1 and Efg1. (A) Hyperfilamentous growth of strains producing Msb2 protein variants ΔD11 and ΔD12. Transformants (encoded variants) included strains ESCa25 (ΔD10), MSCa37 (ΔD11), MSCa45 (ΔD12), MSCa46 (ΔD13), and MSCa48 (ΔD9). (B) Hyphal induction induced by the ΔD11 Msb2 variant in different genetic backgrounds. Resulting transformants included MSCa37 (*msb2* [*ACT1p-MSB2*ΔN$^{514-1087}$]), MSCa38 (wt [*ACT1p-MSB2*ΔN$^{514-1087}$]), MSCa39 (*cek1* [*ACT1p-MSB2*ΔN$^{514-1087}$]), MSCa40 (*czf1* [*ACT1p-MSB2*ΔN$^{514-1087}$]), MSCa41 (*efg1* [*ACT1p-MSB2*ΔN$^{514-1087}$]), MSCa42 (*cph1* [*ACT1p-MSB2*ΔN$^{514-1087}$]), MSCa43 (*tpk1* [*ACT1p-MSB2*ΔN$^{514-1087}$]), MSCa44 (*tpk2* [*ACT1p-MSB2*ΔN$^{514-1087}$]), and MSCa47 (*msb2 sho1* [*ACT1p-MSB2*ΔN$^{514-1087}$]). All cells were grown at 30°C in YPD before staining with calcofluor white and microscopic inspection.

genes according to their functional categories (21; http://www.candidagenome.org/cgi-bin/GO/goTermFinder) revealed that deletion of the Msb2 C-tail had a significant effect on *ALS* genes (*ALS1*, *ALS3*, and *ALS5*), which are responsible for the entry of *C. albicans* into host cells (see Table S3A). GO analysis (Slim Mapper) of the complete regulated gene set assigned 19 genes to stress responses, 16 to cellular protein modification processes, and 15 to responses to chemicals (see Table S3B). To confirm the transcriptional profiling data, we performed qPCR on two selected Msb2 target genes. Transcript levels for the *ALS1* and *ALS3* genes, encoding cell wall proteins, were increased by a factor of 4 or 6 (Fig. 9B). The results confirmed the increased levels of *ALS* gene transcripts in cells producing the ΔD1 variant under caspofungin stress conditions.

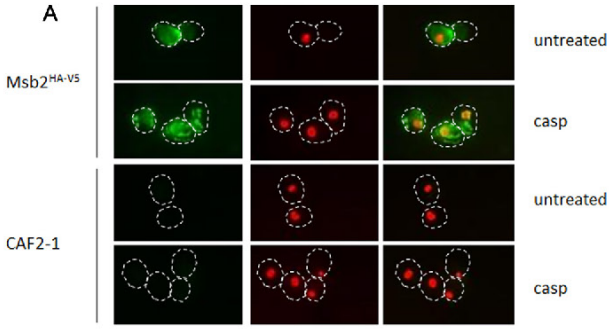

B

condition	CM [%]	intracellular [%]
untreated	98	2
casp	28,6	70,2

FIG 8 Cellular localization of the Msb2 cytoplasmic tail. (A) Fluorescence microscopy was performed on wild-type strain CAF2-1 (wt) and strain ESCa3, producing Msb2^{HA-V5} containing the V5 epitope in its cytoplasmic tail, without and with treatment with 50 ng/ml caspofungin (casp) for 30 min. Fixed cells were treated with mouse anti-V5 antibody, which was detected with FITC-labeled anti-mouse antibody (green signals); staining by DAPI was used to detect nuclei (red signals); and merged signals are shown in yellow. (B) Quantification of cellular localization. Fifty cells were analyzed for V5-FITC staining in the cytoplasmic membrane (CM) or for intracellular localization in the cytoplasm or the nucleus. Fluorescence signals were quantitated using ImageJ software and are indicated as percentages.

The promoter regions of the regulated genes were analyzed using dyad analysis and YeTFaSCo (22, 23), which revealed the following two highly significant transcription factor motifs: GA_2GA_5 (101 sites) and CAC_2AC_2 (46 sites) (Fig. 9C). The identified GA_2GA_5 motif matches the motif for binding of the glucose-induced transcriptional regulator Azf1 in *Saccharomyces cerevisiae* (24). The identified CAC_2AC_2 motif matches the Ace2 binding site in *S. cerevisiae* (23) and in *C. albicans* (L. van Wijlick and J. F. Ernst, unpublished results). Collectively, the transcriptomic results support the notion that the cytoplasmic portion of Msb2 is functional in the nucleus to regulate transcriptional circuits alleviating glycostress. Ace2 was previously identified as contributing to regulation of *PMT* genes (17).

DISCUSSION

The fungal pathogen *C. albicans* is able to adapt to and proliferate in various complex environments of the human host (25). Fungal survival requires stress response pathways to restore cell wall integrity during attack of host immune effectors (26). The signaling mucin Msb2 has dual functions: sensing environmental stress signals and blocking an important aspect of immune defenses by inactivating AMPs (5, 14). Here we showed that different se-

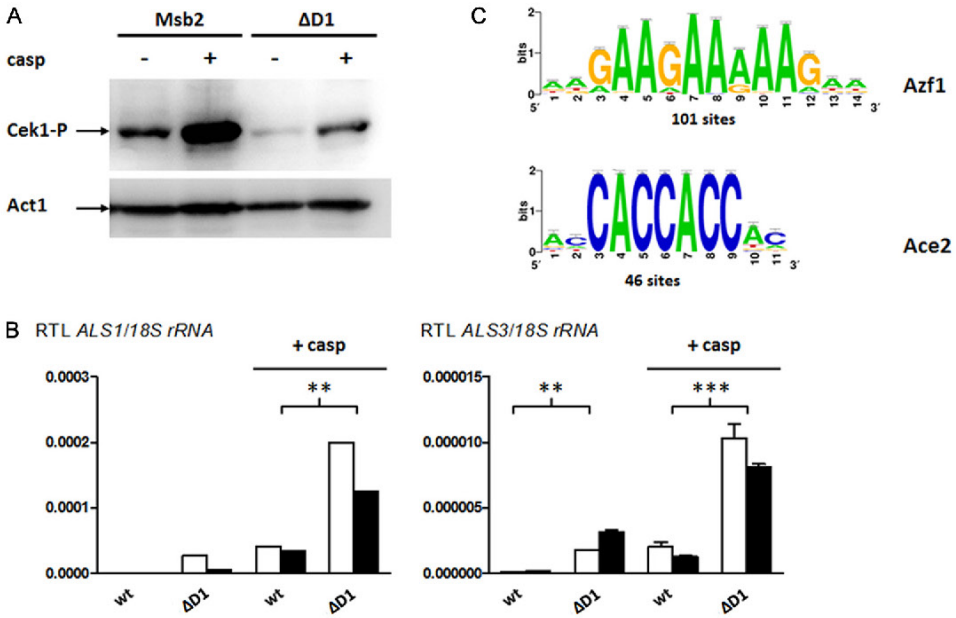

FIG 9 Phosphorylation of Cek1 and regulation of *ALS1* and *MSB2* gene expression by caspofungin treatment. (A) Msb2 C-tail is required for Cek1 phosphorylation during caspofungin treatment. Strains tested include ESCa3 (Msb2; $MSB2^{HA\text{-}V5}$) and mutant strain ESCa38, producing Msb2 lacking the cytoplasmic tail (ΔD1). Cells were grown to stationary phase, diluted in fresh YPD medium, grown to an OD_{600} of 0.8 at 37°C, and incubated further for 30 min in the presence (+) or absence (−) of caspofungin (50 ng/ml). Immunoblot detection of Cek1 and Act1 proteins was performed as described in the legend to Fig. 4. (B) *ALS1* and *ALS3* expression. Transcript levels relative to the 18S rRNA transcript levels in wild-type and ESCa38 mutant cells left untreated or treated with caspofungin (50 ng/ml; 30 min) were determined by qPCR. Means and standard deviations of results for two biological replicates (black and white bars) in triplicate assays are shown. Statistical significance was determined using the *t* test. *, $P < 0.05$; **, $P < 0.01$; ***, $P < 0.001$. (C) Consensus sequences for transcription factors in promoters of genes regulated by the C-tail of Msb2. Genome-wide expression analysis revealed 117 genes regulated by the presence of the Msb2 C-tail (see Table S2 in the supplemental material). Promoter regions were analyzed using dyad analysis (22) and YeTFaSCo (23) to define consensus sequences and revealed binding sites for the Azf1 and Ace2 transcription factors.

quences of Msb2 provide different functions in its proteolytic maturation and in hyphal morphogenesis, basal antifungal resistance, and gene regulation. A scheme depicting the established functional domains of Msb2 is shown in Fig. 10.

Mammalian signaling mucins are known to become proteolytically processed to generate a large extracellular glycodomain as well as a cytoplasmic domain conveying regulatory functions (9). Autoproteolytic cleavage of the MUC1 mucin depends on its internal SEA module, comprising about 120 residues, which cleaves the precursor protein at a G ↑ SVVV motif; the VVV sequence is replaced by other bulky hydrophobic residues in homologs (27). The *C. albicans* Msb2 protein lacks SEA-homologous sequences but contains a G^{1232}SAIY^{1235} sequence N-terminal to its TM region; however, deletion of residues 1231 to 1233 did not abolish shedding of Msb2 (data not shown). Thus, the present evidence suggests that the Msb2 precursor is processed by a separate dedicated protease, as for some mammalian mucins and for the Msb2 protein of *S. cerevisiae*, which is cleaved by the yapsin Yps1 (13). It is currently unclear if, in *C. albicans*, secreted aspartyl proteases (Sap proteins) initiate cleavage and shedding of Msb2 and/or contribute to subsequent degradation of its shed exodomain (8, 19). Here we defined a segment in the Msb2 exodomain, between residues 1084 and 1283, which is essential for the cleavage and shedding of Msb2. This sequence contains several predicted proteolytic cleavage sites (28; http://web.expasy.org/peptide_cutter/) and may contain the relevant site for shedding, or it may ectopically direct the cleavage event. Importantly, we found that the presence of this Msb2 segment is essential for all Msb2-dependent functions.

The Msb2 sensor regulates the activity of the MAP kinase Cek1, which is required for hypha formation on semisolid surfaces (8). Here we showed that glycosylation defects upregulate Cek1 levels, in agreement with the finding that the *CEK1* transcript level is upregulated by tunicamycin (L. van Wijlick and J. F. Ernst, unpublished results). We identified two modes of Msb2 function on Cek1 phosphorylation, which are conveyed by three separate functional Msb2 domains. In unstressed cells, N-terminal sequences (encompassed by the ΔD10 variant) repressed the appearance of phosphorylated Cek1, while under tunicamycin stress, C-terminal sequences flanking the TM region (encompassed by the ΔD1 and ΔD3 variants) mediated induction of Cek1 and its phosphorylated form. Previously, the Mkc1 MAP kinase was described to become activated by surface growth, oxidative stress, and cell wall defects, including caspofungin glycostress (29–32); thus, Msb2 may mediate basal caspofungin resistance by activating both Mkc1 and Cek1. In contrast, increased Mkc1-P levels were not consistently reported for tunicamycin treatment conditions (14, 33), suggesting that defective protein *N*-glycosylation triggers upregulation of Mkc1-P only under as yet undefined conditions (possibly upon prolonged tunicamycin treatment, when cell wall proteins become significantly underglycosylated). The ability to generate hyphae was not correlated with phosphorylated

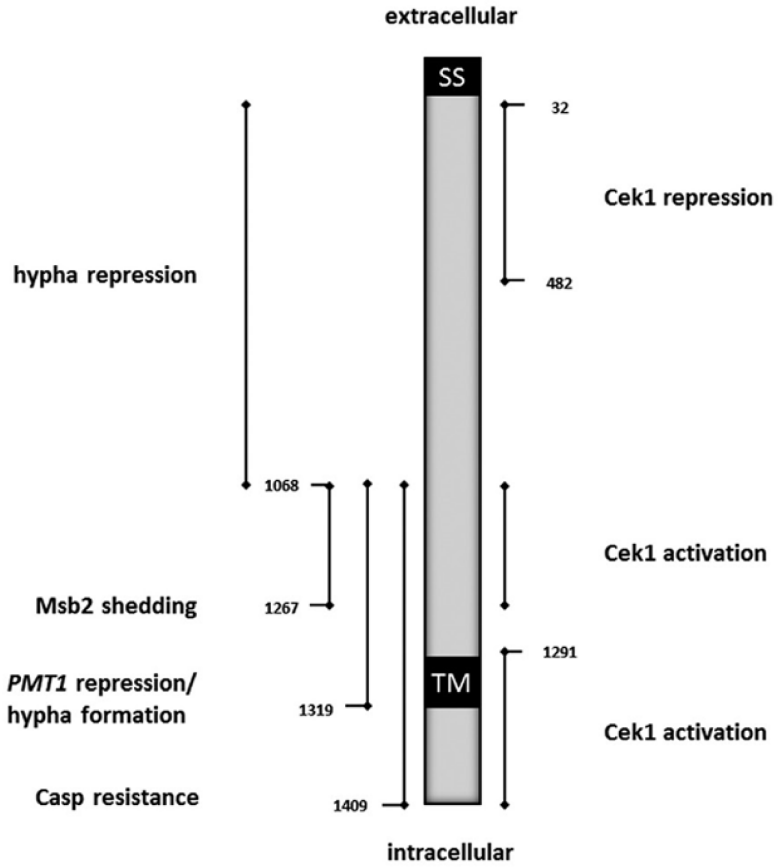

FIG 10 Msb2 domains involved in cellular processes. The schematic of Msb2 indicates the positions of the signal sequence (SS) and the transmembrane region (TM) in the extracellular (shed) and intracellular domains. Bars indicate overlapping subdomains involved in activating/repressing hypha formation and repressing *PMT1* transcripts in unstressed cells. Furthermore, different Msb2 subdomains are indicated that are required for repressing or inducing Cek1 phosphorylation. In unstressed cells, N-terminal sequences mediate repression of Cek1 phosphorylation and activity, while C-terminal sequences allow activation of Cek1 in cells stressed by caspofungin (Casp) and/or tunicamycin.

Cek1, since the ΔD1 variant showed low levels of phosphorylated Cek1 but formed hyphae, while the ΔD4 variant produced high levels of phosphorylated Cek1 but did not undergo filamentation. This result suggests that Msb2 triggers hypha formation, at least partially, independently of Cek1 and/or its state of phosphorylation. Surprisingly, a remarkable hyperfilamentation phenotype was observed when about two-thirds of the N-terminal sequences of Msb2 were deleted (ΔD11 and ΔD12 variants). Strong filamentation occurred in liquid media and led to large hyphal aggregates. Hyperfilamentation was still observed when the cytoplasmic tail of Msb2 was removed but did not occur when the TM region was deleted (ΔD13 variant). Thus, the presence of the TM region and/or its close flanking sequences appears to be sufficient to strongly induce hyphal morphogenesis. Interestingly, the Msb2-generated abnormal hypha formation also occurred in the wild-type genetic background, suggesting the dominance of the Msb2 fragment over full-length Msb2. On the other hand, hyphal formation was not induced in cells carrying the *sho1*, *cek1*, or *efg1* mutation. These results indicate that hyperfilamentation induced by Msb2 sequences in the ΔD11 variant requires a known Msb2 interactor (Sho1) (14) and its downstream kinase (Cek1), but also a transcription factor essential for hypha formation (Efg1) (34). However, the contribution of Msb2 to regular hyphal induction under physiological conditions requires further analysis.

Previous results have implicated the Msb2-Cek1 pathway in fungal basal resistance and cell wall integrity (8, 14, 17). Shed Msb2 binds human AMPs and a peptide antibiotic with high affinity, thereby generating a protective cloud surrounding cells (15). Here we showed that Msb2 sequences that probably are not shed (C-terminal to the proposed cleavage region) also contribute to AMP resistance. C-terminal sequences extending from the cytoplasmic tail to residue 1085 are necessary to increase basal resistance not only to the AMP LL-37 but also to the cell wall-damaging compounds caspofungin and tunicamycin. Although sequences comprising residues 1278 to 1308 are not essential for either Msb2 shedding or Cek1 phosphorylation, they are relevant for basal resistance. The underlying mechanisms are not yet clear, but it appears that extracellular Msb2 sequences that remain after cleavage of the exodomain regulate nuclear activities, as observed in the case of mammalian N-CAM and β-dystroglycan proteins (35, 36).

The transcriptional output of Msb2-Cek1 signaling consists of altered gene expression that restores cell wall integrity. We previ-

ously found that *PMT1* expression is repressed by Msb2-Cek1 proteins during normal growth, while the induction of *PMT2* and *PMT4* genes by inhibition of Pmt1 requires both proteins (17). Since no significant phosphorylation of Cek1 occurs in unstressed cells, it appears that *PMT1* repression requires the presence of Cek1, but not in its phosphorylated form. Msb2 sequences upstream of the TM region, which are also needed to provide basal resistance to caspofungin and tunicamycin, were found to be required for *PMT1* repression, although the latter process was unaffected by absence of the cytoplasmic tail (ΔD1 variant). With regard to the mechanism by which Msb2-Cek1 signaling alters gene expression, we obtained evidence by immunofluorescence microscopy that the C terminus of Msb2 (possibly the cytoplasmic domain, including the TM region) partially relocates to the cytoplasm and the nucleus if cells are stressed by caspofungin. Thus, the carboxy end of Msb2 may enter the nucleus either by itself or as a passenger of the MAP kinase modules and be involved in target gene regulation. Cleavage of type I transmembrane proteins in the membrane, releasing an intracellular fragment capable of transducing nuclear signals, has been described for the Notch-1 protein, ErbB-4, and CN14 (37–39). In two fungal species, the subcellular localization of the Msb2 (*Ustilago maydis*) and MsbA (*Aspergillus nidulans*) C-terminal ends fused to a fluorescent protein is a dynamic process in which the mucin is constantly removed from the membrane and recruited to the vacuole (10, 40). Transcriptomic comparisons of strains containing Msb2 with and without its cytoplasmic tail indeed revealed 117 differentially regulated genes. Intriguingly, the list of genes includes five cell wall genes (*ALS1*, *ALS3*, *ALS5*, *CHT2*, and *PGA14*). Previously, it was shown that caspofungin-induced cell aggregation activates an Efg1-dependent signaling pathway to regulate *ALS1* expression (41). We suggest that Msb2 is an upstream signaling molecule for Efg1-mediated hyphal morphogenesis and for upregulation of *ALS1*. Promoter comparisons of all regulated genes revealed binding motifs for two transcription factors (Ace2 and Azf1) known to activate transcription of genes involved in the maintenance of cell wall integrity. Interestingly, previous results identified Ace2 as an essential protein for regulation of *PMT* genes and for basal antifungal resistance (17). Future research should be directed at clarifying the details of Msb2 processing and its influence in directing environment-regulated gene expression.

ACKNOWLEDGMENTS

We are grateful to C. Davoudi for technical assistance. We thank E. Román and J. Pla for providing the anti-Cek1 antibody.

This work was funded by the Deutsche Forschungsgemeinschaft (grant ER47-13), the Jürgen Manchot Stiftung Düsseldorf, and BMBF-ERA-NET PathoGeNoMics projects "Glycoshield" and "OXYstress."

We declare that we have no conflicts of interest.

REFERENCES

1. Van Der Meer JWM, Van De Veerdonk FL, Joosten LAB, Kullberg BJ, Netea MG. 2010. Severe *Candida* spp. infections: new insights into natural immunity. Int J Antimicrob Agents 36(Suppl 2):S58–S62. http://dx.doi.org/10.1016/j.ijantimicag.2010.11.013.
2. Zipfel PF, Skerka C, Kupka D, Luo S. 2011. Immune escape of the human facultative pathogenic yeast *Candida albicans*: the many faces of the *Candida* Pra1 protein. Int J Med Microbiol 301:423–430. http://dx.doi.org/10.1016/j.ijmm.2011.04.010.
3. Jouault T, Sarazin A, Martinez-Esparza M, Fradin C, Sendid B, Poulain D. 2009. Host responses to a versatile commensal: PAMPs and PRRs interplay leading to tolerance or infection by *Candida albicans*. Cell Microbiol 11:1007–1015. http://dx.doi.org/10.1111/j.1462-5822.2009.01318.x.
4. Mehra T, Koberle M, Braunsdorf C, Mailander-Sanchez D, Borelli C, Schaller M. 2012. Alternative approaches to antifungal therapies. Exp Dermatol 21:778–782. http://dx.doi.org/10.1111/exd.12004.
5. Swidergall M, Ernst JF. 2014. Interplay between *Candida albicans* and the antimicrobial peptide armory. Eukaryot Cell 13:950–957. http://dx.doi.org/10.1128/EC.00093-14.
6. Collette JR, Lorenz MC. 2011. Mechanisms of immune evasion in fungal pathogens. Curr Opin Microbiol 14:668–675. http://dx.doi.org/10.1016/j.mib.2011.09.007.
7. Ernst JF. 2000. Transcription factors in *Candida albicans*—environmental control of morphogenesis. Microbiology 146:1763–1774.
8. Szafranski-Schneider E, Swidergall M, Cottier F, Tielker D, Roman E, Pla J, Ernst JF. 2012. Msb2 shedding protects *Candida albicans* against antimicrobial peptides. PLoS Pathog 8:e1002501. http://dx.doi.org/10.1371/journal.ppat.1002501.
9. Cullen PJ. 2011. Post-translational regulation of signaling mucins. Curr Opin Struct Biol 21:590–596. http://dx.doi.org/10.1016/j.sbi.2011.08.007.
10. Lanver D, Mendoza-Mendoza A, Brachmann A, Kahmann R. 2010. Sho1 and Msb2-related proteins regulate appressorium development in the smut fungus *Ustilago maydis*. Plant Cell 22:2085–2101. http://dx.doi.org/10.1105/tpc.109.073734.
11. Liu W, Zhou X, Li G, Li L, Kong L, Wang C, Zhang H, Xu JR. 2011. Multiple plant surface signals are sensed by different mechanisms in the rice blast fungus for appressorium formation. PLoS Pathog 7:e1001261. http://dx.doi.org/10.1371/journal.ppat.1001261.
12. Perez-Nadales E, Di Pietro A. 2011. The membrane mucin Msb2 regulates invasive growth and plant infection in *Fusarium oxysporum*. Plant Cell 23:1171–1185. http://dx.doi.org/10.1105/tpc.110.075093.
13. Vadaie N, Dionne H, Akajagbor DS, Nickerson SR, Krysan DJ, Cullen PJ. 2008. Cleavage of the signaling mucin Msb2 by the aspartyl protease Yps1 is required for MAPK activation in yeast. J Cell Biol 181:1073–1081. http://dx.doi.org/10.1083/jcb.200704079.
14. Roman E, Cottier F, Ernst JF, Pla J. 2009. Msb2 signaling mucin controls activation of Cek1 mitogen-activated protein kinase in *Candida albicans*. Eukaryot Cell 8:1235–1249. http://dx.doi.org/10.1128/EC.00081-09.
15. Swidergall M, Ernst AM, Ernst JF. 2013. *Candida albicans* mucin Msb2 is a broad-range protectant against antimicrobial peptides. Antimicrob Agents Chemother 57:3917–3922. http://dx.doi.org/10.1128/AAC.00862-13.
16. Whiteway M. 2000. Transcriptional control of cell type and morphogenesis in *Candida* albicans. Curr Opin Microbiol 3:582–588. http://dx.doi.org/10.1016/S1369-5274(00)00144-2.
17. Cantero PD, Ernst JF. 2011. Damage to the glycoshield activates PMT-directed O-mannosylation via the Msb2-Cek1 pathway in *Candida albicans*. Mol Microbiol 80:715–725. http://dx.doi.org/10.1111/j.1365-2958.2011.07604.x.
18. Doedt T, Krishnamurthy S, Bockmuhl DP, Tebarth B, Stempel C, Russell CL, Brown AJ, Ernst JF. 2004. APSES proteins regulate morphogenesis and metabolism in *Candida albicans*. Mol Biol Cell 15:3167–3180. http://dx.doi.org/10.1091/mbc.E03-11-0782.
19. Puri S, Kumar R, Chadha S, Tati S, Conti HR, Hube B, Cullen PJ, Edgerton M. 2012. Secreted aspartic protease cleavage of *Candida albicans* Msb2 activates Cek1 MAPK signaling affecting biofilm formation and oropharyngeal candidiasis. PLoS One 7:e46020. http://dx.doi.org/10.1371/journal.pone.0046020.
20. Nijnik A, Hancock REW. 2009. The roles of cathelicidin LL-37 in immune defences and novel clinical applications. Curr Opin Hematol 16:41–47. http://dx.doi.org/10.1097/MOH.0b013e32831ac517.
21. Inglis DO, Arnaud MB, Binkley J, Shah P, Skrzypek MS, Wymore F, Binkley G, Miyasato SR, Simison M, Sherlock G. 2012. The *Candida* genome database incorporates multiple *Candida* species: multispecies search and analysis tools with curated gene and protein information for *Candida albicans* and *Candida glabrata*. Nucleic Acids Res 40:D667–D674. http://dx.doi.org/10.1093/nar/gkr945.
22. van Helden J, Rios AF, Collado-Vides J. 2000. Discovering regulatory elements in non-coding sequences by analysis of spaced dyads. Nucleic Acids Res 28:1808–1818. http://dx.doi.org/10.1093/nar/28.8.1808.
23. de Boer CG, Hughes TR. 2012. YeTFaSCo: a database of evaluated yeast transcription factor sequence specificities. Nucleic Acids Res 40:D169–D179. http://dx.doi.org/10.1093/nar/gkr993.
24. Newcomb LL, Hall DD, Heideman W. 2002. AZF1 is a glucose-

dependent positive regulator of CLN3 transcription in *Saccharomyces cerevisiae*. Mol Cell Biol 22:1607–1614. http://dx.doi.org/10.1128/MCB.22.5.1607-1614.2002.
25. Yan L, Yang C, Tang J. 2013. Disruption of the intestinal mucosal barrier in *Candida albicans* infections. Microbiol Res 168:389–395. http://dx.doi.org/10.1016/j.micres.2013.02.008.
26. de Dios CH, Roman E, Monge RA, Pla J. 2010. The role of MAPK signal transduction pathways in the response to oxidative stress in the fungal pathogen *Candida albicans*: implications in virulence. Curr Protein Pept Sci 11:693–703. http://dx.doi.org/10.2174/138920310794557655.
27. Maeda T, Inoue M, Koshiba S, Yabuki T, Aoki M, Nunokawa E, Seki E, Matsuda T, Motoda Y, Kobayashi A, Hiroyasu F, Shirouzu M, Terada T, Hayami N, Ishizuka Y, Shinya N, Tatsuguchi A, Yoshida M, Hirota H, Matsuo Y, Tani K, Arakawa T, Carninci P, Kawai J, Hayashizaki Y, Kigawa T, Yokoyama S. 2004. Solution structure of the SEA domain from the murine homologue of ovarian cancer antigen CA125 (MUC16). J Biol Chem 279:13174–13182. http://dx.doi.org/10.1074/jbc.M309417200.
28. Gasteiger E, Hoogland C, Gattiker A, Duvaud Se Wilkins M, Appel R, Bairoch A. 2005. Protein identification and analysis tools on the ExPASy server, p 571–607. *In* Walker J (ed), The proteomics protocols handbook. Humana Press, Totowa, NJ.
29. Navarro-Garcia F, Alonso-Monge R, Rico H, Pla J, Sentandreu R, Nombela C. 1998. A role for the MAP kinase gene *MKC1* in cell wall construction and morphological transitions in *Candida* albicans. Microbiology 144:411–424. http://dx.doi.org/10.1099/00221287-144-2-411.
30. Navarro-Garcia F, Eisman B, Fiuza SM, Nombela C, Pla J. 2005. The MAP kinase Mkc1p is activated under different stress conditions in *Candida albicans*. Microbiology 151:2737–2749. http://dx.doi.org/10.1099/mic.0.28038-0.
31. Kumamoto CA. 2005. A contact-activated kinase signals *Candida albicans* invasive growth and biofilm development. Proc Natl Acad Sci U S A 102:5576–5581. http://dx.doi.org/10.1073/pnas.0407097102.
32. Walker LA, Munro CA, de Bruijn I, Lenardon MD, McKinnon A, Gow NA. 2008. Stimulation of chitin synthesis rescues *Candida albicans* from echinocandins. PLoS Pathog 4:e1000040. http://dx.doi.org/10.1371/journal.ppat.1000040.
33. Cantero PD, Lengsfeld C, Prill SK, Subanovic M, Roman E, Pla J, Ernst JF. 2007. Transcriptional and physiological adaptation to defective protein-*O*-mannosylation in *Candida albicans*. Mol Microbiol 64:1115–1128. http://dx.doi.org/10.1111/j.1365-2958.2007.05723.x.
34. Stoldt VR, Sonneborn A, Leuker CE, Ernst JF. 1997. Efg1p, an essential regulator of morphogenesis of the human pathogen *Candida albicans*, is a member of a conserved class of bHLH proteins regulating morphogenetic processes in fungi. EMBO J 16:1982–1991. http://dx.doi.org/10.1093/emboj/16.8.1982.
35. Oppizzi ML, Akhavan A, Singh M, Fata JE, Muschler JL. 2008. Nuclear translocation of beta-dystroglycan reveals a distinctive trafficking pattern of autoproteolyzed mucins. Traffic 9:2063–2072. http://dx.doi.org/10.1111/j.1600-0854.2008.00822.x.
36. Kleene R, Mzoughi M, Joshi G, Kalus I, Bormann U, Schulze C, Xiao MF, Dityatev A, Schachner M. 2010. NCAM-induced neurite outgrowth depends on binding of calmodulin to NCAM and on nuclear import of NCAM and fak fragments. J Neurosci 30:10784–10798. http://dx.doi.org/10.1523/JNEUROSCI.0297-10.2010.
37. De Strooper B, Annaert W, Cupers P, Saftig P, Craessaerts K, Mumm JS, Schroeter EH, Schrijvers V, Wolfe MS, Ray WJ, Goate A, Kopan R. 1999. A presenilin-1-dependent gamma-secretase-like protease mediates release of Notch intracellular domain. Nature 398:518–522. http://dx.doi.org/10.1038/19083.
38. Lammich S, Okochi M, Takeda M, Kaether C, Capell A, Zimmer AK, Edbauer D, Walter J, Steiner H, Haass C. 2002. Presenilin-dependent intramembrane proteolysis of CD44 leads to the liberation of its intracellular domain and the secretion of an Abeta-like peptide. J Biol Chem 277:44754–44759. http://dx.doi.org/10.1074/jbc.M206872200.
39. Ni CY, Murphy MP, Golde TE, Carpenter G. 2001. γ-Secretase cleavage and nuclear localization of ErbB-4 receptor tyrosine kinase. Science 294:2179–2181. http://dx.doi.org/10.1126/science.1065412.
40. Brown NA, Dos Reis TF, Goinski AB, Savoldi M, Menino J, Almeida MT, Rodrigues F, Goldman GH. 8 October 2014. The *Aspergillus nidulans* signalling mucin MsbA regulates starvation responses, adhesion and affects cellulase secretion in response to environmental cues. Mol Microbiol http://dx.doi.org/10.1111/mmi.12820.
41. Gregori C, Glaser W, Frohner IE, Reinoso-Martin C, Rupp S, Schuller C, Kuchler K. 2011. Efg1 controls caspofungin-induced cell aggregation of *Candida albicans* through the adhesin Als1. Eukaryot Cell 10:1694–1704. http://dx.doi.org/10.1128/EC.05187-11.
42. Sonneborn A, Bockmuhl DP, Gerads M, Kurpanek K, Sanglard D, Ernst JF. 2000. Protein kinase A encoded by *TPK2* regulates dimorphism of *Candida albicans*. Mol Microbiol 35:386–396. http://dx.doi.org/10.1046/j.1365-2958.2000.01705.x.
43. Fonzi WA, Irwin MY. 1993. Isogenic strain construction and gene mapping in *Candida albicans*. Genetics 134:717–728.
44. Csank C, Schroppel K, Leberer E, Harcus D, Mohamed O, Meloche S, Thomas DY, Whiteway M. 1998. Roles of the *Candida albicans* mitogen-activated protein kinase homolog, Cek1p, in hyphal development and systemic candidiasis. Infect Immun 66:2713–2721.
45. Brown DH, Jr, Giusani AD, Chen X, Kumamoto CA. 1999. Filamentous growth of *Candida albicans* in response to physical environmental cues and its regulation by the unique *CZF1* gene. Mol Microbiol 34:651–662. http://dx.doi.org/10.1046/j.1365-2958.1999.01619.x.
46. Lo HJ, Kohler JR, DiDomenico B, Loebenberg D, Cacciapuoti A, Fink GR. 1997. Nonfilamentous *C. albicans* mutants are avirulent. Cell 90:939–949. http://dx.doi.org/10.1016/S0092-8674(00)80358-X.
47. Liu H, Kohler J, Fink GR. 1994. Suppression of hyphal formation in *Candida albicans* by mutation of a *STE12* homolog. Science 266:1723–1726. http://dx.doi.org/10.1126/science.7992058.
48. Bockmuhl DP, Krishnamurthy S, Gerads M, Sonneborn A, Ernst JF. 2001. Distinct and redundant roles of the two protein kinase A isoforms Tpk1p and Tpk2p in morphogenesis and growth of *Candida albicans*. Mol Microbiol 42:1243–1257. http://dx.doi.org/10.1046/j.1365-2958.2001.02688.x.

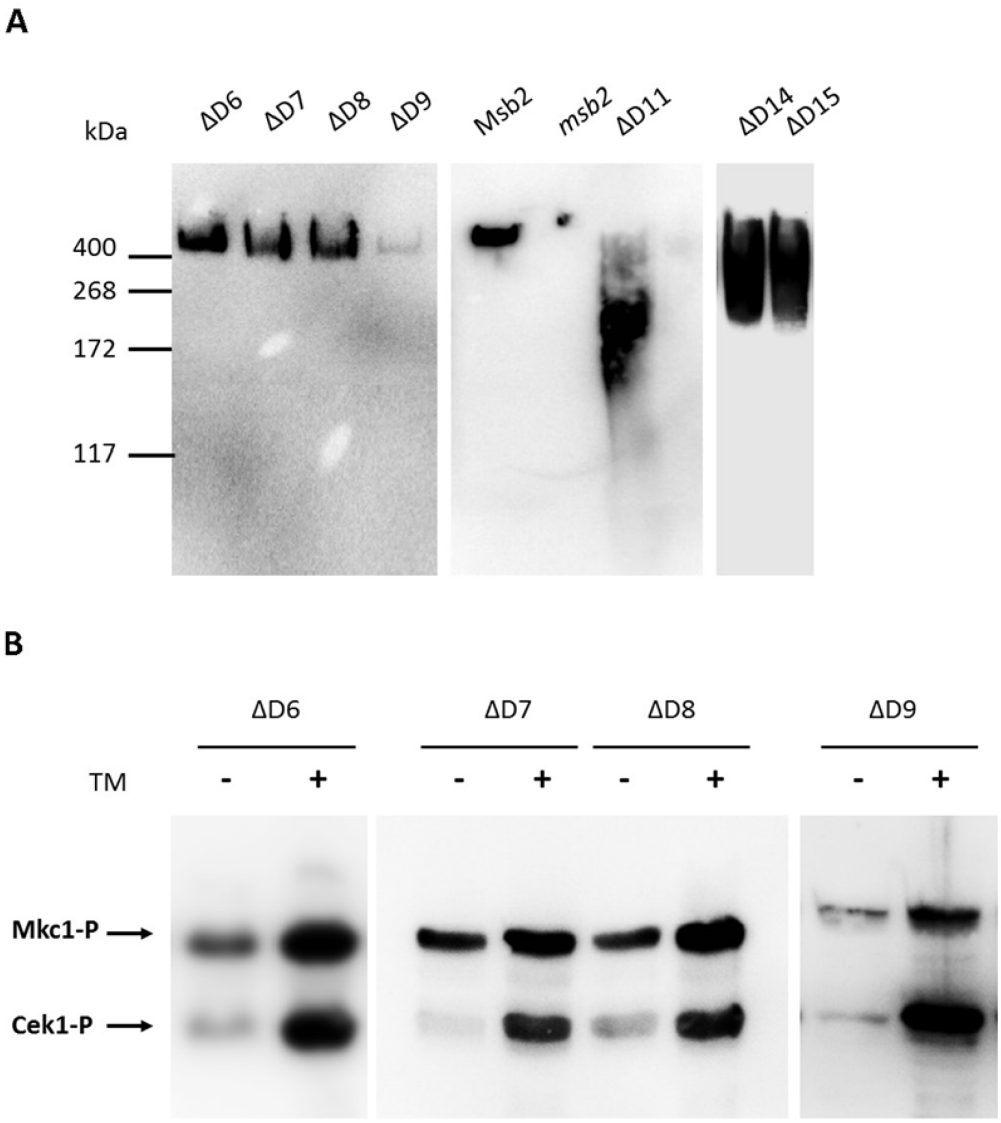

Figure S1. A. Shedding of Msb2 variants. Immunoblot to detect shed HA-tagged Msb2. Proteins in the growth medium (15 µl) were separated by a 4-20 % SDS-PAGE gel and immunoblots were reacted with rat anti-HA antibody. Strains tested included ESCa3 (Msb2; *MSB2*$^{HA\text{-}V5}$), FCCa27 (*msb2*), MSCa34 (ΔD6), MSCa30 (ΔD8), MSCa31 (ΔD7), MSCa48 (ΔD9), MSCa37 (ΔD11), MSCa29 (ΔD14) and MSCa8 (ΔD15). **B. Cek1 activation triggered by Msb2 variants.** Cek1 activation by strains producing variant Msb2 proteins. Cells were grown to stationary phase, diluted in fresh YPD medium, grown to OD_{600} = 0.8 at 37°C and incubated further for 1 h in the presence (+) or absence (–) of tunicamycin (2 µg/ml). Cell extracts (50 µg) were separated by SDS-PAGE and immunoblots were reacted with with anti-phospho-p44/42 MAP kinase antibody, which detects phosphorylated Cek1 (Cek1-P) and Mkc1 (Mkc1-P) proteins. Strains tested included MSCa34 (ΔD6), MSCa30 (ΔD8), MSCa31 (ΔD7) and MSCa48 (ΔD9).

Supplemental Table 1- Oligonucleotides

Name	Sequence
Msb2-15ASDel1 Fwd	5'-GAT TAG TTA CTG ATG ATC AAC AAG TTT CAA TGG ATA TAG TTT CCA ATA C-3'
Msb2-15ASDel1 Rev	5'-GTA TTG GAA ACT ATA TCC ATT GAA ACT TGT TGA TCA TCA GTA ACT AAT C-3'
Msb2-15ASDel2 Fwd	5'-AGT TGC CGA TAA AGG AAG AAT TGC TGG TAT AAC CAT TGG TGC AGC AGC AG-3'
Msb2-15ASDel2 Rev	5'-CTG CTG CTG CAC CAA TGG TTA TAC CAG CAA TTC TTC CTT TAT CGG CAA CT-3'
Msb2 Seq C	5'-CGC CTC GAG CTA ATG ATA CC-3'
Msb2 Seq N	5'-CGC TGT TCT CAC CAG GAT TTA TTG C-3'
Kolo AMP Fwd	5'-GTT GGC CGC AGT GTT ATC-3'
Kolo LEU2 Rev	5'-CACA CTG ATG CTG CTC AGG-3'
Msb2-Del6 Fwd	5'-CCC ACC CAA TCA CCA TCA CAA-3'
Msb2-Del6 Rev	5'- AGG GTT CGC ATA GTC AGG AAC-3'
Msb2-Del7 Fwd	5'-GCT ACA GTT ACT GGT AGT GAA TC-3'
Msb2-Del7 Rev	5'-GGG AAT ATT ACT GCT TTC TG-3'
Msb2-delta PTS Fwd	5'-GTG AAA GCT TTA GGT AGT TTT ATA ACT ACT GCT ATC TAT AGA AAT CCT GAC AGT GTT TTA CAA G-3'
Msb2-delta PTS Rev	5'-CTT GTA AAA CAC TGT CAG GAT TTC TAT AGA TAG CAG TAG TTA TAA AAC TAC CTA AAG CTT TCA C-3'
Msb2-Del9 Fwd	5'-GCT GAG CCA TCA AGT GAA GTT ACC-3'
Msb2-Del9 Rev	5'-GAT TTG TTC AGA TGA TTC TGT AAC-3'
Msb2-Del10 Fwd	5'-CAA ACC GGA ACT TCA GCT GTC-3'
Msb2-Del10 Rev	5'-GGC AAT TGG AGT GGT GGT AGA-3'
Msb2-Del11 Fwd	5'-GAA GTT ACC GCA GTT GCT CCT TC-3'
Msb2-Del11 Rev	5'-CAA TGC AGT TTC AAC TCC ACT TTG-3'
Msb2-Del12 Fwd	5'-GAT AGT AAT CCA TCT ACT AAT TC-3'
Msb2-Del12 Rev	5'-CTC AGC TGA TGC TGG TGG AGA TG-3'
RTACT1 Fwd	5'-CAA CTG GGA CGA TAT GGA AAA AA-3'
RTACT1 Rev	5'-TTC GGT CAA CAA AAC TGG ATG T-3'
RTACT1long Fwd	5'-GAC TTG ACC AAC CAT TTG TCC-3'
RTACT1long Rev	5'-TCA TGA TGG AGT TGA AAG TGG-3'
RTPMT1 Fwd	5'- GCT GCT GAA CCT GTT GAA GA-3'
RTPMT1 Rev	5'- CAT CAG CAA CTT GTG GGT CT-3'
RTALS1 Fwd	5'-GAC TAG TGA ACC AAC AAA TAC CAG A-3'
RTALS1 Rev	5'-CCA GAA GAA ACA GCA GGT GA-3'
18S-rRNA(RT)-f	5'-CGA TGG AAG TTT GAG GCA AT-3'
18S-rRNA(RT)-r	5'-CAC GAC GGA GTT TCA CAA GA-3'

Table S2. Transcriptomal analysis of genes regulated by the C-tail of Msb2. Genes up/down-regulated in response to caspofungin treatment in strain ESCa38 (ΔD1) compared to control strain ESCa3 (Msb2) are listed. Fold regulation is shown for downregulated transcripts (negative values) and upregulated transcripts (positive values). **MSB2* gene expressed from *ACT1*-promoter.

Name	fold regulation	Gene	Description
NOVEL-C121chr7-051	-4.19	*NOVEL TRANSCRIPT 73*	
ORF19.1150	-3.44		Predicted ORF in Assemblies 19, 20 and 21; regulated by Gcn2p and Gcn4p
ORF19.1105	-3.28		
NOVEL-Ca21chr3-021	-2.94	*NOVEL TRANSCRIPT 329*	
ORF19.4575	-2.64		*S. cerevisiae* ortholog YPL109C localizes to mitochondrion
ORF19.7265	-2.56		Hap43p-repressed gene
ORF19.7301	-2.54		
NOVEL-C121chr5-011(+)	-2.49	*NOVEL TRANSCRIPT 58*	
*ORF19.1490**	-2.46	*MSB2**	Adhesin-like protein; mucin family; cell wall damage sensor; N-terminal secretion signal; required for Cek1p phosphorylation in response to cell wall stress; Rim101p-repressed; activation releases extracellular domain into medium
ORF19.3774	-2.41	*PPG1*	Putative protein phosphatase of the Type 2A-related family (serine/threonine-specific), similar to *S. cerevisiae* Ppg1p; possibly an essential gene, disruptants not obtained by UAU1 method
ORF19.5606	-2.36		
ORF19.2201	-2.32		*S. cerevisiae* ortholog CBP6 localizes to mitochondrion
ORF19.3158	-2.32		*S. cerevisiae* ortholog RMD1 localizes to cytoplasm
NOVEL-C121chr2-076	-2.21	*NOVEL TRANSCRIPT 33*	
ORF19.4097	-2.15		
ORF19.7609	-2.10	*PGA11*	Putative GPI-anchored protein
ORF19.3607	-2.06		
ORF19.2436	-2.03		Ortholog of *C. glabrata* CAGL0F03905g
ORF19.5565	-2.02		Putative 3-hydroxyisobutyrate dehydrogenase
NOVEL-Ca21chr1-130	-2.01	*NOVEL TRANSCRIPT 210*	
ORF19.3622	-2.01	*ANP1*	Putative mannosyltransferase of Golgi; member of Mnn9p family; similar to *S. cerevisiae* Anp1p; fungal-specific (no human or murine homolog)
ORF19.6674	-1.91	*BTS1*	Putative geranylgeranyl diphosphate synthase; decreased transcription is observed upon benomyl treatment
NOVEL-Ca21chrR-091	-1.90	*NOVEL TRANSCRIPT 656*	
NOVEL-Ca21chr7-040	-1.90	*NOVEL TRANSCRIPT 570*	
NOVEL-Ca21chr2-025	-1.90	*NOVEL TRANSCRIPT 238*	
ORF19.3229	-1.89		Predicted ORF in Assemblies 19, 20 and 21; transcription detected in high-resolution tiling array experiments
ORF19.2131	-1.86		*S. cerevisiae* ortholog TUL1 has ubiquitin-protein ligase activity, has role in protein ubiquitination, ubiquitin-dependent protein catabolic process via the multivesicular body sorting pathway and localizes to Golgi apparatus
ORF19.4279	-1.86	*MNN1*	Putative alpha-1,3-mannosyltransferase, a component of mannosyltransferase complex; transcription negatively regulated by Rim101p; transcription elevated in chk1 and nik1 null mutants, but not in sln1 null mutant; biofilm-induced gene
ORF19.2809	-1.85	*CTN3*	Predicted peroxisomal carnitine acetyl transferase; Ura+ deletion strain has no obvious metabolic, hyphal, or virulence defects; transcription induced by macrophage

			engulfment, hyphal growth, starvation, or nonfermentable carbon sources
ORF19.1913	-1.82		Late-stage biofilm-induced gene
NOVEL-Ca21chr6-040	-1.81	*NOVEL TRANSCRIPT 530*	
NOVEL-Ca21chr4-004(+)	-1.80	*NOVEL TRANSCRIPT 381*	
ORF19.5622	-1.79	*GLC3*	Putative 1,4-glucan branching enzyme; fluconazole-induced; shows colony morphology-related gene regulation by Ssn6p; stationary phase enriched protein; planktonic growth-induced gene
ORF19.3690.2	-1.78		*S. cerevisiae* ortholog RPL26B has RNA binding, structural constituent of ribosome, has role in translation and localizes to cytosolic large ribosomal subunit
ORF19.644	-1.69	*HGT9*	Putative glucose transporter of the major facilitator superfamily; the C. albicans glucose transporter family comprises 20 members; 12 probable membrane-spanning segments; induced at low (0.2%, compared to 2%) glucose in rich media; intron
ORF19.7660	-1.67	*VPS52*	Protein required for hyphal growth; has similarity to *S. cerevisiae* Vps52p
ORF19.1959	-1.66		*S. cerevisiae* ortholog *OTU2* localizes to ribosome, cytoplasm
C11lfMt26	-1.64		
NOVEL-Ca21chrR-042	-1.62	*NOVEL TRANSCRIPT 614*	
ORF19.5665	-1.60		*S. cerevisiae* ortholog ARA2 has D-arabinose 1-dehydrogenase [NAD(P)+] activity and has role in dehydro-D-arabinono-1,4-lactone biosynthetic process
NOVEL-Ca21chr5-001	-1.58	*NOVEL TRANSCRIPT 447*	
NOVEL-Ca21chr5-042	-1.58	*NOVEL TRANSCRIPT 484*	
ORF19.1636	-1.57	*STE50*	Protein with sterile alpha motif (SAM) and Ras-associated domain (RAD); similar to *S. cerevisiae* Rad50p, which is involved in signal transduction via interaction with and regulation of MAPKKK
ORF19.6462	-1.57		*S. cerevisiae* ortholog AIM27 has role in protein folding in endoplasmic reticulum and localizes to ER membrane protein complex
ORF19.3785	-1.57		
ORF19.4676	-1.56		
ORF19.7370	-1.56		Member of family of putative 7-transmembrane, PQ loop-family of G-protein-coupled receptors (GPCRs) similar to S. pombe Stm1p
ORF19.1536	-1.51		Putative vacuolar transporter; Hap43p-induced gene, required for normal filamentous growth; mRNA binds to She3p and is localized to hyphal tips
ORF19.5736	-1.51	*ALS5*	ALS family adhesin; highly variable; expression in *S. cerevisiae* causes adhesion to human epithelium, endothelium or ECM, endothelial invasiveness by endocytosis and, at high abundance, ECM-induced aggregation; can form amyloid fibrils
ORF19.1428	-1.50	*DUO1*	Subunit of the Dam1 (DASH) complex, which acts in chromosome segregation by coupling kinetochores to spindle microtubules
ORF19.344	-1.50		Predicted ORF in Assemblies 19, 20 and 21; increased transcription is observed upon fluphenazine treatment or in an azole-resistant strain that overexpresses CDR1 and CDR2; possibly transcriptionally regulated by Tac1p
ORF19.4491	3.05	*ERG20*	Putative farnesyl pyrophosphate synthetase involved in isoprenoid and sterol biosynthesis, based on similarity to *S. cerevisiae* Erg20p; likely to be essential for growth, based on an insertional mutagenesis strategy
ORF19.548	2.85	*CDC10*	Septin, required for wild-type cell, hyphal, or chlamydospore morphology; role in virulence and kidney tissue invasion in a mouse model of systemic infection; forms ring at sites of cell division and filaments in mature chlamydospore
NOVEL-Ca21chr4-027	2.59	*NOVEL TRANSCRIPT 401*	

ORF19.1868	2.53	*RNR22*	Putative ribonucleoside diphosphate reductase; shows colony morphology-related gene regulation by Ssn6p; RNA abundance regulated by tyrosol and cell density; Hap43p-repressed gene; biofilm- and planktonic growth-induced
ORF19.5741	2.51	*ALS1*	Adhesin; ALS family of cell-surface glycoproteins; adhesion, virulence roles; immunoprotective; band at hyphal base; amyloid domain; biofilm-induced; Rfg1p, Ssk1p; strain background affects expression; N-term binds fucose-containing glycans
ORF19.6022	2.46	*NRM1*	Transcriptional regulator of cell cycle gene expression; regulates expression of genes involved in DNA replication stress; interacts with Swi4 and Swi6; repressed during core stress response; Spider biofilm repressed
ORF19.2529.1	2.44		
*ORF19.280*_Antisense	2.43	*ANTISENSE-ORF19.280*	
ORF19.257	2.34		Transcription is negatively regulated by Sfu1p; repressed by nitric oxide
ORF19.5419	2.33	*ATP5*	Putative F0-ATP synthase FO subunit B; caspofungin repressed; protein level decreased in stationary phase yeast cultures
ORF19.2640	2.31	*FUR1*	Uracil phosphoribosyltransferase; predicted tetrameric enzyme of pyrimidine salvage; mutations associated with flucytosine resistance in clade I clinical isolates; flucytosine, macrophage-induced protein; levels decrease in stationary phase
ORF19.5586	2.30		*S. cerevisiae* ortholog FIG4 has phosphatidylinositol-3,5-bisphosphate 5-phosphatase activity, has role in phosphatidylinositol dephosphorylation and localizes to fungal-type vacuole membrane, extrinsic to membrane, PAS complex
ORF19.2093	2.28	*RFA1*	Putative DNA replication factor A; RNA abundance regulated by cell cycle, tyrosol and cell density
ORF19.4979	2.24	*KNS1*	*S. cerevisiae* ortholog KNS1 has protein tyrosine kinase activity, protein serine/threonine kinase activity and has role in protein autophosphorylation
ORF19.6753	2.22		Predicted ORF in Assemblies 19, 20 and 21; possibly an essential gene, disruptants not obtained by UAU1 method
ORF19.1353	2.21		Biofilm-and planktonic growth-induced gene; transcription downregulated upon yeast-hyphal switch; Ras1p-regulated
ORF19.4026	2.18	*HIS1*	ATP phosphoribosyl transferase; enzyme of histidine biosynthesis; fungal-specific (no human, murine homolog); upregulated in biofilm; acid upregulated/alkaline downregulated by Rim101p; regulated by Gcn2p, Gcn4p; strain CA9 is a his1 mutant
ORF19.2364	2.18	*MIS11*	Similar to precursor of mitochondrial C1-tetrahydrofolate synthase; putative protein of glycine catabolism; downregulated by Efg1p; fluconazole-induced; stationary phase enriched protein
ORF19.2180	2.14		Ortholog of C. glabrata CAGL0K04433g
ORF19.3055	2.13		Putative RNA polymerase II mediator complex subunit; possibly an essential gene, disruptants not obtained by UAU1 method
ORF19.1678	2.12		Predicted ORF in Assemblies 19, 20 and 21; transcription detected in high-resolution tiling array experiments
ORF19.3583	2.09		
ORF19.3541	2.09	*ERF1*	Putative translation release factor 1, which interacts with stop codons and promotes release of nascent peptides from ribosomes; Hap43p-induced gene
ORF19.4436	2.09	*GPX3*	Planktonic growth-induced gene
ORF19.497	2.09	*EAF7*	Subunit of the NuA4 histone acetyltransferase complex
ORF19.6634	2.08	*VMA2*	Vacuolar H(+)-ATPase; protein present in exponential and stationary growth phase yeast cultures; plasma membrane localized; amphotericin B repressed, caspofungin repressed
ORF19.2947	2.07	*SNZ1*	Stationary phase protein; soluble in hyphae; induced on yeast to hyphal switch, in response to 3-aminotriazole, or in azole-resistant strain overexpressing MDR1; regulated by Gcn4p, macrophage; no human/murine homolog

ORF19.2183	2.06	*KRE30*	YEF3-subfamily ABC family protein, predicted not to be a transporter; downregulated during core stress response; mutation confers hypersensitivity to amphotericin B
ORF19.1652	2.05	*POX1-3*	Predicted acyl-CoA oxidase; farnesol regulated; stationary phase enriched protein
ORF19.7183	2.03		*S. cerevisiae* ortholog EMC4 has role in protein folding in endoplasmic reticulum and localizes to ER membrane protein complex
ORF19.6882	2.02	*OSM1*	Putative flavoprotein subunit of fumarate reductase; soluble protein in hyphae; fungal-specific (no human or murine homolog); caspofungin repressed; stationary phase enriched protein; biofilm-induced gene
ORF19.2309.2	1.99	*RPL2*	Putative 60S ribosomal protein L2; Hap43p-induced gene; shows downregulation in infected rabbit kidney in SC5314, but not NGY152, strain background
ORF19.1816	1.98	*ALS3*	ALS family cell wall adhesin; role in epithelial adhesion, endothelial invasiveness; allelic variation in adhesiveness; immunoprotective in mice; promotes biofilm formation by binding to SspB adhesin of *S. gordonii*; fluconazole-repressed
ORF19.5812	1.94		*S. cerevisiae* ortholog *ETT1* has role in translational termination and localizes to nucleus
ORF19.5747	1.90		*S. cerevisiae* ortholog *MRP4* has structural constituent of ribosome and localizes to mitochondrial small ribosomal subunit
ORF19.825	1.90	*GCD7*	Putative translation initiator; downregulated in the presence of human whole blood or polymorphonuclear (PMN) cells
ORF19.3895	1.87	*CHT2*	GPI-linked chitinase required for normal filamentous growth; downregulated in core caspofungin response; induced in yeast cells; fluconazole, Cyr1p-, Efg1p-, pH-regulated; mRNA binds She3p, is localized to yeast-form buds and hyphal tips
ORF19.3426	1.87	*ANB1*	Translation initiation factor eIF-5A; decreased expression in hyphae vs to yeast-form cells; genes encoding ribosomal subunits, translation factors, tRNA synthetases are downregulated upon phagocytosis by murine macrophage; Hap43p-induced
ORF19.2560	1.87	*CDC60*	Cytosolic leucyl tRNA synthetase; conserved amino acid and ATP binding class I signature, tRNA binding, proofreading motifs; likely essential for growth; interacts with benzoxaborole antifungals; present in exponential and stationary phase
ORF19.5911	1.85	*CMK1*	Putative calcium/calmodulin-dependent protein kinase II; expression regulated upon white-opaque switching; biochemically purified Ca2+/CaM-dependent kinase is soluble, cytosolic, monomeric, and serine-autophosphorylated; Hap43p-repressed
ORF19.4851	1.83	*TFA1*	Protein with polyglutamate motifs and abundant Ser/Thr residues; described as a subunit of TFIIE, which is a basal transcription initiation factor of RNA Polymerase II; possibly an essential gene, disruptants not obtained by UAU1 method
ORF19.1064	1.83	*ACS2*	Acetyl-CoA synthetase; antigenic during human and murine infection; upregulated by Efg1p; macrophage-induced protein; soluble protein in hyphae; gene contains an intron
ORF19.862	1.82		
ORF19.211	1.82		
ORF19.3616	1.81	*ERG9*	Putative farnesyl-diphosphate farnesyl transferase (squalene synthase) involved in the sterol biosynthesis pathway; likely to be essential for growth; regulated by fluconazole and lovastatin; amphotericin B, caspofungin repressed
ORF19.2023	1.81	*HGT7*	Putative glucose transporter, major facilitator superfamily; glucose-, fluconazole-, Snf3p-induced, expressed at high glucose; upregulated in biofilm; C. albicans glucose transporter family comprises 20 members; 12 TM regions predicted
ORF19.5660.1	1.80		*S. cerevisiae* ortholog *TIM11* has structural molecule

			activity, proton-transporting ATPase activity, rotational mechanism and has role in ATP synthesis coupled proton transport, cristae formation, protein oligomerization
ORF19.4558	1.80		ORF|Deleted from Assembly 20
ORF19.5074	1.80		*S. cerevisiae* ortholog *UBA2* has SUMO activating enzyme activity, has role in protein sumoylation and localizes to SUMO activating enzyme complex
ORF19.4865	1.77		*S. cerevisiae* ortholog *SAC1* has role in phosphatidylinositol dephosphorylation
ORF19.5801	1.76	*RNR21*	Putative ribonucleoside-diphosphate reductase; regulated by tyrosol and cell density; transcription upregulated in response to treatment with ciclopirox olamine; fluconazole or flucytosine induced; Hap43p-induced; planktonic growth-induced
ORF19.899	1.76		
ORF19.1505	1.75		
ORF19.4406	1.74		*S. cerevisiae* ortholog *NIF3* localizes to mitochondrion
ORF19.2876	1.74	*CBF1*	Transcription factor that binds upstream of ribosomal protein genes and the rDNA locus, with Tbf1p; also regulates sulfur starvation-response, respiratory, and glycolytic genes; does not bind to centromeres as does *S. cerevisiae* Cbf1p
ORF19.6766	1.74		Hap43p-induced gene; *S. cerevisiae* ortholog *NOP13*, a nucleolar protein found in preribosomal complexes
NOVEL-Ca21chrR-053	1.73	*NOVEL TRANSCRIPT 624*	
ORF19.7178	1.72	*PRE5*	Alpha6 subunit of the 20S proteasome; regulated by Gcn4p; induced in response to amino acid starvation (3-aminotriazole treatment)
ORF19.3861	1.72	*SIS1*	Putative Type II HSP40 co-chaperone; macrophage/pseudohyphal-repressed; heavy metal (cadmium) stress-induced; heterozygous null mutant displays sensitivity to virgineone
ORF19.2328	1.71		
ORF19.88	1.67	*ILV5*	Putative ketol-acid reductoisomerase; antigenic during human/murine infection; regulated by Gcn4p; amino acid starvation (3-AT)-induced; biofilm induced; macrophage-downregulated protein; protein present in exponential and stationary phase
ORF19.968	1.67	*PGA14*	Putative GPI-anchored protein; induced during cell wall regeneration; regulated by Ssn6p
ORF19.5425	1.66		*S. cerevisiae* ortholog *TRZ1* has 3'-tRNA processing endoribonuclease activity, has role in tRNA 3'-trailer cleavage, endonucleolytic and localizes to nucleus, mitochondrion
ORF19.954	1.64		Hap43p-repressed gene
ORF19.5495	1.63		Putative RNA-binding protein; not essential for viability; transcription is induced in response to alpha pheromone in SpiderM medium
ORF19.2728	1.62		*S. cerevisiae* ortholog *RAD24* has DNA clamp loader activity, has role in reciprocal meiotic recombination, DNA damage checkpoint, nucleotide-excision repair and localizes to nucleus, Rad17 RFC-like complex
ORF19.3949	1.61		*S. cerevisiae* ortholog *YTA7* has role in positive regulation of isoprenoid metabolic process, positive regulation of transcription from RNA polymerase II promoter, cellular protein localization
ORF19.7284	1.61	*ASR2*	Gene regulated by cAMP and by osmotic stress; greater mRNA abundance observed in a cyr1 or ras1 homozygous null mutant than in wild type; stationary phase enriched protein
ORF19.6893	1.60		*S. cerevisiae* ortholog *RUD3* has role in ER to Golgi vesicle-mediated transport
ORF19.5982	1.60	*RPL18*	Predicted ribosomal protein; Plc1p-regulated, Tbf1p-activated; genes encoding cytoplasmic ribosomal subunits, translation factors, tRNA synthetases are downregulated upon phagocytosis by murine macrophage; Hap43p-induced gene

ORF19.5943	1.59		*S. cerevisiae* ortholog *PEX28* has role in peroxisome organization and localizes to peroxisomal membrane
ORF19.5285	1.57	*PST3*	Putative flavodoxin; biofilm induced; fungal-specific (no human or murine homolog); stationary phase enriched protein
ORF19.7292	1.57	*ARP2*	Putative component of the Arp2/3 complex; required for virulence, hyphal growth, and cell wall and cytoskeleton organization, but not for endocytosis; mutation confers hypersensitivity to cytochalasin D; regulated by Gcn2p and Gcn4p
ORF19.5854	1.56	*SBP1*	Similar to RNA binding proteins; downregulated upon adherence to polystyrene; stationary-phase enriched protein
ORF19.6403	1.55		*S. cerevisiae* ortholog SIL1 has adenyl-nucleotide exchange factor activity, has role in SRP-dependent cotranslational protein targeting to membrane, translocation and localizes to endoplasmic reticulum
ORF19.6773	1.55	*ECM29*	Protein similar to *S. cerevisiae* Ecm29p; transposon mutation affects filamentous growth
ORF19.3182	1.55	*GIS2*	Putative transcription factor; expression is increased in high iron and reduced upon yeast-hyphal switch; null mutant exhibits sensitivity to sorbitol, 5-fluorocytosine, and cold temperatures
ORF19.4520	1.54		*S. cerevisiae* ortholog YDR248C localizes to cytoplasm
ORF19.1142	1.52		Putative vacuolar transporter of large neutral amino acids; transcription is induced in response to alpha pheromone in SpiderM medium
ORF19.4432	1.51	*KSP1*	Putative serine/threonine protein kinase; mRNA binds to She3p and is localized to hyphal tips; mutation confers hypersensitivity to amphotericin B
ORF19.5467	1.50	*TLO7*	Member of a family of telomere-proximal genes of unknown function; may be spliced in vivo
ORF19.5963	1.50		*S. cerevisiae* ortholog *NUS1* has role in protein glycosylation and localizes to endoplasmic reticulum, lipid particle, nuclear envelope
ORF19.4468	1.50		Putative succinate dehydrogenase; localized to the mitochondrial membrane; Hap43p-repressed gene

Table S3. GO analysis of genes regulated by the C-tail of Msb2. Regulated genes listed in Table S2 were categorized for their functions using GO programs **A.** Term Finder (www.candidagenome.org/cgi-bin/GO/goTermFinder) and **B.** Slim Mapper (www.candidagenome.org/cgi-bin/GO/goTermMapper). In cells lacking the Msb2 C-tail upregulated genes are in red, while downregulated genes are in blue color.

A

GO term	Cluster frequency	Background frequency	Corrected P-value	False discovery rate	Gene(s) annotated to the term
entry into host cell	3 out of 117 genes, 2.6%	4 out of 6473 background genes, 0.1%	0.01352	4.00%	*ALS5*, *ALS1*, *ALS3*
entry into cell of other organism involved in symbiotic interaction	3 out of 117 genes, 2.6%	4 out of 6473 background genes, 0.1%	0.01352	2.00%	*ALS5*, *ALS1*, *ALS3*

B

GO term	Frequency	Gene(s)
response to stress	19 out of 117 genes, 16.2%	*GPX3*, *ORF19.2728*, *STE50*, *MSB2*, *RFA1*, *SIS1*, *ORF19.211*, *GIS2*, *ECM29*, *SBP1*, *CMK1*, *ARP2*, *CHT2*, *AVT4*, *PGA14*, *ORF19.1536*, *VPS52*, *EAF7*, *ERF1*
cellular protein modification process	16 out of 117 genes, 13.6%	*PPG1*, *GPX3*, *ORF19.2436*, *ORF19.5963*, *RFA1*, *KNS1*, *KSP1*, *CMK1*, *ORF19.2131*, *ORF19.1959*, *ACS2*, *MNN1*, *ANP1*, *ANB1*, *UBA2*, *EAF7*
response to chemical	15 out of 117 genes, 12.7%	*GPX3*, *ORF19.2436*, *HGT7*, *STE50*, *NRM1*, *CBF1*, *SIS1*, *GIS2*, *KSP1*, *CMK1*, *KRE30*, *ARP2*, *PGA14*, *ORF19.1536*, *FUR1*

2.6 Manuskript V: A surprising role for the Sch9 protein kinase in chromosome segregation in *Candida albicans*

Neha Varshney, Alida Schaekel, Rima Singha, Tanmoy Chakraborty, **Lasse van Wijlick**, Joachim F. Ernst, Kaustuv Sanyal

Koautor

Beitrag zum Manuskript: 15 %

Lasse van Wijlick hat einen Teil der Experimente durchgeführt und die Daten ausgewertet. Darüber hinaus hat er einen Teil der Abbildungen (Fig.1) erstellt und die entsprechenden Schlussfolgerungen für das Manuskript formuliert.

Veröffentlicht in: Genetics, January 2015; 199(3): 671-674.

Impact Factor: 5.963 (2014)

GENETICS | COMMUNICATIONS

A Surprising Role for the Sch9 Protein Kinase in Chromosome Segregation in *Candida albicans*

Neha Varshney,*,[1] Alida Schaekel,[†,‡,1] Rima Singha,* Tanmoy Chakraborty,*,[2] Lasse van Wijlick,[†,‡] Joachim F. Ernst,[†,‡,3] and Kaustuv Sanyal*,[3]

*Molecular Mycology Laboratory, Jawaharlal Nehru Centre for Advanced Scientific Research, Jakkur, Bangalore 560064, India, and [†]Department Biologie, Molekulare Mykologie and [‡]Manchot Graduate School Molecules of Infection, Heinrich-Heine-Universität, Düsseldorf 40225, Germany

ORCID ID: 0000-0002-6611-4073 (K.S.).

ABSTRACT The AGC kinase Sch9 regulates filamentation in *Candida albicans*. Here, we show that Sch9 binding is most enriched at the centromeres in *C. albicans*, but not in *Saccharomyces cerevisiae*. Deletion of CaSch9 leads to a 150- to 750-fold increase in chromosome loss. Thus, we report a previously unknown role of Sch9 in chromosome segregation.

KEYWORDS kinase, Sch9, centromere, chromosome segregation, kinetochore

TARGET of rapamycin complex 1 (TORC1) is a major regulator of cell growth and a nutrient sensor in all eukaryotic cells. In the pathogenic yeast *Candida albicans*, the AGC kinase Sch9, one of the direct downstream targets of TORC1, represses filamentation in hypoxia and under high CO_2 conditions. Sch9 performs distinct functions in growth and morphogenesis depending on the availability of O_2 and CO_2 (Stichternoth *et al.* 2011). Earlier studies indicated that absence of Sch9 increases the chronological life span of *Saccharomyces cerevisiae* (Fabrizio *et al.* 2001). However, *sch9* mutant cells of *C. albicans* have a reduced longevity only under normoxic conditions and not under hypoxic conditions (Stichternoth *et al.* 2011).

In this study, we sought to determine the genomic binding sites of the HA-tagged Sch9 protein by ChIP on chip (ChIP-chip) experiments under normoxia as well as hypoxia with and without elevated CO_2 levels in *C. albicans*. Remarkably, the major binding peaks of Sch9 coincided with the centromere (*CEN*) regions. Centromeric Sch9 binding was observed under normoxia (Figure 1A) as well as under hypoxia with or without 6% CO_2 (Figure 1B). Under all conditions, a few reproducible Sch9 binding peaks occurred outside the *CEN* regions as well (not shown). The ChIP-chip data were validated by semiquantitative (data not shown) and quantitative PCR (qPCR) analysis using *CEN5*- and *CEN7*-specific primers (Figure 1C).

Enrichment of Sch9 binding at *CEN* regions led us to examine its possible role in the stability of the kinetochore, a multiprotein complex formed on the *CEN* DNA. The centromere–kinetochore complex plays a central role in the microtubule–kinetochore-mediated process of chromosome segregation. First, we analyzed the nuclear morphology in wild-type (CAI4) and mutant cells (CAS1 and CCS3) (strain construction, Southern confirmation, and genotype of strains are described in the Supporting Information, File S1, Figure S1 and Table S1, respectively). Except for a marginal increase in proportion of large-budded cells (at G2/M stage) with the unsegregated nucleus in the *sch9* mutant cells (CAS1 and CCS3) as compared to the wild type (CAI4), no significant difference was evident (Figure S2). A marginal increase observed in the proportion of large-budded mutant cells having an unsegregated nuclear mass as compared to wild type is insignificant, since the wild-type cells also showed unsegregated DNA mass, as expected, during the pre-anaphase stage of the cell cycle. Moreover, a significant delay in G1 in the *sch9* mutant added to the complexity of analysis. Like *S. cerevisiae*, centromeres are clustered

doi: 10.1534/genetics.114.173542
Manuscript received December 11, 2014; accepted for publication January 6, 2015; published Early Online January 15, 2015.
Supporting information is available online at http://www.genetics.org/lookup/suppl/doi:10.1534/genetics.114.173542/-/DC1.
ChIP-chip data have been deposited at http://www.candidagenome.org/download/systematic_results/Chakraborty_2014/.
[1]These authors contributed equally to this work.
[2]Present address: Department of Microbiology, University of Szeged, Ko˝ze´pfasor, Szeged, Hungary 672.
[3]Corresponding authors: Department Biologie, Molekulare Mykologie, Heinrich-Heine-Universität Düsseldorf, Universitätsstr.1/Geb. 26.12, 40225 Düsseldorf, Germany. E-mail: joachim.ernst@uni-duesseldorf.de; Molecular Mycology Laboratory, Molecular Biology and Genetics Unit, Jawaharlal Nehru Centre for Advanced Scientific Research, Jakkur, Bangalore 560064, India. E-mail: sanyal@jncasr.ac.in

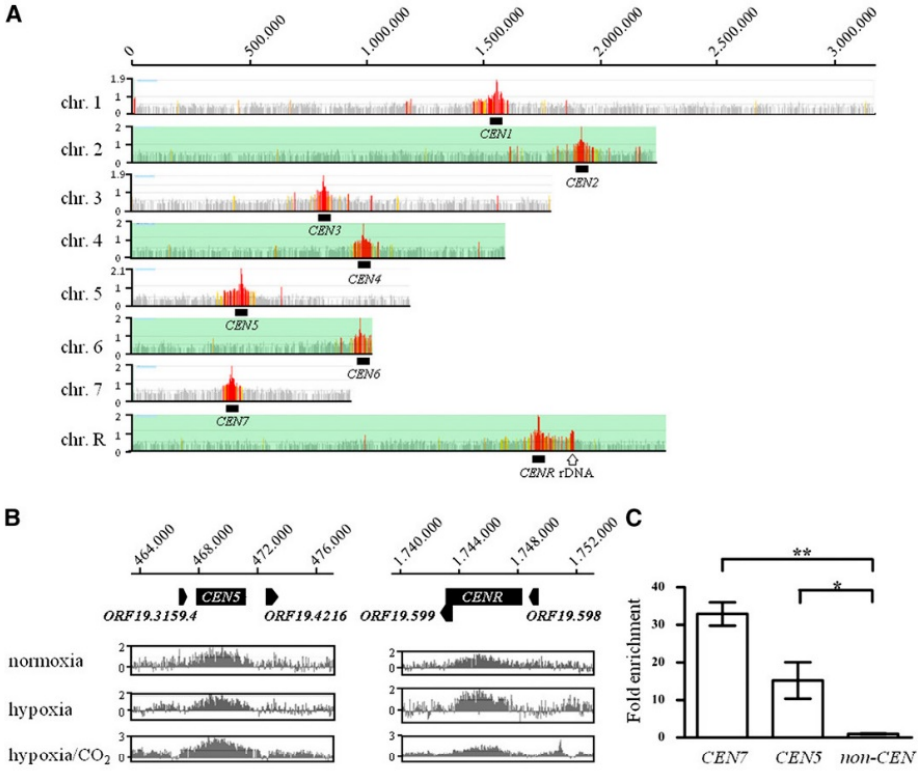

Figure 1 Genomic localization of the Sch9 kinase. The ChIP-chip procedure was carried out essentially as described previously (Lassak *et al.* 2011; Schaekel *et al.* 2013). *C. albicans* genomic tiling microarrays (NimbleGen) were probed pair-wise by immunoprecipitated chromatin of a strain expressing HA-tagged Sch9 (AF1006) and the corresponding control strain (CAS1). Two independent cultures were assayed for each combination of strains. (A) An overview of Sch9 binding. Significant binding peaks were calculated by the NimbleScan software (NimbleGen) and color-coded according to their FDR values in red [false discovery rate (FDR) ≤ 0.05], orange (FDR ≤ 0.1), yellow (FDR 0.1–0.2), and gray (FDR > 0.2). Significant Sch9-binding peaks were detected at centromeres by genomic ChIP-chip on all *C. albicans* chromosomes. In addition, a significant peak occurred at the rDNA locus (open arrow). (B) Examples for centromeric binding of Sch9 at *CEN5* and *CENR*. Scaled $\log_2$ ratios of cells grown in normoxia and hypoxia with or without 6% CO_2 are shown. Note that Sch9 enrichment was obtained for cells grown under normoxia or hypoxia conditions. (C) Enrichment at *CEN7*, *CEN5*, and the noncentromeric region was analyzed using qPCR. qPCR analysis reveals the mean fold enrichment of Sch9 at the centromeres obtained in two independent ChIP experiments (±SD) relative to the no-tag control and normalized to the input samples. The calculation was done with two biological replicates (two ChIP samples), and each measurement was performed in triplicate. Significant difference was observed in Sch9 recruitment at the *CEN5* and *CEN7* region ($P < 0.05$) and ($P < 0.01$), respectively (shown by asterisks).

throughout the cell cycle in *C. albicans* (Roy *et al.* 2011; Sanyal and Carbon 2002; Thakur and Sanyal 2012). Depletion of an essential kinetochore protein leads to centromere declustering and delocalization of the centromere-specific histone Cse4 in *C. albicans* (Thakur and Sanyal 2012). However, we found neither centromere declustering nor any significant change in the centromeric histone Cse4 levels at the kinetochore (Cse4-GFP intensity) in wild-type (strain 8675) and *sch9* mutant (strain 8675T) strains (Figure 2A). To further investigate the role of Sch9 in Cse4 localization at the centromeres, we performed Cse4-ChIP assays with wild-type (J200) and mutant cells (J200T). We analyzed enrichment of Cse4 at *CEN5* and *CEN7* regions both by semiquantitative (Figure S3) and qPCR (Figure 2B) (primer sequences are listed in Table S2). Cse4 binding was found to be similar at the centromeres in the presence or absence of Sch9. Thus, Sch9 does not seem to play a direct role in Cse4-mediated kinetochore integrity in *C. albicans*.

Many kinetochore proteins play crucial but nonessential roles in the process of chromosome segregation (Sanyal *et al.* 1998; Ortiz *et al.* 1999; Poddar *et al.* 1999; Ghosh *et al.* 2001; Measday *et al.* 2002). The centromeric localization of Sch9 prompted us to examine whether Sch9 plays a role in high-fidelity chromosome segregation. One or both of the alleles of *SCH9* were deleted from the diploid genome of the *C. albicans* wild-type strain RM1000AH, which was previously used to study chromosome loss (Sanyal *et al.* 2004). Each homolog of chromosome 7 is marked by the auxotrophic marker *HIS1* or *ARG4* in RM1000AH (Figure 3A). The strains were confirmed by Southern blot analysis (Figure S1). We previously reported that the natural rate of loss of a chromosome in wild-type *C. albicans* (SN148) is $<5 \times 10^{-4}$/cell/generation (Mitra *et al.* 2014). Two independent null (*sch9/sch9*) mutant strains (RMKS2A and RMKS2B) exhibited a 150- to 750-fold increase in chromosome loss as compared to the spontaneous rate of loss of a chromosome (Figure 3B). Even heterozygous (*SCH9/sch9*) mutants of *SCH9* (RMKS1A and RMKS1B) exihibited chromosome loss at a rate higher than the wild type (Figure 3B). This high rate of chromosome loss is comparable to the loss rate exhibited by several *S. cerevisiae* kinetochore mutants. The role of Sch9 in chromosome segregation was further validated by re-integrating the *SCH9* ORF, including its native promoter and terminator sequences at the *RPS10* locus. While the chromosome loss was completely suppressed in re-integrants (RMKS1AR and RMKS1BR) generated in the *SCH9/sch9* mutant background (RMKS1A and RMKS1B), a reduced rate of loss was observed in re-integrants (RMKS2AR and RMKS2BR) in the *sch9/sch9* null mutant background (RMKS2A and RMKS2B) (Figure 3C). While this assay measures the loss of

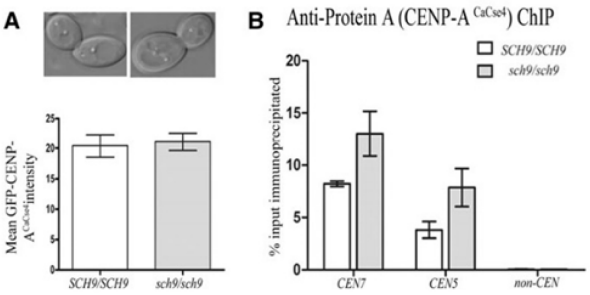

Figure 2 Sch9 is not required for Cse4-mediated kinetochore stability. (A) Microscopy images showing Cse4-GFP signal intensities in wild-type 8675 (*CSE4-GFP/CSE4;SCH9/SCH9*) and mutant 8675T (*CSE4-GFP/CSE4; sch9/sch9*). *C. albicans* wild-type and mutant strains where *CSE4* is GFP-tagged were grown overnight at 30° under normoxic conditions in YPDU (1% yeast extract, 2% peptone, 2% dextrose supplemented with 10mg/100ml uridine) and washed with water, and images were taken using a confocal laser-scanning microscope (LSM 510 META, Carl Zeiss). The brightest GFP signal in each cell was determined using the Image J software as described before (Roy *et al.* 2011). Briefly, an equal area from each cell was selected. The average pixel intensity was measured and corrected for the background by subtracting the lowest pixel intensity value in the field from the average. Then the mean GFP intensity was measured using the Image J software and the graph was plotted using Graph Pad Prism. Measurement was taken from 45 cells in each case. The experiment was performed twice. Standard error of mean (*t*-test) was used to calculate statistical significance ($P < 0.05$). For strain construction (see Supporting Information). (B) Cse4 localization at the centromere is not affected by absence of Sch9. Standard ChIP assays were performed on strains CAKS102 (*CSE4-TAP/CSE4;SCH9/SCH9*) and JZ00T (*CSE4-TAP/Cse4; sch9/sch9*) (grown at 30° under normoxic conditions) using anti-Protein A antibodies. Enrichment at *CEN7*, *CEN5*, and the noncentromeric region was analyzed by qPCR. PCR using total DNA (T) or ChIP DNA fractions with (+) or without (−) antibodies was performed. qPCR analysis revealed the enrichment of Cse4 at the centromere as a percentage of the total chromatin input, and values were plotted as mean of triplicates ±SD. No significant difference was observed in CaCse4 recruitment at the *CEN5* and *CEN7* region ($P > 0.05$). Percentage input was calculated as 100*2^[adjusted input − Ct(IP)] (Mukhopadhyay *et al.* 2008).

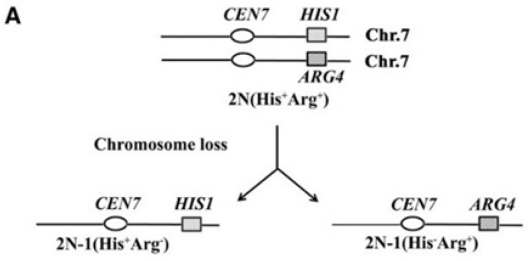

B

Strain name	Genotype	No. of colonies			Chromosome loss rate/ cell/generation
		YPDU	$His^+ Arg^-$	$His^- Arg^+$	
RM1000AH	*SCH9/SCH9*	995	0	0	$<1.0X10^{-3}$
RMKS1A	*SCH9/sch9*	725	3	1	$5.5X10^{-3}$
RMKS1B		1127	1	1	$1.8X10^{-3}$
RMKS2A	*sch9/sch9*	865	8	5	$15.0X10^{-3}$
RMKS2B		989	3	0	$3.0X10^{-3}$

C

Strain name	Genotype	No. of colonies			Chromosome loss rate/ cell/generation
		YPDU	$His^+ Arg^-$	$His^- Arg^+$	
RMKS1AR	*SCH9/sch9/ CIp10-SCH9*	942	0	0	$<1.0X10^{-3}$
RMKS1BR		964	0	0	$<1.0X10^{-3}$
RMKS2AR	*sch9/sch9/ CIp10-SCH9*	1102	6	0	$5.0X10^{-3}$
RMKS2BR		985	0	0	$<1.0X10^{-3}$

Figure 3 Chromosome loss assay. (A) Schematic of chromosome loss assay. (B and C) The chromosome loss assay was performed with two independent transformants of both mutants and revertants, as described before (Sanyal *et al.* 2004). The numbers indicate the summation of colonies patched in independent experiments. Briefly, the strains were grown for ~20 generations on YPDU medium at 30° under normoxic conditions. Subsequently, ~1000 cells were plated on YPDU agar plates for each transformant and incubated at 30° for 2 days. The single colonies were patched on YPDU, SD minimal medium (SD) without arginine (CM−arg), and SD without histidine (CM−his). The chromosome loss rate was calculated by the number of colonies that were unable to grow on selective media divided by the total number of colonies grown on nonselective media.

heterozygosity, the loss of an unlinked single nucleotide polymorphism (SNP) on chromosome 7 along with the loss of a marker gene on the same chromosome could determine the loss of the entire chromosome. We observed that SNPs on chromosome 7 in the strains used in this study are absent, as compared to another *C. albicans* strain reported previously (Forche *et al.* 2009). However, binding of Sch9 to all centromeres combined with a higher rate of loss of the marker gene by the homozygous and heterozygous mutants led us to conclude that absence of Sch9 indeed increases the rate of chromosome loss. This confirms the critical role of Sch9 in the high-fidelity process of chromosome segregation.

To verify if centromere DNA binding of the Sch9 kinase also occurs in other yeast species outside the *Candida*-specific CTG clade, we carried out a genome-wide ChIP-chip experiment to localize HA-tagged ScSch9 (Pascual-Ahuir and Proft 2007) in *S. cerevisiae*. No detectable binding of ScSch9 to any centromere region was found. However, as in *C. albicans*, the ribosomal DNA (rDNA) locus showed significant ScSch9 binding in *S. cerevisiae* (data not shown). We conclude that Sch9 binding to centromeres is not a general feature among Hemiascomycetes fungi and may have arisen specifically in *C. albicans*, a member of the CTG clade, while binding to rDNA remained conserved. It would be tempting to speculate that the association of Sch9 with centromeres might have arisen specifically in the CTG clade. Nevertheless, Sch9 is important for growth in both *S. cerevisiae* and *C. albicans* (Pascual-Ahuir and Proft 2007; Stichternoth *et al.* 2011).

Rapid fungal growth requires effective biosynthetic, metabolic, and regulatory activities of cells. Nutrient abundance is signaled by the Tor1 pathway via the Sch9 AGC kinase. Thus, the remarkable strong binding of Sch9 to centromeres could be related to effective chromosomal replication. Incidentally,

deletion of a centromere-proximal replication origin leads to a moderate increase in chromosome loss (Mitra *et al.* 2014). In addition, phospho-regulation of kinetochore proteins by kinases (such as Aurora B kinase/polo-like kinase 1) has been shown to be critical for proper chromosome segregation (Shang *et al.* 2003; McKinley and Cheeseman 2014). Unlike short 125-bp, genetically determined, sequence-specific point centromeres of *S. cerevisiae*, *C. albicans* chromosomes contain unique sequence-independent epigenetically specified regional centromeres (Sanyal *et al.* 2004; Baum *et al.* 2006; Thakur and Sanyal 2013). While the targets of this AGC kinase Sch9 are largely unknown, centromere binding of this protein selectively in *C. albicans* but not in *S. cerevisiae* provides new insights of functional evolution of a protein in organisms having different types of centromeres.

Acknowledgments

This work was supported by a grant from the Department of Biotechnology, Government of India, and intramural funding from the Jawaharlal Nehru Centre for Advanced Scientific Research (to K.S.) and by grants from the Jürgen Manchot Stiftung Düsseldorf (to A.S. and L.v.W.) and the ERA-NET PathoGenoMics project OXYstress (to J.F.E.). N.V. and R.S. are supported by fellowships from the Council of Scientific and Industrial Research and University Grants Commission (Government of India), respectively.

Literature Cited

Baum, M., K. Sanyal, P. K. Mishra, N. Thaler, and J. Carbon, 2006 Formation of functional centromeric chromatin is specified epigenetically in Candida albicans. Proc. Natl. Acad. Sci. USA 103: 14877–14882.

Fabrizio, P., F. Pozza, S. D. Pletcher, C. M. Gendron, and V. D. Longo, 2001 Regulation of longevity and stress resistance by Sch9 in yeast. Science 292: 288–290.

Forche, A., M. Steinbach, and J. Berman, 2009 Efficient and rapid identification of Candida albicans allelic status using SNP-RFLP. FEMS Yeast Res. 9: 1061–1069.

Ghosh, S. K., A. Poddar, S. Hajra, K. Sanyal, and P. Sinha, 2001 The IML3/MCM19 gene of Saccharomyces cerevisiae is required for a kinetochore-related process during chromosome segregation. Mol. Genet. Genomics 265: 249–257.

Lassak, T., E. Schneider, M. Bussmann, D. Kurtz, J. R. Manak *et al.*, 2011 Target specificity of the Candida albicans Efg1 regulator. Mol. Microbiol. 82: 602–618.

McKinley, K. L., and I. M. Cheeseman, 2014 Polo-like kinase 1 licenses CENP-A deposition at centromeres. Cell 158: 397–411.

Measday, V., D. W. Hailey, I. Pot, S. A. Givan, K. M. Hyland *et al.*, 2002 Ctf3p, the Mis6 budding yeast homolog, interacts with Mcm22p and Mcm16p at the yeast outer kinetochore. Genes Dev. 16: 101–113.

Mitra, S., J. Gomez-Raja, G. Larriba, D. D. Dubey, and K. Sanyal, 2014 Rad51-Rad52 mediated maintenance of centromeric chromatin in Candida albicans. PLoS Genet. 10: e1004344.

Mukhopadhyay, A., B. Deplancke, A. J. Walhout, and H. A. Tissenbaum, 2008 Chromatin immunoprecipitation (ChIP) coupled to detection by quantitative real-time PCR to study transcription factor binding to DNA in Caenorhabditis elegans. Nat. Protoc. 3: 698–709.

Ortiz, J., O. Stemmann, S. Rank, and J. Lechner, 1999 A putative protein complex consisting of Ctf19, Mcm21, and Okp1 represents a missing link in the budding yeast kinetochore. Genes Dev. 13: 1140–1155.

Pascual-Ahuir, A., and M. Proft, 2007 Control of stress-regulated gene expression and longevity by the Sch9 protein kinase. Cell Cycle 6: 2445–2447.

Poddar, A., N. Roy, and P. Sinha, 1999 MCM21 and MCM22, two novel genes of the yeast Saccharomyces cerevisiae are required for chromosome transmission. Mol. Microbiol. 31: 349–360.

Roy, B., L. S. Burrack, M. A. Lone, J. Berman, and K. Sanyal, 2011 CaMtw1, a member of the evolutionarily conserved Mis12 kinetochore protein family, is required for efficient inner kinetochore assembly in the pathogenic yeast Candida albicans. Mol. Microbiol. 80: 14–32.

Sanyal, K., and J. Carbon, 2002 The CENP-A homolog CaCse4p in the pathogenic yeast Candida albicans is a centromere protein essential for chromosome transmission. Proc. Natl. Acad. Sci. USA 99: 12969–12974.

Sanyal, K., S. K. Ghosh, and P. Sinha, 1998 The MCM16 gene of the yeast Saccharomyces cerevisiae is required for chromosome segregation. Mol. Gen. Genet. 260: 242–250.

Sanyal, K., M. Baum, and J. Carbon, 2004 Centromeric DNA sequences in the pathogenic yeast Candida albicans are all different and unique. Proc. Natl. Acad. Sci. USA 101: 11374–11379.

Schaekel, A., P. R. Desai, and J. F. Ernst, 2013 Morphogenesis-regulated localization of protein kinase A to genomic sites in Candida albicans. BMC Genomics 14: 842.

Shang, C., T. R. Hazbun, I. M. Cheeseman, J. Aranda, S. Fields *et al.*, 2003 Kinetochore protein interactions and their regulation by the Aurora kinase Ipl1p. Mol. Biol. Cell 14: 3342–3355.

Stichternoth, C., A. Fraund, E. Setiadi, L. Giasson, A. Vecchiarelli *et al.*, 2011 Sch9 kinase integrates hypoxia and CO2 sensing to suppress hyphal morphogenesis in Candida albicans. Eukaryot. Cell 10: 502–511.

Thakur, J., and K. Sanyal, 2012 A coordinated interdependent protein circuitry stabilizes the kinetochore ensemble to protect CENP-A in the human pathogenic yeast Candida albicans. PLoS Genet. 8: e1002661.

Thakur, J., and K. Sanyal, 2013 Efficient neocentromere formation is suppressed by gene conversion to maintain centromere function at native physical chromosomal loci in Candida albicans. Genome Res. 23: 638–652.

Communicating editor: A. P. Mitchell

GENETICS

Supporting Information
http://www.genetics.org/lookup/suppl/doi:10.1534/genetics.114.173542/-/DC1

A Surprising Role for the Sch9 Protein Kinase in Chromosome Segregation in *Candida albicans*

Neha Varshney, Alida Schaekel, Rima Singha, Tanmoy Chakraborty, Lasse van Wijlick, Joachim F. Ernst, and Kaustuv Sanyal

DOI: 10.1534/genetics.114.173542

File S1

Strain construction

C. albicans strain AF1006 producing C-terminally HA-tagged Sch9 was constructed by transformation of heterozygous strain CAS2 by a tagging cassette generated by oligonucleotides Sch9-HA for/rev, as described (Schaekel *et al.* 2013). Correct chromosomal integration was verified by colony PCR using primers Sch9ver and 3′ test HA-tag. Both alleles of *SCH9* were deleted in *C. albicans* strain RM1000AH (Sanyal *et al.* 2004) and 8675 (Joglekar *et al.* 2008) using the URA blaster method. The construction of the URA blaster deletion cassette for *SCH9* was described previously (Stichternoth *et al.* 2011). After the deletion of the first copy, the heterozygous strains were grown on 5-FOA plate to make the cells auxotroph for *URA3* to obtain RMKS1A, RMKS1B and 8675t. Then the same cassette was again used to disrupt the second allele of the gene, to get strains RMKS2A, RMKS2B and 8675T, respectively. To obtain the re-integrant of Sch9 in heterozygous and homozygous mutant background, the entire ORF along with its promoter and terminator was cloned in *Kpn*I and *Sal*I sites in CIp10 integration vector (Murad *et al.* 2000). Sch9 orf was re-integrated at *RPS10* locus in the *Candida* genome using *Stu*I to obtain RMKS1AR, RMKS1BR, RMKS2AR and RMKS2BR. The correct chromosomal integration of CIp10 was verified by PCR using primers UP-RPS10 and NV207. To check the binding pattern of CENP-A across the centromere in *sch9* mutant by ChIP, one copy of CENP-A was tagged with Prot A using plasmid construct pCaCse4TAPNAT (Thakur and Sanyal 2013). pCaCse4-TAP-NAT was partially digested with *Xho*I and transformed into RMKS2A to get Prot A tagged CENP-A strain.

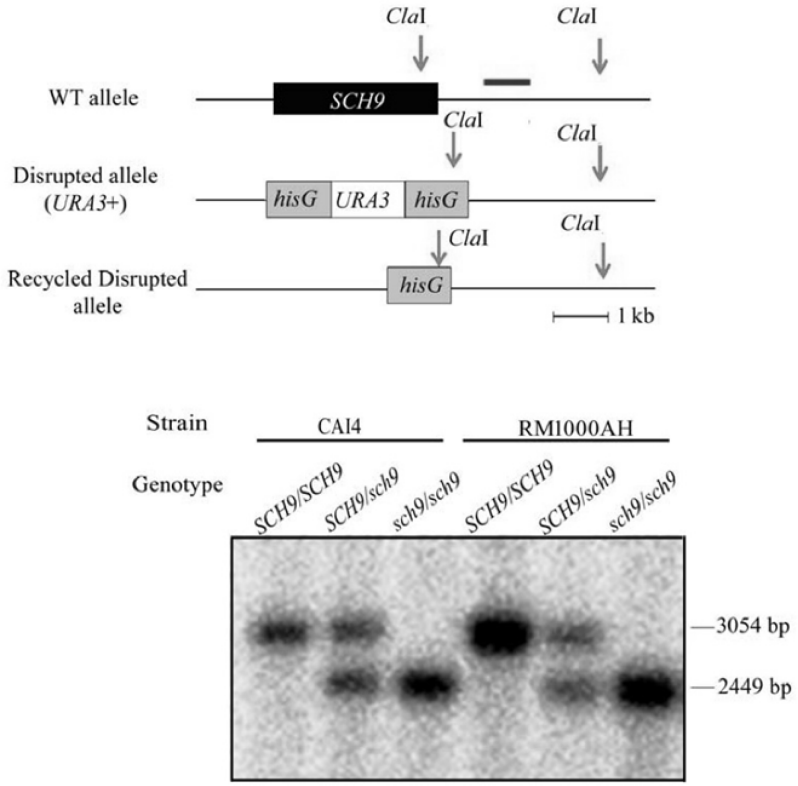

Figure S1 Southern blot analysis. Line diagrams showing wild-type and disrupted alleles of *SCH9*. *Cla*I digested DNA from wild-type strains (CAI4, RM1000AH) and corresponding heterozygous and null mutant strains lacking one or both copies of *SCH9* gene was separated on a agarose gel, blotted and probed with a region marked by the red line. Green arrows indicate *Cla*I sites. Bar, 1 kb.

	Percentage of cells with indicated morphology				Total no. of cells counted
					
CAI4	61.1	24.7	0.4	13.8	247
CAS1	69.1	24.7	0.7	6	133
CCS3	79.2	10.9	1.2	3.6	164

Figure S2 *C. albicans* wild-type (*SCH9/SCH9*), heterozygous (*SCH9/sch9*) and homozygous null mutant (*sch9/sch9*) strains were grown till OD_{600} ~ 1 at 30° in normoxic condition in YPDU and were stained with DAPI. A table showing percentages of cells with indicated morphologies of DAPI-stained nuclei.

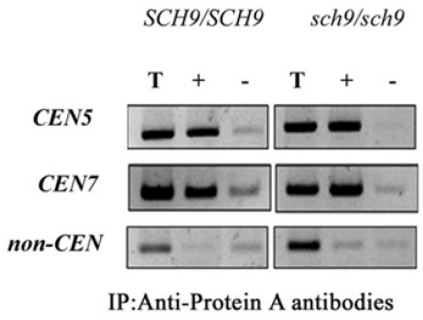

Figure S3 Cse4 localisation at the centromere is not affected by absence of Sch9. Standard ChIP assays were performed on strains CAKS102 (*CSE4-TAP/CSE4;SCH9/SCH9*) and J200T (*CSE4-TAP/Cse4; sch9/sch9*) (grown at 30°) using anti-Protein A (Cse4) antibodies. Enrichment at *CEN7*, *CEN5* and non-centromeric region was analysed using semi- quantitative PCR. PCR using total DNA (T) or ChIP DNA fractions with (+) or without (-) antibodies was performed.

Table S1 Strains used in this study

Name	Parent	Genotype	Reference
CAI4	SC5314	*ura3::imm434/ura3::imm434*	Fonzi *et al* 1993
CAS1	CAI4	as CAI4 but *SCH9/sch9::hisG-URA3-hisG*	Stichternoth *et al*, 2011
CAS2	CAS1	as CAI4 but *SCH9/sch9::hisG*	Stichternoth *et al*, 2011
CCS3	CAS2	as CAI4 but *sch9::hisG/sch9::hisG URA3/ura3::imm434*	Stichternoth *et al*, 2011
AF1006	CAS2	as CAS2 but *SCH9::(3xHA-URA3)/sch9::hisG*	This study
RM1000AH	RM1000	*Δura3::imm434/Δura3::imm434Δhis1::hisG/ Δhis1::hisG arg4::HIS1/ARG4*	Sanyal *et al*, 2004
RMKS1A	RM1000AH	*Δura3::imm434/ Δura3::imm434 Δhis1::hisG/ Δhis1::hisG arg4::HIS1/ARG4 sch9::hisG/SCH9*	This study
RMKS1B	RM1000AH	*Δura3::imm434/ Δura3::imm434 Δhis1::hisG/ Δhis1::hisG arg4::HIS1/ARG4 sch9::hisG/SCH9*	This study
RMKS2A	RMKS1A	*Δura3::imm434/ Δura3::imm434 Δhis1::hisG/ Δhis1::hisG arg4::HIS1/ARG4 sch9::hisG/sch9::hisG-URA3-hisG*	This study
RMKS2B	RMKS1B	*Δura3::imm434/ Δura3::imm434 Δhis1::hisG/ Δhis1::hisG arg4::HIS1/ARG4 sch9::hisG/sch9::hisG-URA3-hisG*	This study
RMKS1AR	RMKS1A	*Δura3::imm434/ Δura3::imm434 Δhis1::hisG/ Δhis1::hisG arg4::HIS1/ARG4 sch9::hisG/SCH9/Cip10-SCH9*	This study
RMKS1BR	RMKS1B	*Δura3::imm434/ Δura3::imm434 Δhis1::hisG/ Δhis1::hisG arg4::HIS1/ARG4 sch9::hisG/SCH9/ Cip10-SCH9*	This study
RMKS2AR	RMKS2A	*Δura3::imm434/ Δura3::imm434 Δhis1::hisG/ Δhis1::hisG arg4::HIS1/ARG4 sch9::hisG/sch9::hisG-URA3-hisG/ Cip10-SCH9*	This study
RMKS2BR	RMKS2B	*Δura3::imm434/ Δura3::imm434 Δhis1::hisG/ Δhis1::hisG arg4::HIS1/ARG4 sch9::hisG/sch9::hisG-URA3-hisG/ Cip10-SCH9*	This study
8675	BWP17	*Δ ura3::λimm434/ Δ ura3::imm434 Δhis1::hisG/Δhis1::hisGΔarg4::hisG/arg4::hisG CSE4/CSE4:GFP:CSE4*	Joglekar*et al*, 2008

8675t	8675	*Δ ura3::λimm434/Δura3::imm434 Δhis1::hisG/Δhis1::hisGΔarg4::hisG/Δarg4:: hisG CSE4/CSE4:GFP:CSE4 sch9::hisG/SCH9*	This study
8675T	8675t	*Δ ura3::λimm434/Δura3::imm434 Δhis1::hisG/Δhis1::hisGΔarg4::hisG/Δarg4:: hisG CSE4/CSE4:GFP:CSE4 sch9::hisG/sch9::hisG-URA3-hisG*	This study
CAKS102	SN148	*Δura3::imm434/Δura3::imm434, Δhis1::hisG/Δhis1::hisG, Δarg4::hisG/Δarg4::hisG, Δleu2::hisG/Δleu2::hisG CSE4/CSE4-TAP(URA3)*	Mitra *et al*, 2014
J200	RM1000AH	*Δura3::imm434/ Δura3::imm434 Δhis1::hisG/ Δhis1::hisG arg4::HIS1/ARG4 CSE4/CSE4TAP-NAT*	Thakur *et al*, 2013
J200T	J200	*ura3::imm434/ ura3::imm434 his1::hisG/his1::hisG arg4::HIS1/ARG4 sch9::hisG/sch9::hisG-URA3-hisG CSE4::CSE4-TAP-NAT*	This study

Table S2 Primers used in this study

Primer name	Sequence	Description
2498-21	CTG GTG CAA GAC CCT CAT AGA AGC	Semi-quantitative ChIP PCR primers for CEN7
2498-22	CCT GAC ACT GTC GTT TCC CAT AGC	Semi-quantitative ChIP PCR primers for CEN7
CEN5e	TGTTCTGACATACTGGGTAGACTTT	Semi-quantitative ChIP PCR primers for CEN5
CEN5f	CGAAGCATTTTGTATAACAGCCC	Semi-quantitative ChIP PCR primers for CEN5
CACH5R1	TTCATGGAAGAGGGGTTTCA	qPCR primers for CEN5
CACH5F1	CCCGCAAATAAGCAAACACT	qPCR primers for CEN5
NCEN7-3	GCATACCTGACACTGTCGTT	qPCR primers for CEN7
NCEN7-4	AACGGTGCTACGTTTTTTTA	qPCR primers for CEN7
Ctrl 7 a	ACTCGCCTTCCCCTCCTTTAAATAG	qPCR and semi-quantitative ChIP PCR primers for non centromeric region
Ctrl 7 b	CCACTACTACGACTGTGGATTCACT	qPCR and semi-quantitative ChIP PCR primers for non centromeric region
Sch9-HA for	GAAGAAGAAGATGAAATGGAAGTTGATGAAGAT CAACATATGGATGATGAATTTGTCAATGGAAGAT TTGATCTTGGTGGTGGTCGGATCCCCGGGTTAAT TAA	HA tagging
Sch9-HA rev	GCACAAAATGGAGAAGGAGAAAAAGTAGGAAC GGAATTCTATTGAATGGAACAGTTTAGTTCTAGA AGGACCACCTTTGATTG	HA tagging
Sch9ver	GTTGATTTCTGGTCATTAGG	Tagging verification primers
3' test HA-tag	CATCGTATGGGTAAAAGATG	Tagging verification primers
NV195	AGTGGTACCGGTCGATGTATAACTTCATTTCAT	CIp10 cloning forward
NV196	ACGCGTCGAGCAC AGA CAT TGG GCA AGA AA	CIp10 cloning reverse
UP-RPS10	TTCTGGTGTTCTCTCACTGTTAAGC	CIp10 integration confirmation forward
NV207	GAGTTATTAGCCCTGCGATCTTTG	CIp10 integration confirmation reverse

Literature Cited

JOGLEKAR, A. P., D. BOUCK, K. FINLEY, X. LIU, Y. WAN *et al.*, 2008 Molecular architecture of the kinetochore-microtubule attachment site is conserved between point and regional centromeres. J Cell Biol **181:** 587-594.

MURAD, A. M., P. R. LEE, I. D. BROADBENT, C. J. BARELLE and A. J. BROWN, 2000 Clp10, an efficient and convenient integrating vector for Candida albicans. Yeast **16:** 325-327.

SANYAL, K., M. BAUM and J. CARBON, 2004 Centromeric DNA sequences in the pathogenic yeast Candida albicans are all different and unique. Proc Natl Acad Sci U S A **101:** 11374-11379.

SCHAEKEL, A., P. R. DESAI and J. F. ERNST, 2013 Morphogenesis-regulated localization of protein kinase A to genomic sites in Candida albicans. BMC Genomics **14:** 842.

STICHTERNOTH, C., A. FRAUND, E. SETIADI, L. GIASSON, A. VECCHIARELLI *et al.*, 2011 Sch9 kinase integrates hypoxia and CO2 sensing to suppress hyphal morphogenesis in Candida albicans. Eukaryot Cell **10:** 502-511.

THAKUR, J., and K. SANYAL, 2013 Efficient neocentromere formation is suppressed by gene conversion to maintain centromere function at native physical chromosomal loci in Candida albicans. Genome Res **23:** 638-652.

3 Diskussion

Der opportunistische humanpathogene Pilz *Candida albicans* ist Teil des Mikrobioms und besiedelt bei den meisten gesunden Menschen als Kommensale die Schleimhaut und den Gastrointestinaltrakt (Huffnagle & Noverr, 2013). In immungeschwächten Patienten kann *C. albicans* den Wechsel vom harmlosen Kommensale zu einem lebensbedrohlichen Pathogen vollziehen, der neben oberflächlichen Mykosen auch häufig letal verlaufende systemische Infektionen verursacht (Pfaller & Diekema, 2007; Brown *et al.*, 2012). *C. albicans* ist der häufigste Verursacher von invasiven Candidosen und stellt damit einen der wichtigsten Pilzpathogene des Menschen dar (Moran *et al.*, 2011; Brown & Netea, 2012). Für die Pathogenität von *C. albicans* ist eine schnelle Anpassungsfähigkeit an die sich ständig ändernde Umwelt von großer Bedeutung. Hoch entwickelte MAPK-Signalwege helfen *C. albicans* auf die verschiedensten Umweltänderungen zu reagieren. Die Anpassung erfolgt in erster Linie in Form von veränderter Genexpression, aber auch durch post-transkriptionelle Mechanismen. Die Pilzzelle wird von einer Zellwand geschützt, einem komplexen und dynamischen Organell, das für die Interaktion des Pilzes mit dem Wirt von großer Bedeutung ist. Die Zellwand besteht aus einem Netzwerk von Kohlenhydrat-basierten Polymeren, die den Pilz vor Angriffen des Immunsystems schützt. Die äußere Schicht der Zellwand besteht im Wesentlichen aus Glykoproteinen, die kovalent mit dem Glukan der inneren Zellwand verknüpft sind. Glykoproteine sind häufig *O*- und *N*-glykosyliert und unterstützen eine Vielzahl von Funktionen, z. B. die Adhäsion, die Biofilmbildung, die Immunerkennung, die Synthese der Zellwand und die Morphogenese (Sheth *et al.*, 2011; Heilmann *et al.*, 2011; Gow & Hube, 2012; Free, 2013; Nobile & Johnson, 2015). Änderungen in der Umwelt werden von spezialisierten Sensoren an der Zelloberfläche von *C. albicans* wahrgenommen und an die Signalwege übermittelt. Die Integrität der Zellwand und insbesondere die Aufrechterhaltung der *O*- und *N*-glykosylierten Mannosepolymere ist entscheidend für die Anpassung von *C. albicans* und das Überleben im Wirt. Der Hauptsignalweg, der bei defekter *O*- und *N*-Glykosylierung aktiviert wird, ist in *C. albicans* der Cek1 MAPK-Signalweg, der sich aus dem Sensorprotein Msb2 und dessen assoziierten Protein Sho1, der PAK Cst20 und dem MAP-Kinase Modul, bestehend aus der MAPKKK Ste11, der MAPKK Hst7 und der MAPK Cek1 zusammensetzt (Roman *et al.*, 2009). Als Zielgene des Cek1-MAPK Signalwegs wurden die *PMT*-Gene identifiziert, die in *C. albicans* für fünf Protein-*O*-Mannosyltransferase-Isoformen kodieren. Pmt-Proteine sind in Eukaryoten konserviert und katalysieren die initiale Verknüpfung eines Mannoserestes an sekretorische Proteine bei der *O*-Glykosylierung

(Cantero & Ernst, 2011; Lengeler *et al.*, 2008). Defekte in der *O*-Glykosylierung führen zu verminderter Virulenz von *C. albicans* und tragen zur Erkennung durch das Immunsystem bei (Prill *et al.*, 2005; Rouabhia *et al.*, 2005; Sheth *et al.*, 2011). Über die Regulation der *PMT*-Gene ist bislang wenig bekannt. Cantero *et al*. (2007) konnten zeigen, dass die Transkription der *PMT*-Gene durch Glykosylierungsdefekte reguliert wird. Eine neuere Studie erbrachte zudem, dass *PMT*-Gene unterschiedlich reguliert werden. Bei defekter *N*-Glykosylierung wird die Expression von *PMT1* de-reprimiert und bei defekter Pmt1-*O*-Mannosylierung erfolgt die kompensatorische Überexpression von *PMT2* und *PMT4* (Cantero & Ernst, 2011). Der Transkriptionsfaktor Ace2 konnte als weiteres Element, das an der Regulation der *PMT*-Gene beteiligt ist, identifiziert werden. Die *ace2*-Mutante wies eine ungewöhnliche Transkription der *PMT*-Gene auf und war nicht in der Lage, sich von der Behandlung mit dem Pmt1-Inhibitor zu erholen (Cantero & Ernst, 2011; Mulhern *et al.*, 2006). Der zugrundeliegende molekulare Mechanismus, über den der Transkriptionsfaktor zur Regulation der *PMT*-Gene beiträgt ist ungeklärt. Auch die Zugehörigkeit des Signalweges ist unklar. Die bisherigen Ergebnisse wiesen darauf hin, dass Ace2 gemeinsam mit dem Sensorprotein Msb2 und der Cek1 MAP-Kinase einen linearen Signalweg bildet. In *S. cerevisiae* wurde Ace2 als Element des RAM-Signalwegs identifiziert, der in allen Hefepilzen konserviert ist und das polarisierte Wachstum und die Zytokinese sicherstellt (Kurischko *et al.*, 2005). Diese Funktion konnte auch in *C. albicans* nachgewiesen werden. Darüber hinaus wurde auch die Interaktion mit dem PKA-Signalweg beschrieben, insbesondere mit dem Hyphenregulator Efg1, der von besonderer Bedeutung für die Hyphenmorphogenese in *C. albicans* ist (Song *et al.*, 2008; Ernst, 2000; Saputo *et al.*, 2014).

Ziele dieser Arbeit bestanden darin die Funktion von Ace2 bei der Regulation der *PMT*-Gene zu klären und den Beitrag von Ace2 an der hypoxischen-Hyphenmorphogenese zu untersuchen. Als Grundlage wurden genomweite ChIP-chip Analysen zur Identifizierung von Ace2-Zielgenen durchgeführt. Auf diese Weise konnte u. a. eine Ace2 abhängige Regulation von Cek1-Signalwegelementen nachgewiesen werden, die auf einen positiven Rückkopplungs-mechanismus hinweist, der unter Glykostress zu einer schnellen Anpassung von *C. albicans* beiträgt. Die Ergebnisse weisen zudem darauf hin, dass auch ein negativer Rückkopplungs-mechanismus, der durch die PAK Cst20 vermittelt wird, zur Inhibierung von Ace2 und dem Cek1-Signalweg beiträgt. Als weitere Elemente, die bei der Antwort auf defekte Glykosylierung an der Regulation von *PMT*-Genen beteiligt sind, konnte der Transkriptionsfaktor Zcf21 und das RNA-Bindeprotein Dom34 identifiziert werden. Die genetische Interaktion von Ace2 mit *ZCF21* trägt zur Reprimierung des *PMT1*-Gens bei,

während für Dom34 eine Funktion bei der Translation von spezifischen Transkripten nachgewiesen werden konnte, zu denen auch die *PMT*-Transkripte zählen.
Die vergleichende Analyse der Ace2-Lokalisation unter hypoxischen Bedingungen, mit identifizierten Efg1-Bindestellen, ergab, dass Ace2 und Efg1 gemeinsam in Abhängigkeit der Temperatur und der Verfügbarkeit von Sauerstoff hyphenspezifische Gene regulieren. Es stellte sich heraus, dass Ace2 ein Aktivator der Hyphenbildung unter hypoxischen Bedingungen ist und der antagonistischen Wirkung von Efg1 als Repressor der Hyphenbildung entgegenwirkt.

3.1 Der Transkriptionsfaktor Ace2 liegt stromabwärts des Cek1-Signalwegs

Um zu klären, ob der Transkriptionsfaktor Ace2 gemeinsam mit dem Sensorprotein Msb2 und der MAP-Kinase Cek1 einen linearen Signalweg bildet, wurde das *ACE2*-Gen in der *msb2*- und der *cek1*-Mutante überexprimiert. Transkriptionelle Analysen ergaben, dass ein genetischer Zusammenhang zwischen dem erhöhten *ACE2*-Transkriptspiegel und der Expression von *PMT2* und *PMT4* besteht (Manuskript I). Die Überexpression von *ACE2* war in der Lage, den Mutanten-Phänotyp der *msb2*-Mutante vollständig zu supprimieren. Auch die Sensitivitäten der *hst7*-Mutante, einem weiteren Element des Cek1-Signalweges, das stromaufwärts der Cek1 MAP-Kinase gelegen ist, konnten teilweise durch die Überexpression von *ACE2* ausgeglichen werden. Im Gegensatz dazu konnte die Überexpression von *ACE2* den Phänotyp der *cek1*-Mutante nicht supprimieren (Manuskript I). Demnach scheint zumindest eine basale Aktivität von Cek1 für die supprimierende Wirkung von Ace2 notwendig zu sein. Ob die Aktivierung von Ace2 durch Phosphorylierung vermittelt wird, verbleibt ungeklärt. Die Untersuchung des Phosphorylierungsstatus des Ace2 Proteins nach der Behandlung der Lambda-Phosphatase in der *cek1*-Mutante konnte im Vergleich zu einem wildtypischen Ace2 Protein keinen erkennbaren Unterschied aufweisen (Manuskript I). Es ist aber auch denkbar, dass Cek1 die Aktivität von Ace2 unabhängig von der Phosphorylierung reguliert. Zahlreiche phosphorylierungsunabhängige Funktionen von MAP-Kinasen wurden bereits beschrieben. Die zu Cek1 homologe MAP-Kinase in *S. cerevisiae* Fus3 ist an der Regulation von Paarungsspezifischen Genen beteiligt und inhibiert durch direkte Bindung den Transkriptionsfaktor Ste12, dem Homolog zu Cph1 in *C. albicans*, und verhindert auf diese Weise die Bildung von Filamenten (Madhani *et al.*, 1997). Eine ähnliche Funktion konnte auch für die MAP-Kinase Kss1 in *S. cerevisiae* nachgewiesen werden (Bardwell *et al.*, 1998).
Ein bekanntes Substrat der Cek1 MAP-Kinase ist der Transkriptionsfaktor Cph1, der in *C. albicans* an der Regulation von Morphogenese-Genen beteiligt ist (Liu *et al.*, 1994). Die *cph1*-Mutante weist zudem Sensitivitäten gegenüber Zellwand-destabilisierenden Substanzen

auf (Eisman *et al.*, 2006). Es wäre deshalb denkbar gewesen, dass auch Cph1 zur Regulation der *PMT*-Gene beiträgt. Weder die Überexpression von *CPH1*, noch der Verlust von *CPH1* führten zu einem Unterschied in der Expression der *PMT*-Gene oder des *ACE2*-Gens (Manuskript I). Die Regulation der *PMT*-Gene im Cek1-Signalweg wird deshalb vermutlich unabhängig von Cph1 vermittelt. Solange die direkte Interaktion zwischen Ace2 und Cek1 nicht bestätigt wird, kann nicht ausgeschlossen werden, dass Ace2 in einem zum Cek1-Signalweg parallelen Signalweg wirkt und die kompensatorischen Effekte auf einer genetischen Verknüpfung der Signalwege beruhen. Die Ergebnisse weisen darauf hin, dass Ace2 stromabwärts von Cek1 liegt und eine basale Aktivität von Cek1 für die Aktivität von Ace2 benötigt wird.

3.2 Die genomweite Bindung von Ace2 enthüllt neue und konservierte Funktionen des Transkriptionsfaktors

Bei der Auswertung der genomweiten Bindeanalysen (ChIP-chip) des Transkriptionsfaktors Ace2 stellte sich heraus, dass Ace2 eine große Anzahl an Bindestellen im Genom unabhängig von den Wachstumsbedingungen bindet. Die Bindestellen traten sowohl unter ungestressten und hypoxischen Wachstumsbedingungen als auch nach der Behandlung mit dem *N*-Glykosylierungs-Inhibitor Tunicamycin auf (Manuskript I und II). Gene, die den identifizierten Bindestellen zugewiesen werden konnten, kodieren für Proteine, die an metabolischen Prozessen, wie der Respiration und der Glykolyse beteiligt sind, aber auch am Proteintransport, der Zellwandsynthese, der Modifikation von Proteinen, dem filamentösen Wachstum, der Translation und dem Zellzyklus. Eine Beteiligung von Ace2 an der Regulation von glykolytischen und respiratorischen Genen war aufgrund von Transkriptomanalysen bereits erwartet worden. Die identifizierten Bindestellen von Ace2 an Promotoren dieser Gene bestätigt dieses Ergebnis (Mulhern *et al.*, 2006). Interessanterweise konnte das identifizierte Ace2-Bindemotiv „GCTGG“ in diesen Binderegionen nicht nachgewiesen werden. Demnach scheint Ace2 entweder indirekt an die Promotoren dieser Gene zu binden oder verfügt über ein weiteres Bindemotiv. Darüber hinaus weist die genomweite Bindeanalyse darauf hin, dass Ace2 ein sehr vielseitiger Transkriptionsfaktor ist, der an zahlreichen Prozessen beteiligt ist. Von besonderem Interesse sind vor allem Gene, die relevant für die Virulenz von *C. albicans* sind. Zu den identifizierten Genen zählen u. a. *EFG1*, *SFL1*, *BRG1*, *WOR1*, *CAS5* und *FLO8*, die jeweils einen großen Einfluss auf die Fähigkeit von *C. albicans* haben zwischen der Hefe- und der Hyphe-Zellform zu wechseln und damit zur Virulenz von *C. albicans* beitragen (Du *et al.*, 2012a; Bruno *et al.*, 2006; Li *et al.*, 2007; Zordan *et al.*, 2007; Du *et al.*, 2012b). Weitere

relevante Prozesse, an denen identifizierte Ace2-Zielgene beteiligt sind, betreffen die Adhäsion an Oberflächen und damit einhergehend die Bildung von Biofilmen (Manuskript II). Interessanterweise weist die *ace2*-Mutante sowohl Defekte bei der Hyphenmorphogenese, der Fähigkeit Biofilme zu bilden, als auch bei der Adhäsion an Plastikoberflächen auf (Kelly *et al.*, 2004; Stichternoth & Ernst, 2009; Finkel *et al.*, 2012). Der Transkriptionsfaktor Ace2 scheint demnach eine deutlich zentralere Rolle bei der Regulation dieser Prozesse zu spielen, als bisher angenommen. Die fehlerhafte Regulation einer oder mehrerer dieser identifizierten Regulatoren könnte für diese Phänotypen verantwortlich sein.

Neben diesen neu-identifizierten Zielgenen von Ace2 konnten auch aus *S. cerevisiae* konservierte Zielgene des zu *C. albicans* homologen Transkriptionsfaktors Ace2, ScAce2 und dessen Paralog Swi5 nachgewiesen werden (Manuskript I und II). Dazu zählt eine Vielzahl von Zellwandproteinen (z. B. *DSE1*, *SCW11*, *PIR1*), wie auch Glukanasen (*ENG1*) und Chitinasen (*CHT2*, *CHT3*). Der Verlust von *ACE2* führt in beiden Organismen zu einem Zellseparationsdefekt, der auf die fehlende Regulation von Chitinasen während der Zellteilung zurückzuführen ist (Doolin *et al.*, 2001; Colman-Lerner *et al.*, 2001). In *S. cerevisiae* konnte als Hauptchitinase Cts1 identifiziert werden, während in *C. albicans* die Chitinase Cht3 hauptverantwortlich für diese Funktion zu sein scheint und eine Ace2-Bindestelle aufweist (O'Conallain *et al.*, 1999; King & Butler, 1998; Kelly *et al.*, 2004). Demnach ist die regulatorische Funktion von Ace2 für einige Prozesse sehr wahrscheinlich in vielen Hefepilzen konserviert. Dies trifft insbesondere auf Gene der Zellwand-Synthese und strukturelle Komponenten der Zellwand zu, deren Expression durch Ace2 vermittelt wird. Auch das identifizierte Ace2-Bindemotiv „GCTGG“ konnte als Konsensus-Sequenz für die homologen Proteine ScAce2 und Swi5 nachgewiesen werden (Badis *et al.*, 2008).

3.3 Ace2 stimuliert die Genexpression von Cek1-Signalwegelementen unter Glykostress-Bedingungen

Unter den Ace2-Zielgenen, die spezifisch unter Glykostress-Bedingungen identifiziert wurden und eine Ace2-Bindestelle aufweisen, befinden sich auch die Gene *MSB2*, *HST7* und *CST20*, die für Elemente des Cek1 MAP-Kinase Signalwegs kodieren und *ACE2* selbst (Roman *et al.*, 2009). Mittels ChIP-qPCR konnte die Bindung von Ace2 an die Promotoren dieser Gene bestätigt werden (Manuskript I). Die Transkriptanalyse der entsprechenden Gene weist darauf hin, dass in Folge von Glykostress die Expression von Genen des Cek1-Signalweges und *ACE2* induziert wird. Obwohl keine direkte Bindung von Ace2 an den Promotor des für die Cek1 MAP-Kinase kodierenden Gens festgestellt werden konnte, ergab die transkriptionelle Analyse,

dass auch *CEK1*, in Abhängigkeit von Ace2 bei Glykostress, hochreguliert wird. Die erstaunlich hohe Expressionssteigerung, um mehr als das 12-Fache, weist daraufhin hin, dass neben der stimulierten Phosphorylierung des Signalweges auch die Biosynthese von Signalwegelementen bei der Anpassung von *C. albicans* an Glykostress von Bedeutung ist. Überaschenderweise konnte die aktivierende Wirkung von Ace2 auf die Expression von Genen des Cek1-Signalwegs nicht in der *msb2*-Mutante beobachtet werden (Manuskript I). Dieses Ergebnis weist darauf hin, dass ein funktionsfähiger Cek1-Signalweg benötigt wird, um Ace2 zu aktivieren und bestärkt damit gleichzeitig die Vermutung, dass Ace2 stromabwärts des Cek1-Signalweges liegt. Darüber hinaus deutet dieses Ergebnis darauf hin, dass der Cek1-Signalweg die Expression seiner Signalwegelemente unter Glykostress-Bedingungen in Form einer positiven Rückkopplungsschleife reguliert, die durch den Ace2 Transkriptionsfaktor geschlossen wird. Auf diese Weise ist *C. albicans* in der Lage die Effektivität der Signalübermittlung zu verstärken und schneller auf Glykostress zu reagieren.
Interessanterweise weist der *MSB2*-Promotor zwei Ace2 Bindestellen auf, die mit zwei nachgewiesenen Transkriptionsstartstellen korrelieren (Sellam *et al.*, 2010; Tuch *et al.*, 2010). Dabei konnte die Bindung von Ace2 an die distale-Bindestelle nur nach der Behandlung mit Tunicamycin nachgewiesen werden, während die proximale-Bindestelle nur unter ungestressten Wachstumsbedingungen auftritt (Manuskript I). Demnach wird unter Glykostress möglicherweise ein um 1.200 Basenpaare längeres *MSB2*-Transkript gebildet. Ein Beispiel für die Verwendung von unterschiedlichen Transkriptionsstartstellen in Abhängigkeit von äußeren Signalen ist das *EFG1*-Gen. Der ungewöhnlich lange *EFG1*-Promotor weist gleich mehrere Transkriptionsstartstellen auf und wird von zahlreichen transkriptionellen Regulatoren gebunden (Lassak *et al.*, 2011; Hernday *et al.*, 2013). Bei dem Wechsel von der Hefe-Zellform in die Opaque-Zellform konnte ein kürzeres Transkript von 2.100 Basenpaaren in Opaque-Zellen und ein etwa 3.330 Basenpaare großes Transkript in Hefe-Zellen nachgewiesen werden (Srikantha *et al.*, 2000). Die Funktion eines solchen Transkripts könnte in einer gesteigerten Translationseffizienz liegen, die zu einer schnellen Synthese des Proteins und damit zu einer schnellen Anpassung führt. Eine detaillierte Analyse des *MSB2*-Promotors könnte Aufschluss über diese Hypothese geben und stellt eine interessante Entdeckung dar.

3.4 Ace2 vermittelt die Transkription von *PMT*-Genen indirekt

Sowohl Transkriptomanalysen, als auch sensitivere transkriptionelle Analysen hatten ergeben, dass der Transkriptionsfaktor Ace2 zur Regulation von *PMT*-Genen beiträgt (Mulhern *et al.*, 2006; Cantero & Ernst, 2011). Überraschenderweise konnte keine direkte Bindung von Ace2

an die Promotoren der *PMT*-Gene durch die genomweite Bindeanalyse nachgewiesen werden (Manuskript I). Zumindest nach der Behandlung mit dem *N*-Glykosylierungs-Inhibitor Tunicamycin war die Bindung von Ace2 an den Promotor des *PMT1* Gens erwartet worden. Bei defekter *N*-Glykosylierung war eine starke Aktivierung des Cek1 MAPK-Signalweges nachgewiesen worden und eine erhöhte Expression des *PMT1*-Gens (Roman *et al.*, 2009; Cantero & Ernst, 2011). In der *ace2*-Mutante konnte die kompensatorische Regulation des *PMT1*-Gens nicht beobachtet werden (Cantero & Ernst, 2011). Zudem hatte die detaillierte Sequenz-Analyse der *PMT*-Promotorsequenzen ergeben, dass die Promotoren (5‘-intergene Regionen) von *PMT1*, *PMT4* und *PMT6* das identifizierte Ace2 Bindemotiv aufweisen (Van Wijlick, 2012). Obwohl eine direkte Bindung von Ace2 an die regulatorischen Sequenzen von *PMT*-Genen unter anderen Wachstumsbedingungen nicht vollständig ausgeschlossen werden kann, weisen die Ergebnisse darauf hin, dass die Regulation der *PMT*-Gene nur indirekt durch Ace2 vermittelt wird. Bestärkt wird diese Vermutung durch Aktivitäts-Analysen des *PMT1*-Promotors mit dem Reportergen *lac*Z. Die Deletion des identifizierten Ace2-Bindemotivs hatte keine Auswirkung auf die Aktivität des Reportergens (Manuskript I). Möglicherweise wäre die Bindeanalyse in einer *pmt1*-Mutante oder nach der Behandlung mit dem Pmt1-Inhibitor aufschlussreicher gewesen, denn bei defekter Pmt1-*O*-Mannosylierung konnte eine verstärkte Expression von sowohl *PMT2*, als auch *PMT4* beobachtet werden, die durch Ace2 vermittelt wird (Cantero *et al.*, 2007; Cantero & Ernst, 2011). Bei defekter *N*-Glykosylierung werden diese beiden Isoformen dagegen nicht reguliert.

Bei der Suche nach weiteren Transkriptionsfaktoren, die an der Regulation von *PMT*-Genen beteiligt sind, konnte der Zink-Finger Transkriptionsfaktor Zcf21 als Repressor von *PMT1* identifiziert werden (Manuskript I). Die Transkriptions-Analysen weisen darauf hin, dass Zcf21 keinen Einfluss auf die Expression von *PMT2* und *PMT4* hat. Zudem steht *ZCF21* selbst unter der Kontrolle des Transkriptionsfaktors Ace2, der die Expression von *ZCF21* bei defekter *N*-Glykosylierung reguliert (Manuskript I). Die inhibierende Wirkung von Zcf21 auf die Transkription des *PMT1*-Gens konnte durch die Überexpression von *ZCF21* in der *pmt4*-Mutante, die bei gleichzeitigem Funktionsverlust der Pmt1-Isoform nicht überlebensfähig ist, bestätigt werden (Prill *et al.*, 2005). Eine aktuelle Studie zeigt zudem, dass Zcf21 die Expression von anderen Mannosyltransferasen, beispielsweise *MNN4* und *MNN22*, beeinflusst. Darüber hinaus scheint Zcf21 hauptsächlich als Repressor seiner Zielgene zu wirken (Bohm *et al.*, 2016). Bestärkt wird diese Vermutung durch den Mannangehalt in der *zcf21*-Mutante, der sich mehr als verdoppelt hatte (Bohm *et al.*, 2016). In einer vorangegangen Studie konnte außerdem gezeigt werden, dass Zcf21 für die Besiedlung von Mausnieren benötigt wird und das

kommensale Wachstum von *C. albicans* unterstützt (Perez & Johnson, 2013). In Anbetracht der neuen Ergebnisse, die Zcf21 als Repressor der *O*-Mannosylierung identifiziert haben, erscheint die intakte Regulation dieses Prozesses maßgeblich für die Virulenz und eine erfolgreiche Interaktion von *C. albicans* mit dem Immunsystem des Wirtes zu sein.

Spezifische Regulatoren für die Expression von *PMT2* und *PMT4* konnten bislang nicht identifiziert werden. Vorläufige Ergebnisse weisen darauf hin, dass der Transkriptionsfaktor Bcr1 möglicherweise daran beteiligt ist. Das Bcr1-Protein wurde, wie auch Ace2, als Zieltranskriptionsfaktor des RAM-Signalweges beschrieben (Gutierrez-Escribano *et al.*, 2012). Die *bcr1*-Mutante wies, anders als die *ace2*-Mutante, keine Sensitivität gegenüber Tunicamycin und dem Pmt1-Inhibitor auf. Die Überexpression von *BCR1* (*ACT1*-Promotor) war aber in der Lage, den Mutanten-Phänotyp einer *msb2*-Mutante zu supprimieren (L. v. Wijlick & J. F. Ernst, unpublizierte Ergebnisse). Die Transkriptanalyse der *PMT*-Gene ergab, dass die Überexpression von *BCR1* zu einem erhöhten Transkriptspiegel von *PMT2* und *PMT4* führt. Die *bcr1*-Mutante wies dagegen keinen signifikanten Unterschied in der Expression der *PMT*-Gene im Vergleich zu einem Kontrollstamm auf. Es stellte sich heraus, dass Bcr1 einen positiven Einfluss auf die Expression von *ACE2* hat und auf diese Weise indirekt an der Regulation der *PMT*-Gene beteiligt ist (siehe auch Manuskript II). Die genetische Interaktion von *ACE2-BCR1* mit den *PMT*-Genen könnte durch die Erzeugung einer Doppelmutante näher geklärt werden; eine indirekte Regulation der *PMT*-Gene ist aber wahrscheinlicher.

3.5 Die zytoplasmatische-Domäne von Msb2 trägt zur Regulation von Glykostress-Zielgenen im Zellkern bei

Neben der Funktion als Sensorprotein konnte für das Mucin Msb2 auch eine direkte Funktion bei der Regulation von Glykostress-Genen nachgewiesen werden, die durch die zytoplasmatische-Domäne des Proteins vermittelt wird (Manuskript IV). Das Msb2 Protein ist über eine Transmembrandomäne in der Zytoplasmamembran verankert. Mucine werden typischerweise proteolytisch prozessiert und in eine extrazelluläre- und eine zytoplasmatische-Domäne gespalten (Cullen, 2011). Die beiden Domänen erfüllen dabei offenbar unterschiedliche Funktionen in *C. albicans*. Die extrazelluläre-Domäne des Msb2 Proteins wird gespalten und in die Umgebung abgegeben und schützt den Pilz vor Angriffen des Immunsystems, beispielsweise vor Antimikrobiellen-Peptiden (Szafranski-Schneider *et al.*, 2012). Die zytoplasmatische-Domäne wird in Folge von Glykostress gespalten und transloziert vom Zytoplasma in den Zellkern (Manuskript IV). Auch in anderen Hefe-Spezies konnte eine zytoplasmatische Lokalisation der zu Msb2 homologen Proteine nachgewiesen werden (Brown

et al., 2014; Lanver *et al.*, 2010). Die Transkriptomanalyse ergab zudem, dass die zytoplasmatische-Domäne von Msb2 zur Regulation von mindestens 117 Genen in *C. albicans* beiträgt. Überraschenderweise konnte in den Promotorsequenzen dieser Gene eine Anreicherung des zuvor identifizierten Ace2-Bindemotivs nachgewiesen werden (Manuskript II) und die Msb2-Zielgene überlappen teilweise mit den identifizierten Ace2-Zielgenen der genomweiten Bindeanalyse (Manuskript I). Unter den Genen, die durch die zytoplasmatische-Domäne des Msb2 Proteins reguliert werden, befand sich auch das *MSB2*-Gen selbst und Mitglieder der *MNN*-Genfamilie (Manuskript IV), die für die katalytisch aktiven α1,3-Mannosyltransferasen kodieren, die an der Kettenverlängerung im Golgi beteiligt sind (Hall *et al.*, 2013). Zudem konnten zahlreiche Gene identifiziert werden, die für Zellwandproteine kodieren. Demnach scheint die zytoplasmatische-Domäne von Msb2 zur Expression von Genen beizutragen, die bei der Antwort auf Glykostress reguliert werden. Cantero *et al*. (2011) hatten zeigen können, dass die Expression des *PMT1*-Gens unter ungestressten Wachstumsbedingungen durch Msb2 und Cek1 reprimiert wird. Überraschenderweise ergab die Transkriptanalyse des *PMT1*-Gens in den Msb2-Deletionsvarianten (ΔD1- ΔD6), dass die zytoplasmatische-Domäne (ΔD1) nicht für die reprimierende-Wirkung von Msb2 benötigt wird (Manuskript IV). Der Mechanismus, über den Msb2 in den Zellkern gelangt, ist ungeklärt, wie auch bei der Relokalisation der Kinase Cst20, die unmittelbar stromabwärts von Msb2 im Cek1-Signalweg lokalisiert ist. Beide Proteine weisen keine konventionelle NLS-Sequenz auf. Die Ergebnisse lassen vermuten, dass beide Proteine gemeinsam an der Regulation von Ace2-Zielgenen beteiligt sind (siehe unten; Manuskript I). Der molekulare Mechanismus, über den Msb2 zur Regulation der Gene beiträgt, ist ebenfalls unklar.

3.6 Die Kinase Cst20 inhibiert Ace2 unter Glykostress-Bedingungen im Zellkern

Unter der Verwendung des Hefe-Zwei-Hybrid Systems konnten neue Interaktionspartner von Ace2 identifiziert werden. Überraschenderweise wurde dabei die Interaktion mit der PAK Cst20, die stromaufwärts der MAPK Cek1 liegt, nachgewiesen. Die Interaktion konnte durch die sensitivere Methode der Ko-Immunpräzipitation bestätigt werden. Interessanterweise konnte das Cst20 Protein nur nach der Behandlung mit Tunicamycin nachgewiesen werden. Die physische Interaktion zwischen Ace2 und Cst20 scheint demnach in Abhängigkeit von Glykostress aufzutreten (Manuskript I). Aus vorangegangen Studien geht hervor, dass Ace2 ausschließlich in Zellkernen von neugebildeten Tochterzellen lokalisiert ist (Kelly *et al.*, 2004; Saputo *et al.*, 2014). Unter Glykostress-Bedingungen konnte eine Anreicherung des Ace2-GFP Proteins auch in den Zellkernen von Mutterzellen beobachtet werden (Manuskript I).

Gleichermaßen wurde auch eine Kolokalisation von Cst20-GFP mit dem Zellkern beobachtet. Diese trat aber nur unter Glykostress-Bedingungen auf (Manuskript I). Unter ungestressten Wachstumsbedingungen konnte eine Lokalisation von Cst20-GFP im Zytoplasma an den Zellpolen von Mutter- und Tochter-Zellen nachgewiesen werden. Damit scheint die Lokalisation von Cst20 unter ungestressten Wachstumsbedingungen mit dem in *S. cerevisiae* homologen Ste20 Protein konserviert zu sein (Peter *et al.*, 1996). Die Ergebnisse zeigen, dass sowohl Ace2, als auch die Kinase Cst20 unter Glykostress-Bedingungen, in den Zellkern lokalisieren und miteinander interagieren. Dieses Ergebnis scheint zunächst überraschend, da die Cst20 Kinase stromaufwärts von Cek1 liegt und möglicherweise für die Signalweiterleitung benötigt wird (Roman *et al.*, 2009). Zudem wies die *cst20*-Mutante erhöhte Sensitivitäten gegenüber Tunicamycin, dem Pmt1-Inhibitor und Caspofungin auf (Manuskript I). Die Deletion von *ACE2* in einem *cst20*-Mutantenhintergrund zeigte keine erhöhte Sensitivität und auch die Überexpression von *ACE2* war in der Lage den Phänotyp der *cst20*-Mutante zu supprimieren. Demnach kann davon ausgegangen werden, dass Ace2 stromabwärts von Cst20 liegt und beide Proteine bei der durch den Cek1-Signalweg vermittelten Antwort auf Glykostress von Bedeutung sind. Die transkriptionelle Analyse ergab außerdem, dass Cst20 ebenfalls für den positiven Rückkopplungsmechanismus des Cek1 MAPK-Signalweges benötigt wird.

Hinweise auf die Relevanz der Interaktion erbrachten Cst20-GFP Proteinfusionen, die mit NLS- und NES-Sequenzen modifiziert wurden. Die gerichtete Lokalisation von Cst20 in den Zellkern führte zu erhöhten Sensitivitäten der Zellen gegenüber den bekannten Glykosylierungsinhibitoren (Manuskript I). Selbst bei der gleichzeitigen Anwesenheit eines nicht modifizierten Cst20 Proteins konnte ein dominant-negativer Effekt des Cst20-NLS Proteins beobachtet werden. Demnach scheint die Zellkern-Lokalisation entgegen der bisher beobachteten positiven Wirkung von Cst20 auf die Signalweiterleitung des Cek1-Signalweges einen negativen Einfluss auf den Signalweg zu haben. Die transkriptionellen Analysen unterstützen diese Hypothese und belegen, dass Cst20 im Zellkern spezifisch Zielgene von Ace2 und des Cek1-Signalweges reprimiert, während das zytoplasmatische Cst20 Protein für die basale Expression dieser Gene benötigt wird. Damit weist die Cst20 Kinase eine duale Funktion bei der Anpassung an Glykostress auf. Einerseits wird Cst20 für die positive Rückkopplungsschleife im Zytoplasma benötigt, andererseits führt die erhöhte Biosynthese von Cst20 im Verlauf der Anpassung an Glykostress zu einer Anreicherung von Cst20 im Zellkern, die zur Inhibierung des Transkriptionsfaktors Ace2 führt. Dieser negative Rückkopplungs-mechanismus wird durch die Interaktion von Cst20 mit Ace2 vermittelt und trägt

möglicherweise zur Wiederherstellung der Sensitivität des Signalweges bei. Auch die Zellkern-Lokalisation von Msb2 könnte einen Einfluss auf diese Funktion haben. Die identifizierten, durch die zytoplasmatische-Msb2 Domäne regulierten Gene, wiesen größtenteils erhöhte Expressionsraten in der verkürzten ΔD1 *msb2*-Mutante auf (Manuskript IV).

Um auszuschließen, dass die Zellkern-Lokalisation von Cst20 zu einer generellen Erhöhung der Zellsensitivität gegenüber anderen Stressfaktoren führt, wurde der Effekt von osmotischem und oxidativem Stress überprüft. Die *cst20*-Mutante und auch ein heterozygoter Stamm, der nur das Cst20-NLS Protein exprimiert, zeigten unter diesen Bedingungen erhöhte Sensitivitäten. Im Gegensatz dazu wiesen die *ace2*-Mutante und ein Stamm der zusätzlich zu dem Cst20-NLS Protein ein wildtypisches Cst20 Protein exprimiert, unter diesen Bedingungen keinen Phänotyp auf (Daten nicht gezeigt). Demnach scheint die Zellkern-Lokalisation von Cst20 nur einen dominanten-negativen Effekt auf Zielgene von Ace2 auszuüben, nicht aber für andere Signalwege, obgleich Cst20 an diesen Signalwegen beteiligt ist. Interessanterweise tritt kein genereller Funktionsverlust von Ace2 auf, denn die Zellen wiesen nicht den für die *ace2*-Mutante typischen Zellseparations-Defekt auf (Kelly *et al.*, 2004). Die Ergebnisse deuten darauf hin, dass Cst20 im Zellkern spezifisch Gene der Glykostress-Antwort reprimiert. Auch für das homologe Ste20 Protein in *S. cerevisiae* und das Säugetier Homolog MST konnte eine Zellkern-Funktion nachgewiesen werden (Ura *et al.*, 2001; Ahn *et al.*, 2005). Bei der Induktion der Apoptose, dem programmierten Zelltod, transloziert die Kinase in den Zellkern und trägt durch Phosphorylierung von Histonen zur Kondensation des Chromatins bei (Radu & Chernoff, 2009). Die Inhibierung von Ace2-Zielgenen könnte demnach durch die Modifikation der regulatorischen Sequenzen auf Chromatin-Ebene realisiert werden. Denkbar wäre zudem, dass Cst20 die Bindung von Ace2 an regulatorische Sequenzen durch die physische Interaktion verhindert. Die Ergebnisse weisen darauf hin, dass auch die Phosphorylierung von Ace2 durch Cst20 eine Rolle spielen könnte. Auch für die PKA-Isoformen Tpk1 und Tpk2 konnte eine Zellkern-Lokalisation nachgewiesen werden (Schaekel *et al.*, 2013). Die Tpk-Proteine sind maßgeblich an der Regulation der Hyphenmorphogenese beteiligt und liegen stromaufwärts des Transkriptionsfaktors Efg1 (Sonneborn *et al.*, 2000; Bockmuhl & Ernst, 2001). Die Studie konnte nachweisen, dass insbesondere Tpk2, unter normalen Wachstumsbedingungen, mit der kodierenden DNA von Efg1-Zielgenen assoziiert und während der Induktion der Hyphenbildung an die regulatorischen Sequenzen dieser Gene bindet. Dieser Mechanismus erlaub eine selektive Regulation von Efg1 und weiteren Transkriptionsfaktoren, direkt an deren Zielgenen. Ein ähnlicher Mechanismus könnte auch für Cst20 und Ace2-Zielgene existieren.

3.7 Dom34 reguliert spezifisch die Translation von Pmt-Isoformen

Neben der transkriptionellen Anpassung an Stressbedingungen sind auch post-transkriptionelle Mechanismen entscheidend für eine schnelle Antwort und das Überleben des Pilzes (Verma-Gaur & Traven, 2016). In Folge von defekter *N*-Glykosylierung kommt es neben der Aktivierung des Cek1-Signalweges auch zur Aktivierung der UPR (*unfolded protein response*)- und des ERAD (*ER associated degradation*)-Signalweges (Cantero *et al.*, 2007; Cantero & Ernst, 2011; Travers *et al.*, 2000). Beide Signalwege sind an der Aufrechterhaltung der Proteinsynthese im ER beteiligt und unterstützen einerseits Proteine bei der Faltung oder helfen andererseits dabei fehl-gefaltete Proteine, die im ER akkumulieren, zu degradieren (Scrimale *et al.*, 2009; Krysan, 2009). Das RNA-Bindeprotein Dom34 ist ein Mitglied der Dom34/Pelota-Familie und ist am *No-Go decay* (NGD) Prozess beteiligt, der die Qualität von mRNA Molekülen während der Translation kontrolliert. Durch die Freisetzung von blockierten Ribosomen von mRNA-Molekülen und durch die Spaltung der mRNA beeinflusst Dom34 die Translation dieser Transkripte (Doma & Parker, 2006; Shoemaker *et al.*, 2010). In vorangegangenen Studien wurde in *S. cerevisiae* die Beteiligung von Dom34 an der *O*-Glykosylierung verschiedener Proteine nachgewiesen (Finck *et al.*, 1996). Eine Verbindung zwischen Dom34 und der Protein-*O*-Mannosylierung konnte in *C. albicans* bestätigt werden (Manuskript III). Dabei stellte sich heraus, dass die Überexpression von *DOM34* zu einer erhöhten Synthese des Pmt1 Proteins führte. Ein erhöhter *PMT1*-Transkriptlevel konnte aber nicht nachgewiesen werden. Demnach scheint Dom34 einen positiven Einfluss auf die Translation von Pmt1 zu haben, nicht aber auf die Transkription des Gens. Die Ergebnisse des Polysomen-Gradienten belegen diese Vermutung. Die Anreicherung des *PMT1*-Transkriptes in den Monosomen-Fraktionen in der *dom34*-Mutante ist ein Hinweis darauf, dass die Translation von Pmt1 in der *dom34*-Mutante gestört ist. Ein genereller Einfluss von Dom34 auf die Translation scheint nicht ausgeschlossen zu sein, aber die Verteilung des *ACT1*-Transkripts im Polysomen-Gradienten weist darauf hin, dass Dom34 nur die Translation von spezifischen Transkripten positiv beeinflusst. Auch das *PMT4*- sowie das *PMT6*-Transkript konnten als Substrate von Dom34 identifiziert werden. Die stimulierte Translation der Pmt4-Isoform könnte auch erklären, weshalb die Überexpression von *DOM34* den Phänotyp der *pmt1*-Mutante supprimieren kann. Cantero *et al*. (2011) hatten gezeigt, dass bei dem Verlust der Pmt1-vermittelten *O*-Mannosylierung die Expression von *PMT2* und *PMT4* zur Kompensation gesteigert wird. Die durch Dom34 vermittelte Translationssteigerung von Pmt4 und möglicherweise auch Pmt2 könnte zu einer effizienten und schnelleren Kompensation der fehlenden Mannosylierung in der *pmt1*-Mutante beitragen. Die Erkennung der Transkripte wird

vermutlich über Sequenzmotive in der 5‘-UTR der Transkripte vermittelt. Bislang konnte aber nur die Bindung von Dom34 an die 5‘-UTR des *PMT1* Transkripts *in vitro* nachgewiesen werden. Als Sequenzmotiv könnte das identifizierte CAAC-Motiv dienen, das in allen *PMT*-Transkripten nachgewiesen werden konnte. Demnach scheint Dom34 ein Translationshelfer von Protein-*O*-Mannosyltransferasen zu sein.

Ein ähnlicher Mechanismus wurde für Transkripte von Genen des UPR- und ERAD-Signalweges beschrieben, die nach der Induktion von ER-Stress (durch DTT) überexprimiert werden. Zu den identifizierten Transkripten gehörten z. B. der Transkriptionsfaktors Hac1, die ER-Oxidoreduktase Ero1 und das Protein Der1, das am Export von fehlgefalteten Proteinen beteiligt ist. In einem Polysomen-Gradienten konnte die Anreicherung dieser Transkripte nach der Behandlung mit DTT in der Polysomen-Fraktion nachgewiesen werden, während die Transkripte in den unbehandelten Zellextrakten ohne induzierten ER-Stress in der Monosomen-Fraktion angereichert waren. Eine generelle Translationssteigerung von Proteinen trat nicht auf. Der regulatorische Mechanismus beruht daher vermutlich auf der Initiierung der Translation von spezifischen mRNA-Molekülen (Payne *et al.*, 2008). Auch die Pmt-Proteine selbst konnten als Komponenten der Protein-Qualitäts-Kontrolle identifiziert werden, die durch die Markierung von fehl-gefalteten Proteinen mit Mannosemolekülen die Translation terminieren (Xu *et al.*, 2013; Xu & Ng, 2015). Der regulatorische Mechanismus könnte daher spezifisch für die Translationsinitiierung von Pmt-Proteinen bei defekter *N*-Glykosylierung sein.

Die Kombination aus der transkriptionellen Anpassung bei der Antwort auf defekte Glykosylierung, die sich in der erhöhten Expression der *PMT*-Gene äußert und der durch Dom34 vermittelten selektiven Translationssteigerung dieser Transkripte, ermöglicht *C. albicans* eine schnelle und effektive Anpassung. Damit ist das RNA-Bindeprotein Dom34 ein wichtiger Faktor bei der Anpassung an defekte Glykosylierung und stellt eine direkte Verbindung zwischen der Translation und der Glykosylierung von Proteinen her. Die regulatorischen Ereignisse, die bei der Antwort auf defekte Glykosylierung aktiviert werden, sind in Abb. 3.1 in Form eines Modells zusammengestellt.

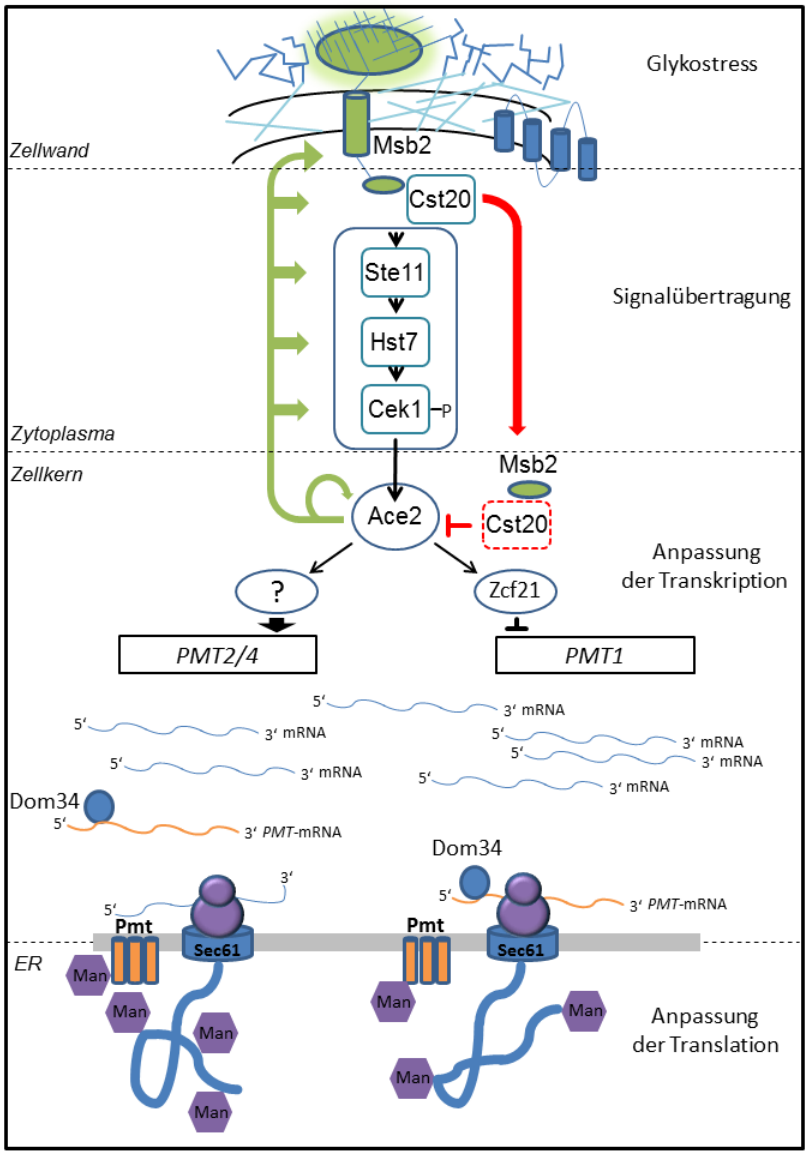

Abb.3.1 Modell zur Regulation der Antwort auf Glykostress in *C. albicans* durch den Cek1-Signalweg. Schäden in den Glykostrukturen der Zellwand werden von dem Membransensorprotein Msb2 an die Kinase Cst20 und das MAP-Kinase Modul des Cek1-Signalwegs übermittelt. Durch die Phosphorylierung der MAPKKK Ste11 wird die MAPKK Hst7 phosphoryliert und aktiviert, die ihrerseits die MAPK Cek1 durch Phosphorylierung aktiviert. Bei defekter *N*-Glykosylierung bindet der Transkriptionsfaktor Ace2 an den Promotor von *ZCF21* und reprimiert dessen Transkription, wodurch der Zcf21 Repressor nicht länger an den Promotor des *PMT1*-Gens bindet und die Transkription von *PMT1* dereprimiert wird. Bei defekter Pmt1-*O*-Mannosylierung reguliert Ace2 einen noch unbekannten Transkriptionsfaktor, der die Transkription von *PMT2* und *PMT4* stimuliert. In Form einer positiven Rückkopplungsschleife stimuliert Ace2 die Transkription von Genen, die für die Elemente des Cek1-Signalwegs kodieren und seine eigene Transkription. Auf diese Weise wird die Signalantwort verstärkt und eine schnelle Anpassung von *C. albicans* ermöglicht. In Folge von anhaltendem Glykostress akkumuliert Cst20 im Zellkern und inhibiert den Transkriptionsfaktor Ace2, wodurch die Homöostase und die Sensitivität des Signalwegs wiederhergestellt werden. Die zytoplasmatische-Domäne des Msb2 Proteins wird abgespalten und trägt zur Regulation von Ace2-Zielgenen im Zellkern bei. Neben dieser transkriptionellen Anpassung unterstützt das RNA-Bindeprotein Dom34 die Translation von spezifischen mRNA-Molekülen, zu denen insbesondere die Transkripte der *PMT*-Gene zählen. Das Zusammenwirken der gesteigerten Transkription von Stressantwort-Genen und deren selektive Translation trägt zur optimalen Anpassung von *C. albicans* bei.

3.8 Ace2 und Efg1 sind Antagonisten bei der hypoxischen Hyphenmorphogenese

Neben der Funktion von Ace2 bei der Antwort auf Glykostress konnte für Ace2 eine weitere Funktion identifiziert werden, die für die Anpassung an die Umwelt wichtig ist. Gemeinsam mit dem Transkriptionsfaktor Efg1, der als Hauptregulator der Hyphenmorphogenese identifiziert werden konnte, trägt Ace2 zur Anpassung an hypoxische Wachstumsbedingungen von *C. albicans* bei (Manuskript II). Beide Transkriptionsfaktoren sind an der Regulation von metabolischen Genen beteiligt und werden für die Induktion von glykolytischen Genen und die Reprimierung von respiratorischen Genen bei niedriger Sauerstoff Verfügbarkeit benötigt (Setiadi *et al.*, 2006; Mulhern *et al.*, 2006). Neben ihrer Funktion zur Aufrechterhaltung des primären Kohlenstoff-Stoffwechsels tragen zudem beide Transkriptionsfaktoren zur Bildung von Hyphen bei. Im Gegensatz zu Ace2 ist diese Funktion bei Efg1 nicht auf hypoxische Wachstumsbedingungen beschränkt. Bei Temperaturen von 36 – 37 °C wird Efg1 für die Bildung von Hyphen unter beiden Wachstumsbedingungen benötigt. Bei Temperaturen unterhalb von 36 °C und bei niedriger Verfügbarkeit von Sauerstoff ändert sich die Funktion von Efg1. Anstelle der induktiven Wirkung reprimiert Efg1 die Bildung von Hyphen (Stoldt *et al.*, 1997, Doedt *et al.*, 2004, Setiadi *et al.*, 2006). Die *ace2*-Mutante wies dagegen nur unter hypoxischen Wachstumsbedingungen einen Defekt in der Hyphenmorphogenese auf (Mulhern *et al.*, 2006; Saputo *et al.*, 2014). Bisher wurde angenommen, dass die Fehlregulation des Metabolismus in der *ace2*-Mutante hauptverantwortlich für den Defekt sei, neuere Studien zeigten aber, dass Efg1, als stromabwärts gelegener Transkriptionsfaktor des cAMP-PKA-Signalwegs, spezifisch die Expression von *ACE2* bei der Initiierung der Hyphenmorphogenese reguliert (Saputo *et al.*, 2014). Interessanterweise konnte unter hypoxischen Wachstumsbedingungen auch die Bindung von Ace2 an den Promotor des *EFG1*-Gens nachgewiesen werden (Manuskript II). Darüber hinaus weisen beide Transkriptionsfaktoren eine Vielzahl von gemeinsamen Binderegionen in regulatorischen Sequenzen von Genen auf, die für bekannte Regulatoren der normoxischen Hyphenmorphogenese kodieren oder dazu beitragen (u. a. *BCR1*, *BRG1*, *EFG1*, *SFL1*, *WOR1*, *EED1*, *TCC1*, *TYE7*). Insgesamt konnten 53 Gene identifiziert werden, die gemeinsam von Ace2 und Efg1 gebunden werden (Manuskript II). Eine genetische Verbindung zwischen Efg1 und *ACE2* war bereits vermutet worden, denn für die Bildung von Hyphen ist es notwendig die Degradierung der Septen zu verhindern, da es andernfalls zur frühzeitigen Zellteilung kommt. Zu den Genen, die für die Degradation des Septinrings verantwortlich sind, gehören vor allem Chitinasen und Glukansen, die unter der transkriptionellen Kontrolle von Ace2 stehen. Durch die Cyclin-abhängige Kinase Cdc28-Hgc1 wird Efg1 phosphoryliert (Position 179), reprimiert Zielgene von Ace2 und

verhindert die Zellteilung während der Bildung von Filamenten (Wang *et al.*, 2009). Interessanterweise konnte für beide Transkriptionsfaktoren das potentielle Bindemotiv CACCAC in hypoxischen-Bindestellen identifiziert werden. Möglicherweise konkurrieren beide Faktoren um die Bindung an dieses Motiv. Die Transkriptanalyse der gemeinsamen Zielgene *BCR1* und *BRG1* ergab, dass Efg1 im Gegensatz zu Ace2 die Expression von *BCR1* stimuliert und *BRG1* reprimiert. In der *ace2*-Mutante war die Expression von *BRG1* dagegen stark vermindert und die Expression von *BCR1* stark erhöht. Überraschenderweise regulieren auch Bcr1 und Brg1 die Expression von *ACE2* und *EFG1* und bilden gemeinsam ein transkriptionelles Netzwerk, dessen Feinregulation einen starken Einfluss auf die Morphogenese von *C. albicans* hat. Damit konnte erstmals bewiesen werden, dass Ace2 einen direkten Einfluss auf die Expression von Hyphenregulatoren ausübt. Gemeinsam mit der transkriptionellen Analyse weisen die Phänotypen der Doppel- und Einzel-Mutanten auf hypheninduzierenden Medien darauf hin, dass Efg1 und Bcr1 als Repressoren der hypoxischen Filamentierung wirken, wohingegen Ace2 und Brg1 als Aktivatoren identifiziert werden konnten (Manuskript II). Ein ähnlicher regulatorischer Mechanismus von Ace2 und Efg1 konnte auch für die gemeinsamen Gene *TYE7*, *EED1* und *ZCF21* unter hypoxischen Wachstumsbedingungen nachgewiesen werden (Manuskript II). Demnach wirken Efg1 und Ace2 als Antagonisten der Hyphenmorphogenese und tragen damit zur Anpassung unter hypoxischen Wachstumsbedingungen bei.

Interessanterweise wird die aktivierende Wirkung von Ace2 auf die Transkription von Hyphengenen durch erhöhte CO_2-Konzentrationen verstärkt (Manuskript II). Erhöhte CO_2-Konzentrationen treten häufig in Verbindung mit Hypoxie auf, besonders an Stellen von Infektionen, und wirken stark induzierend auf die Hyphenbildung von *C. albicans* (Ernst & Tielker, 2009; Grahl & Cramer, 2010). Unter den identifizierten hypoxischen Ace2-Zielgenen befand sich auch das *FLO8*-Gen, das für einen bekannten Sensor der CO_2-induzierten Hyphenmorphogenese kodiert und das *SCH9*-Gen (Du *et al.*, 2012a). Die *sch9*-Mutante zeigt, ähnlich wie die *efg1*-Mutante, bei Temperaturen von 25 °C und niedrigen Sauerstoffkonzentrationen einen hyperfilamentösen Phänotyp, der aber nur bei erhöhter CO_2-Konzentration auftritt (Stichternoth & Ernst, 2009). Der synergistische Effekt von niedriger Verfügbarkeit von Sauerstoff und erhöhter CO_2-Konzentration scheint ausschlaggebend für die Funktion von Ace2 als Aktivator der Hyphenmorphogenese zu sein. Ein ähnlicher Effekt konnte für den Hyphenregulator Ume6 nachgewiesen werden, der in Abhängigkeit von CO_2 und Hypoxie für die Aufrechterhaltung des Hyphenwachstums benötigt wird und überraschenderweise auch als Zielgen von Ace2 identifiziert werden konnte (Lu *et al.*, 2013).

Demnach könnte Ace2 ein wichtiger Zieltranskriptionsfaktor eines CO_2 abhängigen Signalwegs sein, der unter hypoxischen Umweltbedingungen zur Anpassung von *C. albicans* beiträgt.

3.9 Die Genexpression von Cek1-Signalwegelementen wird unter Hypoxie reprimiert

Die Ergebnisse deuten an, dass *C. albicans* unter hypoxischen Wachstumsbedingungen und Temperaturen unterhalb von 36 °C aktiv die Bildung von Filamenten unterdrückt, z. B. durch die reprimierende Wirkung von Efg1 und Bcr1, die der aktivierenden Wirkung von Ace2 und Brg1 entgegenwirken. Neben dem cAMP-PKA-Signalweg wurde auch der Cek1 MAPK-Signalweg als bedeutender Signalweg der normoxischen Hyphenmorphogenese identifiziert (Csank *et al.*, 1998). Zudem konnte Ace2 als Zieltranskriptionsfaktor des Cek1-Signalweges nachgewiesen werden, der die Transkription von Cek1-Signalweg kodierenden Genen bei Glykostress durch einen Rückkopplungsmechanismus reguliert (siehe 3.3 und Manuskript I). Unter hypoxischen Bedingungen konnte eine starke Reprimierung von *CEK1* und dessen Substrat *CPH1* in wildtypischen *C. albicans* Zellen beobachtet werden (Manuskript II). In der *bcr1*- und der *efg1*-Mutante trat dagegen eine starke Dereprimierung beider Transkripte auf, wie auch für das *ACE2*-Transkript. Die verstärkte Phosphorylierung der Cek1 MAP-Kinase in der *efg1*-Mutante unter Hypoxie belegt zudem, dass der Signalweg in der *efg1*-Mutante aktiviert wird. Demnach scheint besonders Efg1 an der Reprimierung des Cek1-Signalwegs unter hypoxischen Bedingungen beteiligt zu sein. Die Überexpression von *CPH1* war außerdem in der Lage diesen reprimierenden Effekt zu supprimieren und die *efg1 cph1*-Doppelmutante war nicht in der Lage, Filamente zu bilden (Manuskript II). Demnach ist der Cek1-Signalweg und der Transkriptionsfaktor Cph1 für den hyperfilamentösen Phänotyp in der *efg1*-Mutante unter Hypoxie verantwortlich. Die Reprimierung von *ACE2* deutet darauf hin, dass Ace2 möglicherweise auch an der transkriptionellen Regulation des Signalwegs unter hypoxischen Bedingungen beteiligt ist.

In Übereinstimmung mit diesen Ergebnissen steht die Beobachtung, dass mit Ausnahme der *pmt1*-Mutante der Hyphendefekt der *PMT*-Gene unter hypoxischen Wachstumsbedingungen nicht auftritt. Die heterozygote *PMT2*/*pmt2*- und die homozygote *pmt4*-Mutante wiesen sogar einen hyperfilamentösen Phänotyp auf (Prill *et al.*, 2005). Defekte in der Glykosylierung führen zur Aktivierung des Cek1-Signalweges und heben offenbar die reprimierende Wirkung von Efg1 auf (Cantero *et al.*, 2007; Cantero & Ernst, 2011). Auch die Behandlung mit Tunicamycin war in der Lage unter hyphenreprimierenden Bedingungen einen hyperfilamentösen Phänotyp zu induzieren (Daten nicht gezeigt). Möglicherweise besteht auch hier ein Zusammenhang

zwischen der durch Efg1 vermittelten Regulation von Cek1-Signalweg kodierenden Genen und dem beobachteten Sensitivitätsphänotyp der *efg1*-Mutante gegenüber Zellwand- und Glykostress verursachender Reagenzien (Sohn *et al.*, 2003). Es ist deshalb wahrscheinlich, dass unterschiedliche Signalwege die Initiierung der Hyphenmorphogenese unter hypoxischen und normoxischen Wachstumsbedingungen regulieren. Die Bildung von Hyphen ist hauptsächlich mit der Virulenz von *C. albicans* assoziiert, während Hefezellen das kommensale Wachstum von *C. albicans* begünstigen. Die Entwicklung eines regulatorischen Mechanismus, der die Hyphenbildung unter hypoxischen Wachstumsbedingungen reprimiert, könnte zum Erfolg von *C. albicans* beitragen als Kommensale in sauerstoffarmen Körpernischen zu überleben.

3.10 Unter Hypoxie binden Ace2 und Sch9 an die Zentromere von Chromosomen

Überraschenderweise traten unter hypoxischen Wachstumsbedingungen Bindestellen von Ace2 innerhalb der Zentromer-Regionen aller acht Chromosomen von *C. albicans* auf (Abb.3.2, Manuskript II). Unter normoxischen Wachstumsbedingungen und auch bei der Induktion von Glykostress mit Tunicamycin konnte keine Bindung von Ace2 an die Zentromere beobachtet werden (Manuskript I, II).

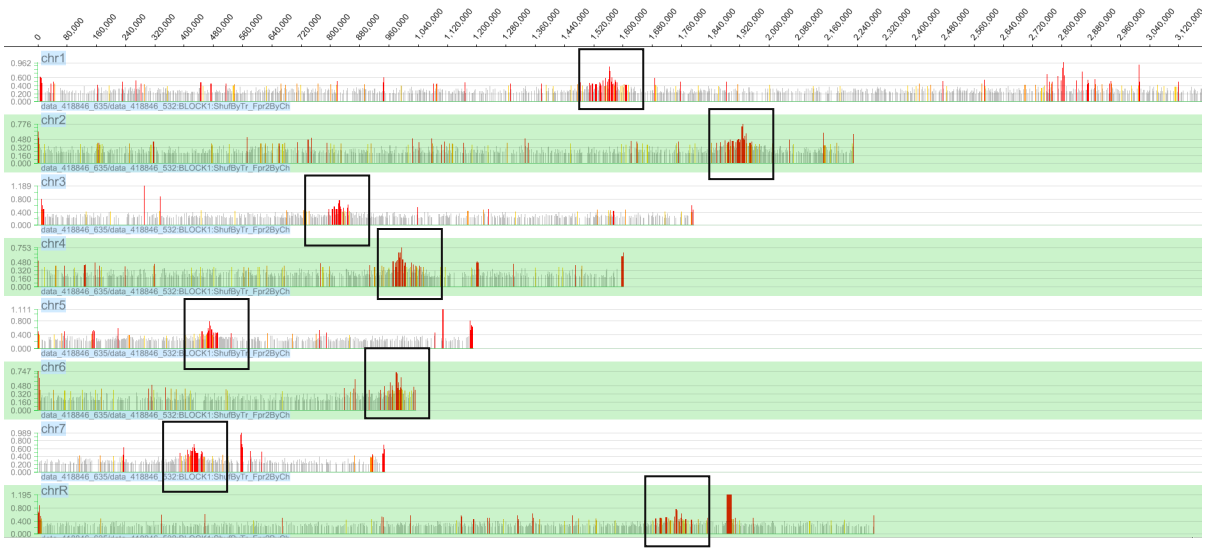

Abb.3.2 Ace2-Bindung an die Zentromere in *C. albicans* unter hypoxischen Wachstumsbedingungen. Gezeigt wird die genomweite Bindung von Ace2-HA unter hypoxischen Wachstumsbedingungen (0.2 % O_2 und 6 % CO_2). Dabei konnte die Bindung an die Zentromere aller acht Chromosomen detektiert werden. Die entsprechenden Binderegionen wurden durch Boxen markiert. Jeder rote Balken entspricht einer signifikanten Bindestelle von Ace2. Graue und gelbe Balken stellen dagegen nicht-signifikante Bindestellen dar. Die Abbildung wurde aus van Wijlick (2012) entnommen und modifiziert.

Die Bindung an die Zentromere scheint demnach spezifisch für Hypoxie oder die erhöhte CO_2-Konzentration zu sein. Die identifizierten Ace2 Bindemotive konnten innerhalb der Zentromer-

DNA nicht nachgewiesen werden. Eine indirekte Bindung ist daher wahrscheinlicher. Im Gegensatz zu Zentromeren in *S. cerevisiae* und *S. pombe* weisen Zentromere in *C. albicans* keine konservierten, sich wiederholenden DNA-Motive auf (Polizzi & Clarke, 1991; Lechner & Ortiz, 1996; Sanyal *et al.*, 2004). Zentromere sind vor allem bei der Segregation der Chromosomen während der Mitose von großer Bedeutung. Katalysiert wird die Segregation durch den mit der Zentromer-DNA assoziierten Kinetochor-Komplex (Pidoux & Allshire, 2000). Die Funktion von Ace2 an den Zentromeren ist bislang ungeklärt und da die Zentromersequenzen frei von offenen Leserastern sind, ist eine transkriptionelle Funktion auszuschließen. Die Organisation der Zentromer-DNA wird weitestgehend durch das Zentromer-spezifische Histon Cse4 (H3) vermittelt und führt zur Bildung von Heterochromatin, das zur Struktur der Zentromere beiträgt (Sanyal & Carbon, 2002; Sanyal *et al.*, 2004). Die Zentromersequenzen umfassen jeweils einen 3.000 bp – 5.000 bp großen Sequenzabschnitt, der für die Ausbildung des Kinetochor-Komplexes essentiell ist (Sanyal *et al.*, 2004). Eine Funktion von Ace2 bei der Modifikation der DNA-Struktur konnte bislang nicht nachgewiesen werden. Die Überexpression von *ACE2* war jedoch in der Lage die Phänotypen einer *snf5*-Mutante zu komplementieren (Finkel *et al.*, 2012). Das Snf5 Protein ist Teil des SWI/SNF-Komplex, der durch die Modifikation von Nukleosomen zur Struktur der DNA und zur Regulation von Genen beiträgt (Geng *et al.*, 2001). Es ist deshalb nicht auszuschließen, dass Ace2 auch eine Funktion bei der Organisation der DNA-Struktur aufweist.

Interessanterweise konnte bei der genomweiten Bindeanalyse der Sch9 Kinase auch die Bindung an die Zentromer-Regionen aller acht Chromosomen identifiziert werden (Manuskript V). Im Gegensatz zu Ace2 trat die Bindung von Sch9 an die Zentromere auch unter normoxischen Wachstumsbedingungen auf. Die Ergebnisse weisen darauf hin, dass Sch9 an der Segregation von Chromosomen beteiligt ist, denn die *sch9*-Mutante wies eine um das 750-fach erhöhte Chromosomenverlustrate auf (Manuskript V). Der zugrundeliegende molekulare Mechanismus ist auch für Sch9 unklar. Eine direkte Regulation des Zentromer-spezifischen Histons Cse4 scheint nicht für den Phänotyp verantwortlich zu sein. Vermutlich interagiert Sch9 mit Elementen des Kinetochor-Komplexes. Die Sch9 Kinase gehört zu den AGC-Kinasen und liegt stromabwärts des TORC1-Signalwegs, der das Zellwachstum in Abhängigkeit des Nährstoffangebotes reguliert (Urban *et al.*, 2007). Darüber hinaus konnte für Sch9 eine Funktion bei der hypoxischen Hyphenmorphogenese nachgewiesen werden (Stichternoth & Ernst, 2009). Wie bereits unter 3.8 beschrieben, scheint die Funktion von Sch9 von einer erhöhten CO_2-Konzentration abhängig zu sein, ähnlich wie für Ace2. Ein Zusammenhang zwischen der Bindung von Sch9 und Ace2 liegt möglicherweise in der Zellteilungsrate, die in

beiden Mutanten unter hypoxischen Wachstumsbedingungen stark reduziert war. Die *sch9*-Mutante weist zudem auch unter normoxischen Wachstumsbedingungen eine langsamere Wachstumsrate auf (Fabrizio *et al.*, 2001; Liu *et al.*, 2010). Die Bindung von Ace2 und Sch9 an die Zentromere wirkt möglicherweise stabilisierend auf den Kinetochor-Komplex. Die Funktion an der Chromosomen-Segregation konnte für das homologe Sch9 Protein in *S. cerevisiae* nicht nachgewiesen werden (Manuskript V). Auch für die homologen Ace2 Proteine gibt es bislang keine Hinweise für die Bindung an Zentromer-Regionen oder eine Funktion an der Segregation von Chromosomen. Um aufzuklären, welche Funktion Ace2 an den Zentromeren besitzt und ob es einen Zusammenhang mit der Bindung von Sch9 gibt, sind weitere Experimente notwendig. Der Einfluss von Ace2 auf die Chromosomen-Segregation in *C. albicans* wird derzeit untersucht (L. v. Wijlick, J. F. Ernst & K. Sanyal, unpublizierte Ergebnisse).

4 Zusammenfassung

Die Fähigkeit, sich schnell an die komplexen Umgebungsbedingungen des menschlichen Wirts anzupassen, macht den Pilz *Candida albicans* zu einem der erfolgreichsten Krankheitserreger. Diese Fähigkeit setzt eine dynamische und intakte Zellwandstruktur des Pilzes voraus. Schäden in den schützenden Glykostrukturen der Zellwand werden vom Sensorprotein Msb2 an den Cek1 MAPK-Signalweg übermittelt, der die Expression von Genen stimuliert, die für Protein-*O*-Mannosyltransferasen (Pmt-Proteine) kodieren. Pmt-Proteine initiieren die *O*-Mannosylierung von Zellwandproteinen und sind dadurch essentiell für das Wachstum und die Virulenz von *C. albicans*. In früheren Arbeiten konnte gezeigt werden, dass der Transkriptionsfaktor Ace2 durch unbekannte Mechanismen zur Regulation von *PMT*-Genen und der Integrität der Zellwand beiträgt.

Die Ergebnisse der genomweiten Bindung von Ace2 weisen darauf hin, dass Ace2 indirekt, über Co-Regulation weiterer Transkriptionsfaktoren, die Transkription von *PMT*-Genen steuert. Als Repressor des *PMT1*-Gens wurde der Transkriptionsfaktor Zcf21 identifiziert, dessen Expression unter nicht-gestressten Wachstumsbedingungen durch Ace2 stimuliert wird und bei defekter Protein-*N*-Glykosylierung reprimiert wird. Zu den neu identifizierten Zielgenen von Ace2 zählen auch die Gene *MSB2*, *CST20*, *HST7* und *CEK1*, die für Elemente des Cek1-Signalwegs kodieren und das *ACE2*-Gen selbst. Transkriptanalysen ergaben, dass ein durch Ace2-Cek1 vermittelter autoregulatorischer Mechanismus zur transkriptionellen Amplifikation des Signalwegs bei defekter *N*-Glykosylierung beiträgt. Unter diesen Bedingungen wurde eine verstärkte Lokalisation einer Cst20-GFP-Fusion im Zellkern beobachtet, die zur Inhibierung von Ace2 und dessen Zielgenen führt. Bei defekter Glykosylierung lokalisierte auch die zytoplasmatische Domäne des Msb2-Proteins im Zellkern. Die Ergebnisse weisen darauf hin, dass der Transkriptionsfaktor Ace2 stromabwärts des Cek1-MAPK-Signalwegs agiert und gemeinsam mit Cst20 und Msb2 sowohl an einem positiven, als auch einem negativen Rückkopplungsmechanismus des Cek1 MAPK-Signalweges beteiligt ist. Die Anpassung an defekte Glykosylierung wird zudem durch das RNA-Bindeprotein Dom34 unterstützt. Das Dom34 Protein gehört zur konservierten Dom34/Pelota-Proteinfamilie und begünstigt spezifisch die Translation von *PMT*-Transkripten. Die Spezifität von Dom34 für Transkripte der *PMT*-Gene wird vermutlich durch ein identifiziertes CAAC-Motiv vermittelt, das in allen 5‘-UTR Sequenzen der *PMT*-mRNAs vorkommt.

Auch bei der Anpassung an hypoxische Umgebungsbedingungen ist der Cek1 MAPK-Signalweg von zentraler Bedeutung. Durch die genomweite Bindeanalyse von Ace2 konnten *BCR1*, *BRG1* und *EFG1*, die für bekannte normoxische Hyphenregulatoren kodieren, als neue Ace2-Zielgene identifiziert werden. Analysen von Transkriptspiegeln und genomischen Bindestellen ergaben, dass die kodierten vier Transkriptionsfaktoren ein regulatorisches Netzwerk bilden, das unter hypoxischen Bedingungen die Hyphenmorphogenese von *C. albicans* reguliert. Dabei konnten Efg1 und Bcr1 als Repressoren und Ace2 und Brg1 als Aktivatoren der Hyphenmorphogenese identifiziert werden. Als Ziele des regulatorischen Netzwerkes wurden unter anderem Gene für Elemente des Cek1-Signalwegs und den stromabwärts agierenden Transkriptionsfaktor Cph1 nachgewiesen. Die komplexen regulatorischen Mechanismen weisen darauf hin, dass *C. albicans* in sauerstoffarmen Körpernischen die Ausbildung von Hyphen durch die Reprimierung des Cek1-Signalwegs unterdrückt, möglicherweise, um Angriffen des Immunsystems zu entgehen und als Kommensale im Wirt zu persistieren. Überraschenderweise konnte unter diesen Wachstumsbedingungen die Bindung von Ace2 und der Kinase Sch9 an die Zentromere aller acht Chromosomen detektiert werden. Die Kinase Sch9 scheint die Segregation von Chromosomen zu unterstützen, während die hypoxische Funktion von Ace2 an den Zentromeren noch aufgeklärt werden muss.

Mit diesen Ergebnissen konnte Ace2 als multifunktionales Regulatorprotein identifiziert werden, das essentiell für die Anpassung und das Überleben von *C. albicans* in wirtspezifischen Umgebungsbedingungen ist.

5 Summary

The ability to promptly respond and adapt to complex host environments of the human body enables *Candida albicans* to become a highly successful pathogen. This ability requires a dynamic and intact cell wall structure of the fungus. Damage of the protecting glyco-structures of the cell wall is sensed by the membrane protein Msb2 and transmitted to the Cek1-MAPK signaling pathway, which stimulates expression of genes encoding protein-*O*-mannosyltransferases (Pmt-proteins). Pmt-proteins initiate *O*-mannosylation of cell wall proteins, which is an essential activity for the growth and virulence of *C. albicans*. Previously it had been shown that the transcription factor Ace2, by unknown mechanisms, contributes to the regulation of *PMT*-genes and the integrity of the cell wall.

Results of the genome-wide binding of Ace2 indicate that Ace2 regulates transcription of *PMT*-genes indirectly, through co-regulation of additional transcription factors. As a repressor of the *PMT1*-gene, the Zcf21 transcription factor was identified, whose expression is stimulated by Ace2 under unstressed growth conditions and repressed during defective protein-*N*-glycosylation. Newly identified Ace2 target genes also included *MSB2*, *CST20*, *HST7* and *CEK1* genes encoding elements of the Cek1 signaling pathway and the *ACE2*-gene itself. Transcript analyses of these genes revealed that an Ace2-Cek1-mediated auto-regulatory mechanism induces transcriptional amplification of the signaling pathway by defective *N*-glycosylation. Under these conditions, increased nuclear localization of a Cst20-GFP fusion was detected leading to inhibition of Ace2 and its target genes. Moreover, defective *N*-glycosylation led to nuclear localization of the cytoplasmic domain of the Msb2-protein. The results suggest that the transcription factor Ace2 acts downstream of the Cek1 signaling pathway and mediates, in concern with Cst20 and Msb2, positive as well as negative feedback regulation of Cek1 MAPK signaling pathway. Furthermore, adaptation to defective glycosylation is supported by the RNA binding protein Dom34. The Dom34 protein is a member of the Dom34/Pelota protein family and specifically promotes translation of *PMT*-transcripts. Specificity of Dom34 for transcripts of *PMT*-genes is possibly mediated through an identified CAAC-motif, which is present in all 5'-UTR sequences of *PMT*-mRNAs.

The Cek1 MAPK signaling pathway is also of crucial importance for adaption to hypoxic conditions. Exploring genome-wide binding of Ace2 identified *BCR1*, *BRG1* and *EFG1*, encoding known normoxic hyphal-regulators as novel Ace2 target genes. Analysis of transcript levels and genomic binding sites revealed that the encoded four transcription factors form a regulatory network that controls hyphal morphogenesis of *C. albicans* under hypoxic conditions. Hereby, Efg1 and Bcr1 were identified as repressors and Ace2 and Brg1 as activators of hyphal morphogenesis. Targets of the identified regulatory network include genes encoding elements of the Cek1 signaling pathway and the downstream acting transcription factor Cph1. The complex regulatory mechanisms occurring under hypoxia suggest that *C. albicans* actively represses hyphal development in oxygen-poor body niches through repression of Cek1 signaling, presumably in an attempt to avoid immune response and to persist as a commensal in the human host. Surprisingly, under these conditions binding of Ace2 and the kinase Sch9 was detected to centromeres of all eight chromosomes. For the Sch9 kinase, a novel function in chromosome segregation was identified, while the function of Ace2 at the centromeres under hypoxia remains to be elucidated.

By these results, Ace2 was identified to be a multifunctional regulator protein, which is essential for adaptation and survival of *C. albicans* in specific host niches.

6 Literaturverzeichnis

Ahn, S.H., W.L. Cheung, J.Y. Hsu, R.L. Diaz, M.M. Smith & C.D. Allis, (2005) Sterile 20 kinase phosphorylates histone H2B at serine 10 during hydrogen peroxide-induced apoptosis in S. cerevisiae. *Cell* **120**: 25-36.

Almeida, R.S., S. Brunke, A. Albrecht, S. Thewes, M. Laue, J.E. Edwards, S.G. Filler & B. Hube, (2008) the hyphal-associated adhesin and invasin Als3 of Candida albicans mediates iron acquisition from host ferritin. *PLoS Pathog* **4**: e1000217.

Apweiler, R., H. Hermjakob & N. Sharon, (1999) On the frequency of protein glycosylation, as deduced from analysis of the SWISS-PROT database. *Biochim Biophys Acta* **1473**: 4-8.

Arroyo, J., J. Hutzler, C. Bermejo, E. Ragni, J. Garcia-Cantalejo, P. Botias, H. Piberger, A. Schott, A.B. Sanz & S. Strahl, (2011) Functional and genomic analyses of blocked protein O-mannosylation in baker's yeast. *Mol Microbiol* **79**: 1529-1546.

Bacher, P., A. Steinbach, O. Kniemeyer, A. Hamprecht, M. Assenmacher, M.J. Vehreschild, J.J. Vehreschild, A.A. Brakhage, O.A. Cornely & A. Scheffold, (2015) Fungus-specific CD4(+) T cells for rapid identification of invasive pulmonary mold infection. *Am J Respir Crit Care Med* **191**: 348-352.

Badis, G., E.T. Chan, H. van Bakel, L. Pena-Castillo, D. Tillo, K. Tsui, C.D. Carlson, A.J. Gossett, M.J. Hasinoff, C.L. Warren, M. Gebbia, S. Talukder, A. Yang, S. Mnaimneh, D. Terterov, D. Coburn, A. Li Yeo, Z.X. Yeo, N.D. Clarke, J.D. Lieb, A.Z. Ansari, C. Nislow & T.R. Hughes, (2008) A library of yeast transcription factor motifs reveals a widespread function for Rsc3 in targeting nucleosome exclusion at promoters. *Mol Cell* **32**: 878-887.

Bardwell, L., J.G. Cook, D. Voora, D.M. Baggott, A.R. Martinez & J. Thorner, (1998) Repression of yeast Ste12 transcription factor by direct binding of unphosphorylated Kss1 MAPK and its regulation by the Ste7 MEK. *Genes Dev* **12**: 2887-2898.

Barresi, R. & K.P. Campbell, (2006) Dystroglycan: from biosynthesis to pathogenesis of human disease. *J Cell Sci* **119**: 199-207.

Bates, S., H.B. Hughes, C.A. Munro, W.P. Thomas, D.M. MacCallum, G. Bertram, A. Atrih, M.A. Ferguson, A.J. Brown, F.C. Odds & N.A. Gow, (2006) Outer chain N-glycans are required for cell wall integrity and virulence of Candida albicans. *J Biol Chem* **281**: 90-98.

Bharucha, N., Y. Chabrier-Rosello, T. Xu, C. Johnson, S. Sobczynski, Q. Song, C.J. Dobry, M.J. Eckwahl, C.P. Anderson, A.J. Benjamin, A. Kumar & D.J. Krysan, (2011) A large-scale complex haploinsufficiency-based genetic interaction screen in Candida albicans: analysis of the RAM network during morphogenesis. *PLoS Genet* **7**: e1002058.

Bockmuhl, D.P. & J.F. Ernst, (2001) A potential phosphorylation site for an A-type kinase in the Efg1 regulator protein contributes to hyphal morphogenesis of Candida albicans. *Genetics* **157**: 1523-1530.

Bohm, L., P. Muralidhara & J.C. Perez, (2016) A Candida albicans regulator of disseminated infection operates primarily as a repressor and governs cell surface remodeling. *Mol Microbiol* **100**: 328-344.

Bourens, M., W. Racki, A.M. Becam, C. Panozzo, S. Boulon, E. Bertrand & C.J. Herbert, (2008) Mutations in a small region of the exportin Crm1p disrupt the daughter cell-specific nuclear localization of the transcription factor Ace2p in Saccharomyces cerevisiae. *Biol Cell* **100**: 343-354.

Brace, J., J. Hsu & E.L. Weiss, (2011) Mitotic exit control of the Saccharomyces cerevisiae Ndr/LATS kinase Cbk1 regulates daughter cell separation after cytokinesis. *Mol Cell Biol* **31**: 721-735.

Brock, M., (2009) Fungal metabolism in host niches. *Curr Opin Microbiol* **12**: 371-376.

Brown, G.D., D.W. Denning, N.A. Gow, S.M. Levitz, M.G. Netea & T.C. White, (2012) Hidden killers: human fungal infections. *Sci Transl Med* **4**: 165rv113.

Brown, G.D. & M.G. Netea, (2012) Exciting developments in the immunology of fungal infections. *Cell Host Microbe* **11**: 422-424.

Brown, N.A., T.F. Dos Reis, A.B. Goinski, M. Savoldi, J. Menino, M.T. Almeida, F. Rodrigues & G.H. Goldman, (2014) The Aspergillus nidulans signalling mucin MsbA regulates starvation responses, adhesion and affects cellulase secretion in response to environmental cues. *Mol Microbiol*.

Bruno, V.M., S. Kalachikov, R. Subaran, C.J. Nobile, C. Kyratsous & A.P. Mitchell, (2006) Control of the C. albicans cell wall damage response by transcriptional regulator Cas5. *PLoS Pathog* **2**: e21.

Buurman, E.T., C. Westwater, B. Hube, A.J. Brown, F.C. Odds & N.A. Gow, (1998) Molecular analysis of CaMnt1p, a mannosyl transferase important for adhesion and virulence of Candida albicans. *Proc Natl Acad Sci U S A* **95**: 7670-7675.

Calderon-Norena, D.M., A. Gonzalez-Novo, S. Orellana-Munoz, P. Gutierrez-Escribano, Y. Arnaiz-Pita, E. Duenas-Santero, M.B. Suarez, M.E. Bougnoux, F. Del Rey, G. Sherlock, C. d'Enfert, J. Correa-Bordes & C.R. de Aldana, (2015) A single nucleotide polymorphism uncovers a novel function for the transcription factor Ace2 during Candida albicans hyphal development. *PLoS Genet* **11**: e1005152.

Canivenc-Gansel, E., I. Imhof, F. Reggiori, P. Burda, A. Conzelmann & A. Benachour, (1998) GPI anchor biosynthesis in yeast: phosphoethanolamine is attached to the alpha1,4-linked mannose of the complete precursor glycophospholipid. *Glycobiology* **8**: 761-770.

Cantero, P.D., (2010) Proteinglykosylierung bei Candida albicans: Regulatorische Signalwege und Virulenzeigenschaften. *Dissertation, Heinrich-Heine Universität Düsseldorf.*

Cantero, P.D. & J.F. Ernst, (2011) Damage to the glycoshield activates PMT-directed O-mannosylation via the Msb2-Cek1 pathway in Candida albicans. *Mol Microbiol* **80**: 715-725.

Cantero, P.D., C. Lengsfeld, S.K. Prill, M. Subanovic, E. Roman, J. Pla & J.F. Ernst, (2007) Transcriptional and physiological adaptation to defective protein-O-mannosylation in Candida albicans. *Mol Microbiol* **64**: 1115-1128.

Cassone, A. & R. Cauda, (2012) Candida and candidiasis in HIV-infected patients: where commensalism, opportunistic behavior and frank pathogenicity lose their borders. *AIDS* **26**: 1457-1472.

Chaffin, W.L., (2008) Candida albicans cell wall proteins. *Microbiol Mol Biol Rev* **72**: 495-544.

Chaffin, W.L., J.L. Lopez-Ribot, M. Casanova, D. Gozalbo & J.P. Martinez, (1998) Cell wall and secreted proteins of Candida albicans: identification, function, and expression. *Microbiol Mol Biol Rev* **62**: 130-180.

Cheng, S.C., F.L. van de Veerdonk, M. Lenardon, M. Stoffels, T. Plantinga, S. Smeekens, L. Rizzetto, L. Mukaremera, K. Preechasuth, D. Cavalieri, T.D. Kanneganti, J.W. van der Meer, B.J. Kullberg, L.A. Joosten, N.A. Gow & M.G. Netea, (2011) The dectin-1/inflammasome pathway is responsible for the induction of protective T-helper 17 responses that discriminate between yeasts and hyphae of Candida albicans. *J Leukoc Biol* **90**: 357-366.

Childers, D.S., V. Mundodi, M. Banerjee & D. Kadosh, (2014) A 5' UTR-mediated translational efficiency mechanism inhibits the Candida albicans morphological transition. *Mol Microbiol* **92**: 570-585.

Cleary, I.A., A.L. Lazzell, C. Monteagudo, D.P. Thomas & S.P. Saville, (2012) BRG1 and NRG1 form a novel feedback circuit regulating Candida albicans hypha formation and virulence. *Mol Microbiol* **85**: 557-573.

Clemente-Blanco, A., A. Gonzalez-Novo, F. Machin, D. Caballero-Lima, L. Aragon, M. Sanchez, C.R. de Aldana, J. Jimenez & J. Correa-Bordes, (2006) The Cdc14p phosphatase affects late cell-cycle events and morphogenesis in Candida albicans. *J Cell Sci* **119**: 1130-1143.

Collier, E., J.L. Carpentier, L. Beitz, H. Carol, S.I. Taylor & P. Gorden, (1993) Specific glycosylation site mutations of the insulin receptor alpha subunit impair intracellular transport. *Biochemistry* **32**: 7818-7823.

Colman-Lerner, A., T.E. Chin & R. Brent, (2001) Yeast Cbk1 and Mob2 activate daughter-specific genetic programs to induce asymmetric cell fates. *Cell* **107**: 739-750.

Cottier, F. & F.A. Muhlschlegel, (2009) Sensing the environment: response of Candida albicans to the X factor. *FEMS Microbiol Lett* **295**: 1-9.

Csank, C., C. Makris, S. Meloche, K. Schroppel, M. Rollinghoff, D. Dignard, D.Y. Thomas & M. Whiteway, (1997) Derepressed hyphal growth and reduced virulence in a VH1 family-related protein phosphatase mutant of the human pathogen Candida albicans. *Mol Biol Cell* **8**: 2539-2551.

Csank, C., K. Schroppel, E. Leberer, D. Harcus, O. Mohamed, S. Meloche, D.Y. Thomas & M. Whiteway, (1998) Roles of the Candida albicans mitogen-activated protein kinase homolog, Cek1p, in hyphal development and systemic candidiasis. *Infect Immun* **66**: 2713-2721.

Cullen, P.J., (2011) Post-translational regulation of signaling mucins. *Curr Opin Struct Biol* **21**: 590-596.

Cullen, P.J., W. Sabbagh, Jr., E. Graham, M.M. Irick, E.K. van Olden, C. Neal, J. Delrow, L. Bardwell & G.F. Sprague, Jr., (2004) A signaling mucin at the head of the Cdc42- and MAPK-dependent filamentous growth pathway in yeast. *Genes Dev* **18**: 1695-1708.

Cullen, P.J., J. Schultz, J. Horecka, B.J. Stevenson, Y. Jigami & G.F. Sprague, Jr., (2000) Defects in protein glycosylation cause SHO1-dependent activation of a STE12 signaling pathway in yeast. *Genetics* **155**: 1005-1018.

Cullen, P.J., R. Xu-Friedman, J. Delrow & G.F. Sprague, (2006) Genome-wide analysis of the response to protein glycosylation deficiency in yeast. *FEMS Yeast Res* **6**: 1264-1273.

Cutler, J.E., (1991) Putative virulence factors of Candida albicans. *Annu Rev Microbiol* **45**: 187-218.

Da Silva, C.A., C. Chalouni, A. Williams, D. Hartl, C.G. Lee & J.A. Elias, (2009) Chitin is a size-dependent regulator of macrophage TNF and IL-10 production. *J Immunol* **182**: 3573-3582.

Darwazeh, A.M., P.J. Lamey, L.P. Samaranayake, T.W. MacFarlane, B.M. Fisher, S.M. Macrury & A.C. MacCuish, (1990) The relationship between colonisation, secretor status and in-vitro adhesion of Candida albicans to buccal epithelial cells from diabetics. *J Med Microbiol* **33**: 43-49.

Dennehy, K.M., G. Ferwerda, I. Faro-Trindade, E. Pyz, J.A. Willment, P.R. Taylor, A. Kerrigan, S.V. Tsoni, S. Gordon, F. Meyer-Wentrup, G.J. Adema, B.J. Kullberg, E. Schweighoffer, V. Tybulewicz, H.M. Mora-Montes, N.A. Gow, D.L. Williams, M.G. Netea & G.D. Brown, (2008) Syk kinase is required for collaborative cytokine production induced through Dectin-1 and Toll-like receptors. *Eur J Immunol* **38**: 500-506.

Doedt, T., S. Krishnamurthy, D.P. Bockmuhl, B. Tebarth, C. Stempel, C.L. Russell, A.J. Brown & J.F. Ernst, (2004) APSES proteins regulate morphogenesis and metabolism in Candida albicans. *Mol Biol Cell* **15**: 3167-3180.

Doma, M.K. & R. Parker, (2006) Endonucleolytic cleavage of eukaryotic mRNAs with stalls in translation elongation. *Nature* **440**: 561-564.

Doolin, M.T., A.L. Johnson, L.H. Johnston & G. Butler, (2001) Overlapping and distinct roles of the duplicated yeast transcription factors Ace2p and Swi5p. *Mol Microbiol* **40**: 422-432.

Du, H., G. Guan, J. Xie, F. Cottier, Y. Sun, W. Jia, F.A. Muhlschlegel & G. Huang, (2012a) The transcription factor Flo8 mediates CO2 sensing in the human fungal pathogen Candida albicans. *Mol Biol Cell* **23**: 2692-2701.

Du, H., G. Guan, J. Xie, Y. Sun, Y. Tong, L. Zhang & G. Huang, (2012b) Roles of Candida albicans Gat2, a GATA-type zinc finger transcription factor, in biofilm formation, filamentous growth and virulence. *PLoS One* **7**: e29707.

Dube, A.K., M. Belanger, I. Gagnon-Arsenault & Y. Bourbonnais, (2015) N-terminal entrance loop of yeast Yps1 and O-glycosylation of substrates are determinant factors controlling the shedding activity of this GPI-anchored endopeptidase. *BMC Microbiol* **15**: 50.

Ecker, M., R. Deutzmann, L. Lehle, V. Mrsa & W. Tanner, (2006) Pir proteins of Saccharomyces cerevisiae are attached to beta-1,3-glucan by a new protein-carbohydrate linkage. *J Biol Chem* **281**: 11523-11529.

Eggimann, P. & D. Pittet, (2006) Postoperative fungal infections. *Surg Infect (Larchmt)* **7 Suppl 2**: S53-56.

Eisman, B., R. Alonso-Monge, E. Roman, D. Arana, C. Nombela & J. Pla, (2006) The Cek1 and Hog1 mitogen-activated protein kinases play complementary roles in cell wall biogenesis and chlamydospore formation in the fungal pathogen Candida albicans. *Eukaryot Cell* **5**: 347-358.

Ejzykowicz, D.E., M.M. Cunha, S. Rozental, N.V. Solis, F.N. Gravelat, D.C. Sheppard & S.G. Filler, (2009) The Aspergillus fumigatus transcription factor Ace2 governs pigment production, conidiation and virulence. *Mol Microbiol* **72**: 155-169.

Ernst, J.F., (2000) Transcription factors in Candida albicans - environmental control of morphogenesis. *Microbiology* **146 (Pt 8)**: 1763-1774.

Ernst, J.F. & S.K. Prill, (2001) O-glycosylation. *Med Mycol* **39 Suppl 1**: 67-74.

Ernst, J.F. & D. Tielker, (2009) Responses to hypoxia in fungal pathogens. *Cell Microbiol* **11**: 183-190.

Espitia, C., L. Servin-Gonzalez & R. Mancilla, (2010) New insights into protein O-mannosylation in actinomycetes. *Mol Biosyst* **6**: 775-781.

Fabrizio, P., F. Pozza, S.D. Pletcher, C.M. Gendron & V.D. Longo, (2001) Regulation of longevity and stress resistance by Sch9 in yeast. *Science* **292**: 288-290.

Feng, Q., E. Summers, B. Guo & G. Fink, (1999) Ras signaling is required for serum-induced hyphal differentiation in Candida albicans. *J Bacteriol* **181**: 6339-6346.

Finck, M., N. Bergmann, B. Jansson & J.F. Ernst, (1996) Defective threonine-linked glycosylation of human insulin-like growth factor in mutants of the yeast Saccharomyces cerevisiae. *Glycobiology* **6**: 313-320.

Finkel, J.S., W. Xu, D. Huang, E.M. Hill, J.V. Desai, C.A. Woolford, J.E. Nett, H. Taff, C.T. Norice, D.R. Andes, F. Lanni & A.P. Mitchell, (2012) Portrait of Candida albicans adherence regulators. *PLoS Pathog* **8**: e1002525.

Fischer, G., (2012) Chronic vulvovaginal candidiasis: what we know and what we have yet to learn. *Australas J Dermatol* **53**: 247-254.

Free, S.J., (2013) Fungal cell wall organization and biosynthesis. *Adv Genet* **81**: 33-82.

Gantner, B.N., R.M. Simmons & D.M. Underhill, (2005) Dectin-1 mediates macrophage recognition of Candida albicans yeast but not filaments. *EMBO J* **24**: 1277-1286.

Geng, F., Y. Cao & B.C. Laurent, (2001) Essential roles of Snf5p in Snf-Swi chromatin remodeling in vivo. *Mol Cell Biol* **21**: 4311-4320.

Ghannoum, M.A., R.J. Jurevic, P.K. Mukherjee, F. Cui, M. Sikaroodi, A. Naqvi & P.M. Gillevet, (2010) Characterization of the oral fungal microbiome (mycobiome) in healthy individuals. *PLoS Pathog* **6**: e1000713.

Giusani, A.D., M. Vinces & C.A. Kumamoto, (2002) Invasive filamentous growth of Candida albicans is promoted by Czf1p-dependent relief of Efg1p-mediated repression. *Genetics* **160**: 1749-1753.

Gow, N.A., (2013) A developmental program for Candida commensalism. *Nat Genet* **45**: 967-968.

Gow, N.A. & B. Hube, (2012) Importance of the Candida albicans cell wall during commensalism and infection. *Curr Opin Microbiol* **15**: 406-412.

Grahl, N. & R.A. Cramer, Jr., (2010) Regulation of hypoxia adaptation: an overlooked virulence attribute of pathogenic fungi? *Med Mycol* **48**: 1-15.

Gudlaugsson, O., S. Gillespie, K. Lee, J. Vande Berg, J. Hu, S. Messer, L. Herwaldt, M. Pfaller & D. Diekema, (2003) Attributable mortality of nosocomial candidemia, revisited. *Clin Infect Dis* **37**: 1172-1177.

Guha-Niyogi, A., D.R. Sullivan & S.J. Turco, (2001) Glycoconjugate structures of parasitic protozoa. *Glycobiology* **11**: 45R-59R.

Gutierrez-Escribano, P., A. Gonzalez-Novo, M.B. Suarez, C.R. Li, Y. Wang, C.R. de Aldana & J. Correa-Bordes, (2011) CDK-dependent phosphorylation of Mob2 is essential for hyphal development in Candida albicans. *Mol Biol Cell* **22**: 2458-2469.

Gutierrez-Escribano, P., U. Zeidler, M.B. Suarez, S. Bachellier-Bassi, A. Clemente-Blanco, J. Bonhomme, C.R. Vazquez de Aldana, C. d'Enfert & J. Correa-Bordes, (2012) The NDR/LATS kinase Cbk1 controls the activity of the transcriptional regulator Bcr1 during biofilm formation in Candida albicans. *PLoS Pathog* **8**: e1002683.

Hall, R.A., S. Bates, M.D. Lenardon, D.M. Maccallum, J. Wagener, D.W. Lowman, M.D. Kruppa, D.L. Williams, F.C. Odds, A.J. Brown & N.A. Gow, (2013) The Mnn2 mannosyltransferase family modulates mannoprotein fibril length, immune recognition and virulence of Candida albicans. *PLoS Pathog* **9**: e1003276.

Hall, R.A. & N.A. Gow, (2013) Mannosylation in Candida albicans: role in cell wall function and immune recognition. *Mol Microbiol* **90**: 1147-1161.

Heilmann, C.J., A.G. Sorgo, A.R. Siliakus, H.L. Dekker, S. Brul, C.G. de Koster, L.J. de Koning & F.M. Klis, (2011) Hyphal induction in the human fungal pathogen Candida albicans reveals a characteristic wall protein profile. *Microbiology* **157**: 2297-2307.

Hernday, A.D., M.B. Lohse, P.M. Fordyce, C.J. Nobile, J.L. DeRisi & A.D. Johnson, (2013) Structure of the transcriptional network controlling white-opaque switching in Candida albicans. *Mol Microbiol* **90**: 22-35.

Hewitt, J.E., (2009) Abnormal glycosylation of dystroglycan in human genetic disease. *Biochim Biophys Acta* **1792**: 853-861.

Hostetter, M.K., (1994) Adhesins and ligands involved in the interaction of Candida spp. with epithelial and endothelial surfaces. *Clin Microbiol Rev* **7**: 29-42.

Huang, G., (2012) Regulation of phenotypic transitions in the fungal pathogen Candida albicans. *Virulence* **3**: 251-261.

Huffnagle, G.B. & M.C. Noverr, (2013) The emerging world of the fungal microbiome. *Trends Microbiol* **21**: 334-341.

Jaeken, J., (2010) Congenital disorders of glycosylation. *Ann N Y Acad Sci* **1214**: 190-198.

Jimenez-Lopez, C. & M.C. Lorenz, (2013) Fungal immune evasion in a model host-pathogen interaction: Candida albicans versus macrophages. *PLoS Pathog* **9**: e1003741.

Kamran, M., A.M. Calcagno, H. Findon, E. Bignell, M.D. Jones, P. Warn, P. Hopkins, D.W. Denning, G. Butler, T. Rogers, F.A. Muhlschlegel & K. Haynes, (2004) Inactivation of transcription factor gene ACE2 in the fungal pathogen Candida glabrata results in hypervirulence. *Eukaryot Cell* **3**: 546-552.

Karababa, M., E. Valentino, G. Pardini, A.T. Coste, J. Bille & D. Sanglard, (2006) CRZ1, a target of the calcineurin pathway in Candida albicans. *Mol Microbiol* **59**: 1429-1451.

Kelly, M.T., D.M. MacCallum, S.D. Clancy, F.C. Odds, A.J. Brown & G. Butler, (2004) The Candida albicans CaACE2 gene affects morphogenesis, adherence and virulence. *Mol Microbiol* **53**: 969-983.

King, L. & G. Butler, (1998) Ace2p, a regulator of CTS1 (chitinase) expression, affects pseudohyphal production in Saccharomyces cerevisiae. *Curr Genet* **34**: 183-191.

Klis, F.M., P. de Groot & K. Hellingwerf, (2001) Molecular organization of the cell wall of Candida albicans. *Med Mycol* **39 Suppl 1**: 1-8.

Klis, F.M., P. Mol, K. Hellingwerf & S. Brul, (2002) Dynamics of cell wall structure in Saccharomyces cerevisiae. *FEMS Microbiol Rev* **26**: 239-256.

Koh, A.Y., (2013) Murine models of Candida gastrointestinal colonization and dissemination. *Eukaryot Cell* **12**: 1416-1422.

Krysan, D.J., (2009) The cell wall and endoplasmic reticulum stress responses are coordinately regulated in Saccharomyces cerevisiae. *Commun Integr Biol* **2**: 233-235.

Kullberg, B.J. & M.C. Arendrup, (2015) Invasive Candidiasis. *N Engl J Med* **373**: 1445-1456.

Kurischko, C., G. Weiss, M. Ottey & F.C. Luca, (2005) A role for the Saccharomyces cerevisiae regulation of Ace2 and polarized morphogenesis signaling network in cell integrity. *Genetics* **171**: 443-455.

Lanver, D., A. Mendoza-Mendoza, A. Brachmann & R. Kahmann, (2010) Sho1 and Msb2-related proteins regulate appressorium development in the smut fungus Ustilago maydis. *Plant Cell* **22**: 2085-2101.

Lassak, T., E. Schneider, M. Bussmann, D. Kurtz, J.R. Manak, T. Srikantha, D.R. Soll & J.F. Ernst, (2011) Target specificity of the Candida albicans Efg1 regulator. *Mol Microbiol* **82**: 602-618.

Leberer, E., D. Harcus, D. Dignard, L. Johnson, S. Ushinsky, D.Y. Thomas & K. Schroppel, (2001) Ras links cellular morphogenesis to virulence by regulation of the MAP kinase and cAMP signalling pathways in the pathogenic fungus Candida albicans. *Mol Microbiol* **42**: 673-687.

Lechner, J. & J. Ortiz, (1996) The Saccharomyces cerevisiae kinetochore. *FEBS Lett* **389**: 70-74.

Lee, B.N. & E.A. Elion, (1999) The MAPKKK Ste11 regulates vegetative growth through a kinase cascade of shared signaling components. *Proc Natl Acad Sci U S A* **96**: 12679-12684.

Lee, C.G., C.A. Da Silva, J.Y. Lee, D. Hartl & J.A. Elias, (2008) Chitin regulation of immune responses: an old molecule with new roles. *Curr Opin Immunol* **20**: 684-689.

Lenardon, M.D., C.A. Munro & N.A. Gow, (2010) Chitin synthesis and fungal pathogenesis. *Curr Opin Microbiol* **13**: 416-423.

Lengeler, K.B., D. Tielker & J.F. Ernst, (2008) Protein-O-mannosyltransferases in virulence and development. *Cell Mol Life Sci* **65**: 528-544.

Li, Y., C. Su, X. Mao, F. Cao & J. Chen, (2007) Roles of Candida albicans Sfl1 in hyphal development. *Eukaryot Cell* **6**: 2112-2121.

Lionakis, M.S. & M.G. Netea, (2013) Candida and host determinants of susceptibility to invasive candidiasis. *PLoS Pathog* **9**: e1003079.

Lipke, P.N. & R. Ovalle, (1998) Cell wall architecture in yeast: new structure and new challenges. *J Bacteriol* **180**: 3735-3740.

Liu, H., J. Kohler & G.R. Fink, (1994) Suppression of hyphal formation in Candida albicans by mutation of a STE12 homolog. *Science* **266**: 1723-1726.

Liu, W., J. Zhao, X. Li, Y. Li & L. Jiang, (2010) The protein kinase CaSch9p is required for the cell growth, filamentation and virulence in the human fungal pathogen Candida albicans. *FEMS Yeast Res* **10**: 462-470.

Lo, H.J., J.R. Kohler, B. DiDomenico, D. Loebenberg, A. Cacciapuoti & G.R. Fink, (1997) Nonfilamentous C. albicans mutants are avirulent. *Cell* **90**: 939-949.

Lu, Y., C. Su, N.V. Solis, S.G. Filler & H. Liu, (2013) Synergistic regulation of hyphal elongation by hypoxia, CO(2), and nutrient conditions controls the virulence of Candida albicans. *Cell Host Microbe* **14**: 499-509.

Lyalin, D., K. Koles, S.D. Roosendaal, E. Repnikova, L. Van Wechel & V.M. Panin, (2006) The twisted gene encodes Drosophila protein O-mannosyltransferase 2 and genetically interacts with the rotated abdomen gene encoding Drosophila protein O-mannosyltransferase 1. *Genetics* **172**: 343-353.

MacCallum, D.M., H. Findon, C.C. Kenny, G. Butler, K. Haynes & F.C. Odds, (2006) Different consequences of ACE2 and SWI5 gene disruptions for virulence of pathogenic and nonpathogenic yeasts. *Infect Immun* **74**: 5244-5248.

Madhani, H.D., C.A. Styles & G.R. Fink, (1997) MAP kinases with distinct inhibitory functions impart signaling specificity during yeast differentiation. *Cell* **91**: 673-684.

Maggi, D., G. Andraghetti, J.L. Carpentier & R. Cordera, (1998) Cys860 in the extracellular domain of insulin receptor beta-subunit is critical for internalization and signal transduction. *Endocrinology* **139**: 496-504.

Mahne, M., A. Tauch, A. Puhler & J. Kalinowski, (2006) The Corynebacterium glutamicum gene pmt encoding a glycosyltransferase related to eukaryotic protein-O-mannosyltransferases is essential for glycosylation of the resuscitation promoting factor (Rpf2) and other secreted proteins. *FEMS Microbiol Lett* **259**: 226-233.

Maidan, M.M., L. De Rop, J. Serneels, S. Exler, S. Rupp, H. Tournu, J.M. Thevelein & P. Van Dijck, (2005) The G protein-coupled receptor Gpr1 and the Galpha protein Gpa2 act through the cAMP-protein kinase A pathway to induce morphogenesis in Candida albicans. *Mol Biol Cell* **16**: 1971-1986.

Martchenko, M., A.M. Alarco, D. Harcus & M. Whiteway, (2004) Superoxide dismutases in Candida albicans: transcriptional regulation and functional characterization of the hyphal-induced SOD5 gene. *Mol Biol Cell* **15**: 456-467.

Mazanka, E. & E.L. Weiss, (2010) Sequential counteracting kinases restrict an asymmetric gene expression program to early G1. *Mol Biol Cell* **21**: 2809-2820.

Mendonca, F.H., S.S. Santos, S. Faria Ida, C.R. Goncalves e Silva, A.O. Jorge & M.V. Leao, (2012) Effects of probiotic bacteria on Candida presence and IgA anti-Candida in the oral cavity of elderly. *Braz Dent J* **23**: 534-538.

Miller, M.G. & A.D. Johnson, (2002) White-opaque switching in Candida albicans is controlled by mating-type locus homeodomain proteins and allows efficient mating. *Cell* **110**: 293-302.

Miramon, P., L. Kasper & B. Hube, (2013) Thriving within the host: Candida spp. interactions with phagocytic cells. *Med Microbiol Immunol* **202**: 183-195.

Mora-Montes, H.M., S. Bates, M.G. Netea, L. Castillo, A. Brand, E.T. Buurman, D.F. Diaz-Jimenez, B. Jan Kullberg, A.J. Brown, F.C. Odds & N.A. Gow, (2010) A multifunctional mannosyltransferase family in Candida albicans determines cell wall mannan structure and host-fungus interactions. *J Biol Chem* **285**: 12087-12095.

Mora-Montes, H.M., S. Bates, M.G. Netea, D.F. Diaz-Jimenez, E. Lopez-Romero, S. Zinker, P. Ponce-Noyola, B.J. Kullberg, A.J. Brown, F.C. Odds, A. Flores-Carreon & N.A. Gow, (2007) Endoplasmic reticulum alpha-glycosidases of Candida albicans are required for N glycosylation, cell wall integrity, and normal host-fungus interaction. *Eukaryot Cell* **6**: 2184-2193.

Moran, G.P., D.C. Coleman & D.J. Sullivan, (2011) Comparative genomics and the evolution of pathogenicity in human pathogenic fungi. *Eukaryot Cell* **10**: 34-42.

Morschhauser, J., (2010) Regulation of white-opaque switching in Candida albicans. *Med Microbiol Immunol* **199**: 165-172.

Mulhern, S.M., M.E. Logue & G. Butler, (2006) Candida albicans transcription factor Ace2 regulates metabolism and is required for filamentation in hypoxic conditions. *Eukaryot Cell* **5**: 2001-2013.

Munro, C.A., S. Bates, E.T. Buurman, H.B. Hughes, D.M. Maccallum, G. Bertram, A. Atrih, M.A. Ferguson, J.M. Bain, A. Brand, S. Hamilton, C. Westwater, L.M. Thomson, A.J. Brown, F.C. Odds & N.A. Gow, (2005) Mnt1p and Mnt2p of Candida albicans are partially redundant alpha-1,2-mannosyltransferases that participate in O-linked mannosylation and are required for adhesion and virulence. *J Biol Chem* **280**: 1051-1060.

Munro, C.A. & N.A. Gow, (2001) Chitin synthesis in human pathogenic fungi. *Med Mycol* **39 Suppl 1**: 41-53.

Munro, C.A., D.A. Schofield, G.W. Gooday & N.A. Gow, (1998) Regulation of chitin synthesis during dimorphic growth of Candida albicans. *Microbiology* **144 (Pt 2)**: 391-401.

Naglik, J.R., S.J. Challacombe & B. Hube, (2003) Candida albicans secreted aspartyl proteinases in virulence and pathogenesis. *Microbiol Mol Biol Rev* **67**: 400-428, table of contents.

Navarro-Garcia, F., M. Sanchez, J. Pla & C. Nombela, (1995) Functional characterization of the MKC1 gene of Candida albicans, which encodes a mitogen-activated protein kinase homolog related to cell integrity. *Mol Cell Biol* **15**: 2197-2206.

Nelson, B., C. Kurischko, J. Horecka, M. Mody, P. Nair, L. Pratt, A. Zougman, L.D. McBroom, T.R. Hughes, C. Boone & F.C. Luca, (2003) RAM: a conserved signaling network that regulates Ace2p transcriptional activity and polarized morphogenesis. *Mol Biol Cell* **14**: 3782-3803.

Netea, M.G., G.D. Brown, B.J. Kullberg & N.A. Gow, (2008) An integrated model of the recognition of Candida albicans by the innate immune system. *Nat Rev Microbiol* **6**: 67-78.

Netea, M.G., N.A. Gow, C.A. Munro, S. Bates, C. Collins, G. Ferwerda, R.P. Hobson, G. Bertram, H.B. Hughes, T. Jansen, L. Jacobs, E.T. Buurman, K. Gijzen, D.L. Williams, R. Torensma, A. McKinnon, D.M. MacCallum, F.C. Odds, J.W. Van der Meer, A.J. Brown & B.J. Kullberg, (2006) Immune sensing of Candida albicans requires cooperative recognition of mannans and glucans by lectin and Toll-like receptors. *J Clin Invest* **116**: 1642-1650.

Neubert, P., A. Halim, M. Zauser, A. Essig, H.J. Joshi, E. Zatorska, I.S. Larsen, M. Loibl, J. Castells-Ballester, M. Aebi, H. Clausen & S. Strahl, (2016) Mapping the O-Mannose Glycoproteome in Saccharomyces cerevisiae. *Mol Cell Proteomics* **15**: 1323-1337.

Nguyen, M.H., M.C. Wissel, R.K. Shields, M.A. Salomoni, B. Hao, E.G. Press, R.M. Shields, S. Cheng, D. Mitsani, A. Vadnerkar, F.P. Silveira, S.B. Kleiboeker & C.J. Clancy, (2012) Performance of Candida real-time polymerase chain reaction, beta-D-glucan assay, and blood cultures in the diagnosis of invasive candidiasis. *Clin Infect Dis* **54**: 1240-1248.

Nobile, C.J. & A.D. Johnson, (2015) Candida albicans Biofilms and Human Disease. *Annu Rev Microbiol* **69**: 71-92.

Nobile, C.J., J.E. Nett, D.R. Andes & A.P. Mitchell, (2006) Function of Candida albicans adhesin Hwp1 in biofilm formation. *Eukaryot Cell* **5**: 1604-1610.

O'Conallain, C., M.T. Doolin, C. Taggart, F. Thornton & G. Butler, (1999) Regulated nuclear localisation of the yeast transcription factor Ace2p controls expression of chitinase (CTS1) in Saccharomyces cerevisiae. *Mol Gen Genet* **262**: 275-282.

Odds, F.C., (1988) Candida and Candidosis. . *Bailliere Tindall* **2nd Edition**.

Pande, K., C. Chen & S.M. Noble, (2013) Passage through the mammalian gut triggers a phenotypic switch that promotes Candida albicans commensalism. *Nat Genet* **45**: 1088-1091.

Pappas, P.G., C.A. Kauffman, D. Andes, D.K. Benjamin, Jr., T.F. Calandra, J.E. Edwards, Jr., S.G. Filler, J.F. Fisher, B.J. Kullberg, L. Ostrosky-Zeichner, A.C. Reboli, J.H. Rex, T.J. Walsh, J.D. Sobel & A. Infectious Diseases Society of, (2009) Clinical practice guidelines for the management of candidiasis: 2009 update by the Infectious Diseases Society of America. *Clin Infect Dis* **48**: 503-535.

Payne, T., C. Hanfrey, A.L. Bishop, A.J. Michael, S.V. Avery & D.B. Archer, (2008) Transcript-specific translational regulation in the unfolded protein response of Saccharomyces cerevisiae. *FEBS Lett* **582**: 503-509.

Perez, J.C. & A.D. Johnson, (2013) Regulatory circuits that enable proliferation of the fungus Candida albicans in a mammalian host. *PLoS Pathog* **9**: e1003780.

Perfect, J.R., (2013) Fungal diagnosis: how do we do it and can we do better? *Curr Med Res Opin* **29 Suppl 4**: 3-11.

Peter, M., A.M. Neiman, H.O. Park, M. van Lohuizen & I. Herskowitz, (1996) Functional analysis of the interaction between the small GTP binding protein Cdc42 and the Ste20 protein kinase in yeast. *EMBO J* **15**: 7046-7059.

Petersen, R.F., G. Marinoni, M.L. Nielsen & J. Piskur, (2000) Molecular approaches for analyzing diversity and phylogeny among yeast species. *Contrib Microbiol* **5**: 15-35.

Petrescu, A.J., A.L. Milac, S.M. Petrescu, R.A. Dwek & M.R. Wormald, (2004) Statistical analysis of the protein environment of N-glycosylation sites: implications for occupancy, structure, and folding. *Glycobiology* **14**: 103-114.

Pfaller, M.A. & D.J. Diekema, (2007) Epidemiology of invasive candidiasis: a persistent public health problem. *Clin Microbiol Rev* **20**: 133-163.

Phan, Q.T., P.H. Belanger & S.G. Filler, (2000) Role of hyphal formation in interactions of Candida albicans with endothelial cells. *Infect Immun* **68**: 3485-3490.

Pidoux, A.L. & R.C. Allshire, (2000) Centromeres: getting a grip of chromosomes. *Curr Opin Cell Biol* **12**: 308-319.

Pierce, J.V. & C.A. Kumamoto, (2012) Variation in Candida albicans EFG1 expression enables host-dependent changes in colonizing fungal populations. *MBio* **3**: e00117-00112.

Polizzi, C. & L. Clarke, (1991) The chromatin structure of centromeres from fission yeast: differentiation of the central core that correlates with function. *J Cell Biol* **112**: 191-201.

Prill, S.K., B. Klinkert, C. Timpel, C.A. Gale, K. Schroppel & J.F. Ernst, (2005) PMT family of Candida albicans: five protein mannosyltransferase isoforms affect growth, morphogenesis and antifungal resistance. *Mol Microbiol* **55**: 546-560.

Radu, M. & J. Chernoff, (2009) The DeMSTification of mammalian Ste20 kinases. *Curr Biol* **19**: R421-425.

Reed, U.C., (2009) Congenital muscular dystrophy. Part II: a review of pathogenesis and therapeutic perspectives. *Arq Neuropsiquiatr* **67**: 343-362.

Richard, M., P. De Groot, O. Courtin, D. Poulain, F. Klis & C. Gaillardin, (2002) GPI7 affects cell-wall protein anchorage in Saccharomyces cerevisiae and Candida albicans. *Microbiology* **148**: 2125-2133.

Roman, E., D.M. Arana, C. Nombela, R. Alonso-Monge & J. Pla, (2007) MAP kinase pathways as regulators of fungal virulence. *Trends Microbiol* **15**: 181-190.

Roman, E., I. Correia, A. Salazin, C. Fradin, T. Jouault, D. Poulain, F.T. Liu & J. Pla, (2016) The Cek1mediated MAP kinase pathway regulates exposure of alpha1,2 and beta1,2mannosides in the cell wall of Candida albicans modulating immune recognition. *Virulence* **7**: 558-577.

Roman, E., F. Cottier, J.F. Ernst & J. Pla, (2009) Msb2 signaling mucin controls activation of Cek1 mitogen-activated protein kinase in Candida albicans. *Eukaryot Cell* **8**: 1235-1249.

Rouabhia, M., M. Schaller, C. Corbucci, A. Vecchiarelli, S.K. Prill, L. Giasson & J.F. Ernst, (2005) Virulence of the fungal pathogen Candida albicans requires the five isoforms of protein mannosyltransferases. *Infect Immun* **73**: 4571-4580.

Ruhnke, M., V. Rickerts, O.A. Cornely, D. Buchheidt, A. Glockner, W. Heinz, R. Hohl, R. Horre, M. Karthaus, P. Kujath, B. Willinger, E. Presterl, P. Rath, J. Ritter, A. Glasmacher, C. Lass-Florl, A.H. Groll, S. German Speaking Mycological & C. Paul-Ehrlich-Society for, (2011) Diagnosis and therapy of Candida infections: joint recommendations of the German Speaking Mycological Society and the Paul-Ehrlich-Society for Chemotherapy. *Mycoses* **54**: 279-310.

Saijo, S. & Y. Iwakura, (2011) Dectin-1 and Dectin-2 in innate immunity against fungi. *Int Immunol* **23**: 467-472.

Sanyal, K., M. Baum & J. Carbon, (2004) Centromeric DNA sequences in the pathogenic yeast Candida albicans are all different and unique. *Proc Natl Acad Sci U S A* **101**: 11374-11379.

Sanyal, K. & J. Carbon, (2002) The CENP-A homolog CaCse4p in the pathogenic yeast Candida albicans is a centromere protein essential for chromosome transmission. *Proc Natl Acad Sci U S A* **99**: 12969-12974.

Saputo, S., Y. Chabrier-Rosello, F.C. Luca, A. Kumar & D.J. Krysan, (2012) The RAM network in pathogenic fungi. *Eukaryot Cell* **11**: 708-717.

Saputo, S., A. Kumar & D.J. Krysan, (2014) Efg1 directly regulates ACE2 expression to mediate cross talk between the cAMP/PKA and RAM pathways during Candida albicans morphogenesis. *Eukaryot Cell* **13**: 1169-1180.

Sbia, M., E.J. Parnell, Y. Yu, A.E. Olsen, K.L. Kretschmann, W.P. Voth & D.J. Stillman, (2008) Regulation of the yeast Ace2 transcription factor during the cell cycle. *J Biol Chem* **283**: 11135-11145.

Schaekel, A., P.R. Desai & J.F. Ernst, (2013) Morphogenesis-regulated localization of protein kinase A to genomic sites in Candida albicans. *BMC Genomics* **14**: 842.

Schroppel, K., K. Sprosser, M. Whiteway, D.Y. Thomas, M. Rollinghoff & C. Csank, (2000) Repression of hyphal proteinase expression by the mitogen-activated protein (MAP) kinase phosphatase Cpp1p of Candida albicans is independent of the MAP kinase Cek1p. *Infect Immun* **68**: 7159-7161.

Scrimale, T., L. Didone, K.L. de Mesy Bentley & D.J. Krysan, (2009) The unfolded protein response is induced by the cell wall integrity mitogen-activated protein kinase signaling cascade and is required for cell wall integrity in Saccharomyces cerevisiae. *Mol Biol Cell* **20**: 164-175.

Sellam, A., H. Hogues, C. Askew, F. Tebbji, M. van Het Hoog, H. Lavoie, C.A. Kumamoto, M. Whiteway & A. Nantel, (2010) Experimental annotation of the human pathogen Candida albicans coding and noncoding transcribed regions using high-resolution tiling arrays. *Genome Biol* **11**: R71.

Setiadi, E.R., T. Doedt, F. Cottier, C. Noffz & J.F. Ernst, (2006) Transcriptional response of Candida albicans to hypoxia: linkage of oxygen sensing and Efg1p-regulatory networks. *J Mol Biol* **361**: 399-411.

Shepherd, M.G., (1987) Cell envelope of Candida albicans. *Crit Rev Microbiol* **15**: 7-25.

Sheth, C.C., R. Hall, L. Lewis, A.J. Brown, F.C. Odds, L.P. Erwig & N.A. Gow, (2011) Glycosylation status of the C. albicans cell wall affects the efficiency of neutrophil phagocytosis and killing but not cytokine signaling. *Med Mycol* **49**: 513-524.

Shoemaker, C.J., D.E. Eyler & R. Green, (2010) Dom34:Hbs1 promotes subunit dissociation and peptidyl-tRNA drop-off to initiate no-go decay. *Science* **330**: 369-372.

Smits, G.J., H. van den Ende & F.M. Klis, (2001) Differential regulation of cell wall biogenesis during growth and development in yeast. *Microbiology* **147**: 781-794.

Sobel, J.D., (1988) Pathogenesis and epidemiology of vulvovaginal candidiasis. *Ann N Y Acad Sci* **544**: 547-557.

Sohn, K., C. Urban, H. Brunner & S. Rupp, (2003) EFG1 is a major regulator of cell wall dynamics in Candida albicans as revealed by DNA microarrays. *Mol Microbiol* **47**: 89-102.

Song, Y., S.A. Cheon, K.E. Lee, S.Y. Lee, B.K. Lee, D.B. Oh, H.A. Kang & J.Y. Kim, (2008) Role of the RAM network in cell polarity and hyphal morphogenesis in Candida albicans. *Mol Biol Cell* **19**: 5456-5477.

Sonneborn, A., D.P. Bockmuhl & J.F. Ernst, (1999) Chlamydospore formation in Candida albicans requires the Efg1p morphogenetic regulator. *Infect Immun* **67**: 5514-5517.

Sonneborn, A., D.P. Bockmuhl, M. Gerads, K. Kurpanek, D. Sanglard & J.F. Ernst, (2000) Protein kinase A encoded by TPK2 regulates dimorphism of Candida albicans. *Mol Microbiol* **35**: 386-396.

Spiro, R.G., (2002) Protein glycosylation: nature, distribution, enzymatic formation, and disease implications of glycopeptide bonds. *Glycobiology* **12**: 43R-56R.

Srikantha, T., L.K. Tsai, K. Daniels & D.R. Soll, (2000) EFG1 null mutants of Candida albicans switch but cannot express the complete phenotype of white-phase budding cells. *J Bacteriol* **182**: 1580-1591.

Staab, J.F. & P. Sundstrom, (1998) Genetic organization and sequence analysis of the hypha-specific cell wall protein gene HWP1 of Candida albicans. *Yeast* **14**: 681-686.

Staib, P. & J. Morschhauser, (2007) Chlamydospore formation in Candida albicans and Candida dubliniensis--an enigmatic developmental programme. *Mycoses* **50**: 1-12.

Stichternoth, C. & J.F. Ernst, (2009) Hypoxic adaptation by Efg1 regulates biofilm formation by Candida albicans. *Appl Environ Microbiol* **75**: 3663-3672.

Stoldt, V.R., A. Sonneborn, C.E. Leuker & J.F. Ernst, (1997) Efg1p, an essential regulator of morphogenesis of the human pathogen Candida albicans, is a member of a conserved class of bHLH proteins regulating morphogenetic processes in fungi. *EMBO J* **16**: 1982-1991.

Sudbery, P.E., (2011) Growth of Candida albicans hyphae. *Nat Rev Microbiol* **9**: 737-748.

Swidergall, M., A.M. Ernst & J.F. Ernst, (2013) Candida albicans mucin Msb2 is a broad-range protectant against antimicrobial peptides. *Antimicrob Agents Chemother* **57**: 3917-3922.

Szafranski-Schneider, E., M. Swidergall, F. Cottier, D. Tielker, E. Roman, J. Pla & J.F. Ernst, (2012) Msb2 shedding protects Candida albicans against antimicrobial peptides. *PLoS Pathog* **8**: e1002501.

Szafranski-Schneider, M.E., (2011) Charakterisierung des Msb2 Sensorproteins in Candida albicans. *Dissertation, Heinrich-Heine-Universität Düsseldorf*.

Tanner, W. & L. Lehle, (1987) Protein glycosylation in yeast. *Biochim Biophys Acta* **906**: 81-99.

Tebarth, B., T. Doedt, S. Krishnamurthy, M. Weide, F. Monterola, A. Dominguez & J.F. Ernst, (2003) Adaptation of the Efg1p morphogenetic pathway in Candida albicans by negative autoregulation and PKA-dependent repression of the EFG1 gene. *J Mol Biol* **329**: 949-962.

Timpel, C., S. Strahl-Bolsinger, K. Ziegelbauer & J.F. Ernst, (1998) Multiple functions of Pmt1p-mediated protein O-mannosylation in the fungal pathogen Candida albicans. *J Biol Chem* **273**: 20837-20846.

Timpel, C., S. Zink, S. Strahl-Bolsinger, K. Schroppel & J. Ernst, (2000) Morphogenesis, adhesive properties, and antifungal resistance depend on the Pmt6 protein mannosyltransferase in the fungal pathogen candida albicans. *J Bacteriol* **182**: 3063-3071.

Travers, K.J., C.K. Patil, L. Wodicka, D.J. Lockhart, J.S. Weissman & P. Walter, (2000) Functional and genomic analyses reveal an essential coordination between the unfolded protein response and ER-associated degradation. *Cell* **101**: 249-258.

Tuch, B.B., Q.M. Mitrovich, O.R. Homann, A.D. Hernday, C.K. Monighetti, F.M. De La Vega & A.D. Johnson, (2010) The transcriptomes of two heritable cell types illuminate the circuit governing their differentiation. *PLoS Genet* **6**: e1001070.

Ura, S., N. Masuyama, J.D. Graves & Y. Gotoh, (2001) Caspase cleavage of MST1 promotes nuclear translocation and chromatin condensation. *Proc Natl Acad Sci U S A* **98**: 10148-10153.

Urban, J., A. Soulard, A. Huber, S. Lippman, D. Mukhopadhyay, O. Deloche, V. Wanke, D. Anrather, G. Ammerer, H. Riezman, J.R. Broach, C. De Virgilio, M.N. Hall & R. Loewith, (2007) Sch9 is a major target of TORC1 in Saccharomyces cerevisiae. *Mol Cell* **26**: 663-674.

van der Graaf, C.A., M.G. Netea, I. Verschueren, J.W. van der Meer & B.J. Kullberg, (2005) Differential cytokine production and Toll-like receptor signaling pathways by Candida albicans blastoconidia and hyphae. *Infect Immun* **73**: 7458-7464.

van Reeuwijk, J., M. Janssen, C. van den Elzen, D. Beltran-Valero de Bernabe, P. Sabatelli, L. Merlini, M. Boon, H. Scheffer, M. Brockington, F. Muntoni, M.A. Huynen, A. Verrips, C.A. Walsh, P.G. Barth, H.G. Brunner & H. van Bokhoven, (2005) POMT2 mutations cause alpha-dystroglycan hypoglycosylation and Walker-Warburg syndrome. *J Med Genet* **42**: 907-912.

Van Wijlick, L., (2012) Funktion des Transkriptionsfaktors Ace2 bei der Regulation von *PMT*-Genen in *C. albicans*. *Diplomarbeit, Heinrich-Heine-Universität Düsseldorf.*

Vazquez-Torres, A. & E. Balish, (1997) Macrophages in resistance to candidiasis. *Microbiol Mol Biol Rev* **61**: 170-192.

Verma-Gaur, J. & A. Traven, (2016) Post-transcriptional gene regulation in the biology and virulence of Candida albicans. *Cell Microbiol* **18**: 800-806.

Wachtler, B., D. Wilson & B. Hube, (2011) Candida albicans adhesion to and invasion and damage of vaginal epithelial cells: stage-specific inhibition by clotrimazole and bifonazole. *Antimicrob Agents Chemother* **55**: 4436-4439.

Waldman, A., A. Gilhar, L. Duek & I. Berdicevsky, (2001) Incidence of Candida in psoriasis--a study on the fungal flora of psoriatic patients. *Mycoses* **44**: 77-81.

Wang, A., P.P. Raniga, S. Lane, Y. Lu & H. Liu, (2009) Hyphal chain formation in Candida albicans: Cdc28-Hgc1 phosphorylation of Efg1 represses cell separation genes. *Mol Cell Biol* **29**: 4406-4416.

Weber, Y., S.K. Prill & J.F. Ernst, (2004) Pmt-mediated O mannosylation stabilizes an essential component of the secretory apparatus, Sec20p, in Candida albicans. *Eukaryot Cell* **3**: 1164-1168.

Willer, T., W. Amselgruber, R. Deutzmann & S. Strahl, (2002) Characterization of POMT2, a novel member of the PMT protein O-mannosyltransferase family specifically localized to the acrosome of mammalian spermatids. *Glycobiology* **12**: 771-783.

Wimalasena, T.T., B. Enjalbert, T. Guillemette, A. Plumridge, S. Budge, Z. Yin, A.J. Brown & D.B. Archer, (2008) Impact of the unfolded protein response upon genome-wide expression patterns, and the role of Hac1 in the polarized growth, of Candida albicans. *Fungal Genet Biol* **45**: 1235-1247.

Xu, C. & D.T. Ng, (2015) Glycosylation-directed quality control of protein folding. *Nat Rev Mol Cell Biol* **16**: 742-752.

Xu, C., S. Wang, G. Thibault & D.T. Ng, (2013) Futile protein folding cycles in the ER are terminated by the unfolded protein O-mannosylation pathway. *Science* **340**: 978-981.

Yoshikawa, F.S., R. Yabe, Y. Iwakura, S.R. de Almeida & S. Saijo, (2016) Dectin-1 and Dectin-2 promote control of the fungal pathogen Trichophyton rubrum independently of IL-17 and adaptive immunity in experimental deep dermatophytosis. *Innate Immun* **22**: 316-324.

Zipfel, P.F., C. Skerka, D. Kupka & S. Luo, (2011) Immune escape of the human facultative pathogenic yeast Candida albicans: the many faces of the Candida Pra1 protein. *Int J Med Microbiol* **301**: 423-430.

Zordan, R.E., M.G. Miller, D.J. Galgoczy, B.B. Tuch & A.D. Johnson, (2007) Interlocking transcriptional feedback loops control white-opaque switching in Candida albicans. *PLoS Biol* **5**: e256.

7 Abkürzungsverzeichnis

%	Prozent
°C	Grad Celsius
Abb.	Abbildung
ATP	Adenosintriphosphat
Asn	Asparagin
A. fumigatus	*Aspergillus fumigatus*
bHLH	basic-Helix-Loop-Helix
Bp	Basenpaare
bzw.	Beziehungsweise
Ca	*Candida albicans*
cAMP	cyclisches Adenosinmonophosphat
CO_2	Kohlenstoffdioxid
DC-SIGN	Dendritic-Cell specific ICAM-3-grabbing non-integrin-1
DNA	Desoxyribonukleinsäure
Dol-P	Dolichol-Phosphat
ER	Endoplasmatisches Retikulum
ERAD	ER-Assoziierte Degradation
GEF	Guanosintriphosphat-Exchange Faktor
GlcNAc	N-Acetyl-D-Glukosamin
GPI	Glycosyl Phosphatidyl Inositol
GTP	Guanosintriphosphat
GUT	Gastrointestinally-Induced Transition
HIV	Humane Immundefizienz-Virus
HOG	High-Osmolarity Glycerol
IL	Interleukin
MAPK	Mitogen-Aktivierte Proteinkinase
Mincle	Makrophagen-induzierte C-Typ-Lektine
mRNA	messenger Ribonukleinsäure
MRP	Mannose Rezeptorprotein
NES	Nuclear Export Sequence
NLS	Nuclear Localization Sequence
PAK	p51-activated Kinase
PAMPs	Pathogen-Associated Molecular Patterns

PCR	Polymerase-Ketten-Reaktion
Pir	Protein with internal repeats
PKA	Proteinkinase A
PKC	Proteinkinase C
Pmt	Protein-*O*-Mannosyltransferase
PRRs	Pattern Recognition Receptors
RAM	Regulation of Ace2 and Morphogenesis
Sc	*Saccharomyces cerevisiae*
Scwp	Soluble cell wall proteins
Ser	Serin
spp.	species pluralis
SVG	Sterile Vegetative Growth
Thr	Threonin
TLR	Toll-Like Rezeptor
TM	Transmembran
TOR	Target of Rapamycin
u. a.	unter anderem
UPR	Unfolded-Protein-Response
UTR	untranslatierte Region
z. B.	zum Beispiel

8 Lebenslauf und Publikationen

Lebenslauf

Name	Lasse van Wijlick
Geburtsdatum	27.08.1986
Geburtsort	Viersen
Nationalität	deutsch
Ausbildung	
04.2013 – 09.2016	Heinrich-Heine-Universität Düsseldorf Promotion, Molekulare Mykologie
10.2006 – 03.2012	Heinrich-Heine-Universität Düsseldorf Diplomstudium der Biologie
08.1997 – 07.2006	Städtische Gesamtschule Hardt Mönchengladbach Abitur

Publikationen

Varshney N, Schaekel A, Singha R, Chakraborty T, **van Wijlick L**, Ernst JF, Sanyal K. A Surprising Role for the Sch9 Protein Kinase in Chromosome Segregation in *Candida albicans*. Genetics 2015 Mar, 199(3):671-4.

Swidergall M, **van Wijlick L**, Ernst JF. Signaling domains of mucin Msb2 in *Candida albicans*. Eukaryot Cell 2015 Apr, EC.00264-14;14(4):359-70.

Desai PR*, **van Wijlick L***, Kurtz D, Juchimiuk M, Ernst JF (*shared first authors). Hypoxia and Temperature Regulated Morphogenesis in *Candida albicans*. PLoS Genet 2015 Aug, 14;11(8):e1005447.

van Wijlick L, Swidergall M, Brandt P, Ernst JF. *Candida albicans* responds to glycostructure damage by Ace2-mediated feedback regulation of Cek1 signaling. Mol Microbiol 2016 Sep, doi: 10.1111/mmi.13494.

van Wijlick L, Geissen R, Hilbig JS, Lagadec Q, Cantero PD, Pfeifer E, Juchimiuk M, Kluge S, Wickert S, Alepuz P, Ernst JF. Dom34 links translation to protein *O*-mannosylation. PLoS Genet 2016 Oct, 12(10): e1006395.

Präsentationen

van Wijlick L, Ernst JF
Hypoxic function of the transcription factor Ace2 in *Candida albicans*
Oxystress and human fungal pathogens, 19 – 20 November 2013, Innsbruck, Austria

van Wijlick L, Ernst JF
Cell surface regulation in *Candida albicans* by the Ace2 signaling pathway
1st MOI II Symposium, 24 – 25 September 2014, Cologne, Germany

van Wijlick L, Desai PR, Ernst JF
Novel mechanisms of hypoxic regulators in *C. albicans*
Oxystress and human fungal pathogens, 06 – 07 November 2014, Valencia, Spain

van Wijlick L, Swidergall M, Ernst JF
Glycoshield regulation in *Candida albicans* by the Ace2 signaling pathway
Statusworkshop DGHM Fachgruppe Eukaryontische Krankheitserreger, 26 – 27 February 2015, Erlangen, Germany

van Wijlick L, Ernst JF
Cell surface regulation in *Candida albicans* by the Ace2 signaling pathway
2nd MOI II Symposium, 17 – 19 September 2015, Düsseldorf, Germany

van Wijlick L, Ernst JF
Candida albicans responds to glycostructure damage by Ace2-mediated feedback regulation of Cek1 signaling
3rd MOI II Symposium, 21 – 23 September 2016, Geldern, Germany

Poster

van Wijlick L, Ernst JF
Cell surface regulation in *Candida albicans* by the Ace2 signaling pathway
12th ASM Conference on Candida and Candidiasis, 26 – 30 March 2014, New Orleans, Louisiana USA

van Wijlick L, Swidergall M, Ernst JF
Glycoshield regulation by the Ace2 signaling pathway in *Candida albicans*
67. Jahrestagung der DGHM, 27 – 30 September 2015, Münster, Germany

van Wijlick L, Swidergall M, Ernst JF
Glycoshield regulation by the Ace2 signaling pathway in *Candida albicans*
Fungal Cell Wall, 26 – 28 October 2015, Paris, France

9 Danksagung

Nach nun mehr drei Jahren intensiver Forschung ist es an der Zeit mich bei all denjenigen zu bedanken, die mich während meiner Promotionszeit unterstützt haben.

An erster Stelle möchte ich mich herzlich bei Prof. Joachim Ernst bedanken. Zum einen für das interessante Thema, aber auch die gewährte Freiheit, die es mir ermöglicht hat meinen eigenen Weg zu finden und dem damit entgegengebrachten Vertrauen. Sein ansteckender Wissensdrang hat wesentlich zum Gelingen dieser Arbeit beigetragen und für die ein oder andere Überraschung gesorgt. Er stand mir zu jeder Zeit für Fragen und Diskussionen zur Seite. Auch wenn Du nun im Ruhestand bist, bin ich mir sicher, dass dich Dein Forschergeist auch die nächsten Jahre auf Trab halten wird. Ich habe mich immer sehr wohl in deiner Arbeitsgruppe gefühlt.

Bei Prof. Walter Däubener und Prof. Joachim Morschhäuser möchte ich mich für die Übernahme des Koreferats meiner Dissertation und das Interesse an meinem Projekt bedanken.

Auch bei Dr. Christoph Bürth möchte ich mich bedanken, insbesondere in der Schlussphase meiner Promotionszeit stand er mir mit Ratschlägen zur Seite.

Ein besonderer Dank gilt auch Dr. Inge Krümpelbeck, für ihre Arbeit und Unterstützung als Koordinatorin meiner Graduiertenschule, aber auch für das darüber hinaus entgegengebrachte Interesse an meinem Projekt.

Natürlich möchte ich mich auch herzlich bei meinen Arbeitskollegen für eine wundervolle Zeit im Labor und auch außerhalb des Labors bedanken. Allen voran danke ich Michaela Gerads, Maya Kunigo und Pilar Dominguez, die mich in ihrem Labor willkommen hießen. Zudem danke ich Dr. Mateusz Juchimiuk, Evelyn Wetjen, Silas Janßen, Dr. Isabel Eichhof, Dr. Theresia Lassak und Dr. René Geißen für ihre Unterstützung meiner Arbeit und die gemeinsame Zeit im Labor. Ein besonderer Dank gilt Dr. Alida Schäkel und Prashant Desai, gemeinsam haben wir über die Jahre die Hoch- und Tiefpunkte der Forschungsarbeit erlebt. Ohne euch wäre es nicht halb so schön gewesen. Bei Mario Kapitan und Silke Jankowski möchte ich mich insbesondere für die fröhlichen Aktivitäten bedanken.

Lieber Marc, zusammen haben wir Deutschland und die Welt bereist. Auf zahlreichen Konferenzen standen wir uns zur Seite. Ich danke Dir für Deine unverblümte Ehrlichkeit, Dein großes Interesse an der Forschung und unsere unzähligen Diskussionen. Für die Weltforschung!

Außerdem möchte ich mich an dieser Stelle bei meinen Studenten bedanken, die durch ihre Arbeit und ihr Interesse zu unseren Forschungsprojekten beigetragen haben. Danke, Corinna, Jonas, Meltem, Daniela und Philipp, für eure Hilfe.

Lieber Philipp, dank unserer Abmachung, ich würde für jede beantwortete Frage Zehn Euro erhalten, wäre ich inzwischen Multimillionär. Hiermit erlasse ich Dir deine Schulden und wünsche Dir noch alles Gute auf Deiner Reise.

Besonderer Dank gilt auch meinen Eltern und meiner Familie, die mich auf jede erdenkliche Weise unterstützt haben. Bei euch habe ich einen Ort zum Durchatmen.

Ein außerordentlicher Dank gilt meiner Ellen, die mich durch mein gesamtes Studium und die Promotionszeit getragen und ertragen hat. Mein Glück, dass ich Dich habe.

Eidesstattliche Erklärung

Ich versichere an Eides Statt, dass die Dissertation von mir selbständig und ohne unzulässige fremde Hilfe unter Beachtung der „Grundsätze zur Sicherung guter wissenschaftlicher Praxis an der Heinrich-Heine-Universität Düsseldorf“ erstellt worden ist. Sie wurde weder in dieser noch in ähnlicher Form bei einer anderen Institution vorgelegt. Ich habe keinen Doktorgrad an einer anderen Hochschule erworben oder zu erwerben versucht. Zitate wurden kenntlich gemacht.

Düsseldorf, _____ _____

(Lasse van Wijlick)

Teile dieser Arbeit wurden veröffentlicht:

Varshney N, Schaekel A, Singha R, Chakraborty T, van Wijlick L, Ernst JF, Sanyal K.
A Surprising Role for the Sch9 Protein Kinase in Chromosome Segregation in *Candida albicans*. Genetics 2015 Mar, 199(3):671-4.

Swidergall M, van Wijlick L, Ernst JF. Signaling domains of mucin Msb2 in *Candida albicans*. Eukaryot Cell 2015 Apr, EC.00264-14;14(4):359-70.

Desai PR*, van Wijlick L*, Kurtz D, Juchimiuk M, Ernst JF (*shared first authors). Hypoxia and Temperature Regulated Morphogenesis in *Candida albicans*. PLoS Genet 2015 Aug, 14;11(8):e1005447.

van Wijlick L, Swidergall M, Brandt P, Ernst JF. *Candida albicans* responds to glycostructure damage by Ace2-mediated feedback regulation of Cek1 signaling. Mol Microbiol 2016 Sep, doi: 10.1111/mmi.13494.

van Wijlick L, Geissen R, Hilbig JS, Lagadec Q, Cantero PD, Pfeifer E, Juchimiuk M, Kluge S, Wickert S, Alepuz P, Ernst JF. Dom34 links translation to protein *O*-mannosylation. PLoS Genet 2016 Oct, 12(10): e1006395.